

Stony Brook University



OFFICIAL COPY

The official electronic file of this thesis or dissertation is maintained by the University Libraries on behalf of The Graduate School at Stony Brook University.

© All Rights Reserved by Author.

**Development of novel antimicrobial agents through inhibition of cytokinetic protein FtsZ
in Mycobacterium tuberculosis and sphingolipid GlcCer in fungi**

A Dissertation Presented

By

Krupanandan Haranahalli

To

The Graduate School
In Partial Fulfillment of the
Requirements
For the Degree of

Doctor of Philosophy

in

Chemistry

Stony Brook University

August 2016

Stony Brook University

The Graduate School

Krupanandan Haranahalli Raghunandan

We, the dissertation committee for the above candidate for the
Doctor of Philosophy degree, hereby recommend
acceptance of this dissertation.

Iwao Ojima – Dissertation Advisor

Distinguished Professor, Department of Chemistry

Peter J. Tonge – Chairperson of Defense

Professor, Department of Chemistry

Dale G. Drueckhammer – Third Member

Professor, Department of Chemistry

Maurizio Del Poeta – Outside member

Professor, Department of Molecular Genetics & Microbiology,

Stony Brook University, Stony Brook, NY

This dissertation is accepted by the Graduate School

Nancy Goroff

Interim Dean of the Graduate School

Abstract of the dissertation

**Development of novel antimicrobial agents through inhibition of cytokinetic protein FtsZ
in Mycobacterium tuberculosis and sphingolipid GlcCer in fungi**

by

Krupanandan Haranahalli

Doctor of Philosophy

in

Chemistry

Stony Brook University

2016

In 2014, an estimated 480,000 people developed MDR-TB and 190,000 people died as a result of it. Approximately 9.7 % of people with MDR-TB are estimated to have XDR-TB. With the increase in the number of MDR-TB and XDR-TB cases, there is a dire need for the development of new anti-TB agents with novel mechanism of action. FtsZ, a crucial bacterial cytokinesis protein is a potential target for the development of new anti-TB agents. Previously a library of 2,5,6- and 2,5,7-trisubstituted benzimidazoles were synthesized and tested for their anti-TB activity. The lead molecules inhibited the assembly of Mycobacterium tuberculosis FtsZ by enhancing the GTPase activity. Based on the SAR studies, a new series of 2,5,6-trisubstituted benzimidazole library containing a dimethylamino group at the 6-position and various modifications at the 2-position was designed and synthesized. Trisubstituted indole analogs of the lead benzimidazoles were also synthesized as a part of SAR studies.

Fungal infections affect an estimated 300 million people globally. With existing drugs displaying drawbacks like drug-drug interactions, toxicity and narrow spectrum of activity and emergence of fungal infections resistant to current drugs, new antifungal agents with novel targets are crucial. In this context, fungal sphingolipids is a promising target as it is essential for their virulence in alkaline environment. Screening of a library of 49,120 compounds from ChemBridge against *C. neoformans*, led to the identification of two hits, BHBM and D0 with MFC of 4 $\mu\text{g}/\text{mL}$ and 1.2 $\mu\text{g}/\text{mL}$ respectively. Further screening found three more hit compounds, which exhibited potent antifungal activity (MIC₈₀ 0.03 $\mu\text{g}/\text{mL}$). Based on these results, a new library of aromatic acylhydrazides has been designed and synthesized for SAR studies. Synthesis, biological activity, and SAR study of the new library of anti-fungal acylhydrazones will be presented.

Table of contents

Chapter 1

Novel trisubstituted benzimidazoles as anti-tubercular agents that inhibit ftsz

1.1. Introduction.....	3
1.1.1. Filamentous temperature sensitive protein Z (FtsZ).....	5
1.1.2. Development of Mtb FtsZ inhibitors	6
1.1.2.1. Taxanes as a starting point.....	6
1.1.2.2. Benzimidazoles as FtsZ inhibitors.....	7
1.1.2.3. 2-alkoxycarbonylaminopyridines and 2-carbamoylpteridines as Mtb FtsZ inhibitors.....	7
1.1.2.4. Trisubstituted benzimidazoles	8
1.2. Results and Discussion	13
1.2.1. Synthesis of 2,5,6-trisubstituted benzimidazoles.....	13
1.2.1.1. Library synthesis.....	14
1.2.1.2. Hits from the library at 5 µg/mL.....	15
1.2.1.3. Resynthesis of hits from library.....	17
1.2.1.3.1. 2-Benzylbenzimidazoles.....	17
1.2.1.3.2. 2-Cyclopentylbenzimidazoles.....	18
1.2.1.3.3. 2-(3-pentyl)benzimidazoles	19
1.2.1.3.4. 2-Isopropyl and 2-Thienyl benzimidazoles	20
1.2.1.3. Synthesis of 2-tetrahydropyranyl benzimidazoles.....	21
1.2.1.4. Synthesis of 2- α,α -difluorophenylacetyl benzimidazoles.....	24
1.2.1.5. 2-Morpholinyl benzimidazoles	25
1.2.2. SAR of 2-position of 2,5,6-trisubstituted benzimidazoles.....	26
1.2.3. Metabolic stability of 2,5,6-trisubstituted benzimidazoles.....	27
1.2.4. Human ether a-go-go-related gene (hERG) inhibitor	28
1.2.4.1. Synthesis of 3-pentyl analogs of lead benzimidazoles	30
1.2.4.2. Synthesis of polar trisubstituted benzimidazoles.....	30
1.2.5. Exploration of trisubstituted indoles as antibacterial scaffold.....	33
1.2.5.1. Indole analogs of SB-P17G-A37 and SB-P17G-A55.....	34
1.2.5.2. Tetrasubstituted indoles	37

1.2.5.3. Trisubstituted indoles with phenyl substitution at the 2-position	37
1.2.5.4. Accurate MIC of the synthesized indoles	38
1.3. Conclusion	39
1.4. Experimental Section	39
1.5. References	75

Chapter 2

Synthesis of acyl hydrazones as antimicrobial agents targeting fungal GlcCer

2.1. Introduction	81
2.1.1. Preliminary SAR	83
2.2. Results and discussion	85
2.2.1. Synthesis of acyl hydrazides	85
2.2.2. Synthesis of 3-Bromobenzoic hydrazide	85
2.2.3. Synthesis of quinolone-3-carbohydrazide	86
2.2.4. Resynthesis of hits from initial screening	86
2.2.5. Synthesis of ¹³ C analog of BHBM	88
2.2.6. Acyl hydrazone library synthesis	89
2.3. Conclusion	90
2.4. Experimental Section	90
2.5. References	97

Chapter 3

Development of novel inhibitors of botulinum neurotoxins A and E

3.1. Introduction	100
3.1.1. Molecular foot-print based rescoring methodology	100
3.1.2. Molecular dynamics	102

3.1.3. BoNT/E Inhibitors	103
3.2 Results and discussion	103
3.2.1. Synthesis of hybrid compound.....	103
3.2.2. Resynthesis of 5-chloroethyl-3-(4-trifluoromethylphenyl)-[1,2,4]oxadiazole	107
3.2.3. Synthesis of C562-1101-D-Ile	109
3.3. Conclusion	110
3.4. Experimental section.....	110
3.5. References.....	116

Chapter 4

Resynthesis of SB-RA-5001

4.1. Introduction.....	119
4.2. Results and discussion	119
4.3. Conclusion	120
4.4. Experimental Section	120
4.5. References.....	123
Bibliography	124
Appendix	132

List of Figures

Figure 1: Global TB incidence rates in 2013	3
Figure 2: First line drugs for treatment of TB.....	4
Figure 3: Drugs for MDR-TB.....	5
Figure 4: Division of a bacterial cell.....	6
Figure 5: Taxanes that inhibit FtsZ.....	7
Figure 6: Albendazole, thiabendazole and SRI compounds	8
Figure 7: SAR studies of 2,5,6-trisubstituted benzimidazoles.....	10
Figure 8: Structure of SB-P17G-C2.....	10
Figure 9: Lead trisubstituted benzimidazoles with benzamide at 5-position.....	11
Figure 10: (A)- Inhibition of Mtb FtsZ by SB-P17G-C2 in a dose dependent manner	12
Figure 11: TEM images of Mtb FtsZ.....	12
Figure 12: Proposed library of 2,5,6-trisubstituted benzimidazoles.....	13
Figure 13: Hits from library at 5 µg/mL.....	17
Figure 14: Structure of hERG channel.....	28
Figure 15: Interaction of drug spiroperidone with hERG channel	29
Figure 16: Mass spectrum of 14 and possible structure for dimer.....	36
Figure 2.1: Structures of fungal and mammalian GlcCer.....	81
Figure 2.2: Identification of BHBM and D0 as GlcCer inhibitors.....	82
Figure 2.3: Structures of BHBM and D0.....	83
Figure 2.4: GlcCer inhibition by BHBM and D0. ¹ Copied from Reference 1.....	83
Figure 2.5: Kill characteristics of BHBM (A) and D0 (B). ¹ Copied from reference 1.....	83
Figure 2.6: Screening of BHBM and D0 analogs.....	84
Figure 2.7: Additional hits from initial screening.....	84
Figure 2.8: Resynthesis of BHBM and other hit compounds.....	87
Figure 2.9: Compounds from initial library.....	89
Figure 2.10: Library of 96 compounds.....	90
Figure 3.1: Use of FPS score in virtual screening (a) Reference ligand (red). (b) Comparison between the reference (red) and candidate molecule (green) from the virtual screen	100
Figure 3.2: 2D chemical structure and 3D docked structures of hit compounds.....	101
Figure 3.3: Molecular dynamics simulation studies of hybrid compound.....	102

Figure 3.4: Predicted binding pose and footprint of the hybrid compound.	102
Figure 3.5: Footprint of RIME and ZINC20284316 with BoNT/E.	103

List of tables

Table 1: Second line drugs for TB.....	5
Table 2: Antimicrobial activities of some trisubstituted benzimidazoles against Mtb.....	9
Table 3: Accurate MIC of 2-benzylbenzimidazoles.....	18
Table 4: Accurate MIC of 2-cyclopentylbenzimidazoles.....	19
Table 5: Accurate MIC of 2-(3-pentyl)benzimidazoles.....	20
Table 6: Accurate MIC of 2-Isopropyl and 2-Thienyl benzimidazoles.....	21
Table 7: Accurate MIC of 2-tetrahydropyranyl analogs of lead benzimidazoles.....	24
Table 8: Synthesis of α,α -difluorophenylacetamide.....	25
Table 9: SAR of 2-position of 2,5,6-trisubstituted benzimidazoles.....	27
Table 10: Metabolic stability of 2,5,6-trisubstituted benzimidazoles.....	28
Table 11: hERG inhibition by trisubstituted benzimidazoles.....	30
Table 12: 3-pentyl analogs of lead benzimidazoles.....	30
Table 13: hERG inhibitory prediction results from LabMol.....	31
Table 14: Accurate MIC of indoles against Mtb H37Rv.....	39

List of schemes

Scheme 1: Synthesis of 2,5,6-trisubstituted benzimidazoles.	14
Scheme 2: Library synthesis.	15
Scheme 3: General procedure for the re-synthesis of hit amides and carbamates.	17
Scheme 4: Synthesis of 2-tetrahydropyranyl benzimidazoles.	22
Scheme 5: Synthesis of 2-tetrahydropyranyl benzimidazoles.	22
Scheme 6: Synthesis of 2-tetrahydropyranyl analogs of lead benzimidazoles.	23
Scheme 7: Synthesis of α,α -difluorophenylacetamide.	24
Scheme 8: Synthesis of 2- α,α -difluorophenylacetamide analog of SB-P17G-A20.	25
Scheme 9: Synthesis of morpholinylamide.	25
Scheme 10: Synthesis of trifluoroacetamides.	32
Scheme 11: Synthesis of 5-amidobenzimidazoles.	32
Scheme 12: Synthesis of trisubstituted indoles with methyl substitution at the 2-position.	33
Scheme 13: Synthesis of trisubstituted indoles with cyclohexyl substitution at the 2-position.	34
Scheme 14: Synthesis of indole analogs of SB-P17G-A38 and SB-P17G-A55.	35
Scheme 15: Synthesis of indole analogs of SB-P17G-A38 and SB-P17G-A55.	37
Scheme 16: Synthesis of tetrasubstituted indoles.	37
Scheme 17: Synthesis of trisubstituted indoles with phenyl substitution at the 2-position.	38
Scheme 2.1: Synthesis of 2,3-difluorobenzoic hydrazide.	85
Scheme 2.2: Synthesis of 3-Bromobenzoic hydrazide.	85
Scheme 2.4: Synthesis of substituted phenyl carbohydrazides.	86
Scheme 2.5: Synthesis of acyl hydrazones.	88
Scheme 2.6: Synthesis of ^{13}C analog of BHBM.	88
Scheme 2.7: Synthesis of ^{13}C analog of BHBM.	88
Scheme 2.8: Acyl hydrazone library synthesis.	89
Scheme 3.1: Synthesis of (6,8-dioxo-5,8-dihydro[1,3]dioxolo[4,5-g]quinazolin-7(6H)- yl)ethanol.	104
Scheme 3.2: Oxidation of alcohol to aldehyde.	105
Scheme 3.3: Proposed synthesis of aldehyde 6.	105
Scheme 3.4: Synthesis of acetal.	106

Scheme 3.5: Synthesis of weinreb amide 12.....	106
Scheme 3.6: Reduction of weinreb amide and ester to aldehyde.....	107
Scheme 3.7: Fukuyama reduction to synthesize 6.....	107
Scheme 3.8: Synthesis of 5-chloroethyl-3-(4-trifluoromethylphenyl)-[1,2,4]oxadiazole.	108
Scheme 3.9: Synthesis of 5-chloroethyl-3-(4-trifluoromethylphenyl)-[1,2,4]oxadiazole.	108
Scheme 3.10: Proposed synthesis of 12.....	108
Scheme 3.11: Synthesis of 13.	109
Scheme 3.12: Synthesis of C562-1101-D-Ile	110
Scheme 4.1: Synthesis of SB-RA-5001.....	119

List of abbreviations

AcCN	Acetonitrile
AIDS	Acquired immune deficiency syndrome
ATP	Adenosine triphosphate
CDC	Center for disease control and prevention
CDI	Carbonyldiimidazole
Cu(OAc) ₂	Cupric acetate
¹³ C NMR	Carbon-13 nuclear magnetic resonance
DCM	Dichloromethane
DIPEA	Diisopropylethylamine
DMAP	Dimethylaminopyridine
DMF	Dimethylformamide
DMSO	Dimethylsulfoxide
DNA	Deoxynucleic acid
<i>E. coli</i>	<i>Escherichia coli</i>
EDC·HCl	1-Ethyl-3-(3-dimethylaminopropyl)carbodiimide hydrochloride
EMB	Ethambutol
EtOAc	Ethyl acetate
EtOH	ethanol
FDA	Food and drug administration
FtsZ	Filamentous temperature sensitive protein Z
GDP	Guanosine diphosphate
GTP	Guanosine triphosphate
GTPase	Guanosine triphosphatase
HCl	Hydrochloric acid
hERG	Human ether-a-go-go-related gene
HF	Hydrogen flouride
HIV	Human immunodeficiency virus
¹ H NMR	Proton nuclear magnetic resonance
HPLC	High pressure liquid chromatography
HRMA	High resolution mass spectrometry
INH	Isoniazid
IP	Intraperitoneal
IPA	Isopropyl alcohol

mp	Melting point
MABA	Microplate Alamar blue assay
MDR-TB	Multidrug resistant tuberculosis
MeCN	Acetonitrile
MeOH	Methanol
MIC	Minimum inhibitory concentration
<i>Mtb</i>	<i>Mycobacterium tuberculosis</i>
PO	Per oral
PZA	Pyrazinamide
RIF	Rifampicin
SAR	Structure-activity relationship
SEM	Scanning Electron Microscopy
SRI	Southern Research Institute
TB	Tuberculosis
TEM	Transmission electron microscopy
TEA	Triethylamine
TES-Cl	Triethylsilyl chloride
TFA	Trifluoroacetic acid
TFAA	Trifluoroacetic anhydride
THF	Tetrahydrofuran
TLC	Thin layer chromatography
USFDA	United States Food and Drug Administration
WHO	World Health Organization
XDR-TB	Extensively drug-resistant tuberculosis

**Dedicated to my late Godfather
Mr. Venkatesh Murthy**

Chapter 1

Novel trisubstituted benzimidazoles as anti-tubercular agents that inhibit ftsz

1.1. Introduction.....	3
1.1.1. Filamentous temperature sensitive protein Z (FtsZ).....	5
1.1.2. Development of Mtb FtsZ inhibitors	6
1.1.2.1. Taxanes as a starting point.....	6
1.1.2.2. Benzimidazoles as FtsZ inhibitors.....	7
1.1.2.3. 2-alkoxycarbonylaminopyridines and 2-carbamoylpteridines as Mtb FtsZ inhibitors.....	7
1.1.2.4. Trisubstituted benzimidazoles	8
1.2. Results and Discussion	13
1.2.1. Synthesis of 2,5,6-trisubstituted benzimidazoles.....	13
1.2.1.1. Library synthesis.....	14
1.2.1.2. Hits from the library at 5 µg/mL.....	15
1.2.1.3. Resynthesis of hits from library.....	17
1.2.1.3.1. 2-Benzylbenzimidazoles	17
1.2.1.3.2. 2-Cyclopentylbenzimidazoles.....	18
1.2.1.3.3. 2-(3-pentyl)benzimidazoles	19
1.2.1.3.4. 2-Isopropyl and 2-Thienyl benzimidazoles	20
1.2.1.3. Synthesis of 2-tetrahydropyranyl benzimidazoles.....	21
1.2.1.4. Synthesis of 2- α,α -difluorophenylacetyl benzimidazoles.....	24
1.2.1.5. 2-Morpholinyl benzimidazoles	25
1.2.2. SAR of 2-position of 2,5,6-trisubstituted benzimidazoles.....	26
1.2.3. Metabolic stability of 2,5,6-trisubstituted benzimidazoles.....	27
1.2.4. Human ether a-go-go-related gene (hERG) inhibitor	28
1.2.4.1. Synthesis of 3-pentyl analogs of lead benzimidazoles	30
1.2.4.2. Synthesis of polar trisubstituted benzimidazoles.....	30
1.2.5. Exploration of trisubstituted indoles as antibacterial scaffold.....	33
1.2.5.1. Indole analogs of SB-P17G-A37 and SB-P17G-A55	34
1.2.5.2. Tetrasubstituted indoles	37
1.2.5.3. Trisubstituted indoles with phenyl substitution at the 2-position	37

1.2.5.4. Accurate MIC of the synthesized indoles	38
1.3. Conclusion	39
1.4. Experimental Section	39
1.5. References	75

1. Novel trisubstituted benzimidazoles as anti-tubercular agents that inhibit FtsZ

1.1. Introduction

Tuberculosis (TB) is an infectious disease caused by the bacteria, *Mycobacterium tuberculosis* (Mtb).¹ In 2014, an estimated 9.6 million people fell ill by contracting TB, and 1.5 million people died as a result of TB infection.² Globally TB is more prevalent in Asia and Africa (Figure 1).² The most common form of TB is pulmonary TB. Owing to its airborne nature, the disease spreads from one person to another, when an infected person coughs or sneezes.² Extrapulmonary TB which affects organs such as pleura, lymph nodes, joints, bones, spine, genitourinary system and abdomen,³ occurs to a lesser extent, and is mainly seen in immune compromised patients or children.^{2,4} About 1/3 of the world's population has latent TB,⁵ which means the bacteria inhaled remains dormant and people infected with TB do not show any symptoms of the disease. A person infected with TB has a 10 % lifetime risk to develop active infection.² People with compromised immune systems, such as HIV patients and malnourished individuals, are at a greater risk of falling ill.^{2,6} Some of the symptoms of pulmonary TB include persistent cough with sputum and blood, fever, chills, weight loss, weakness and chest pains.⁷

Estimated TB incidence rates, 2013

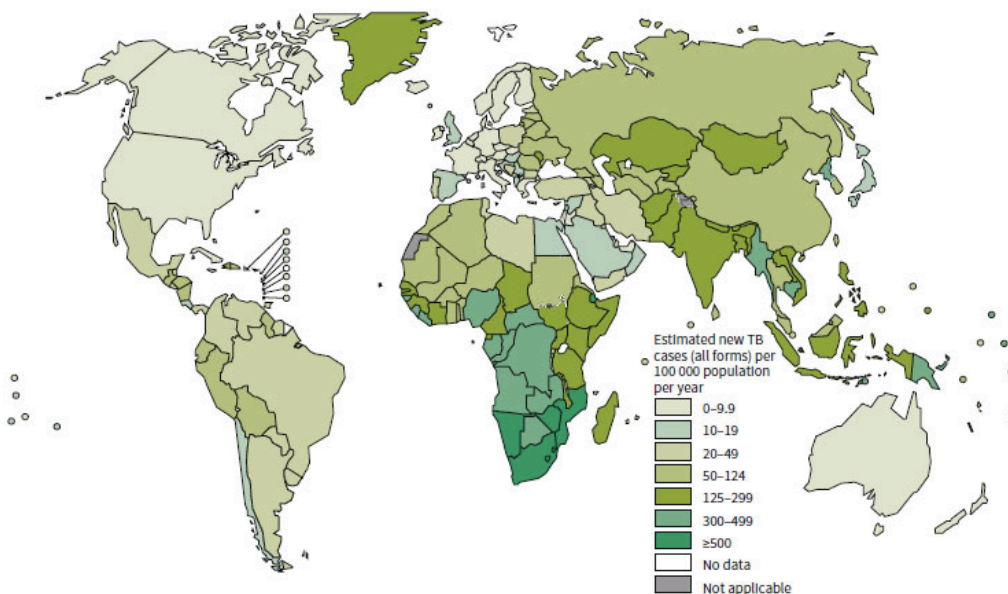


Figure 1: Global TB incidence rates in 2013²

TB is diagnosed by identifying the presence of Mtb in a clinical sample (ex. Sputum), chest X-ray, Tuberculin Skin Test.⁸ The initial treatment for TB comprises a cocktail of antibiotics, also

known as first line drugs which include, isoniazid (INH), rifampicin (RIF), ethambutol (EMB) and pyrazinamide (PZA) (Figure 2) for 2 months, followed by INH and RIF for 4 months.⁹

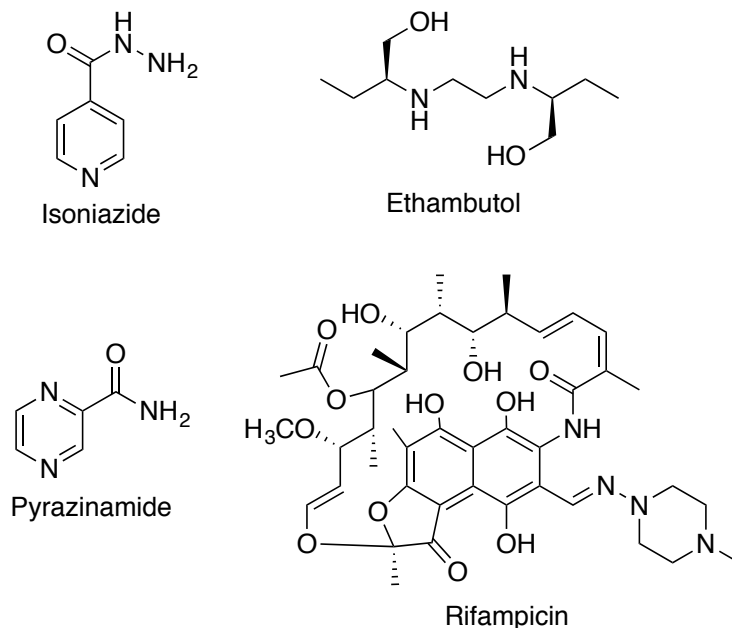


Figure 2: First line drugs for treatment of TB.

Resistant strains of Mtb are seen either due to mutations or patient incompletion owing to the prolonged period needed for treatment. Strains of TB, which are resistant to INH and RIF are termed as Multi Drug Resistant Tuberculosis (MDR-TB).¹⁰ According to WHO, in 2014, an estimated 480,000 people developed MDR-TB and 190,000 people died as a result of it.¹¹ MDR-TB is treated with a combination of second line drugs shown in table 1.¹² Treatment for MDR-TB can take up to 2 years. When MDR-TB develops resistance to fluoroquinolones and one of the three injectable second line drugs, it is referred to as extensively drug resistant (XDR) TB.¹³ Approximately 9.7 % of people with MDR-TB are estimated to have XDR-TB.²

Injectables	Kanamycin, amikacin, capreomycin
Fluoroquinolones	Ofloxacin, moxifloxacin, levofloxacin
Oral bacteriostatic agents	Para amino salicylic acid, cycloserine, thionamide, protionamide

Table 1: Second line drugs for TB.

The treatment options available for MDR-TB are scarce. With the increase in emergence of resistant strains of TB, there is a need for new drugs.¹⁴ Recent advances in the understanding of molecular biology of TB has revived research for new anti-TB drugs.¹⁵ For the first time in about 50 years, two new drugs delamanid and bedaquiline have been approved for the treatment of MDR-TB by the European Medicines Agency and the USFDA respectively (Figure 3).^{16,17} Delamanid inhibits mycolic acid synthesis, while bedaquiline inhibits ATP synthase in Mtb.¹⁶ Both the drugs cause QT prolongation, as a result of which they have been approved for MDR-TB only when no other effective treatment regimen can be provided.^{18,19} A recent study showed that the combination of delamanid and bedaquiline could completely cure XDR-TB.²⁰

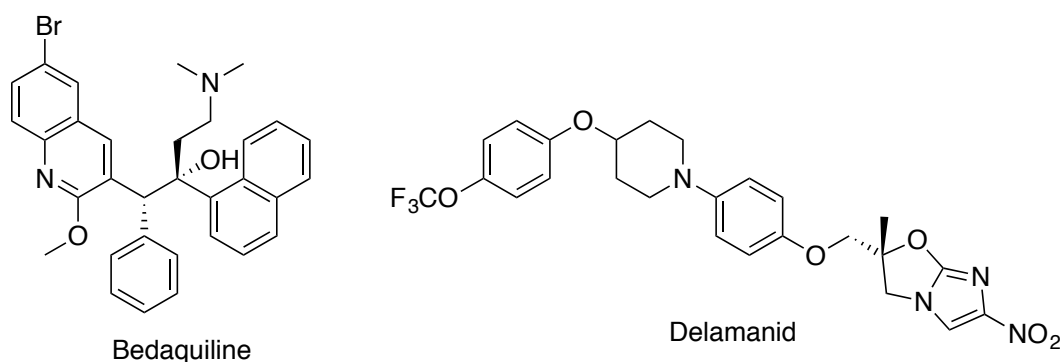


Figure 3: Drugs for MDR-TB.

With the increasing cases of MDR-TB and XDR-TB and new drugs displaying life threatening side effects, there is a dire need for the development of new anti-tubercular agents that would not only make it difficult for the bacteria to develop resistance, but are also safe. In this context, filamentous temperature sensitive protein Z (FtsZ), a bacterial cell division protein seems to be a promising target.²¹

1.1.1. Filamentous temperature sensitive protein Z (FtsZ)

FtsZ, a homolog of tubulin, is a prokaryotic cell division protein, sharing ~ 7 % sequence identity but high structural similarity with tubulin.^{22,23} FtsZ is a guanosine triphosphate (GTP) dependent protein, in the presence of which, it polymerizes into protofilaments.^{24,25} These protofilaments assemble together to form the Z-ring, which is a highly dynamic ring, at the center of the cell.^{24,25} With the aid of other proteins, the Z-ring forms a septum, which results in cytokinesis.²⁶ While FtsZ polymerizes, GTP is hydrolyzed to GDP, which causes the polymers to bend, resulting in constriction of the Z-ring (Figure 4).^{27,28} Further, contraction of the septum

results in cell division.²⁶ Thus, inhibition of FtsZ would affect the Z-ring assembly, hindering septum formation and cell division, leading to bacterial cell death.²⁹ Since FtsZ is highly conserved in prokaryotes,³⁰ agents that inhibit FtsZ, could potentially lead to broad spectrum antibiotics.

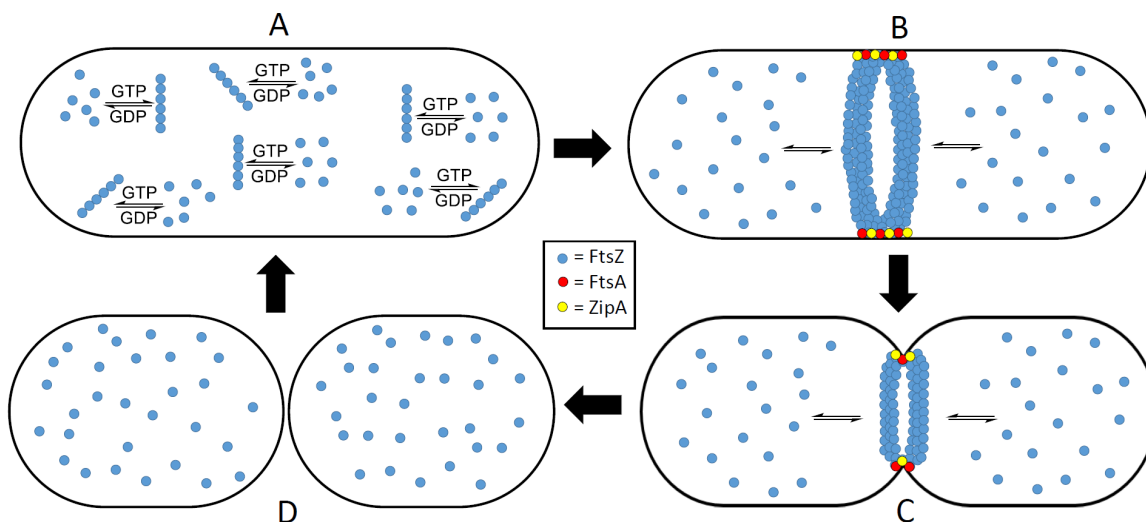


Figure 4: Division of a bacterial cell. A) FtsZ monomers and protofilaments are in equilibrium. GTP binding initiates polymerization bidirectionally. B) FtsA and ZipA are recruited to form the Z-ring. C) Hydrolysis of GTP to GDP causes a contraction of the septum, and cytokinesis begins. D) Cytokinesis finishes and the initial parent cell is split into two daughter cells.²⁸

Currently, there are no drugs available in the market that target FtsZ. A variety of potent inhibitors have been identified by several research groups, as agents that specifically target FtsZ in certain bacteria, or as broad spectrum antibiotics. However, the only groups working on inhibitors for Mtb FtsZ are the Southern Research Institute and the Ojima lab.

1.1.2. Development of Mtb FtsZ inhibitors

1.1.2.1. Taxanes as a starting point

Since FtsZ and tubulin share some homology, agents that inhibit/stabilize tubulin/microtubules afford a good starting point for the development of FtsZ inhibitors.^{31,32} With pioneering work on taxanes in Ojima lab, it was natural to start with taxanes, in the quest to identify FtsZ inhibitors. Taxanes that displayed anti-tubercular activity were strategically modified such that, their specificity towards tubulin was completely reversed (Figure 5).³¹ Filamentation was seen in scanning electron microscopy (SEM) images of Mtb cells treated with SB-RA-5001, which is a phenotypic response of FtsZ inhibition.³¹

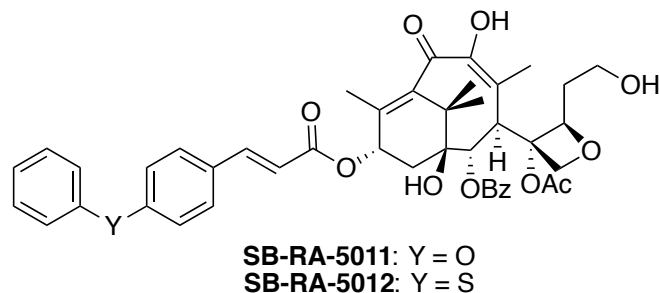


Figure 5: Taxanes that inhibit FtsZ.

1.1.2.2. Benzimidazoles as FtsZ inhibitors

Albendazole and Thiabendazole (Figure 6), which are known tubulin inhibitors, also displayed inhibitory activity against FtsZ in *E. coli*, which was seen through filamentation.³³ Later, Slayden et al. tested albendazole and thiabendazole against *Mtb*, and found the minimum inhibitory concentration (MIC) to be 60-120 μM and 80-160 μM respectively. The viability of *Mtb* cells treated with 60 μM of albendazole and 80 μM of thiabendazole was reduced by ~ 4 and ~ 3 log units respectively.³⁴ SEM analysis of *Mtb* cells treated with albendazole and thiabendazole displayed a length of 6 and 9 μM respectively, as compared to untreated cells which measured 2 μM .³⁴ These results suggest albendazole and thiabendazole inhibit the division of *Mtb* cells by targeting FtsZ. The disadvantage of using albendazole and thiabendazole as FtsZ inhibitors, without any modification is cytotoxicity that will result from their ability to inhibit tubulin.

1.1.2.3. 2-alkoxycarbonylaminopyridines and 2-carbamoylpteridines as *Mtb* FtsZ inhibitors

Researchers at the Southern Research Institute (SRI) assayed a library of tubulin inhibitors against *Mtb* and identified 2 inhibitors SRI-3072 and SRI-7614, which displayed MIC of 0.15 and 6.25 $\mu\text{g/mL}$ respectively.³⁵ SRI-3072 showed specificity towards *Mtb* FtsZ over tubulin at 100 μM concentration. 2-carbamoylpteridine analog of SRI-3072 was also synthesized which displayed an eight-fold improved activity over SRI-3072 (Figure 6).³⁶

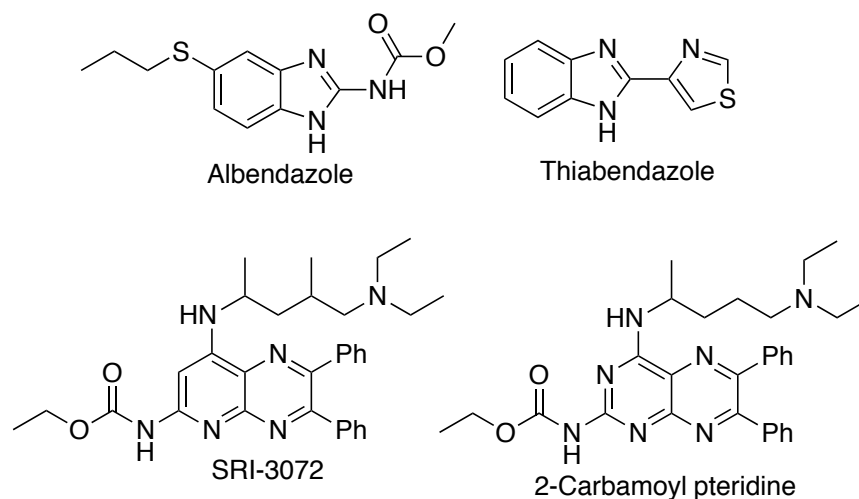
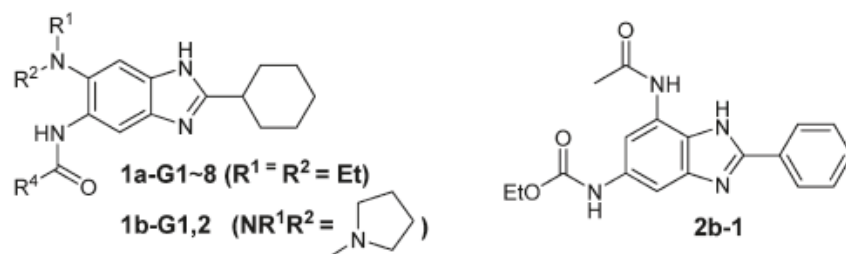


Figure 6: Albendazole, thiabendazole and SRI compounds.

1.1.2.4. Trisubstituted benzimidazoles

Using the benzimidazole core, and following the substitution pattern from SRI compounds, Ojima lab synthesized a library of 349 novel 2,5,6- and 2,5,7 trisubstituted benzimidazoles and tested against Mtb H37Rv (Table2).²¹ Out of these, 26 compounds displayed MIC values $\leq 5 \mu\text{g/mL}$, and 9 out of the 25 hits displayed MIC of 0.5-6.1 $\mu\text{g/mL}$ in alamar blue assay. The 9 hit compounds consisted of a diethylamine substitution at the 6-position and a cyclohexyl substitution at the 2-position of the benzimidazole. Based on these results, a new library of 238 trisubstituted benzimidazoles with varying dialkyl amines at the 6-position, while retaining cyclohexyl group at the 2-position were synthesized. 54 compounds, from this second library displayed MIC values $\leq 5 \mu\text{g/mL}$. Along with H37Rv, 5 compounds from this series, were found to be effective against resistant strains of Mtb (Table2). 2 most potent hits were 1a-G7 (SB-P3G2) and 1b-G1 (SB-P8B2) that displayed MIC of 0.63 and 0.39 $\mu\text{g/mL}$ in alamar blue assay.²¹



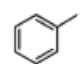
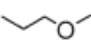
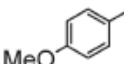
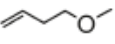
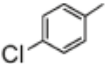
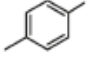
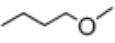
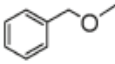

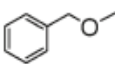
Entry	Benzimidazole	R_4	MIC ₉₉ (μM) <i>Mtb</i> strains						Cytotoxicity (IC ₅₀ μM) Vero cells
			H37Rv	W210	NHN20	NHN335	NHN382	TN587	
1	1a-G1		7.9						>400
2	1a-G2		4.3						>400
3	1a-G3		7.4						>400
4	1a-G4		4.2	4.2	4.2	4.2	4.2	4.2	>400
5	1a-G5		14.1						>400
6	1a-G6		15.1						>400
7	1a-G7		2.0	4.0	4.0	4.0	2.0	4.0	>400
8	1a-G8		3.8						>400
9	1b-G1		1.0	1.0	1.0	1.0	1.0	1.0	>200
10	1b-G2		3.7	3.7	3.7	3.7	3.7	3.7	>200
11	2b-1	Me	2.3	4.6	2.3	2.3	2.3	2.3	>200

Table2: Antimicrobial activities of some trisubstituted benzimidazoles against *Mtb*.²¹

Additionally, 63 2,5,6-trisubstituted benzimidazoles containing a cyclohexyl substitution at the 6-position, various dialkylamino groups at the 6-position and the 5-position consisting of carbamates, urea, alkyl and benzyl amides were synthesized and tested against *Mtb*

H37RV (Figure 7). SB-P17G-C2 from this series, which contains a dimethylamine substitution at the 6-position, was extremely potent with an MIC of 0.06 $\mu\text{g}/\text{mL}$ against Mtb H37Rv (Figure 8).³⁷

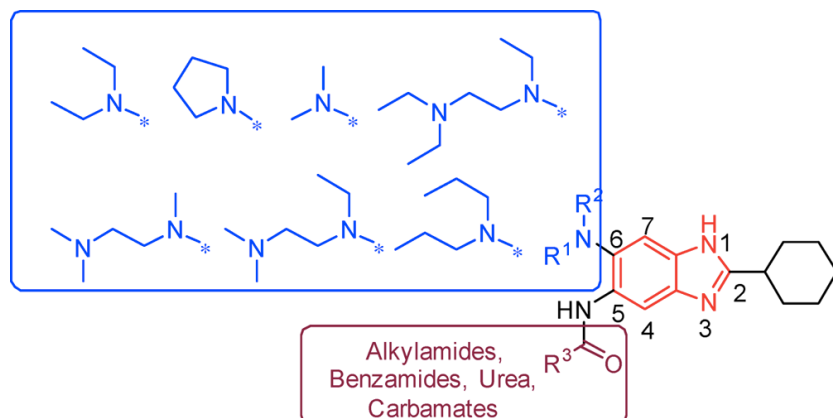


Figure 7: SAR studies of 2,5,6-trisubstituted benzimidazoles.³⁷

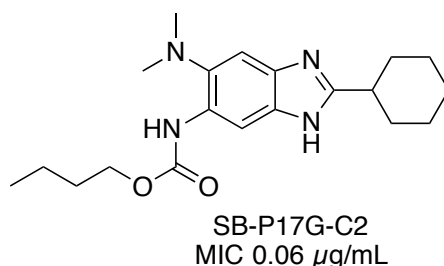


Figure 8: Structure of SB-P17G-C2.³⁷

Though SB-P3G2, SB-P8B2 and SB-P17G-C2 are extremely potent, the carbamate moiety at the 5-position makes them highly metabolically labile. Metabolic stability studies conducted by Sanofi showed that the carbamate moiety was hydrolyzed to generate the final intermediate amine. This amine did not possess any anti-tubercular activity. Along with the amine, other possible metabolic products were also synthesized and tested for anti-tubercular activity, but none of them were active. To synthesize more stable compounds, the carbamate moiety was replaced by urea, aliphatic and aromatic amides at the 5-position. Unfortunately, urea substitution was detrimental for activity.³⁷ Compounds with aliphatic amide were not active, but ones with benzamide showed good inhibitory activity.³⁷ Some of the lead benzamide compounds include SB-P17G-A20, SB-P17G-A38 and SB-P17G-A42 (Figure 9).^{37,38} Compounds with a fluorine at the 2-position of benzamide had improved metabolic stability as opposed to their unsubstituted counterparts. SB-P3G2 and SB-P17G-A20 when tested in vivo against immune compromised GKO mice, reduced the bacterial load by 0.71 \log_{10} CFU in the lung, 0.41 \log_{10} CFU in the spleen and 1.73 \log_{10} CFU in the lung, 2.68 \log_{10} CFU in the spleen respectively.^{39,40} SB-P17G-A38 and SB-P17G-A42

reduced the bacterial load in the lung by 5.7-6.3 \log_{10} CFU and in the spleen by 3.9-5.0 \log_{10} CFU respectively.³⁸

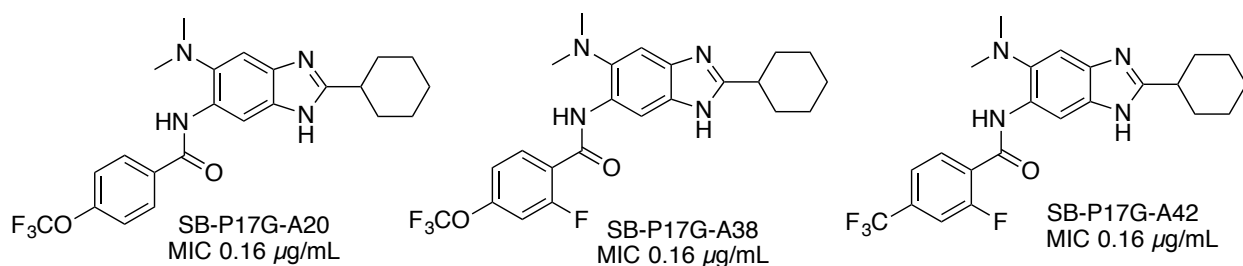
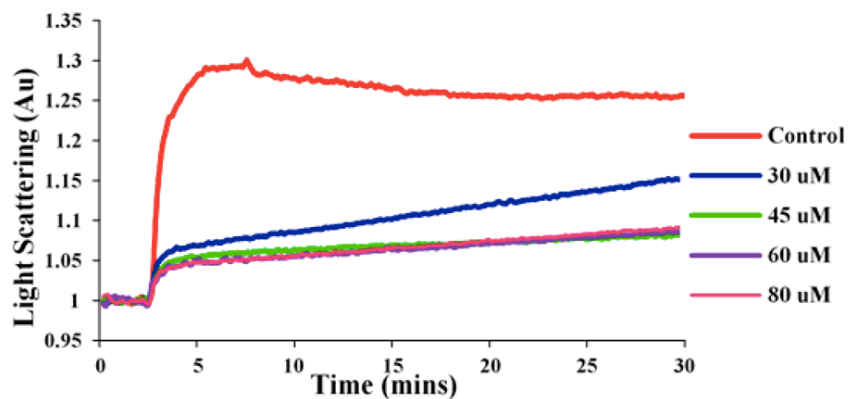
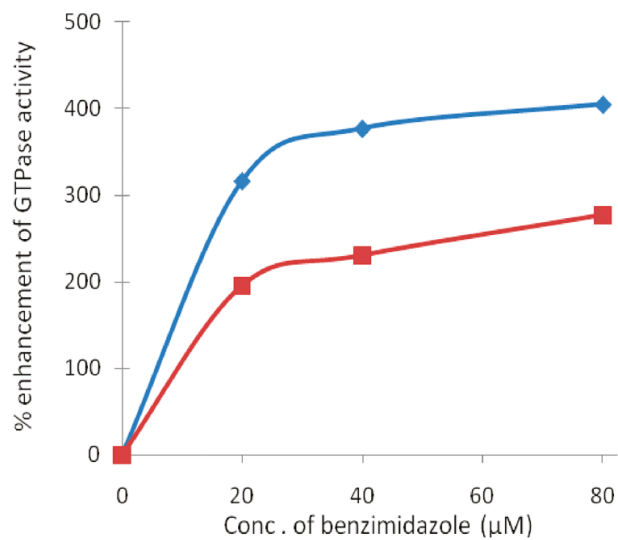


Figure 9: Lead trisubstituted benzimidazoles with benzamide at 5-position.

In order to confirm the hypothesis that antibacterial activity of trisubstituted benzimidazoles was due to their FtsZ inhibitory activity, target validation studies like polymerization assay, GTPase assay and Transmission Electron Microscopy (TEM) imaging were carried out.^{21,37} SB-P17G-C2 inhibited the polymerization of Mtb FtsZ in a dose dependent manner (Figure 10 A).³⁷ Malachite green assay (GTPase assay) of SB-P3G2 and 1a-G4 (Figure 10 B), showed that the trisubstituted benzimidazoles increase the GTPase activity i.e they promote hydrolysis of GTP to GDP thus rendering the FtsZ polymer unstable.^{21,32} TEM images of Mtb FtsZ treated with SB-P17G-C2 showed that not only did the compound inhibit the formation of polymers, but also brought about depolymerization, when preformed FtsZ polymers were treated with the compound (Figure 11). All these results strongly suggest that the trisubstituted benzimidazoles target FtsZ. Based on computational studies using the crystal structure of GTP γ S bound Mtb FtsZ, it has been hypothesized that the binding site of trisubstituted benzimidazoles is close to the GTP binding site present between the two FtsZ monomers.⁴¹



A



B

Figure 10: (A)- Inhibition of Mtb FtsZ by SB-P17G-C2 in a dose dependent manner.³⁷ (B)- GTPase assay of SB-P3G2 (blue) and 1a-G4 (red).²¹

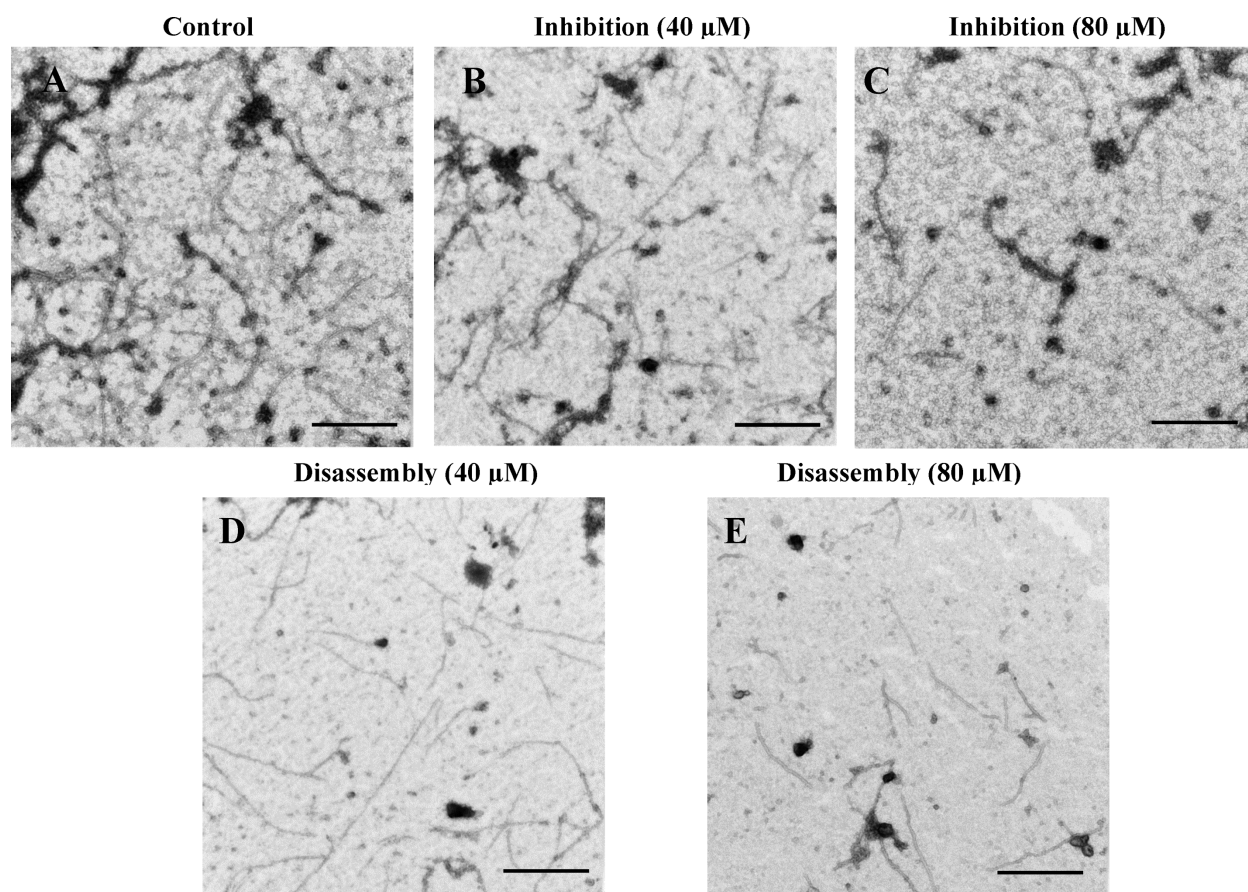


Figure 11: TEM images of Mtb FtsZ. 5 µM FtsZ was polymerized with 25 µM GTP, in the absence

(A), and presence of SB-P17G-C2 40 μM (B) and 80 μM (C). Preformed FtsZ polymers were treated with SB-P17G-C2 40 μM (D) and 80 μM (E).³⁷

Based on these results, a new series of benzimidazoles with modified 2-position were designed and synthesized.

1.2. Results and Discussion

So far with the 2,5,6-trisubstituted benzimidazoles we have seen that, substituting a dimethyl amine group at the 6-position improves the activity drastically, and the presence of benzamides is essential for stability and certain benzamide compounds like SB-P17G-A38 and SB-P17G-A42 are highly active. However, not much has been explored with respect to the 2-position of benzimidazoles. So far, all the compounds that have been synthesized have a cyclohexyl substitution at the 2-position. In order to diversify our library, benzimidazoles with dimethylamine at the 6-position and varying 2-position substitutions were synthesized and tested against Mtb H37Rv (Figure 12).

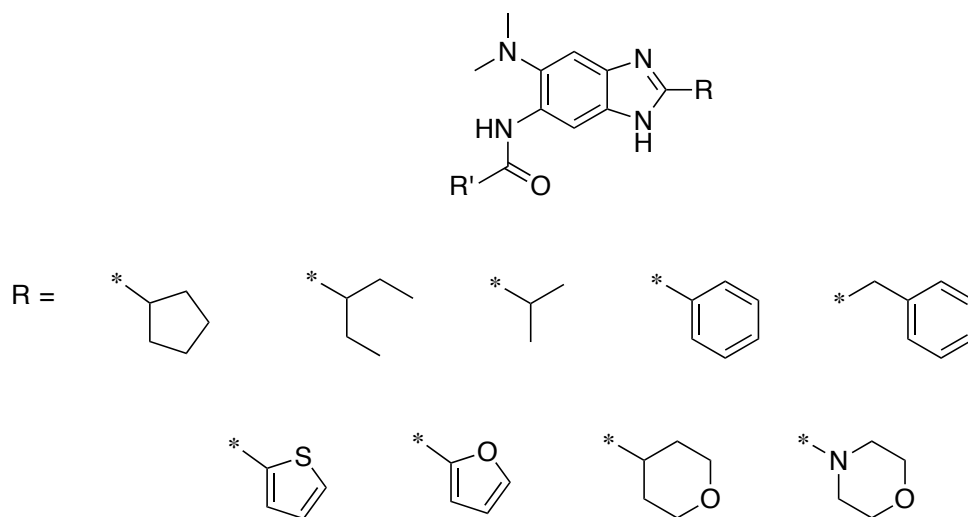
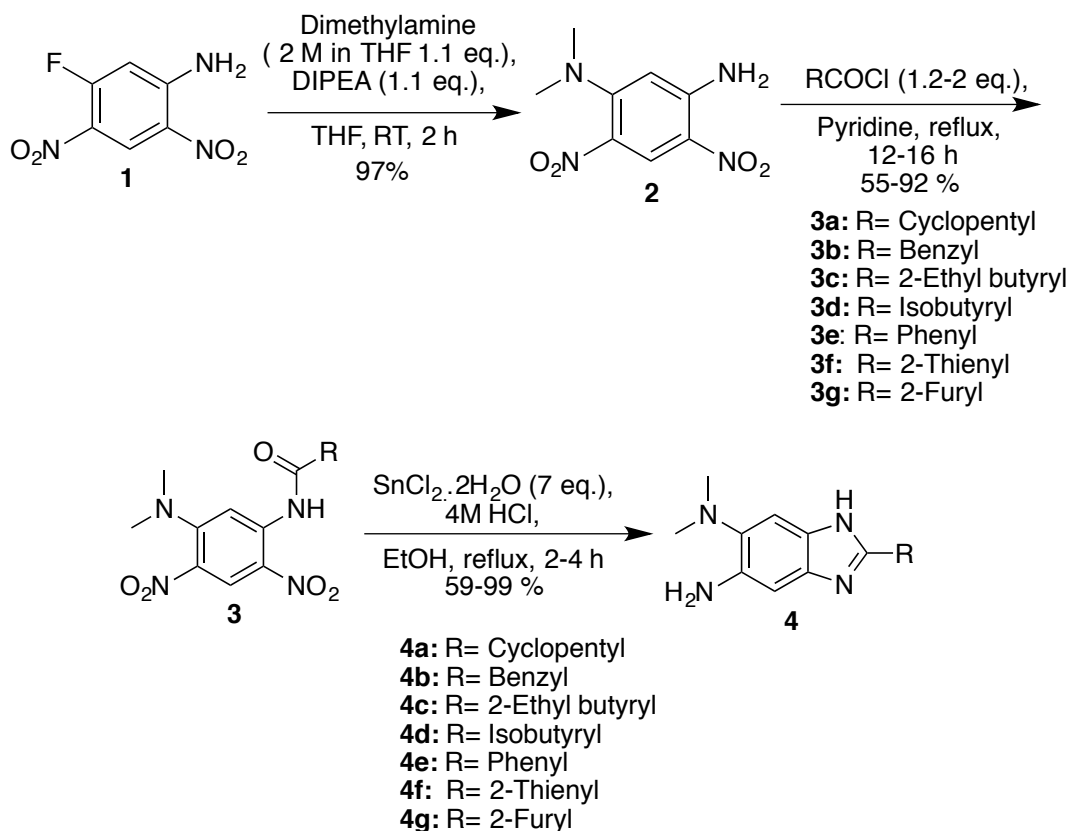


Figure 12: Proposed library of 2,5,6-trisubstituted benzimidazoles.

1.2.1. Synthesis of 2,5,6-trisubstituted benzimidazoles

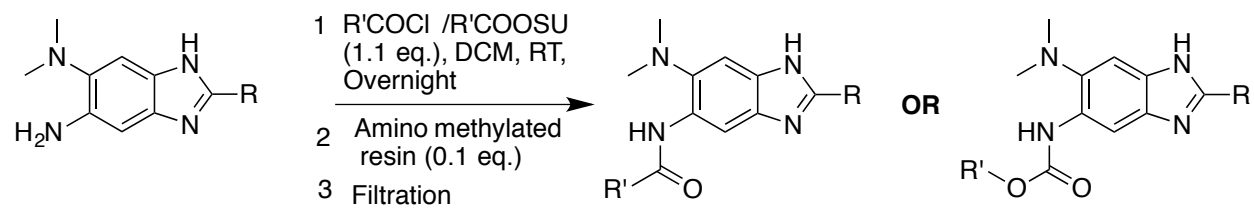
Commercially available 2,4-dinitro-5-fluoroaniline **1** was subjected to nucleophilic aromatic substitution with dimethylamine in the presence of diisopropylethylamine (DIPEA) as base to give **2** in 97% yield. Acylation of **2** with various carbonyl chlorides afforded **3a-g**, in yields ranging from 55% to 96%. Reduction followed by acid-catalyzed cyclization of **3a-g** with stannous chloride dihydrate and hydrochloric acid (HCl), resulted in 5-aminobenzimidazoles **4a-g** in 50-99% yields (Scheme 1).



Scheme 1: Synthesis of 2,5,6-trisubstituted benzimidazoles.

1.2.1.1. Library synthesis

The seven final intermediates **4a-g** were treated with 35 different acyl chlorides/ ROSu (succinate ester) in dichloromethane (DCM) at room temperature. This was followed by treatment with amino methylated resin in order to remove any unreacted acyl chloride. Finally, the reaction mixture was filtered using millipore filter to remove the resin. This resulted in 245 final compounds containing either an amide or carbamate functionality at 5-position of 2,5,6-trisubstituted benzimidazoles (Scheme 2). The synthesized library was screened against Mtb H37Rv in triplicates, in a 96 well format. 53 compounds were active at 5 $\mu\text{g/mL}$ concentration. Unsubstituted final intermediates were also used for biological testing (Figure 13).



R' =

Scheme 2: Library synthesis.

1.2.1.2. Hits from the library at 5 µg/mL

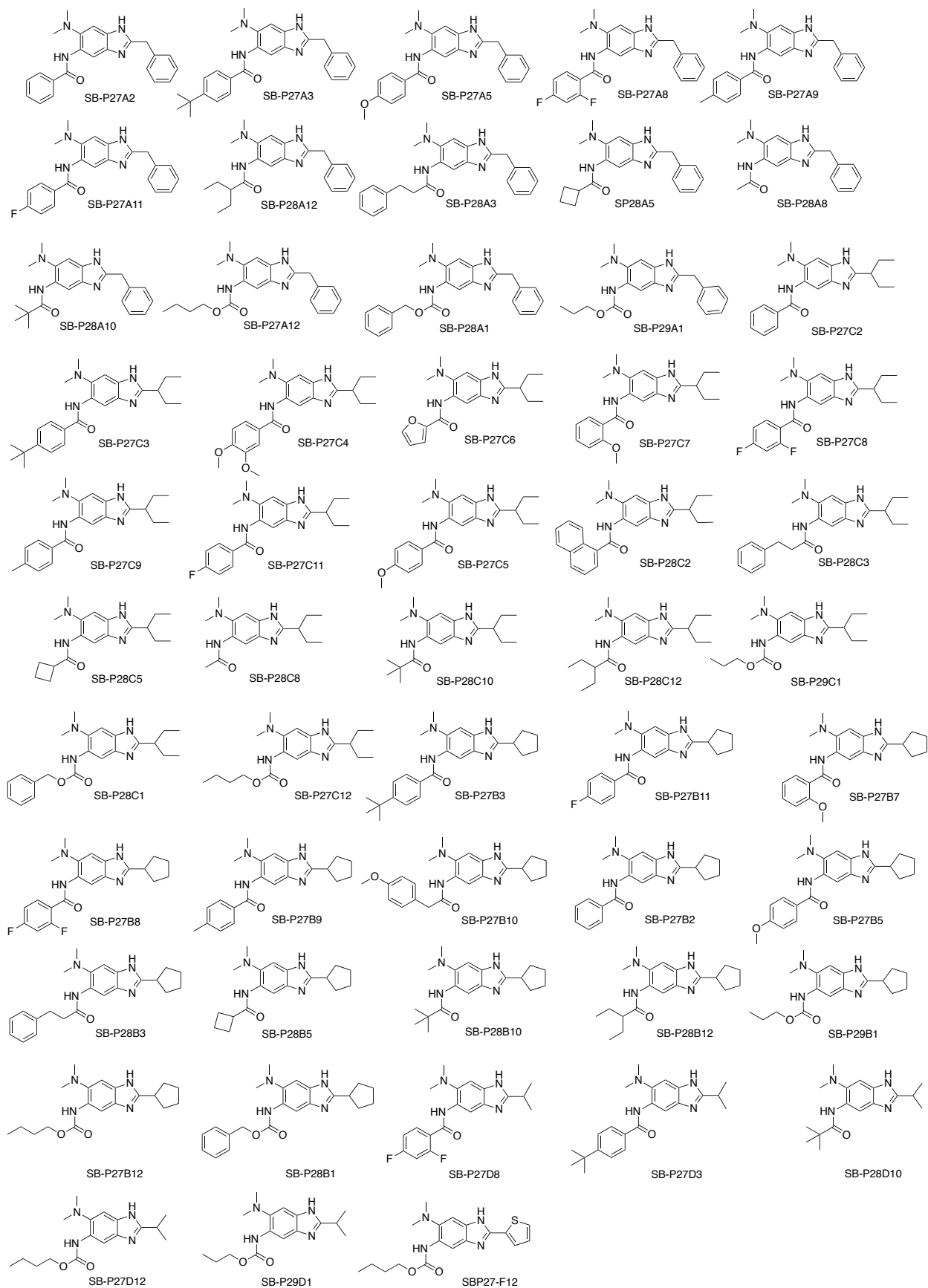
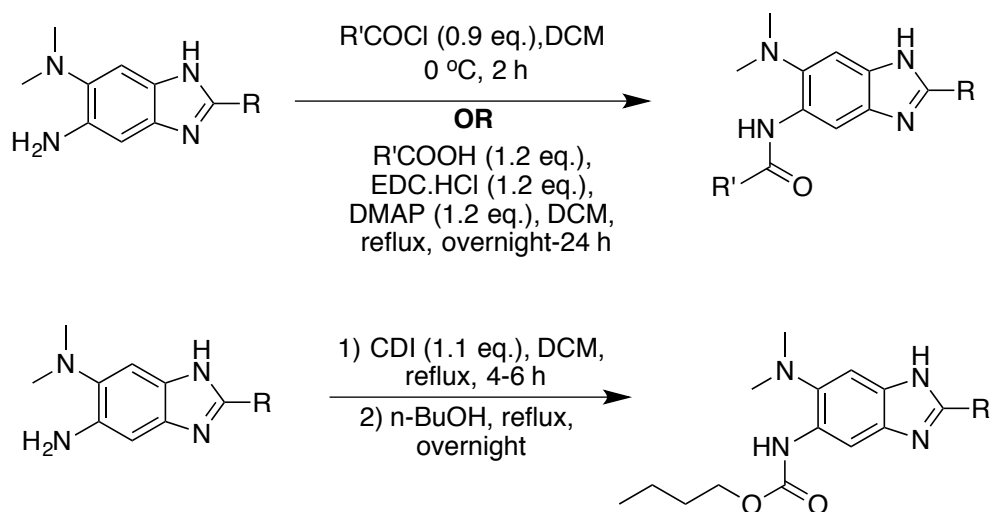


Figure 13: Hits from library at 5 $\mu\text{g/mL}$.

1.2.1.3. Resynthesis of hits from library

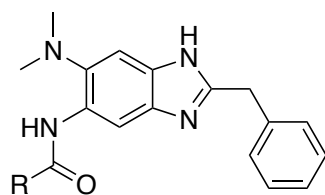
The hits from the library were resynthesized to measure the accurate MIC. Not all compounds with aliphatic amide at the 5-position were resynthesized as they are not as active compared to the benzamide counterparts. Along with hits from library, analogs of lead benzimidazoles SB-P17G-A20, A38 and A42 were also synthesized for some compounds. The final intermediates **4a-g** were either treated with acyl chloride at 0 °C in DCM for two hours or coupled with respective acids in the presence of N-(3-Dimethylaminopropyl)-N'-ethylcarbodiimide hydrochloride (EDC.HCl) and diisopropylethylamine (DIPEA) and refluxed in DCM overnight. In case of carbamates, the final intermediate was refluxed with carbonyldiimidazole (CDI) for 4-6 hours in DCM, followed by addition of n-butanol and the the reaction mixture was refluxed overnight (Scheme 3).



Scheme 3: General procedure for the re-synthesis of hit amides and carbamates.

1.2.1.3.1. 2-Benzylbenzimidazoles

Substitution of a benzyl group at the 2-position of benzimidazoles resulted in a large number of hits. As expected, butyl carbamate at the 5-position resulted in the most active compound in this series. p-substituted benzamide was more active than the un-substituted counterpart. Even though some aliphatic amides came up as hits from the initial screening, they did not possess any activity when they were resynthesized and tested. Since SB-P17G-A20 was the lead compound at that point, A20 analog with 2-benzyl substitution was synthesized as well (Table 3).



Compound	R	MIC		Compound	R	MIC	
		Yield (%)	Mtb H37Rv ($\mu\text{g/mL}$)			Yield (%)	Mtb H37Rv ($\mu\text{g/mL}$)
SB-P27A2		57	1.25	SB-P27A11		89	0.63
SB-P27A3		79	0.33	SB-P27A12		44	<0.078
SB-P27A5		55	1.25	SB-P27A-A20		66	1.25
SB-P27A8		92	0.63	SB-P27A10		92	>10
SB-P27A9		68	1.56	SB-P28A12		67	>10

Table 3: Accurate MIC of 2-benzylbenzimidazoles.

1.2.1.3.2. 2-Cyclopentylbenzimidazoles

Since cyclopentyl group is very similar to cyclohexyl group, it was interesting to see its effect on anti-Mtb activity. Surprisingly, the carbamate analog of 2-cyclopentyl benzimidazole SB-P27B12 with an MIC of 0.31 $\mu\text{g/mL}$, was 5 times less active compared to the cyclohexyl congener SB-P17GC2 that displayed MIC of 0.06 $\mu\text{g/mL}$. p-substituted benzamides at the 5-position, were more active than o-substituted or un-substituted compounds (Table 4).

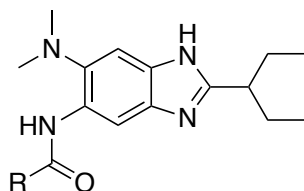
Compound	R	Yield (%)	MIC		Compound	R	Yield (%)	MIC	
			Mtb H37Rv (µg/mL)	(µg/mL)				Mtb H37Rv (µg/mL)	(µg/mL)
SB-P27B2		94	1.56		SB-P27B10		94	50	
SB-P27B3		80	0.78		SB-P27B11		78	0.78	
SB-P27B5		53	1.25		SB-P27B12		70	0.31	
SB-P27B7		76	12.5		SB-P27B-A20		64	1.56	
SB-P27B8		92	0.625		SB-P28B5		75	>10	
SB-P27B9		76	0.625		SB-P28B12		66	>50	

Table 4: Accurate MIC of 2-cyclopentylbenzimidazoles.

1.2.1.3.3. 2-(3-pentyl)benzimidazoles

3-pentyl substitution at the 2-position of benzimidazole resulted in the maximum number of hits from the initial library screening. The butyl carbamate analog displayed similar activity as

SB-P17G-C2, while the SB-P17G-A20 analog was 50 % less active with an MIC of 0.31 $\mu\text{g/mL}$ (Table 5).



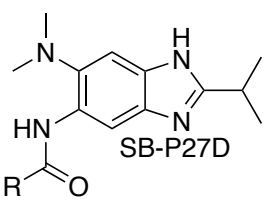
Compound	R	Yield (%)	MIC	Compound	R	Yield (%)	MIC
			Mtb H37Rv ($\mu\text{g/mL}$)				Mtb H37Rv ($\mu\text{g/mL}$)
SB-P27C2		85	1.56	SB-P27C12		70	0.078
SB-P27C4		58	12.5	SB-P27C-A20		76	0.31
SB-P27C7		60	1.56	SB-P28C2		64	>10
SB-P27C9		61	0.5	SB-P28C3		65	1.56
SB-P27C8		62	0.71	SB-P27C-A1		69	>10
SB-P27C11		44	0.78				

Table 5: Accurate MIC of 2-(3-pentyl)benzimidazoles.

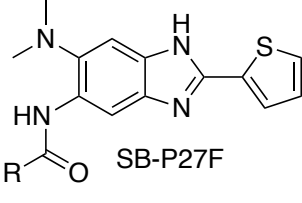
1.2.1.3.4. 2-Isopropyl and 2-Thienyl benzimidazoles

2-isopropyl and 2-thienyl substitutions did not result in as many hits. Surprisingly in case of 2-isopropyl benzimidazoles, the p-tert-butyl benzamide at the 5-position SB-P27D3 was more

active than the 5-butyl carbamate analog, SB-P27D12. The 5-carbamate analog with thiophene substitution at the 2-position was not active (Table 6).



SB-P27D



SB-P27F

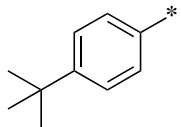
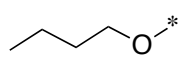
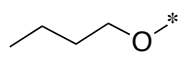
Compound	R	Yield (%)	MIC Mtb H37Rv (µg/mL)
SB-P27D3		87	0.78
SB-P27D12		79	1.25
SB-P27F12		55	>10

Table 6: Accurate MIC of 2-Isopropyl and 2-Thienyl benzimidazoles.

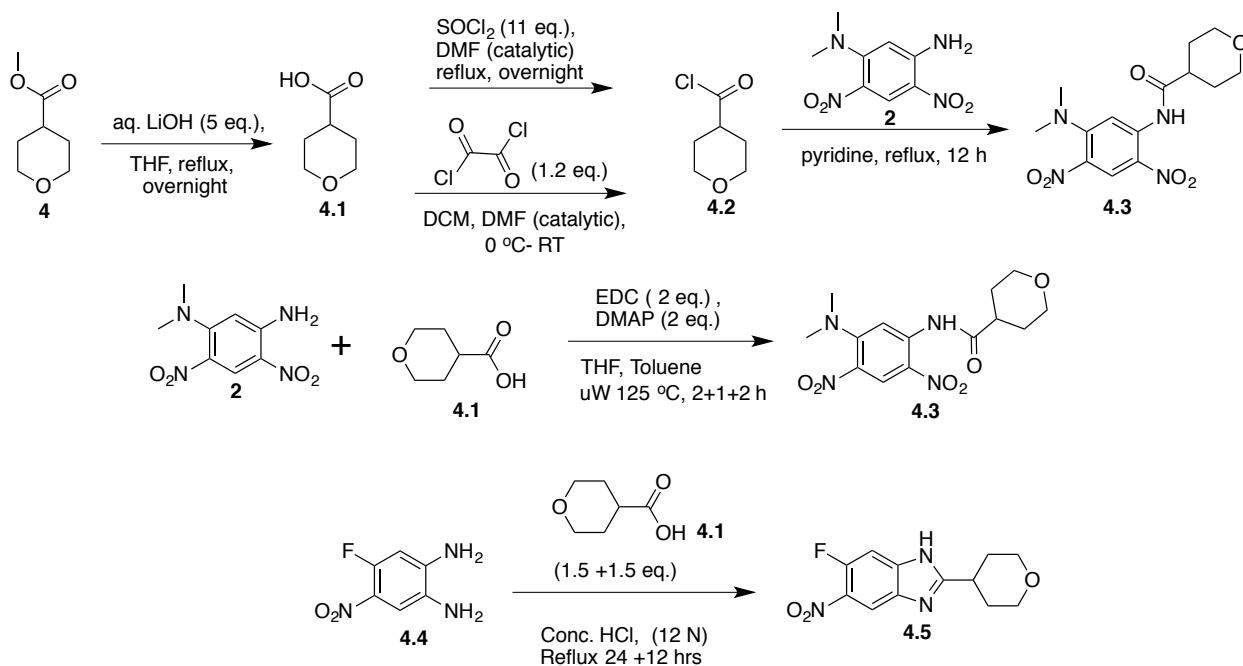
1.2.1.3. Synthesis of 2-tetrahydropyranyl benzimidazoles

Benzimidazoles containing a tetrahydropyran substitution at the 2-position were also a part of the initial plan. Unfortunately, the final intermediate could not be synthesized in time and hence it wasn't a part of the library. However, efforts towards the synthesis of 2-tetrahydropyranyl benzimidazoles were continued, and finally succeeded. Since the 5-position of the benzimidazoles had been optimized by then, instead of synthesizing another library, analogs of the lead compounds were synthesized.

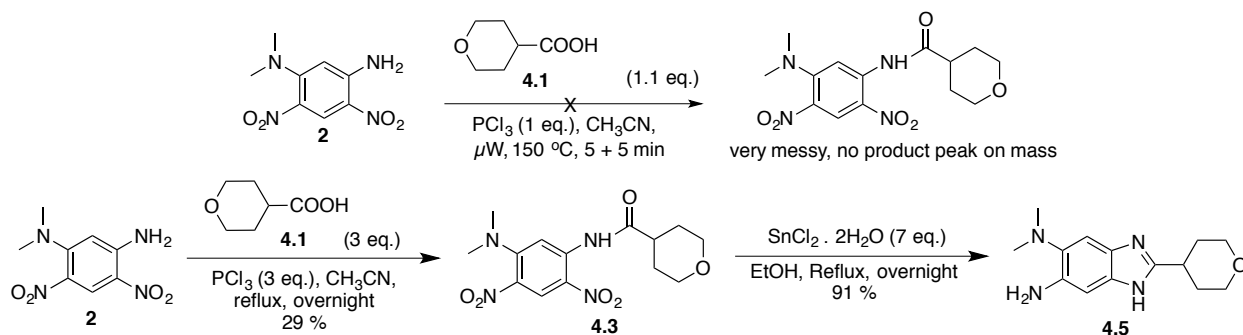
Commercially available methyl ester of tetrahydropyran-4-carboxylic acid was hydrolyzed using lithium hydroxide to give the corresponding acid. Attempts were made to convert the acid **4.1** to the acyl chloride either using thionyl chloride or oxalyl chloride in the presence of catalytic amount of dimethylformamide (DMF). When the reaction was carried out using thionyl chloride, the reaction did not go to completion and it was difficult to separate the starting material **2** from the product **4.3**. With oxalyl chloride, the reaction barely proceeded with a very faint spot for the product **4.3** seen. Attempt to directly couple the acid **4.1** with compound **2** using EDC.HCl and DMAP also resulted in a mixture with difficulty in isolating the product from the starting material. The reaction did not go to completion in spite of subjecting the reaction mixture to microwave irradiation. Compound **4.4** was refluxed with the acid **4.1** in the presence 12 N HCl overnight.

Molecular ion peak was seen on mass spectrometer. Faint spot for the product was seen. Column chromatography resulted in only 3 mg of the product (Scheme 4).

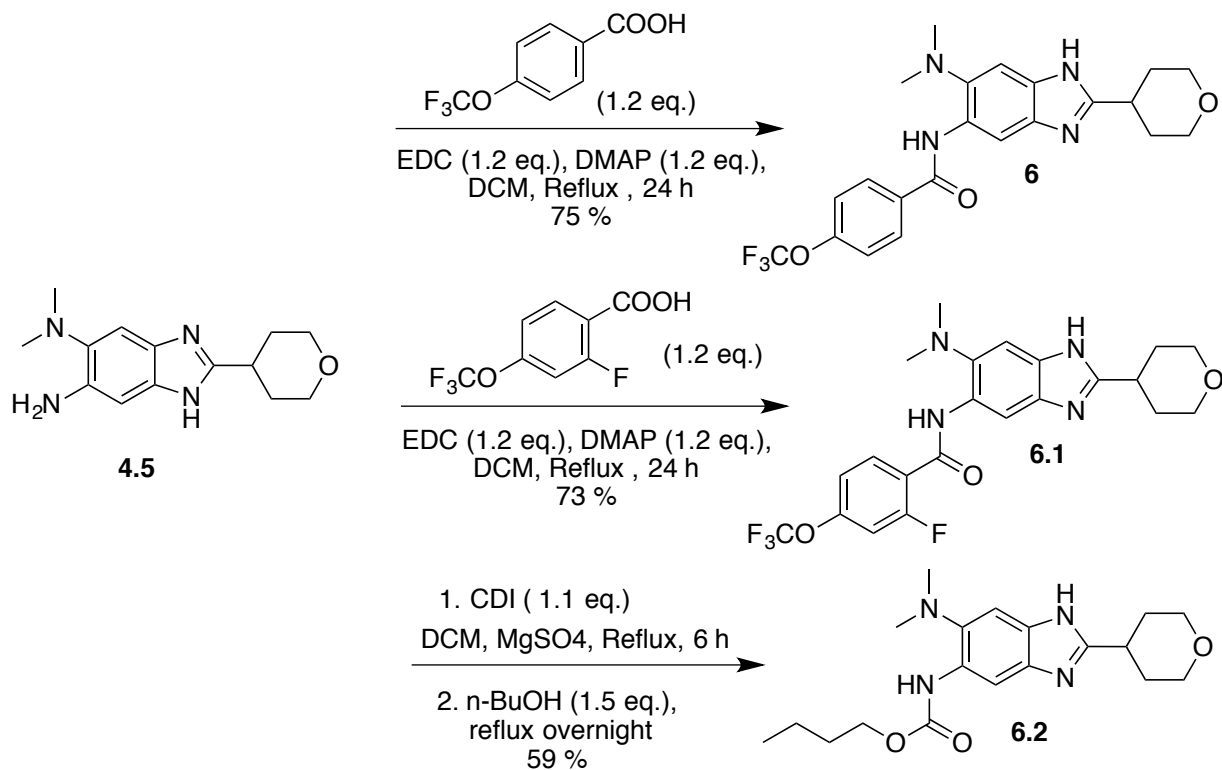
The amine **2** and the acid **4.1** were treated with PCl_3 in acetonitrile in a microwave reactor. The acid would react with PCl_3 to generate the acyl chloride in situ which in turn would react with the amine to give the amide.⁴² Unfortunately, the reaction was extremely messy. The same reaction was tried again but by conventional refluxing instead of using a microwave reactor, and the reaction finally worked giving the desired product **4.3**. Once the amide was formed, it was subjected to reduction, cyclization using tin chloride dihydrate and HCl, to give the final intermediate **4.5** (Scheme 5). The amine **4.5** was treated with acids or CDI and n-butanol to synthesize the analogs of lead benzimidazoles (Scheme 6).



Scheme 4: Synthesis of 2-tetrahydropyranyl benzimidazoles.



Scheme 5: Synthesis of 2-tetrahydropyranyl benzimidazoles.



Scheme 6: Synthesis of 2-tetrahydropyranyl analogs of lead benzimidazoles.

Accurate MIC of the 2-tetrahydropyranyl analogs of lead benzimidazoles was determined against Mtb H37Rv. Surprisingly none of the benzamide compounds were active. The carbamate analog though was slightly active; it was not as active as the lead SB-P17G-C2 which has an MIC of 0.06 $\mu\text{g/mL}$. Addition of an oxygen on the cyclohexyl ring seems to have a drastic effect on the activity (Table 7).

Compound	R	MIC Mtb H37Rv ($\mu\text{g/mL}$)
SB-OL5-A20 (6)	<chem>Fc1ccc(cc1)C(=O)O</chem> *	>10

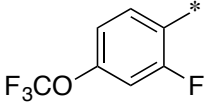
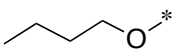
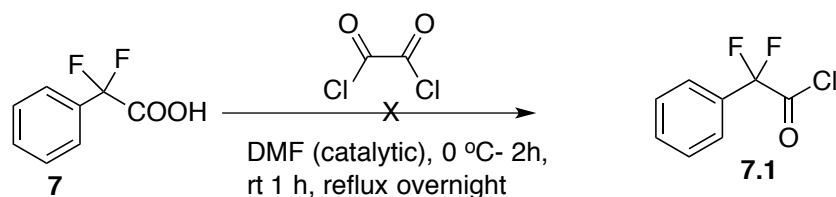
SB-OL5-A38 (6.1)		10
SB-OL5-C2 (6.2)		>2.5

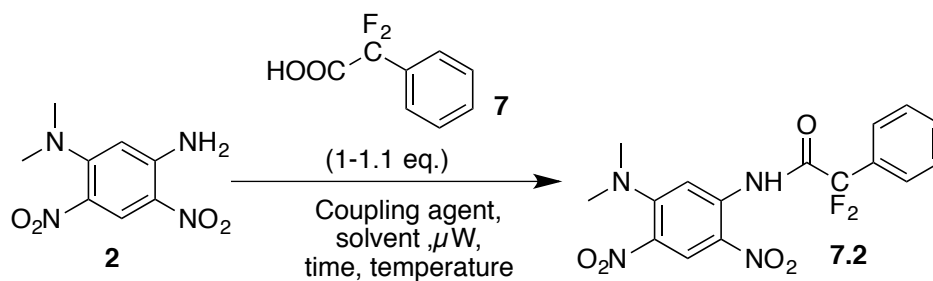
Table 7: Accurate MIC of 2-tetrahydropyranyl analogs of lead benzimidazoles.

1.2.1.4. Synthesis of 2- α,α -difluorophenylacetyl benzimidazoles

Since the 2-benzyl benzimidazoles resulted in a number of active compounds, it was interesting to see the effect of addition of two fluorine atoms on the methylene group. Initial trial to convert α,α -difluorophenylacetic acid to the corresponding acyl chloride failed (Scheme 7). Direct coupling of the acid **7** with the amine **2** succeeded after several trials (Table 8). The difficulty in the synthesis of amide **7.2** could have been due to the fact that the difluoromethylene group which has a large electron cloud, may repel the electrons from the approaching nucleophile. The amide **7.2** was subjected to reduction and cyclization using tin chloride dihydrate and HCl, which was in turn coupled with 4-trifluoromethoxy benzoic acid in the presence of EDC.HCl and DMAP to give the **SB-P17G-A20** analog, **SB-OL6-A20** (Scheme 8). However, the compound was not active with an MIC >10 $\mu\text{g/mL}$ against Mtb H37Rv.



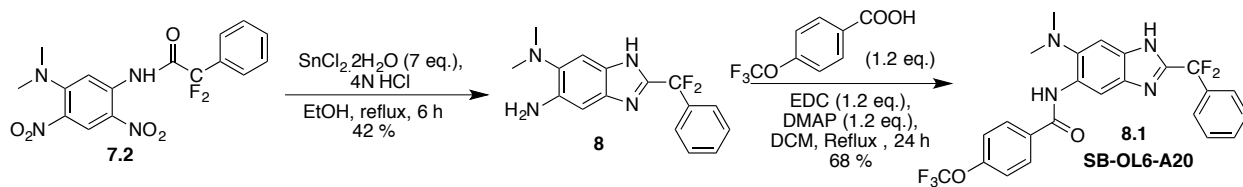
Scheme 7: Synthesis of α,α -difluorophenylacetamide.



Coupling agent	Solvent	Time, temperature	Result
EDC.HCl	Toluene	3 h, 100 °C	No product

EDC.HCl	DMF	2h, 100 °C, 3 h, 125 °C	No product
PCl ₃	Acetonitrile	5 min, 150 °C	Product seen (51 % yield)

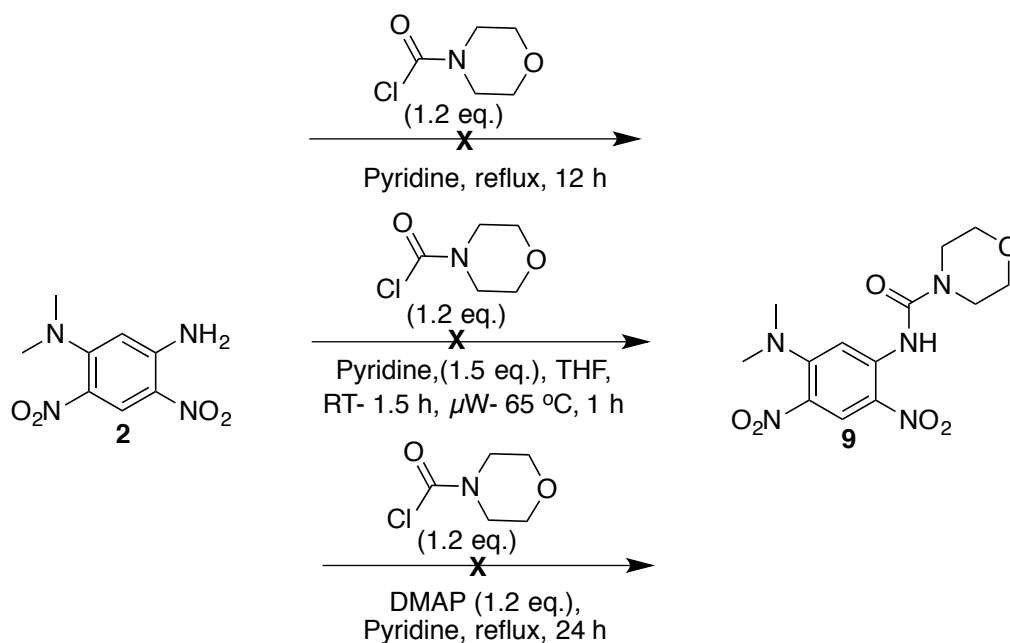
Table 8: Synthesis of α,α -difluorophenylacetamide.



Scheme 8: Synthesis of 2- α,α -difluorophenylacetamide analog of SB-P17G-A20.

1.2.1.5. 2-Morpholinyl benzimidazoles

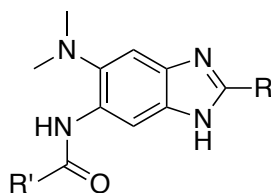
Attempts were made to synthesize compounds with morpholinyl substitution at the 2-position of benzimidazoles. Compound **2** was refluxed with morpholinoyl chloride in pyridine, but unfortunately the reaction did not proceed. The reaction was also carried out using pyridine as base in microwave reactor and finally using DMAP as base with pyridine as solvent. But all the attempts to synthesize **9** failed. This could be due to the poor reactivity of the 4-morpholinecarbonyl chloride (Scheme 9).



Scheme 9: Synthesis of morpholinylamide.

1.2.2. SAR of 2-position of 2,5,6-trisubstituted benzimidazoles

The 2-position of trisubstituted benzimidazoles seems to be sensitive to minor changes. Replacement of cyclohexyl group with a tetrahydropyran resulted in reduction of activity by ~40 times. Substitution of a cyclopentyl group reduced the activity by half as opposed to the cyclohexyl group. This could be because, the cyclopentyl group being more rigid than cyclohexyl, may not be able to interact with the same amino acids in the binding pocket. Activity of C2 analog with 3-pentyl substitution at the 2-position, was very similar to SB-P17G-C2. This could be attributed to the flexibility of the 3-pentyl group, as a result of which it might mimic the binding pose of the cyclohexyl group. Isopropyl substitution diminished the activity indicating the importance of the carbon chain length at the 2-position. The butyl carbamate analog with benzyl substitution at the 2-position was very similar in activity to SB-P17G-C2, but the A38 analog was less active compared to the cyclohexyl lead. Substitution of an aromatic group like 2-thiophene, resulted in loss of activity. Also, since there were no hits with 2-phenyl or 2-furyl substitutions from the initial library; it was very clear that an sp² carbon at the 2-position is highly unfavorable. Substitution of α,α -difluorophenylacetyl group at the 2-position was detrimental for activity, indicating the importance of an sp³ hybridized hydrocarbon (Table 9).



Compound	R	R'	MIC Mtb H37RV ($\mu\text{g/mL}$)
SB-P17G-C2	*-		0.06
SB-P17G-A20	*-		0.16
SB-OL5-C2	*-		>2.5
SB-P27B12	*-		0.31

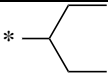
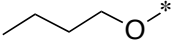
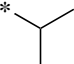
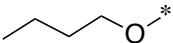
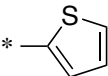
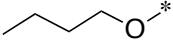
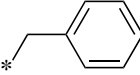
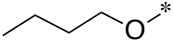
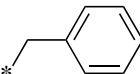
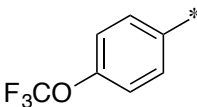
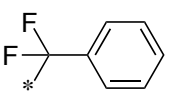
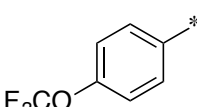
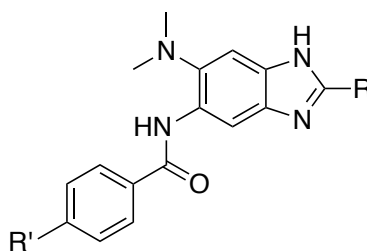
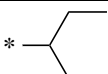
SB-P27C12			0.078
SB-P27D12			1.25
SB-P27F12			>10
SB-P27A12			<0.078
SB-P27A-A20			1.25
SBB-OL6-A20			>10

Table 9: SAR of 2-position of 2,5,6-trisubstituted benzimidazoles.

1.2.3. Metabolic stability of 2,5,6-trisubstituted benzimidazoles

Metabolic stability studies of trisubstituted benzimidazoles was carried out in human and mouse liver microsomes. p – substitution on the benzamide at the 5-position is essential to block the metabolism. Among methyl, methoxy and trifluoromethoxy substitutions at the p- position of the benzamide, trifluoromethoxy group seems to have the largest effect in improving the metabolic stability. The 3-pentyl group at the 2-position seems to be the most metabolically labile. Benzyl substituted compounds at the 2-position were more stable in human plasma than mouse plasma. 2-cyclopentyl compounds displayed reasonable stability (Table 10).



R	R'	Microsomal stability	
		Human	Mouse
	H	99 %	95 %
	F	99 %	93 %

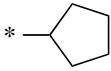
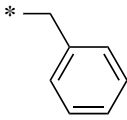
	CH ₃	94 %	81 %
	OCF ₃	68 %	45 %
	CH ₃	71 %	73 %
	OCH ₃	46 %	41 %
	OCF ₃	36 %	30 %
	CH ₃	75 %	97 %
	OCH ₃	53 %	92 %
	OCF ₃	27 %	49 %

Table 10: Metabolic stability of 2,5,6-trisubstituted benzimidazoles.

1.2.4. Human ether a-go-go-related gene (hERG) inhibitor

Human ether a-go-go-related gene (hERG) encodes for voltage gated potassium channels in the nervous system and smooth muscles including that of heart.⁴³ It is a homotetramer and each subunit is made of six α -helical segments (S1-S6), out of which S1-S4 form the voltage sensing transmembrane domain, S5 forms the P-loop and S6 forms the K⁺ selective pore (Figure 14).⁴⁴ When the electrical conduction across the channel is blocked either through drugs or mutation, it leads to prolongation of QT interval which in turn results in ventricular arrhythmia and finally death.^{45,46} Recently, several drugs have been withdrawn from the market owing to their undesirable hERG related cardiac toxicity.⁴⁴ As a result, pre-clinical assessment of QT prolongation is an essential step in drug discovery.⁴⁷

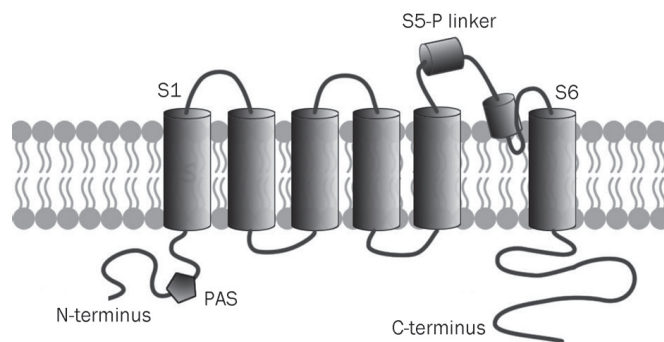


Figure 14: Structure of hERG channel.

Non specific binding of a wide range of drugs to the hERG channel is mainly attributed to interaction of drugs with tyrosine 652 and phenyl alanine 656.⁴⁸ Mutation studies and homology models suggest that Y652 is responsible for pi-pi stacking with neutral aromatic ligands and pi-

cation interactions with basic amine ligands, and F656 causes hydrophobic interactions (Figure 15).⁴⁹ Ways to mitigate the undesired interaction of ligands with hERG channel include formation of zwitterions, reduction of logP and attenuation of pKa.⁴⁹

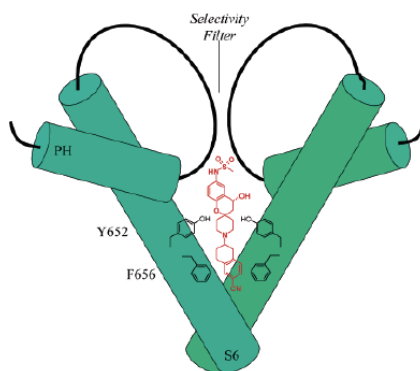
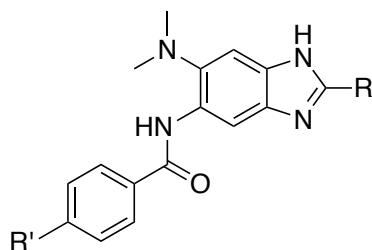


Figure 15: Interaction of drug spiroperidone with hERG channel.⁴⁹

Our collaborator Sanofi identified that the lead trisubstituted benzimidazoles, though display potent inhibitory activity against Mtb, they possess strong affinity towards hERG channel as well, thus displaying a potential for cardiotoxicity. One of the lead compounds, SB-P17G-A38 inhibited hERG 83 % at 1 μ M and 94 % at 10 μ M respectively. In order to make trisubstituted benzimidazoles more drug like, it is highly essential to overcome this undesired hERG inhibition. Some of the 3-pentyl substituted compounds at the 2-position displayed reduced hERG inhibition, analogs of lead compounds SB-P17G-A34, 38 and 42 were synthesized (Table 11). Unfortunately, these compounds could not be tested by Sanofi.



Compound	R	R'	hERG inhibition (%)
			1/10 μ M
SB-P17G-A38	*		83/94
SB-P27C9	*		2/34

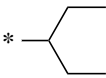
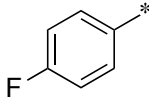
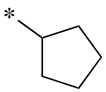
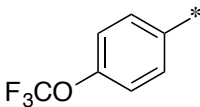
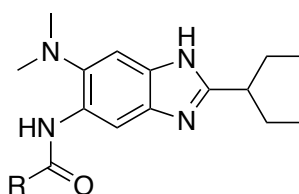
SB-P27C11			18/39
SB-P27B-A20			74/100

Table 11: hERG inhibition by trisubstituted benzimidazoles.

1.2.4.1. Synthesis of 3-pentyl analogs of lead benzimidazoles

The final intermediate 4c was coupled with different acids in the presence of EDC.HCl and DMAP to give the respective amides (Table 12).



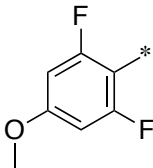
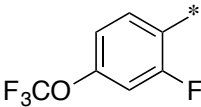
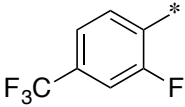
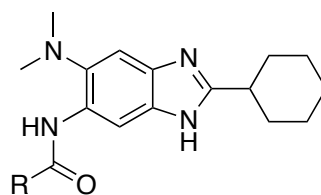
Compound	R	Yield (%)	MIC
			Mtb H37Rv ($\mu\text{g/mL}$)
SB-P27C-A34		63	2.5
SB-P27C-A38		39	1.25
SB-P27C-A42		66	0.625

Table 12: 3-pentyl analogs of lead benzimidazoles

1.2.4.2. Synthesis of polar trisubstituted benzimidazoles

Since the crystal structure of hERG is not known, efforts were made to synthesize compounds with reduced hERG inhibition using LabMol hERG prediction program.⁵⁰ Based on the results from the program, it is the benzamide and the substitutions on the benzamide at the 5-position of the trisubstituted benzimidazole that mainly affect hERG affinity. The initial lead compound SB-P17G-C2 displayed good anti-tubercular activity and reduced hERG inhibitory

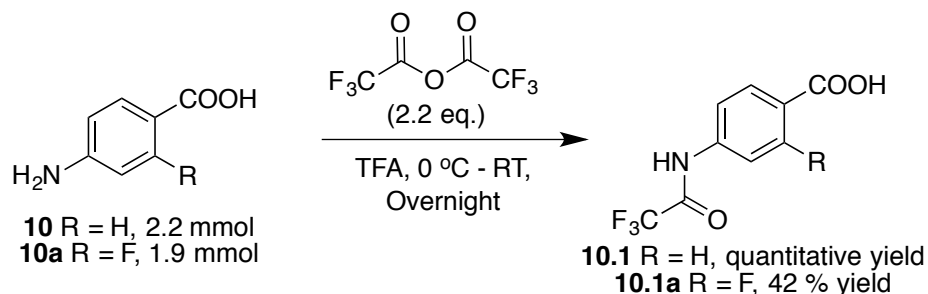
activity, but the carbamate substitution at the 5-position of the benzimidazole was extremely labile in the plasma. On the other hand, the benzamide lead SB-P17G-A38 displayed good metabolic stability and anti-tubercular activity but high hERG inhibitory activity. Compounds displaying a fine balance between anti-tubercular activity, metabolic stability and reduced hERG inhibitory activity need to be designed. Addition of trifluoroacetamide group on the benzamide at the 5-position and replacement of benzamide with nicotinamide derivatives were carried out to increase the polarity of compounds by reducing the cLogP. Unfortunately none of the more polar compounds synthesized were nearly as active as the lead compounds (Table 13).



Compound	R	Binary prediction		cLogP	MIC
		LabMol	Probability		Mtb H37Rv μg/mL
SB-P17G-C2		Non-blocker	0.69	6.1	0.0019
SB-P17G-A38		Blocker	0.6	6.7	<0.024
SB-P17G-A59		Non-blocker	0.53	6.1	3.19
SB-P17G-A60		Non-blocker	0.53	5.9	0.78
SB-P17G-A61		Non-blocker	0.64	4.5	6.25
SB-P17G-A62		Non-blocker	0.66	4.5	12.5

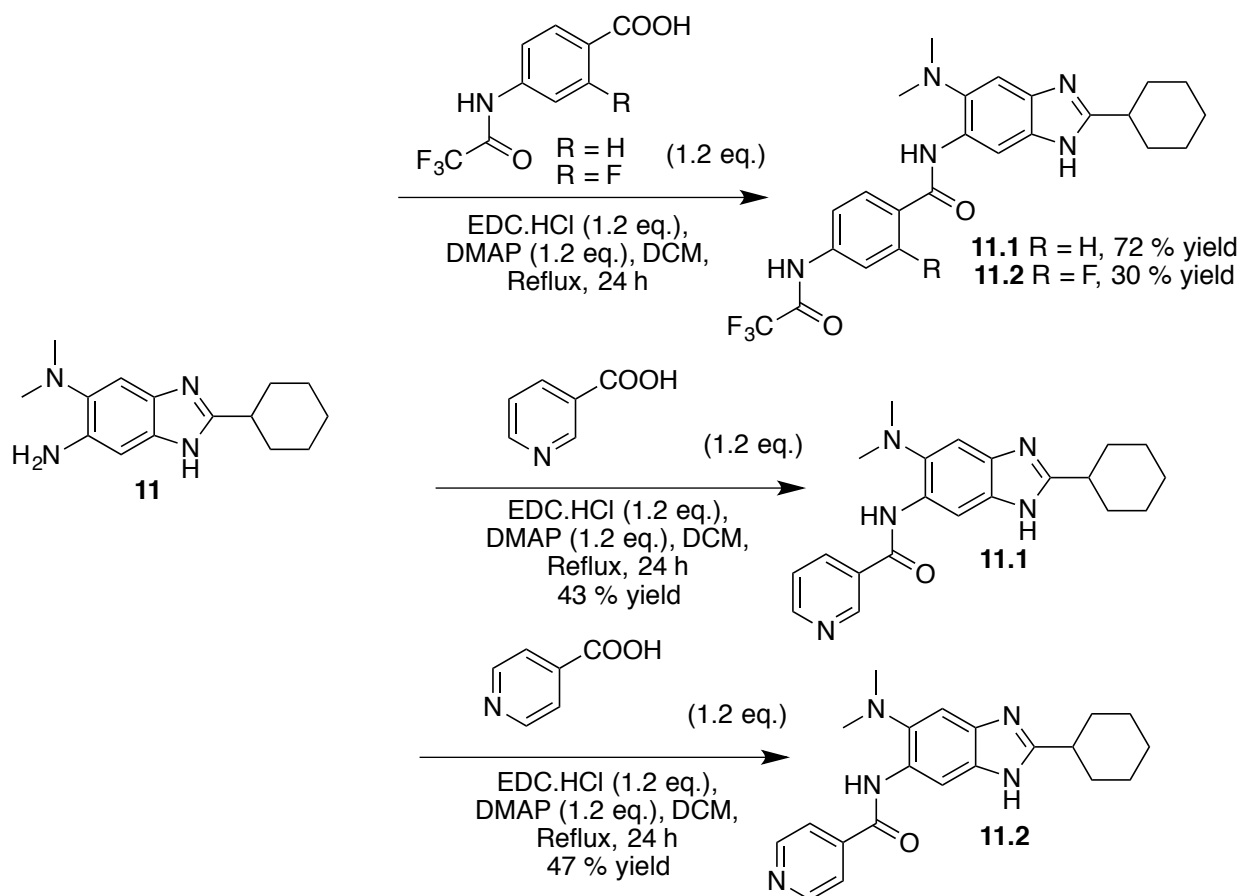
Table 13: hERG inhibitory prediction results from LabMol.

Commercially available 4-aminobenzoic acid and 2-fluoro-4-aminobenzoic acid was treated with trifluoroacetic anhydride at 0 °C, and the reaction mixture was stirred at room temperature overnight to give respective trifluoroacetamides (Scheme 10).



Scheme 10: Synthesis of trifluoroacetamides.

Amine **11** was coupled with different acids using EDC.HCl and DMAP to give respective amides (Scheme 11).

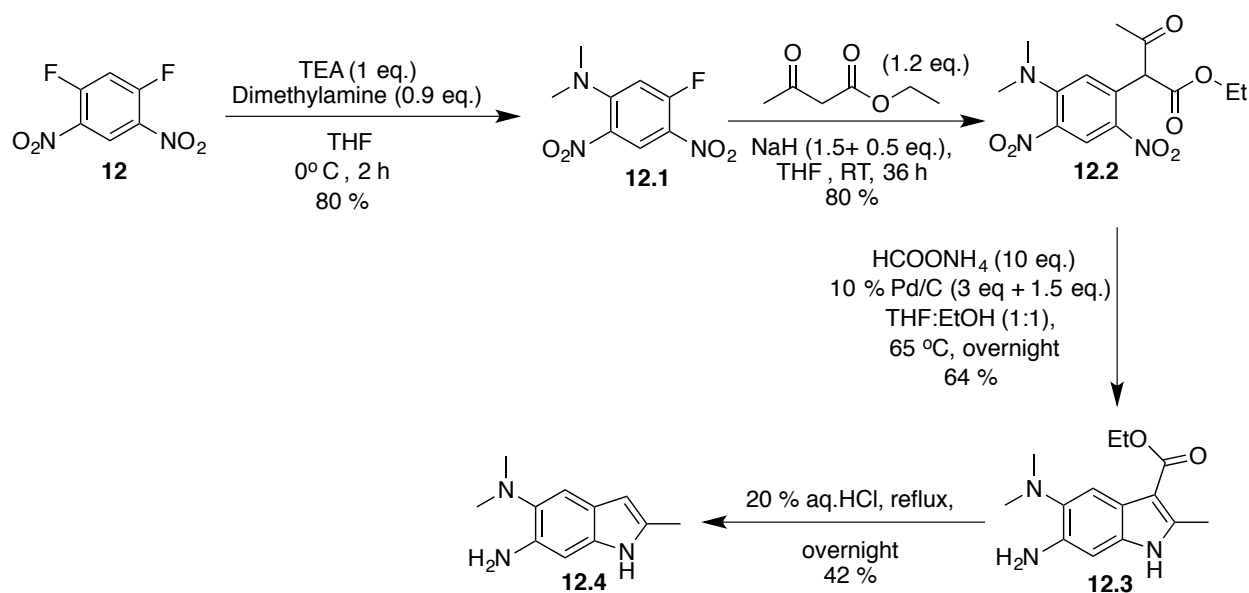


Scheme 11: Synthesis of 5-amidobenzimidazoles.

1.2.5. Exploration of trisubstituted indoles as antibacterial scaffold

In order to diversify our trisubstituted benzimidazole library and better understand the SAR, 2,5,6- trisubstituted indoles were proposed as anti-tubercular agents. Replacement of -N with -CH₂ would constitute a good bioisostere. Also, like benzimidazoles, indole is also a very well studied core, as it is present in a variety of drug classes like anticancer, antihypertensive, antiemetic, anti-HIV etc, thus making it a good drug like core.⁵¹

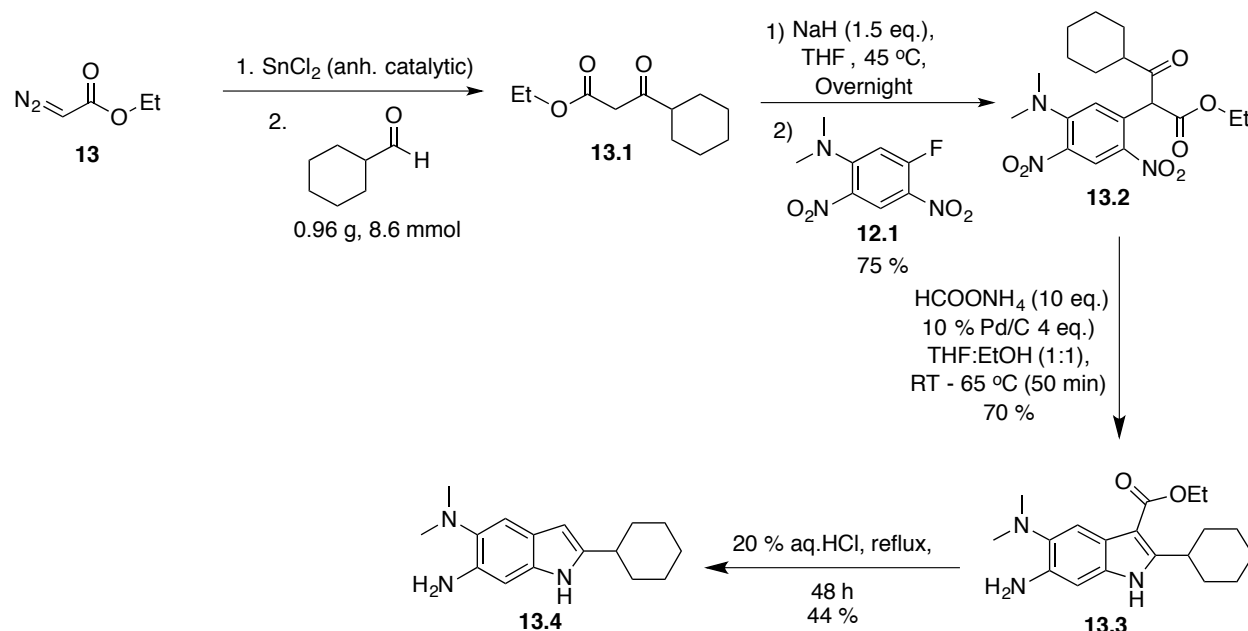
For the ease of synthesis, trisubstituted indole with a methyl substitution at the 2-position was attempted, as ethyl acetoacetate was readily available in the lab. Aromatic nucleophilic substitution of 1,5-difluoro-2,4-dinitrobenzene **12**, was carried out with dimethyl amine with the aid of triethylamine as the base in THF at 0 °C for 2 hours give compound **12.1**, followed by treatment with ethyl acetoacetate in the presence of sodium hydride in THF to give **12.2**. Reduction and cyclization of **12.2** was brought about by using ammonium formate and palladium on carbon in a mixture of THF: ethanol (1:1) at 65 °C to give **12.3**. Decarboxylation of **12.3** was carried out by refluxing with 20 % aqueous HCl overnight to give **12.4** (Scheme 12). However, **12.4** was found to be unstable as it degraded soon.



Scheme 12: Synthesis of trisubstituted indoles with methyl substitution at the 2-position.

Since the lead trisubstituted benzimidazoles have a cyclohexyl substitution at the 2-position, trisubstituted indoles with cyclohexyl substitution at the 2-position would be a good comparison to see the effect to replacing a -N with a -CH group. Ethyl diazoacetate **13**, was treated with catalytic amount of anhydrous tin chloride followed by cyclohexane aldehyde to give

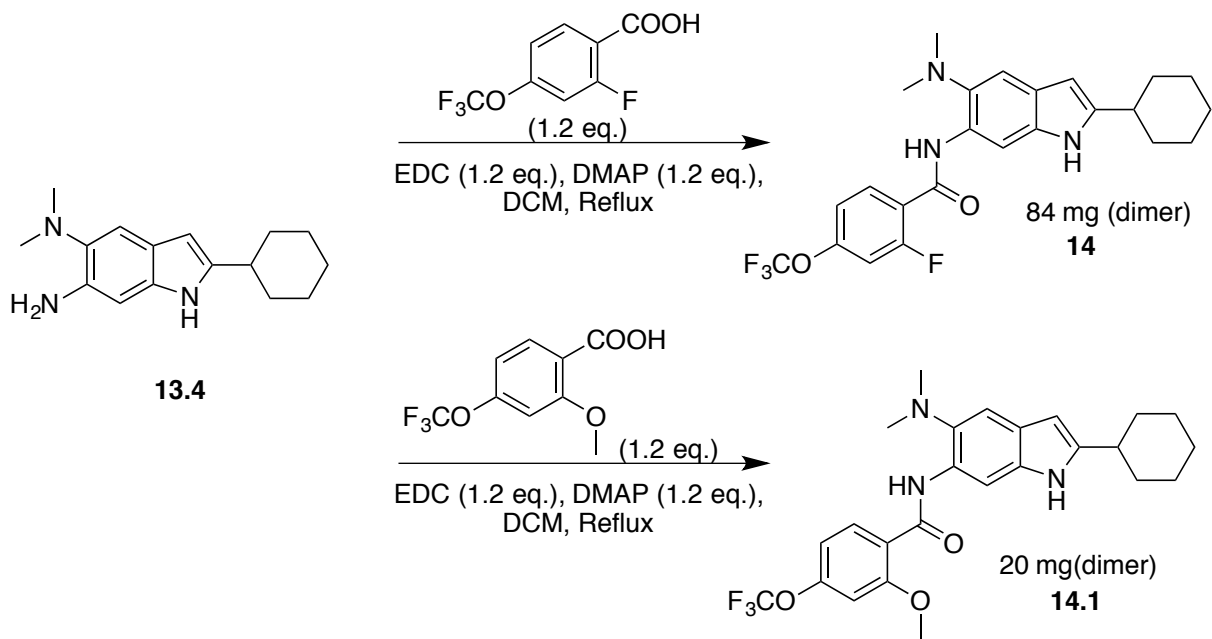
compound **13.1**. **13.1** was initially treated with sodium hydride (NaH) to generate the enolate, which was in turn treated with 5-dimethylamino-2,4-dinitro-fluoro benzene **12.1**, in THF to give **13.2**. This was followed by reduction and cyclization of **13.2** using ammonium formate and palladium on carbon in a mixture of THF: ethanol (1:1) at 65 °C to give **13.3**. Decarboxylation of **13.3** was carried out by refluxing with 20 % aqueous HCl overnight to give **13.4** (Scheme 13).



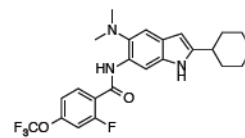
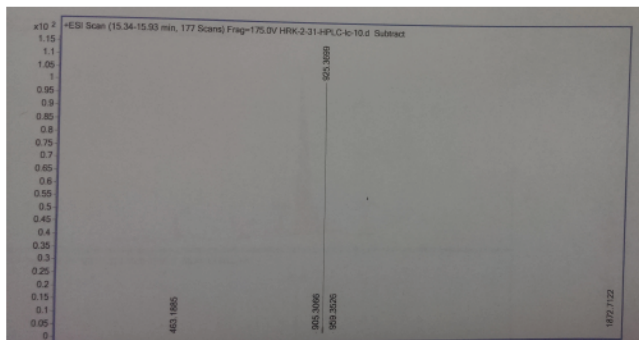
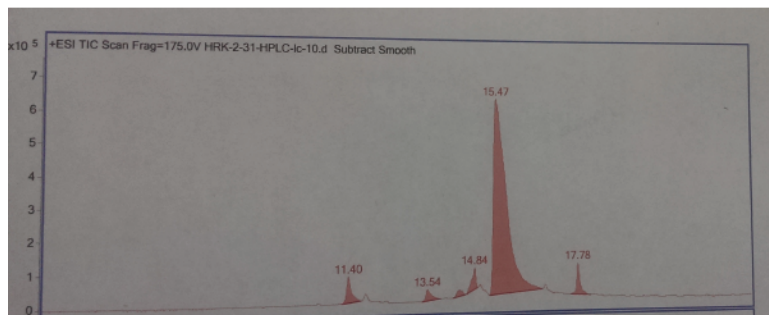
Scheme 13: Synthesis of trisubstituted indoles with cyclohexyl substitution at the 2-position.

1.2.5.1. Indole analogs of SB-P17G-A37 and SB-P17G-A55

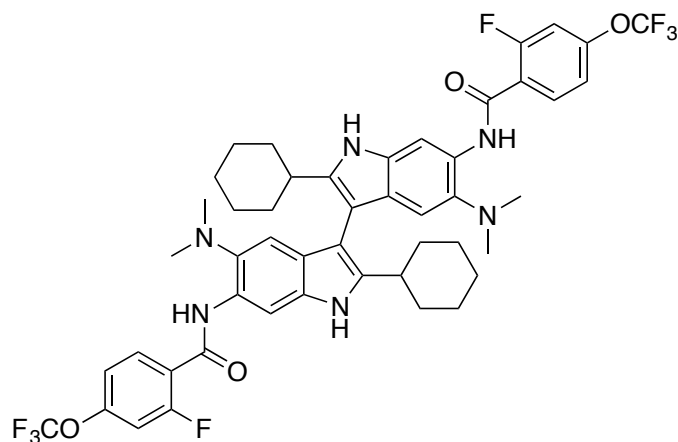
Compound **13.4** was coupled with 2 different acids in the presence of EDC.HCl and DMAP to give compounds **14** and **14.1** (Scheme 14). Surprisingly the mass of compounds **14** and **14.1** showed the molecular ion peak for a covalent dimer, twice the desired mass with the loss of two protons. The peak at 15.47 min corresponds to a covalent dimer with molecular weight 925.36 (Figure 16), which is twice the required molecular weight minus 2 hydrogens. Also, on the proton NMR, the -CH proton at the 3-position was missing which leads to speculate the possible structure as shown in Figure 16.



Scheme 14: Synthesis of indole analogs of SB-P17G-A38 and SB-P17G-A55.



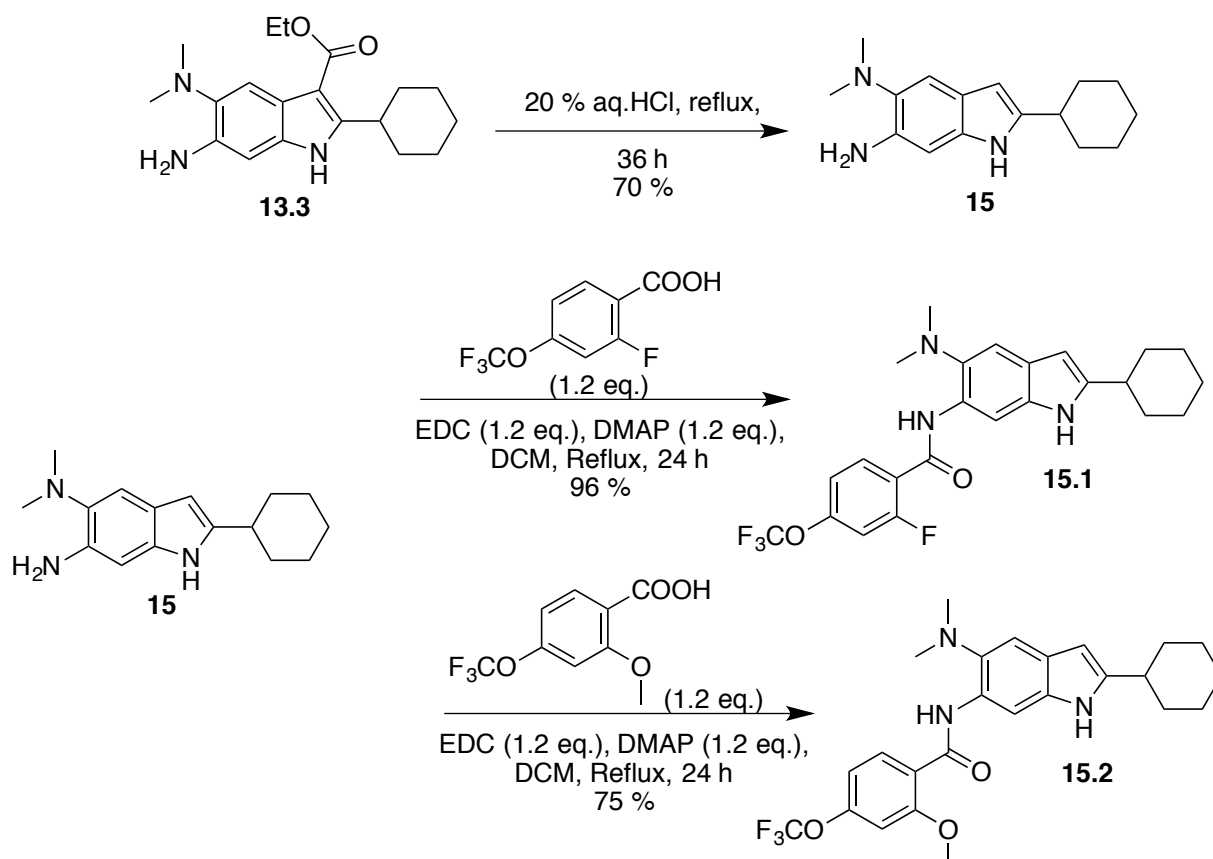
Exact Mass: 463.19



Possible dimer

Figure 16: Mass spectrum of 14 and possible structure for dimer.

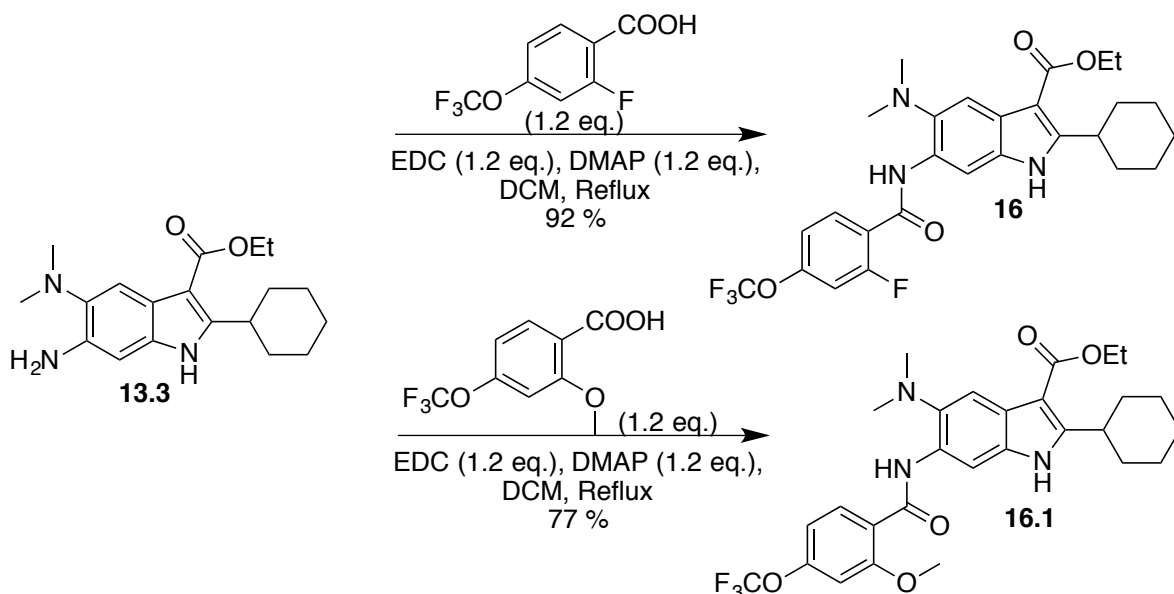
In order to get trisubstituted indoles and not the dimers, product **15** after decarboxylation was purified and the structure was confirmed by NMR by the presence of a new aromatic peak corresponding to the 3-position of the indole. **15** was coupled with acids in the presence of EDC.HCl and DMAP to give compounds **15.1** and **15.2**. Mass showed the presence of desired product and not the dimer (Scheme 15).



Scheme 15: Synthesis of indole analogs of SB-P17G-A38 and SB-P17G-A55.

1.2.5.2. Tetrasubstituted indoles

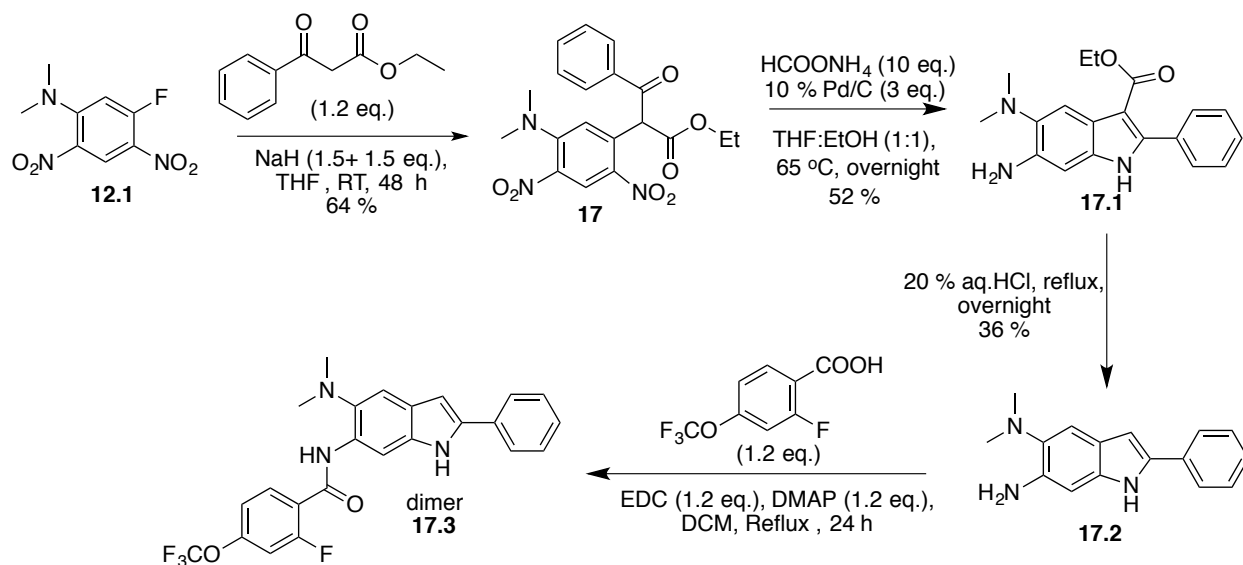
Since our lead trisubstituted benzimidazoles display hERG inhibitory activity, tetrasubstituted indole analogs of SB-P17G-A38 and SB-P17G-A55 were also synthesized, as the ester group on the 3-position of indoles would render the compounds polar. SB-P17G-A55, though not very potent with an MIC of 5 $\mu\text{g/mL}$, displayed reduced hERG inhibition. Tetrasubstituted indole **13.3** was coupled with 2-fluoro-4-trifluoromethoxy benzoic acid and 2-methoxy-4-trifluoromethoxy benzoic acid to give compounds **16** and **16.1** respectively (Scheme 16).



Scheme 16: Synthesis of tetrasubstituted indoles.

1.2.5.3. Trisubstituted indoles with phenyl substitution at the 2-position

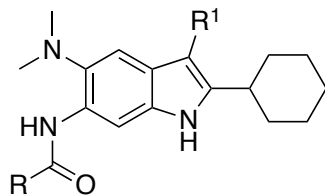
In order to diversify the compounds for SAR, trisubstituted indoles with a phenyl substitution at the 3-position were synthesized following the same procedure as 2-methyl substituted indoles in scheme 12. After decarboxylation, compound **17.2** was then coupled with 2-fluoro-4-trifluoromethoxy benzoic acid in the presence of EDC.HCl and DMAP to give **17.3**. Like compounds **14** and **14.1**, compound **17.3** showed the molecular ion peak for a dimer on the mass spectrum as well.



Scheme 17: Synthesis of trisubstituted indoles with phenyl substitution at the 2-position.

1.2.5.4. Accurate MIC of the synthesized indoles

The trisubstituted and tetrasubstituted indoles were tested against Mtb H37Rv to check for their inhibitory activity (Table 14). Unfortunately, none of the indole analogs were as active as the benzimidazole counter parts. The indole may bind to a different binding pocket than benzimidazole. Extensive SAR is required to identify potent molecules. The A38 analog of indole was inactive suggesting the importance of N at the 3-position.



Compound	R	R ¹	MIC($\mu\text{g/mL}$) H37Rv
SB-IND1-A38 (4)		H	>13.5 $\mu\text{g/mL}$
SB-IND1-A55 (4.1)		H	>29 $\mu\text{g/mL}$

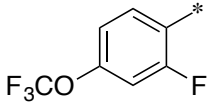
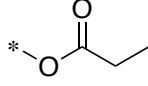
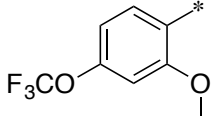
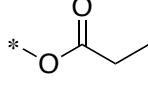
SB-IND1-A38-C3-1 (5)			>10 µg/mL
SB-IND1-A55-C3-1 (5.1)			>10 µg/mL

Table 14: Accurate MIC of indoles against Mtb H37Rv.

1.3. Conclusion

3-pentyl and benzyl substitutions at the 2-position of 2,5,6-trisubstituted benzimidazoles resulted in a large number of hits from initial screening against Mtb H37Rv. SB-P17G-A38 analogs of 2-(3-pentyl) and 2-benzyl benzimidazoles displayed similar activity as the cyclohexyl lead. Unfortunately, none of the 2-position modified compounds were more active than cyclohexyl group. More SAR needs to be carried out to optimize the 2-position. But the issue that needs to be addressed immediately is the design of compounds with a balance between Mtb inhibitory activity and reduced hERG inhibition. Trisubstituted indoles are in an early stage of discovery. Extensive SAR needs to be carried out to identify lead compounds. The MIC results suggest that replacing a –N of imidazole with –CH in indole greatly affects the Mtb inhibitory activity.

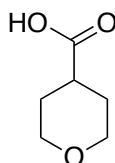
1.4. Experimental Section

Methods. ¹H and ¹³C NMR spectra were measured on Bruker 300, 400 or 500 MHz NMR spectrometer. Melting points were measured on a Thomas Hoover Capillary melting point apparatus and are uncorrected. TLC was performed on silica coated aluminum sheets (thickness 200 µm) or alumina coated (thickness 200 µm) aluminum sheets supplied by Sorbent Technologies and column chromatography was carried out on Siliaflash® P60 silica gel, 40-63 µm (230-400 mesh) supplied by Silicycle. Aluminum oxide, activated, neutral, Brockmann Grade I, 58 Å, was supplied by Alfa Aesar. High-resolution mass spectra were obtained from the Mass Spectrometry Laboratory, University of Illinois at Urbana-Champaign, Urbana, IL. Purity of synthesized compounds was determined by a Shimadzu LC-2010A HT series HPLC assembly or Agilent 1100 series HPLC assembly. Four analytical conditions were used and noted as a part of the characterization data for synthesized compounds. HPLC (1): Adsorbosphere Silica 5 µ, 250 × 4.6 mm column, isopropanol and hexanes, flow rate of 1 mL/min, t = 0-40 min, gradient of 5-50% isopropanol. HPLC (3): Kinetex PFP, 2.6 µm, 4.6 mm × 100 mm column, methanol and water, flow rate of 0.2 mL/min, t = 0-30 min, gradient of 20-80% MeOH. HPLC. Measurements were

made at 254 nm and 303 nm.

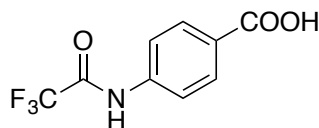
Materials. Solvents (HPLC grade or better), and all the other chemicals were purchased from Fisher Scientific Co. (Pittsburgh, PA). The chemicals were purchased from Aldrich Co., Synquest Inc. and Sigma. Tetrahydrofuran (THF) was freshly distilled from sodium metal and benzophenone. Dichloromethane was also distilled immediately prior to use under nitrogen from calcium hydride.

Synthesis of tetrahydro-2H-pyran-4-carboxylic acid (4.1)⁵²



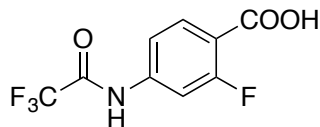
Methyl tetrahydropyran-4-carboxylate (35 mmol) was dissolved in THF: methanol (2:1), and refluxed with lithium hydroxide monohydrate (5 eq.) overnight. After the reaction was complete, the reaction mixture was concentrated in a rotary evaporator. The crude reaction mixture was neutralized with 2 M HCl, and extracted with ethyl acetate to give the crude product. Recrystallization using hexanes:ethyl acetate resulted in pure white crystals (92% yield); ¹H NMR (500 MHz, CDCl₃) δ 1.75 – 1.88 (m, 4 H), 2.54 – 2.60 (m, 1 H), 3.42 – 3.47 (m, 2 H), 3.95 – 3.99 (m, 2 H), 11.24 (br. s, 1 H). The analytical data was consistent with literature.⁵²

Synthesis of 4-Trifluoroacetamido benzoic acid⁵³



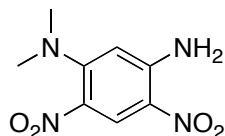
p-Aminobenzoic acid (2.2 mmol) was dissolved in trifluoroacetic acid, followed by addition of trifluoroacetic anhydride at 0 °C. The reaction mixture was stirred overnight at room temperature. After the reaction was complete, the reaction mixture was poured in to ice cold water, and extracted with ethyl acetate (30 mL X 3). The organic layers were combined, dried over anhydrous magnesium sulfate, filtered, concentrated in a rotary evaporator, and dried under vacuum to afford the acid as a brown solid (quantitative yield); ¹H NMR (300 MHz, Acetone-D₆) δ 7.79 (d, 2 H, J = 7 Hz), 8.06 (d, 2 H, J = 8.7 Hz), 9.44 (s, 1 H). The analytical data was consistent with literature.⁵³ Same procedure was used for the synthesis of 2-fluoro-4-trifluoroacetamido benzoic acid.

Synthesis of 2-fluoro-4-trifluoroacetamido benzoic acid



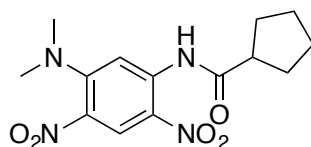
Recrystallization with hexane: ethyl acetate resulted in pure acid as brown solid (43% yield); ^1H NMR (300 MHz, Acetone- D_6) δ 7.61 (d, 1 H, $J = 8.6$ Hz), 7.74 (d, 1 H, $J = 12.6$ Hz), 8.01 (t, 1 H, $J = 8.4$ Hz), 10.64 (s, 1 H), 11.55 (br. s, 1 H).

5-N,N-Dimethylamino-2,4-dinitroaniline (**2**)²¹



To a solution of 2,4-dinitro-5-fluoroaniline (9.92 g, 49 mmol) and DIPEA (54 mmol) in tetrahydrofuran (150 mL) was added a solution of dimethylamine (2 M in THF, 54 mmol) in tetrahydrofuran (10 mL), drop wise and the mixture was stirred at room temperature for 4 h. After completion of reaction, the reaction mixture was diluted with dichloromethane, transferred to a separatory funnel and washed with water (30 mL x 3), dried over anhydrous magnesium sulfate, filtered, rotary evaporated and dried under vacuum to afford **1.1** as a yellow solid (97% yield); mp 162-165 °C; ^1H NMR (400 MHz, CDCl_3) δ 2.94 (s, 6 H), 6.01 (s, 1 H), 6.41 (s, 2 H), 8.80 (s, 1 H). The analytical data was consistent with literature.²¹

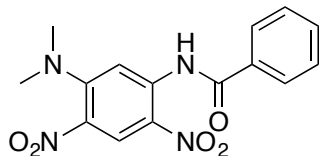
1-(Cyclopentanecarboxamido)-5-N,N-dimethylamino-2,4-dinitrobenzene (**3a**)



A solution of **1.1** (1 g, 4.42 mmol) and cyclopentanecarbonyl chloride (5.30 mmol) in pyridine (4 mL) was refluxed overnight. After the starting material disappeared, the reaction mixture was evaporated to get a brown residue. It was then triturated with methanol to obtain the product **3a** as yellow solid (70% yield); mp 118-120 °C; ^1H NMR (400 MHz, CDCl_3) δ 1.62-1.71 (m, 2 H), 1.74-1.81 (m, 2 H), 1.82-1.93 (m, 2 H), 1.99-2.07 (m, 2 H), 2.81- 2.90 (p, 1 H, $J = 8.08$ Hz), 3.04 (s, 6 H), 8.57 (s, 1 H), 8.83 (s, 1 H), 10.96 (s, 1 H); ^{13}C NMR (100 MHz, CDCl_3) δ 26.0, 30.4, 42.7, 48.2, 106.2, 125.2, 127.7, 131.6, 138.9, 150.4, 176.4; MS (ESI) m/z 323.1 ($\text{M}+1$)⁺.

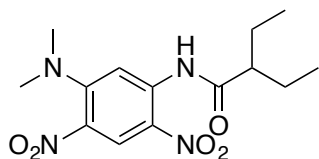
Same procedure was used for the synthesis of **3b-g**, **4.3** and **7.2**.

1-Benzamido-5-N,N-dimethylamino-2,4-dinitrobenzene (**3b**)



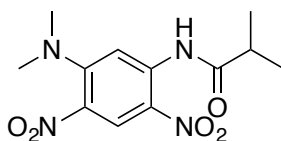
Yellow solid (96% yield); mp 190-193 °C; ^1H NMR (400 MHz, CDCl_3) δ 3.1 (s, 6 H), 7.52-7.56 (m, 2 H), 7.60-7.64 (m, 1 H), 7.96-7.99 (m 2 H), 8.75 (s, 1 H), 8.87 (s, 1 H), 11.88 (s, 1 H); ^{13}C NMR (100 MHz, CDCl_3) δ 42.8, 106.2, 125.4, 127.5, 127.8, 129.3, 131.8, 133.2, 133.7, 139.0, 150.4, 166.3; MS (ESI) m/z 331.1 ($\text{M}+1$) $^+$.

1-(Ethylbutanamido)-5-N,N-dimethylamino-2,4-dinitrobenzene (3c)



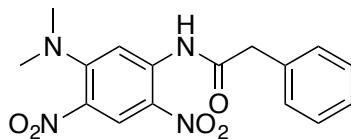
Yellow solid (92% yield); mp 98-100 °C; ^1H NMR (400 MHz, CDCl_3) δ 0.97 (t, 6 H $J = 7.4$ Hz), 1.58-1.79 (m, 4 H), 2.19-2.27 (m, 1 H), 3.06 (s, 3 H), 8.63 (s, 1 H), 8.85 (s, 1 H), 10.96 (s, 1 H); ^{13}C NMR (100 MHz, CDCl_3) δ 12.1, 25.8, 42.7, 53.6, 106.3, 125.2, 127.7, 131.7, 138.7, 150.4, 176.3; MS (ESI) m/z 325.2 ($\text{M}+1$) $^+$.

1-(Isobutyramido)-5-N,N-dimethylamino-2,4-dinitrobenzene (3d)



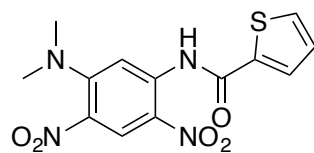
Yellow solid (74% yield); mp 105-107 °C; ^1H NMR (400 MHz, CDCl_3) δ 1.30 (d 6 H, J 6.96 Hz), 2.62-2.72 (m, 1 H), 2.93 (s 1 H), 3.05 (s, 6 H), 8.57 (s, 1 H), 8.78 (s, 1 H), 10.99 (s, 1 H); ^{13}C NMR (100 MHz, CDCl_3) δ 19.4, 38.0, 42.7, 106.2, 125.2, 127.6, 131.6, 138.8, 150.3, 177.0; MS (ESI) m/z 297.2 ($\text{M}+1$) $^+$.

1-(Phenylacetamido)-5-N,N-dimethylamino-2,4-dinitrobenzene (3e)



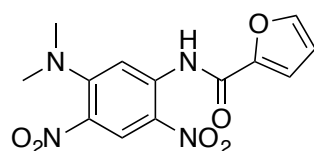
Yellow solid (55% yield); mp 125-128 °C; ^1H NMR (400 MHz, CDCl_3) δ 3.02 (s, 6 H), 3.82 (s, 2 H), 7.33-7.37 (m, 3 H), 7.37-7.43 (m, 2 H), 8.53 (s, 1 H), 8.75 (s, 1 H), 10.82 (s, 1 H); ^{13}C NMR (100 MHz, CDCl_3) δ 42.7, 46.1, 106.2, 125.1, 127.5, 128.2, 129.5, 129.7, 131.6, 133.0, 138.4, 150.2, 171.1; MS (ESI) m/z 345.1 ($\text{M}+1$) $^+$.

1-(Thiophene-2-carboxamido)-5-N,N-dimethylamino-2,4-dinitrobenzene (3f)



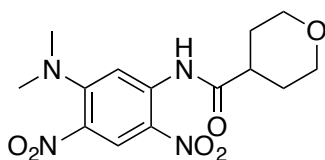
Yellow solid (91% yield); mp 212-215 °C; ^1H NMR (400 MHz, CDCl_3) δ 3.08 (s, 6 H), 7.18-7.20 (m, 1 H), 7.67 (s, 1 H), 7.76 (s, 1 H), 8.64 (s, 1 H), 8.87 (s, 1 H), 11.82 (s, 1 H); ^{13}C NMR (400 MHz, CDCl_3) δ 42.8, 106.1, 125.2, 127.8, 128.6, 129.6, 131.8, 133.1, 138.8, 138.9, 150.3, 160.9; MS (ESI) m/z 337.1 ($\text{M}+1$) $^+$.

1-(Furan-2-carboxamido)-5-N,N-dimethylamino-2,4-dinitrobenzene (3g)



Yellow solid (81% yield); mp 185-188 °C; ^1H NMR (400 MHz, CDCl_3) δ 3.07 (s, 6 H), 6.06-6.61 (dd, 1 H), 7.29-7.30 (dd, 1 H), 7.63 (s, 1 H), 8.65 (s, 1 H), 8.85 (s, 1 H), 11.88 (s, 1 H); ^{13}C NMR (100 MHz, CDCl_3) δ 42.7, 106.3, 113.1, 117.1, 125.3, 127.7, 131.7, 138.4, 146.0, 147.1, 150.2, 157.0; MS (ESI) m/z 321.1 ($\text{M}+1$) $^+$.

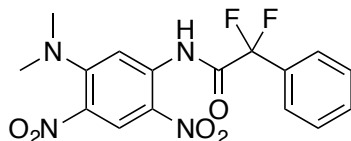
1-(Tetrahydropyranamido)-5-N,N-dimethylamino-2,4-dinitrobenzene (4.3)



To a solution of **2** (0.44 mmol) in acetonitrile was added tetrahydropyran-4-carboxylic acid (3 eq.) and phosphorus trichloride (3 eq.). The reaction mixture was refluxed overnight. After the completion of the reaction, solvent from the reaction mixture was evaporated under vacuum to give the crude reaction mixture, which was washed with sodium bicarbonate (30 mL X 3) and water (30 mL X 3). The product was extracted with ethyl acetate (30 mL X 3) and dichloromethane (30 mL X 3). The organic layers were combined and dried over anhydrous MgSO_4 , filtered and rotary evaporated to give the crude product. Purification of the crude product by flash chromatography on silica gel using DCM and hexanes (9:1), followed by 100 % ethyl acetate as eluent afforded **4.3** as yellow solid (47 % yield); ^1H NMR (500 MHz, CDCl_3) δ 1.79 – 1.93 (m, 4 H), 2.61 – 2.67 (m, 1 H), 3.06 (s, 6 H), 3.46 – 3.51 (m, 2 H), 4.05 – 4.09 (m, 2 H), 8.56 (s, 1 H),

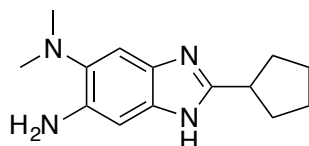
8.83 (s, 1 H), 11.06 (s, 1 H); ^{13}C NMR (125 MHz, CDCl_3) δ 29.06, 42.77, 44.23, 67.20, 106.36, 127.72, 138.65, 150.37, 174.26; MS (ESI) m/z 339.1 ($\text{M}+1$) $^+$.

1-(α,α -difluorophenylacetamido)-5-N,N-dimethylamino-2,4-dinitrobenzene (**7.2**)



A solution of **2** (2.2 mmol) in acetonitrile was treated with α,α -difluorophenylacetic acid (1.1 eq.) and phosphorus trichloride (1.1 eq.) in a microwave reactor at 150 $^\circ\text{C}$, 200 watts and 250 psi for 5 minutes. After the completion of the reaction, solvent from the reaction mixture was evaporated under vacuum to give the crude reaction mixture, which was washed with sodium bicarbonate (30 mL X 3) and water (30 mL X 3). The product was extracted with ethyl acetate (30 mL X 3). The organic layers were combined and dried over anhydrous MgSO_4 , filtered and rotary evaporated to give the crude product as a yellow oil. Pure product **7.2** crashed out from the oil after addition of methanol (5 mL) and hexanes (15 mL) as yellow solid (51% yield); ^1H NMR (500 MHz, CDCl_3) δ 3.05 (s, 6 H), 7.48 – 7.67 (m, 3 H), 7.68 – 7.69 (m, 2 H), 8.45 (s, 1 H), 8.84 (s, 1 H), 11.94 (s, 1 H); ^{13}C NMR (125 MHz, CDCl_3) δ 42.79, 106.89, 114.56, 116.59, 125.53, 125.61, 126.66, 125.71, 127.67, 129.16, 131.62, 131.94, 132.15, 132.25, 132.35, 136.92, 150.08, 163.43, 163.69, 163.95; MS (ESI) m/z 381.1 ($\text{M}+1$) $^+$.

5-Amino-6-N,N-dimethylamino-2-cyclopentyl-1H-benzo[d]imidazole (**4a**)

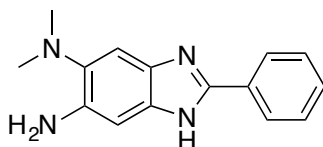


To a solution of **3a** (1.4 g, 4.5 mmol) in ethanol (25 mL), solid stannous chloride dihydrate ($\text{SnCl}_2 \cdot 2\text{H}_2\text{O}$) (7.1 g, 31.6 mmol) was added. Concentrated hydrochloric acid (18 mL) was added to the reaction mixture such that the final concentration of HCl was 4 N in the reaction flask. The reaction mixture was refluxed for 4 h. Upon completion, the reaction mixture was basified with 30% sodium hydroxide solution. Excess stannous chloride formed a soluble salt in presence of excess base. It was then extracted with dichloromethane (30 ml X 3), dried over anhydrous MgSO_4 , filtered and rotary evaporated to give a dark brown oil. The brown oil was purified by flash chromatography on alumina using 100% ethyl acetate as eluent to afford **4a** as a pale brown solid (87% yield); mp 100-103 $^\circ\text{C}$; ^1H NMR (400 MHz, CDCl_3) δ 1.54-1.64 (m, 2 H), 1.68-1.79 (m, 2

H), 1.86-1.95 (m, 2 H), 2.04- 2.12 (m, 2 H), 2.61 (s, 6 H), 3.19- 3.27 (p, 1 H, J 8.47 Hz), 6.78 (s, 1 H), 7.22 (s, 1 H); ^{13}C NMR (100 MHz, CDCl_3) δ 25.5, 32.4, 39.6, 44.6, 98.5, 106.5, 132.9, 134.2, 138.0, 138.2, 157.2; HRMS (ESI) m/z calcd for $\text{C}_{14}\text{H}_{20}\text{N}_4\text{H}^+$: 245.1687, Found: 245.1759 ($\Delta = 0.38$ ppm).

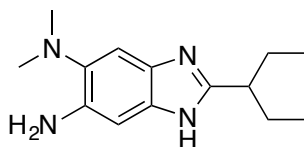
Same procedure was used for the synthesis of **4b-g**, **4.5** and **8**.

5-Amino-6-N,N-dimethylamino-2-phenyl-1H-benzo[d]imidazole (**4b**)



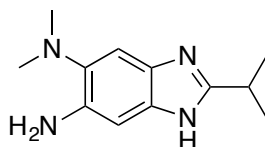
Brown solid (96% yield); mp 90-93 °C; ^1H NMR (400 MHz, CDCl_3) δ 2.57 (s, 6 H), 6.77 (s, 1 H), 7.22 (s, 1 H), 7.29-7.33 (m, 3 H), 8.06-8.09 (m, 2 H); ^{13}C NMR (100 MHz, CDCl_3) δ 44.4, 98.9, 107.4, 126.4, 128.9, 129.3, 130.4, 134.5, 138.8, 139.1, 150.6, 171.3; HRMS (ESI) m/z calcd for $\text{C}_{15}\text{H}_{16}\text{N}_4\text{H}^+$: 253.1376, Found: 253.1449 ($\Delta = -0.47$ ppm).

5-Amino-6-N,N-dimethylamino-2-(pentan-3-yl)-1H-benzo[d]imidazole (**4c**)



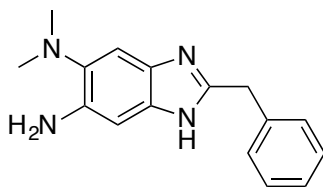
Brown solid (87 % yield); mp 80-82 °C; ^1H NMR (400 MHz, CDCl_3) δ 0.86-0.90 (t, 6 H, J = 7.4 Hz), 1.71-1.89 (m, 4 H), 2.62 (s, 6 H), 2.71-2.79 (m, 1 H), 6.81 (s, 1 H), 7.23 (s, 1 H); ^{13}C NMR (100 MHz, CDCl_3) δ 12.3, 27.7, 44.1, 44.6, 98.7, 106.5, 133.1, 134.4, 137.8, 138.0, 157.1; HRMS (ESI) m/z calcd for $\text{C}_{14}\text{H}_{22}\text{N}_4\text{H}^+$: 247.1845, Found: 247.1918 ($\Delta = -0.35$ ppm).

5-Amino-6-N,N-dimethylamino-2-isopropyl-1H-benzo[d]imidazole (**4d**)



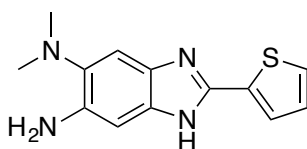
Brown solid (69% yield); mp 83-85 °C; ^1H NMR (400 MHz, CDCl_3) δ 1.38 (d, 6 H, J = 6.96 Hz), 2.62 (s, 6 H), 3.11-3.22 (m, 1 H), 3.50 (s, 1 H), 6.79 (s, 1 H), 7.23 (s, 1 H); ^{13}C NMR (100 MHz, CDCl_3) δ 21.8, 29.1, 44.7, 98.7, 106.8, 133.1, 134.3, 138.1, 138.3, 158.8; HRMS (ESI) m/z calcd for $\text{C}_{12}\text{H}_{18}\text{N}_4\text{H}^+$: 219.1530, Found: 219.1603 ($\Delta = 0.68$ ppm).

5-Amino-6-N,N-dimethylamino-2-benzyl-1H-benzo[d]imidazole (**4e**)



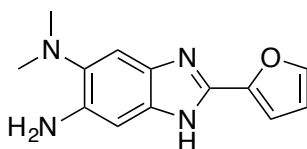
Brown Solid (59% yield); 80-83 °C; ^1H NMR (400 MHz, CDCl_3) δ 2.61 (s, 6 H), 4.09 (s, 2 H), 6.68 (s, 1 H), 7.16-7.24 (m, 6 H); ^{13}C NMR (100 MHz, CDCl_3) δ 35.6, 44.5, 98.7, 106.6, 126.9, 128.7, 128.9, 133.1, 134.6, 137.0, 138.1, 138.4, 151.8; HRMS (ESI) m/z calcd for $\text{C}_{16}\text{H}_{18}\text{N}_4\text{H}^+$: 267.1527, Found: 267.1600 ($\Delta = 1.73$ ppm).

5-Amino-6-N,N-dimethylamino-2-(thiophen-2-yl)-1H-benzo[d]imidazole (4f)



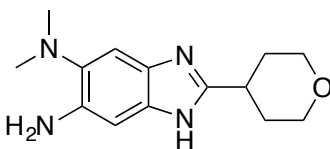
Brown solid (87% yield); mp 100-102 °C; ^1H NMR (400 MHz, CDCl_3) δ 2.58 (s, 6 H), 6.77 (s, 1 H), 6.94-6.96 (m, 1 H), 7.21 (s, 1 H), 7.23-7.25 (m, 1 H), 7.62-7.63 (m, 1 H); ^{13}C NMR (100 MHz, CDCl_3) δ 44.4, 98.3, 107.0, 125.8, 127.0, 127.9, 133.9, 134.9, 138.9, 139.1, 146.1; HRMS (ESI) m/z calcd for $\text{C}_{13}\text{H}_{14}\text{N}_4\text{SH}^+$: 259.0941, Found: 259.1013 ($\Delta = -0.89$ ppm).

5-Amino-6-N,N-dimethylamino-2-(furan-2-yl)-1H-benzo[d]imidazole (4g)



Yellow solid (99% yield); mp 92-95 °C; ^1H NMR (400 MHz, CDCl_3) δ 2.62 (s, 6 H), 6.42 (s 1 H), 6.80 (s, 1 H), 7.02 (d, 1 H, J 4 Hz), 7.25 (s, 1 H), 7.38 (s, 1 H); ^{13}C NMR (100 MHz, CDCl_3) δ 44.4, 98.4, 107.2, 109.2, 112.1, 134.3, 139.9, 139.2, 142.6, 143.0, 145.9; HRMS (ESI) m/z calcd for $\text{C}_{13}\text{H}_{14}\text{N}_4\text{OH}^+$: 243.1159, Found: 243.1232 ($\Delta = 3.44$ ppm).

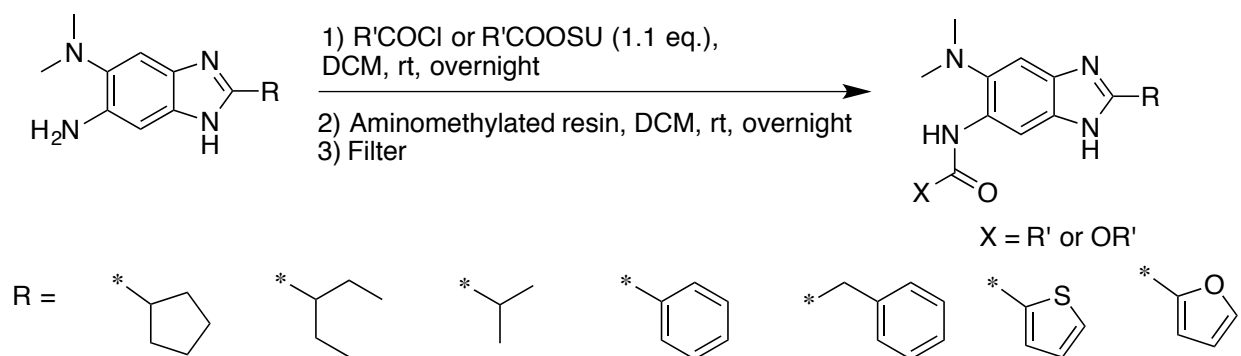
5-Amino-6-N,N-dimethylamino-2-tetrahydropyranyl-1H-benzo[d]imidazole (4.5)



Brown solid (91% yield); ^1H NMR (300 MHz, CDCl_3) δ 1.94 – 2.01 (m, 4 H), 2.66 (s, 6 H), 3.02 – 3.14 (m, 1 H), 3.48 – 3.56 (m, 2 H), 4.04 – 4.08 (m, 2 H), 5.29 (s, 1 H), 6.82 (s, 1 H), 7.29 (s, 1 H); HRMS (ESI) m/z calcd for $\text{C}_{14}\text{H}_{20}\text{N}_4\text{OH}^+$: 261.171, Found: 261.1708 ($\Delta = 0.69$ ppm).

Synthesis of 2,5,6-trisubstituted benzimidazole library (Plates 27, 28, 29)

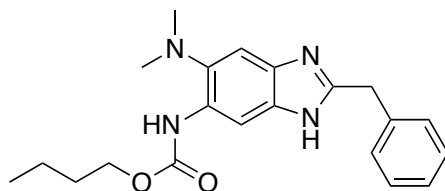
A solution of the final intermediates 4a-g (0.01 mmol) in DCM was transferred to 96 well plates to which was added acyl chlorides or OSU ester (1.1 eq.), and the plate was shaken at room temperature overnight. Aminomethylated polystyrene resin EHL (200-400 mesh), 2 % DVB (10 eq.) was added to the reaction mixture in each well and shaken at room temperature overnight. The reaction mixture was then filtered using a Millipore filter to give the library of 2,5,6-trisubstituted benzimidazoles.



R' =

Synthesis of 2,5,6-trisubstituted benzimidazoles with carbamate substitution at the 5-position

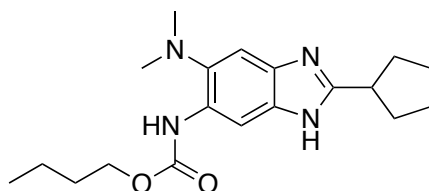
5-Butyloxycarbonylamino-2-benzyl-6-N,N-dimethylamino-1H-benzo[d]imidazole (SB-P27A12):



To a solution of **4b** (0.4 mmol) in DCM, carbonyldiimidazole (1.1 eq.) was added. The reaction mixture was refluxed for 4 hours. This was followed by the addition of n-BuOH (1.5 eq.), and the reaction mixture was refluxed overnight. After the completion of the reaction, the reaction mixture was washed with NaHCO₃ (50 ml X 2), water (50 ml X 2). The organic layer was collected, dried with MgSO₄, filtered and concentrated on a rotary evaporator, to get the crude product. Column chromatography using alumina and Hexane: EtOAc (1:1) as solvent system resulted in **SB-P27A12** as a light brown solid (44% yield); ¹H NMR (400 MHz, CDCl₃) δ 0.95 (t, 3 H, J = 7.4 Hz), 1.37 – 1.51 (sext, 2 H, J = 11.3 Hz), 1.63 – 1.70 (quin, 2 H, J = 7.2 Hz), 2.63 (s, 6 H), 4.14 – 4.19 (m, 4 H), 7.21 – 7.30 (m, 5 H), 7.44 (s, 1 H), 8.15 (s, 1 H), 9.71 (s, 1 H); ¹³C NMR (125 MHz, CDCl₃) δ 13.98, 19.32, 31.26, 36.09, 45.79, 65.11, 99.63, 111.09, 127.40, 129.13, 129.18, 130.05, 136.68, 139.14, 153.12, 154.26; HRMS (ESI) m/z calcd for C₂₁H₂₆N₄O₂H⁺: 367.2129, Found: 367.2122 (Δ = 1.82 ppm).

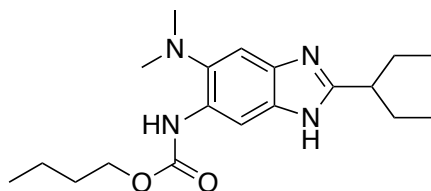
The same procedure was followed for the synthesis of **SB-P27B12**, **SB-P27C12**, **SB-P27-D12**, **SB-P27-F12**, **SB-OL5-C2**.

5-Butyloxycarbonylamino-2-cyclopentyl-6-N,N-dimethylamino-1H-benzo[d]imidazole (SB-P27B12):

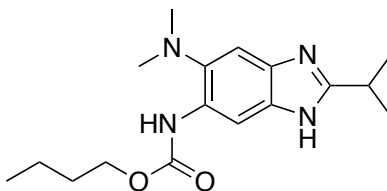


White solid (70% yield); ¹H NMR (500 MHz, CDCl₃) δ 0.95 (t, 3 H, J = 7.4 Hz), 1.43 (sext, 2 H, J = 7.5 Hz), 1.63 – 1.71 (m, 4 H), 1.75 – 1.82 (m, 2 H), 1.87 – 1.95 (m, 2 H), 2.07 – 2.13 (m, 2 H), 2.62 (s, 6 H), 3.23 (quin, 1 H, J = 8.4 Hz), 4.18 (t, 2 H, J = 6.7 Hz), 7.5 (s, 1 H), 8.19 (s, 2 H), 9.99 (s, 1 H); ¹³C NMR (125 MHz, CDCl₃) δ 13.96, 19.31, 25.73, 31.26, 32.45, 39.80, 45.82, 65.13, 99.65, 110.74, 129.52, 131.32, 138.82, 154.43, 158.73; HRMS (ESI) m/z calcd for C₁₉H₂₈N₄O₂H⁺: 345.2285, Found: 345.2279 (Δ = 1.87 ppm).

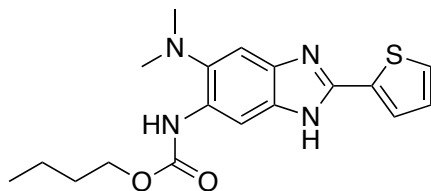
5-Butyloxycarbonylamino-2-(3-pentyl)-6-N,N-dimethylamino-1H-benzo[d]imidazole (SB-

P27C12):

Light brown solid (57 % yield); mp ; ^1H NMR (500 MHz, CDCl_3) δ 0.83 (t, 6 H, $J = 7.4$ Hz), 0.95 (t, 3 H, $J = 7.3$ Hz), 1.44 (sext, 2 H, $J = 6$ Hz), 1.68 (quin, 2 H, $J = 7.0$ Hz), 1.72 – 1.81 (m, 4 H), 2.62 (s, 1 H), 2.68 (s, 1 H), 4.19 (t, 2 H, $J = 6.7$ Hz), 7.25 (s, 1 H), 7.51 (s, 1 H), 8.19 (s, 1 H), 10.18 (s, 1 H); ^{13}C NMR (125 MHz, CDCl_3) δ 12.31, 13.95, 19.29, 27.70, 31.23, 44.21, 45.78, 65.12, 99.80, 110.75, 129.42, 131.01, 138.72, 138.84, 154.48, 158.28; HRMS (ESI) m/z calcd for $\text{C}_{19}\text{H}_{30}\text{N}_4\text{O}_2\text{H}^+$: 347.2442, Found: 347.2434 ($\Delta = 2.12$ ppm).

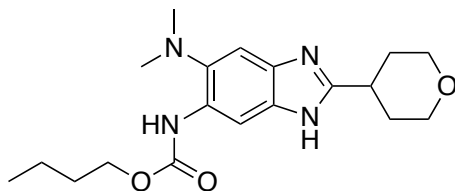
5-Butyloxycarbonylamino-2-isopropyl-6-N,N-dimethylamino-1H-benzo[d]imidazole (SB-P27D12):

Brown solid (79% yield); ^1H NMR (500 MHz, CDCl_3) δ 0.90 (t, 3 H, $J = 7.4$ Hz), 1.38 (sext, 2 H, $J = 7.5$ Hz), 1.58 – 1.64 (m, 8 H), 2.61 (s, 6 H), 3.76 (quin, 1 H, $J = 7$ Hz), 4.09 (t, 2 H, $J = 6.7$ Hz), 3.73 – 3.78 (m, 1 H), 4.09 (t, 2 H, $J = 6.9$ Hz), 7.64 (s, 1 H), 8.01 (s, 1 H), 8.48 (s, 1 H), 14.7 (s, 1 H); ^{13}C NMR (125 MHz, CDCl_3) δ 13.93, 19.26, 21.18, 27.82, 31.10, 45.25, 65.46, 102.62, 106.26, 126.35, 128.40, 132.77, 141.99, 153.70, 157.84; HRMS (ESI) m/z calcd for $\text{C}_{17}\text{H}_{26}\text{N}_4\text{O}_2\text{H}^+$: 319.2129, Found: 319.2121 ($\Delta = 2.27$ ppm).

5-Butyloxycarbonylamino-2-thienyl-6-N,N-dimethylamino-1H-benzo[d]imidazole (SB-P27F12):

White solid (% yield); ^1H NMR (500 MHz, CDCl_3) δ 0.94 (t, 3 H, $J = 7.4$ Hz), 1.42 (sextet, 2 H, $J = 7.5$ Hz), 1.68 (p, 2 H, $J = 7.1$ Hz), 2.64 (s, 6 H), 4.18 (t, 2 H, $J = 6.7$ Hz), 7.04 (m, 1 H), 7.37 (d, 2 H, $J = 6.1$ Hz), 7.54 (s, 1 H), 7.56 (s, 1 H), 8.23 (s, 1 H), 8.26 (s, 1 H), 10.32 (s, 1 H); ^{13}C NMR (125 MHz, CDCl_3) δ 13.98, 19.31, 31.23, 45.78, 65.32, 99.74, 111.24, 125.87, 127.83, 128.06, 130.60, 131.71, 133.74, 139.45, 139.74, 147.15, 154.47.

5-Butyloxycarbonylamino-2-tetrahydropyranyl-6-N,N-dimethylamino-1H-benzo[d]imidazole (SB-OL5-C2):

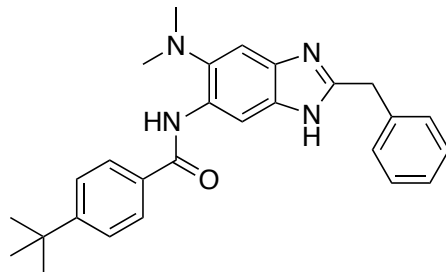


White solid (59% yield); ^1H NMR (500 MHz, CDCl_3) δ 0.96 (t, 3 H, $J = 7.4$ Hz), 1.41 – 1.48 (m, 2 H), 1.67 – 1.72 (m, 2 H), 2.00 – 2.03 (m, 4 H), 2.64 (s, 6 H), 3.14 – 3.20 (m, 1 H), 3.52 – 3.57 (m, 2 H), 4.06 – 4.09 (m, 2 H), 4.20 (t, 2 H, $J = 6.7$ Hz), 7.50 (s, 1 H), 8.17 (s, 1 H), 8.25 (s, 1H); ^{13}C NMR (100 MHz, CDCl_3) δ 14.00, 19.35, 31.26, 31.51, 35.85, 45.80, 65.25, 67.70, 130.24, 139.43, 154.36, 156.75; HRMS (ESI) m/z calcd for $\text{C}_{19}\text{H}_{28}\text{N}_4\text{O}_3\text{H}^+$: 361.2234, Found: 361.2229 ($\Delta = 1.56$ ppm).

General procedure for the synthesis of 2,5,6-trisubstituted benzimidazoles with amide substitution at the 5-position using acyl chlorides

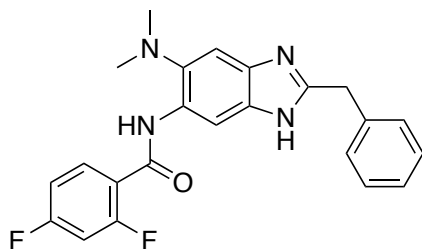
A solution of final intermediate **4a-g** (0.4 mmol) and acyl chloride (0.9 eq.) in DCM was stirred at 0 °C for two hours. After the completion of reaction, the reaction mixture was washed with NaHCO_3 (20 mL X 2) followed by water (20 mL X 2). The organic layer was collected, dried with MgSO_4 , filtered and concentrated on a rotary evaporator to get the crude product. Column chromatography on alumina using hexanes: ethyl acetate (1:1) as eluent resulted in the pure product.

5-(4-t-Butylbenzamido)-2-benzyl-6-N,N-dimethylamino-1-H-benzo[d]imidazole (SB-P27A3):



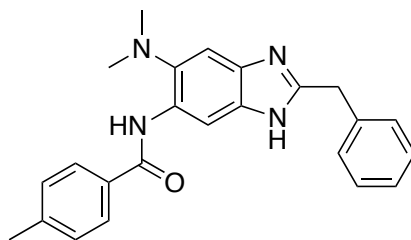
Beige solid (79% yield); ^1H NMR (400 MHz, CDCl_3) δ 1.35 (s, 9 H), 2.73 (s, 6 H), 4.16 (s, 2 H), 7.15-7.25 (m, 5 H), 7.51 (d, 2 H, $J = 8.5$ Hz), 7.59 (br. s, 1 H), 7.86 (d, 2 H, $J = 8.5$ Hz), 8.82 (s, 1 H), 9.85 (s, 1 H), 10.45 (s, 1 H); ^{13}C NMR (100 MHz, CDCl_3) δ 31.38, 35.2, 35.97, 46.08, 101.62, 111.03, 126.05, 127.04, 127.12, 128.94, 128.99, 129.71, 131.82, 132.89, 136.94, 139.66, 139.95, 153.72, 155.50, 165.54; HRMS (ESI) m/z calcd for $\text{C}_{27}\text{H}_{30}\text{N}_4\text{OH}^+$: 427.2492, Found: 427.2496 ($\Delta = 1.51$ ppm).

5-(2,4-Difluorobenzamido)-2-benzyl-6-N,N-dimethylamino-1-H-benzo[d]imidazole (SB-P27A8):



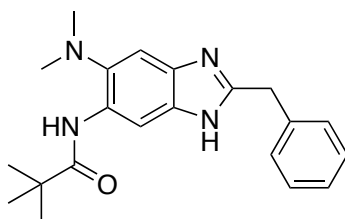
Light yellow solid (92% yield); ^1H NMR (500 MHz, CDCl_3) δ 2.68 (s, 6 H), 4.11 (s, 2 H), 6.90 – 6.94 (m, 1 H), 6.95 – 6.99 (m, 1 H), 7.11 – 7.16 (m, 5 H), 7.49 (s, 1 H), 8.13 – 8.18 (m, 1 H), 8.80 (s, 1 H), 10.27 (s, 1 H); ^{13}C NMR (125 MHz, CDCl_3) δ 36.04, 45.91, 102.07, 104.44, 104.65, 104.87, 111.15, 112.55, 112.57, 112.72, 112.74, 118.82, 118.94, 127.32, 129.03, 129.11, 129.95, 133.97, 136.69, 140.04, 153.80, 159.87, 159.97, 160.32, 161.87, 161.97, 163.98, 164.08, 166.01, 166.11; HRMS (ESI) m/z calcd for $\text{C}_{23}\text{H}_{20}\text{F}_2\text{N}_4\text{OH}^+$: 407.1678, Found: 407.1672 ($\Delta = 1.49$ ppm).

5-(4-Methylbenzamido)-2-benzyl-6-N,N-dimethylamino-1-H-benzo[d]imidazole (SB-P27A9):



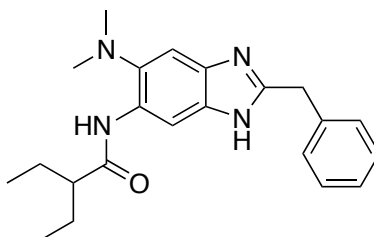
Off white solid (68% yield); mp ; ^1H NMR (400 MHz, CDCl_3) δ 2.43 (s, 3 H), 2.73 (s, 6 H), 4.12 (s, 2 H), 7.12-7.22 (m, 5 H), 7.29 (d, 2 H, $J = 7.9$ Hz), 7.58 (s, 1 H), 7.82 (d, 2 H, $J = 8.2$ Hz), 8.82 (s, 1 H), 9.85 (s, 1 H), 11.02 (s, 1 H); ^{13}C NMR (100 MHz, CDCl_3) δ 21.70, 35.88, 46.07, 101.77, 110.94, 126.95, 127.14, 128.86, 129.53, 129.77, 131.81, 132.93, 137.06, 139.57, 139.99, 142.46, 153.89, 165.61;

5-(4-*t*-Butylamido) -2-benzyl -6-*N,N*-dimethylamino-1-*H*-benzo[d]imidazole (SB-P27A10):



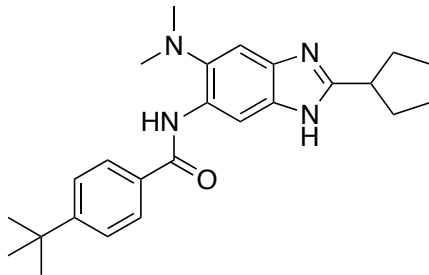
White solid (92% yield); ^1H NMR (400 MHz, CDCl_3) δ 1.33 (s, 9 H), 2.65 (s, 6 H), 4.12 (s, 2 H), 7.16 (m, 5 H), 7.47 (s, 1 H), 8.54 (s, 1 H), 9.29 (s, 1 H), 11.24 (s, 1 H); ^{13}C NMR (100 MHz, CDCl_3) δ 27.86, 35.76, 40.11, 45.71, 101.72, 110.46, 126.90, 128.82, 128.90, 129.38, 131.56, 137.08, 139.52, 153.78, 176.71 HRMS (ESI) m/z calcd for $\text{C}_{21}\text{H}_{26}\text{N}_4\text{OH}^+$: 351.2179, Found: 351.2172 ($\Delta = 2.18$ ppm).

5-(3-Pentylamido) -2-benzyl -6-*N,N*-dimethylamino-1-*H*-benzo[d]imidazole (SB-P27A12):



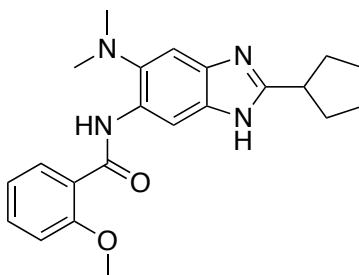
White solid (67% yield); ^1H NMR (500 MHz, CDCl_3) δ 0.95 (t, 6 H, $J = 7.4$ Hz), 1.53 – 1.62 (m, 2 H), 1.66 – 1.75 (m, 2 H), 2.09 – 2.16 (m, 1 H), 7.21 – 7.30 (m, 5 H), 7.54 (br. s, 1 H), 8.58 (s, 1 H), 8.91 (s, 1 H), 10.09 (s, 1 H); ^{13}C NMR (125 MHz, CDCl_3) δ 12.37, 26.26, 36.05, 45.89, 53.11, 101.71, 110.84, 127.24, 129.00, 128.08, 129.47, 131.48, 136.90, 139.37, 139.67, 153.51, 174.36; HRMS (ESI) m/z calcd for $\text{C}_{27}\text{H}_{30}\text{N}_4\text{OH}^+$: 365.2336, Found: 365.2331 ($\Delta = 1.42$ ppm).

5-(4-*t*-Butylbenzamido)-2-cyclopentyl-6-*N,N*-dimethylamino-1-*H*-benzo[d]imidazole (SB-P27B3):



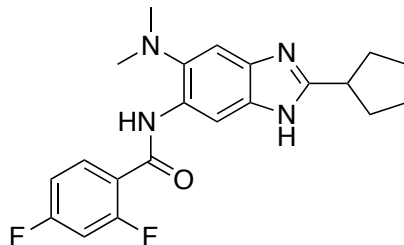
Beige solid (80% yield); ^1H NMR (400 MHz, CDCl_3) δ 1.38 (s, 9 H), 1.65-1.70 (m, 2 H), 1.82-1.85 (m, 2 H), 1.87-1.93 (m, 4 H), 2.73 (s, 6 H), 3.03- 3.12 (p, 1 H, $J = 8.4$ Hz), 7.56 (d, 2 H, $J = 8.3$ Hz), 7.61 (s, 1 H), 7.91 (d, 2 H, $J = 8.4$ Hz), 8.96 (s, 1 H), 9.96 (s, 1 H), 11.39 (s, 1H); ^{13}C NMR (100 MHz, CDCl_3) δ 25.56, 31.37, 32.50, 35.20, 39.92, 46.16, 101.69, 110.74, 126.01, 127.00, 129.08, 131.85, 133.08, 139.23, 139.90, 155.50, 159.59, 165.86; HRMS (ESI) m/z calcd for $\text{C}_{25}\text{H}_{32}\text{N}_4\text{OH}^+$: 405.2649, Found: 405.2641 ($\Delta = 1.87$ ppm).

5-(2-Methoxybenzamido)-2-cyclopentyl-6-N,N-dimethylamino-1-H-benzo[d]imidazole (SB-P27B7):



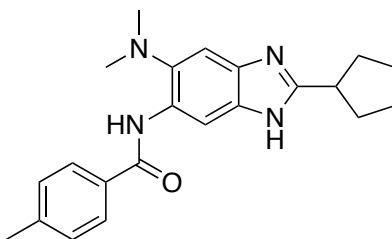
White solid (76% yield); ^1H NMR (400 MHz, CDCl_3) δ 1.39-1.48 (m, 2 H), 1.57-1.65 (m, 2 H), 1.80-1.89 (m, 2 H), 1.91 1.99 (m, 2 H), 2.73 (s, 6 H), 3.09 (p, 1 H, $J = 8.5$ Hz), 4.07 (s, 3 H), 7.06 (d, 1 H, $J = 8.3$ Hz), 7.14 (t, 1 H, $J = 7.5$ Hz), 7.51 (t, 1 H, $J = 7.1$ Hz), 7.57 (s, 1 H), 8.37 (dd, 1 H, $J = 9.6, 6$ Hz), 9.04 (s, 1 H), 11.19 (s, 1 H), 11.39 (s, 1 H); ^{13}C NMR (100 MHz, CDCl_3) δ 25.53, 32.51, 39.93, 46.07, 55.92, 102.62, 110.40, 111.64, 121.44, 122.62, 129.85, 131.66, 132.42, 133.26, 139.72, 139.86, 157.61, 159.49, 163.62; HRMS (ESI) m/z calcd for $\text{C}_{22}\text{H}_{26}\text{N}_4\text{O}_2\text{H}^+$: 379.2129, Found: 379.2119 ($\Delta = 2.62$ ppm).

5-(2,4-Difluorobenzamido)-2-cyclopentyl-6-N,N-dimethylamino-1-H-benzo[d]imidazole (SB-P27B8):



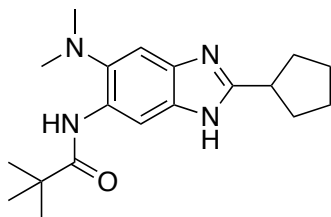
White solid (92% yield); ^1H NMR (500 MHz, CDCl_3) δ 1.62-1.64 (m, 2 H), 1.76-1.79 (m, 2 H), 1.88-1.95 (m, 2 H), 2.05 -2.12 (m, 2 H), 2.71 (s, 6 H), 3.21 (p, 1 H, $J = 8.2$ Hz), 6.95 (t, 2 H, $J = 9.3$ Hz), 7.04 – 7.07 (m, 1 H), 7.61 (s, 1 H), 8.21-8.26 (m, 1 H), 8.79 (s, 1 H), 9.83 (s, 1 H), 10.33 (d, 1H, $J = 11.8$ Hz); ^{13}C NMR (125 MHz, CDCl_3) δ 25.63, 32.48, 39.90, 45.97, 102.11, 104.54, 104.76, 104.97, 110.87, 112.52, 112.54, 112.69, 112.71, 118.91, 118.94, 119.01, 119.03, 129.34, 131.45, 133.74, 133.80, 139.69, 140.01, 159.58, 159.85, 159.95, 160.54, 161.85, 161.95, 164.00, 164.09, 166.03, 166.13 HRMS (ESI) m/z calcd for $\text{C}_{21}\text{H}_{22}\text{F}_2\text{N}_4\text{OH}^+$: 385.1834, Found: 385.1829 ($\Delta = 1.46$ ppm).

5-(4-Methylbenzamido)-2-cyclopentyl-6-N,N-dimethylamino-1-H-benzo[d]imidazole (SB-P27B9):



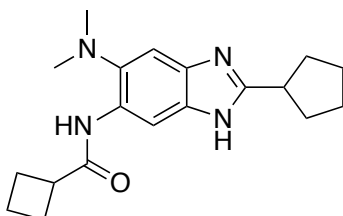
White solid 976% yield); ^1H NMR (500 MHz, CDCl_3) δ 1.47-1.48 (m, 2 H), 1.66-1.76 (m, 2 H), 1.87-1.93 (m, 4 H), 2.44 (s, 3 H), 2.72 (s, 6 H), 3.04- 3.11 (p, 1 H, $J = 8.3$ Hz), 7.34 (d, 2 H, $J = 7.7$ Hz), 7.60 (s, 1 H), 7.87 (d, 2 H, $J = 7.9$ Hz), 8.92 (s, 1 H), 9.92 (s, 1 H), 11.52 (s, 1H); ^{13}C NMR (125 MHz, CDCl_3) δ 21.66, 25.52, 32.48, 39.87, 46.09, 101.73, 110.60, 127.11, 128.94, 129.69, 131.79, 133.01, 139.23, 139.84, 142.43, 159.62, 165.79; HRMS (ESI) m/z calcd for $\text{C}_{22}\text{H}_{26}\text{N}_4\text{OH}^+$: 363.2179, Found: 363.2171 ($\Delta = 2.3$ ppm).

5-(4-t-Butylamido)-2-cyclopentyl-6-N,N-dimethylamino-1-H-benzo[d]imidazole (SB-P27B10):



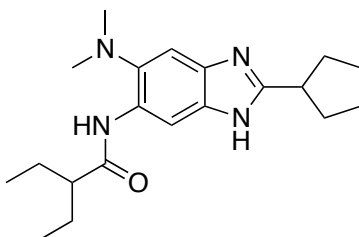
White solid (94% yield); ^1H NMR (500 MHz, CDCl_3) δ 1.34 (s, 9H), 1.55 - 1.57 (m, 2 H), 1.68 - 1.76 (m, 2 H), 1.85-1.90 (m, 2 H), 1.99 - 2.05 (m, 2 H), 2.64 (s, 6 H), 3.19 (p, 1 H, $J = 8.4$ Hz), 7.46 (s, 1 H), 8.53 (s, 1 H), 9.25 (s, 1 H); ^{13}C NMR (125 MHz, CDCl_3) δ 25.60, 27.84, 32.44, 39.74, 40.09, 45.70, 102.03, 109.98, 128.79, 131.65, 139.30, 159.41, 176.74; HRMS (ESI) m/z calcd for $\text{C}_{19}\text{H}_{28}\text{N}_4\text{OH}^+$: 329.2336, Found: 329.2327 ($\Delta = 2.83$ ppm).

5-Cyclobutamido-2-cyclopentyl-6-N,N-dimethylamino-1-H-benzo[d]imidazole(SB-P28B5):



Brown solid (75% yield); ^1H NMR (400 MHz, CDCl_3) δ 1.64 - 1.69 (m, 2 H), 1.76 - 1.84 (m, 2 H), 1.88-1.99 (m, 3 H), 2.01 - 2.13 (m, 3 H), 2.26 - 2.34 (m, 2 H), 2.37 - 2.47 (m, 2 H), 2.64 (s, 6 H), 3.21 - 3.34 (m, 2 H), 7.51 (s, 1 H), 8.59 (s, 1 H), 8.87 (s, 1 H), 10.63 (s, 1 H); ^{13}C NMR (100 MHz, CDCl_3) δ 18.27, 25.76, 25.80, 32.52, 39.84, 41.60, 45.84, 101.73, 110.50, 128.89, 131.36, 139.14, 159.27, 176.32; HRMS (ESI) m/z calcd for $\text{C}_{19}\text{H}_{26}\text{N}_4\text{OH}^+$: 327.2179, Found: 327.2171 ($\Delta = 2.65$ ppm).

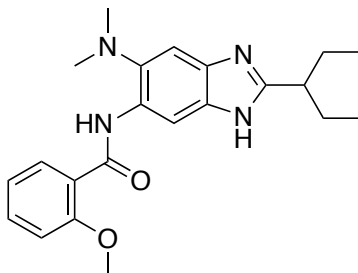
5-(3-Pentylamido)-2-cyclopentyl-6-N,N-dimethylamino-1-H-benzo[d]imidazole (SB-P27B12):



Beige solid (66% yield); ^1H NMR (400 MHz, CDCl_3) δ 0.99 (t, 6 H, $J = 7.4$ Hz), 1.59 - 1.79 (m, 6 H), 1.81 - 1.86 (m, 2 H), 1.92 - 2.01 (m, 2 H), 2.09 - 2.21 (m, 3 H), 2.67 (s, 6 H), 3.26 (quin, 1 H, $J = 8.3$ Hz), 7.57 (s, 1 H), 8.59 (s, 1 H), 8.91 (s, 1 H), 9.84 (s, 1 H); ^{13}C NMR (100 MHz, CDCl_3)

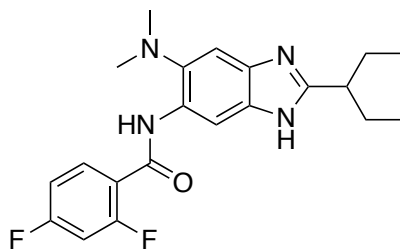
δ 12.4, 25.78, 26.23, 32.54, 39.82, 45.95, 53.12, 101.54, 110.70, 129.19, 131.15, 139.19, 139.52, 159.05, 174.32.

5-(2-Methoxybenzamido)-2-(3-pentyl)-6-N,N-dimethylamino-1-H-benzo[d]imidazole (SB-P27C7):



Light brown solid (60% yield); mp 214-215 °C; ^1H NMR (500 MHz, CDCl_3) δ 0.75 (t, 6 H, $J = 7.3$ Hz), 1.59 – 1.77 (m, 4 H), 2.53 – 2.59 (m, 1 H), 2.74 (s, 6 H), 4.08 (s, 3 H), 7.18 – 7.21 (m, 1 H), 7.27 – 7.30 (m, 3 H), 7.07 (d, 1 H, $J = 8.3$ Hz), 7.15 (t, 1 H, $J = 7.4$ Hz), 7.52 (t, 1 H, $J = 8.5$ Hz), 7.58 (s, 1 H), 8.37 (dd, 1 H, $J = 6.05, 9.6$ Hz), 9.01 (s, 1 H), 10.60 (s, 1 H), 11.36 (s, 1 H); ^{13}C NMR (125 MHz, CDCl_3): δ 12.23, 27.52, 44.08, 46.04, 55.94, 102.57, 110.51, 111.65, 121.51, 122.66, 129.97, 131.10, 132.58, 133.24, 139.76, 139.95, 157.66, 158.95, 163.57; HRMS (ESI) m/z calcd for $\text{C}_{22}\text{H}_{28}\text{N}_4\text{O}_2\text{H}^+$: 381.2285, Found: 381.228 ($\Delta = 1.24$ ppm).

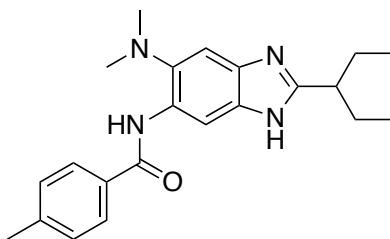
5-(2,4-Difluorobenzamido)-2-(3-pentyl)-6-N,N-dimethylamino-1-H-benzo[d]imidazole (SB-P27C8):



Beige solid (62 % yield); mp 207-210 °C; ^1H NMR (500 MHz, CDCl_3) δ 0.81 (t, 6 H, $J = 7.2$ Hz), 1.69 – 1.78 (m, 4 H), 2.59 – 2.66 (m, 1 H), 2.70 (s, 6 H), 6.96 (t, 1 H, $J = 9.5$ Hz), 7.05 (t, 1 H, $J = 9.2$ Hz), 7.60 (s, 1H), 8.21 – 8.26 (m, 1H), 8.83 (s, 1 H), 10.32 – 10.37 (m, 2 H); ^{13}C NMR (125 MHz, CDCl_3) δ 12.27, 27.59, 44.22, 45.94, 102.12, 104.53, 104.74, 104.96, 111.02, 112.54, 112.56, 112.71, 118.97, 119.03, 129.41, 131.01, 133.85, 139.71, 140.09, 159.03, 159.88, 159.98, 160.52, 161.88, 161.98, 164.01, 164.11, 166.05, 166.14; HRMS (ESI) m/z calcd for $\text{C}_{21}\text{H}_{24}\text{F}_2\text{N}_4\text{OH}^+$: 387.1991, Found: 387.1988 ($\Delta = 0.76$ ppm).

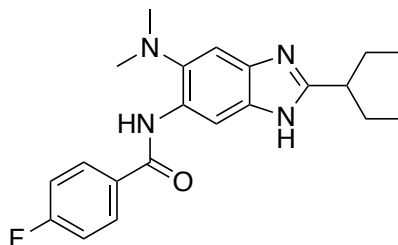
5-(4-Methylbenzamido)-2-(3-pentyl)-6-N,N-dimethylamino-1-H-benzo[d]imidazole (SB-

P27C9):



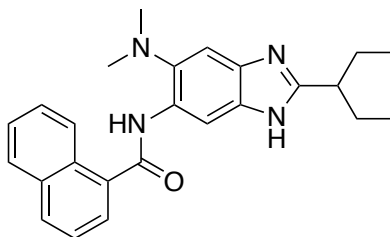
White solid (61% yield); mp > 230 °C; ¹H NMR (500 MHz, CDCl₃) δ 0.76 (t, 6 H, J = 7 Hz), 1.61 – 1.75 (m, 4 H), 2.45 (s, 3 H), 2.54 – 2.60 (m, 1 H), 2.73 (s, 6 H), 7.36 (d, 2 H, J = 7.8 Hz), 7.61 (s, 1 H), 7.86 (d, 2 H, J = 8 Hz), 8.89 (s, 1 H), 9.89 (s, 1 H), 10.91 (s, 1 H); ¹³C NMR (125 MHz, CDCl₃) δ 12.22, 21.71, 27.52, 44.03, 46.10, 101.74, 110.79, 127.23, 129.05, 129.74, 131.28, 133.00, 139.30, 140.01, 142.45, 159.17, 165.75; HRMS (ESI) m/z calcd for C₂₂H₂₈N₄OH⁺: 365.2336, Found: 365.2332 (Δ = 1.02 ppm).

5-(4-Fluorobenzamido)-2-(3-pentyl)-6-N,N-dimethylamino-1-H-benzo[d]imidazole (SB-P27C11):



White solid (44 % yield); mp 192-195 °C; ¹H NMR (500 MHz, CDCl₃) δ 0.77 (t, 6 H, J = 7.4 Hz), 1.63 – 1.69 (m, 2 H), 1.71 – 1.78 (m, 2 H), 2.58 – 2.62 (m, 1H), 2.71 (s, 6 H), 7.21 (t, 2 H, J = 8.5 Hz), 7.59 (s, 1H), 7.95 – 7.98 (m, 2 H), 8.83 (s, 1 H), 9.86 (s, 1 H), 11.1 (bs, 1 H); ¹³C NMR (125 MHz, CDCl₃) δ 12.24, 27.51, 44.11, 46.06, 101.79, 110.73, 116.03, 116.21, 128.82, 129.43, 129.5, 131.29, 131.89, 131.91, 139.33, 139.96, 159.28, 164.01, 164.48, 166.02; HRMS (ESI) m/z calcd for C₂₁H₂₅FN₄OH⁺: 369.2085, Found: 369.2082 (Δ = 0.84 ppm).

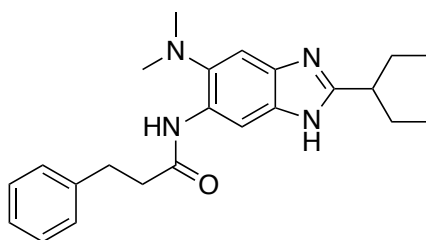
5-(1-Naphthamido)-2-(3-pentyl)-6-N,N-dimethylamino-1-H-benzo[d]imidazole (SB-P28C2):



Brown solid (64 % yield); mp 211-214 °C; ¹H NMR (500 MHz, CDCl₃) δ 0.43 (t, 6 H, J = 7.3

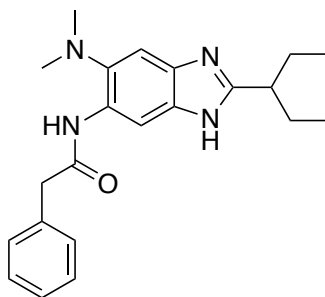
Hz), 1.07 – 1.59 (m, 2 H), 1.18 – 1.27 (m, 2 H), 1.78 – 1.83 (m, 1 H), 2.65 (s, 6 H), 7.55 – 7.60 (m, 3 H), 7.61 (s, 1 H), 7.80 (d, 1 H, $J = 6$ Hz), 7.96 – 7.98 (m, 1 H), 8.04 (d, 1 H, $J = 8.3$ Hz), 8.45 – 8.46 (m, 1 H), 9.21 (s, 1 H), 9.68 (s, 1 H), 11.30 (s, 1 H); ^{13}C NMR (125 MHz, CDCl_3) δ 11.88, 27.07, 43.58, 46.16, 102.13, 110.94, 124.89, 125.24, 125.62, 127.01, 127.72, 128.72, 129.03, 130.46, 131.00, 131.74, 134.12, 135.71, 139.08, 140.32, 159.40, 168.30; HRMS (ESI) m/z calcd for $\text{C}_{25}\text{H}_{28}\text{N}_4\text{OH}^+$: 401.2336, Found: 401.2334 ($\Delta = 0.53$ ppm).

5-Phenylpropanamido-2-(3-pentyl)-6-N,N-dimethylamino-1-H-benzo[d]imidazole (SB-P28C3):



Brown solid (65 % yield); mp 181-183 °C; ^1H NMR (500 MHz, CDCl_3) δ 0.85 (t, 6 H, $J = 7.4$ Hz), 1.74 – 1.88 (m, 4 H), 2.54 (s, 6 H), 2.71 – 2.75 (m, 1 H), 2.79 (t, 2 H, $J = 7.6$ Hz), 3.12 (t, 2 H, $J = 7.7$ Hz), 7.18 – 7.21 (m, 1 H), 7.27 – 7.30 (m, 3 H), 7.53 (s, 1 H), 8.63 (s, 1 H), 8.88 (s, 1 H), 10.51 (s, 1 H); ^{13}C NMR (125 MHz, CDCl_3) δ 12.36, 27.75, 32.20, 40.36, 44.33, 45.76, 101.78, 110.52, 126.60, 128.47, 128.79, 128.83, 131.11, 139.03, 139.78, 140.58, 158.93, 170.51; HRMS (ESI) m/z calcd for $\text{C}_{23}\text{H}_{30}\text{N}_4\text{OH}^+$: 379.2492, Found: 379.2491 ($\Delta = 0.29$ ppm).

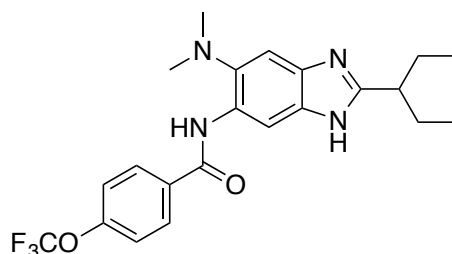
5-Phenylethanamido-2-(3-pentyl)-6-N,N-dimethylamino-1-H-benzo[d]imidazole (SB-P27C-A1):



Brown solid (69 % yield); mp 187-189 °C; ^1H NMR (300 MHz, CDCl_3) δ 0.85 (t, 6 H, $J = 7.3$ Hz), 1.73 – 1.91 (m, 4 H), 2.31 (s, 6 H), 2.67 – 2.76 (m, 1 H), 3.86 (s, 2 H), 7.25 – 7.44 (m, 6 H), 8.71 (s, 1 H), 9.07 (s, 1 H), 11.72 (s, 1 H); ^{13}C NMR (125 MHz, CDCl_3) δ 12.39, 27.81, 44.42, 45.48, 45.83, 101.36, 110.65, 127.80, 128.92, 129.35, 129.90, 131.41, 134.74, 139.10, 158.94, 169.37;

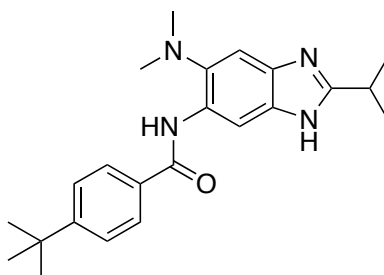
HRMS (ESI) m/z calcd for $C_{22}H_{28}N_4OH^+$: 365.2336, Found: 365.2334 ($\Delta = 0.43$ ppm).

5-(4-Trifluoromethoxybenzamido)-2-(3-pentyl)-6-N,N-dimethylamino-1-H-benzo[d]imidazole (SB-P27C-A20):



White solid (76% yield); 1H NMR (500 MHz, $CDCl_3$) δ 0.80 (t, 6 H, $J = 7.35$ Hz), 1.69-1.80 (m, 4 H), 2.58-2.64 (m, 1 H), 2.74 (s, 1 H), 7.38 (d, 2 H, $J = 8.25$ Hz), 7.64 (s, 1 H), 8.00 (d, 2 H, $J = 8.7$ Hz), 8.79 (s, 1 H), 9.9 (s, 1 H), 10.26 (s, 1 H); ^{13}C NMR (125 MHz, $CDCl_3$) δ 12.25, 27.59, 44.21, 46.17, 101.56, 111.12, 119.54, 121.18, 121.59, 129.08, 131.09, 134.23, 139.42, 140.12, 151.83, 159.06, 164.20; HRMS (ESI) m/z calcd for $C_{22}H_{25}F_3N_4O_2H^+$: 435.2002, Found: 435.2 ($\Delta = 0.62$ ppm).

5-(4-t-Butylbenzamido)-2-isopropyl-6-N,N-dimethylamino-1-H-benzo[d]imidazole (SB-P27 D3):



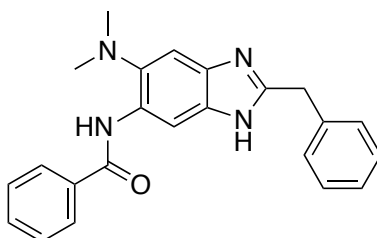
White solid (87% yield); 1H NMR (500 MHz, $CDCl_3$) δ 1.31 (s, 6 H), 1.38 (s, 9 H), 2.72 (s, 6 H), 3.02 (s, 1 H), 7.56 (d, 2 H, $J = 7.7$ Hz), 7.62 (s, 1 H), 7.90 (d, 2 H, $J = 8.1$ Hz), 8.90 (s, 1 H), 9.96 (s, 1 H), 10.87 (s, 1 H); ^{13}C NMR (125 MHz, $CDCl_3$) δ 21.71, 29.12, 31.39, 35.23, 46.15, 101.75, 110.88, 126.02, 127.07, 129.28, 131.56, 133.01, 139.39, 139.71, 155.53, 160.73, 165.85; HRMS (ESI) m/z calcd for $C_{23}H_{30}N_4OH^+$: 379.2492, Found: 379.2495 ($\Delta = 1.89$ ppm).

General procedure for the synthesis of 2,5,6-trisubstituted benzimidazoles with amide substitution at the 5-position using acids.

The final intermediates 4a-g, 4.5 and 8 (0.4 mmol) were each dissolved in dichloromethane. To this solution was added acid (1.2 eq.), EDC.HCl (1.2 eq.), DMAP (1.2 eq.), and the reaction

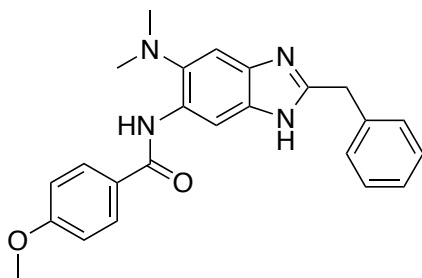
mixture was refluxed overnight or until starting material disappeared. The reaction mixture was then washed with NaHCO₃ (20 ml X 2) followed by water (20 ml X 2). The organic layer was collected, dried with MgSO₄, filtered and concentrated in a rotary evaporator to get the crude product. Column chromatography of the crude product on silica using Hexane: EtOAc (1:1) as eluent resulted in the pure product.

5-Benzamido-2-benzyl-6-N,N-dimethylamino-1-H-benzo[d]imidazole (SB-P27A2):



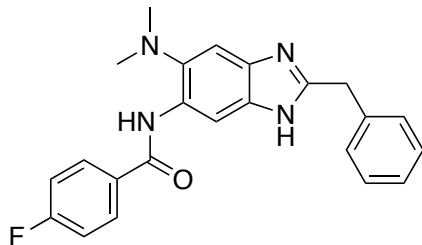
Light yellow solid (57% yield); ¹H NMR (500 MHz, CDCl₃) δ 2.72 (s, 6 H), 4.12 (s, 2 H), 7.13-7.23 (m, 5 H), 7.48 - 7.51 (m, 2 H), 7.54 - 7.57 (m, 2 H), 7.93 (d, 2 H, J = 8.5 Hz), 8.8 (s, 1 H), 9.89 (s, 1 H), 10.99 (s, 1 H); ¹³C NMR (125 MHz, CDCl₃) δ 35.89, 46.07, 101.79, 110.99, 127.00, 127.13, 128.88, 128.90, 129.10, 129.44, 131.93, 135.75, 136.99, 139.65, 140.05, 153.96, 165.54; HRMS (ESI) m/z calcd for C₂₃H₂₂N₄OH⁺: 371.1866, Found: 371.1864 (Δ = 0.7 ppm).

5-(4-Methoxybenzamido)-2-benzyl-6-N,N-dimethylamino-1-H-benzo[d]imidazole (SB-P27A5):



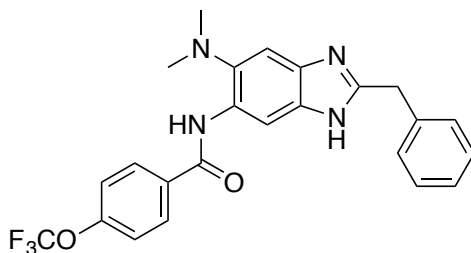
Light yellow solid (55% yield); ¹H NMR (400 MHz, CDCl₃) δ 2.71 (s, 6 H), 3.85 (s, 3 H), 4.11 (s, 2 H), 6.97 (d, 2 H, J = 8.8 Hz), 7.12-7.20 (m, 5 H), 7.55 (s, 1 H), 7.88 (d, 2 H, J = 8.7 Hz), 8.82 (s, 1 H), 9.80 (s, 1 H), 11.26 (bs, 1 H); ¹³C NMR (100 MHz, CDCl₃) δ 35.81, 46.02, 55.64, 101.74, 110.84, 114.27, 126.89, 127.90, 128.82, 128.95, 129.51, 131.82, 137.12, 139.57, 139.86, 153.88, 162.57, 165.08; HRMS (ESI) m/z calcd for C₂₄H₂₄N₄O₂H⁺: 401.1972, Found: 401.1967 (Δ = 1.26 ppm).

5-(4-Fluorobenzamido)-2-benzyl-6-N,N-dimethylamino-1-H-benzo[d]imidazole (SB-P27A11):



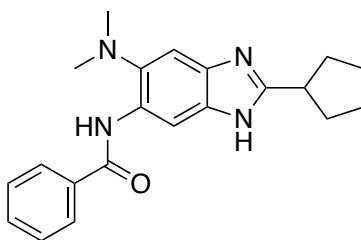
Yellow solid (89% yield); ^1H NMR (400 MHz, CDCl_3) δ 2.71 (s, 6 H), 4.16 (s, 2 H), 7.14 – 7.25 (m, 7 H), 7.89 – 7.93 (m, 2 H), 8.73 (s, 1 H), 9.79 (s, 1 H), 10.62 (br. s, 1 H); ^{13}C NMR (100 MHz, CDCl_3) δ 35.92, 46.06, 101.76, 111.11, 116.01, 116.23, 127.15, 128.93, 129.0, 129.41, 129.49, 131.79, 131.81, 136.85, 139.71, 153.93, 163.77, 164.28, 166.28; HRMS (ESI) m/z calcd for $\text{C}_{23}\text{H}_{21}\text{FN}_4\text{OH}^+$: 389.1772, Found: 389.1764 ($\Delta = 2.18$ ppm).

5-(4-Trifluoromethoxybenzamido)-2-benzyl-6-N,N-dimethylamino-1-H-benzo[d]imidazole (SB-P27A-A20):



Light yellow solid (66 % yield); ^1H NMR (500 MHz, CDCl_3) δ 2.71 (s, 6 H), 4.12 (s, 2 H), 7.11-7.19 (m, 5 H), 7.32 (d, 2 H, $J = 8.2$ Hz), 7.53 (s, 1 H), 7.94 (d, 2 H, $J = 8.6$ Hz), 8.76 (s, 1 H), 11.4(br. s, 1 H); ^{13}C NMR (125 MHz, CDCl_3) δ 35.63, 45.90, 101.72, 110.78, 117.28, 119.34, 120.92, 121.40, 123.45, 126.85, 128.67, 129.04, 131.72, 133.83, 136.78, 139.55, 151.62, 154.04, 163.80; HRMS (ESI) m/z calcd for $\text{C}_{24}\text{H}_{21}\text{F}_3\text{N}_4\text{O}_2\text{H}^+$: 228.0881, Found: 228.0886 ($\Delta = -2.23$ ppm).

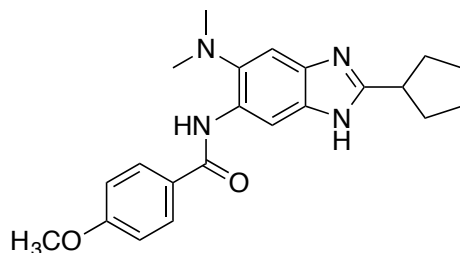
5-Benzamido-2-cyclopentyl-6-N,N-dimethylamino-1-H-benzo[d]imidazole (SB-P27B2):



Off white solid (94% yield); ^1H NMR (500 MHz, CDCl_3) δ 1.46-1.48 (m, 2 H), 1.62-1.68 (m, 2 H), 1.83-1.96 (m, 4 H), 2.72 (s, 6 H), 3.09 (p, 1 H, $J = 8.5$ Hz), 7.52-7.58 (m, 3 H), 7.61 (s, 1 H), 7.97 (d, 2 H, $J = 7.1$ Hz), 8.94 (s, 1 H), 9.98 (s, 1 H), 11.66 (s, 1H); ^{13}C NMR (125 MHz, CDCl_3)

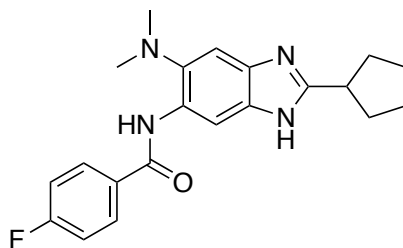
δ 25.50, 32.47, 39.85, 46.10, 101.76, 110.62, 127.06, 128.85, 129.04, 131.80, 131.90, 135.80, 139.25, 139.90, 159.74, 165.74; HRMS (ESI) m/z calcd for $C_{21}H_{24}N_4OH^+$: 349.2023, Found: 349.2013 ($\Delta = 2.78$ ppm).

5-(4-Methoxybenzamido)-2-cyclopentyl-6-N,N-dimethylamino-1-H-benzo[d]imidazole (SB-P27B5):



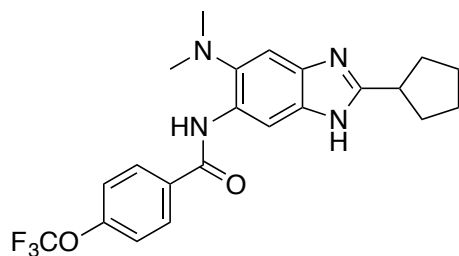
White solid (53% yield); mp 205-208 °C; 1H NMR (400 MHz, $CDCl_3$) δ 1.60-1.65 (m, 2 H), 1.71-1.81 (m, 2 H), 1.87-1.95 (m, 2 H), 2.04-2.06 (m, 2 H), 2.73 (s, 6 H), 3.14-3.21 (p, 1 H, $J = 6.7$ Hz), 3.89 (s, 3 H), 7.03 (d, 2 H, $J = 7$ Hz), 7.59 (s, 1 H), 7.93 (d, 2 H, $J = 7$ Hz), 8.81 (s, 1 H), 9.80 (s, 1 H); ^{13}C NMR (100 MHz, $CDCl_3$) δ 25.70, 32.49, 39.86, 46.12, 55.71, 101.35, 110.87, 114.25, 128.04, 129.02, 129.51, 139.45, 159.13, 162.59, 165.08; HRMS (ESI) m/z calcd for $C_{22}H_{26}N_4O_2H^+$: 379.2129, Found: 379.2129 ($\Delta = -0.19$ ppm).

5-(4-Fluorobenzamido)-2-cyclopentyl-6-N,N-dimethylamino-1-H-benzo[d]imidazole (SB-P27B11):



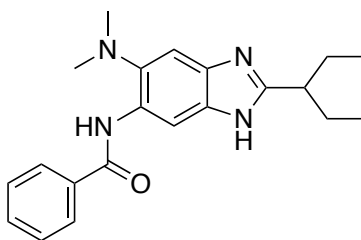
White solid (75% yield); 1H NMR (500 MHz, $CDCl_3$) δ 1.47-1.54 (m, 2 H), 1.68-1.70 (m, 2 H), 1.84-1.88 (m, 2 H), 1.90-1.96 (m, 2 H), 2.71 (s, 6 H), 3.09-3.15 (p, 1 H, $J = 8.6$ Hz), 7.21 (t, 2 H, $J = 8.3$ Hz), 7.59 (s, 1 H), 7.95-7.98 (m, 2 H), 8.82 (s, 1 H), 9.90 (s, 1 H), 11.36 (s, 1H); ^{13}C NMR (125 MHz, $CDCl_3$) δ 25.57, 32.47, 39.88, 46.11, 101.67, 110.71, 116.04, 116.21, 128.83, 129.39, 129.46, 131.69, 131.88, 131.90, 139.32, 139.89, 159.70, 164.00, 164.51, 166.01; HRMS (ESI) m/z calcd for $C_{21}H_{23}FN_4OH^+$: 367.1929, Found: 367.1919 ($\Delta = 2.51$ ppm).

5-(4-Trifluoromethoxybenzamido)-2-cyclopentyl-6-N,N-dimethylamino-1-H-benzo[d]imidazole (SB-P27B-A20):



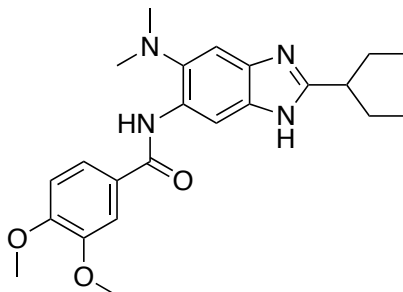
White solid (50% yield); White solid (50 % yield); mp 182-186 °C; ^1H NMR (500 MHz, CDCl_3) δ 1.53 – 1.57 (m, 2 H), 1.68 – 1.75 (m, 2 H), 1.86 – 1.93 (m, 2H), 1.97 – 2.03 (m, 2H), 2.73 (s, 6 H), 3.11 – 3.18 (m, 1 H), 7.38 (d, 2 H, $J = 8.1$ Hz), 7.62 (s, 1 H), 8.0 (d, 2 H, $J = 8.7$ Hz), 8.81 (s, 1 H), 9.94 (s, 1 H), 10.77 (s, 1 H); ^{13}C NMR (125 MHz, CDCl_3) δ 25.61, 32.48, 39.90, 46.18, 101.58, 110.97, 117.46, 119.52, 121.14, 121.57, 123.63, 131.58, 134.22, 139.41, 140.02, 151.83, 159.63, 164.22; HRMS (ESI) m/z calcd for $\text{C}_{22}\text{H}_{23}\text{F}_3\text{N}_4\text{O}_2\text{H}^+$: 433.1846, Found: 433.1843 ($\Delta = 0.77$ ppm).

5-Benzamido-2-(3-pentyl)-6-N,N-dimethylamino-1-H-benzo[d]imidazole (SB-P27C2):



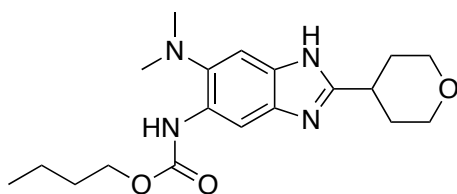
White solid (85 % yield); mp 208-210 °C; ^1H NMR (400 MHz, CDCl_3) δ 0.76 (t, $J=7.40$ Hz, 6 H), 1.58 - 1.82 (m, 4 H), 2.57 (m, 1 H), 2.74 (s, 6 H), 7.52 - 7.61 (m, 3 H), 7.63 (s, 1 H), 7.97 (dd, $J = 7.91$ Hz, 2 H), 8.91 (s, 1 H), 9.94 (s, 1 H), 10.99 (s, 1 H); ^{13}C NMR (100MHz, CDCl_3) δ 12.22, 27.52, 44.05, 46.13, 101.78, 110.86, 127.21, 128.97, 129.11, 131.33, 131.94, 135.88, 139.32, 140.14, 159.27, 165.79; HRMS (ESI) m/z calcd for $\text{C}_{21}\text{H}_{26}\text{N}_4\text{OH}^+$: 351.2179, Found: 351.2173 ($\Delta = 1.94$ ppm).

5-(3,4-Dimethoxybenzamido)-2-(3-pentyl)-6-N,N-dimethylamino-1-H-benzo[d]imidazole (SB-P27C4):



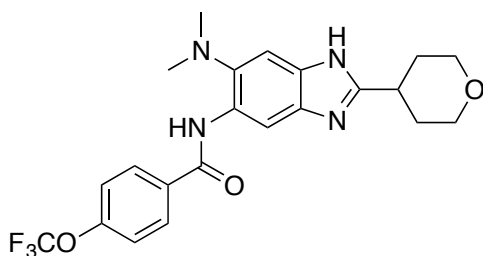
White solid (58 % yield); mp 184-186 °C; ^1H NMR (500 MHz, CDCl_3) δ 0.77 (t, 6 H, $J = 7.4$ Hz), 1.64 – 1.79 (m, 4 H), 2.56 – 2.62 (m, 1 H), 2.73 (s, 6 H), 3.97 (s, 6 H), 6.99 (d, 1 H, $J = 8.4$ Hz), 7.49 (dd, 1 H, $J = 10.25, 6.45$ Hz), 7.60 (s, 2 H), 8.80 (s, 1 H), 9.85 (s, 1 H), 10.40 (s, 1 H); ^{13}C NMR (125 MHz, CDCl_3) δ 12.25, 27.56, 44.16, 46.08, 56.22, 56.30, 101.45, 110.80, 110.84, 110.85, 119.68, 128.31, 129.21, 131.14, 139.28, 139.83, 149.44, 152.22, 158.94, 165.17; HRMS (ESI) m/z calcd for $\text{C}_{23}\text{H}_{30}\text{N}_4\text{O}_3\text{H}^+$: 411.2391, Found: 411.2387 ($\Delta = 0.79$ ppm).

5-Butyloxycarbonylamino-2-tetrahydropyranyl-6-N,N-dimethylamino-1H-benzo[d]imidazole (SB-OL5-C2):



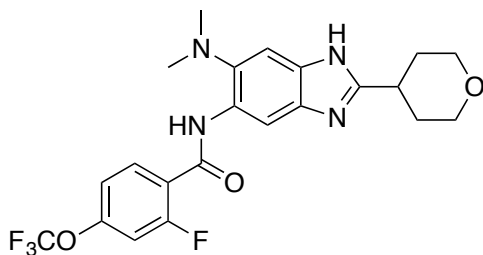
White solid (59% yield); ^1H NMR (500 MHz, CDCl_3) δ 0.96 (t, 3 H, $J = 7.4$ Hz), 1.41 – 1.48 (m, 2 H), 1.67 – 1.72 (m, 2 H), 2.00 – 2.03 (m, 4 H), 2.64 (s, 6 H), 3.14 – 3.20 (m, 1 H), 3.52 – 3.57 (m, 2 H), 4.06 – 4.09 (m, 2 H), 4.20 (t, 2 H, $J = 6.7$ Hz), 7.50 (s, 1 H), 8.17 (s, 1 H), 8.25 (s, 1H). ^{13}C NMR (100 MHz, CDCl_3) δ 14.00, 19.35, 31.26, 31.51, 35.85, 45.80, 65.25, 67.70, 130.24, 139.43, 154.36, 156.75; HRMS (ESI) m/z calcd for $\text{C}_{19}\text{H}_{28}\text{N}_4\text{O}_3\text{H}^+$: 361.2234, Found: 361.229 ($\Delta = 1.56$ ppm).

5-(4-Trifluoromethoxybenzamido)-2tetrahydropyranyl-6-N,N-dimethylamino-1-H-benzo[d]imidazole (SB-OL5-A20):



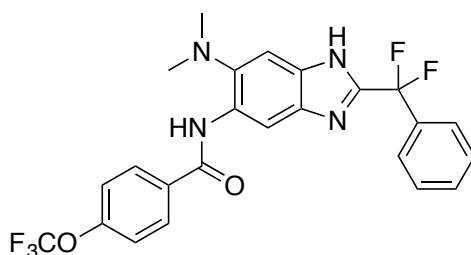
White solid (75% yield); ^1H NMR (500 MHz, CDCl_3) δ 1.96 – 2.07 (m, 4 H), 2.73 (s, 6 H), 3.09 – 3.14 (m, 1 H), 3.42 – 3.47 (m, 2 H), 4.00 – 4.03 (m, 2 H), 7.40 (d, 2 H, $J = 8.05$ Hz), 7.59 (bs, 1 H), 8.00 (d, 2 H, $J = 8.75$ Hz), 9.88 (br. s, 1 H); ^{13}C NMR (100 MHz, CDCl_3) δ 31.5, 36.05, 46.13, 67.68, 102.46, 110.51, 119.53, 121.24, 121.58, 123.64, 129.03, 129.31, 134.09, 139.84, 151.90, 151.92, 157.97, 164.26; HRMS (ESI) m/z calcd for $\text{C}_{22}\text{H}_{23}\text{F}_3\text{N}_4\text{O}_3\text{H}^+$: 449.1795, Found: 449.1792 ($\Delta = 0.57$ ppm).

5-(2-Fluoro-4-trifluoromethoxybenzamido)-2-tetrahydropyranyl-6-N,N-dimethylamino-1-H-benzo[d]imidazole (SB-OL5-A38):



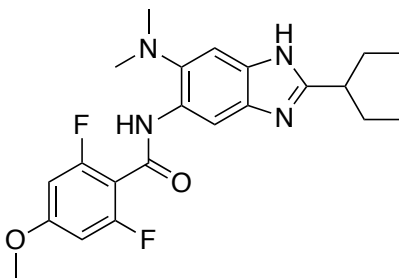
White solid (73% yield); ^1H NMR (500 MHz, CDCl_3) δ 1.59 – 2.15 (m, 4 H), 2.71 (s, 6 H), 3.12 – 3.54 (m, 1 H), 3.47 – 3.54 (m, 2 H), 4.03 – 4.07 (m, 2 H), 7.12 (d, 1 H, $J = 16.2$ Hz), 7.22 (d, 1 H, $J = 11.1$ Hz), 7.58 (s, 1 H), 8.26 (t, 1 H, $J = 10.9$ Hz), 8.82 (s, 1 H), 10.33 (d, 1 H, $J = 14.5$ Hz); ^{13}C NMR (100 MHz, CDCl_3) δ 31.52, 36.07, 45.97, 67.71, 109.07, 109.36, 117.12, 119.12, 120.90, 121.02, 121.71, 129.83, 133.56, 133.59, 140.18, 152.25, 152.35, 157.79, 159.29, 160.20, 160.24, 161.78; HRMS (ESI) m/z calcd for $\text{C}_{22}\text{H}_{22}\text{F}_4\text{N}_4\text{O}_3\text{H}^+$: 467.1701, Found: 467.1699 ($\Delta = 0.47$ ppm).

5-(4-Trifluoromethoxybenzamido)-2-(α,α -difluorobenzyl)-6-N,N-dimethylamino-1-H-benzo[d]imidazole (SB-OL6-A20):



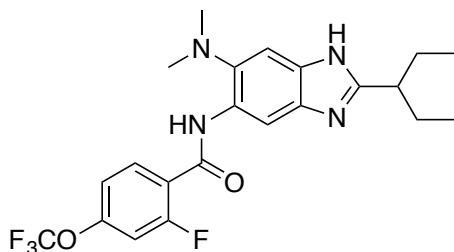
Yellow solid (68 % yield); ^1H NMR (500 MHz, CDCl_3) δ 2.79 (s, 6 H), 7.37 – 7.38 (m, 2 H), 7.54 – 7.59 (m, 2 H), 7.63 – 7.67 (m, 1 H), 7.84 (s, 1 H), 8.02 – 8.04 (m, 2 H), 8.66 – 8.68 (m, 2 H), 8.92 (s, 1 H), 9.9 (s, 1 H), 10.64 (s, 1 H); ^{13}C NMR (125 MHz, CDCl_3) δ 45.59, 46.05, 101.90, 113.882, 121.14, 128.69, 128.75, 129.13, 131.30, 131.37, 131.58, 133.18, 133.66, 133.85, 135.79, 140.51, 141.99, 148.40, 152.02, 164.19, 183.42; MS (ESI) m/z 491.1 ($\text{M}+1$) $^+$

5-(2,6-Difluoro-4-methylbenzamido)-2(3-pentyl)-6-N,N-dimethylamino-1-H-benzo[d]imidazole (SB-P27C-A34):



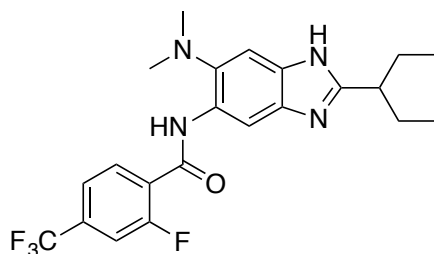
Beige solid (63% yield); ^1H NMR (500 MHz, CDCl_3) δ 0.78 (t, 6 H, $J = 7.4$ Hz), 1.62 – 1.73 (m, 4 H), 2.56 – 2.62 (m, 1 H), 2.67 (s, 6 H), 3.85 (s, 3 H), 6.57 (d, 2 H, $J = 9.7$ Hz), 7.58 (s, 1 H), 8.89 (s, 1 H), 9.56 (s, 1 H); ^{13}C NMR (125 MHz, CDCl_3) δ 12.23, 27.50, 44.14, 46.09, 98.72, 98.95, 102.57, 107.78, 107.94, 108.09, 110.46, 128.90, 139.27, 158.53, 159.26, 160.34, 160.42, 162.34, 152.42, 162.49, 162.60, 162.71; HRMS (ESI) m/z calcd for $\text{C}_{22}\text{H}_{26}\text{F}_2\text{N}_4\text{O}_2\text{H}^+$: 417.2097, Found: 417.2092 ($\Delta = 0.99$ ppm).

5-(2-Fluoro-4-trifluoromethoxybenzamido)-2(3-pentyl)-6-N,N-dimethylamino-1-H-benzimidazole (SB-P27C-A38):



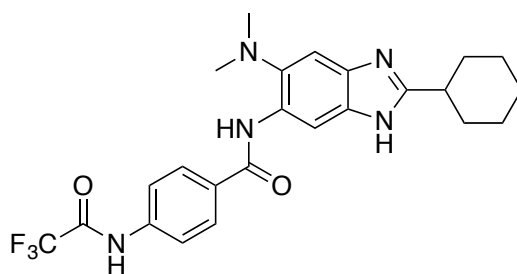
White solid (39% yield); ^1H NMR (500 MHz, CDCl_3) δ 0.85 (t, 6 H, $J = 7.6$ Hz), 1.74 – 1.81 (m, 4 H), 2.71 (s, 7 H), 7.10 (d, 1 H, $J = 11.8$ Hz), 7.19 (d, 1 H, $J = 8.9$ Hz), 7.59 (s, 1 H), 8.26 (t, 1 H, $J = 8.7$ Hz), 8.81 (s, 1 H), 10.29 (d, 1 H, $J = 11.5$ Hz); ^{13}C NMR (125 MHz, CDCl_3) δ 12.28, 27.64, 44.21, 45.95, 109.06, 109.29, 117.02, 119.39, 120.98, 121.08, 121.45, 123.52, 129.68, 133.71, 133.73, 140.00, 152.15, 152.25, 158.77, 159.53, 160.06, 160.09, 162.53; HRMS (ESI) m/z calcd for $\text{C}_{22}\text{H}_{24}\text{F}_4\text{N}_4\text{O}_2\text{H}^+$: 453.1908, Found: 453.1903 ($\Delta = 1.18$ ppm).

5-(2-Fluoro-4-trifluoromethylbenzamido)-2(3-pentyl)-6-N,N-dimethylamino-1-H-benzimidazole (SB-P27C-A42):



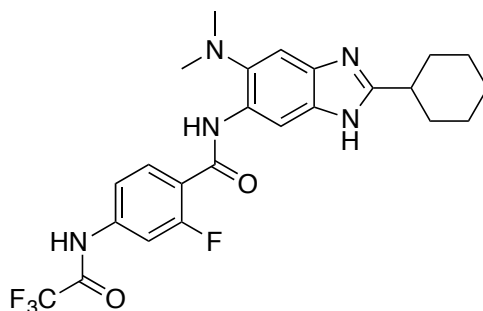
White solid (66% yield); ^1H NMR (500 MHz, CDCl_3) δ 0.86 (t, 6 H, $J = 7.4$ Hz), 1.75-1.89 (m, 4 H), 2.70 (s, 6 H), 2.79-2.83 (m, 1 H), 7.48 (d, 1 H, $J = 9$ Hz), 7.58 (d, 1 H, $J = 9$ Hz), 7.60 (s, 1 H), 8.29 (t, 1 H, $J = 7.8$ Hz), 8.84 (s, 1 H), 10.31 (d, 1 H, $J = 11$ Hz); ^{13}C NMR (125 MHz, CDCl_3) δ 12.31, 27.62, 44.05, 45.88, 103.47, 109.53, 1114.09, 114.12, 114.31, 114.34, 121.91, 121.93, 121.96, 124.06, 125.74, 125.84, 129.82, 131.72, 133.23, 135.17, 135.23, 135.43, 135.50, 140.40, 158.84, 159.00, 159.85, 159.88, 160.99; HRMS (ESI) m/z calcd for $\text{C}_{22}\text{H}_{24}\text{F}_4\text{N}_4\text{OH}^+$: 437.1959, Found: 437.1956 ($\Delta = 0.61$ ppm).

5-(4-Trifluoroacetamidobenzamido)-2-cyclohexyl-6-N,N-dimethylamino-1-H-benzo[d]imidazole (SB-P17G-A59):



Beige solid (72 % yield); ^1H NMR (500 MHz, Acetone- D_6) δ 1.26 – 1.35 (m, 1 H), 1.38 – 1.47 (m, 2 H), 1.65 – 1.74 (m, 3 H), 1.82 – 1.86 (m, 2 H), 2.05 – 2.11 (m, 2 H), 2.75 (s, 6 H), 2.87 – 2.93 (m, 1 H), 7.48 (s, 1 H), 7.93 (d, 2 H, $J = 8.8$ Hz), 8.04 (d, 2 H, $J = 8.9$ Hz), 8.7 (s, 1 H), 9.86 (s, 1 H), 10.58 (s, 1 H); ^{13}C NMR (125 MHz, Acetone- D_6) δ 26.77, 32.53, 39.25, 46.1, 115.76, 118.05, 121.61, 128.87, 130.07, 133.56, 140.22, 140.36, 155.58, 155.85, 156.15, 156.44, 160.14, 163.94; HRMS (ESI) m/z calcd for $\text{C}_{24}\text{H}_{26}\text{F}_3\text{N}_5\text{O}_2\text{H}^+$: 474.2111, Found: 474.2118 ($\Delta = -0.61$ ppm).

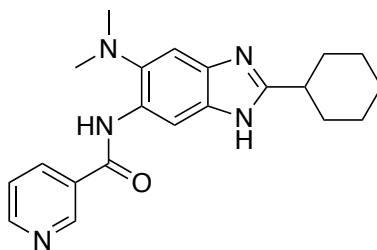
5-(2-Fluoro-4-trifluoroacetamidobenzamido)-2-cyclohexyl-6-N,N-dimethylamino-1-H-benzo[d]imidazole (SB-P17G-A60)



Beige solid (30 % yield); ^1H NMR (500 MHz, Acetone- D_6) δ 1.26 – 1.35 (m, 1 H), 1.38 – 1.47 (m, 2 H), 1.65 – 1.74 (m, 3 H), 1.81 – 1.85 (m, 2 H), 2.09 – 2.11 (m, 2 H), 2.73 (s, 6 H), 2.87 – 2.93 (m, 1 H), 7.48 (s, 1 H), 7.69 (d, 1 H, $J = 8.7$ Hz), 7.87 (dd, 1 H, $J = 15.6$ Hz, 12 Hz), 8.18 (t,

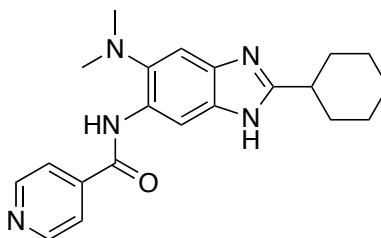
1 H, J = 8.8 Hz), 8.78 (s, 1 H), 10.21 (d, 1 H, J = 12.3 Hz), 10.8 (s, 1 H); ^{13}C NMR (125 MHz, Acetone-D6) δ 26.77, 32.53, 39.25, 46.07, 104.99, 108.92, 109.17, 115.60, 117.69, 117.71, 117.89, 120.04, 120.14, 130.36, 133.53, 133.56, 140.18, 141.85, 141.94, 155.76, 156.06, 156.36, 156.66, 160.23, 160.34, 160.37, 162.18; HRMS (ESI) m/z calcd for $\text{C}_{24}\text{H}_{25}\text{F}_4\text{N}_5\text{O}_2\text{H}^+$: 492.2017, Found: 492.2025 ($\Delta = -1.61$ ppm).

5-Nicotinamido-2-cyclohexyl-6-N,N-dimethylamino-1-H-benzo[d] imidazole (SB-P17G-A61):



Beige solid (43 % yield); ^1H NMR (500 MHz, Acetone-D6) δ 1.26 – 1.34 (m, 1 H), 1.38 – 1.47 (m, 2 H), 1.65 – 1.73 (m, 3 H), 1.81 – 1.85 (m, 2 H), 2.09 – 2.11 (m, 2 H), 2.75 (s, 6 H), 2.88 – 2.94 (m, 1 H), 7.5 (s, 1 H), 7.54 – 7.57 (m, 1 H), 8.32 (dd, 1 H, J = 10 Hz, 5.9 Hz), 8.68 (s, 1 H), 8.77 (d, 1 H, J = 6 Hz), 9.15 (s, 1 H), 9.93 (b.s. 1 H), 11.25 (b.s. 1 H); ^{13}C NMR (125 MHz, Acetone-D6) δ 26.76, 32.53, 39.26, 46.10, 124.60, 129.79, 132.04, 135.50, 140.39, 149.08, 153.10, 160.35, 163.37; HRMS (ESI) m/z calcd for $\text{C}_{21}\text{H}_{25}\text{N}_5\text{OH}^+$: 364.2132, Found: 364.2135 ($\Delta = -0.99$ ppm).

5-Isonicotinamido-2-cyclohexyl-6-N,N-dimethylamino-1-H-benzo[d] imidazole (SB-P17G-A62):

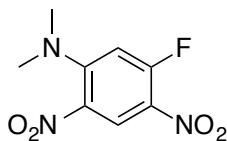


Beige solid (47 % yield); ^1H NMR (500 MHz, Acetone-D6) δ 1.27 – 1.35 (m, 1 H), 1.39 – 1.47 (m, 2 H), 1.66 – 1.73 (m, 3 H), 1.82 – 1.85 (m, 2 H), 2.08 – 2.11 (m, 2 H), 2.75 (s, 6 H), 2.88 – 2.94 (m, 1 H), 7.5 (s, 1 H), 7.85 (s, 1 H), 8.67 (s, 1 H), 8.78 (d, 1 H, J = 6 Hz), 10.0 (s, 1 H), 11.18 (b.s. 1 H); ^{13}C NMR (125 MHz, Acetone-D6) δ 28.76, 31.85, 38.56, 45.45, 120.99, 128.85, 139.65,

142.67, 151.03, 159.64, 162.37; HRMS (ESI) m/z calcd for $C_{21}H_{25}N_5OH^+$: 364.2132, Found: 364.2135 ($\Delta = -0.96$ ppm).

Synthesis of trisubstituted indoles

1,1-dimethylamino-5-fluoro-2,4-dinitrobenzene (**12.1**)⁵⁴

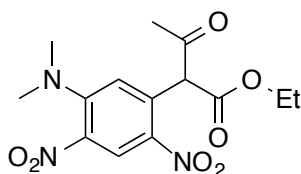


To a solution of **12** (1 g, 4.9 mmol) in THF was added dimethylamine (0.9 eq.) dissolved in THF drop wise over a period of 2 hours at 0 °C. The solvent was evaporated under reduced pressure to give the crude product. Column chromatography of the crude product using silica and Hexanes: EtOAc (2:1) as the eluent resulted in product as yellow solid (0.89g, 80 % yield); ¹H NMR (300 MHz, CDCl₃) δ 3.04 (s, 6 H), 6.71 (d, 1 H, $J = 13.9$ Hz), 8.69 (d, 1 H, $J = 8.0$ Hz); ¹³C NMR (100 MHz, CDCl₃) δ 42.73, 104.52, 104.74, 125.84, 125.90, 127.54, 132.59, 150.10, 150.20, 157.25, 159.39. The analytical data was consistent with literature.⁵⁴

General procedure for the aromatic nucleophilic substitution using alkyl or arylacetoacetate

Sodium hydride 60 % dispersion in mineral oil (180 mg, 4.6 mmol) was carefully transferred into a clean and dry round bottomed flask to which dry THF was immediately added and stirred. Alkyl/aryl acetoacetate in THF was added drop wise. The reaction mixture was stirred at room temperature for 20 minutes. This was followed by the addition of **12.1**, and the reaction mixture was stirred at room temperature overnight. The solvent was evaporated under reduced pressure to give the crude product, which was then dissolved in water and neutralized with 2 M HCl. The product was extracted with ethyl acetate, washed with brine (20 mL x 2). The organic layer was collected, dried with MgSO₄, filtered and concentrated in a rotary evaporator to give the crude product.

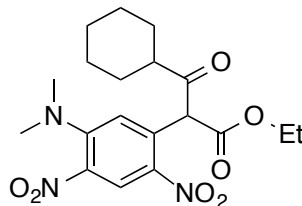
1-(ethyl-3-oxobutanoyl)-5-dimethylamino-2,4-dinitrobenzene (**12.2**)



Recrystallization of the crude product using silica and Hexanes and ethyl acetate resulted in product as yellow solid (0.8 g, 80 % yield); ¹H NMR (500 MHz, CDCl₃) δ 1.13 (t, 3 H, $J = 7.1$

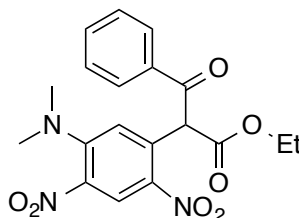
Hz), 1.91 (s, 3 H), 3.99 – 4.06 (m, 1 H), 4.21 – 4.28 (m, 1 H), 6.74 (s, 1 H), 8.69 (s, 1 H), 12.99 (s, 1 H); MS (ESI) m/z 340.1 (M+1)⁺.

1-(ethyl-3-cyclohexanoyl)-5-dimethylamino-2,4-dinitrobenzene (13.2)



Recrystallization of the crude product using silica and hexanes: ethyl acetate resulted in product as yellow solid (1 g, 72 % yield); ¹H NMR (300 MHz, CDCl₃) δ 1.03- 1.28 (m, 6 H), 1.54 – 1.60 (m, 4 H), 1.67 – 1.79 (m, 4 H), 2.06 – 2.15 (m, 1 H), 3.03 (s, 6 H), 3.94 – 4.05 (m, 1 H), 4.18 – 4.29 (m, 1 H), 6.71 (s, 1 H), 8.69 (s, 1 H), 13.12 (s, 1 H); ¹³C NMR (125 MHz, CDCl₃) δ 14.15, 25.67, 25.73, 29.27, 29.97, 41.99, 42.63, 61.32, 100.06, 121.25, 125.97, 135.13, 136.16, 137.78, 147.62, 171.23, 179.07; MS (ESI) m/z 408.2 (M+1)⁺.

1-(ethyl-3-benzoyl)-5-dimethylamino-2,4-dinitrobenzene (17)

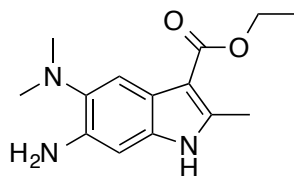


Recrystallization of the crude product using silica and hexanes and ethyl acetate resulted in product as yellow solid (0.67 g, 64 % yield); mp 113-116 °C; ¹H NMR (500 MHz, CDCl₃) δ 1.26 (t, 3 H, J = 7.1 Hz), 4.23 – 4.29 (m, 2 H), 6.68 (s, 1 H), 6.95 (s, 1 H), 7.48 (t, 2 H, J = 7.9 Hz), 7.59 (t, 1 H, J = 7.5 Hz), 7.95 (d, 2 H, J = 7.2 Hz), 8.75 (s, 1 H); ¹³C NMR (100 MHz, CDCl₃) δ 14.22, 42.54, 56.19, 62.65, 119.61, 126.86, 129.0, 129.26, 134.07, 134.39, 135.09, 135.56, 135.91, 147.94, 167.95, 192.82; MS (ESI) m/z 402.1 (M+1)⁺.

General procedure for reduction and cyclization

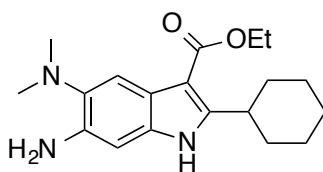
A mixture of dinitro compound (1.5 – 2.5 mmol), ammonium formate (10 eq.) and 10 % palladium on carbon (4 eq.) was refluxed in THF: Ethanol (1:1) for 1.5 hours. The reaction mixture was cooled to room temperature and filtered on celite. The solvent was evaporated under reduced pressure to give the crude product, which was dissolved in ethyl acetate and washed with water (20 mL x 2). The organic layer was collected, dried with MgSO₄, filtered and rotary evaporated.

6-amino-5-(dimethylamino)-3-ethylcarboxyl-2-methyl-1H-indole (12.3)



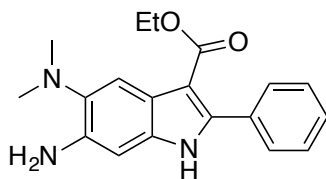
Column chromatography on alumina using EtOAc: Hexanes (8:2) as eluent resulted in the pure product **12.3** as a brown solid (0.37 g, 64 % yield); $^1\text{H NMR}$ (300 MHz, CDCl_3) δ 1.44 (t, 3 H, $J = 7.0$ Hz), 2.64 (s, 3 H), 2.70 (s, 6 H), 4.03 (br. s, 2 H), 4.37 (q, 2 H, $J = 7.0$ Hz), 6.66 (s, 1 H), 7.77 (s, 1 H), 8.08 (s, 1 H); MS (ESI) m/z 262.2 ($\text{M}+1$) $^+$.

6-amino-5-(dimethylamino)-3-ethylcarboxyl-2-cyclohexyl-1H-indole (13.3)



Column chromatography on alumina using EtOAc: Hexanes (1:1) as eluent resulted in the pure product **13.3** as a brown solid (0.6 g, 70 % yield); $^1\text{H NMR}$ (300 MHz, CDCl_3) δ 1.20 – 1.47 (m, 8 H), 1.74 – 1.85 (m, 3 H), 2.00 – 2.03 (m, 2 H), 2.70 (s, 6 H), 3.65 – 3.72 (m, 1 H), 4.06 (s, 2 H), 4.34 – 4.41 (q, 2 H), 6.63 (s, 1 H), 7.81 (s, 1 H), 8.28 (s, 1 H); MS (ESI) m/z 330.2 ($\text{M}+1$) $^+$.

6-amino-5-(dimethylamino)-3-ethylcarboxyl-2-phenyl-1H-indole (17.1)

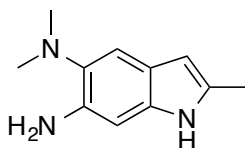


Brown solid (52 % yield); $^1\text{H NMR}$ (300 MHz, CDCl_3) δ 1.27 (t, 3 H, $J = 7$ Hz), 3.74 (s, 2 H), 4.24 (q, 2 H, $J = 7.1$ Hz), 6.49 (s, 1 H), 7.33 – 7.35 (m, 3 H), 7.53 – 7.55 (m, 2 H), 7.88 (s, 1 H), 8.90 (s, 1 H); MS (ESI) m/z 324.2 ($\text{M}+1$) $^+$.

General procedure for decarboxylation

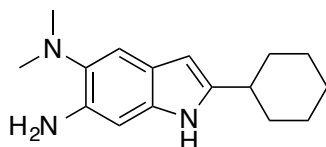
The tetrasubstituted indole was refluxed with 20 % aq. HCl overnight to bring about decarboxylation. The reaction mixture was neutralized with 30 % NaOH to pH 8, and extracted with ethyl acetate. The organic layer was dried with MgSO_4 , filtered and rotary evaporated to give crude product.

6-amino-5-(dimethylamino)-2-methyl-1H-indole (12.4)



Column chromatography on alumina using EtOAc: Hexanes (1:1) as eluent resulted in the pure product **12.4** as a brown solid (0.09 g, 44 % yield) ^1H NMR (300 MHz, CDCl_3) δ 2.35 (s, 3 H), 2.68 (s, 6 H), 3.63 (br. s, 2 H), 6.03 (s, 1 H), 6.63 (s, 1 H), 7.17 (s, 1 H), 7.54 (s, 1 H); MS (ESI) m/z 190.1 ($\text{M}+1$) $^+$.

6-amino-5-(dimethylamino)-2-cyclohexyl-1H-indole (**15**)

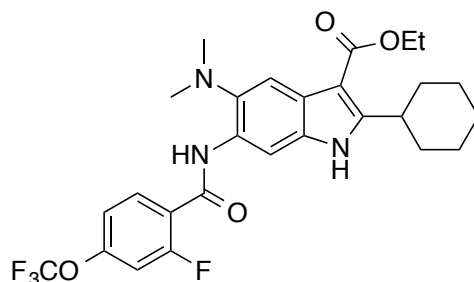


Column chromatography on alumina using EtOAc: Hexanes (1:1) as eluent resulted in the pure product **15** as a brown solid (0.13 g, 44 % yield); ^1H NMR (300 MHz, CDCl_3) δ 1.24 – 1.50 (m, 5 H), 1.71 – 1.84 (m, 3 H), 2.01 – 2.05 (m, 2 H), 2.59 – 2.64 (m, 1 H), 2.68 (s, 6 H), 4.0 (s, 2 H), 6.05 (s, 1 H), 6.66 (s, 1 H), 7.20 (s, 1 H), 7.58 (s, 1 H); ^{13}C NMR (125 MHz, CDCl_3) δ 26.36, 26.49, 33.28, 37.53, 45.17, 96.36, 97.08, 110.63, 121.52, 133.46, 136.89, 137.66, 143.20; MS (ESI) m/z 258.2 ($\text{M}+1$) $^+$.

General procedure for amide synthesis

To a solution of the amine in DCM, was added acid (1.2 eq.), EDC.HCl (1.2 eq.) and DMAP (1.2 eq.). The reaction mixture was refluxed overnight or until starting material disappeared. The reaction mixture was then washed with NaHCO_3 (20 ml X 2) followed by water (20 ml X 2). The organic layer was collected, dried with MgSO_4 , filtered and rotary evaporated to get the crude product.

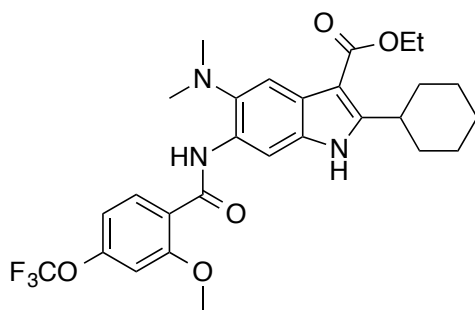
6-(2-fluoro-4-trifluoromethoxybenzamido)-5-(dimethylamino)-3-ethoxycarbonyl-2-cyclohexyl-1H-indole (SB-IND1-A38-C3-1)



Column chromatography on silica using Hexanes: EtOAc (80:20) as eluent resulted in the pure product **SB-IND1-A38-C3-1** as a white solid (112 mg, 92 % yield); ^1H NMR (400 MHz, CDCl_3) δ 1.13 – 1.21 (m, 1 H), 1.33 – 1.50 (m, 7 H), 1.60 – 1.83 (m, 3 H), 2.03 (d, 2 H, $J = 9$ Hz), 2.75 (s, 6 H), 3.69 – 3.72 (m, 1 H), 4.39 (q, 2 H, $J = 6$ Hz), 7.09 (d, 1H, $J = 9.5$ Hz), 7.18 (d, 1 H, $J = 7.2$ Hz), 8.02(s, 1 H), 8.27 (t, 1 H, $J = 7$ Hz), 8.68 (s, 1 H), 8.71 (s, 1 H), 10.31 (d, 1 H, $J = 9.7$ Hz); ^{13}C NMR (100 MHz, CDCl_3) δ 14.73, 26.20, 26.67, 32.56, 36.75, 45.98, 59.61, 102.43, 103.04, 109.0, 109.24, 113.28, 116.99, 119.39, 120.99, 121.09, 121.46, 123.82, 129.64, 131.88, 133.85, 139.64, 152.08, 152.18, 153.18, 159.54, 160.0, 161.54, 166.01; HRMS (ESI) m/z calcd for $\text{C}_{27}\text{H}_{29}\text{F}_4\text{N}_3\text{O}_4\text{H}^+$: 536.2167, Found: 536.2169 ($\Delta = -0.39$ ppm).

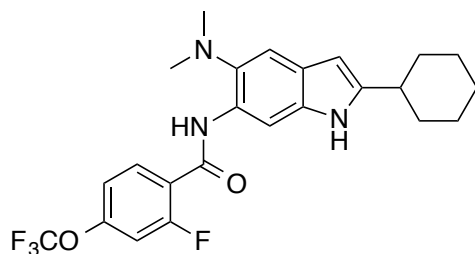
The same procedure was used for the synthesis of **SB-IND1-A55-C3-1**.

6-(2-methoxy-4-trifluoromethoxybenzamido)-5-(dimethylamino)-3-ethoxycarbonyl-2-cyclohexyl-1H-indole (SB-IND1-A55-C3-1):



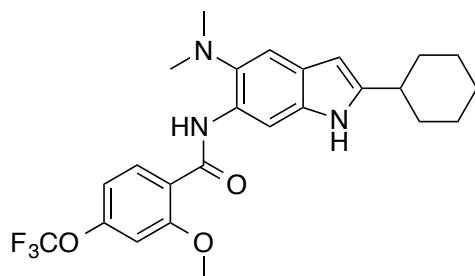
Column chromatography on silica using Hexanes: EtOAc (80:20) as eluent resulted in the pure product **16.1** as a white solid (83 mg, 77 % yield); ^1H NMR (400 MHz, CDCl_3) δ 0.86 – 0.90 (m, 1 H), 1.24 – 1.41 (m, 4 H), 1.44 (t, 3 H, $J = 7.1$ Hz), 1.60 – 1.67 (m, 3 H), 1.90 – 1.92 (m, 2 H), 2.77 (s, 6 H), 3.61 – 3.67 (m, 1 H), 4.10 (s, 3 H), 4.37 (q, 2 H, $J = 7.1$ Hz), 6.89 (s, 1 H), 6.99 – 7.01 (m, 1 H), 7.98 (s, 1 H), 8.42 (d, 1 H, $J = 8.8$ Hz), 8.90 (s, 1 H), 9.30 (s, 1 H), 11.24 (s, 1 H); ^{13}C NMR (125 MHz, CDCl_3) δ 14.74, 25.91, 26.61, 32.41, 36.64, 46.04, 56.36, 59.44, 102.61, 103.22, 104.54, 112.74, 113.09, 119.52, 121.28, 121.58, 123.60, 129.85, 132.21, 134.40, 139.73, 152.61, 153.31, 158.48, 162.31, 166.18; HRMS (ESI) m/z calcd for $\text{C}_{28}\text{H}_{32}\text{F}_3\text{N}_3\text{O}_5\text{H}^+$: 548.2367, Found: 549.237 ($\Delta = -0.51$ ppm).

6-(2-fluoro-4-trifluoromethoxybenzamido)-5-(dimethylamino)-2-cyclohexyl-1H-indole (SB-IND1-A38):



Column chromatography on silica using EtOAc: Hexanes (3:7) as eluent resulted in the pure product **4** as a yellow solid (0.12 g, 96 % yield); ^1H NMR (400 MHz, CDCl_3) δ 1.20 – 1.50 (m, 5 H), 1.71 – 1.84 (m, 3 H), 2.03 – 2.06 (m, 2 H), 2.64 – 2.68 (m, 1 H), 2.69 (s, 6 H), 6.15 (s, 1 H), 7.08 (d, 1 H, $J = 12$ Hz), 7.18 (d, 1 H, $J = 9$ Hz), 7.40 (s, 1 H), 8.10 (s, 1 H), 8.28 (t, 1 H, $J = 9$ Hz), 8.68 (s, 1 H), 10.33 (d, 1 H, $J = 12$ Hz); ^{13}C NMR (100 MHz, CDCl_3) δ 26.28, 26.44, 37.61, 46.15, 97.31, 102.13, 108.94, 109.23, 111.47, 116.94, 119.16, 121.29, 121.41, 121.74, 124.90, 128.76, 133.05, 133.76, 133.80, 137.84, 146.07, 151.88, 152.01, 159.25, 159.55, 159.59, 161.74; HRMS (ESI) m/z calcd for $\text{C}_{24}\text{H}_{25}\text{F}_4\text{N}_3\text{O}_2\text{H}^+$: 464.1956, Found: 464.1953 ($\Delta = 0.47$ ppm).

6-(2-methoxy-4-trifluoromethoxybenzamido)-5-(dimethylamino)-2-cyclohexyl-1H-indole (SB-IND1-A55):



Column chromatography on silica using EtOAc: Hexanes (2:8) as eluent resulted in the pure product **SB-IND1-A55** as a yellow solid (0.09 g, 75 % yield); ^1H NMR (500 MHz, CDCl_3) δ 1.14 – 1.26 (m, 3 H), 1.37 – 1.43 (m, 2 H), 1.66 – 1.75 (m, 3 H), 1.97 – 2.00 (m, 2 H), 2.58 – 2.62 (m, 1 H), 2.74 (s, 6 H), 6.11 (s, 1 H), 6.88 (s, 1 H), 7.01 (d, 1 H, $J = 8.3$ Hz), 7.37 (s, 1 H), 8.43 (s, 1 H, $J = 8.6$ Hz), 8.62 (s, 1 H), 8.85 (s, 1 H), 11.23 (s, 1 H); ^{13}C NMR (100 MHz, CDCl_3) δ 26.19, 26.39, 33.19, 37.62, 46.25, 56.29, 96.81, 102.69, 104.52, 110.97, 113.04, 119.55, 121.60, 121.64, 124.61, 129.14, 133.29, 134.20, 137.86, 146.08, 152.37, 158.40, 161.71; HRMS (ESI) m/z calcd for $\text{C}_{25}\text{H}_{28}\text{F}_3\text{N}_3\text{O}_3\text{H}^+$: 476.2156, Found: 476.2151 ($\Delta = 1.05$ ppm).

1.5. References

- (1) Kumar, V.; Abbas, K. A.; Aster, J. Robbins Basic Pathology, 8TH ed.; Elsevier, 2007.
- (2) World Health Organization (WHO). Global Tuberculosis Report 2015; 2015; Vol. 1.
- (3) Cucunawangsih; Wiwing, V.; Widysanto, A.; Lugito, N. P. H. Mycobacterium Tuberculosis Resistance Pattern against First-Line Drugs in Patients from Urban Area. *Int. J. Mycobacteriology* **2015**, 4 (4), 302–305.
- (4) Lee, J. Y. Diagnosis and Treatment of Extrapulmonary Tuberculosis. *Tuberc. Respir. Dis. (Seoul)*. **2015**, 78 (2), 47.
- (5) Hauck, F. R.; Neese, B. H.; Panchal, A. S.; El-Amin, W. Identification and Management of Latent Tuberculosis Infection. *Am. Fam. Physician* **2009**, 79 (10), 879–886.
- (6) Swaminathan, S.; Padmapriyadarsini, C.; Narendran, G. Diagnosis & Treatment of Tuberculosis in HIV Co-Infected Patients. *Indian J. Med. Res.* **2011**, 134 (6), 850.
- (7) CDC. Signs and symptoms of TB
<http://www.cdc.gov/tb/topic/basics/signsandsymptoms.htm> (accessed Jan 1, 2016).
- (8) CDC. Diagnosis of Tuberculosis Disease
<http://www.cdc.gov/tb/publications/factsheets/testing/diagnosis.htm>.
- (9) Poce, G.; Cocozza, M.; Consalvi, S.; Biava, M. SAR Analysis of New Anti-TB Drugs Currently in Pre-Clinical and Clinical Development. *Eur. J. Med. Chem.* **2014**, 86, 335–351.
- (10) Babu, G. R.; Laxminarayan, R. The Unsurprising Story of MDR-TB Resistance in India. *Tuberculosis* **2012**, 92 (4), 301–306.
- (11) WHO/Int/TB/data. Tuberculosis (Mdr-Tb). **2015**, No. November, 2014–2015.
- (12) TB Drugs – First line, second line & new TB drugs <http://www.tbfacts.org/tb-drugs/>.
- (13) CDC. TB Elimination Extensively Drug-Resistant Tuberculosis (XDR TB).
- (14) Lienhardt, C.; Vernon, A.; Raviglione, M. C. New Drugs and New Regimens for the Treatment of Tuberculosis: Review of the Drug Development Pipeline and Implications for National Programmes. *Curr. Opin. Pulm. Med.* **2010**, 16 (3), 186–193.
- (15) Mdluli, K.; Kaneko, T.; Upton, A. The Tuberculosis Drug Discovery and Development Pipeline and Emerging Drug Targets. *Cold Spring Harb. Perspect. Med.* **2015**, 5 (6), a021154–a021154.
- (16) Brigden, G.; Hewison, C.; Varaine, F. New Developments in the Treatment of Drug-

- Resistant Tuberculosis: Clinical Utility of Bedaquiline and Delamanid. *Infect. Drug Resist.* **2015**, 8, 367–378.
- (17) European Medicines Agency recommends two new treatment options for tuberculosis http://www.ema.europa.eu/ema/index.jsp?curl=pages/news_and_events/news/2013/11/news_detail_001972.jsp&mid=WC0b01ac058004d5c1.
- (18) Leibert, E. New Drugs to Treat Multidrug-Resistant Tuberculosis; the Case for Bedaquiline.pdf. **2014**, 597–602.
- (19) Szumowski, J. D.; Lynch, J. B. Profile of Delamanid for the Treatment of Multidrug-Resistant Tuberculosis. *Drug Des. Devel. Ther.* **2015**, 9, 677–682.
- (20) Tadolini, M.; Lingsang, R. D.; Tiberi, S.; Enwerem, M.; D'Ambrosio, L.; Sadutshang, T. D.; Centis, R.; Migliori, G. B. First Case of Extensively Drug-Resistant Tuberculosis Treated with Both Delamanid and Bedaquiline: TABLE 1. *Eur. Respir. J.* **2016**, ERJ – 00637–02016.
- (21) Kumar, K.; Awasthi, D.; Lee, S. Y.; Zanardi, I.; Ruzsicska, B.; Knudson, S.; Tonge, P. J.; Slayden, R. a.; Ojima, I. Novel Trisubstituted Benzimidazoles, Targeting Mtb FtsZ, as a New Class of Antitubercular Agents. *J. Med. Chem.* **2011**, 54 (1), 374–381.
- (22) Mukherjee, A.; Lutkenhaus, J. Guanine Nucleotide-Dependent Assembly of FtsZ into Filaments. *J. Bacteriol.* **1994**, 176 (9), 2754–2758.
- (23) Nogales, E.; Wolf, S. G.; Downing, K. H. Structure of the Alpha Beta Tubulin Dimer by Electron Crystallography. *Nature* **1998**, 391 (6663), 199–203.
- (24) Leung, A. K. W.; Lucile White, E.; Ross, L. J.; Reynolds, R. C.; DeVito, J. A.; Borhani, D. W. Structure of Mycobacterium Tuberculosis FtsZ Reveals Unexpected, G Protein-like Conformational Switches. *J. Mol. Biol.* **2004**, 342 (3), 953–970.
- (25) Goehring, N. W.; Beckwith, J. Diverse Paths to Midcell: Assembly of the Bacterial Cell Division Machinery. *Curr. Biol.* **2005**, 15 (13), R514–R526.
- (26) Errington, J.; Daniel, R. A.; Scheffers, D.-J. Cytokinesis in Bacteria. *Microbiol. Mol. Biol. Rev.* **2003**, 67 (1), 52–65.
- (27) Kumar, K.; Awasthi, D.; Berger, W. T.; Tonge, P. J.; Slayden, R. A.; Ojima, I. Discovery of Anti-TB Agents That Target the Cell-Division Protein FtsZ. *Future Med. Chem.* **2010**, 2 (8), 1305–1323.
- (28) Haranahalli, K.; Tong, S.; Ojima, I. Recent Advances in the Discovery and Development

- of Antibacterial Agents Targeting the Cell-Division Protein FtsZ. *Bioorg. Med. Chem.* **2016**.
- (29) Erickson, H. P.; Anderson, D. E.; Osawa, M. FtsZ in Bacterial Cytokinesis: Cytoskeleton and Force Generator All in One. *Microbiol. Mol. Biol. Rev.* **2010**, *74* (4), 504–528.
- (30) Margolin, W. FtsZ and the Division of Prokaryotic Cells and Organelles. *Nat. Rev. Mol. Cell Biol.* **2005**, *6* (11), 862–871.
- (31) Huang, Q.; Kirikae, F.; Kirikae, T.; Pepe, A.; Amin, A.; Respicio, L.; Slayden, R. A.; Tonge, P. J.; Ojima, I. Targeting FtsZ for Antituberculosis Drug Discovery: Noncytotoxic Taxanes as Novel Antituberculosis Agents. *J. Med. Chem.* **2006**, *49* (2), 463–466.
- (32) Ojima, I.; Kumar, K.; Awasthi, D.; Vineberg, J. G. Drug Discovery Targeting Cell Division Proteins, Microtubules and FtsZ. *Bioorg. Med. Chem.* **2014**, *22* (18), 5060–5077.
- (33) Sarcina, M.; Mullineaux, C. W. Effects of Tubulin Assembly Inhibitors on Cell Division in Prokaryotes in Vivo. *FEMS Microbiol. Lett.* **2000**, *191* (1), 25–29.
- (34) Slayden, R. a.; Knudson, D. L.; Belisle, J. T. Identification of Cell Cycle Regulators in *Mycobacterium Tuberculosis* by Inhibition of Septum Formation and Global Transcriptional Analysis. *Microbiology* **2006**, *152* (6), 1789–1797.
- (35) White, E. L. 2-Alkoxy-carbonylaminopyridines: Inhibitors of *Mycobacterium Tuberculosis* FtsZ. *J. Antimicrob. Chemother.* **2002**, *50* (1), 111–114.
- (36) Reynolds, R. C.; Srivastava, S.; Ross, L. J.; Suling, W. J.; White, E. L. A New 2-Carbamoyl Pteridine That Inhibits *Mycobacterial* FtsZ. *Bioorg. Med. Chem. Lett.* **2004**, *14* (12), 3161–3164.
- (37) Awasthi, D.; Kumar, K.; Knudson, S. E.; Slayden, R. A.; Ojima, I. SAR Studies on Trisubstituted Benzimidazoles as Inhibitors of *Mtb* FtsZ for the Development of Novel Antitubercular Agents. *J. Med. Chem.* **2013**, *56* (23), 9756–9770.
- (38) Knudson, S. E.; Awasthi, D.; Kumar, K.; Carreau, A.; Goullieux, L.; Lagrange, S.; Vermet, H.; Ojima, I.; Slayden, R. A. Cell Division Inhibitors with Efficacy Equivalent to Isoniazid in the Acute Murine *Mycobacterium Tuberculosis* Infection Model. *J. Antimicrob. Chemother.* **2015**, *70* (11), 3070–3073.
- (39) Knudson, S. E.; Awasthi, D.; Kumar, K.; Carreau, A.; Goullieux, L.; Lagrange, S.; Vermet, H.; Ojima, I.; Slayden, R. A. A Trisubstituted Benzimidazole Cell Division Inhibitor with Efficacy against *Mycobacterium Tuberculosis*. *PLoS One* **2014**, *9* (4),

e93953.

- (40) Knudson, S. E.; Kumar, K.; Awasthi, D.; Ojima, I.; Slayden, R. A. In Vitro–in Vivo Activity Relationship of Substituted Benzimidazole Cell Division Inhibitors with Activity against Mycobacterium Tuberculosis. *Tuberculosis* **2014**, 94 (3), 271–276.
- (41) Ojima, I.; Awasthi, D.; Wei, L.; Haranahalli, K. Strategic Incorporation of Fluorine in the Drug Discovery of New-Generation Antitubercular Agents Targeting Bacterial Cell Division Protein FtsZ. *J. Fluor. Chem.* **2016**.
- (42) Colombo, M.; Bossolo, S.; Aramini, A. Phosphorus Trichloride-Mediated and Microwave-Assisted Synthesis of a Small Collection of Amides Bearing Strong Electron-Withdrawing Group Substituted Anilines. *J. Comb. Chem.* **2009**, 11 (3), 335–337.
- (43) Sanguinetti, M. C.; Tristani-Firouzi, M. hERG Potassium Channels and Cardiac Arrhythmia. *Nature* **2006**, 440 (7083), 463–469.
- (44) Wang, S.; Li, Y.; Xu, L.; Li, D.; Hou, T. Recent Developments in Computational Prediction of hERG Blockage. *Curr. Top. Med. Chem.* **2013**, 13 (11), 1317–1326.
- (45) Hedley, P. L.; Jørgensen, P.; Schlamowitz, S.; Wangari, R.; Moolman-Smook, J.; Brink, P. A.; Kanters, J. K.; Corfield, V. A.; Christiansen, M. The Genetic Basis of Long QT and Short QT Syndromes: A Mutation Update. *Hum. Mutat.* **2009**, 30 (11), 1486–1511.
- (46) Nogawa, H.; Kawai, T. hERG Trafficking Inhibition in Drug-Induced Lethal Cardiac Arrhythmia. *Eur. J. Pharmacol.* **2014**, 741, 336–339.
- (47) Jing, Y.; Easter, A.; Peters, D.; Kim, N.; Enyedy, I. J. In Silico Prediction of hERG Inhibition. *Future Med. Chem.* **2015**, 7 (5), 571–586.
- (48) Zhou, P. Z.; Babcock, J.; Liu, L. Q.; Li, M.; Gao, Z. B. (20) Activation of Human Ether-a-Go-Go Related Gene (hERG) Potassium Channels by Small Molecules. *Acta Pharmacol Sin* **2011**, 32 (6), 781–788.
- (49) Jamieson, C.; Moir, E. M.; Rankovic, Z.; Wishart, G. Medicinal Chemistry of hERG Optimizations: Highlights and Hang-Ups. *J. Med. Chem.* **2006**, 49 (17), 5029–5046.
- (50) Braga, R. C.; Alves, V. M.; Silva, M. F. B.; Muratov, E.; Fourches, D.; Lião, L. M.; Tropsha, A.; Andrade, C. H. Pred-hERG: A Novel Web-Accessible Computational Tool for Predicting Cardiac Toxicity. *Mol. Inform.* **2015**, 34 (10), 698–701.
- (51) Biswal, S.; Sahoo, U.; Sethy, S.; Kumar, H. K. S.; Banerjee, M.; Hooker, J. Indole: The Molecule of Diverse Biological Activities. *Asian J. Pharm. Clin. Res.* **2012**, 5 (1), 2–7.

- (52) Liu, L.; Norman, M. H.; Lee, M.; Xi, N.; Siegmund, A.; Boezio, A. A.; Booker, S.; Choquette, D.; D'Angelo, N. D.; Germain, J.; et al. Structure-Based Design of Novel Class II c-Met Inhibitors: 2. SAR and Kinase Selectivity Profiles of the Pyrazolone Series. *J. Med. Chem.* **2012**, 55 (5), 1868–1897.
- (53) Ban, H.; Gavriluk, J.; Barbas Carlos F. Tyrosine Bioconjugation through Aqueous Ene-Type Reactions: A Click-Like Reaction for Tyrosine. *J. Am. Chem. Soc.* **2010**, 132 (5), 1523–1525.
- (54) Xie, X.; Yan, Y.; Zhu, N.; Liu, G. Benzothiazoles Exhibit Broad-Spectrum Antitumor Activity: Their Potency, Structure–activity and Structure–metabolism Relationships. *Eur. J. Med. Chem.* **2014**, 76, 67–78.

Chapter 2

Synthesis of acyl hydrazones as antimicrobial agents targeting fungal GlcCer

2.1. Introduction.....	81
2.1.1. Preliminary SAR.....	83
2.2. Results and discussion.....	85
2.2.1. Synthesis of acyl hydrazides.....	85
2.2.2. Synthesis of 3-Bromobenzoic hydrazide.....	85
2.2.3. Synthesis of quinolone-3-carbohydrazide.....	86
2.2.4. Resynthesis of hits from initial screening.....	86
2.2.5. Synthesis of ¹³ C analog of BHBM.....	88
2.2.6. Acyl hydrazone library synthesis.....	89
2.3. Conclusion.....	90
2.4. Experimental Section.....	90
2.5. References.....	97

2. Synthesis of acyl hydrazones as antimicrobial agents targeting fungal Glc Cer

2.1. Introduction

Recent statistics suggest fungal infections affect nearly 300 million people, globally.^{1,2} Fungal infections can be classified as allergic reactions towards fungal proteins or fungal toxins and mycoses.³ Life threatening invasive fungal infections include candidiasis, aspergillosis, cryptococcosis and pneumocystosis.¹ While Increased incidences of fungal infections are seen in immune compromised patients including HIV patients or immune suppressed patients like ones receiving organ transplant or cancer patients receiving chemotherapy,⁴ majority of fungal infection related deaths are seen in HIV patients.⁵ Current antifungal drug classes such as azoles and polyenes possess a variety of drawbacks, including narrow spectrum of activity, and, drug-drug interactions with immunosuppressants and chemotherapy agents.¹ The emerging resistant strains of fungi, either natural or acquired,⁶ calls for new antifungal agents with fewer side effects.

Glucosylceramide (GlcCer), a glycosphingolipid, can be seen in plants, animals and fungi.⁷ GlcCer is known to play a role in cell adhesion, cell growth, signal transduction and apoptosis.^{8,9} Owing to the structural differences between mammalian and microbial GlcCer, it makes a novel target for antimicrobial drug discovery.⁸ Fungal GlcCer possesses a C9-methyl group and a trans unsaturation on C8 on the sphingoid base, which is absent in mammalian GlcCer (Figure 2.1).

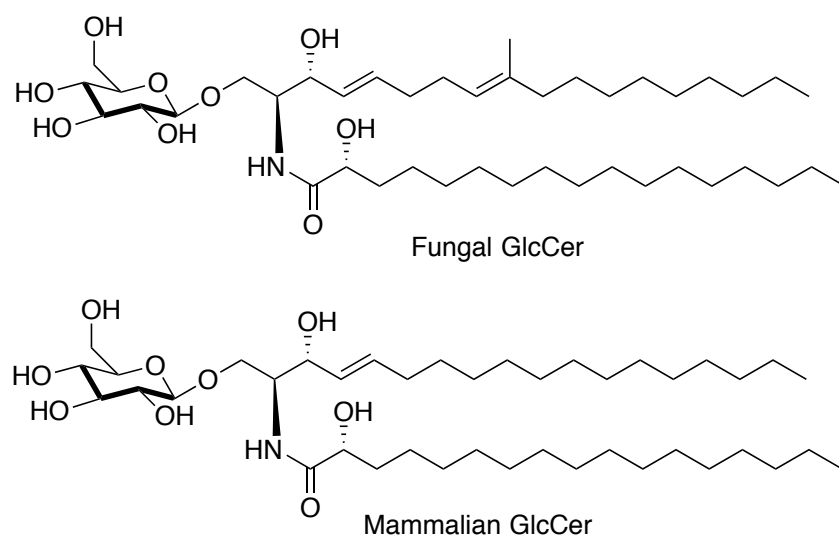


Figure 2.1: Structures of fungal and mammalian GlcCer.

Fungal GlcCer controls cell division in neutral and alkaline environment such as blood, cerebrospinal fluid and alveolar space.^{1,10,11} In case of *Cryptococcus neoformans* (Cn), GlcCer

mutant strain Δ gcs1 failed to divide in neutral or alkaline pH, displaying the importance of GlcCer for fungal virulence.¹⁰ Thus, GlcCer is a novel target for new antifungal drug discovery. Screening of ~50,000 compounds from ChemBridge library (Figure 2.2), resulted in 2 hits BHBM and D0 (Figure 2.3).¹

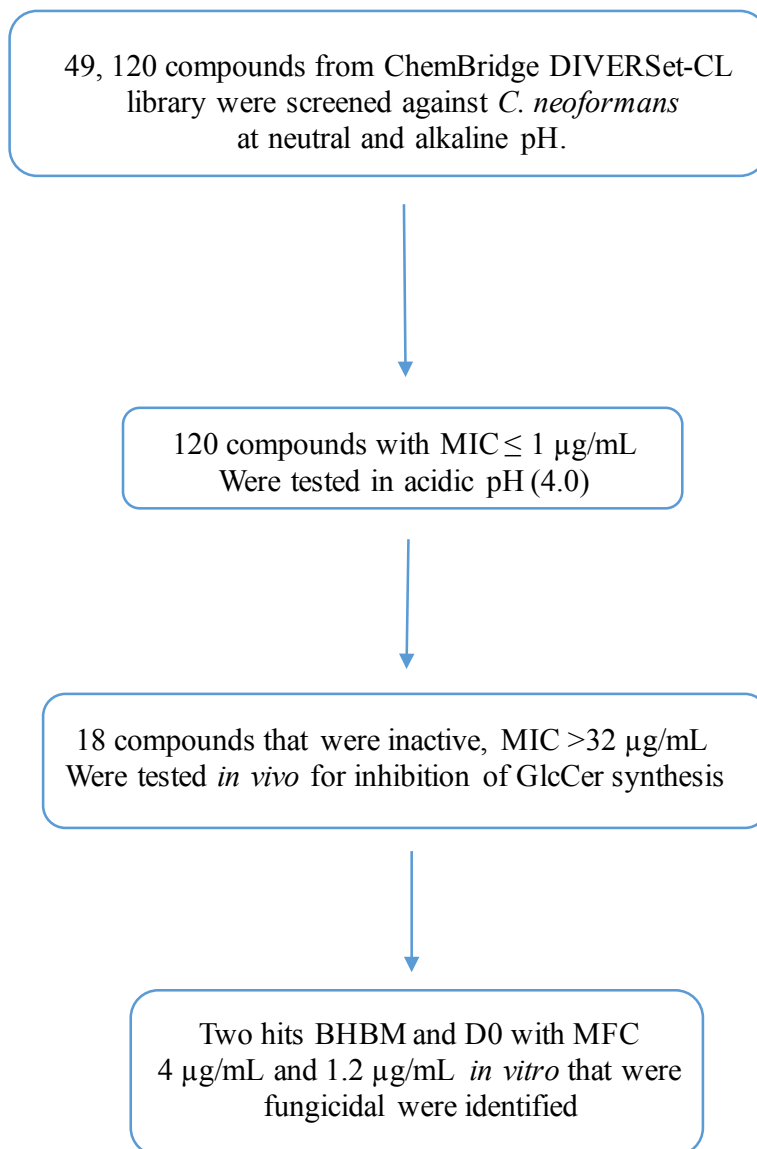


Figure 2.2: Identification of BHBM and D0 as GlcCer inhibitors.

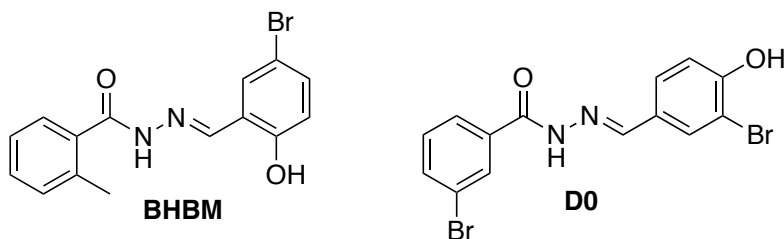


Figure 2.3: Structures of BHBM and D0.

Both BHBM and D0 inhibited *C. neoformans* (Cn), but not mammalian (J774) GlcCer (Figure 2.4) proving they are not cytotoxic.¹ Kill characteristics of BHBM and D0 showed that, BHBM killed *C. neoformans* in a concentration dependent manner, while D0 killed in a time dependent manner (Figure 2.5).¹ BHBM and D0 did not display any antibacterial activity with MIC >160 µg/mL.¹

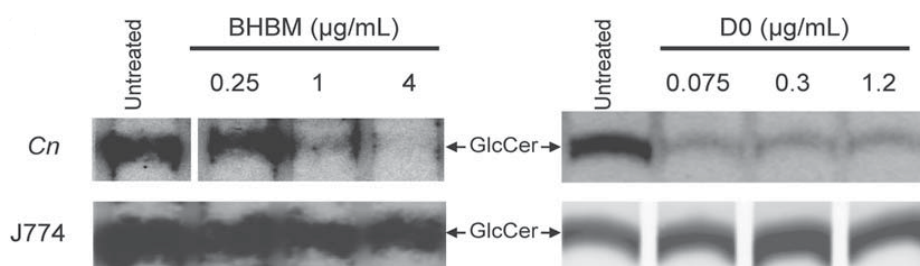


Figure 2.4: GlcCer inhibition by BHBM and D0.¹ Copied from Reference 1.

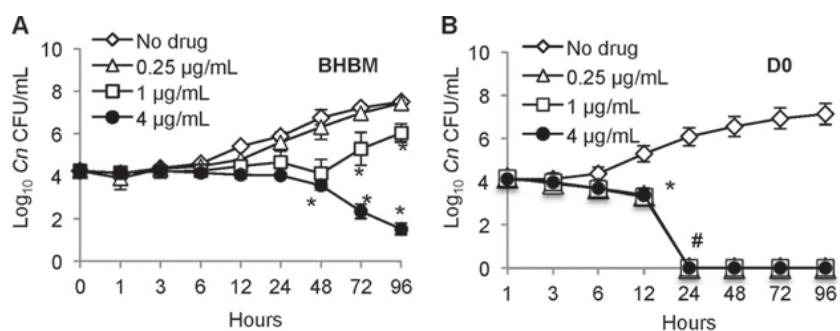
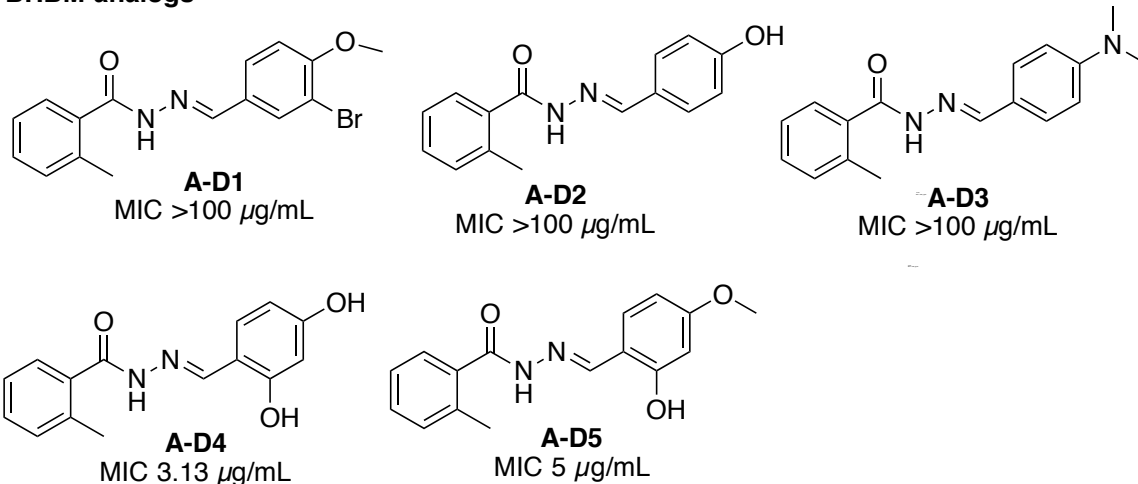


Figure 2.5: Kill characteristics of BHBM (A) and D0 (B).¹ Copied from reference 1.

2.1.1. Preliminary SAR

Based on promising results of BHBM and D0, several analogs were tested in vitro against *C. neoformans* as well. Preliminary SAR studies suggest that presence of a hydroxyl group ortho to imine is essential for activity as seen in A-D4, A-D5, B-D4 and B-D5 (Figure 2.6).

BHBM analogs



D0 analogs

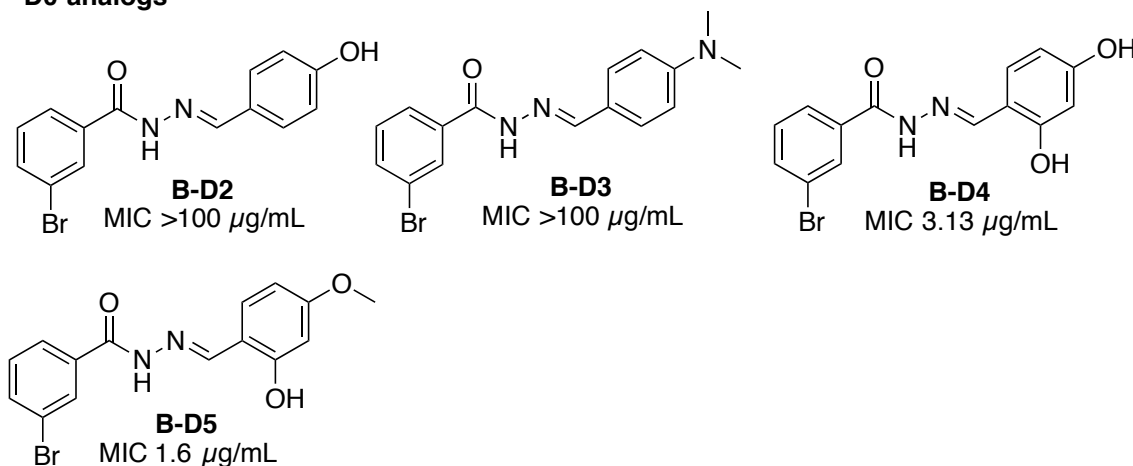


Figure 2.6: Screening of BHBM and D0 analogs.

While screening for more compounds, three additional hits D2, D13 and D17 with $MIC_{80} < 0.03$ µg/mL and D6 with MIC_{80} 0.12 µg/mL against *C. neoformans* were identified (Figure 2.7). These results also highlight the significance of a 2-hydroxyl substitution on the hydrazine moiety.

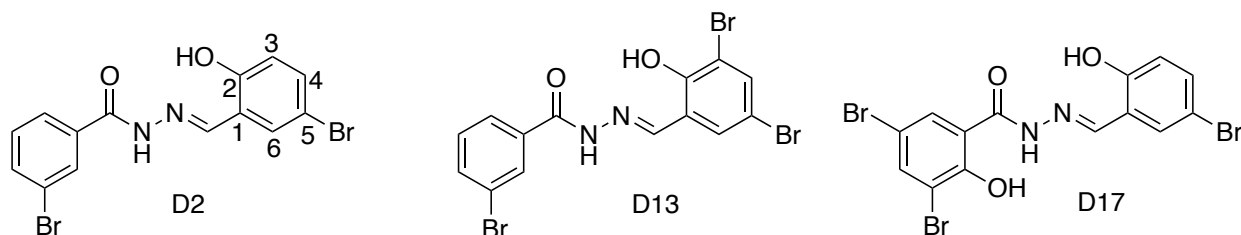
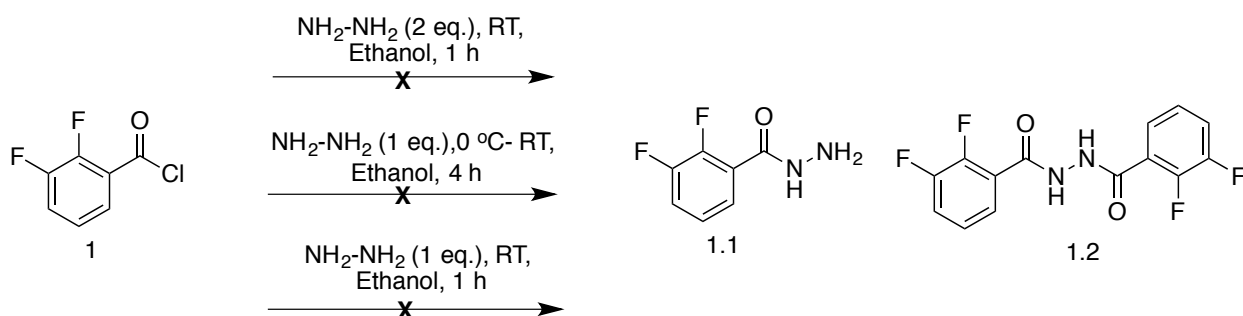


Figure 2.7: Additional hits from initial screening.

Based on these results, a new library of acyl hydrazones were designed and synthesized.

2.2. Results and discussion

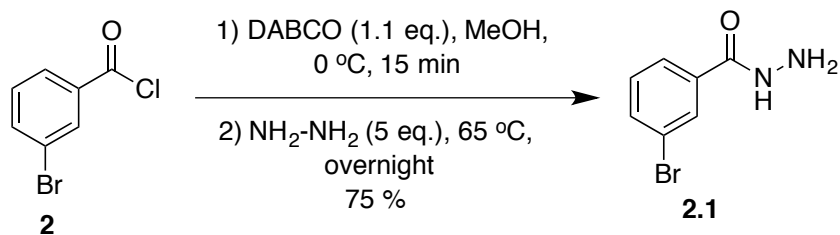
2.2.1. Synthesis of acyl hydrazides



Scheme 2.1: Synthesis of 2,3-difluorobenzoyl hydrazide.

2,3-difluorobenzoyl chloride (1) was treated with hydrazine (2 eq.) in ethanol. The reaction mixture was stirred at room temperature for 1 hour. Mass spectrum of the reaction mixture after 1 hour showed molecular ion peak for the dimer (1.2). The same reaction was tried by adding hydrazine (1 eq.) drop wise using a syringe pump at 0 °C, over a period of 1 hour to a solution of 2,3-difluorobenzoyl chloride in ethanol. After addition, the reaction mixture was allowed to stir at room temperature. The reaction mixture was checked after 1 hour, 3 hours and 4 hours respectively using TLC and mass spectrometer. Molecular ion peak for the product was not seen, instead a peak for molecular weight of the product + 76 was seen. The peaks for dimer or ester were not seen. The reaction was also tried by adding hydrazine (1 eq.) to drop wise using a syringe pump at room temperature over a period of 1 hour to a solution of 2,3-difluorobenzoyl chloride (1) in tetrahydrofuran. Mass spectrum of the reaction mixture after addition showed molecular ion peak for the dimer (1.2). The formation of dimer could have been due to the high reactivity of the acyl chloride.

2.2.2. Synthesis of 3-Bromobenzoic hydrazide

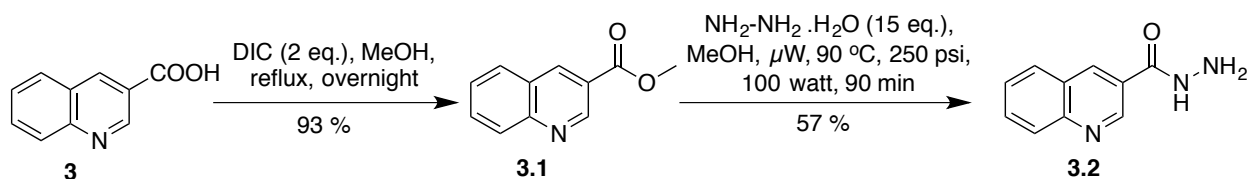


Scheme 2.2: Synthesis of 3-Bromobenzoic hydrazide.

3-Bromobenzoyl chloride (2) was treated with DABCO (1.1 eq.) in methanol at 0 °C to form ethyl 3-bromobenzoate, which was then refluxed with hydrazine (5 eq.) at 65 °C in methanol, overnight to give 3-Bromobenzoic hydrazide (2.1).

Since the reaction of acyl chloride with hydrazine resulted in disubstitution under various reaction conditions, synthesis of carbohydrazides was carried out using phenyl esters instead of acyl chlorides.

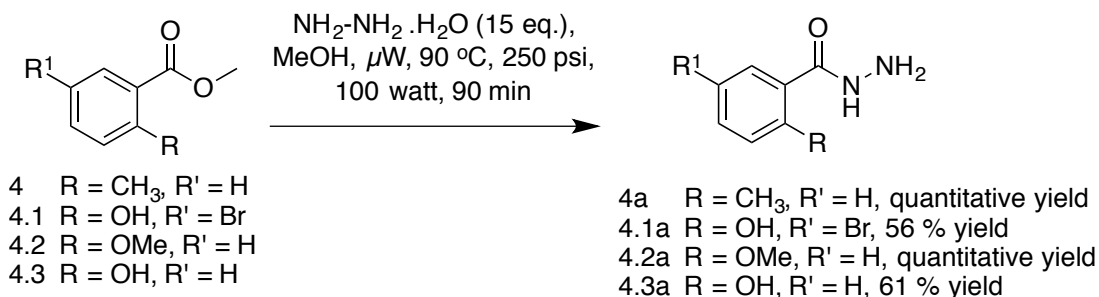
2.2.3. Synthesis of quinolone-3-carbohydrazide



Scheme 2.3: Synthesis of quinolone-3-carbohydrazide.

Commercially available quinoline-3-carboxylic acid was refluxed with DIC (2 eq.) in methanol overnight to give methyl quinolone-3-carboxylate (3.1), which was then treated with hydrazine monohydrate in methanol in a microwave reactor at 90 °C for 90 minutes, at 100 watts and 250 psi to give quinolone-3-carbohydrazide.

Other carbohydrazides were synthesized by treating commercially available substituted phenyl esters with hydrazine monohydrate, following the above mentioned method (Scheme 2.4).



Scheme 2.4: Synthesis of substituted phenyl carbohydrazides.

2.2.4. Resynthesis of hits from initial screening

Initial in vitro screening of 220 compounds resulted in 18 hits that were tested in vivo, out of which 2 compounds, BHBM and D0 were found to be active. All the compounds that were tested were purchased from ChemDiv. But when BHBM was purchased the second time, it was noticed that the structure of BHBM given by ChemDiv originally was wrong (BHBM-1). Change in the

hydroxyl substitution from 2-position in BHBM to 4-position in BHBM-1 resulted in loss of activity. This could possibly be attributed to the fact that the oxygen of carbonyl group, the nitrogen and the hydroxyl group at the 2-position chelate with a copper ion to exert antifungal activity. In order to confirm the correct structure of BHBM, both the analogs BHBM and BHBM-1 were synthesized. Along with BHBM, other active compounds D2 and D6 were resynthesized to be tested as well (Figure 2.8).

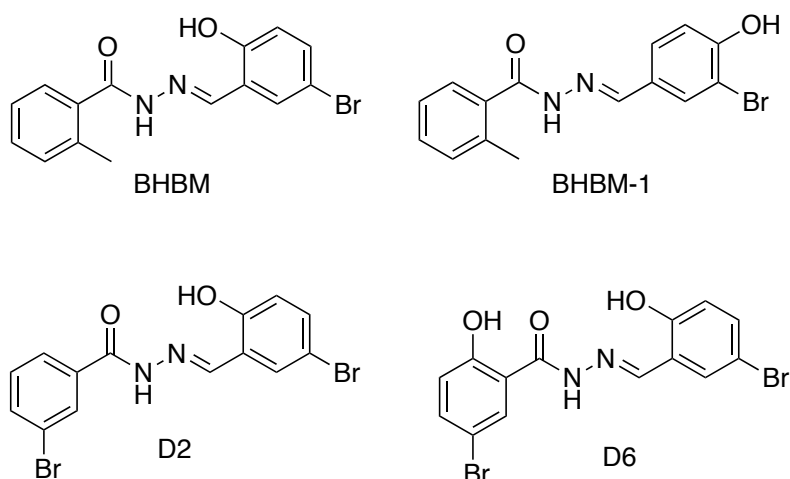
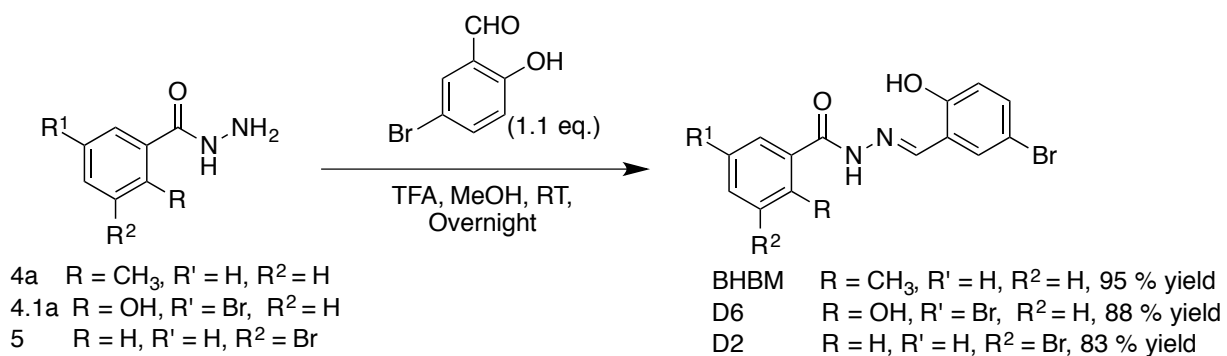
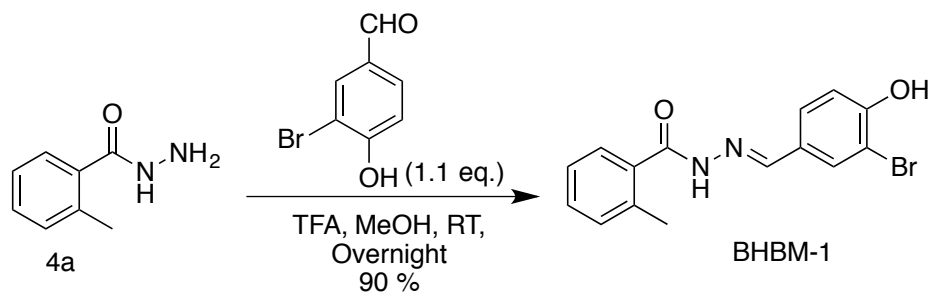


Figure 2.8: Resynthesis of BHBM and other hit compounds.

Carboxydrazides were treated with corresponding aldehydes in methanol, in the presence of catalytic amount of trifluoroacetic acid. The reaction mixture was stirred at room temperature overnight to give respective acyl hydrazones (Scheme 2.5).

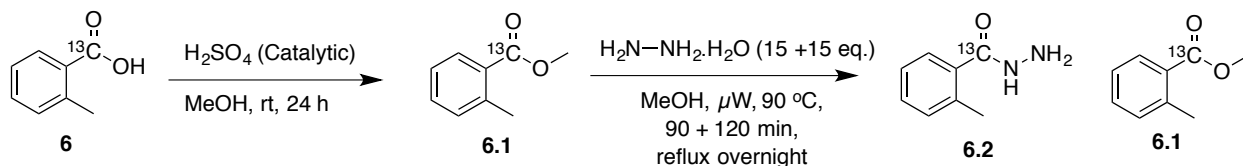




Scheme 2.5: Synthesis of acyl hydrazones.

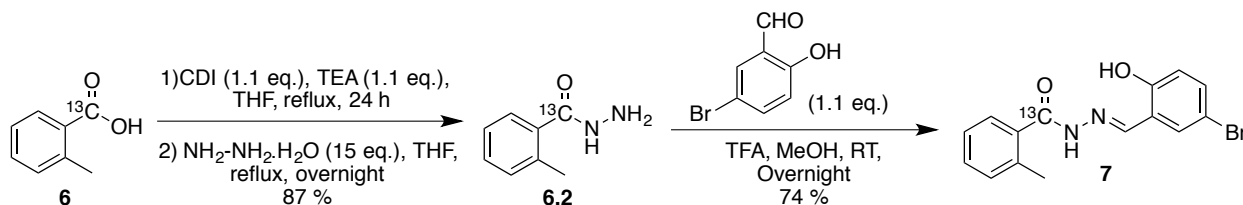
2.2.5. Synthesis of ^{13}C analog of BHBM

In order to identify different metabolites of BHBM, ^{13}C analog of BHBM was synthesized. ^{13}C O-toluic acid was treated with methanol in the presence of sulfuric acid at room temperature to give methyl o-toluate. The first time methyl o-toluate was made, all the product was lost when dried under vacuum overnight. The reaction was carried out again and the crude product was immediately treated with hydrazine monohydrate under microwave irradiation in methanol, without further drying, unfortunately the reaction did not go to completion in spite of subjecting to microwave irradiation repeatedly and refluxing overnight (Scheme 2.6).



Scheme 2.6: Synthesis of ^{13}C analog of BHBM.

The next time, ^{13}C O-toluic acid was refluxed with CDI in the presence of TEA, in THF for 24 hours to give an anhydride, which was refluxed with hydrazine monohydrate in THF, overnight to give desired ^{13}C O-toluyldiazide. The diazide was then treated with 2-hydroxy-5-bromobenzaldehyde in the presence of catalytic amount of trifluoroacetic acid in methanol at room temperature, overnight to give ^{13}C -BHBM analog (Scheme 2.7).



Scheme 2.7: Synthesis of ^{13}C analog of BHBM.

2.2.6. Acyl hydrazone library synthesis

To study the structure activity relationships of acyl hydrazones as inhibitors of fungal GluCer, libraries of compounds had to be synthesized. A quick and efficient way to carry out this, was through combinatorial library synthesis. An initial library of 8 compounds was synthesized to optimize the reaction conditions (Figure 2.9). Once the conditions were optimized, a library of 96 compounds was synthesized.

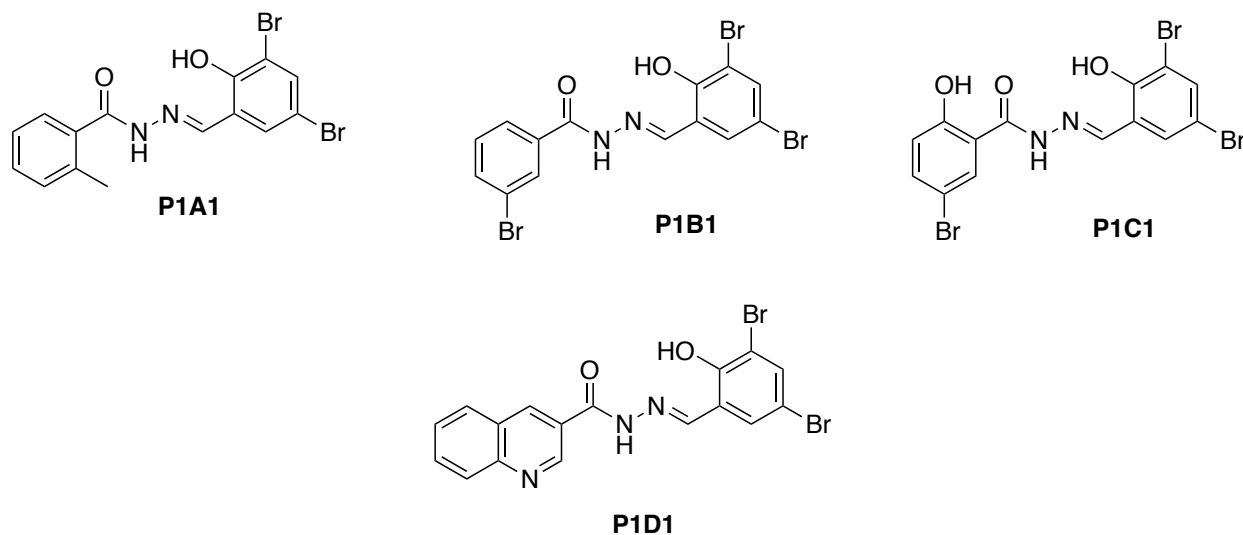
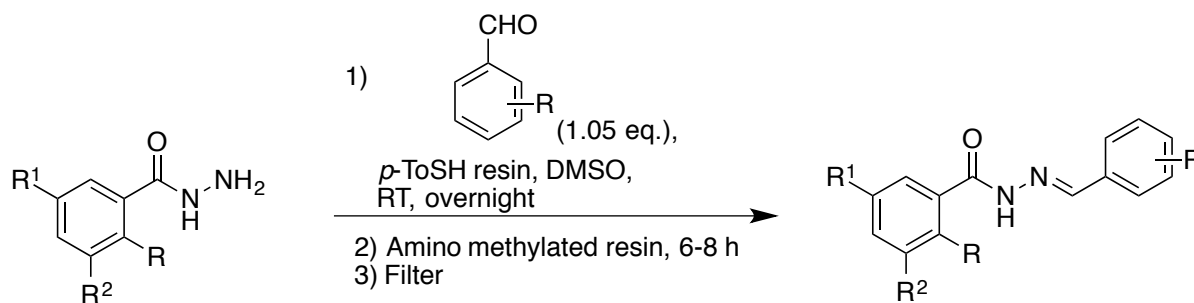


Figure 2.9: Compounds from initial library.

Aryl hydrazide was dissolved in DMSO and treated with various aldehydes in the presence of *p*-toluene sulfonic acid (*p*-ToSH) resin, as catalyst at room temperature overnight. This was followed by the addition of amino methylated resin, in order to remove excess aldehyde. At the end, the reaction mixture was filtered using a millipore filter in order to remove *p*-ToSH resin and the amino methylated resin (Scheme 2.8).



Scheme 2.8: Acyl hydrazone library synthesis.

Eight aryl hydrazides were treated with sixteen aldehydes to give 96 compounds (Figure 2.10).

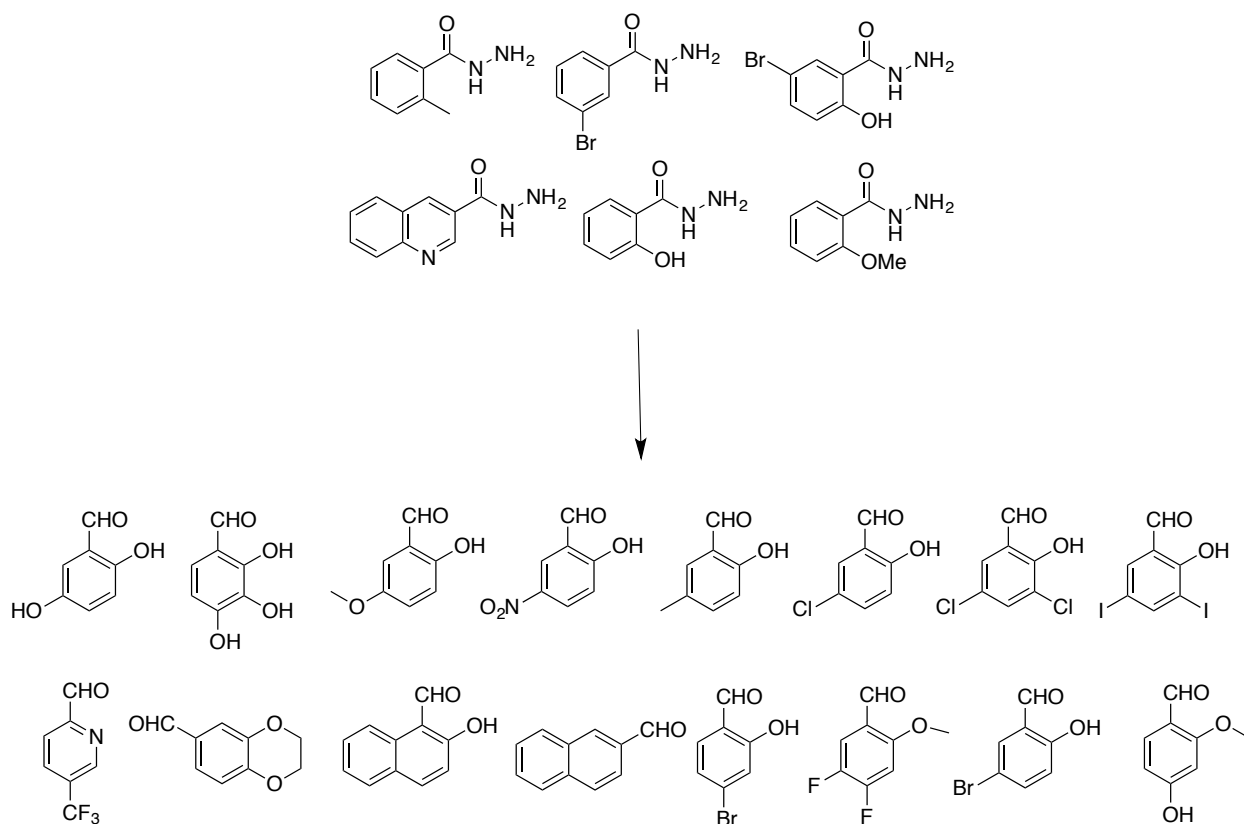


Figure 2.10: Library of 96 compounds.

2.3. Conclusion

The initial hits BIBM, D2 and their derivatives seem to be promising leads for the development of new fungal GlcCer inhibitors. This project is in a very nascent stage. MIC results from the library of compounds synthesized will give a better idea of the SAR. Based on those results, compounds can be further modified if necessary.

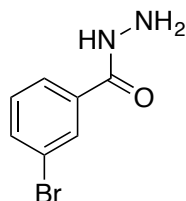
2.4. Experimental Section

Methods. ^1H and ^{13}C NMR spectra were measured on Bruker 300, 400 or 500 MHz NMR spectrometer. Melting points were measured on a Thomas Hoover Capillary melting point apparatus and are uncorrected. TLC was performed on silica coated aluminum sheets (thickness 200 μm) or alumina coated (thickness 200 μm) aluminum sheets supplied by Sorbent Technologies and column chromatography was carried out on Siliacflash® P60 silica gel, 40-63 μm (230-400 mesh) supplied by Silicycle. Aluminum oxide, activated, neutral, Brockmann Grade I, 58 Å, was supplied by Alfa Aesar. High-resolution mass spectra were obtained from the ICB&DD Mass Spectrometry Laboratory at Stony Brook University.

Materials. Solvents (HPLC grade or better), and all the other chemicals were purchased from

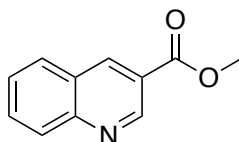
Fisher Scientific Co. (Pittsburgh, PA). The chemicals were purchased from Aldrich Co., Synquest Inc. and Sigma. Tetrahydrofuran (THF) was freshly distilled from sodium metal and benzophenone. Dichloromethane was also distilled immediately prior to use under nitrogen from calcium hydride.

3-Bromobenzoic hydrazide (5.2)¹²



DABCO (2.5 mmol) was transferred to a three neck round bottom flask. Three cycles of vacuum and nitrogen were alternately passed through the flask. This was followed by the addition of methanol (15 mL) and 3-bromobenzoyl chloride (2.3 mmol) at 0 °C. The reaction mixture was stirred at 0 °C for 15 minutes, followed by the addition of hydrazine (34 mmol) at room temperature. The reaction mixture was stirred at 65 °C overnight, and then cooled to room temperature. This was followed by the addition of water, which caused white solid to crash out. The solid was filtered and dried, to give desired product as a white solid (75 % yield), ¹H NMR (300 MHz, DMSO-d₆) δ 4.5 (s, 2 H), 7.41 (t, 1 H, J = 7.9 Hz), 7.70 (d, 1 H, J = 7.7 Hz), 7.80 (d, 1 H, J = 7.7 Hz), 7.96 (s, 1 H), 9.88 (s, 1 H). Analytical data matches the reported results.¹²

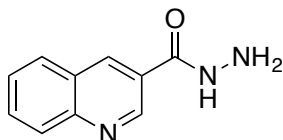
Methyl quinolone-3-carboxylate (3.1)¹³



Quinoline-3-carboxylic acid (2.9 mmol) was transferred to a round bottom flask, followed by the addition of DIC (5.8 mmol) and methanol (5 mL). The reaction mixture was refluxed overnight. After completion of the reaction, the reaction mixture was concentrated in a rotary evaporator. The crude reaction mixture was washed with water (25 mL X 3) and extracted with ethyl acetate (25 mL X 3). The organic layer was collected, dried over anhydrous magnesium sulfate, filtered and concentrated in a rotary evaporator to give the crude product. Flash chromatography of the crude product using silica gel and hexanes: ethyl acetate (1:1) as eluent, resulted in pure product as a white solid (93 % yield), ¹H NMR (300 MHz, CDCl₃) δ 4.01 (s, 3H), 7.62 (t, 1 H, J = 7.53 Hz),

7.83 (t, 1 H, J = 7.3 Hz), 7.93 (d, 1 H, J = 8.04 Hz), 8.16 (d, 1 H, J = 8.4 Hz), 8.84 (s, 1 H), 9.44 (s, 1H). Analytical data matches the reported results.¹³

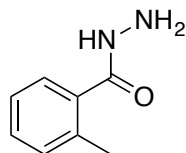
Synthesis of quinolone-3-carbohydrazide (3.2)¹⁴



A mixture of Methyl quinolone-3-carboxylate (1.87 mmol), hydrazine monohydrate (28 mmol) and methanol (3 mL) was irradiated in a microwave reactor at 90 °C, for 90 minutes at 100 watts and 250 psi. After the reaction was complete, the reaction mixture was allowed to cool to room temperature and product crystallized from the reaction mixture. The solid was filtered and dried to give pure product as white solid (57 % yield), ¹H NMR (300 MHz, DMSO-d₆) δ 4.63 (s, 2 H), 7.67 (t, 1 H, J = 7.5 Hz), 7.85 (t, 1 H, J = 7 Hz), 8.04 – 8.08 (m, 2 H), 8.78 (s, 1 H), 9.24 (s, 1 H), 10.11 (s, 1 H). Analytical data matches the reported results.¹⁴

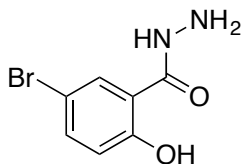
Compounds **4a**, **4.1a**, **4.2a** and **4.3a** were synthesized following the same procedure.

2-Methylbenzoic hydrazide (4a)¹⁵



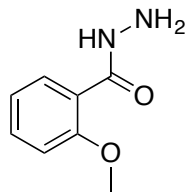
White solid (quantitative yield); ¹H NMR (300 MHz, CDCl₃) δ 2.43 (s, 3 H), 4.09 (s, 2 H), 7.10 (s, 1 H), 7.13 – 7.26 (m, 2 H), 7.31 – 7.35 (m, 2 H). Analytical data matches the reported results.¹⁵

2-hydroxy-5-bromobenzoic hydrazide (4.1a)¹⁶



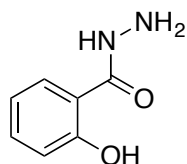
White solid (56 % yield); ¹H NMR (500 MHz, DMSO-d₆) δ 4.66 (br. s, 2 H), 6.87 (d, 1 H, J = 8.8 Hz), 7.48 – 7.51 (m, 1 H), 7.97 (s, 1 H), 10.08 (br. s, 1 H), 12.45 (br. s, 1 H). Analytical data matches the reported results.¹⁶

2-methoxybenzoic hydrazide (4.2a)¹⁷



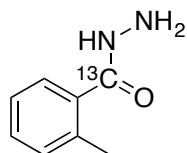
White solid (quantitative yield); $^1\text{H NMR}$ (300 MHz, CDCl_3) δ 3.83 (s, 3 H), 4.14 (br. s, 2 H), 6.87 (d, 1 H, $J = 8.3$ Hz), 6.98 (t, 1 H, $J = 7.5$ Hz), 7.36 (t, 1 H, $J = 7$ Hz), 8.09 (d, 1 H, $J = 7.8$ Hz), 8.91 (s, 1 H). Analytical data matches the reported results.¹⁷

2-hydroxybenzoic hydrazide (4.3a)¹⁵



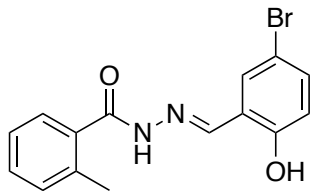
White solid (61 % yield); $^1\text{H NMR}$ (300 MHz, CDCl_3) δ 4.10 (s, 2 H), 6.85 (t, 1 H, $J = 7.6$ Hz), 7.0 (d, 1 H, $J = 8.3$ Hz), 7.33 (d, 1 H, $J = 7.9$ Hz), 7.41 (t, 1 H, $J = 7.7$ Hz), 7.77 (s, 1 H), 11.76 (br. s, 1 H). Analytical data matches the reported results.¹⁵

(^{13}C) O- toluylhydrazide (6.2)¹⁵



To a solution of (^{13}C) O- toluic acid (1.45 mmol) in THF (6 mL), was added CDI (1.6 mmol) and triethylamine (1.6 mmol). The reaction mixture was refluxed overnight, to form the anhydride. To the same reaction mixture was added hydrazine monohydrate (22 mmol) and refluxed for 4 hours. After the completion of reaction, the reaction mixture was concentrated in vacuo, followed by the addition of water and extraction with dichloromethane (30 mL X 3). The organic layer was collected, dried with magnesium sulfate, filtered, evaporated and dried under vacuum to give the product as white solid (87 % yield); $^1\text{H NMR}$ (300 MHz, CDCl_3) δ 2.43 (s, 3 H), 4.10 (s, 2 H), 7.04 – 7.30 (m, 3 H), 7.31 – 7.57 (m, 2 H). Analytical data matches the reported results.¹⁵

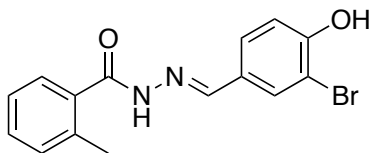
Synthesis of 2-Methylbenzoic acid -[1-(2-hydroxy-5-bromophenyl)methylidene]hydrazide (BHBM)



To a solution of 2-methylbenzoic hydrazide (0.66 mmol), 2-hydroxy-5-bromobenzaldehyde (0.72 mmol) in methanol (3 mL) was added 3 drops of glacial acetic acid. The reaction mixture was stirred at room temperature overnight. Addition of water to the reaction mixture resulted in precipitation of the product, which was filtered, washed with water and dried to give pure product as white solid (95 % yield); ^1H NMR (300 MHz, DMSO- d_6) δ 2.38 (s, 3 H), 6.76 (s, 1 H), 7.29 – 7.47 (m, 6 H), 7.77 (s, 1 H), 8.46 (s, 1 H), 11.19 (s, 1 H), 12.05 (s, 1 H); ^{13}C NMR (100 MHz, DMSO- d_6) δ 19.10, 19.42, 110.52, 118.51, 118.73, 121.36, 121.53, 125.46, 125.75, 126.92, 127.61, 129.26, 129.54, 129.95, 130.28, 130.47, 130.79, 133.30, 133.66, 134.20, 134.58, 135.67, 136.19, 141.45, 145.36, 155.68, 156.42, 165.20, 171.23; HRMS (ESI) m/z calcd for $\text{C}_{15}\text{H}_{13}\text{BrN}_2\text{O}_2\text{H}^+$: 333.0233, Found: 333.0225 ($\Delta = 2.31$ ppm).

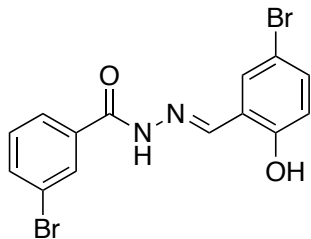
The same procedure was followed for the synthesis of **BHBM-1**, **D2**, **D6** and ^{13}C **BHBM**.

2-Methylbenzoic acid -[1-(3-bromo-4-hydroxyphenyl)methylidene]hydrazide (**BHBM-1**)



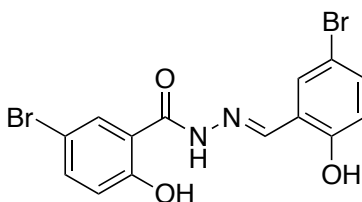
White solid (90 % yield); ^1H NMR (500 MHz, DMSO- d_6) δ 2.35 (s, 3 H), 7.0 (d, 1 H, $J = 8.4$ Hz), 7.25 – 7.29 (m, 3 H), 7.36 – 7.41 (m, 2 H), 7.51 – 7.53 (dd, 1 H, $J = 7$ Hz, 10.3 Hz), 7.84 (s, 1 H), 8.15 (s, 1 H); ^{13}C NMR (100 MHz, DMSO- d_6) δ 19.30, 109.74, 109.85, 116.55, 125.07, 125.64, 126.89, 127.01, 127.41, 127.93, 128.97, 129.67, 130.59, 131.36, 135.38, 135.83, 142.41, 146.02, 155.49, 155.82, 165.13; HRMS (ESI) m/z calcd for $\text{C}_{15}\text{H}_{13}\text{BrN}_2\text{O}_2\text{H}^+$: 333.0233, Found: 333.0226 ($\Delta = 2.03$ ppm).

3-Bromobenzoic acid -[1-(5-bromo-2-hydroxyphenyl)methylidene]hydrazide (**D2**)



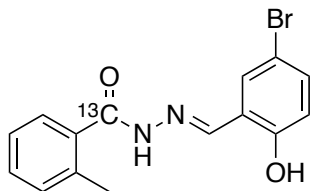
White solid (83 % yield); ^1H NMR (500 MHz, DMSO- d_6) δ 6.89 (d, 1 H, $J = 8.7$ Hz), 7.43 (dd, 1 H, $J = 11.1$ Hz, 6.4 Hz), 7.50 (t, 1 H, $J = 7.9$ Hz), 7.79 – 7.81 (m, 2 H), 9.83 (d, 1 H, $J = 7.8$ Hz), 8.11 (s, 1 H), 8.60 (s, 1 H), 11.17 (s, 1 H), 12.21 (s, 1 H); ^{13}C NMR (125 MHz, DMSO- d_6) δ 110.48, 118.68, 121.33, 121.77, 126.91, 130.17, 130.82, 133.72, 134.71, 134.96, 145.83, 156.40, 161.43; HRMS (ESI) m/z calcd for $\text{C}_{14}\text{H}_{10}\text{Br}_2\text{N}_2\text{O}_2\text{H}^+$: 396.9182, Found: 396.917 ($\Delta = 2.99$ ppm).

5-Bromo-2-hydroxybenzoic acid -[1-(5-bromo-2-hydroxyphenyl)methylidene]hydrazide (D6)



White solid (88 % yield); ^1H NMR (500 MHz, DMSO- d_6) δ 6.90 (d, 1 H, $J = 8.8$ Hz), 6.95 (d, 1 H, $J = 8.8$ Hz), 7.43 (dd, 1 H, $J = 11.1$ Hz, 6.4 Hz), 7.58 (dd, 1 H, $J = 11.1$ Hz, 6.5 Hz), 7.78 (s, 1 H), 8.01 (s, 1 H), 8.61 (s, 1 H), 11.12 (s, 1 H), 11.80 (s, 1 H), 12.07 (s, 1 H); ^{13}C NMR (125 MHz, DMSO- d_6) δ 110.02, 110.5, 118.16, 118.71, 119.58, 121.23, 130.14, 130.79, 133.90, 136.19, 146.41, 156.46, 157.91, 163.17; HRMS (ESI) m/z calcd for $\text{C}_{14}\text{H}_{10}\text{Br}_2\text{N}_2\text{O}_3\text{H}^+$: 412.9131, Found: 412.912 ($\Delta = 2.64$ ppm).

(^{13}C) 2-Methylbenzoic acid -[1-(5-bromo-2-hydroxyphenyl)methylidene]hydrazide (^{13}C BHBM)



White solid (74 % yield); ^1H NMR (500 MHz, DMSO- d_6) δ 2.38 (s, 3 H), 6.89 (d, 1 H, $J = 8.8$ Hz), 7.27 – 7.31 (m, 2 H), 7.39 – 7.46 (m, 3 H), 7.77 (s, 1 H), 8.46 (s, 1 H), 11.19 (s, 1 H), 12.05 (s, 1 H); ^{13}C NMR (125 MHz, DMSO- d_6) δ 110.44, 118.43, 118.65, 121.31, 121.51, 125.37,

125.64, 125.68, 126.87, 127.55, 129.17, 129.40, 129.89, 130.19, 130.38, 130.69, 130.72, 133.21, 133.56, 134.15, 134.29, 134.81, 135.37, 135.89, 136.12, 136.13, 141.21, 141.26, 145.19, 145.23, 155.62, 156.36; HRMS (ESI) m/z calcd for C₁₄¹³CH₁₃BrN₂O₂H⁺: 334.0267, Found: 334.0264 (Δ = 0.91 ppm).

Library synthesis

A solution of phenyl carbohydrazide (4 mg) in DMSO was added into each well in a 96 well plate, followed by a solution of aldehyde (1.1 eq.) in DMSO. The final volume was made up to 1 mL using DMSO. p-TOSH resin was added as a catalyst to each well. The plate was shaken at room temperature overnight. This was followed by the addition of 0.1 eq. of amino methylated resin to each well, to quench any unreacted hydrazide, and the reaction mixture was shaken at room temperature for 6 hours. The reaction mixture was filtered through a millipore filter to remove the resin and afford the desired library. The in vitro inhibitory activity of these compounds are currently being tested in Professor Maurizio Del Poeta's lab.

2.5. References

- (1) Mor, V.; Rella, A.; Farnoud, A. M.; Singh, A.; Munshi, M.; Bryan, A.; Naseem, S.; Konopka, J. B.; Ojima, I.; Bullesbach, E.; et al. Identification of a New Class of Antifungals Targeting the Synthesis of Fungal Sphingolipids. *MBio* **2015**, 6 (3), e00647.
- (2) Brown, G. D.; Denning, D. W.; Gow, N. A. R.; Levitz, S. M.; Netea, M. G.; White, T. C. Hidden Killers: Human Fungal Infections. *Sci. Transl. Med.* **2012**, 4 (165), 165rv13–rv165rv13.
- (3) Kathiravan, M. K.; Salake, A. B.; Chothe, A. S.; Dudhe, P. B.; Watode, R. P.; Mukta, M. S.; Gadhwe, S. The Biology and Chemistry of Antifungal Agents: A Review. *Bioorg. Med. Chem.* **2012**, 20 (19), 5678–5698.
- (4) Babazadeh-Qazijahani, M.; Badali, H.; Irannejad, H.; Afsarian, M. H.; Emami, S. Imidazolylchromanones Containing Non-Benzylic Oxime Ethers: Synthesis and Molecular Modeling Study of New Azole Antifungals Selective against *Cryptococcus Gattii*. *Eur. J. Med. Chem.* **2014**, 76, 264–273.
- (5) Armstrong-James, D.; Meintjes, G.; Brown, G. D. A Neglected Epidemic: Fungal Infections in HIV/AIDS. *Trends Microbiol.* **2014**, 22 (3), 120–127.
- (6) Spitzer, M.; Robbins, N.; Wright, G. D. Combinatorial Strategies For Combating Invasive Fungal Infections. *Virulence* **2016**, 5594 (July), 0.
- (7) Rella, A.; Farnoud, A. M.; Del Poeta, M. Plasma Membrane Lipids and Their Role in Fungal Virulence. *Prog. Lipid Res.* **2016**, 61, 63–72.
- (8) Nimrichter, L.; Rodrigues, M. L.; Rodrigues, E. G.; Travassos, L. R. The Multitude of Targets for the Immune System and Drug Therapy in the Fungal Cell Wall. *Microbes Infect.* **2005**, 7 (4), 789–798.
- (9) Hakomori, S. Structure, Organization, and Function of Glycosphingolipids in Membrane. *Curr. Opin. Hematol.* **2003**, 10 (1), 16–24.
- (10) Rittershaus, P. C.; Kechichian, T. B.; Allegood, J. C.; Merrill, A. H.; Hennig, M.; Luberto, C.; Del Poeta, M. Glucosylceramide Synthase Is an Essential Regulator of Pathogenicity of *Cryptococcus Neoformans*. *J. Clin. Invest.* **2006**, 116 (6), 1651–1659.
- (11) Saito, K.; Takakuwa, N.; Ohnishi, M.; Oda, Y. Presence of Glucosylceramide in Yeast and Its Relation to Alkali Tolerance of Yeast. *Appl. Microbiol. Biotechnol.* **2006**, 71 (4), 515–521.

- (12) Ashiq, U.; Ara, R.; Mahroof-Tahir, M.; Maqsood, Z. T.; Khan, K. M.; Khan, S. N.; Siddiqui, H.; Choudhary, M. I. Synthesis, Spectroscopy, and Biological Properties of Vanadium(IV)–Hydrazide Complexes. *Chem. Biodivers.* **2008**, 5 (1), 82–92.
- (13) Han, E.-G.; Kim, H. J.; Lee, K.-J. Quinolines from Morita–Baylis–Hillman Acetates of 2-Azidobenzaldehydes. *Tetrahedron* **2009**, 65 (46), 9616–9625.
- (14) Monga, V.; Nayyar, A.; Vaitilingam, B.; Palde, P. B.; Singh Jhamb, S.; Kaur, S.; Singh, P. P.; Jain, R. Ring-Substituted Quinolines. Part 2: Synthesis and Antimycobacterial Activities of Ring-Substituted Quinolincarbohydrazide and Ring-Substituted Quinolincarboxamide Analogues. *Bioorg. Med. Chem.* **2004**, 12 (24), 6465–6472.
- (15) Saha, A.; Kumar, R.; Kumar, R.; C, D. Development and Assessment of Green Synthesis of Hydrazides. *Indian J. Chem.* **2010**, 49b, 526–531.
- (16) Rida, S.; Saudi, M.; Youssef, A.; Halim, M. Synthesis and Biological Evaluation of the Pyrazole Class of Cyclooxygenase- 2-Inhibitors. *Lett. Org. Chem.* **2009**, 6 (4), 282–288.
- (17) Hou, J.-L.; Shao, X.-B.; Chen, G.-J.; Zhou, Y.-X.; Jiang, X.-K.; Li, Z.-T. Hydrogen Bonded Oligohydrazide Foldamers and Their Recognition for Saccharides. *J. Am. Chem. Soc.* **2004**, 126 (39), 12386–12394.

Chapter 3

Development of novel inhibitors of botulinum neurotoxins A and E

3.1. Introduction.....	100
3.1.1. Molecular foot-print based rescoring methodology.....	100
3.1.2. Molecular dynamics.....	102
3.1.3. BoNT/E Inhibitors	103
3.2 Results and discussion	103
3.2.1. Synthesis of hybrid compound.....	103
3.2.2. Resynthesis of 5-chloroethyl-3-(4-trifluoromethylphenyl)-[1,2,4]oxadiazole	107
3.2.3. Synthesis of C562-1101-D-Ile	109
3.3. Conclusion	110
3.4. Experimental section.....	110
3.5. References.....	116

3. Development of Novel Inhibitors of Botulinum Neurotoxins A and E

3.1. Introduction

Botulinum neurotoxins (BoNTs), known to be the most potent neurotoxins, are produced by anaerobic bacteria *Clostridium botulinum*.^{1,2} The Centers for Disease Control and prevention (CDC) classifies BoNTs as class A bioterrorism agents.³ They exist as eight distinct serotypes (A-H).⁴ While botulinum neurotoxins A, B, E and F (BoNT/A, B, E, F) are all responsible for human botulism, BoNT/A is the most potent with an LD₅₀ of 1.3 ng/kg.^{1,5,6} BoNT/A is a two-chain polypeptide made up of a heavy and a light chain, which are linked to each other by a disulfide linkage.³ Under normal physiological conditions, the family of SNARE proteins which include synaptobrevin, SNAP-25 and syntaxin, form a complex⁷ and promote the fusion of synaptic vesicle to the neuronal cell membrane. This causes the release of acetyl choline in the synaptic cleft, making it available to bind to receptors to cause muscle contractions.⁵ BoNT heavy chain targets the ganglioside, bringing about endocytosis of the toxin, while the light chain gets released into the cytosol and cleaves the SNARE proteins.⁵ BoNTs/A,C and E cleave SNAP-25.⁵ The limited availability of therapeutic treatment and their low LD₅₀ makes BoNTs highly potential weapons for biological warfare. Thus there is a need for the development of agents that inhibit BoNTs.

3.1.1. Molecular foot-print based rescoring methodology

Traditional screening programs such as DOCK utilize van der Waals (VDW) and electrostatic (ES) terms to rank order the compatibility of ligands with target.⁸ A new scoring function called the molecular foot print similarity (FPS) score was used to identify inhibitors for BoNT. The FPS scoring method identifies compounds that are energetically most similar to the known reference (Figure 3.1).

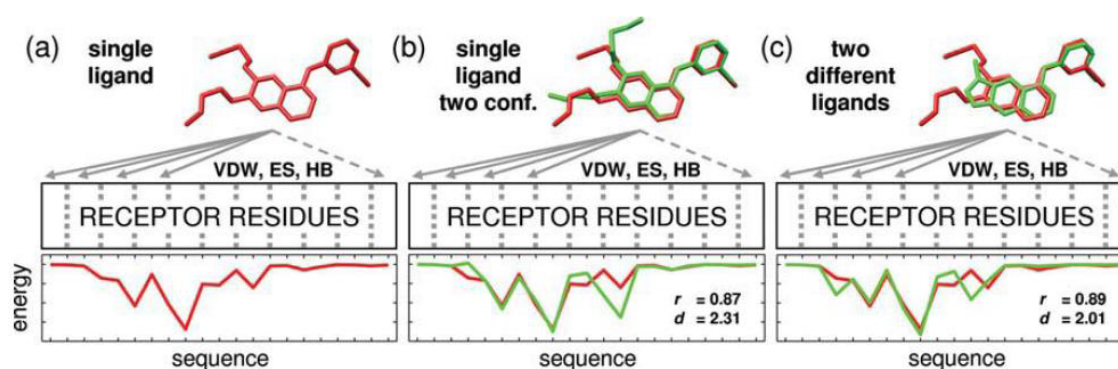


Figure 3.1: Use of FPS score in virtual screening (a) Reference ligand (red). (b) Comparison

between the reference (red) and candidate molecule (green) from the virtual screen.⁸

Peptidomimetics was used for the initial attempts to identify inhibitors for BoNT/A.³ 8 of the available co-crystal structures of BoNT/A with inhibitors were overlaid to determine favorable vs unfavorable interaction energies.⁹ Polypeptide RRGC was found to have the best overall fit in 7 out of 8 co-crystal structures. Thus polypeptide RRGC, which has a K_i of 157 nM against BoNT-A, was used a reference ligand for virtual screening.³

In order to identify new Botulinum neurotoxin light chain-A (BoNT/LC-A) inhibitors, virtual screening of over one million commercially available compounds was carried out of which 99 compounds were selected, purchased from Chem-Div.³ The 99 compounds were assayed in vitro using a high throughput SNAPtide assay, which resulted in the identification of 2 hit compounds ChemDiv 5762-1843/ZINC20036308 (IC_{50} 24 μ M) and ChemDiv E843-1064/ZINC21873993 (IC_{50} 27 μ M).³ 3D docked structures of ChemDiv 5762-1843 and ChemDiv E843-1064 show that the compounds interact with Zinc ion and Aspartic acid 370. The coordination group for ChemDiv 5762-1843 is urea and that for ChemDiv E843-1064 is 1,2,4-oxadiazole (Figure 3.2).³

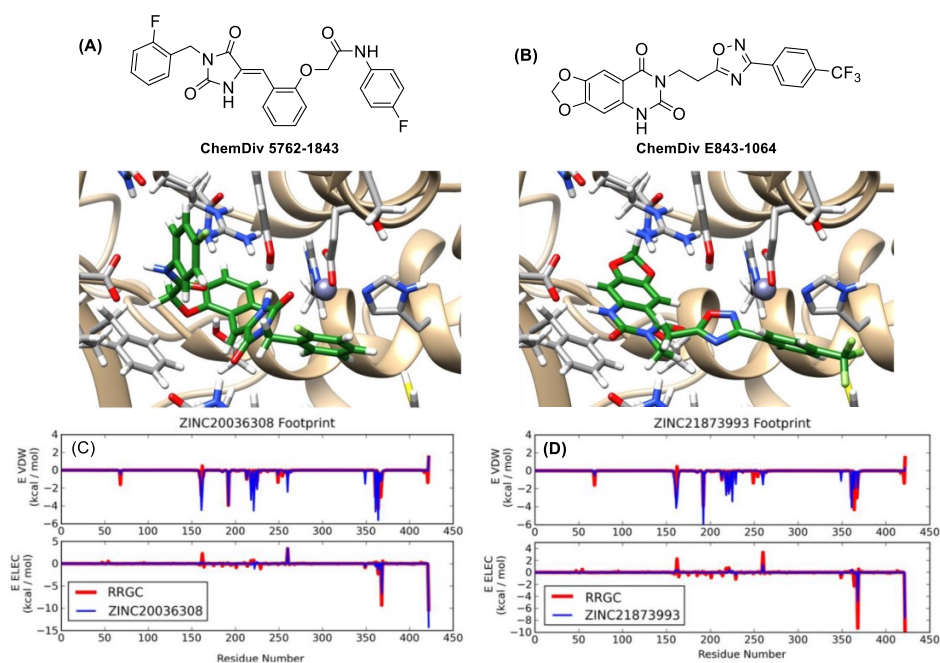


Figure 3.2: 2D chemical structure and 3D docked structures of hit compounds (A) ChemDiv ID 5762-1843 and (B) ChemDiv ID E843-1064. The Vander wals (VDW) and Electrostatic (ES) footprint overlay of RRGC (red) and hit compounds (blue) (C) ChemDiv ID 5762-1843 and (D) ChemDiv ID E843-1064.³

3.1.2. Molecular dynamics

Molecular dynamics simulation studies showed that, a hybrid compound composed of 1,3-dioxoloquinazolinone portion from ChemDiv 5762-1843 and fluorobenzyl imidazolinone portion of ChemDiv E843-1064 displayed better stability and improved chelation with zinc as compared to the two ChemDiv compounds (Figure 3.3). The predicted binding pose and footprint of the hybrid compound are shown in figure 3.4. Several attempts were made to synthesize the hybrid compound.

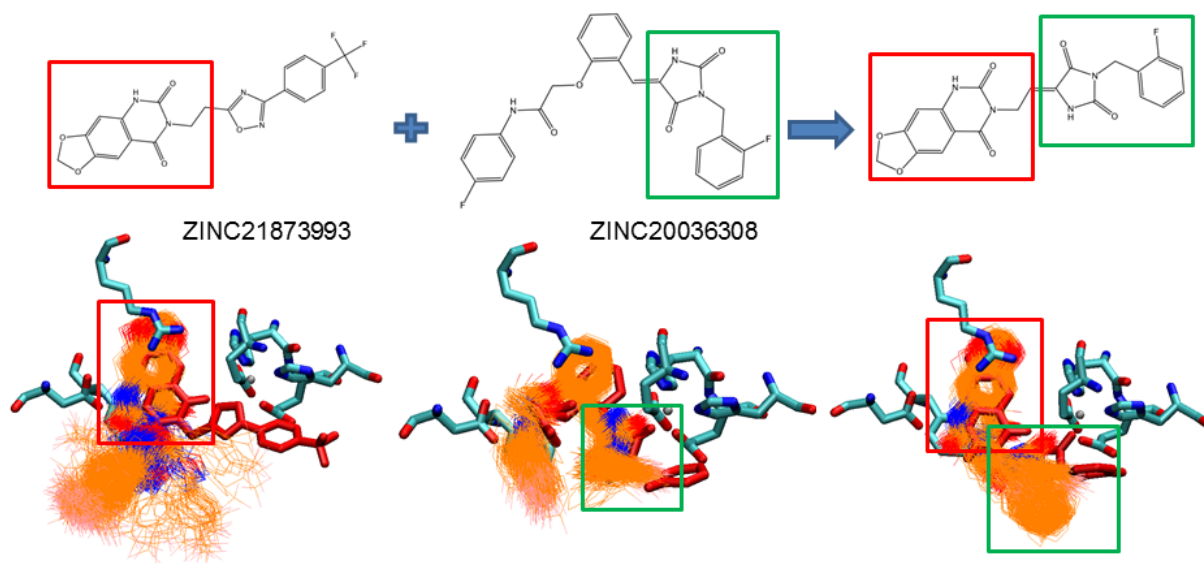


Figure 3.3: Molecular dynamics simulation studies of hybrid compound.

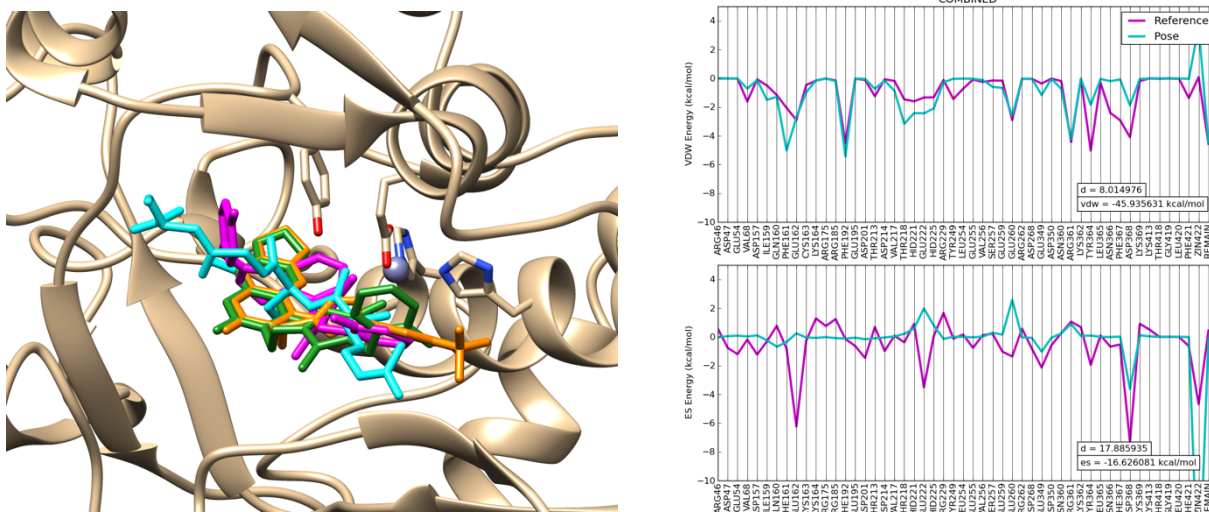


Figure 3.4: Predicted binding pose and footprint of the hybrid compound.

3.1.3. BoNT/E Inhibitors

In order to identify potential lead compounds for BoNT/E inhibition, virtual screening of commercial structure library (ChemDiv Inc.) against BoNT/E was carried out. Tetrapeptide RIME, a known BoNT/E binding peptide, was used as footprint binding baseline. ZINC20284316 was identified as the top scoring lead compound, and in vitro assay of ZINC20284316 exhibited 70% inhibition at 100 μ M against BoNT/E (Figure 3.5).

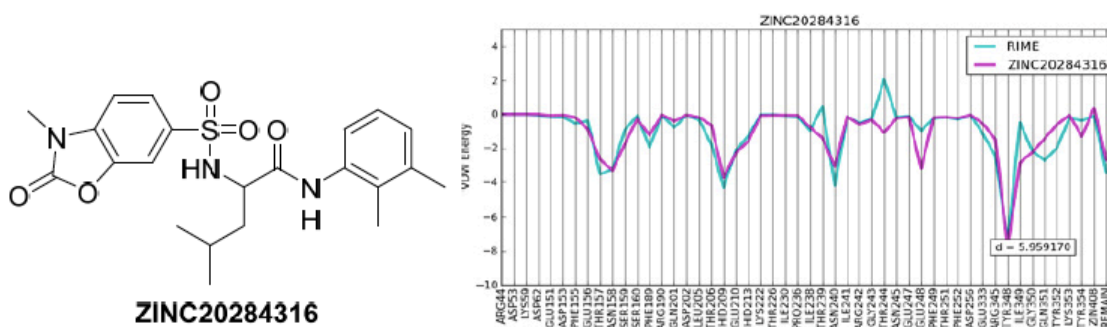


Figure 3.5: Footprint of RIME and ZINC20284316 with BoNT/E.

Previously leucine analog of ZINC20284316 was synthesized as BoNT/E inhibitor. Since the natural ligand RIME has isoleucine, an isoleucine analog of ZINC20284316 was synthesized.

3.2 Results and discussion

3.2.1. Synthesis of hybrid compound

Based on the results of compounds ChemDiv 5762-1843 and ChemDiv E843-1064 a hybrid compound (A) was proposed. The compound A could essentially be synthesized by combining the two pieces via a condensation reaction (Figure 3.6).

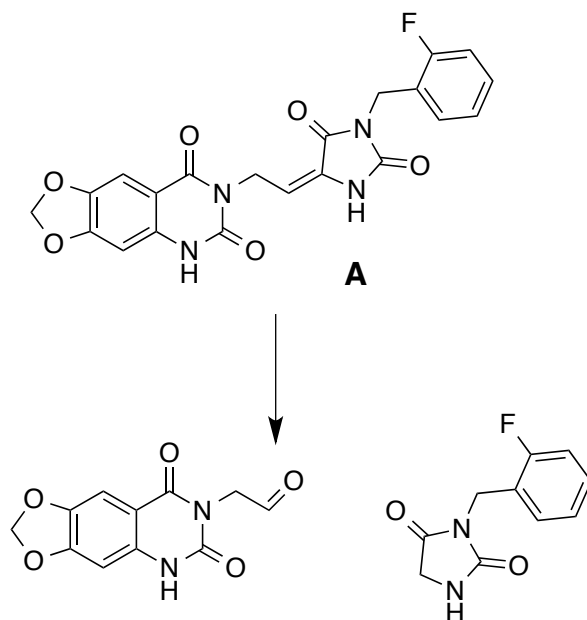
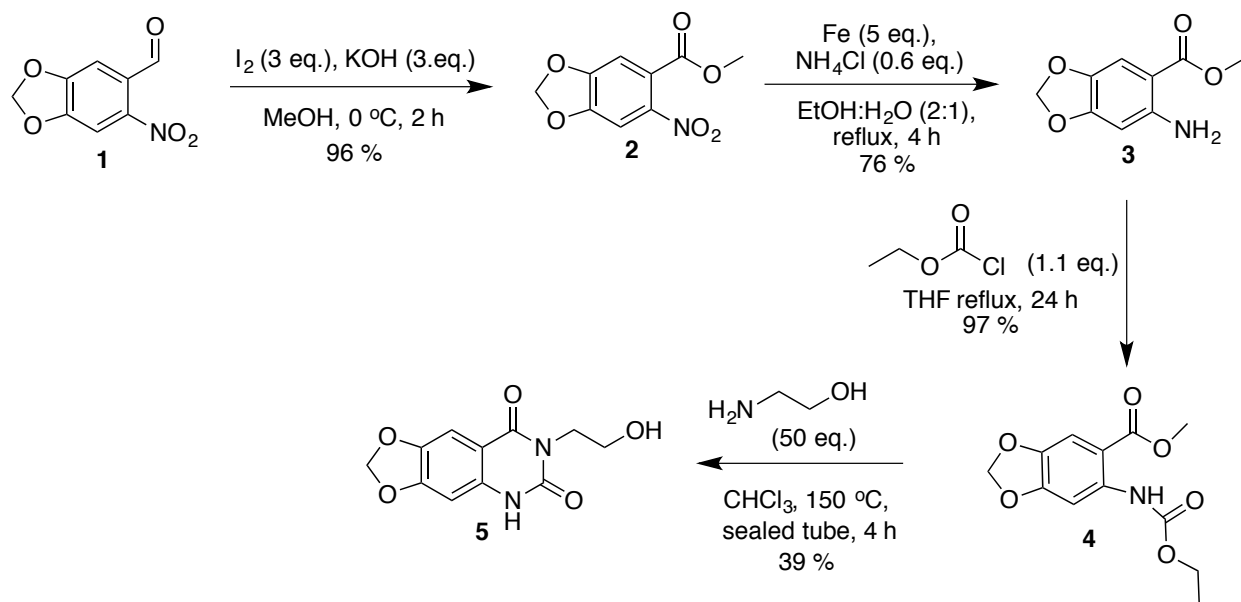


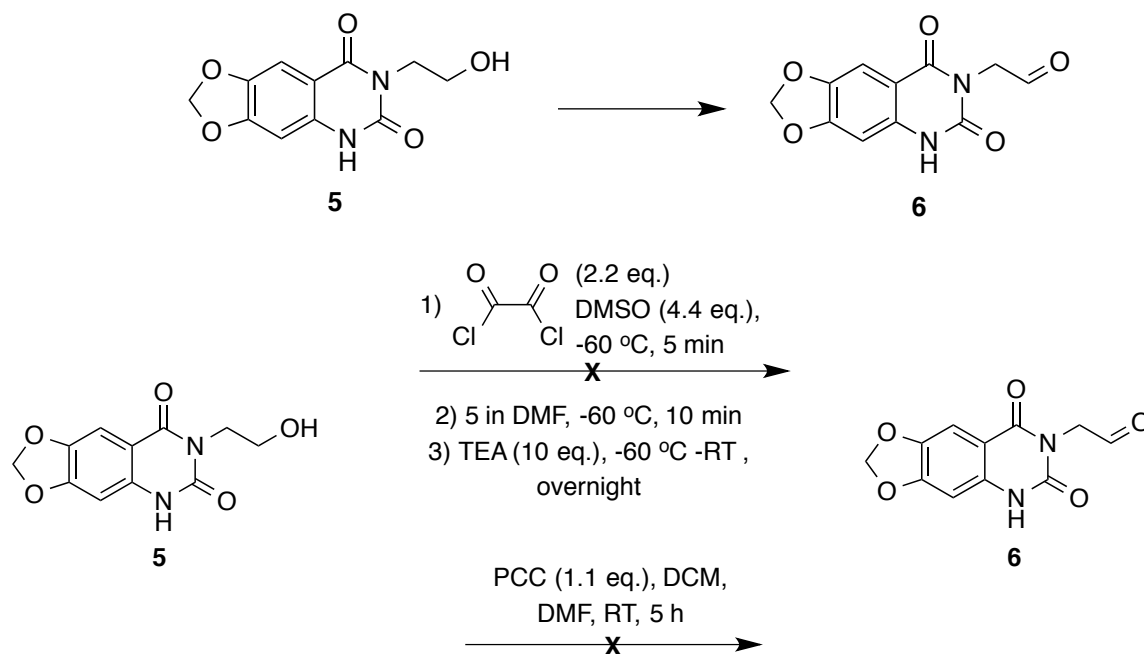
Figure 3.6: Retro synthesis of hybrid compound A.

6-Nitropiperonal was treated with iodine and KOH on methanol at 0 °C for 2 hours to give compound **2**. Reduction of compound **2** was brought about by refluxing in metallic iron and ammonium chloride with a mixture of ethanol: water (2:1) for 4 hours.³ The amine **3** was refluxed in THF with ethyl chloroformate to yield carbamate **4**. Compound **4** was heated in a sealed tube with chloroform and excess ethanolamine for 4 hours to yield the alcohol **5**.¹⁰ Subsequent trials of reaction **4** to **5** did not work. It is not clear as to why the results are not reproducible.



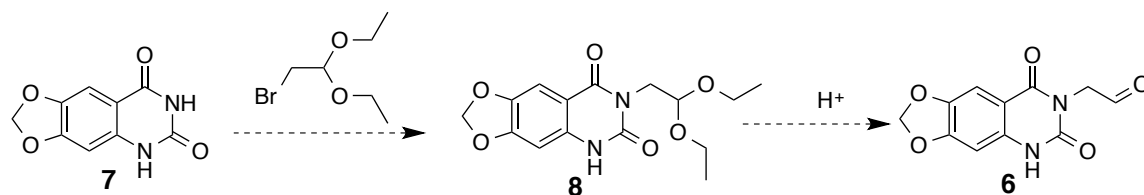
Scheme 3.1: Synthesis of (6,8-dioxo-5,8-dihydro[1,3]dioxolo[4,5-g]quinazolin-7(6H)-yl)ethanol

Two different methods were tried for the oxidation of **5** to **6**. The first method was by Swern oxidation, but the reaction did not proceed and starting material was recovered. The second method was by using Pyridinium chlorochromate (PCC). Starting material was consumed and a new baseline spot was seen. Mass did not correspond to that of desired product. Further literature search suggested that the reaction of alcohol with PCC in the presence of DMF would most likely result in corresponding acid instead of aldehyde (Scheme 3.2).



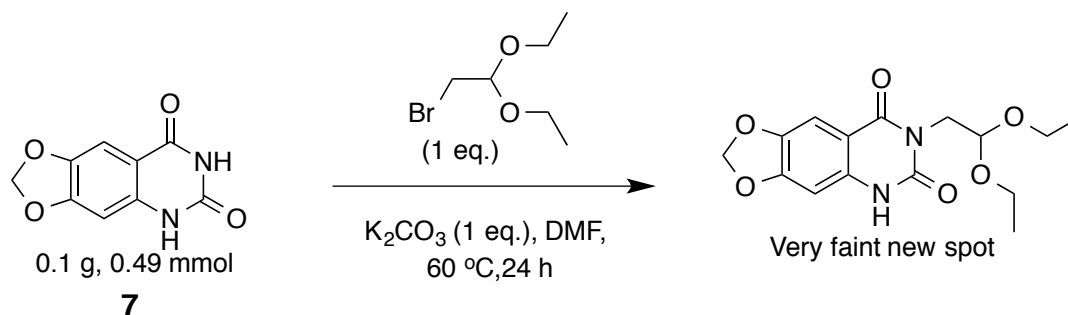
Scheme 3.2: Oxidation of alcohol to aldehyde.

Another possible route for the synthesis of compound **6** was to treat compound **7** with bromoacetaldehyde diethyl acetal to get the acetal product **8** and deprotect the acetal with an acid to give compound **6** (Scheme 3.3).



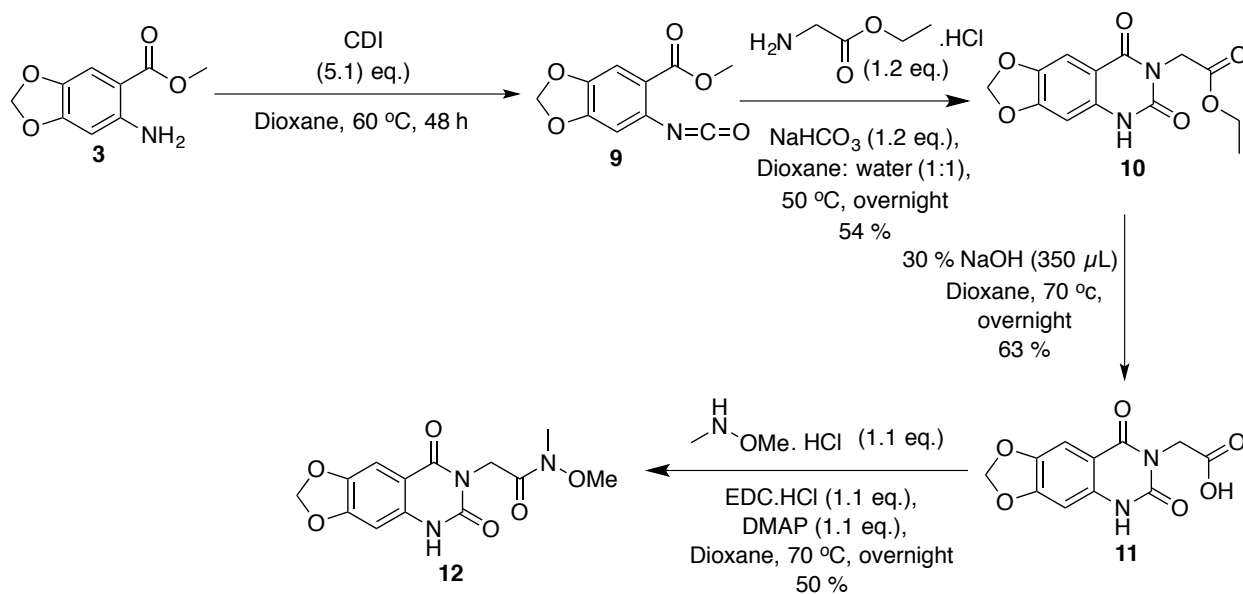
Scheme 3.3: Proposed synthesis of aldehyde **6**.

Compound **7** when treated with bromoacetaldehyde diethyl acetal in the presence of potassium carbonate and DMF as solvent, a very faint new spot was formed. The reaction did not seem to proceed even after heating for 24 hours. It might be due to reduced reactivity of the acetal towards the -NH of **7**.

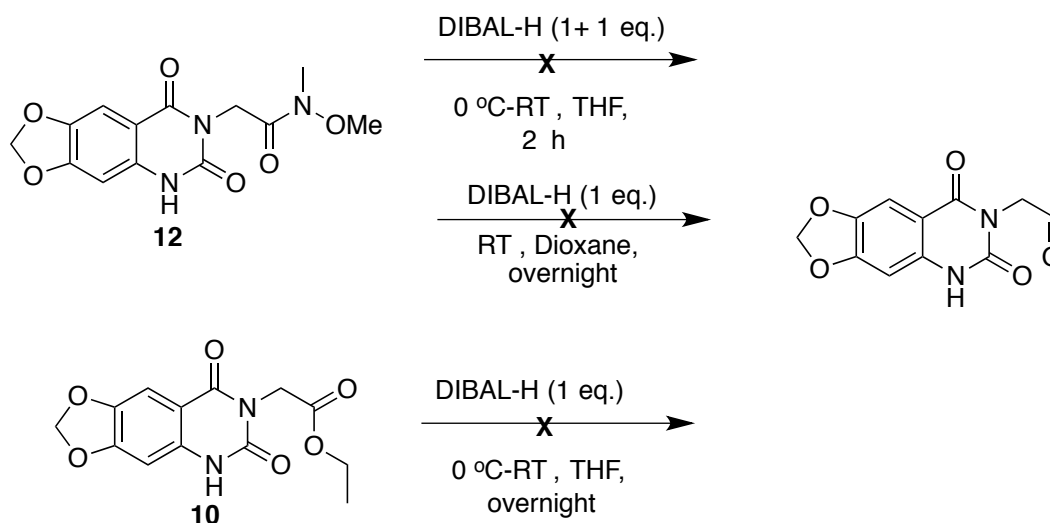


Scheme 3.4: Synthesis of acetal.

An alternative route was carried out wherein the amine **3**, was treated with CDI to form the isocyanate **9**, which was in turn treated with glycine ethyl ester hydrochloride to give 1,3-dioxoloquinazolidinedione ethyl ester **10**. Since Weinreb amides are known to give only aldehydes on reduction and not alcohols, the ester was reduced to an acid **11** using 30 % aqueous sodium hydroxide solution which was then coupled with N,O-Dimethylhydroxylamine hydrochloride to form the Weinreb amide **12** (Scheme 3.5). Unfortunately, neither the Weinreb amide nor the ester could be reduced to aldehyde using DIBAL-H (Scheme 3.6).

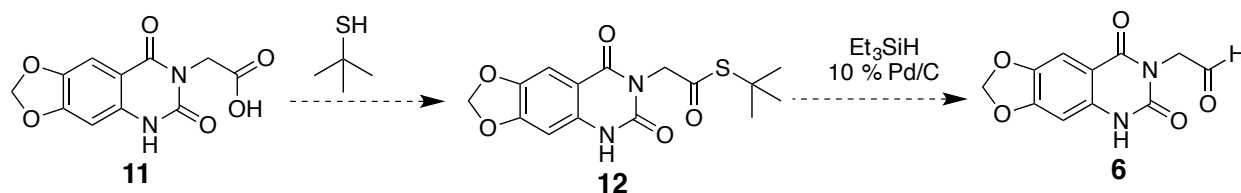


Scheme 3.5: Synthesis of Weinreb amide **12**.



Scheme 3.6: Reduction of Weinreb amide and ester to aldehyde.

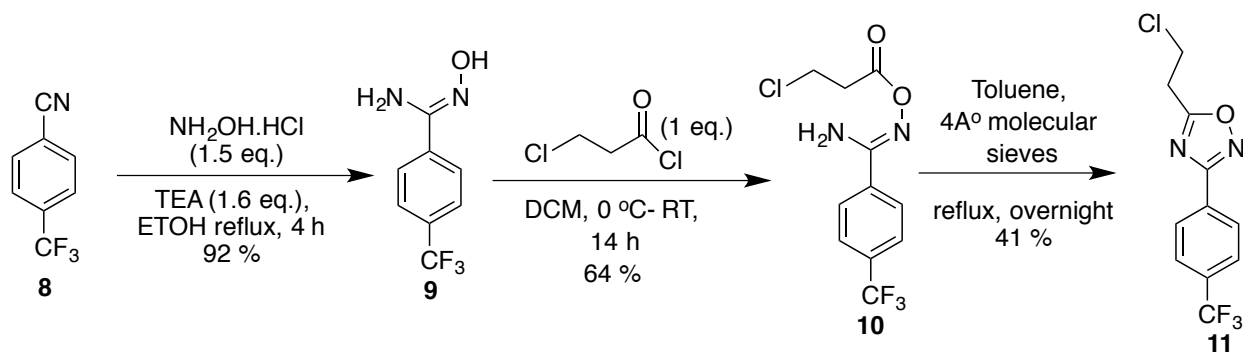
Another plausible route that might be worth trying would be worth trying is treatment of acid **11** with t-butyl thiol to give **12** which can be subjected to Fukuyama reduction to give the aldehyde **6** (Scheme 3.7).¹¹



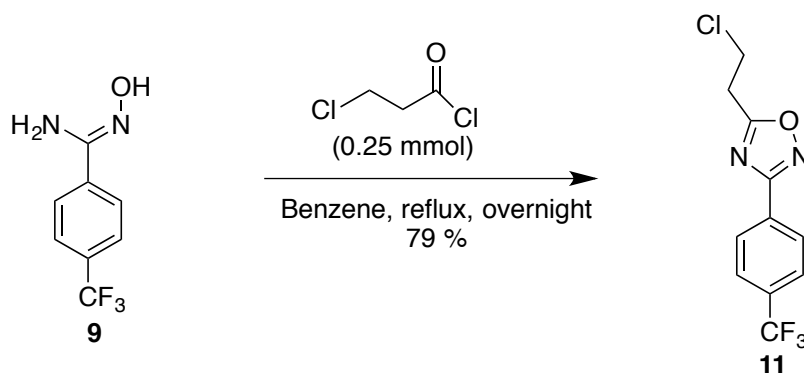
Scheme 3.7: Fukuyama reduction to synthesize **6**.

3.2.2. Resynthesis of 5-chloroethyl-3-(4-trifluoromethylphenyl)-[1,2,4]oxadiazole

5-chloroethyl-3-(4-trifluoromethylphenyl)-[1,2,4]oxadiazole had to be resynthesized to get the analytical data such as NMR and HRMS. 4-trifluoromethylbenzotrile was treated with hydroxylamine hydrochloride in the presence of triethylamine and ethanol to give **9** in 92 % yield. **8** was treated with chloropropionyl chloride in DCM to give the acylated product **10** in 64 % yield. Compound **10** was refluxed in toluene overnight with molecular sieves to aid cyclisation and dehydration resulting in **11** in 41 % yield (Scheme 3.8).

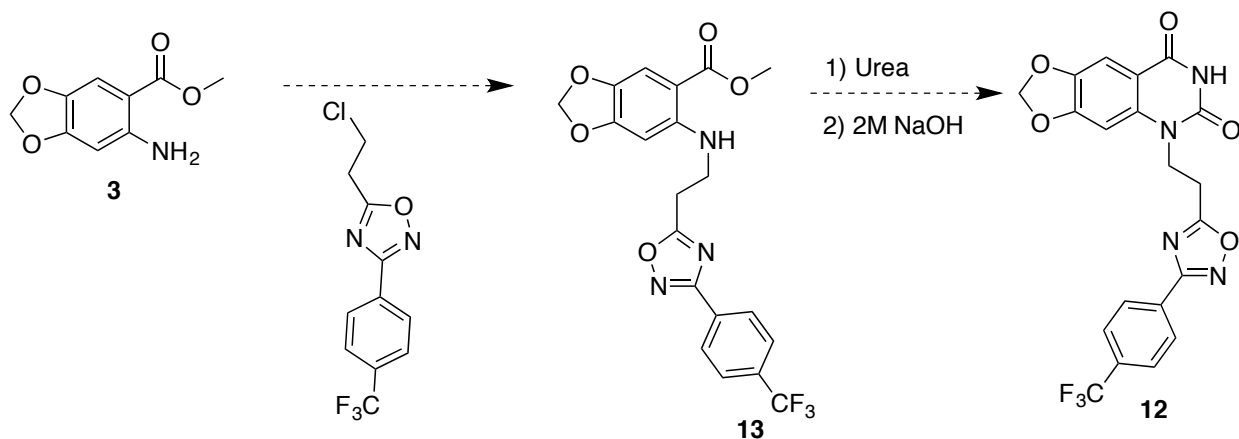


Scheme 3.8: Synthesis of 5-chloroethyl-3-(4-trifluoromethylphenyl)-[1,2,4]oxadiazole. Alternately, compound **11** could be synthesized directly for compound **9** by refluxing with chloroacetyl chloride and benzene as solvent (Scheme 3.9).¹²



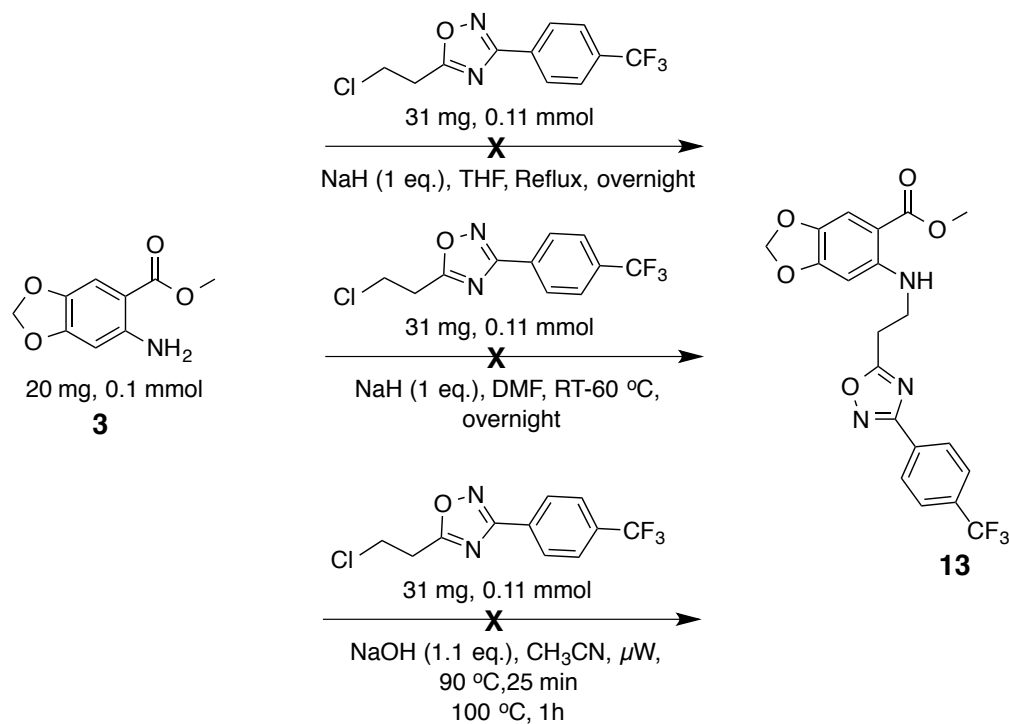
Scheme 3.9: Synthesis of 5-chloroethyl-3-(4-trifluoromethylphenyl)-[1,2,4]oxadiazole.

Since ChemDiv E843-1064 had good inhibitory activity against BoNT/A, its regioisomer **12** might be an interesting molecule to synthesize in order to understand the SAR. The plan was to carry out a nucleophilic substitution on **11** using **3** in the presence of a base. Then compound **3** would be treated with urea and NaOH to undergo cyclisation to give compound **12**.



Scheme 3.10: Proposed synthesis of **12**.

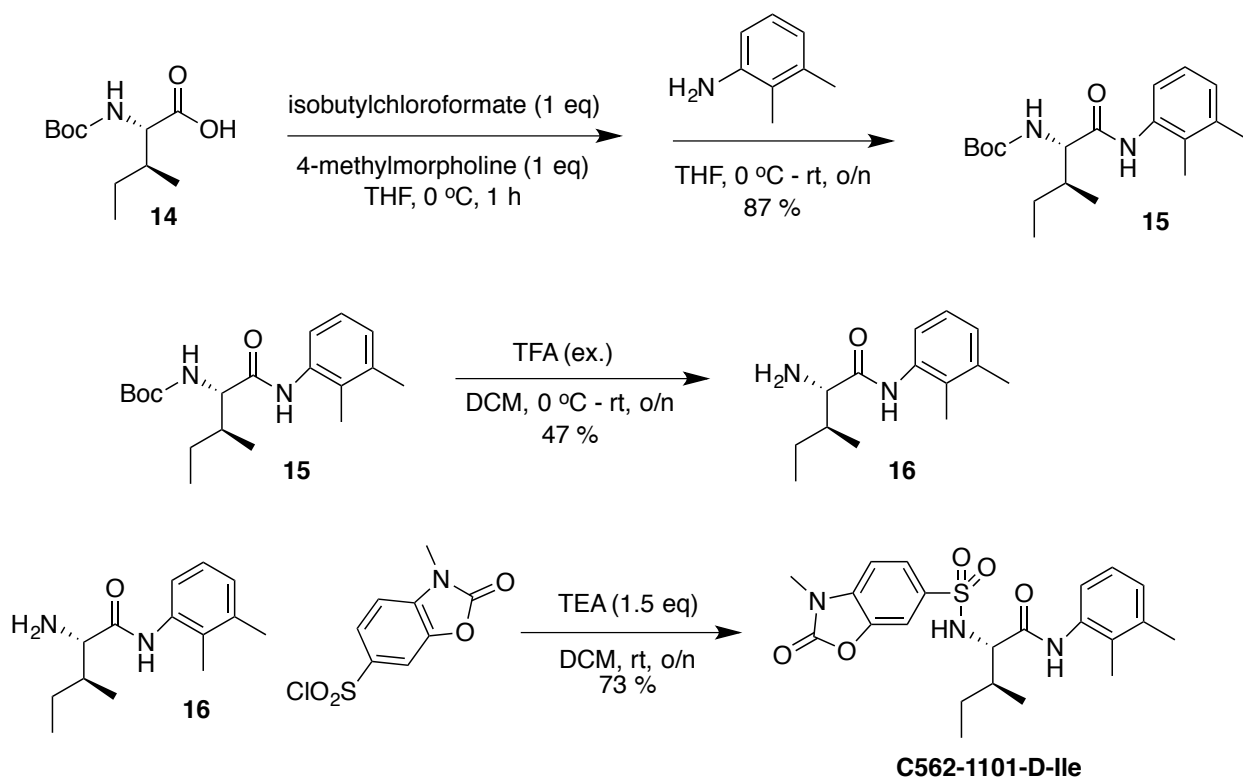
Several attempts were made for the synthesis of intermediate **13**. Compound **3** was treated with **11** in the presence of sodium hydride (NaH) and refluxed with solvents like THF and DMF, but none of them worked. The reaction was also carried out in the microwave reactor with acetonitrile as solvent. Unfortunately, the reaction did not proceed and starting material was recovered. The amine might not have been sufficiently nucleophilic to attack the halogen and bring about a substitution reaction.



Scheme 3.11: Synthesis of **13**.

3.2.3. Synthesis of C562-1101-D-Ile

Previously leucine analog of ZINC20284316 was synthesized as BoNT/E inhibitor. Since the natural ligand RIME has isoleucine, an isoleucine analog of ZINC20284316 was synthesized and tested. Unfortunately, there was not much of a difference in the inhibitory activity. (R)-Le-C562-1101 displayed IC₅₀ of 14 μM, while (R)-Ile-C562-1101 displayed IC₅₀ of 16 μM against BoNT/E.¹³ Modification of Isoleucine started with N-Boc-IsoLeu. The carboxylic acid was activated with isobutylchloroformate to generate the mixed-anhydride, and then treated with 2,3-dimethylaniline to furnish the amide in excellent yield. Boc protecting group was removed with TFA to give the free amine in quantitative yield. The free amine was reacted with N-methylbenzoxalinonylsulfonyl chloride to give the final compound (Scheme 3.12).¹³



Scheme 3.12: Synthesis of C562-1101-D-Ile

3.3. Conclusion

Several attempts were made towards the synthesis of aldehyde 6. Unfortunately none of them resulted in the desired product. Fukuyama reaction might be a good alternative route to carry out the synthesis of 6.

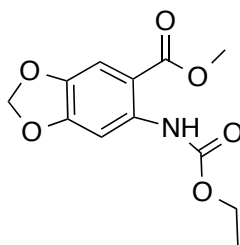
3.4. Experimental section

Methods. ^1H and ^{13}C NMR spectra were measured on Bruker 300, 400 or 500 MHz NMR spectrometer. Melting points were measured on a Thomas Hoover Capillary melting point apparatus and are uncorrected. TLC was performed on silica coated aluminum sheets (thickness 200 μm) or alumina coated (thickness 200 μm) aluminum sheets supplied by Sorbent Technologies and column chromatography was carried out on Siliaflash® P60 silica gel, 40-63 μm (230-400 mesh) supplied by Silicycle. Aluminum oxide, activated, neutral, Brockmann Grade I, 58 Å , was supplied by Alfa Aesar. High-resolution mass spectrometric analyses were carried out by ICB&DD at Stony Brook University using Agilent LC-UV-TOF. Analytical HPLC in reverse phase was carried out with a Shimadzu LC-2010AHT HPLC system using a Waters Nova-Pak C18 (60 Å , 4 μm , 3.9 mm, 150 mm) analytical column with water/acetonitrile as mobile phase. Chiral HPLC was carried out in normal phase with a Shimadzu LC-2010AHT HPLC system using

CHIRALCEL-ODH (5 μ m, 4.6 mm, 150 mm) column with isopropylalcohol as mobile phase.

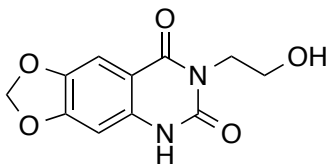
Materials. Solvents (HPLC grade or better), and all the other chemicals were purchased from Fisher Scientific Co. (Pittsburgh, PA). The chemicals were purchased from Aldrich Co., Synquest Inc. and Sigma. Tetrahydrofuran (THF) was freshly distilled from sodium metal and benzophenone. Dichloromethane was also distilled immediately prior to use under nitrogen from calcium hydride.

Methyl -6- (ethoxycarbonyl)amino-1,3-benzodioxole-5-carboxylate (4)



Methyl-6-amino-1,3-benzodioxole-5-carboxylate (0.1 g, 0.5 mmol), was dissolved in THF and heated at 85 °C, followed by the addition of ethyl chloroformate (0.77 mmol, 1.5 eq.) and the reaction mixture was refluxed at 85 °C overnight. The reaction mixture was cooled to room temperature and the solvent was removed by rotary evaporation to give the crude product. Recrystallization of the crude product using DCM: Hexanes as solvent resulted in pure brown solid (0.13 g, 97 % yield). ¹H NMR (300 MHz, CDCl₃) δ 1.31 (t, 3 H, J = 7.1 Hz), 3.87 (s, 3 H), 4.21 (q, 2 H, J = 7.1 Hz), 5.99 (s, 2 H), 7.39 (s, 1 H), 8.04 (s, 1 H), 10.66 (br. s, 1 H).

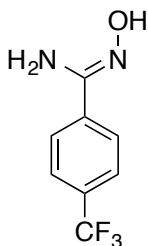
3- (2-Hydroxyethyl)-6,7-methylenedioxy-quinazoline-2,4(1H,3H)-dione (5)



Methyl -6- (ethoxycarbonyl)amino-1,3-benzodioxole-5-carboxylate (0.15 g, 0.56 mmol) was dissolved in chloroform in a sealed tube followed by the addition of ethanol amine (1.7 g, 50 eq.). The reaction mixture was heated at 150 °C for 4 hours. Solid crashed out when the reaction mixture was cooled down to room temperature. The reaction mixture was diluted with water and neutralized with 12 N HCl to pH 6. The solid product was filtered and washed with isopropyl alcohol to give white solid (55 mg, 39 % yield). ¹H NMR (300 MHz, DMSO-D₆) δ 3.51 (t, 2 H, J

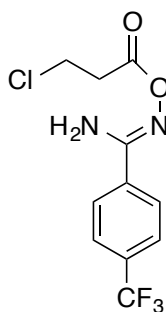
= 6.5 Hz), 3.93 (t, 2 H, J = 6.5 Hz), 4.75 (br. s, 1 H), 6.11 (s, 2 H), 6.63 (s, 1 H), 7.24 (s, 1 H). MS (ESI) m/z 249.05 (M-1)⁺.

4-Trifluoromethyl-N-hydroxybenzamidine (9)



A mixture of 4-trifluoromethyl benzonitrile (0.5 g, 3 mmol), hydroxylamine hydrochloride (4.38 mmol, 1.5 eq.) and triethylamine (4.67 mmol, 1.6 eq.) was refluxed in ethanol at 88 °C for 4 hours. Solvent was removed by concentrating in vacuo. The crude product was washed with brine (3x 25 mL), water (3x 25 mL) and extracted with dichloromethane. The organic layer was dried with magnesium sulfate, filtered and evaporated. Column chromatography of the crude product on silica gel using hexanes: ethyl acetate (1:1) as eluent resulted in pure white solid (550 mg, 92 % yield). ¹H NMR (300 MHz, CDCl₃) δ 4.95 (br. s, 2 H), 7.65 (d, 2 H, J = 8.2 Hz), 7.75 (d, 2 H, J = 8.5 Hz), 8.99 (br. s, 1 H). ¹³C NMR (100 MHz, CDCl₃) δ 120.78, 122.94, 125.11, 125.85, 125.91, 126.45, 126.66, 127.27, 131.77, 132.03, 132.29, 132.55, 135.98, 151.74. MS (ESI) m/z 205.05 (M+1)⁺. The analytical data was consistent with literature data.³

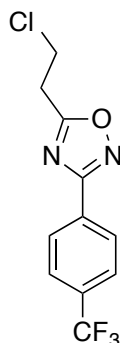
(Z)-N²-(2-Chloropropanoyloxy)benzimidamide (10)



4-trifluoromethyl-N-hydroxybenzamidine (0.5 g, 2.45 mmol) was dissolved in dichloromethane followed by the addition of chloropropionyl chloride (2.45 mmol, 1 eq.) at 0 °C. The reaction mixture was gradually allowed to warm up to room temperature overnight. The reaction mixture was washed with sodium bicarbonate (30 mL X 2), brine (25 mL X 2), water (25 mL) and extracted with dichloromethane. The organic layer was dried with magnesium sulfate, filtered and

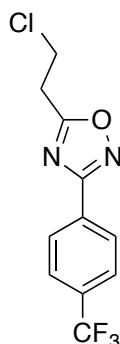
evaporated. Column chromatography of the crude product on silica gel using hexanes: ethyl acetate (1:1) as eluent resulted in pure white solid (0.46 g, 64 %). ^1H NMR (500 MHz, CDCl_3) δ 3.01 (t, 2 H, $J = 6.6$ Hz), 3.86 (t, 2 H, $J = 6.6$ Hz), 5.2 (br. s, 2 H), 7.68 (d, 2 H, $J = 8.3$ Hz), 7.82 (d, 2 H, $J = 8.2$ Hz). ^{13}C NMR (100 MHz, CDCl_3) δ 36.82, 39.19, 120.56, 122.73, 124.9, 125.96, 126.02, 127.07, 127.45, 132.89, 133.15, 133.41, 133.67, 134.56, 155.7, 168.2.

5-Chloroethyl-3-(4-trifluoromethylphenyl)-[1,2,4]Oxadiazole (11)



(*Z*)-*N*'-(2-chloropropanoyloxy)benzimidamide (0.4 g, 1.4 mmol) was refluxed in toluene in the presence of 4 Å molecular sieves for 24 hours. The reaction mixture was concentrated in vacuo and purified via column chromatography using silica gel and DCM: Hexanes (gradient 20 % - 50 % DCM) to give product as colorless oil (0.14 g, 42 % yield). ^1H NMR (500 MHz, CDCl_3) δ 3.45 (t, 2 H, $J = 6.9$ Hz), 4.0 (t, 2 H, $J = 6.9$ Hz), 7.75 (d, 2 H, $J = 8.2$ Hz), 8.21 (d, 2 H, $J = 8.1$ Hz). ^{13}C NMR (100 MHz, CDCl_3) δ 30.53, 39.57, 120.70, 122.87, 125.03, 126.06, 126.09, 126.12, 126.15, 127.2, 128.05, 130.18, 132.85, 133.11, 133.37, 133.63, 167.73, 177.02; HRMS (ESI) m/z calcd for $[\text{M}+\text{H}]^+$ $\text{C}_{11}\text{H}_9\text{ClF}_3\text{N}_2\text{O}$: 277.0350, found 277.0348 (Δ 0.7 ppm).

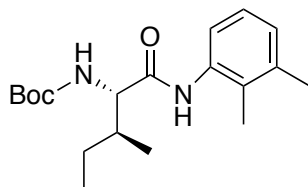
5-Chloroethyl-3-(4-trifluoromethylphenyl)-[1,2,4]Oxadiazole (11)



4-trifluoromethyl-*N*-hydroxybenzimidine (0.1 g, 0.5 mmol) was dissolved in benzene to which chloropropionyl chloride (0.25 mmol, 0.5 eq.) dissolved in benzene was added drop wise. The reaction mixture was refluxed overnight at 90 °C. The reaction mixture was concentrated in vacuo

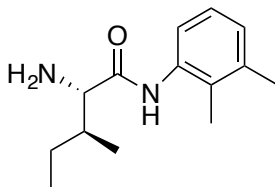
and purified via column chromatography using silica gel and DCM: Hexanes (gradient 20 % - 50 % DCM) to give product as colorless oil (0.05 g, 79 % yield). ^1H NMR (500 MHz, CDCl_3) δ 3.45 (t, 2 H, $J = 6.9$ Hz), 4.0 (t, 2 H, $J = 6.9$ Hz), 7.75 (d, 2 H, $J = 8.2$ Hz), 8.21 (d, 2 H, $J = 8.1$ Hz). ^{13}C NMR (100 MHz, CDCl_3) δ 30.53, 39.57, 120.70, 122.87, 125.03, 126.06, 126.09, 126.12, 126.15, 127.2, 128.05, 130.18, 132.85, 133.11, 133.37, 133.63, 167.73, 177.02; HRMS (ESI) m/z calcd for $[\text{M}+\text{H}]^+$ $\text{C}_{11}\text{H}_9\text{ClF}_3\text{N}_2\text{O}$: 277.0350, found 277.0348 (Δ 0.7 ppm).³

N-Boc-D-isoleu-N'-(2,3-dimethylphenyl)amide (15)



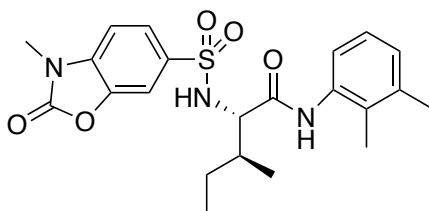
To a solution of N-Boc-Isoleucine (0.500 g, 2.16 mmol) in THF (10 mL) was added 4-methylmorpholine (0.219 g, 2.16 mmol) and the solution was cooled to 0 °C. Isobutylchloroformate (0.295 g, 2.16 mmol) in THF (3 mL) was added to the reaction mixture, and was stirred at 0 °C for 30 min. The aniline (0.262 g, 2.16 mmol) in THF (2 mL) was added to the reaction mixture, which was stirred at room temperature overnight. The volatiles were removed in vacuo, and the residue was dissolved in EtOAc, and then the organic layer was washed with Sat. NaHCO_3 , water, brine, dried over MgSO_4 , and concentrated to afford the product as off-white solid (0.625 g, 87 %): mp: 158-160 °C; ^1H NMR (500 MHz, CDCl_3) δ 7.74 (s, 1H), 7.48 (d, $J = 7.6$ Hz, 1H), 7.08 (t, $J = 7.4$ Hz, 1H), 7.0 (d, $J = 7$ Hz, 1H), 5.13 (s, 1H), 4.08 (t, $J = 7.2$ Hz, 1H), 2.27 (s, 3H), 2.12 (s, 3H), 2.06 – 2.04 (m, 1H), 1.60 – 1.58 (m, 1H), 1.45 (s, 9 H), 1.22 – 1.18 (m, 1H), 1.03 (d, $J = 6.5$ Hz, 3H), 0.94 (t, $J = 7.2$ Hz, 3H); ^{13}C NMR (101 MHz, CDCl_3) δ 170.35, 156.28, 137.61, 135.21, 129.38, 127.59, 126.02, 122.11, 80.42, 60.29, 36.77, 28.52, 25.01, 20.77, 16.05, 13.88, 11.58; HRMS (ESI-TOF) m/z calcd for $[\text{M}+\text{H}]^+$ $\text{C}_{19}\text{H}_{30}\text{N}_2\text{O}_3$: 335.2329, found 335.2336 (Δ -1.95 ppm).

D-Isoleu-N'-(2,3-dimethylphenyl)amide (16)



N-Boc-isoleu-N'-(2,3-dimethylphenyl)amide (0.63 g, 1.87 mmol) in DCM (20 mL) was cooled to 0 °C, and TFA (1 mL) was added drop wise and the reaction mixture was allowed to warm to room temperature and stirred overnight. Water was added to the reaction mixture, and K₂CO₃ was added in small portions until evolution of gas stopped. Organic layer was separated and then washed with water, brine, dried over MgSO₄, and concentrated to afford the title compound as off-white solid (0.2 g, 47 %): m.p: 82–85 °C; ¹H NMR (400 MHz, CDCl₃) δ 9.53 (s, 1H), 7.82 (d, J = 6.4 Hz, 1H), 7.10 (t, J = 6.3 Hz, 1H), 6.95 (d, J = 6 Hz, 1H), 3.49 (s, 1H), 2.29 (s, 3H), 2.16- 2.11 (m, 4H), 1.72 (br. s, 2H), 1.51 – 1.41 (m, 1H), 1.21 – 1.11 (m, 1H), 1.03 (d, J = 6 Hz, 3H), 0.92 (t, J = 9.8 Hz, 3H); ¹³C NMR (100 MHz, CDCl₃) δ 172.47, 137.28, 135.90, 127.39, 126.52, 126.12, 126.18, 60.58, 38.07, 23.92, 20.85, 16.56, 13.70, 12.11; HRMS (ESI-TOF) m/z calcd for [M+H]⁺ C₁₄H₂₂N₂O: 235.1805, found 235.1813 (Δ -3.48 ppm).

C562-1101-D-Ile



Isoleu-N'-(2,3-dimethylphenyl)amide (0.12 g, 0.53 mmol) and sulfonyl chloride (0.159-0.2 g, 0.64-0.8 mmol) in DCM (10 mL) was added TEA (0.065-0.08 g, 0.64-0.8 mmol) and the reaction mixture was stirred overnight. The reaction mixture was diluted with DCM/MeOH, and then washed with water, brine, dried over MgSO₄, and concentrated. The product was recrystallized from DCM/MeOH to afford the title compound as white solid (0.17 g, 73%): mp: >250 °C; ¹H NMR (400 MHz, DMSO) δ 9.36 (s, 1H), 8.07 (d, J = 9.6 Hz, 1H), 7.70 – 7.68 (m, 1 H), 7.36 (d, J = 8.7 Hz, 1H), 6.90 (d, J = 7.6 Hz, 1H), 6.82 (t, J = 7.7 Hz, 1H), 6.47 (d, J = 7.8 Hz, 1H), 3.79 (t, J = 8.8 Hz, 1H), 3.32 (s, 3H), 2.16 (s, 3H), 1.88 (s, 3H), 1.61 – 1.72 (m, 1H), 1.59 – 1.47 (m, 1H), 1.22 – 1.06 (m, 1H), 0.87 (d, J = 6.8 Hz, 3H), 0.81 (t, J = 7.4 Hz, 3H); ¹³C NMR (100 MHz, CDCl₃) δ 169.00, 153.81, 141.22, 136.80, 135.28, 135.04, 134.99, 130.27, 126.64, 124.54, 123.36, 122.58, 108.88, 108.16, 60.91, 37.09, 28.31, 24.34, 20.05, 15.25, 13.65, 10.60. HRMS (ESI-TOF) m/z calcd for [M+H]⁺ C₂₂H₂₇N₃O₅S: 446.1744, found : 446.175 (Δ = -1.33 ppm).

3.5. References

- (1) Nigam, P.; Nigam, A. Botulinum Toxin. *Indian J. Dermatol.* **2010**, *55* (1), 8.
- (2) Dennis, D. T.; Inglesby, T. V.; Henderson, D. a; Bartlett, J. G.; Ascher, M. S.; Eitzen, E.; Fine, a D.; Friedlander, a M.; Hauer, J.; Layton, M.; et al. Tularemia as a Biological Weapon: Medical and Public Health Management. *JAMA* **2001**, *285* (21), 2763–2773.
- (3) Teng, Y.-H. G.; Berger, W. T.; Nesbitt, N. M.; Kumar, K.; Balius, T. E.; Rizzo, R. C.; Tonge, P. J.; Ojima, I.; Swaminathan, S. Computer-Aided Identification, Synthesis, and Biological Evaluation of Novel Inhibitors for Botulinum Neurotoxin Serotype A. *Bioorg. Med. Chem.* **2015**, *23* (17), 5489–5495.
- (4) Zhang, Y.; Lou, J.; Jenko, K. L.; Marks, J. D.; Varnum, S. M. Simultaneous and Sensitive Detection of Six Serotypes of Botulinum Neurotoxin Using Enzyme-Linked Immunosorbent Assay-Based Protein Antibody Microarrays. *Anal. Biochem.* **2012**, *430* (2), 185–192.
- (5) Arnon, S. S.; Schechter, R.; Inglesby, T. V.; Henderson, D. A.; Bartlett, J. G.; Ascher, M. S.; Eitzen, E.; Fine, A. D.; Hauer, J.; Layton, M.; et al. Botulinum Toxin as a Biological Weapon. *JAMA* **2001**, *285* (8), 1059.
- (6) Benoit, R. M.; Frey, D.; Wieser, M. M.; Thielges, K. M.; Jaussi, R.; Capitani, G.; Kammerer, R. A. Structure of the BoNT/A1 – Receptor Complex. *Toxicon* **2015**, *107*, 25–31.
- (7) Rossetto, O.; Pirazzini, M.; Montecucco, C. Botulinum Neurotoxins: Genetic, Structural and Mechanistic Insights. *Nat. Rev. Microbiol.* **2014**, *12* (8), 535–549.
- (8) Balius, T. E.; Mukherjee, S.; Rizzo, R. C. Implementation and Evaluation of a Docking-Rescoring Method Using Molecular Footprint Comparisons. *J. Comput. Chem.* **2011**, *32* (10), 2273–2289.
- (9) Kumaran, D.; Rawat, R.; Ludivico, M. L.; Ahmed, S. A.; Swaminathan, S. Structure- and Substrate-Based Inhibitor Design for Clostridium Botulinum Neurotoxin Serotype A. *J. Biol. Chem.* **2008**, *283* (27), 18883–18891.
- (10) Li, Z.; Zhu, A.; Yang, J. One-Pot Three-Component Mild Synthesis of 2-Aryl-3-(9-Alkylcarbazol-3-Yl)thiazolin-4-Ones. *J. Heterocycl. Chem.* **2012**, *49* (Scheme 1), 1458–1461.
- (11) Oyama, H.; Orimoto, K.; Niwa, T.; Nakada, M. Highly Enantioselective Catalytic

Asymmetric Mukaiyama-Michael Reactions of Cyclic α -Alkylidene β -Oxo Imides.
Tetrahedron Asymmetry **2015**, 26 (5-6), 262–270.

- (12) Dürüst, Y.; Karakuş, H.; Kaiser, M.; Tasdemir, D. Synthesis and Anti-Protozoal Activity of Novel dihydropyrrolo[3,4-d][1,2,3]triazoles. Eur. J. Med. Chem. **2012**, 48, 296–304.
- (13) Zhou, Y.; McGillick, B. E.; Teng, Y.-H. G.; Haranahalli, K.; Ojima, I.; Swaminathan, S.; Rizzo, R. C. Identification of Small Molecule Inhibitors of Botulinum Neurotoxin Serotype E via Footprint Similarity. Bioorg. Med. Chem. **2016**.

Chapter 4

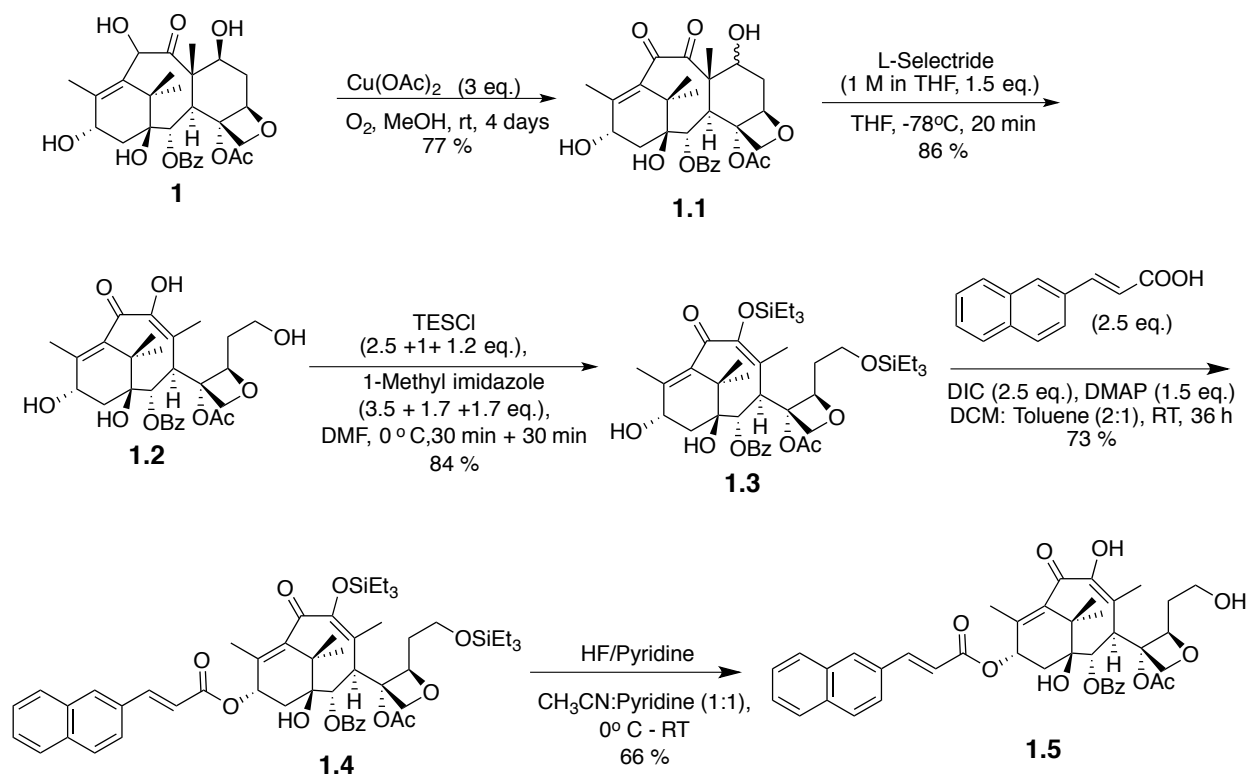
Resynthesis of SB-RA-5001

4.1. Introduction.....	119
4.2. Results and discussion	119
4.3. Conslusion	120
4.4. Expremental Section	120
4.5. References.....	123

4. Resynthesis of SB-RA-5001

4.1. Introduction

Tubulin and FtsZ share 10-18 % sequence similarity, tubulin inhibitors were used as a starting point to identify inhibitors for FtsZ. A library of compounds containing taxol-like compounds and noncytotoxic taxane multidrug reversal agents were tested for antibacterial activity. SB-RA-2001 and SB-T-0032 were selected for further studies based on MIC and cytotoxicity results. The C-seco baccation analogue of taxane IDN5390 was found to be less cytotoxic than paclitaxel. Hence C-seco analogues of SB-RA-2001 were made and were found to have good Mtb activity (MIC 1.25-2.5 μM) and less cytotoxic activity ($\text{IC}_{50} > 80 \mu\text{M}$).¹ SB-RA-5001 had to be resynthesized for one of our collaborators in Spain.



Scheme 4.1: Synthesis of SB-RA-5001.

4.2. Results and discussion

Oxidation of 10-DAB III in the presence of copper acetate resulted in **5.1** a mixture of the C-7 epimerized hydroxyl group. The epimers when treated with L-selectride underwent retro-aldol reductive fragmentation to give **5.2**. C-7, C-9 di-TES protection of **5.2** was done using TES-Cl. Di-TES product was separated from the mon-TES compound. **5.3** was coupled with 3-(2-Naphthyl)acrylic acid followed by treatment HF/pyridine to give **SB-RA-5001**.

4.3. Conclusion

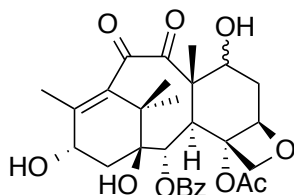
SB-RA-5001 was successfully synthesized and sent to the collaborator in Spain.

4.4. Experimental Section

Methods. ^1H and ^{13}C NMR spectra were measured on Bruker 300, 400 or 500 MHz NMR spectrometer. Melting points were measured on a Thomas Hoover Capillary melting point apparatus and are uncorrected. TLC was performed on silica coated aluminum sheets (thickness 200 μm) or alumina coated (thickness 200 μm) aluminum sheets supplied by Sorbent Technologies and column chromatography was carried out on Siliaflash® P60 silica gel, 40-63 μm (230-400 mesh) supplied by Silicycle. Aluminum oxide, activated, neutral, Brockmann Grade I, 58 Å, was supplied by Alfa Aesar. High-resolution mass spectra were obtained from the ICB&DD Mass Spectrometry Laboratory at Stony Brook University.

Materials. Solvents (HPLC grade or better), and all the other chemicals were purchased from Fisher Scientific Co. (Pittsburgh, PA). The chemicals were purchased from Aldrich Co., Synquest Inc. and Sigma. Tetrahydrofuran (THF) was freshly distilled from sodium metal and benzophenone. Dichloromethane was also distilled immediately prior to use under nitrogen from calcium hydride.

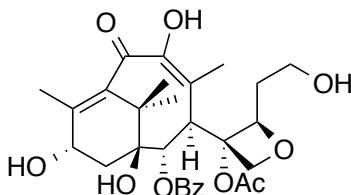
10-Dehydro-10-deacetylbaccatin (1.1)¹



10-DAB (0.7 g, 1.3 mmol) was suspended in methanol (25 mL), and $\text{Cu}(\text{OAc})_2$ (0.7 g, 4 mmol) was added in small portions, with vigorous mechanical stirring, over ca. 10 min. The reaction mixture was stirred unstoppered to allow contact with air. After 72 h, the reaction mixture was concentrated under vacuum and the residue was purified by column chromatography on silica gel, with a dichloromethane: methanol (95:5) resulted in 5 as beige solid (553 mg, 77 %). ^1H NMR (300 MHz, CDCl_3) δ 1.04 - 1.30 (m, 18 H), 1.67 - 1.73 (m, 6 H), 1.77 - 2.13 (m, 18 H), 2.23 - 2.40 (m, 12 H), 2.49 - 2.64 (m, 2 H), 3.65 (d, $J = 6.87$ Hz, 1 H), 3.84 (d, $J = 6.87$ Hz, 1 H), 4.29 - 4.34 (m, 2 H), 4.40 - 4.44 (m, 0.5 H), 4.61 (d, $J = 10.71$ Hz, 0.5 H), 4.87 - 5.03 (m, 4 H), 5.72 - 5.84 (m, 2 H), 7.46 - 7.54 (m, 4 H), 7.59 - 7.67 (m, 2 H), 8.07 - 8.15 (m, 4 H). Analytical data matches

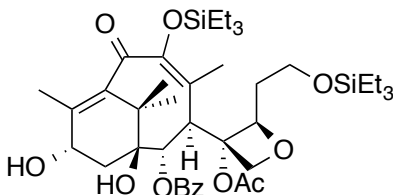
the reported results.¹

10-Dehydro-C-seco-10-deacetylbaecatin (1.2)¹



Compound 5.1 (0.4 g, 0.74 mmol) was suspended in dry THF. The suspension was cooled to -78 °C with vigorous stirring, followed by the addition of L-selectride (1.0 M in THF, 1.84 mL) drop wise. After addition. The reaction mixture was removed from the cold bath and worked up by the addition of ethyl acetate and 2 N H₂SO₄ (1.5 mL). The organic layer was washed with 2 N H₂SO₄ and brine. The crude material was purified by column chromatography on silica gel using dichloromethane: methanol (95:5) to give 5.2 as white solid (171 mg, 86 %), ¹H NMR (300 MHz, CDCl₃) δ 0.96 - 1.20 (m, 9 H), 1.80 (br. s., 6 H), 1.92 (s, 3 H), 2.00 - 2.17 (m, 2 H), 2.30 - 2.54 (m, 3 H), 2.61 - 2.94 (m, 3 H), 3.75 (d, J = 19.23 Hz, 2 H), 4.29 (br. s., 2 H), 4.83 - 4.96 (m, 1 H), 5.19 (br. s., 2 H), 5.56 (d, J = 9.07 Hz, 1 H), 6.50 (br. s., 1 H), 7.39 - 7.50 (m, 2 H), 7.53 - 7.62 (m, 1 H), 7.91 - 8.07 (m, 2 H). Analytical data matches the reported results.¹

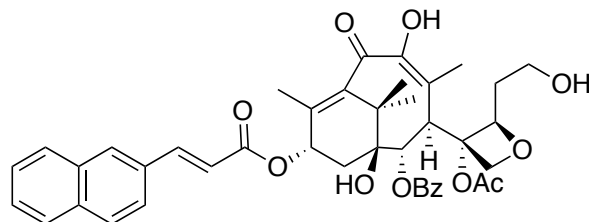
7,9-Bis(triethylsilyl)-10-dehydro-C-seco-10-deacetylbaecatin (1.3)¹



Compound 5.2 (0.16 g, 0.29 mmol) was dissolved in DMF and maintained at 0 °C, to this was added 1-Methylimidazole (109.7 μL, 1.38 mmol) and TESC1 (154 μL, 0.92 mmol). The reaction mixture was stirred for 30 min and was worked up by the addition of ethyl acetate and washed with water. The organic layer was collected, dried with magnesium sulfate, filtered and concentrated under vacuum to get the crude product. Column chromatography of the crude product using silica gel and Hexnes: EtOAc (2:1) as eluent resulted in 5.3 as pure white solid (0.13 g, 84 % conversion yield). ¹H NMR (300 MHz, CDCl₃) δ 0.53 - 0.83 (m, 12 H), 0.97 (q, J = 7.51 Hz, 18 H), 1.13 (d, J = 6.87 Hz, 6 H), 1.63 - 2.16 (m, 10 H), 3.51 - 3.92 (m, 2 H), 4.07 - 4.60 (m, 2 H), 4.91 (q, J = 7.69 Hz, 1 H), 5.20 (bs, 2 H), 5.57 (d, J = 9.07 Hz, 1 H), 7.43 - 7.52 (m, 2 H), 7.58 -

7.66 (m, 1 H), 8.01 (bs, 2 H). Analytical data matches the reported results.¹

Synthesis of SB-RA-5001 (5.5)¹



To a mixture of 1.3 (0.12 g, 0.16 mmol), acid (0.08 g, 0.4 mmol), DMAP (30 mg, 0.24 mmol) in dichloromethane: toluene (2:1) was added DIC (51 mg, 0.4 mmol) drop wise at room temperature. The reaction mixture was stirred at room temperature overnight, and the solvent was evaporated in vacuo. The residue was washed with brine (15 mL X 5) and extracted with ethyl acetate. The organic layer was collected, dried with magnesium sulfate, filtered and concentrated under vacuum to get the crude product. Purification of the crude product by short silica gel chromatography using ethyl acetate/hexane (2:3) as eluent afforded TES protected C-13 coupling product contaminated by DIC-acid complex, which was directly used in the next step.

The TES protected product in a mixture of pyridine: acetonitrile was cooled to 0 °C followed by the addition of HF/Pyridine (1.2 mL) drop wise. The reaction mixture was stirred overnight at room temperature. the reaction was quenched with NaHCO₃ solution and extracted with ethyl acetate and then dried over magnesium sulfate. Column chromatography of the crude product using silica gel and Hexnes: EtOAc (2:1) as eluent followed by recrystallization resulted in 5.5 as pure white solid (56 mg, 66 % yield).

¹H NMR (300 MHz, CDCl₃) δ 1.02 - 1.32 (m, 9 H), 1.79 - 2.38 (m, 15 H), 3.90 (br. s., 2 H), 4.36 (br. s., 2 H), 5.18 - 5.52 (m, 2 H), 5.65 (d, J = 9.07 Hz, 1 H), 6.09 - 6.23 (m, 1 H), 6.53 (s, 1 H), 6.71 (d, J = 15.38 Hz, 1 H), 7.39 - 8.21 (m, 13 H). Analytical data matches the reported results.¹

4.5. References

- (1) Huang, Q.; Kirikae, F.; Kirikae, T.; Pepe, A.; Amin, A.; Respicio, L.; Slayden, R. A.; Tonge, P. J.; Ojima, I. Targeting FtsZ for Antituberculosis Drug Discovery: Noncytotoxic Taxanes as Novel Antituberculosis Agents. *J. Med. Chem.* **2006**, 49 (2), 463–466.

Bibliography

Chapter 1

- (1) Kumar, V.; Abbas. K, A.; Aster, J. Robbins Basic Pathology, 8TH ed.; Elsevier, 2007.
- (2) World Health Organization (WHO). Global Tuberculosis Report 2015; 2015; Vol. 1.
- (3) Cucunawangsih; Wiwing, V.; Widysanto, A.; Lugito, N. P. H. Mycobacterium Tuberculosis Resistance Pattern against First-Line Drugs in Patients from Urban Area. *Int. J. Mycobacteriology* **2015**, 4 (4), 302–305.
- (4) Lee, J. Y. Diagnosis and Treatment of Extrapulmonary Tuberculosis. *Tuberc. Respir. Dis. (Seoul)*. **2015**, 78 (2), 47.
- (5) Hauck, F. R.; Neese, B. H.; Panchal, A. S.; El-Amin, W. Identification and Management of Latent Tuberculosis Infection. *Am. Fam. Physician* **2009**, 79 (10), 879–886.
- (6) Swaminathan, S.; Padmapriyadarsini, C.; Narendran, G. Diagnosis & Treatment of Tuberculosis in HIV Co-Infected Patients. *Indian J. Med. Res.* **2011**, 134 (6), 850.
- (7) CDC. Signs and symptoms of TB
<http://www.cdc.gov/tb/topic/basics/signsandsymptoms.htm> (accessed Jan 1, 2016).
- (8) CDC. Diagnosis of Tuberculosis Disease
<http://www.cdc.gov/tb/publications/factsheets/testing/diagnosis.htm>.
- (9) Poce, G.; Coccozza, M.; Consalvi, S.; Biava, M. SAR Analysis of New Anti-TB Drugs Currently in Pre-Clinical and Clinical Development. *Eur. J. Med. Chem.* **2014**, 86, 335–351.
- (10) Babu, G. R.; Laxminarayan, R. The Unsurprising Story of MDR-TB Resistance in India. *Tuberculosis* **2012**, 92 (4), 301–306.
- (11) WHO/Int/TB/data. Tuberculosis (Mdr-Tb). **2015**, No. November, 2014–2015.
- (12) TB Drugs – First line, second line & new TB drugs <http://www.tbfacts.org/tb-drugs/>.
- (13) CDC. TB Elimination Extensively Drug-Resistant Tuberculosis (XDR TB).
- (14) Lienhardt, C.; Vernon, A.; Raviglione, M. C. New Drugs and New Regimens for the Treatment of Tuberculosis: Review of the Drug Development Pipeline and Implications for National Programmes. *Curr. Opin. Pulm. Med.* **2010**, 16 (3), 186–193.
- (15) Mdluli, K.; Kaneko, T.; Upton, A. The Tuberculosis Drug Discovery and Development Pipeline and Emerging Drug Targets. *Cold Spring Harb. Perspect. Med.* **2015**, 5 (6), a021154–a021154.

- (16) Brigden, G.; Hewison, C.; Varaine, F. New Developments in the Treatment of Drug-Resistant Tuberculosis: Clinical Utility of Bedaquiline and Delamanid. *Infect. Drug Resist.* **2015**, *8*, 367–378.
- (17) European Medicines Agency recommends two new treatment options for tuberculosis http://www.ema.europa.eu/ema/index.jsp?curl=pages/news_and_events/news/2013/11/news_detail_001972.jsp&mid=WC0b01ac058004d5c1.
- (18) Leibert, E. New Drugs to Treat Multidrug-Resistant Tuberculosis; the Case for Bedaquiline.pdf. **2014**, 597–602.
- (19) Szumowski, J. D.; Lynch, J. B. Profile of Delamanid for the Treatment of Multidrug-Resistant Tuberculosis. *Drug Des. Devel. Ther.* **2015**, *9*, 677–682.
- (20) Tadolini, M.; Lingsang, R. D.; Tiberi, S.; Enwerem, M.; D’Ambrosio, L.; Sadutshang, T. D.; Centis, R.; Migliori, G. B. First Case of Extensively Drug-Resistant Tuberculosis Treated with Both Delamanid and Bedaquiline: TABLE 1. *Eur. Respir. J.* **2016**, ERJ – 00637–02016.
- (21) Kumar, K.; Awasthi, D.; Lee, S. Y.; Zanardi, I.; Ruzsicska, B.; Knudson, S.; Tonge, P. J.; Slayden, R. a.; Ojima, I. Novel Trisubstituted Benzimidazoles, Targeting Mtb FtsZ, as a New Class of Antitubercular Agents. *J. Med. Chem.* **2011**, *54* (1), 374–381.
- (22) Mukherjee, A.; Lutkenhaus, J. Guanine Nucleotide-Dependent Assembly of FtsZ into Filaments. *J. Bacteriol.* **1994**, *176* (9), 2754–2758.
- (23) Nogales, E.; Wolf, S. G.; Downing, K. H. Structure of the Alpha Beta Tubulin Dimer by Electron Crystallography. *Nature* **1998**, *391* (6663), 199–203.
- (24) Leung, A. K. W.; Lucile White, E.; Ross, L. J.; Reynolds, R. C.; DeVito, J. A.; Borhani, D. W. Structure of Mycobacterium Tuberculosis FtsZ Reveals Unexpected, G Protein-like Conformational Switches. *J. Mol. Biol.* **2004**, *342* (3), 953–970.
- (25) Goehring, N. W.; Beckwith, J. Diverse Paths to Midcell: Assembly of the Bacterial Cell Division Machinery. *Curr. Biol.* **2005**, *15* (13), R514–R526.
- (26) Errington, J.; Daniel, R. A.; Scheffers, D.-J. Cytokinesis in Bacteria. *Microbiol. Mol. Biol. Rev.* **2003**, *67* (1), 52–65.
- (27) Kumar, K.; Awasthi, D.; Berger, W. T.; Tonge, P. J.; Slayden, R. A.; Ojima, I. Discovery of Anti-TB Agents That Target the Cell-Division Protein FtsZ. *Future Med. Chem.* **2010**, *2* (8), 1305–1323.

- (28) Haranahalli, K.; Tong, S.; Ojima, I. Recent Advances in the Discovery and Development of Antibacterial Agents Targeting the Cell-Division Protein FtsZ. *Bioorg. Med. Chem.* **2016**.
- (29) Erickson, H. P.; Anderson, D. E.; Osawa, M. FtsZ in Bacterial Cytokinesis: Cytoskeleton and Force Generator All in One. *Microbiol. Mol. Biol. Rev.* **2010**, 74 (4), 504–528.
- (30) Margolin, W. FtsZ and the Division of Prokaryotic Cells and Organelles. *Nat. Rev. Mol. Cell Biol.* **2005**, 6 (11), 862–871.
- (31) Huang, Q.; Kirikae, F.; Kirikae, T.; Pepe, A.; Amin, A.; Respicio, L.; Slayden, R. A.; Tonge, P. J.; Ojima, I. Targeting FtsZ for Antituberculosis Drug Discovery: Noncytotoxic Taxanes as Novel Antituberculosis Agents. *J. Med. Chem.* **2006**, 49 (2), 463–466.
- (32) Ojima, I.; Kumar, K.; Awasthi, D.; Vineberg, J. G. Drug Discovery Targeting Cell Division Proteins, Microtubules and FtsZ. *Bioorg. Med. Chem.* **2014**, 22 (18), 5060–5077.
- (33) Sarcina, M.; Mullineaux, C. W. Effects of Tubulin Assembly Inhibitors on Cell Division in Prokaryotes in Vivo. *FEMS Microbiol. Lett.* **2000**, 191 (1), 25–29.
- (34) Slayden, R. a.; Knudson, D. L.; Belisle, J. T. Identification of Cell Cycle Regulators in Mycobacterium Tuberculosis by Inhibition of Septum Formation and Global Transcriptional Analysis. *Microbiology* **2006**, 152 (6), 1789–1797.
- (35) White, E. L. 2-Alkoxy-carbonylaminopyridines: Inhibitors of Mycobacterium Tuberculosis FtsZ. *J. Antimicrob. Chemother.* **2002**, 50 (1), 111–114.
- (36) Reynolds, R. C.; Srivastava, S.; Ross, L. J.; Suling, W. J.; White, E. L. A New 2-Carbamoyl Pteridine That Inhibits Mycobacterial FtsZ. *Bioorg. Med. Chem. Lett.* **2004**, 14 (12), 3161–3164.
- (37) Awasthi, D.; Kumar, K.; Knudson, S. E.; Slayden, R. A.; Ojima, I. SAR Studies on Trisubstituted Benzimidazoles as Inhibitors of Mtb FtsZ for the Development of Novel Antitubercular Agents. *J. Med. Chem.* **2013**, 56 (23), 9756–9770.
- (38) Knudson, S. E.; Awasthi, D.; Kumar, K.; Carreau, A.; Goullieux, L.; Lagrange, S.; Vermet, H.; Ojima, I.; Slayden, R. A. Cell Division Inhibitors with Efficacy Equivalent to Isoniazid in the Acute Murine Mycobacterium Tuberculosis Infection Model. *J. Antimicrob. Chemother.* **2015**, 70 (11), 3070–3073.
- (39) Knudson, S. E.; Awasthi, D.; Kumar, K.; Carreau, A.; Goullieux, L.; Lagrange, S.; Vermet, H.; Ojima, I.; Slayden, R. A. A Trisubstituted Benzimidazole Cell Division

- Inhibitor with Efficacy against Mycobacterium Tuberculosis. *PLoS One* **2014**, 9 (4), e93953.
- (40) Knudson, S. E.; Kumar, K.; Awasthi, D.; Ojima, I.; Slayden, R. A. In Vitro–in Vivo Activity Relationship of Substituted Benzimidazole Cell Division Inhibitors with Activity against Mycobacterium Tuberculosis. *Tuberculosis* **2014**, 94 (3), 271–276.
- (41) Ojima, I.; Awasthi, D.; Wei, L.; Haranahalli, K. Strategic Incorporation of Fluorine in the Drug Discovery of New-Generation Antitubercular Agents Targeting Bacterial Cell Division Protein FtsZ. *J. Fluor. Chem.* **2016**.
- (42) Colombo, M.; Bossolo, S.; Aramini, A. Phosphorus Trichloride-Mediated and Microwave-Assisted Synthesis of a Small Collection of Amides Bearing Strong Electron-Withdrawing Group Substituted Anilines. *J. Comb. Chem.* **2009**, 11 (3), 335–337.
- (43) Sanguinetti, M. C.; Tristani-Firouzi, M. hERG Potassium Channels and Cardiac Arrhythmia. *Nature* **2006**, 440 (7083), 463–469.
- (44) Wang, S.; Li, Y.; Xu, L.; Li, D.; Hou, T. Recent Developments in Computational Prediction of hERG Blockage. *Curr. Top. Med. Chem.* **2013**, 13 (11), 1317–1326.
- (45) Hedley, P. L.; Jørgensen, P.; Schlamowitz, S.; Wangari, R.; Moolman-Smook, J.; Brink, P. A.; Kanters, J. K.; Corfield, V. A.; Christiansen, M. The Genetic Basis of Long QT and Short QT Syndromes: A Mutation Update. *Hum. Mutat.* **2009**, 30 (11), 1486–1511.
- (46) Nogawa, H.; Kawai, T. hERG Trafficking Inhibition in Drug-Induced Lethal Cardiac Arrhythmia. *Eur. J. Pharmacol.* **2014**, 741, 336–339.
- (47) Jing, Y.; Easter, A.; Peters, D.; Kim, N.; Enyedy, I. J. In Silico Prediction of hERG Inhibition. *Future Med. Chem.* **2015**, 7 (5), 571–586.
- (48) Zhou, P. Z.; Babcock, J.; Liu, L. Q.; Li, M.; Gao, Z. B. (20) Activation of Human Ether-a-Go-Go Related Gene (hERG) Potassium Channels by Small Molecules. *Acta Pharmacol Sin* **2011**, 32 (6), 781–788.
- (49) Jamieson, C.; Moir, E. M.; Rankovic, Z.; Wishart, G. Medicinal Chemistry of hERG Optimizations: Highlights and Hang-Ups. *J. Med. Chem.* **2006**, 49 (17), 5029–5046.
- (50) Braga, R. C.; Alves, V. M.; Silva, M. F. B.; Muratov, E.; Fourches, D.; Lião, L. M.; Tropsha, A.; Andrade, C. H. Pred-hERG: A Novel Web-Accessible Computational Tool for Predicting Cardiac Toxicity. *Mol. Inform.* **2015**, 34 (10), 698–701.
- (51) Biswal, S.; Sahoo, U.; Sethy, S.; Kumar, H. K. S.; Banerjee, M.; Hooker, J. Indole: The

- Molecule of Diverse Biological Activities. *Asian J. Pharm. Clin. Res.* **2012**, 5 (1), 2–7.
- (52) Liu, L.; Norman, M. H.; Lee, M.; Xi, N.; Siegmund, A.; Boezio, A. A.; Booker, S.; Choquette, D.; D'Angelo, N. D.; Germain, J.; et al. Structure-Based Design of Novel Class II c-Met Inhibitors: 2. SAR and Kinase Selectivity Profiles of the Pyrazolone Series. *J. Med. Chem.* **2012**, 55 (5), 1868–1897.
- (53) Ban, H.; Gavrilyuk, J.; Barbas Carlos F. Tyrosine Bioconjugation through Aqueous Ene-Type Reactions: A Click-Like Reaction for Tyrosine. *J. Am. Chem. Soc.* **2010**, 132 (5), 1523–1525.
- (54) Xie, X.; Yan, Y.; Zhu, N.; Liu, G. Benzothiazoles Exhibit Broad-Spectrum Antitumor Activity: Their Potency, Structure–activity and Structure–metabolism Relationships. *Eur. J. Med. Chem.* **2014**, 76, 67–78.

Chapter 2

- (1) Mor, V.; Rella, A.; Farnoud, A. M.; Singh, A.; Munshi, M.; Bryan, A.; Naseem, S.; Konopka, J. B.; Ojima, I.; Bullesbach, E.; et al. Identification of a New Class of Antifungals Targeting the Synthesis of Fungal Sphingolipids. *MBio* **2015**, 6 (3), e00647.
- (2) Brown, G. D.; Denning, D. W.; Gow, N. A. R.; Levitz, S. M.; Netea, M. G.; White, T. C. Hidden Killers: Human Fungal Infections. *Sci. Transl. Med.* **2012**, 4 (165), 165rv13–rv165rv13.
- (3) Kathiravan, M. K.; Salake, A. B.; Chothe, A. S.; Dudhe, P. B.; Watode, R. P.; Mukta, M. S.; Gadhwe, S. The Biology and Chemistry of Antifungal Agents: A Review. *Bioorg. Med. Chem.* **2012**, 20 (19), 5678–5698.
- (4) Babazadeh-Qazijahani, M.; Badali, H.; Irannejad, H.; Afsarian, M. H.; Emami, S. Imidazolylchromanones Containing Non-Benzyl Oxime Ethers: Synthesis and Molecular Modeling Study of New Azole Antifungals Selective against *Cryptococcus Gattii*. *Eur. J. Med. Chem.* **2014**, 76, 264–273.
- (5) Armstrong-James, D.; Meintjes, G.; Brown, G. D. A Neglected Epidemic: Fungal Infections in HIV/AIDS. *Trends Microbiol.* **2014**, 22 (3), 120–127.
- (6) Spitzer, M.; Robbins, N.; Wright, G. D. Combinatorial Strategies For Combating Invasive Fungal Infections. *Virulence* **2016**, 5594 (July), 0.
- (7) Rella, A.; Farnoud, A. M.; Del Poeta, M. Plasma Membrane Lipids and Their Role in Fungal Virulence. *Prog. Lipid Res.* **2016**, 61, 63–72.

- (8) Nimrichter, L.; Rodrigues, M. L.; Rodrigues, E. G.; Travassos, L. R. The Multitude of Targets for the Immune System and Drug Therapy in the Fungal Cell Wall. *Microbes Infect.* **2005**, 7 (4), 789–798.
- (9) Hakomori, S. Structure, Organization, and Function of Glycosphingolipids in Membrane. *Curr. Opin. Hematol.* **2003**, 10 (1), 16–24.
- (10) Rittershaus, P. C.; Kechichian, T. B.; Allegood, J. C.; Merrill, A. H.; Hennig, M.; Luberto, C.; Del Poeta, M. Glucosylceramide Synthase Is an Essential Regulator of Pathogenicity of *Cryptococcus Neoformans*. *J. Clin. Invest.* **2006**, 116 (6), 1651–1659.
- (11) Saito, K.; Takakuwa, N.; Ohnishi, M.; Oda, Y. Presence of Glucosylceramide in Yeast and Its Relation to Alkali Tolerance of Yeast. *Appl. Microbiol. Biotechnol.* **2006**, 71 (4), 515–521.
- (12) Ashiq, U.; Ara, R.; Mahroof-Tahir, M.; Maqsood, Z. T.; Khan, K. M.; Khan, S. N.; Siddiqui, H.; Choudhary, M. I. Synthesis, Spectroscopy, and Biological Properties of Vanadium(IV)–Hydrazide Complexes. *Chem. Biodivers.* **2008**, 5 (1), 82–92.
- (13) Han, E.-G.; Kim, H. J.; Lee, K.-J. Quinolines from Morita–Baylis–Hillman Acetates of 2-Azidobenzaldehydes. *Tetrahedron* **2009**, 65 (46), 9616–9625.
- (14) Monga, V.; Nayyar, A.; Vaitilingam, B.; Palde, P. B.; Singh Jhamb, S.; Kaur, S.; Singh, P. P.; Jain, R. Ring-Substituted Quinolines. Part 2: Synthesis and Antimycobacterial Activities of Ring-Substituted Quinolincarbohydrazide and Ring-Substituted Quinolincarboxamide Analogues. *Bioorg. Med. Chem.* **2004**, 12 (24), 6465–6472.
- (15) Saha, A.; Kumar, R.; Kumar, R.; C, D. Development and Assessment of Green Synthesis of Hydrazides. *Indian J. Chem.* **2010**, 49b, 526–531.
- (16) Rida, S.; Saudi, M.; Youssef, A.; Halim, M. Synthesis and Biological Evaluation of the Pyrazole Class of Cyclooxygenase- 2-Inhibitors. *Lett. Org. Chem.* **2009**, 6 (4), 282–288.
- (17) Hou, J.-L.; Shao, X.-B.; Chen, G.-J.; Zhou, Y.-X.; Jiang, X.-K.; Li, Z.-T. Hydrogen Bonded Oligohydrazide Foldamers and Their Recognition for Saccharides. *J. Am. Chem. Soc.* **2004**, 126 (39), 12386–12394.

Chapter 3

- (1) Nigam, P.; Nigam, A. Botulinum Toxin. *Indian J. Dermatol.* **2010**, 55 (1), 8.
- (2) Dennis, D. T.; Inglesby, T. V.; Henderson, D. a; Bartlett, J. G.; Ascher, M. S.; Eitzen, E.; Fine, a D.; Friedlander, a M.; Hauer, J.; Layton, M.; et al. Tularemia as a Biological

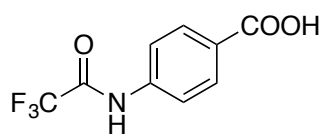
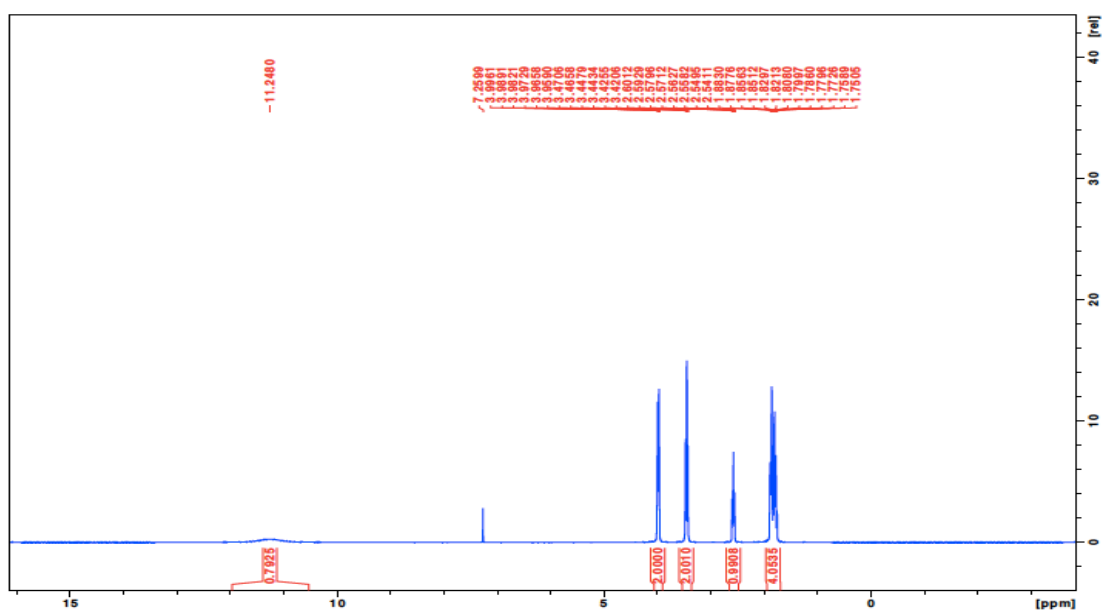
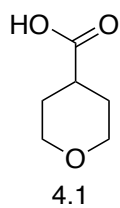
- Weapon: Medical and Public Health Management. *JAMA* **2001**, 285 (21), 2763–2773.
- (3) Teng, Y.-H. G.; Berger, W. T.; Nesbitt, N. M.; Kumar, K.; Balius, T. E.; Rizzo, R. C.; Tonge, P. J.; Ojima, I.; Swaminathan, S. Computer-Aided Identification, Synthesis, and Biological Evaluation of Novel Inhibitors for Botulinum Neurotoxin Serotype A. *Bioorg. Med. Chem.* **2015**, 23 (17), 5489–5495.
- (4) Zhang, Y.; Lou, J.; Jenko, K. L.; Marks, J. D.; Varnum, S. M. Simultaneous and Sensitive Detection of Six Serotypes of Botulinum Neurotoxin Using Enzyme-Linked Immunosorbent Assay-Based Protein Antibody Microarrays. *Anal. Biochem.* **2012**, 430 (2), 185–192.
- (5) Arnon, S. S.; Schechter, R.; Inglesby, T. V.; Henderson, D. A.; Bartlett, J. G.; Ascher, M. S.; Eitzen, E.; Fine, A. D.; Hauer, J.; Layton, M.; et al. Botulinum Toxin as a Biological Weapon. *JAMA* **2001**, 285 (8), 1059.
- (6) Benoit, R. M.; Frey, D.; Wieser, M. M.; Thielges, K. M.; Jaussi, R.; Capitani, G.; Kammerer, R. A. Structure of the BoNT/A1 – Receptor Complex. *Toxicon* **2015**, 107, 25–31.
- (7) Rossetto, O.; Pirazzini, M.; Montecucco, C. Botulinum Neurotoxins: Genetic, Structural and Mechanistic Insights. *Nat. Rev. Microbiol.* **2014**, 12 (8), 535–549.
- (8) Balius, T. E.; Mukherjee, S.; Rizzo, R. C. Implementation and Evaluation of a Docking-Rescoring Method Using Molecular Footprint Comparisons. *J. Comput. Chem.* **2011**, 32 (10), 2273–2289.
- (9) Kumaran, D.; Rawat, R.; Ludivico, M. L.; Ahmed, S. A.; Swaminathan, S. Structure- and Substrate-Based Inhibitor Design for Clostridium Botulinum Neurotoxin Serotype A. *J. Biol. Chem.* **2008**, 283 (27), 18883–18891.
- (10) Li, Z.; Zhu, A.; Yang, J. One-Pot Three-Component Mild Synthesis of 2-Aryl-3-(9-Alkylcarbazol-3-Yl)thiazolin-4-Ones. *J. Heterocycl. Chem.* **2012**, 49 (Scheme 1), 1458–1461.
- (11) Oyama, H.; Orimoto, K.; Niwa, T.; Nakada, M. Highly Enantioselective Catalytic Asymmetric Mukaiyama-Michael Reactions of Cyclic α -Alkylidene β -Oxo Imides. *Tetrahedron Asymmetry* **2015**, 26 (5-6), 262–270.
- (12) Dürüst, Y.; Karakuş, H.; Kaiser, M.; Tasdemir, D. Synthesis and Anti-Protozoal Activity of Novel dihydropyrrolo[3,4-d][1,2,3]triazoles. *Eur. J. Med. Chem.* **2012**, 48, 296–304.

- (13) Zhou, Y.; McGillick, B. E.; Teng, Y.-H. G.; Haranahalli, K.; Ojima, I.; Swaminathan, S.; Rizzo, R. C. Identification of Small Molecule Inhibitors of Botulinum Neurotoxin Serotype E via Footprint Similarity. *Bioorg. Med. Chem.* **2016**.

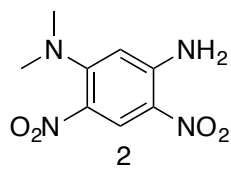
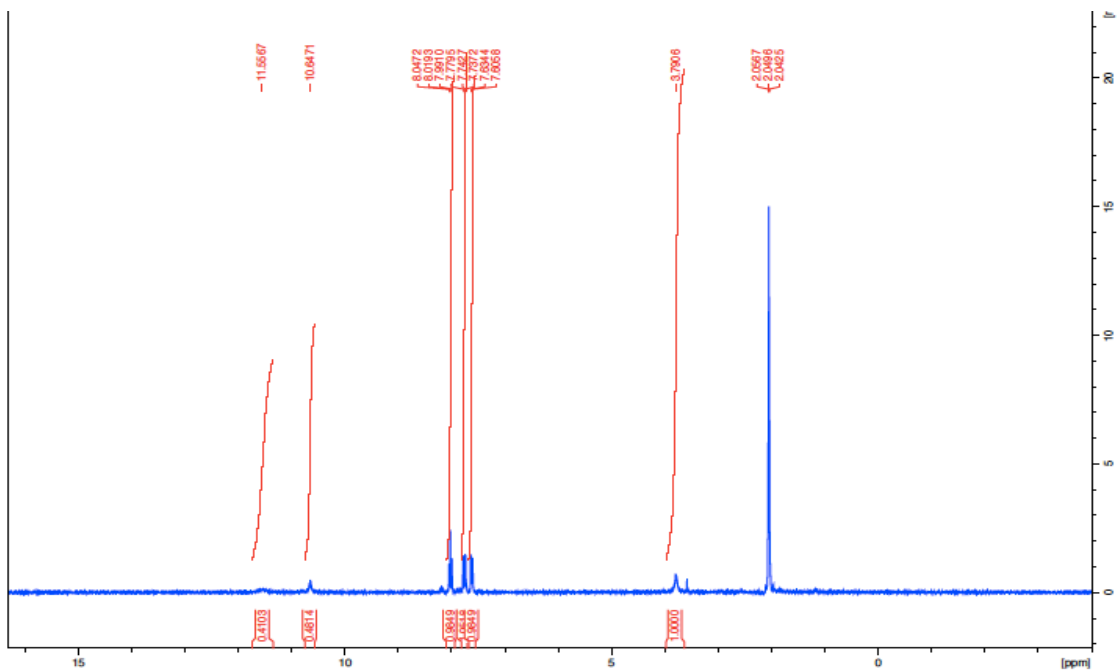
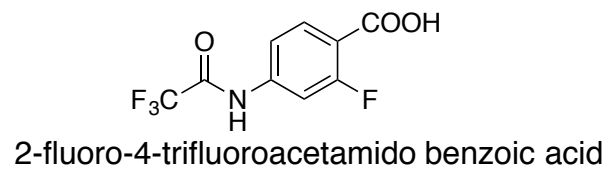
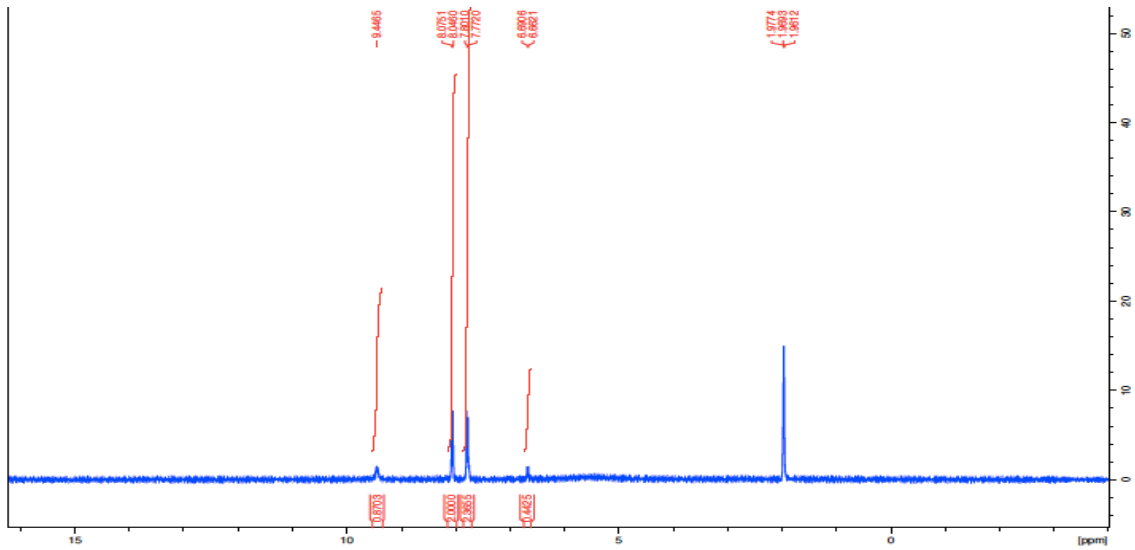
Chapter 4

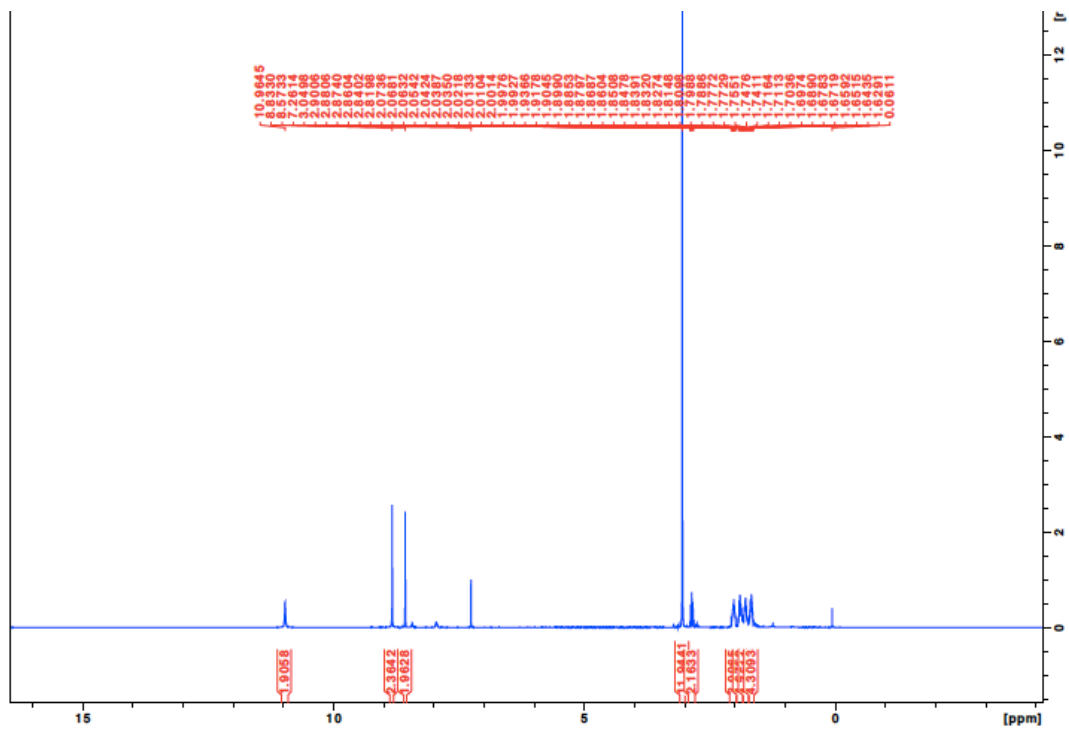
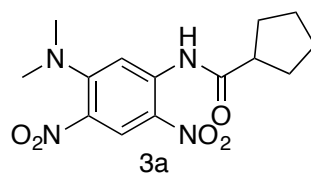
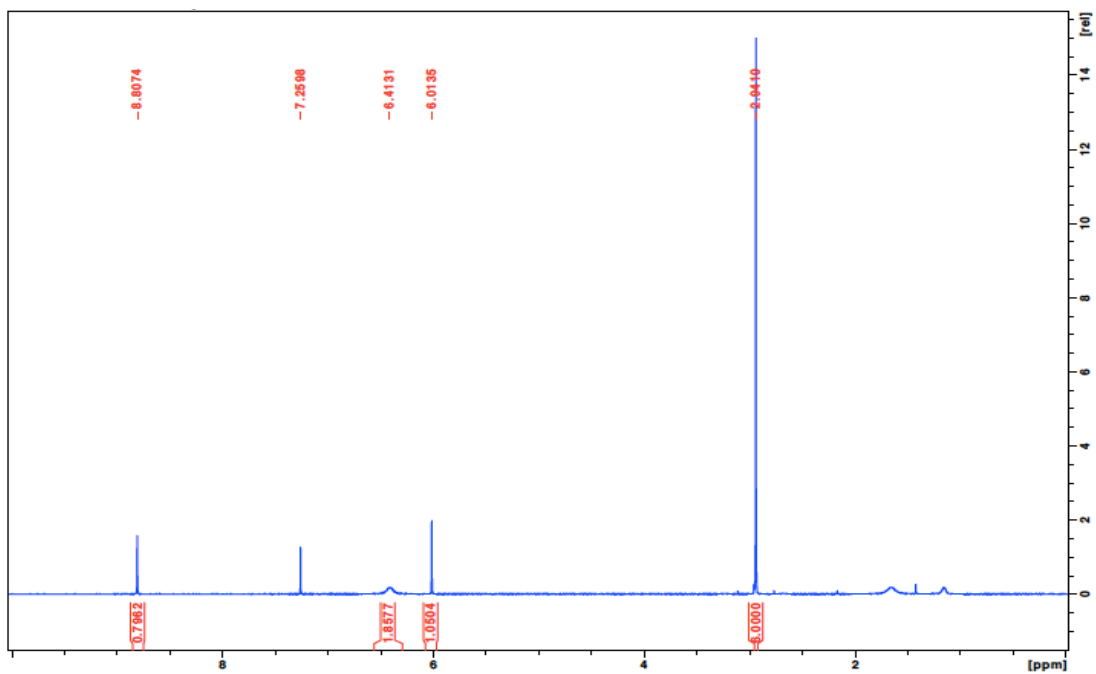
- (1) Huang, Q.; Kirikae, F.; Kirikae, T.; Pepe, A.; Amin, A.; Respicio, L.; Slayden, R. A.; Tonge, P. J.; Ojima, I. Targeting FtsZ for Antituberculosis Drug Discovery: Noncytotoxic Taxanes as Novel Antituberculosis Agents. *J. Med. Chem.* **2006**, 49 (2), 463–466.

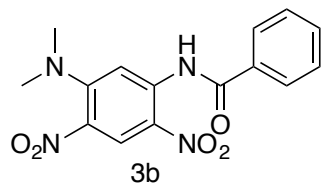
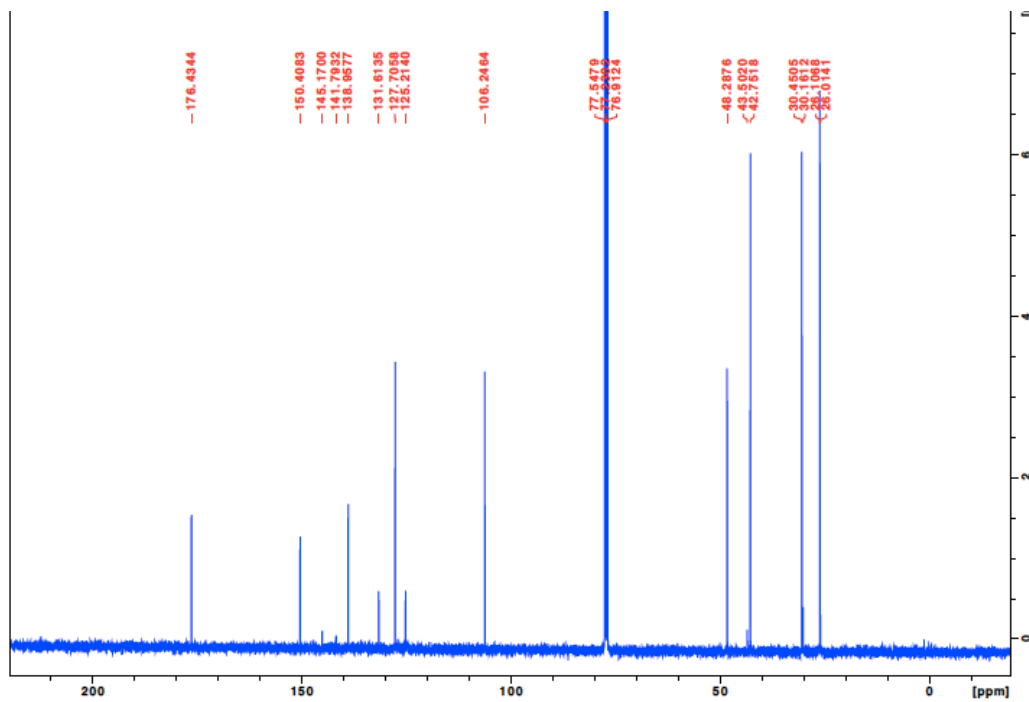
Appendix
Chapter 1

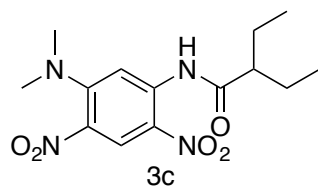
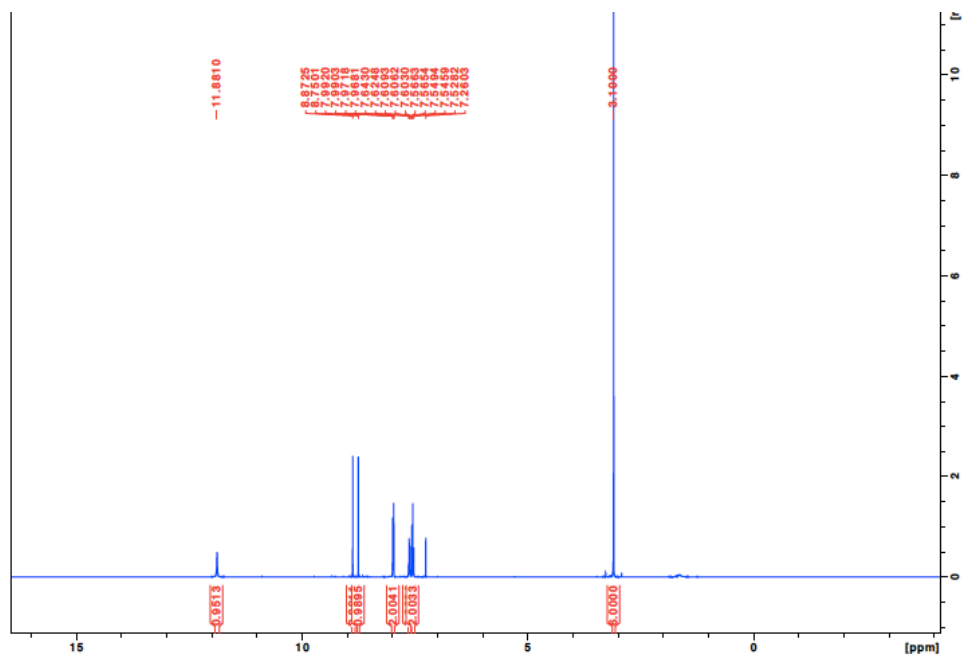
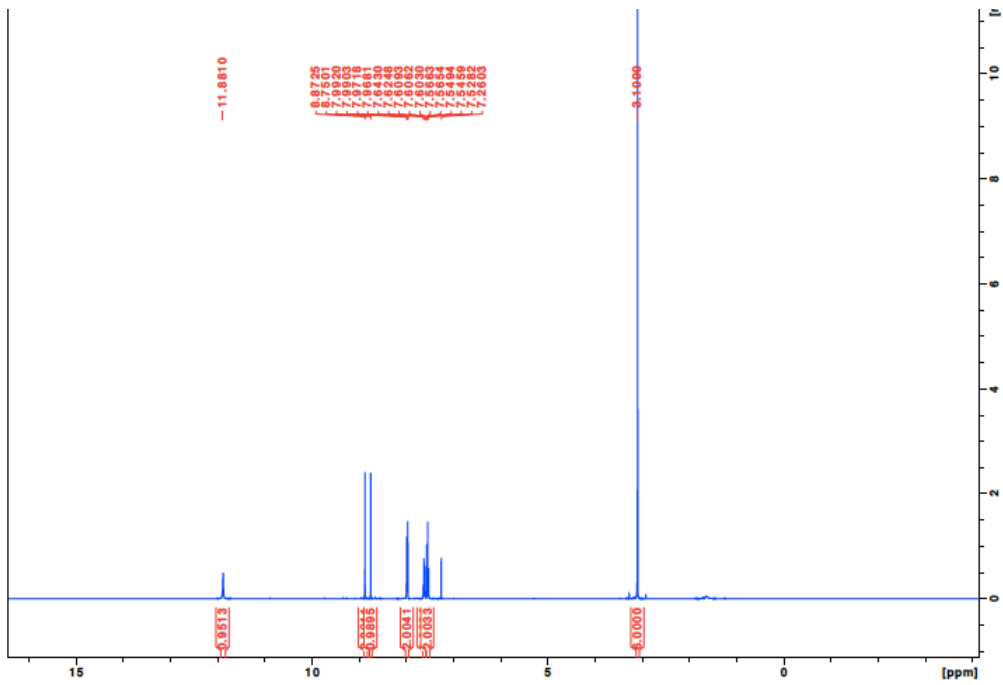


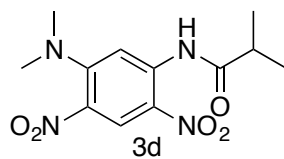
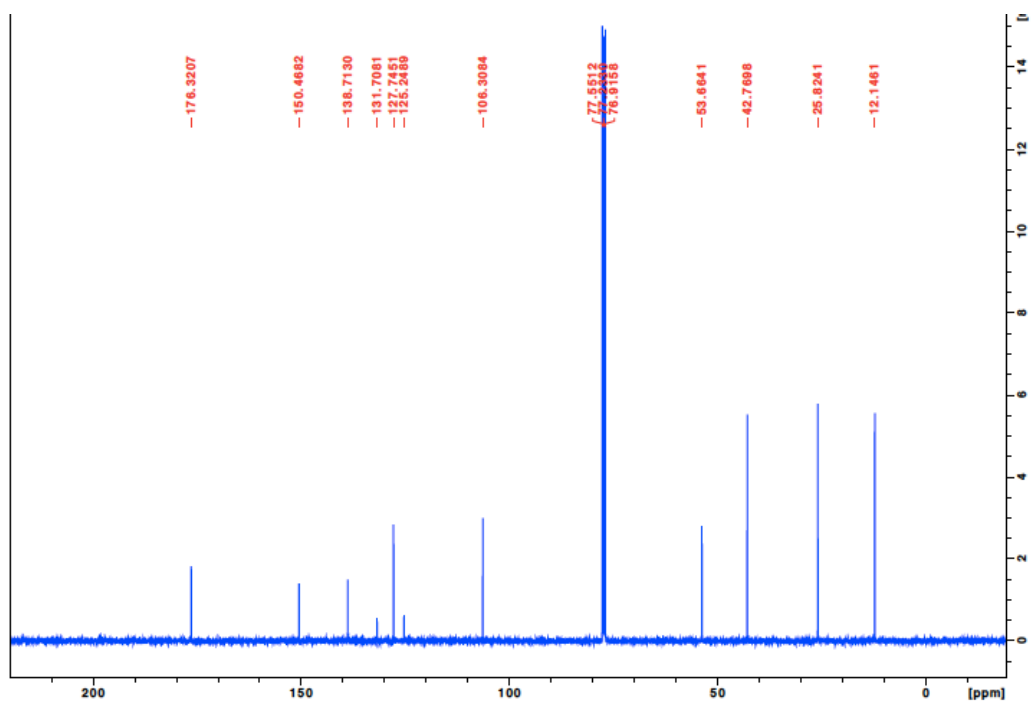
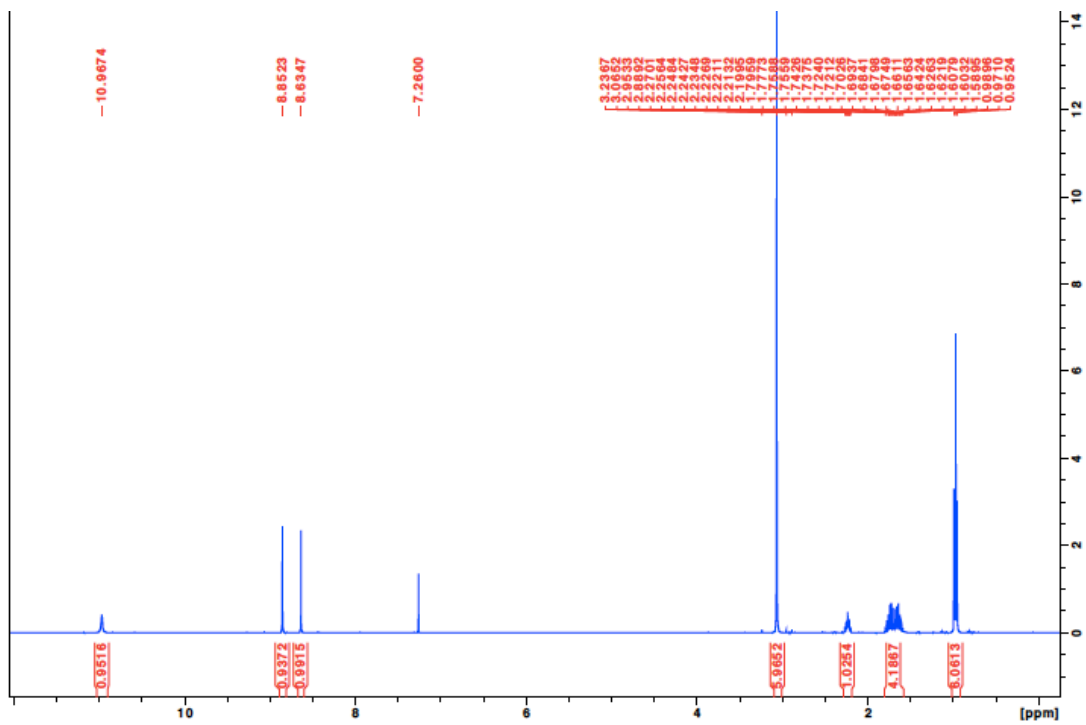
4-Trifluoroacetamido benzoic acid

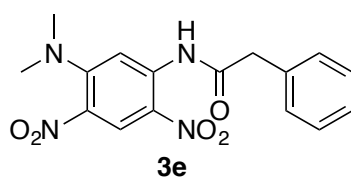
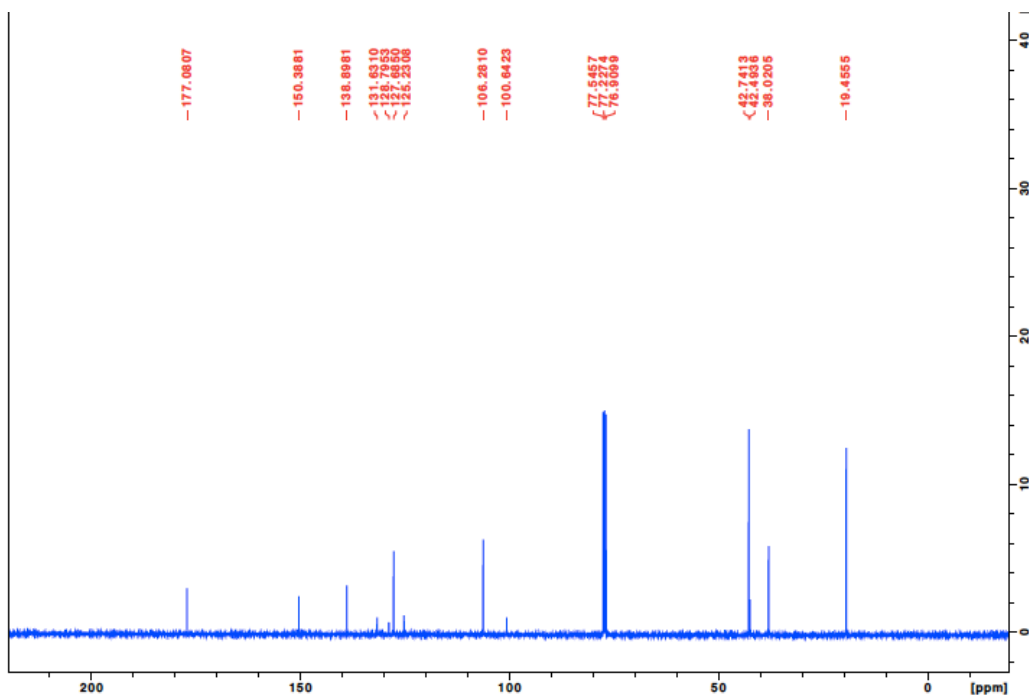
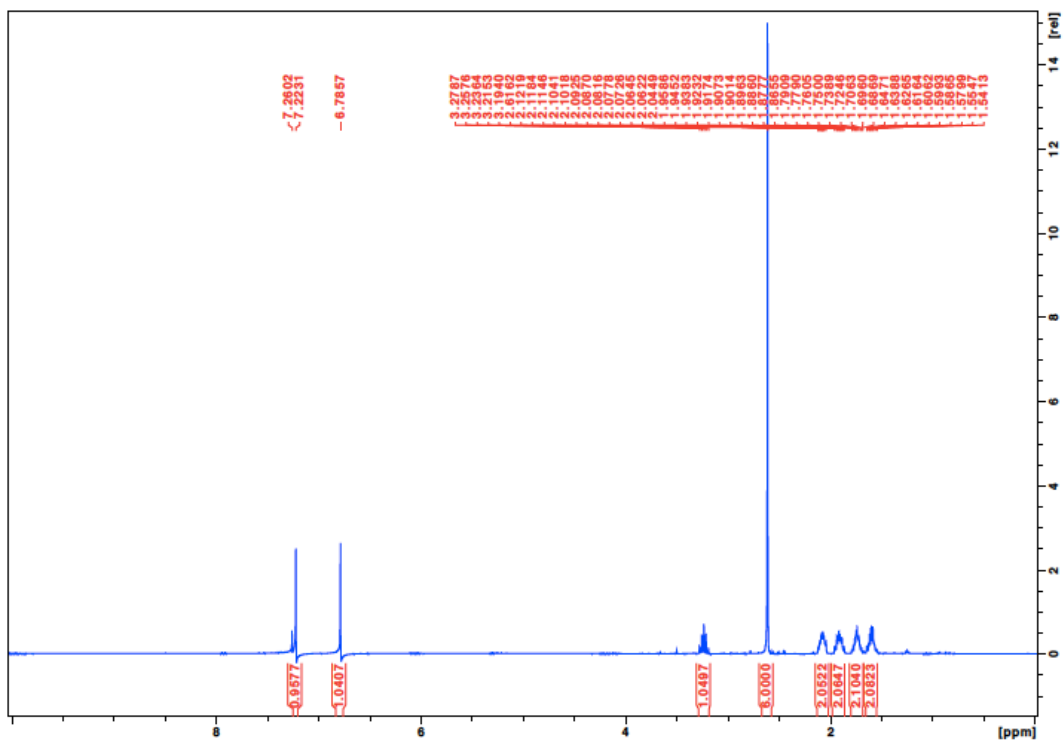


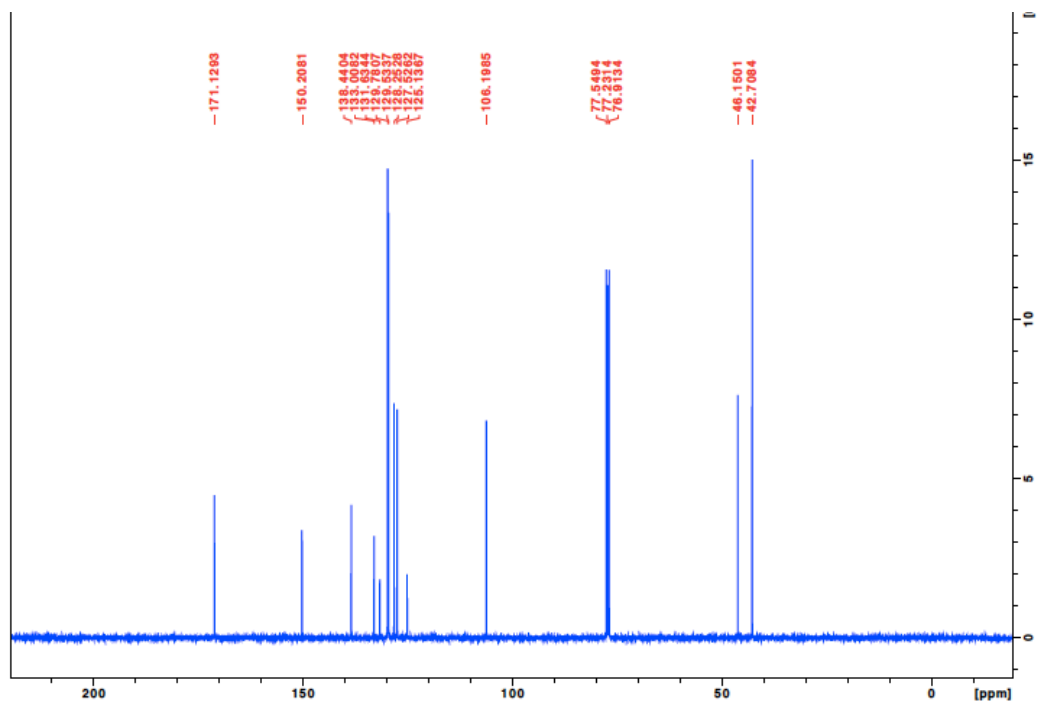
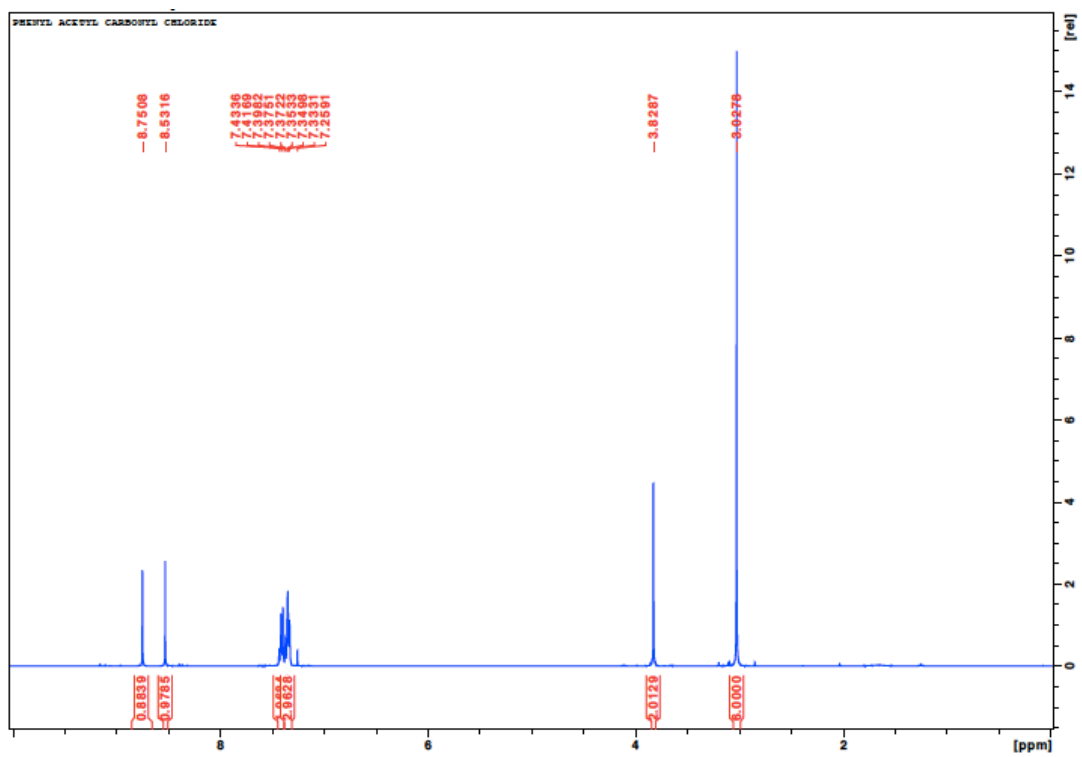


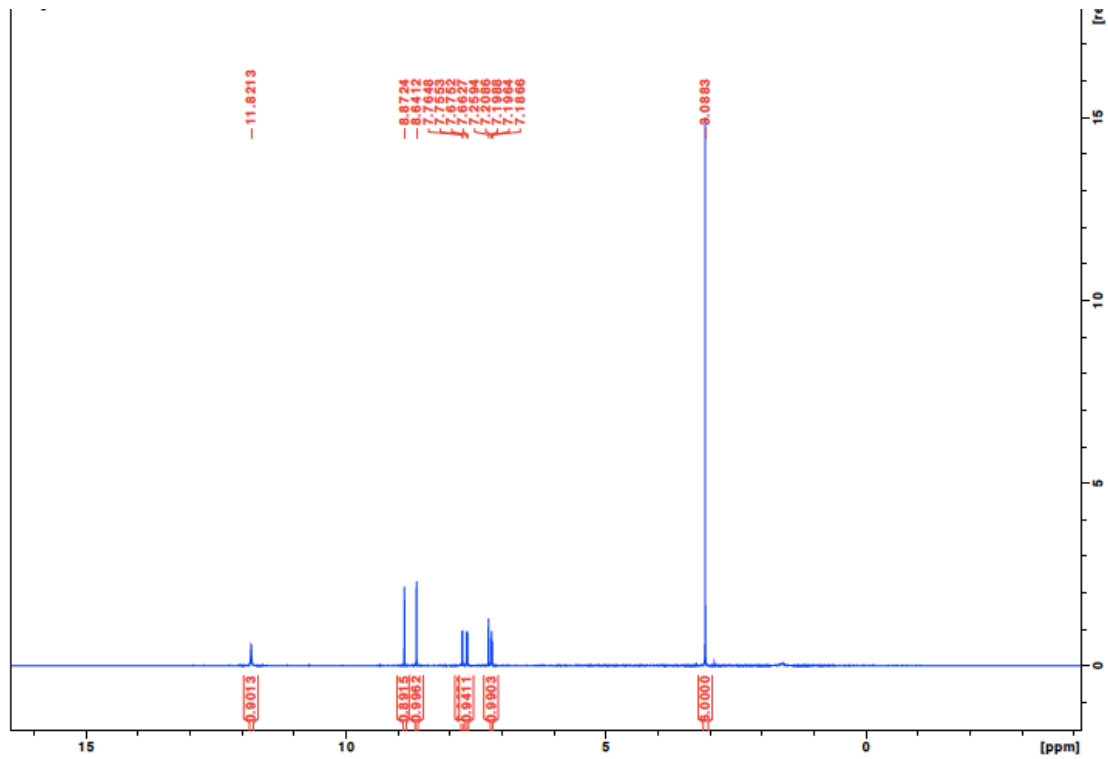
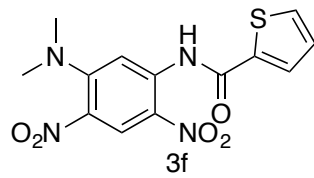


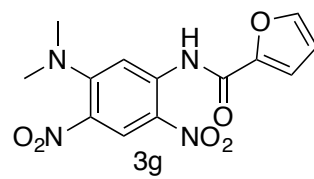
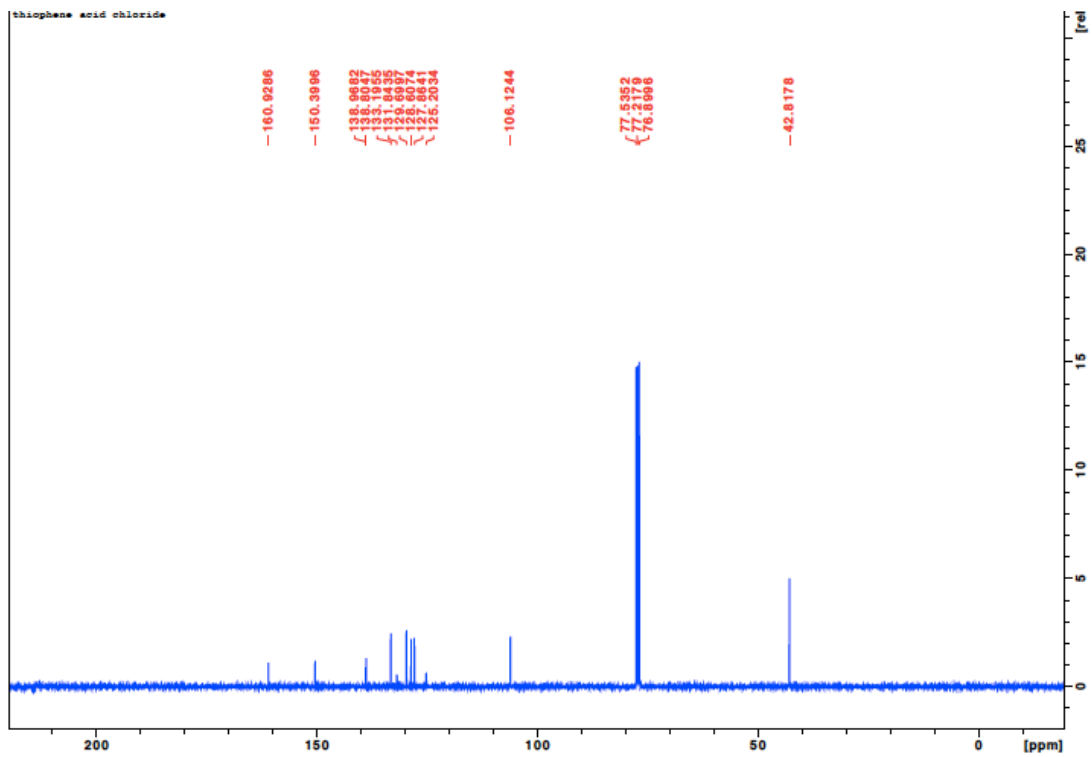


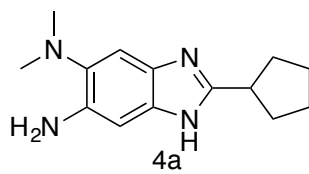
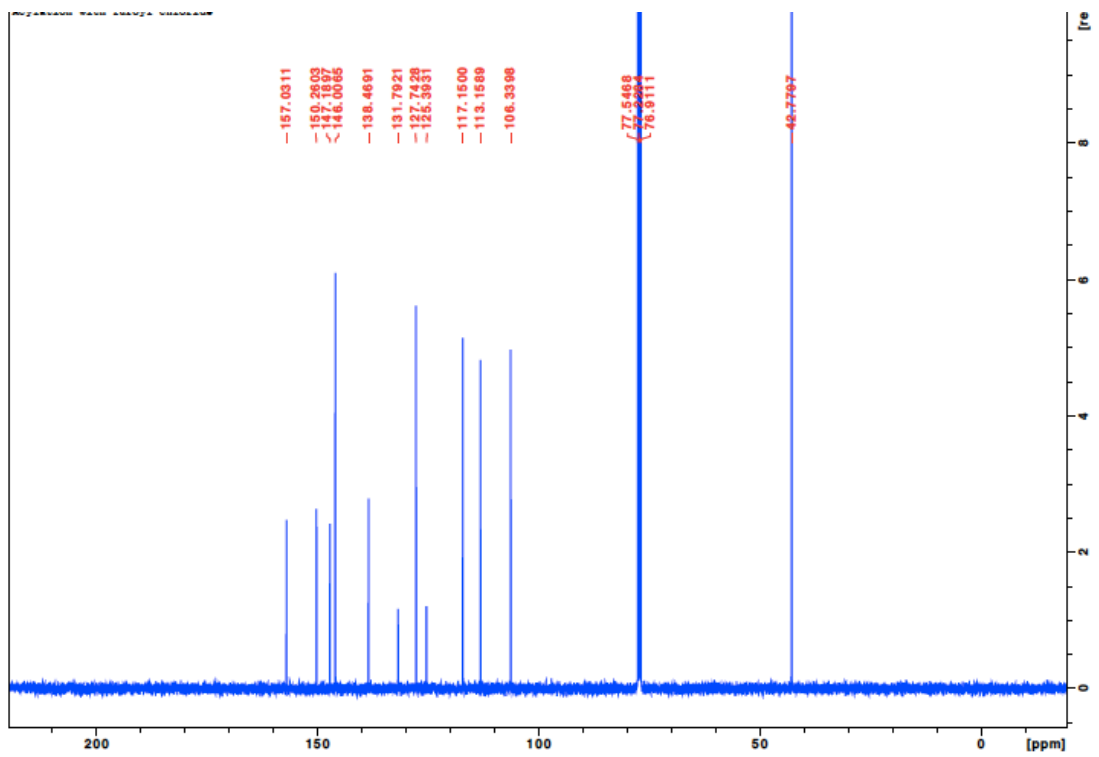
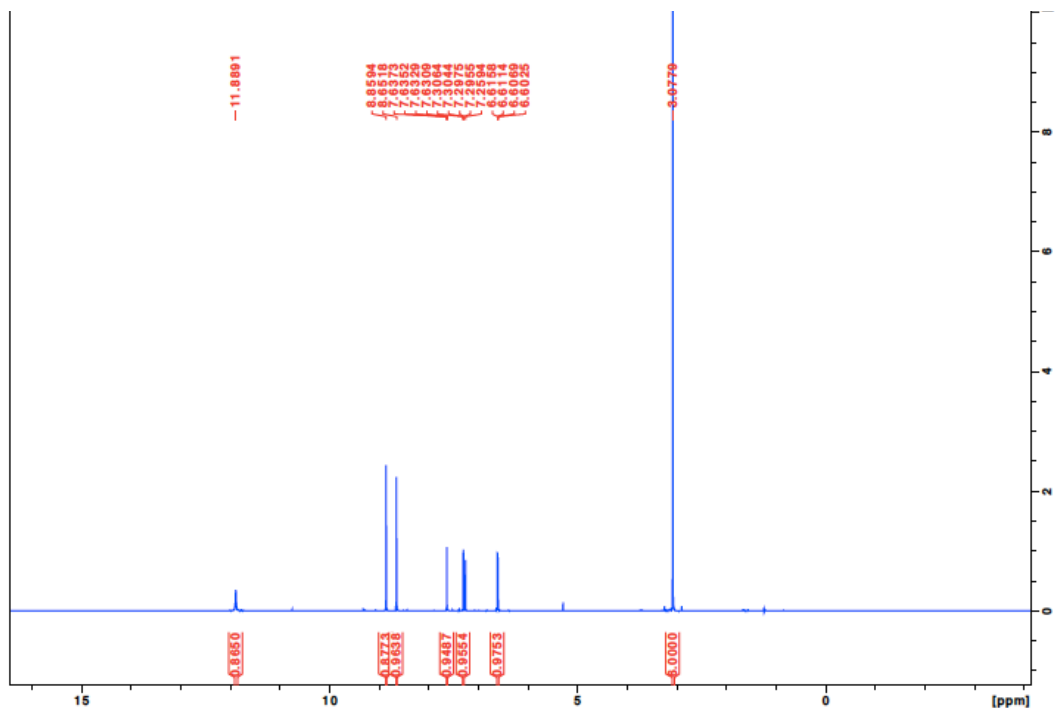


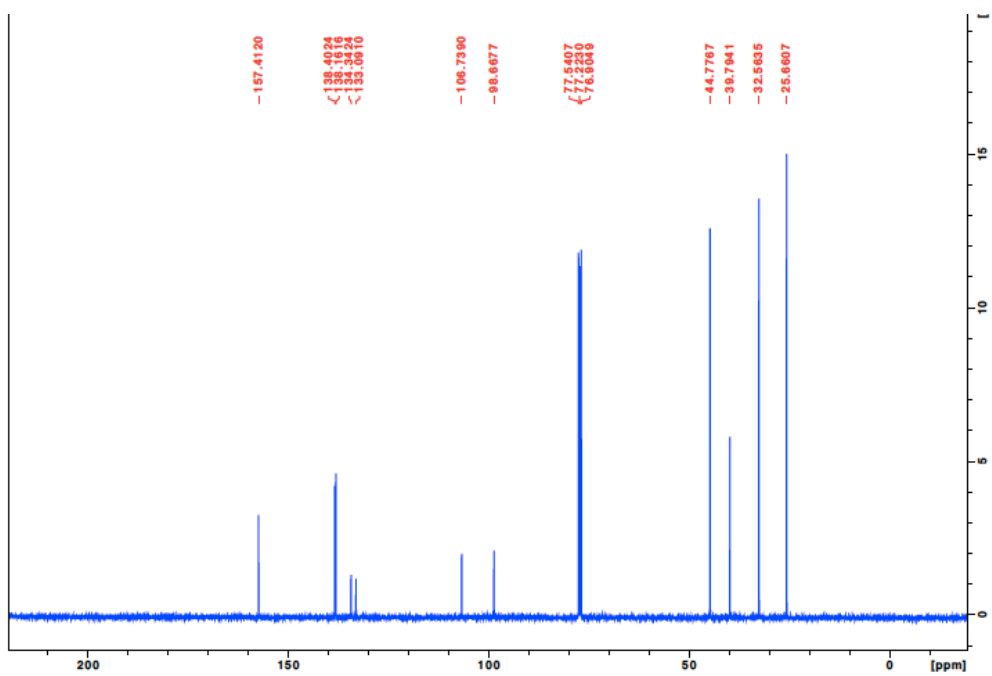
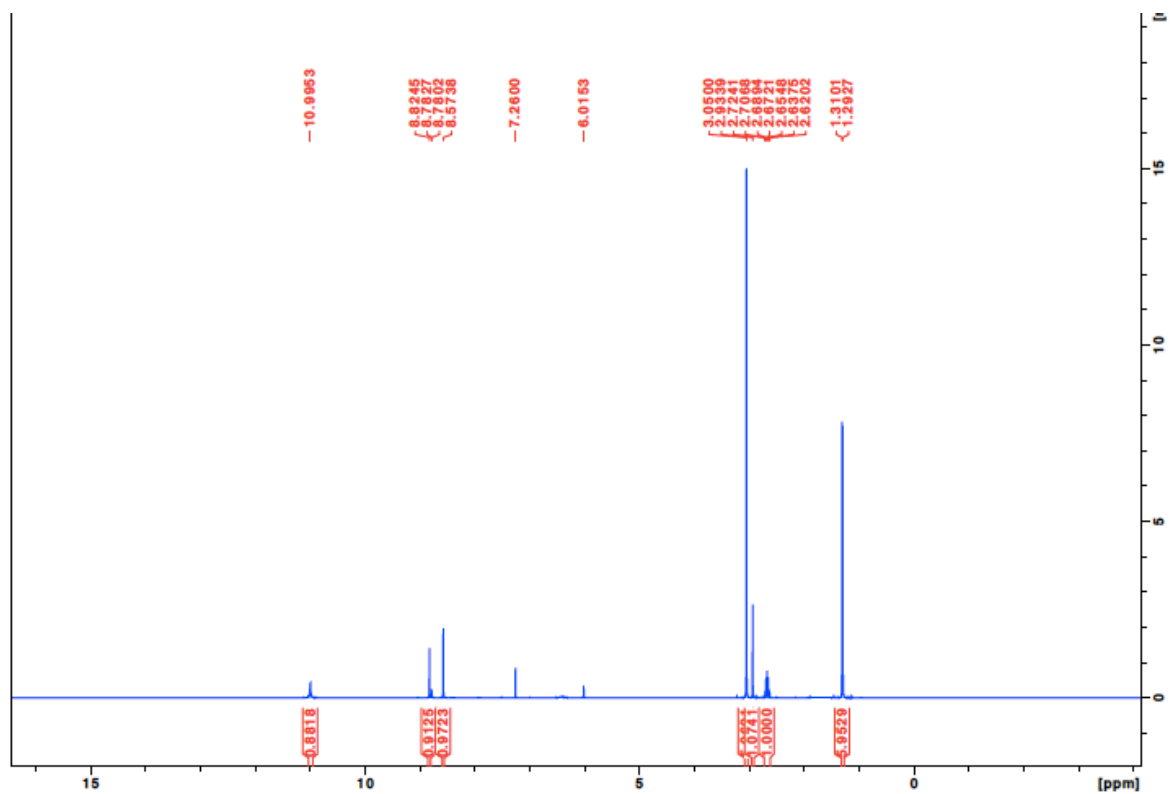


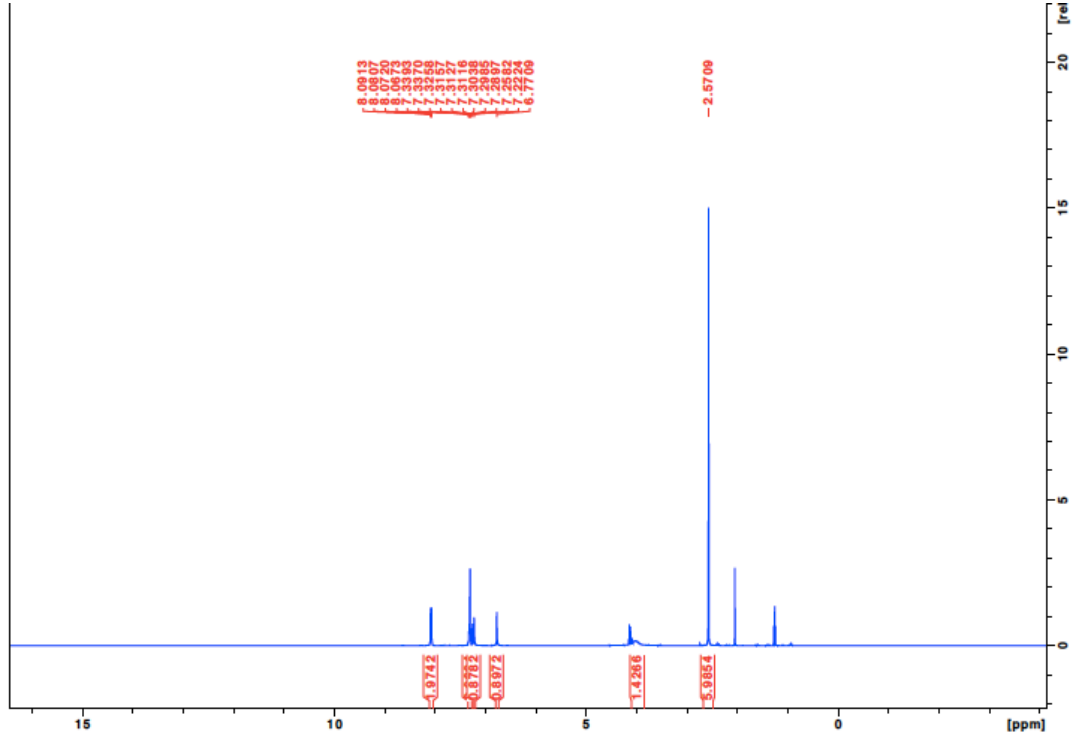
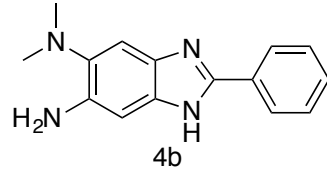


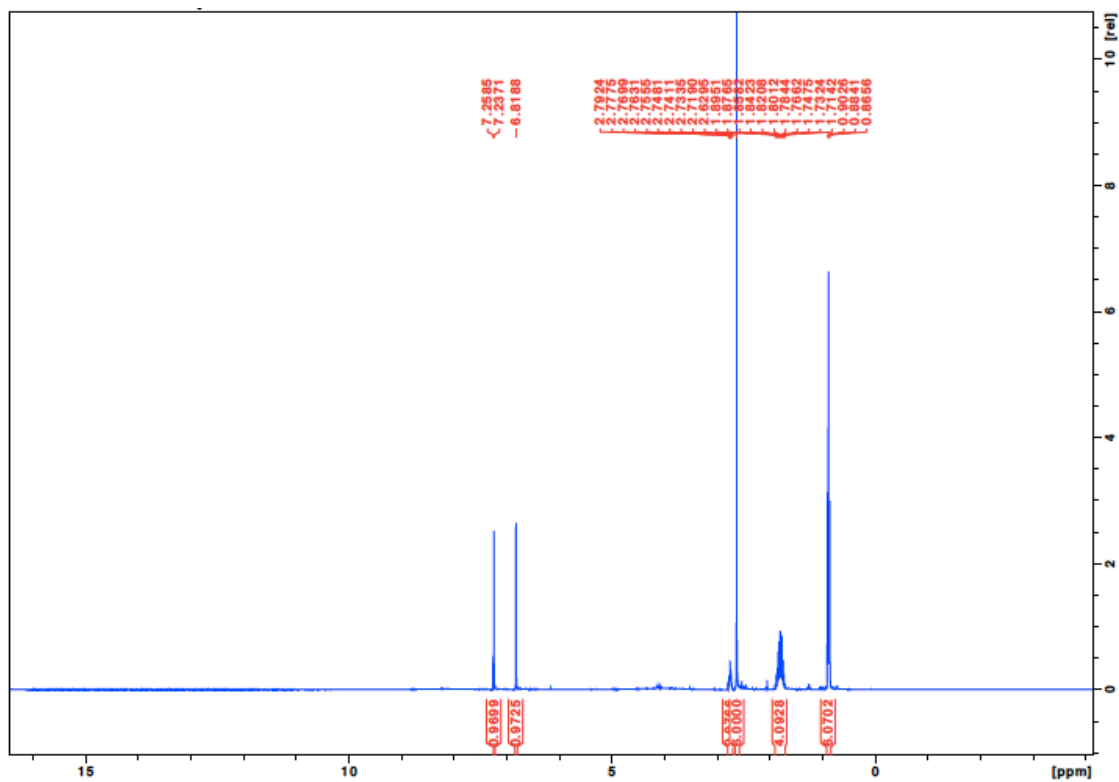
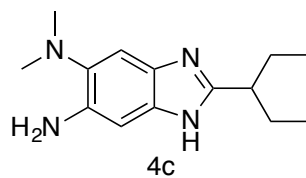
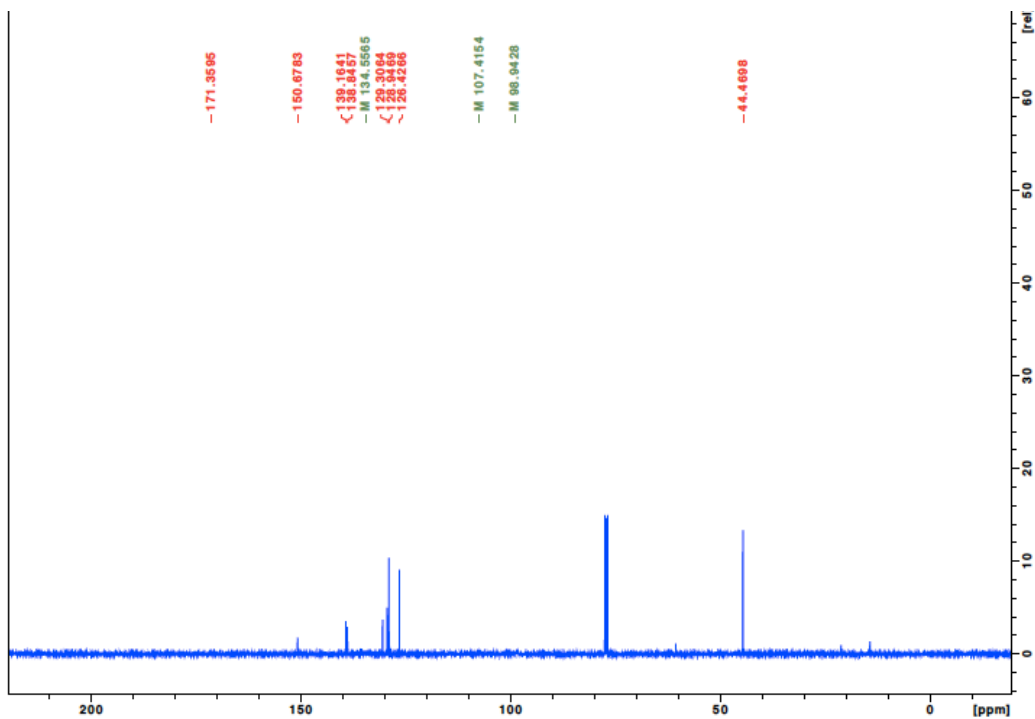


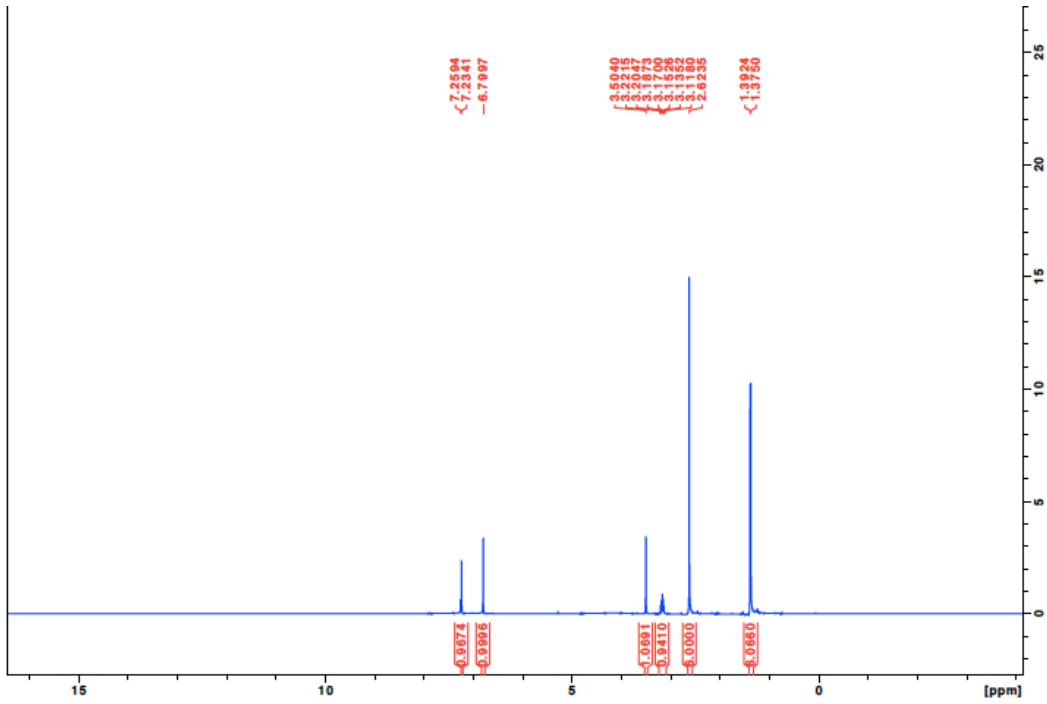
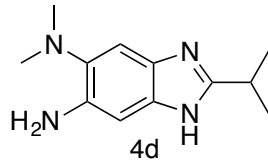
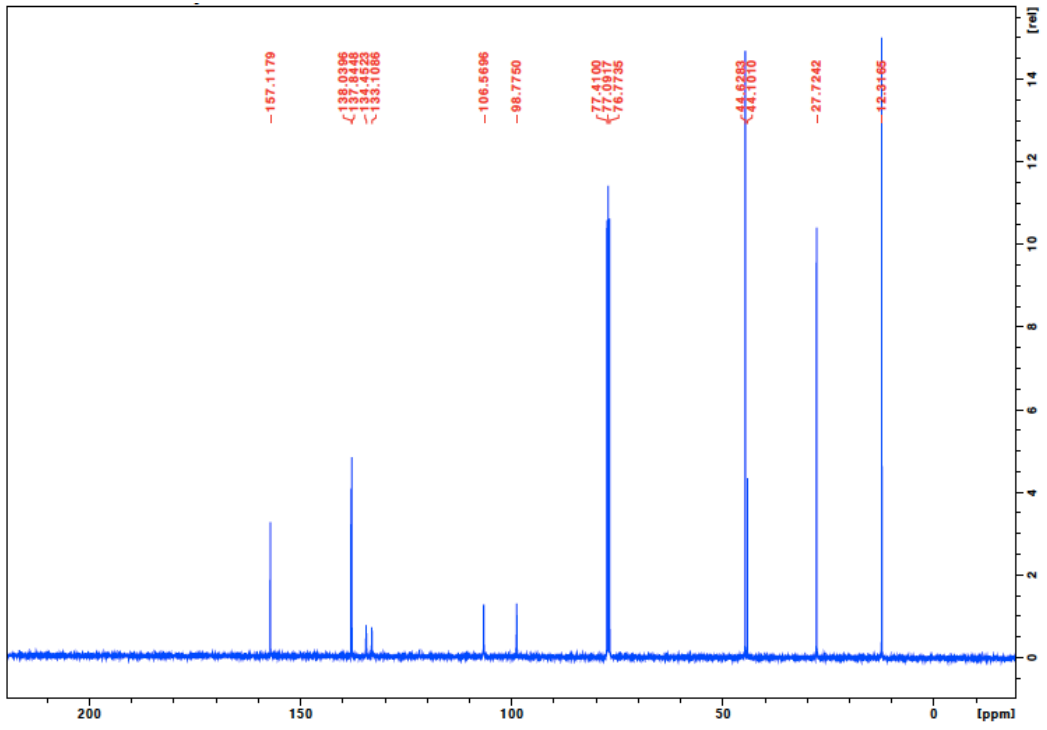


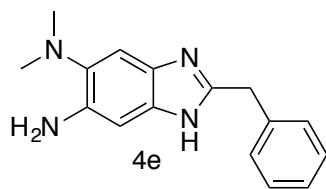
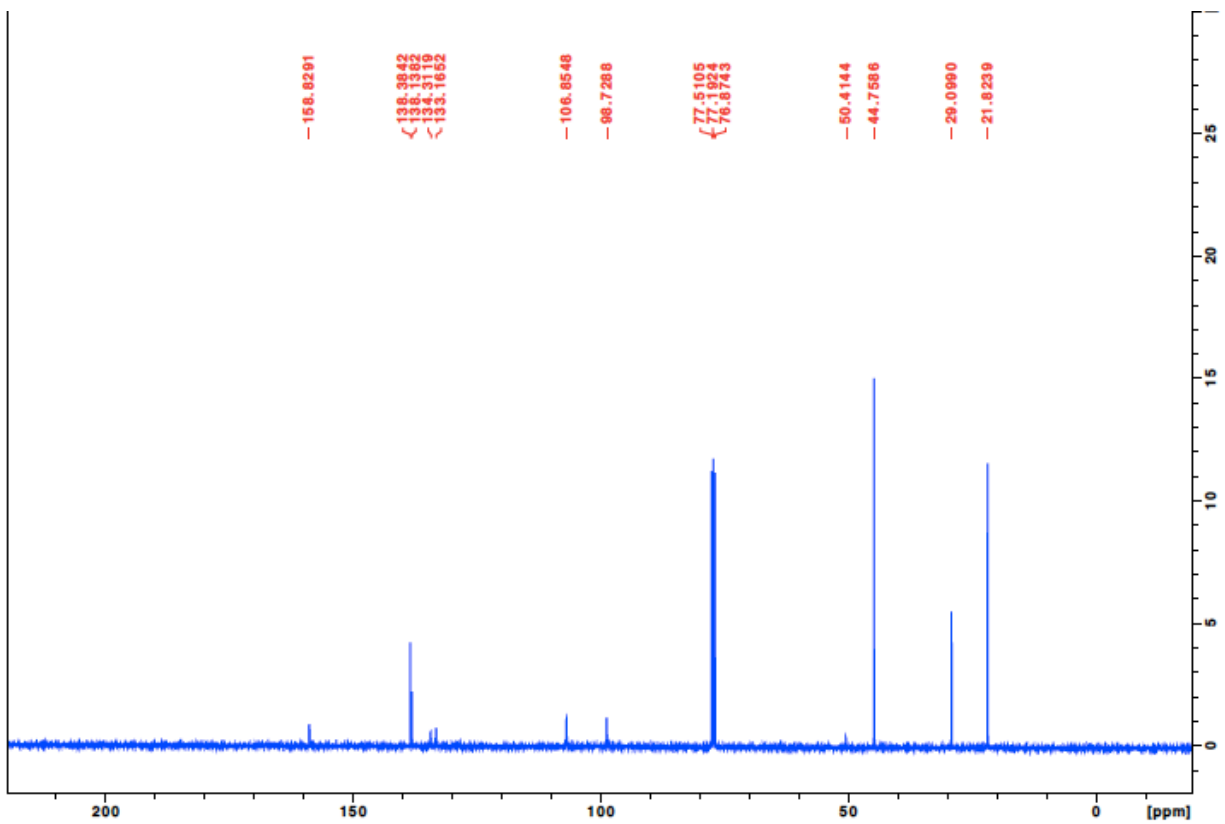


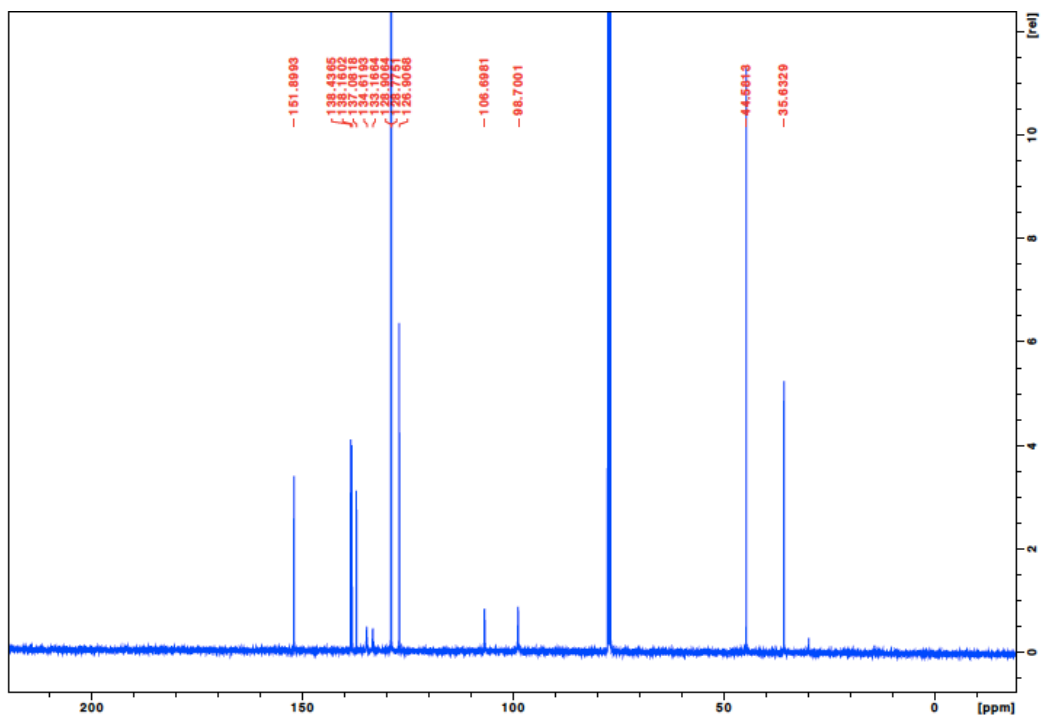
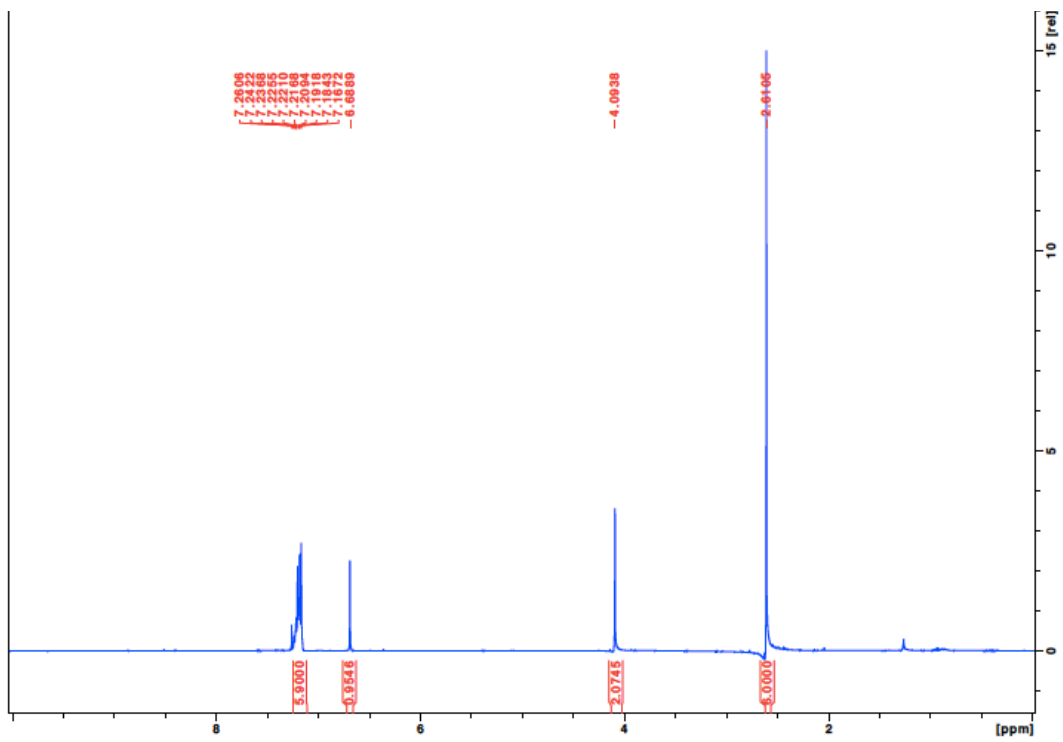


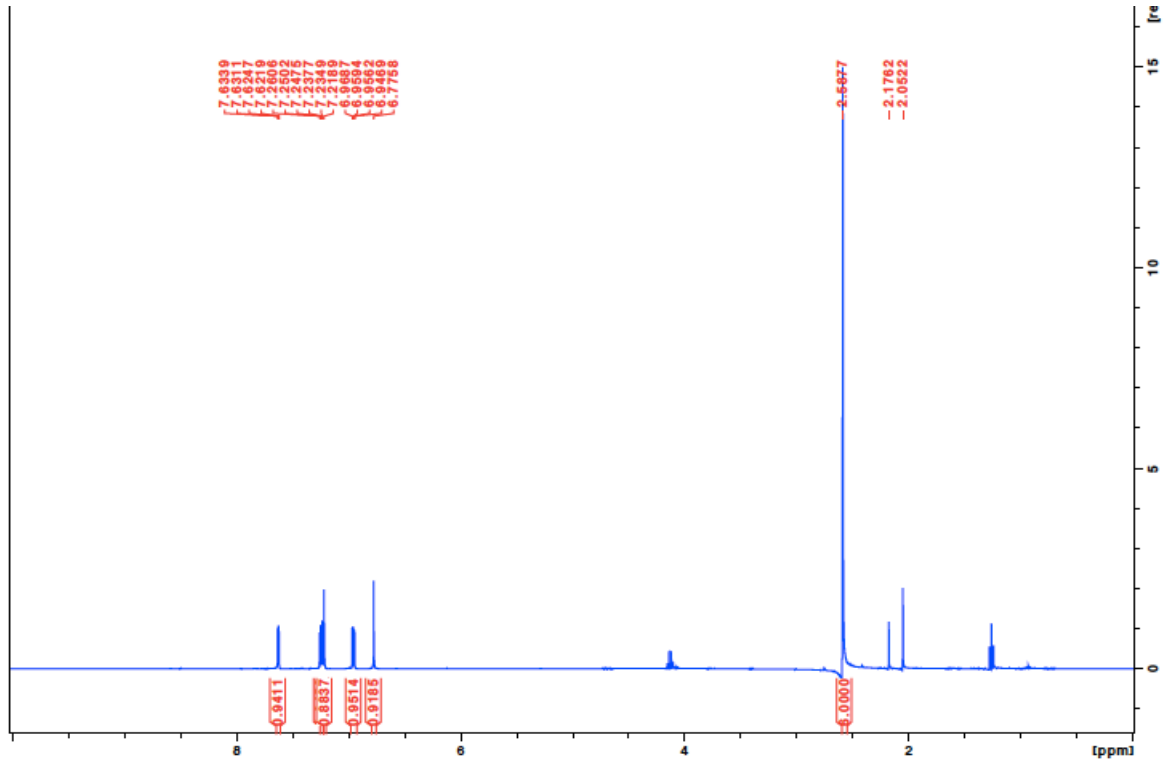
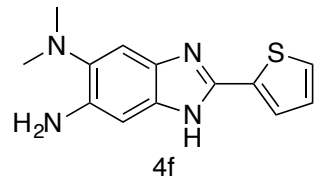


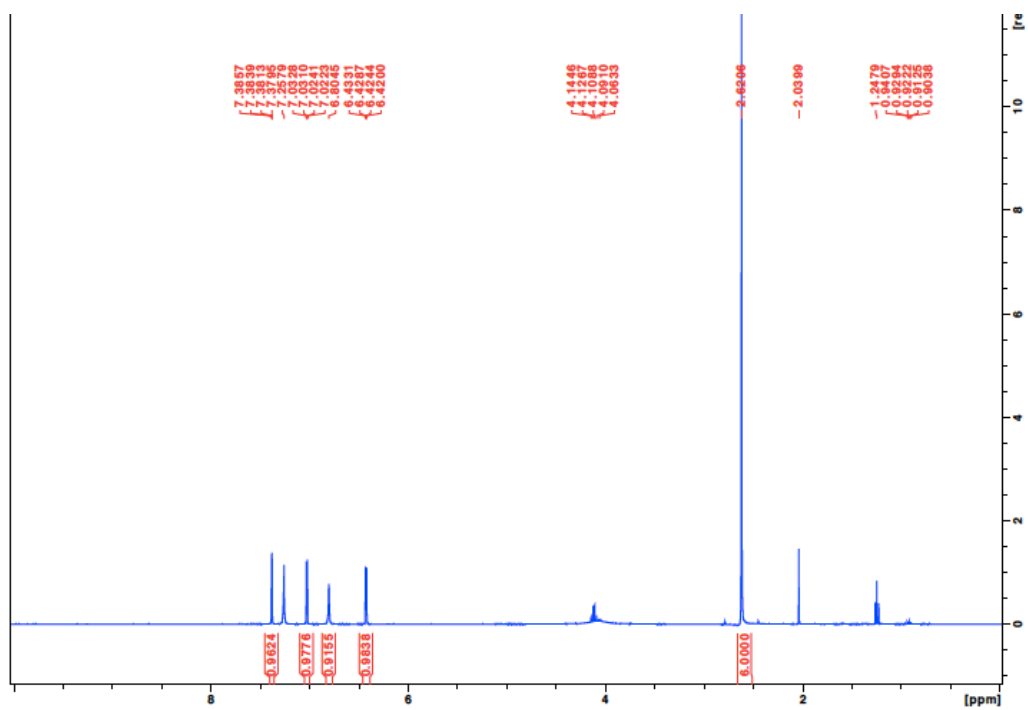
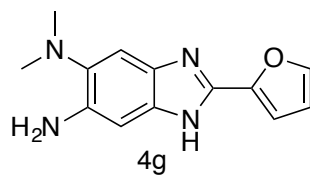
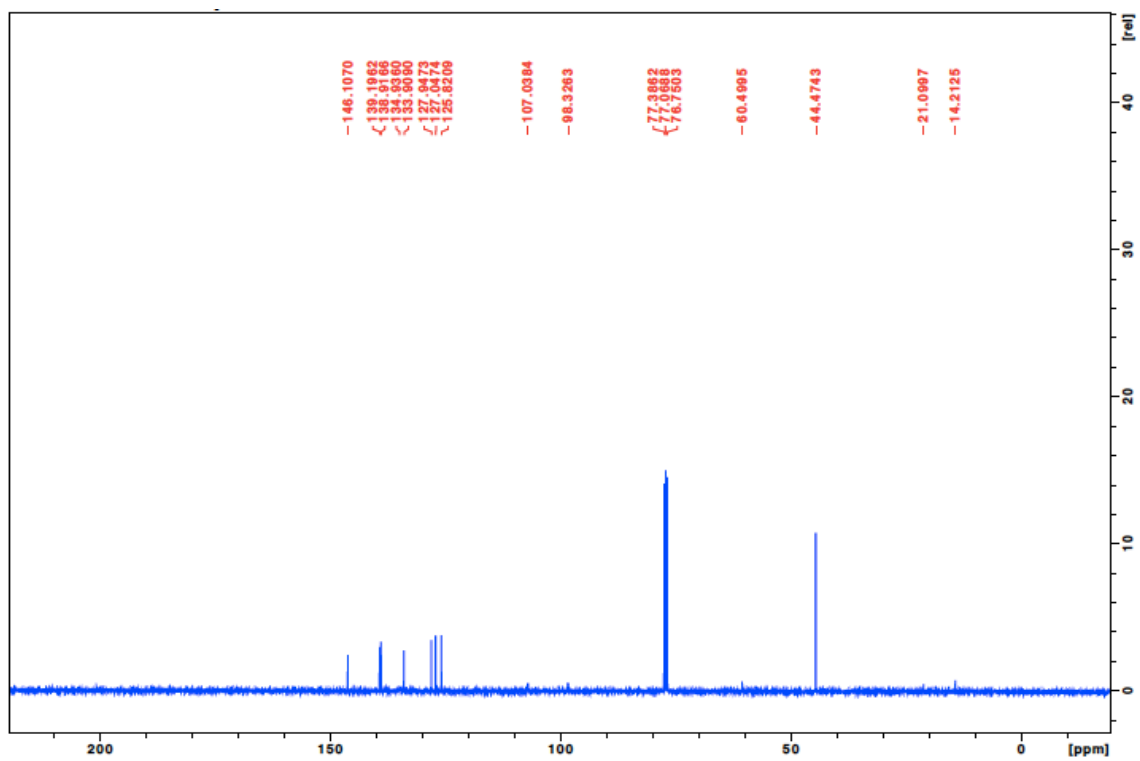


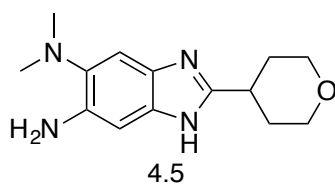
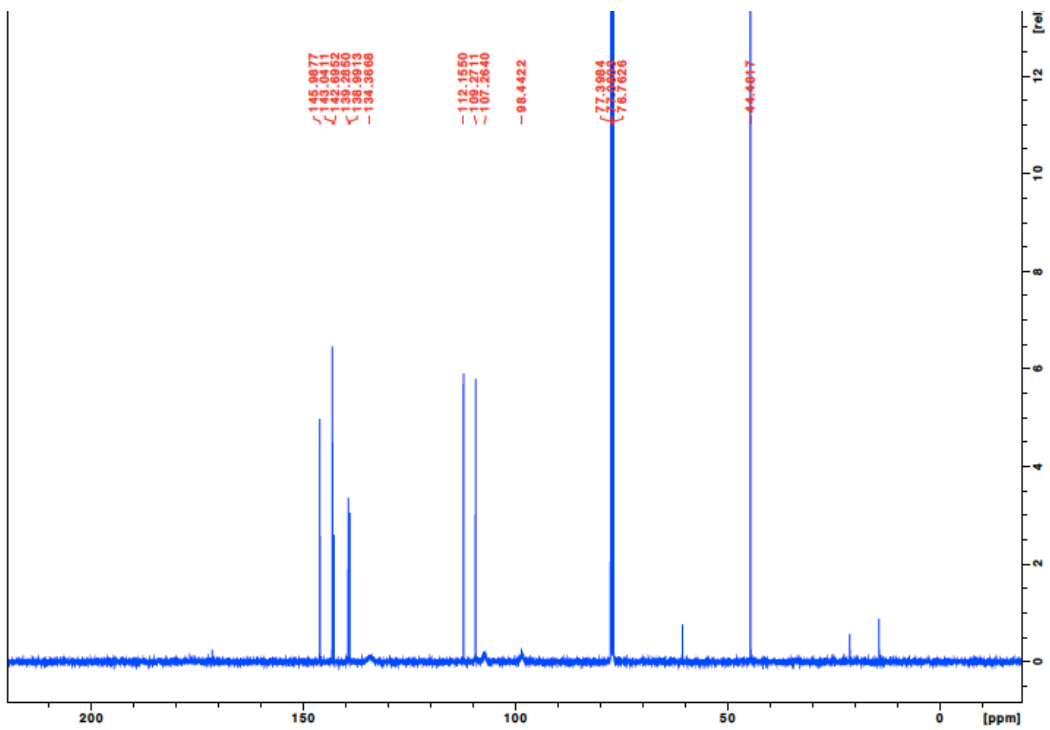


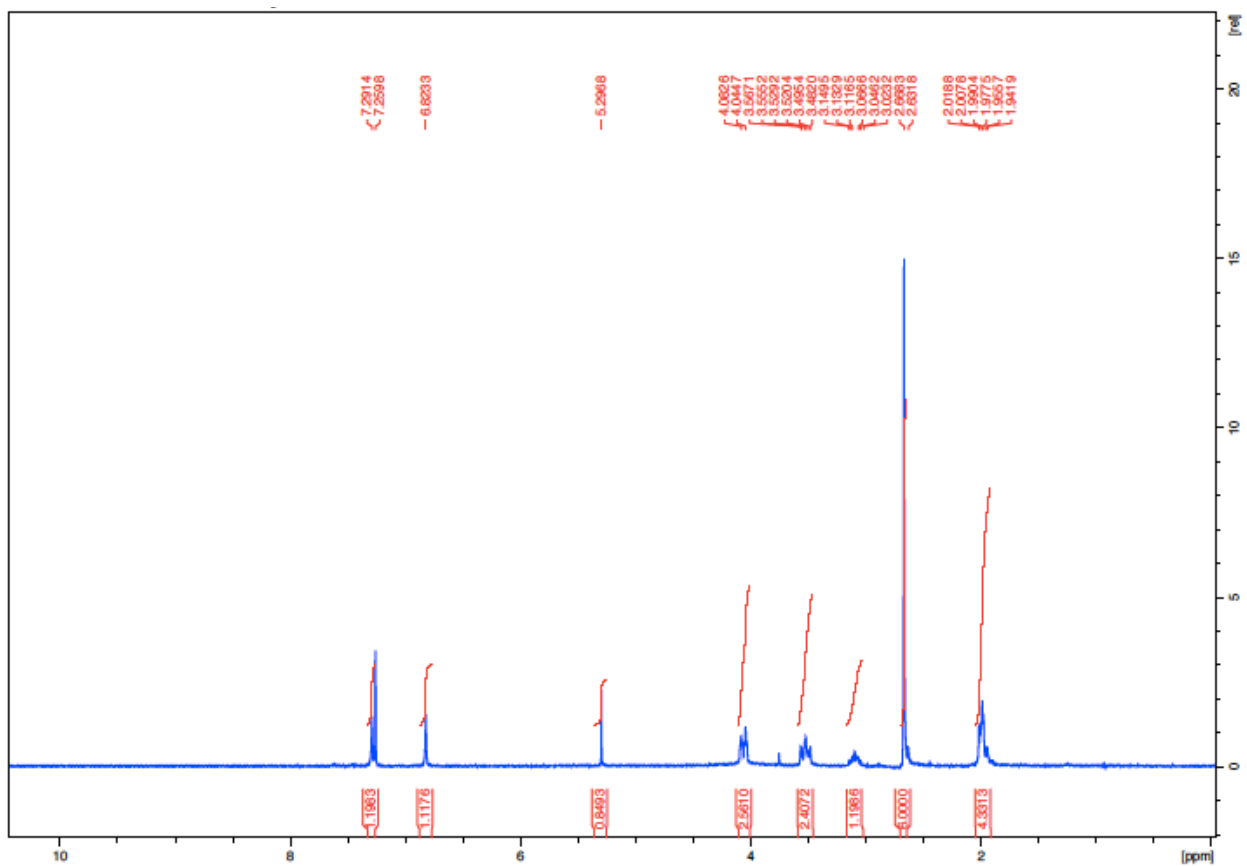


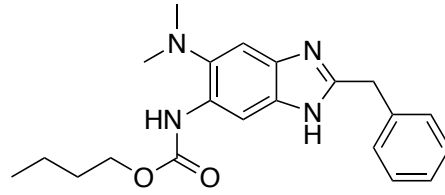




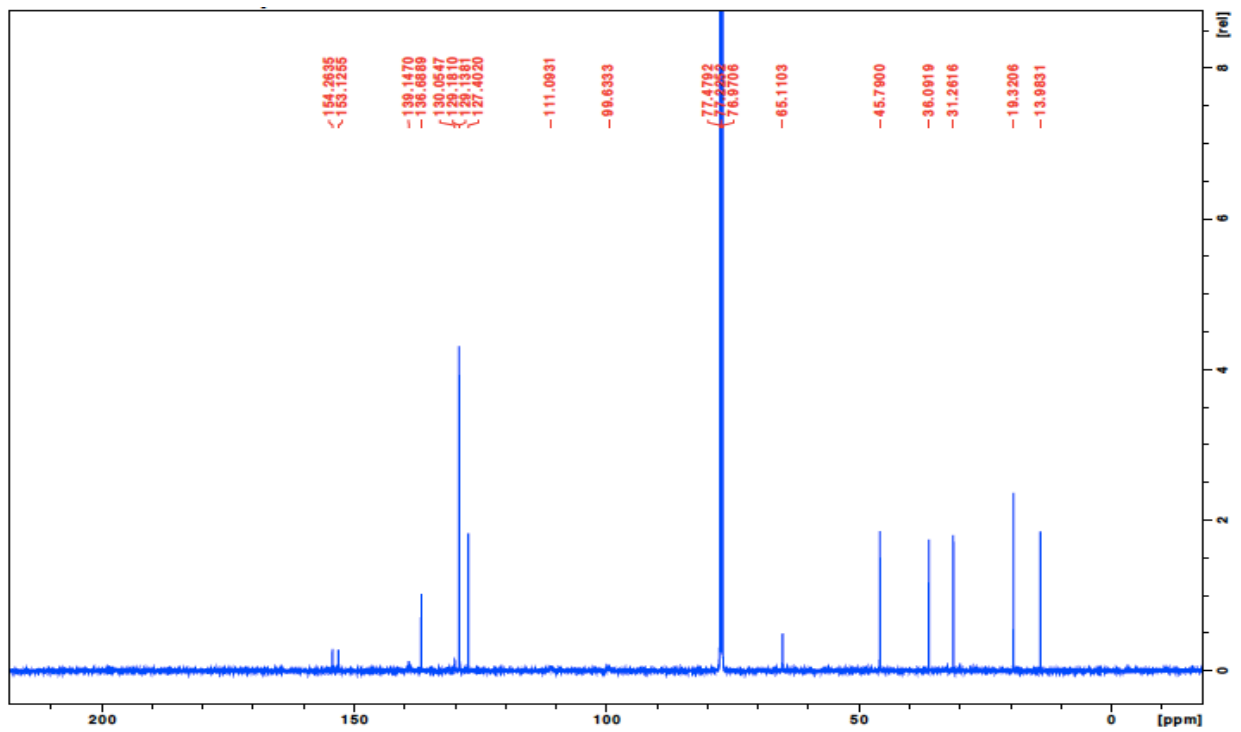
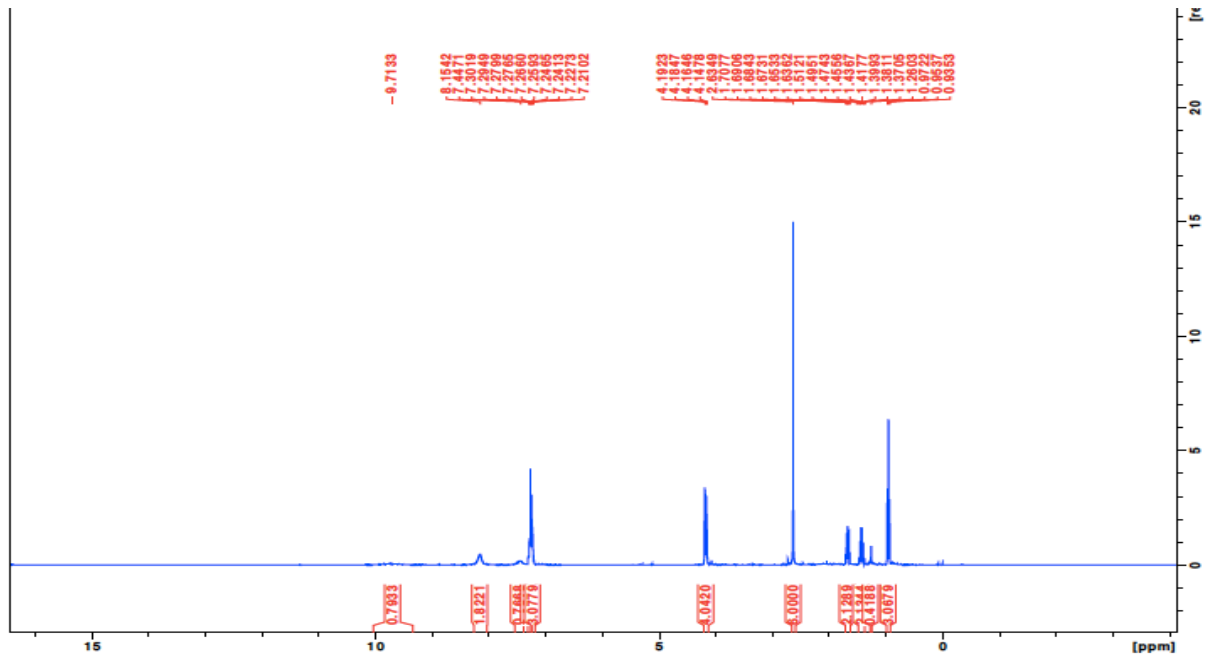


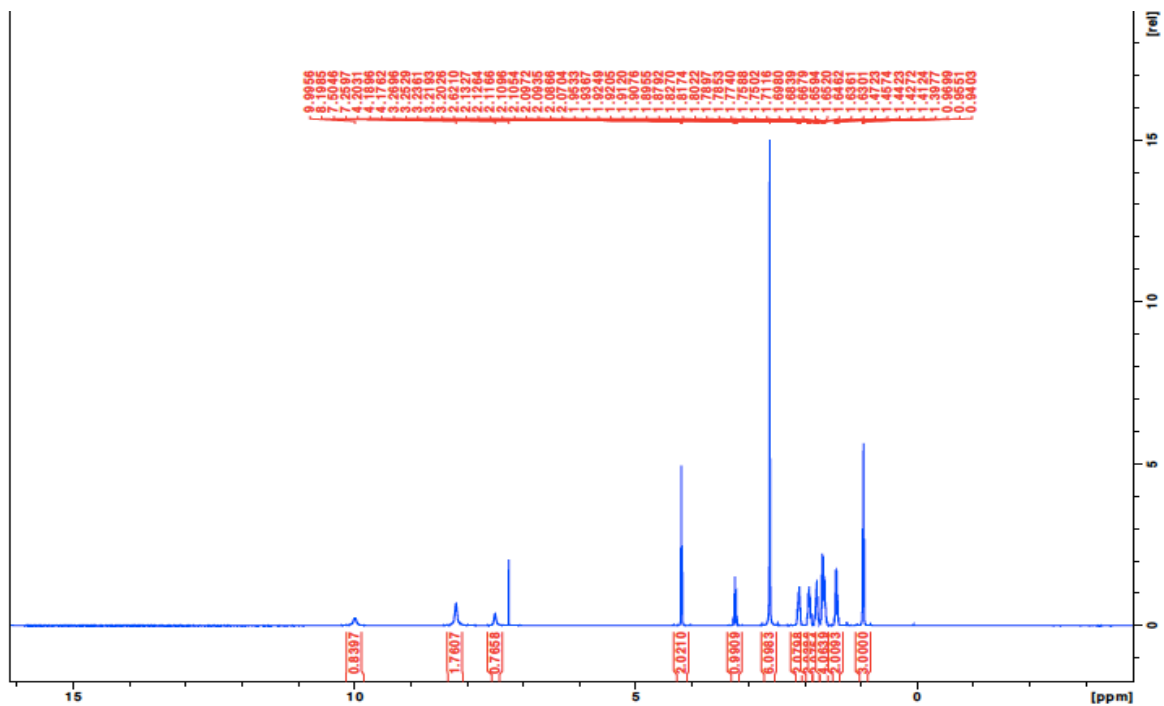
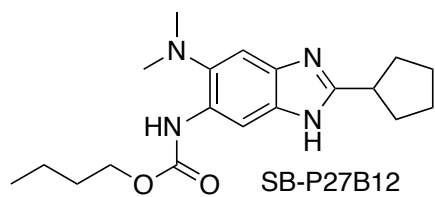


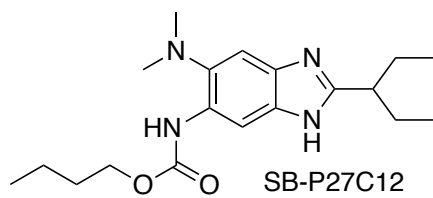
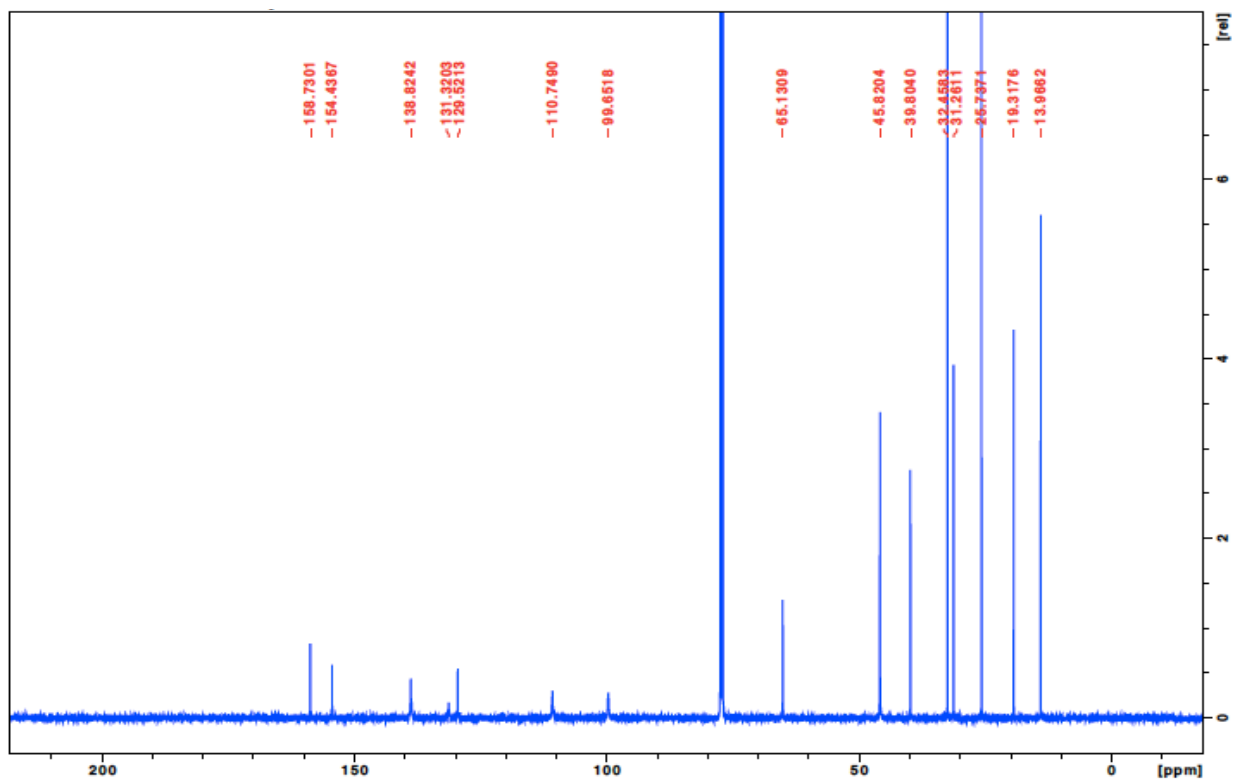


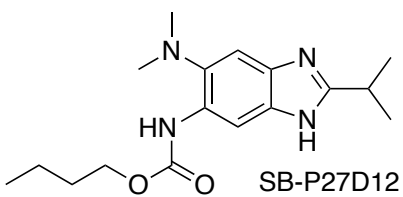
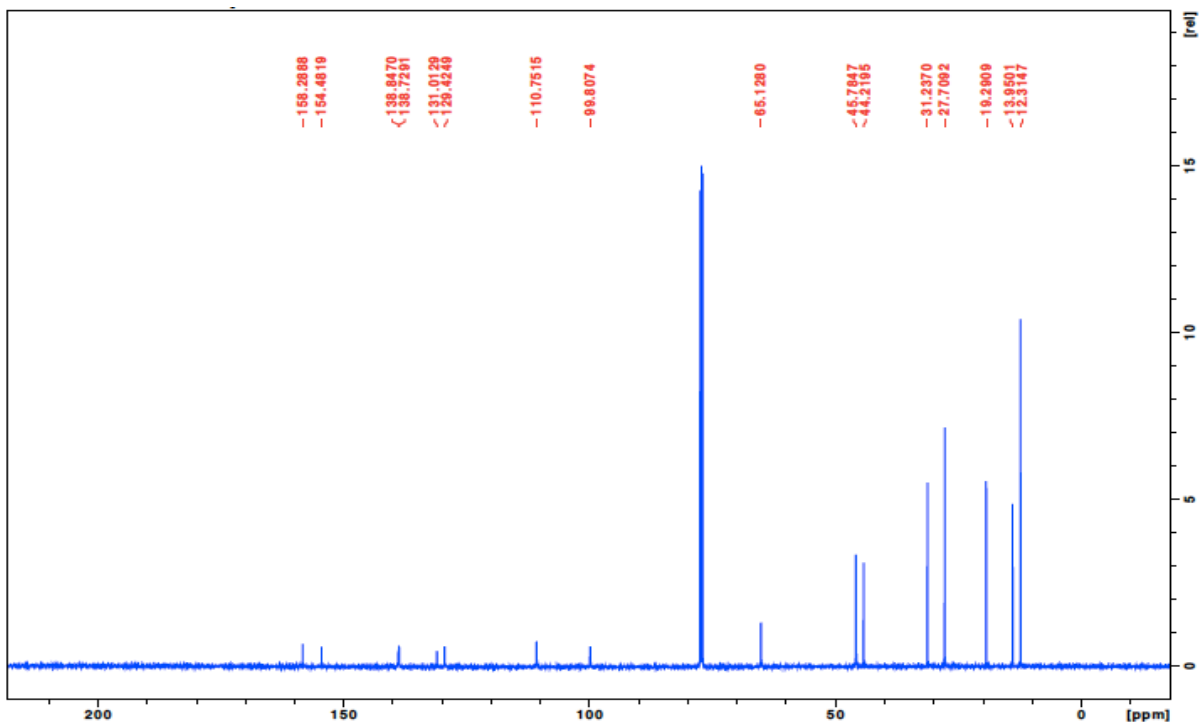
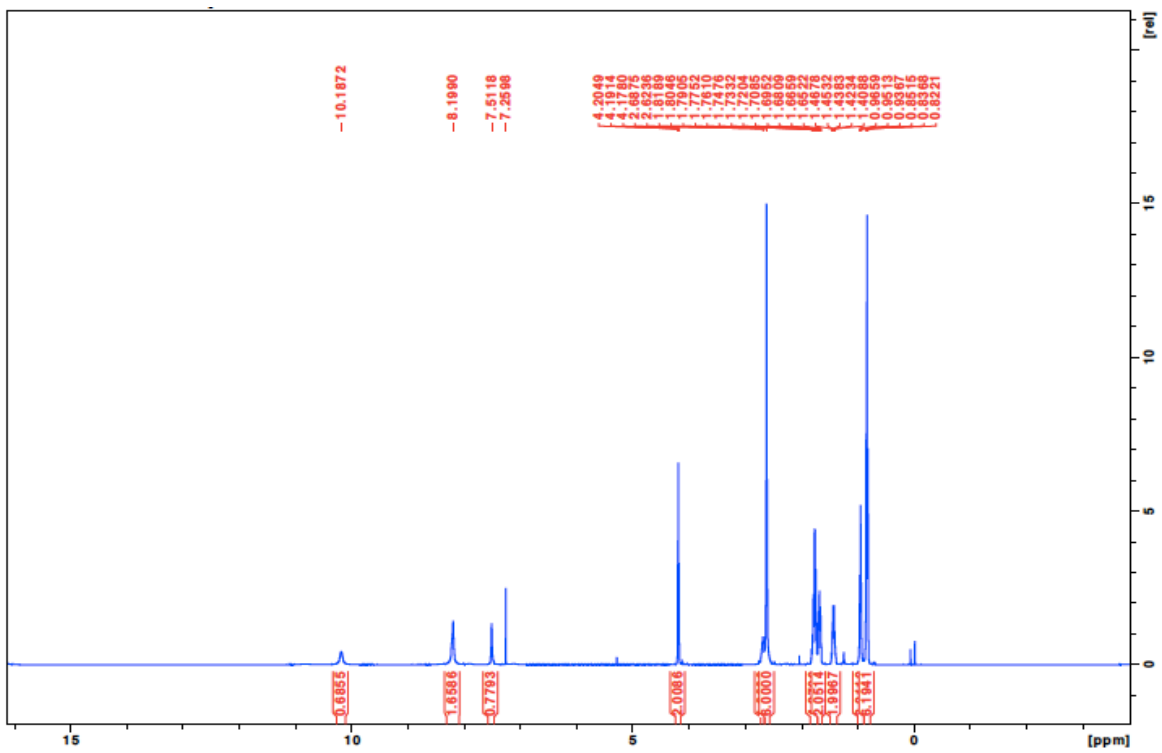


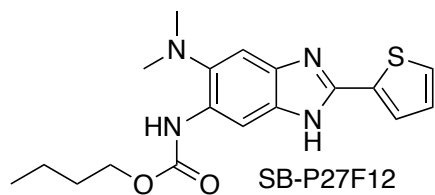
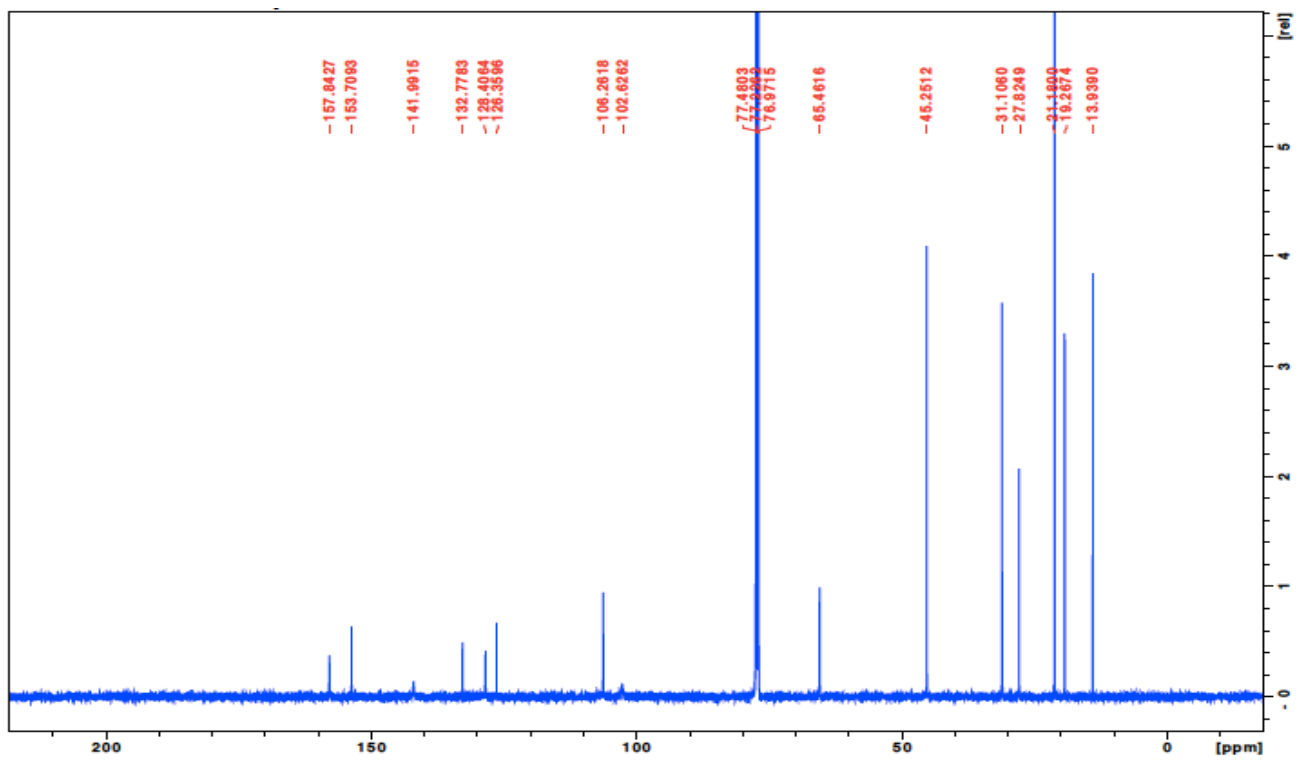
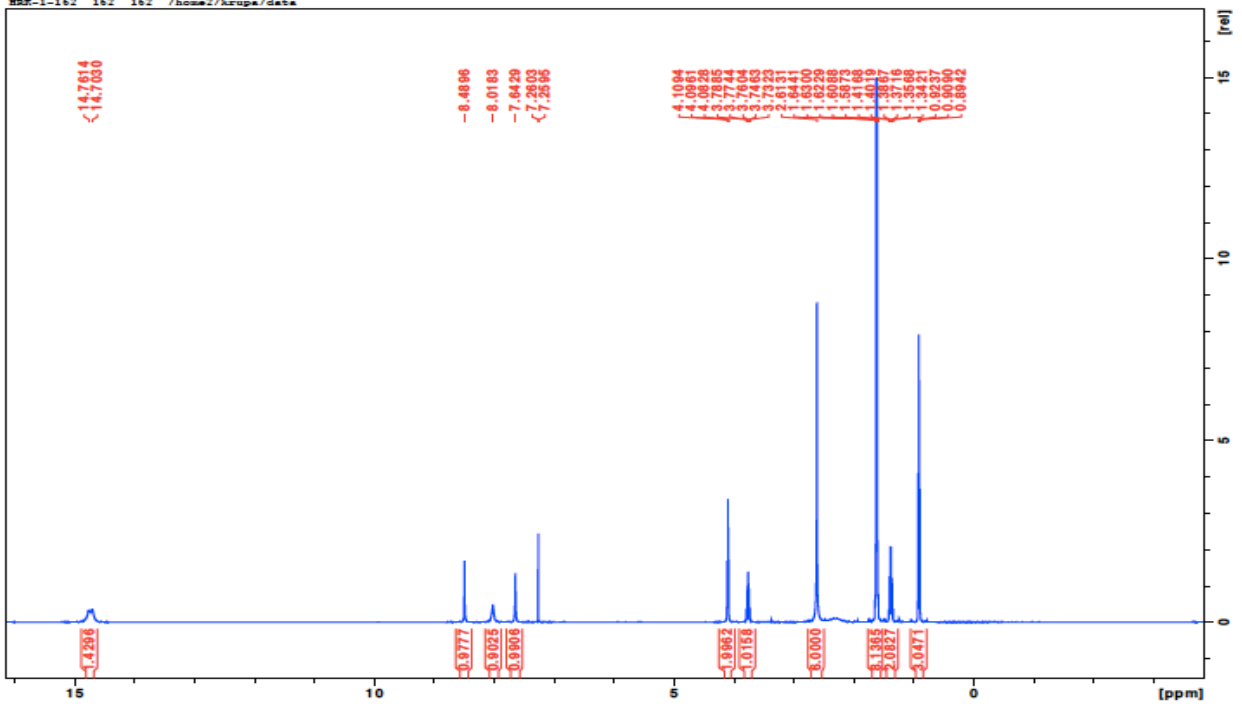
SB-P27A12

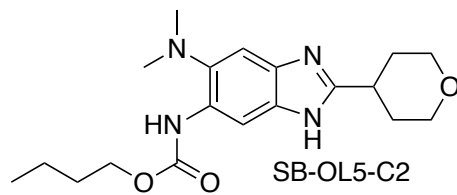
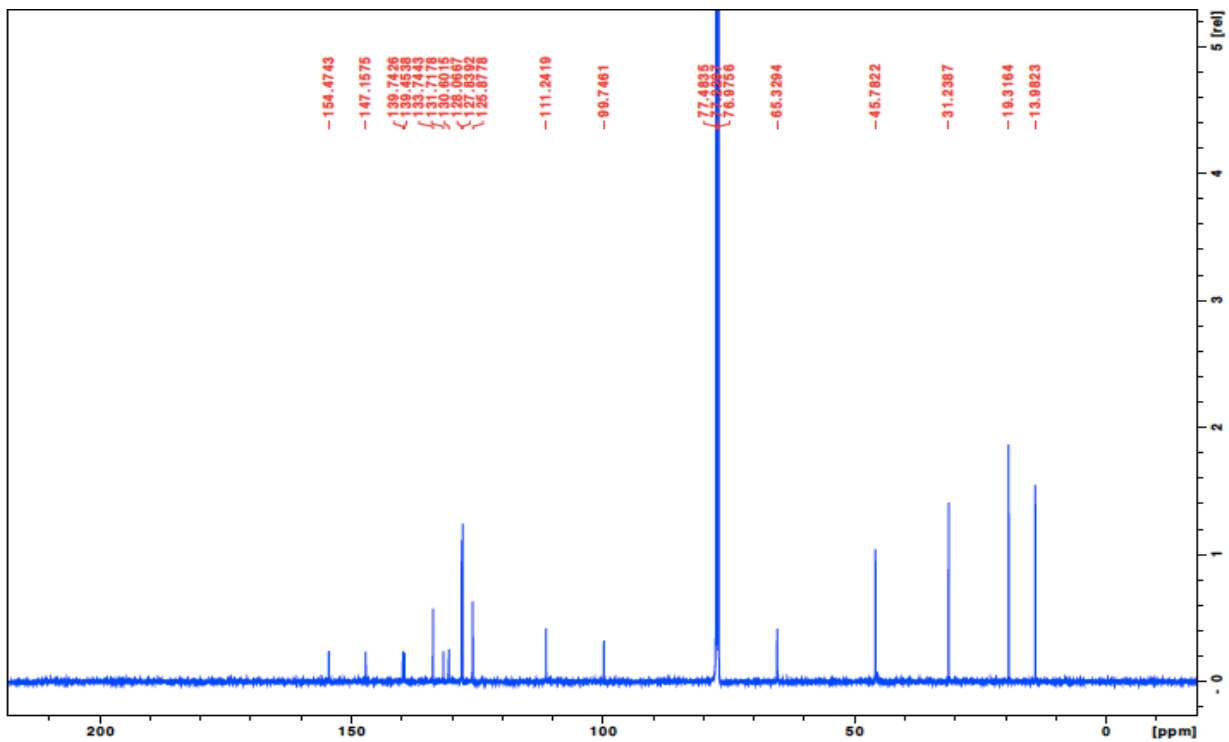
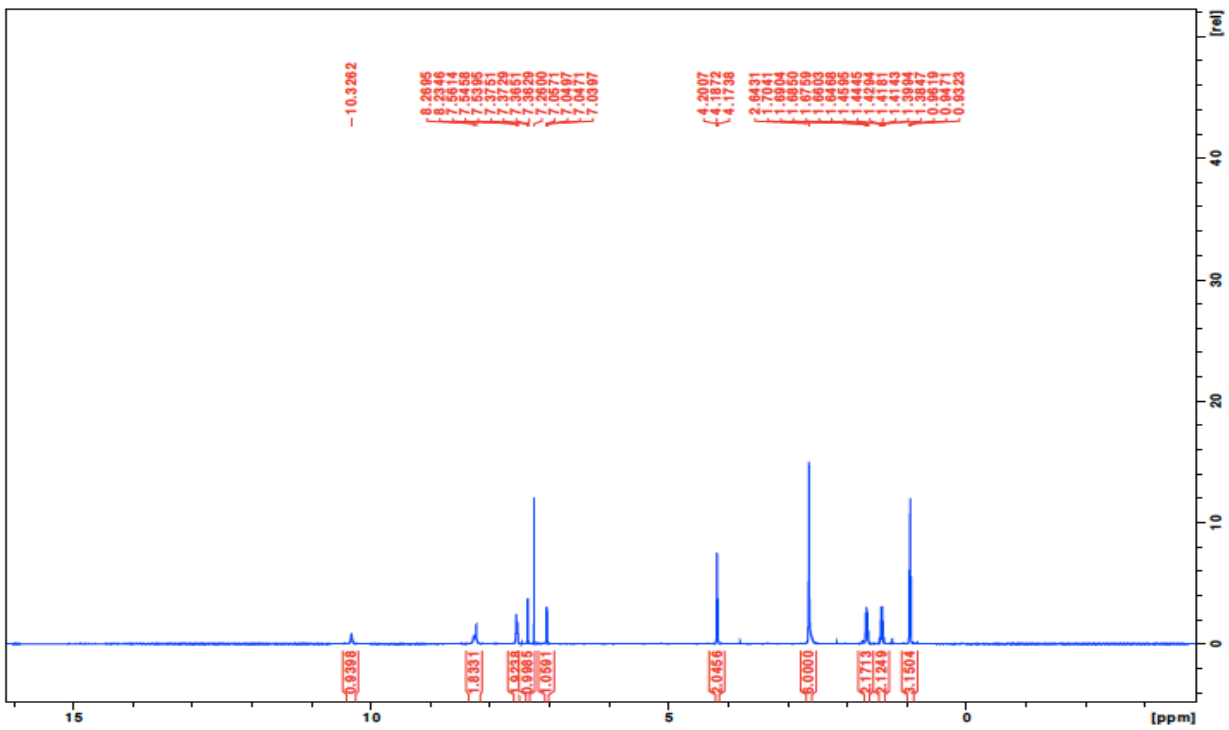


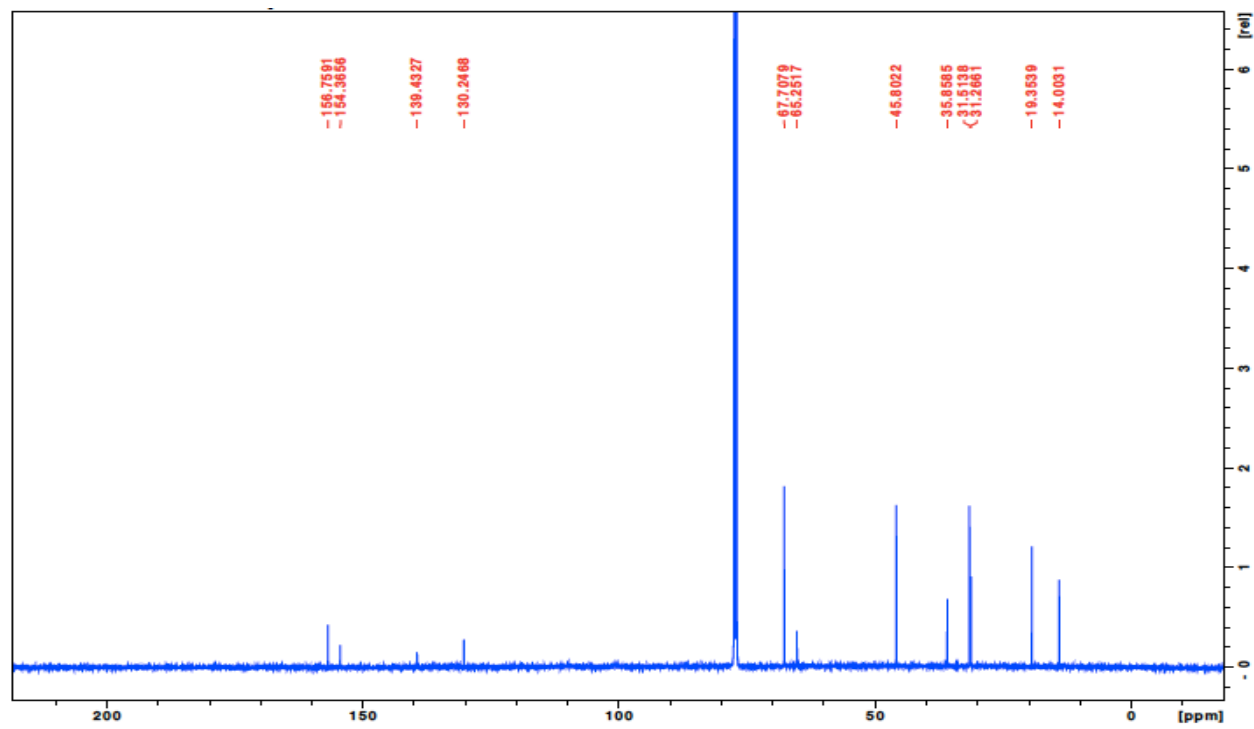
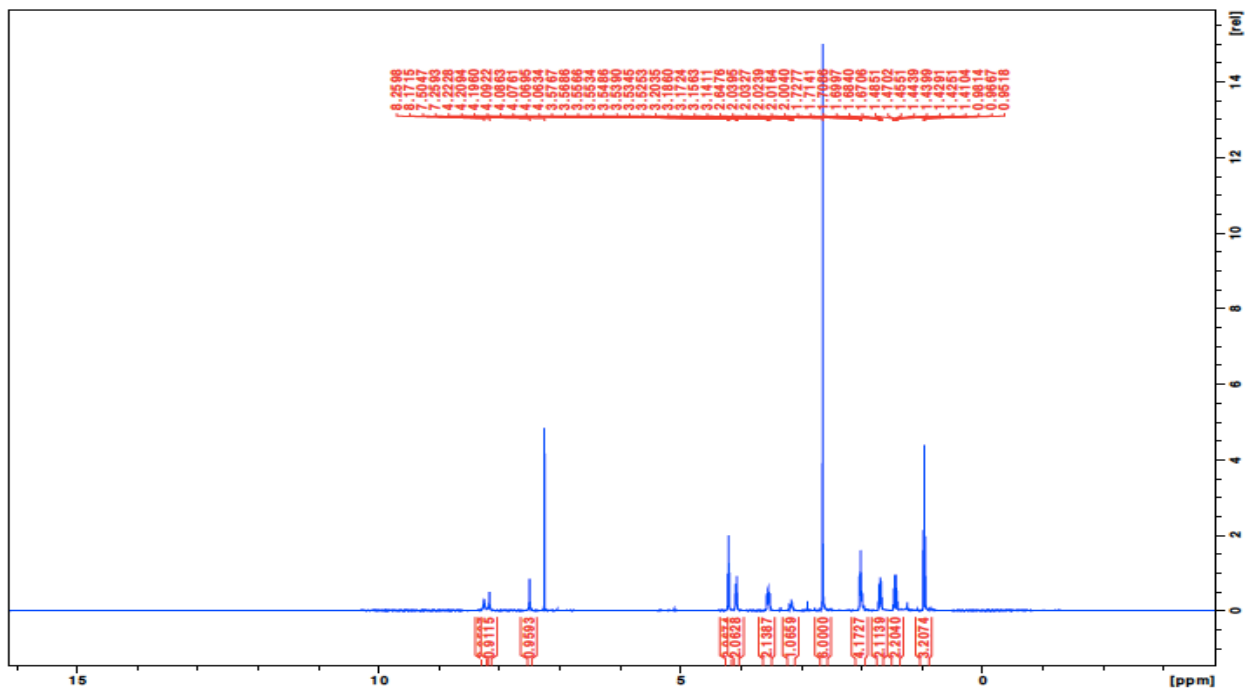


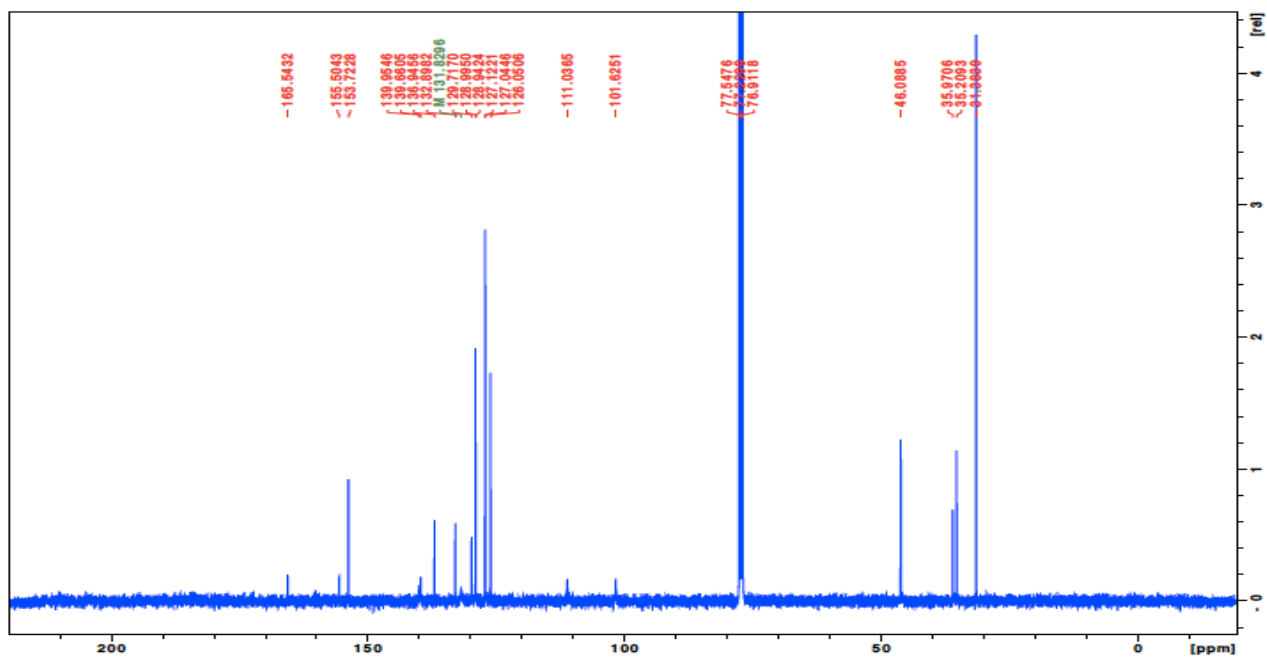
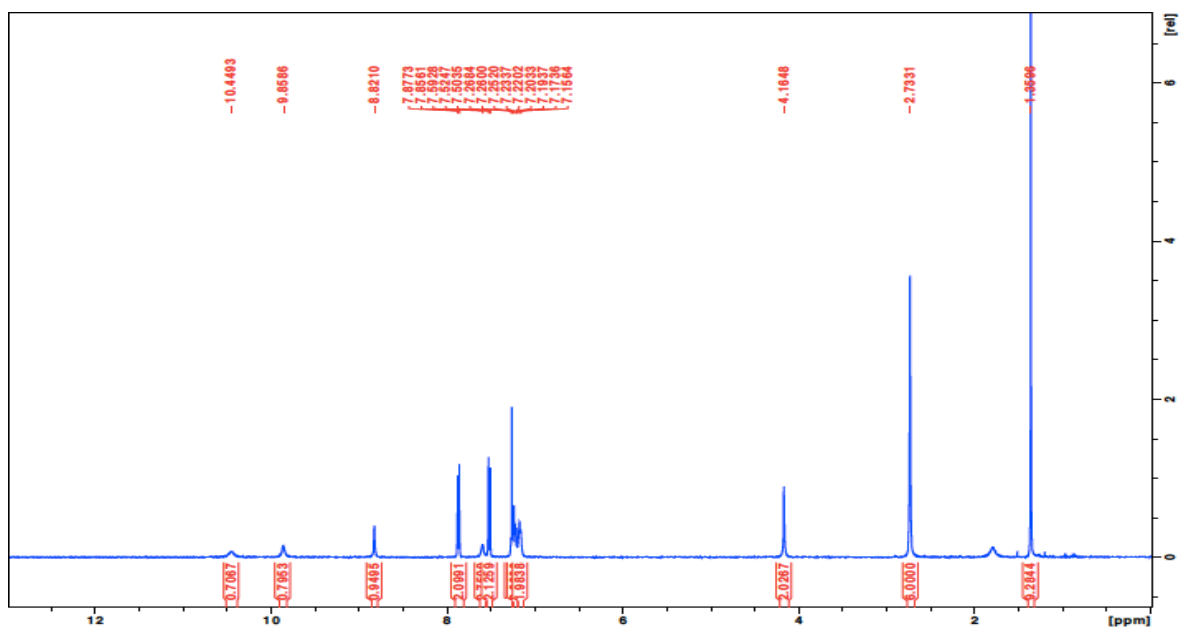
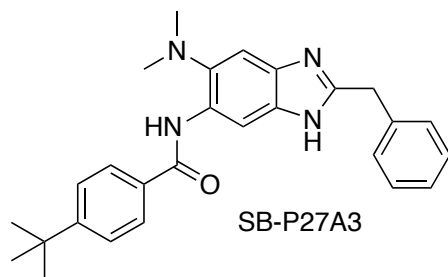


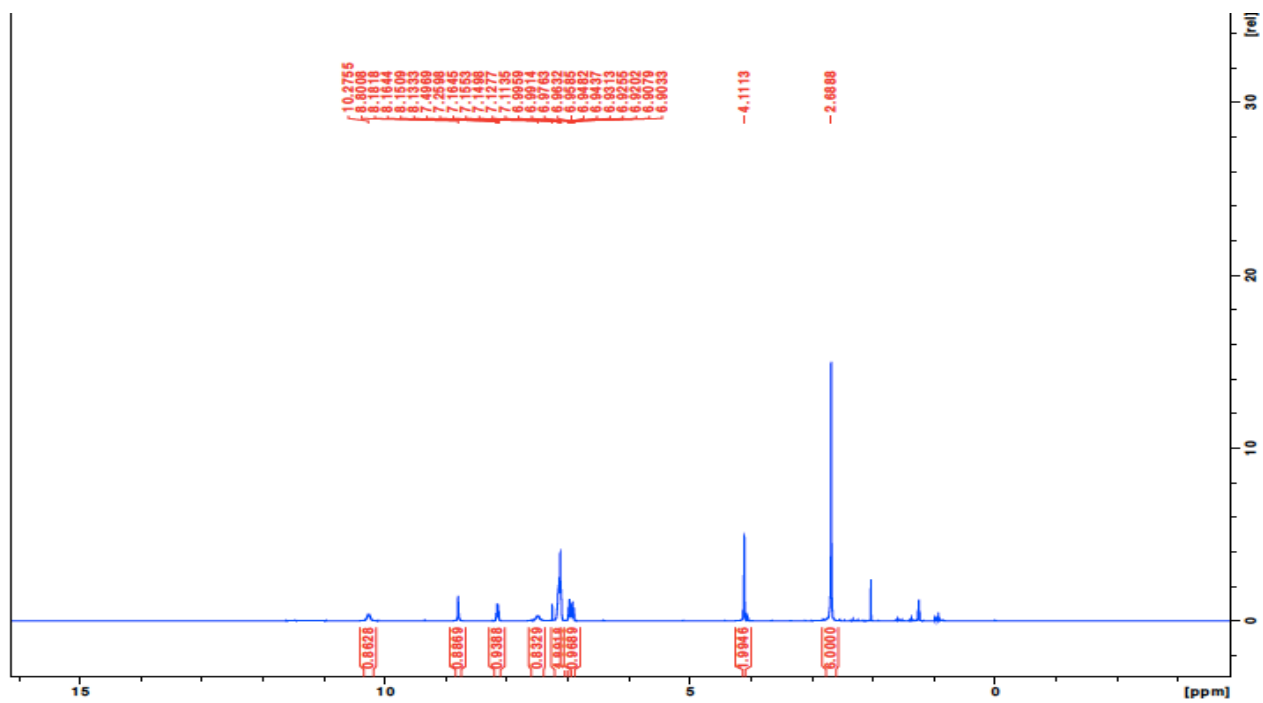
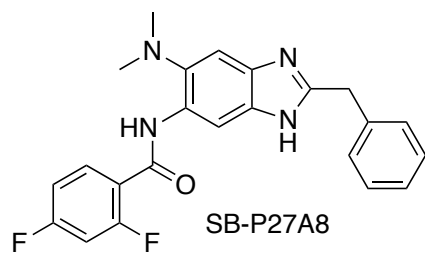


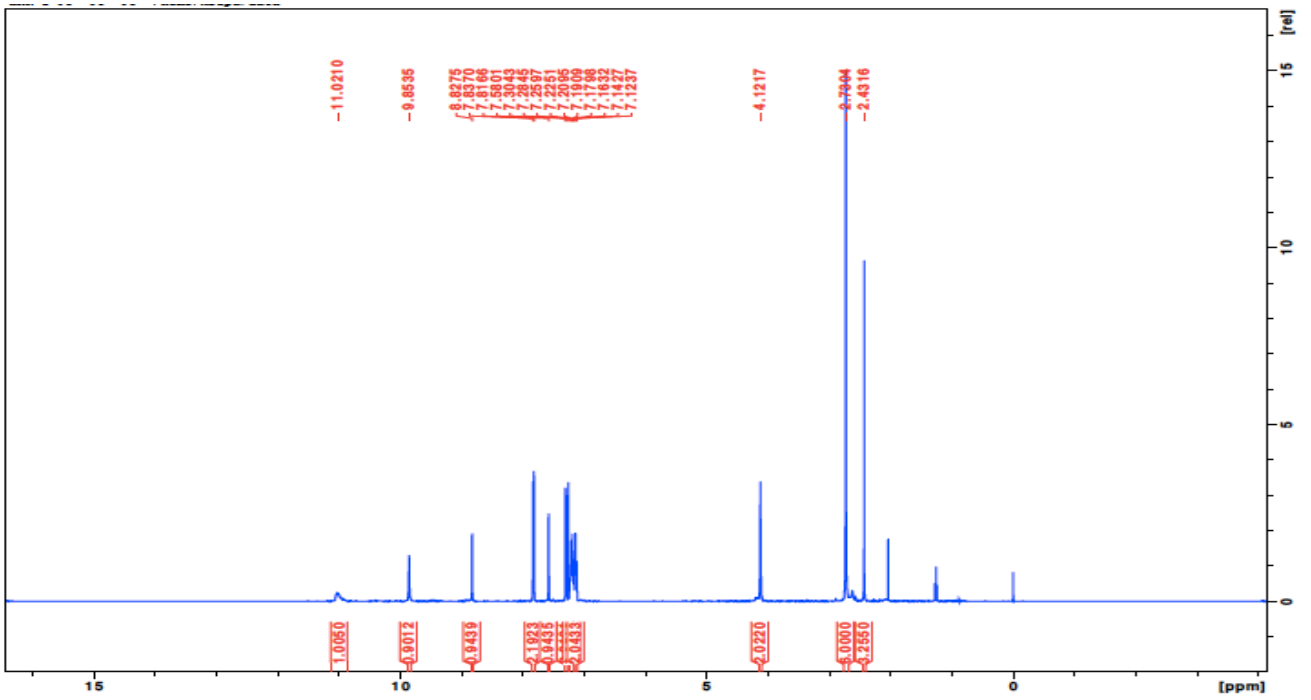
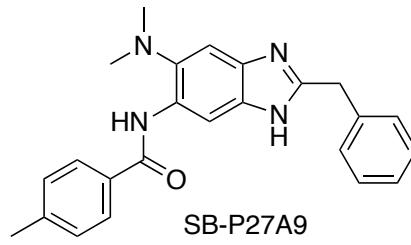
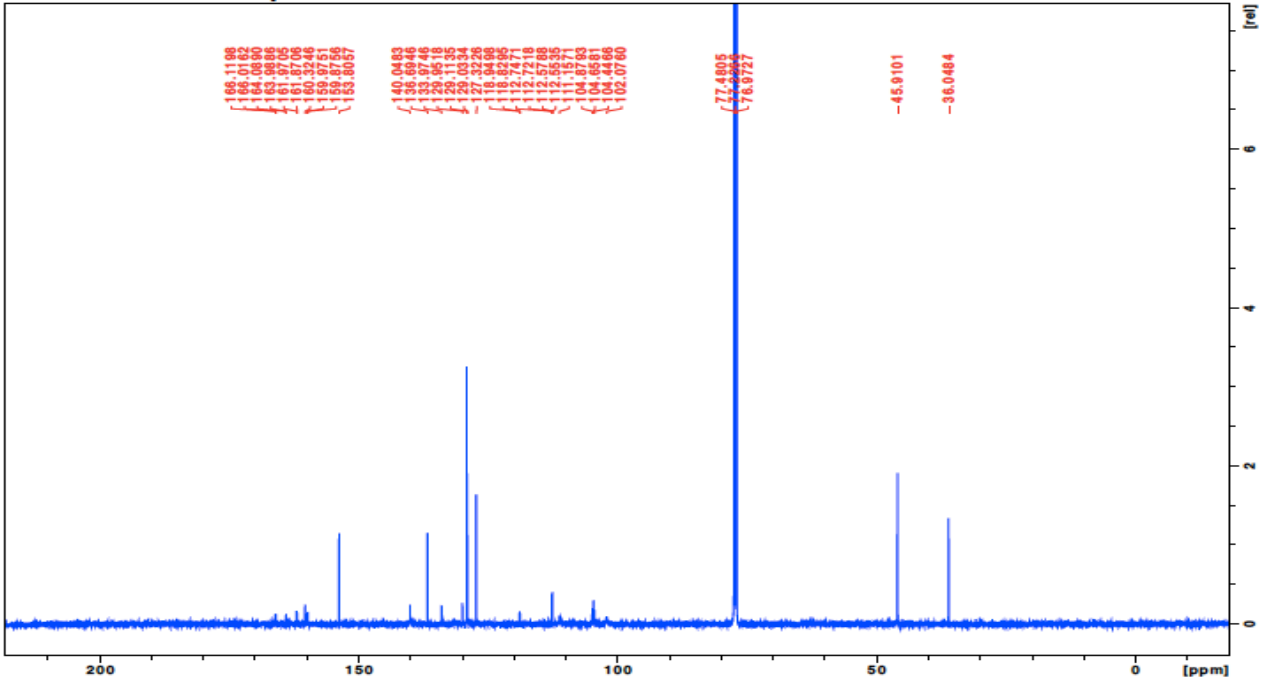


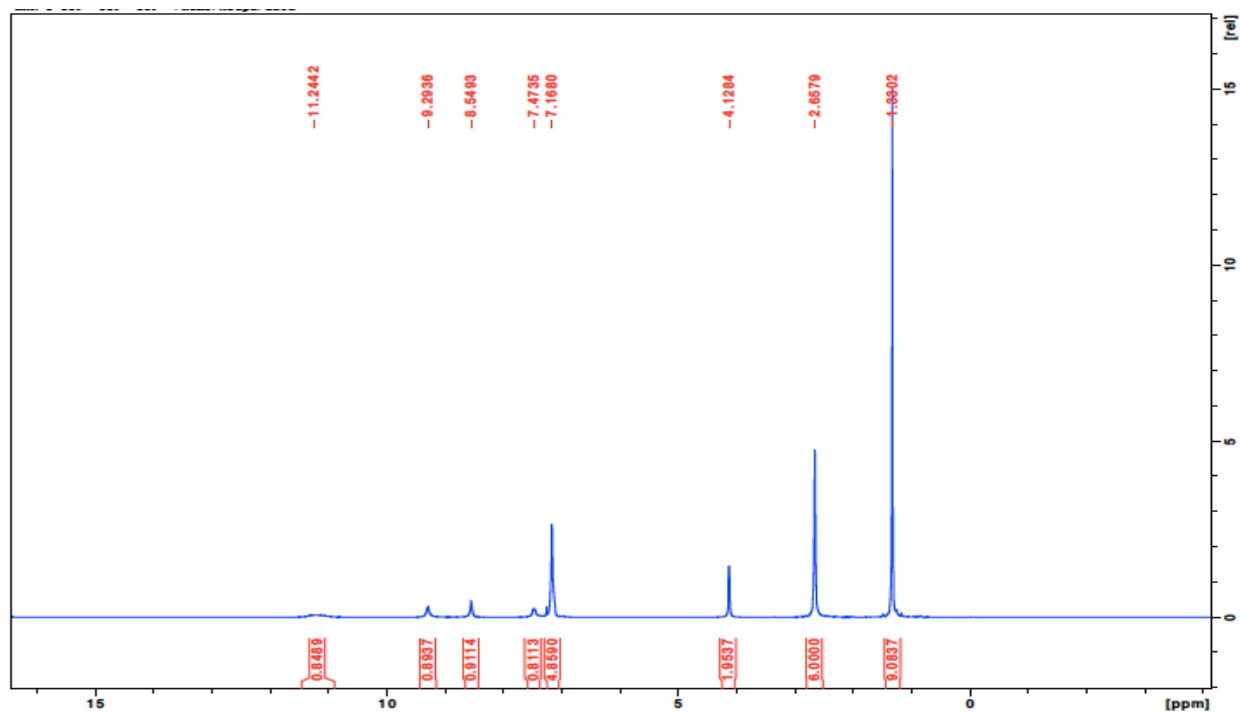
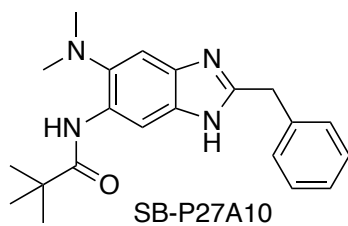
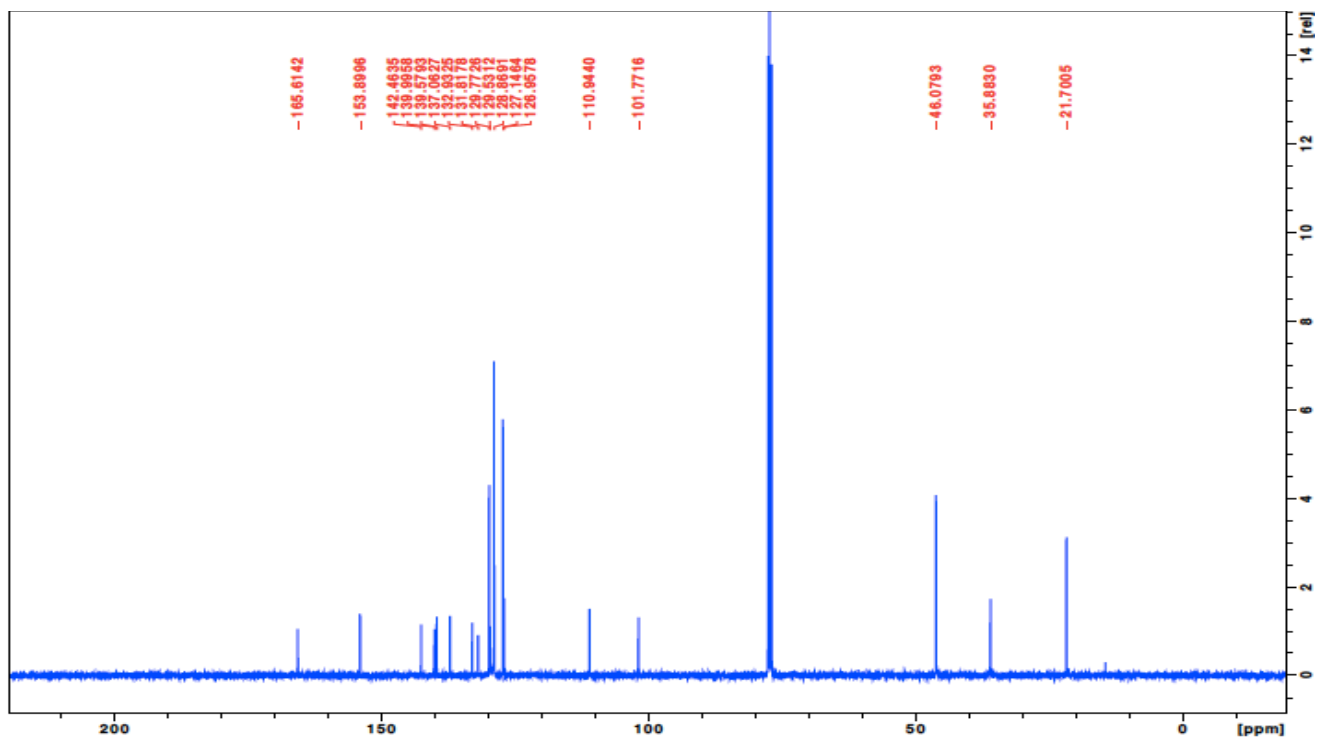


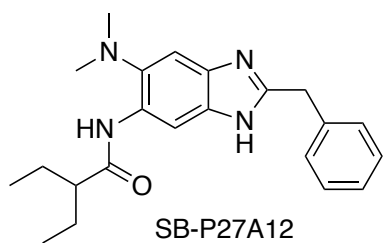
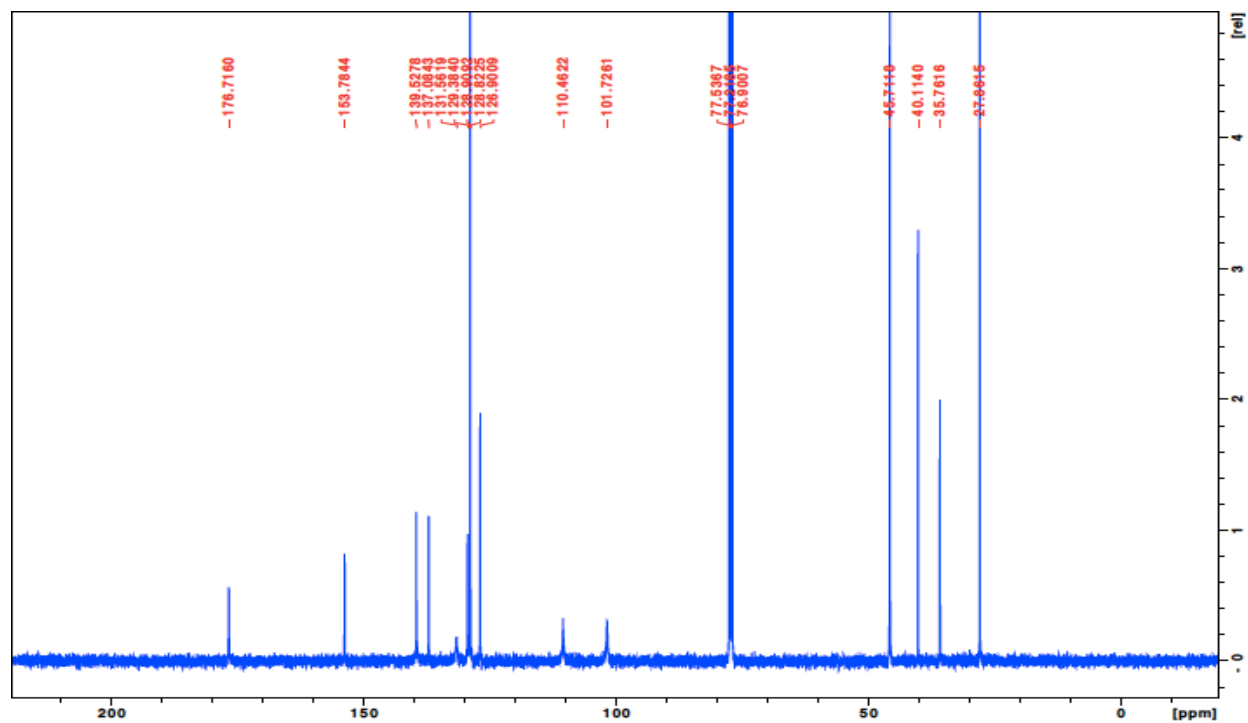


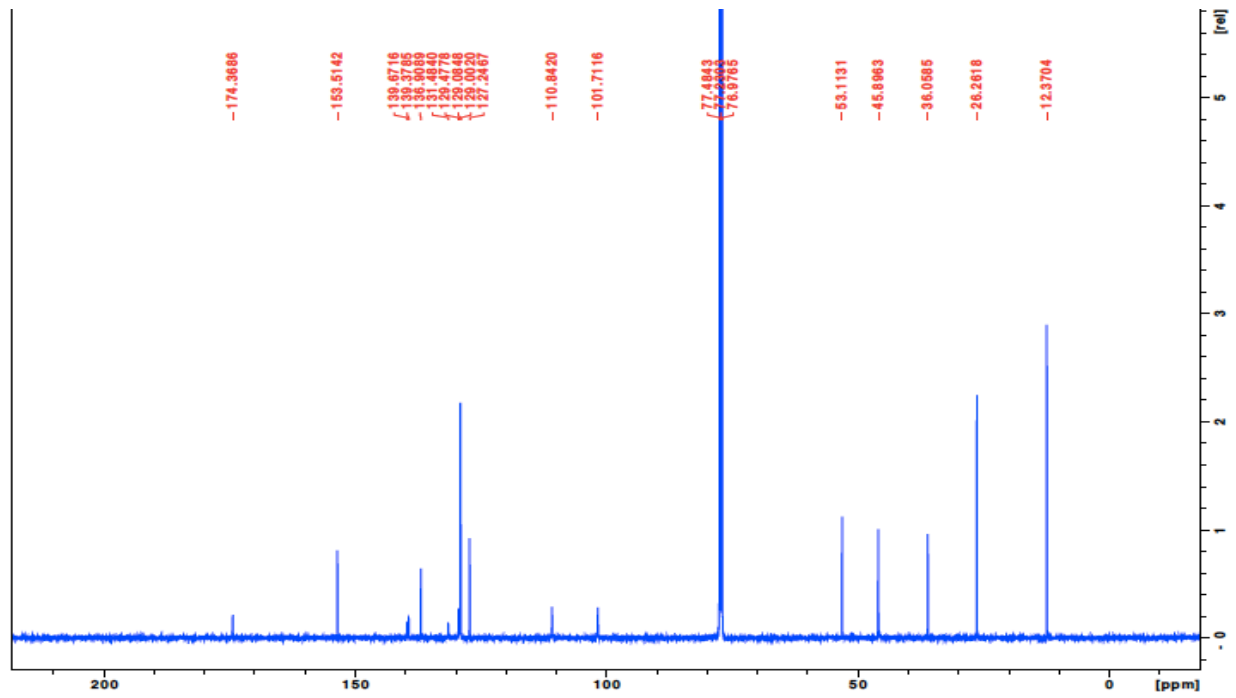
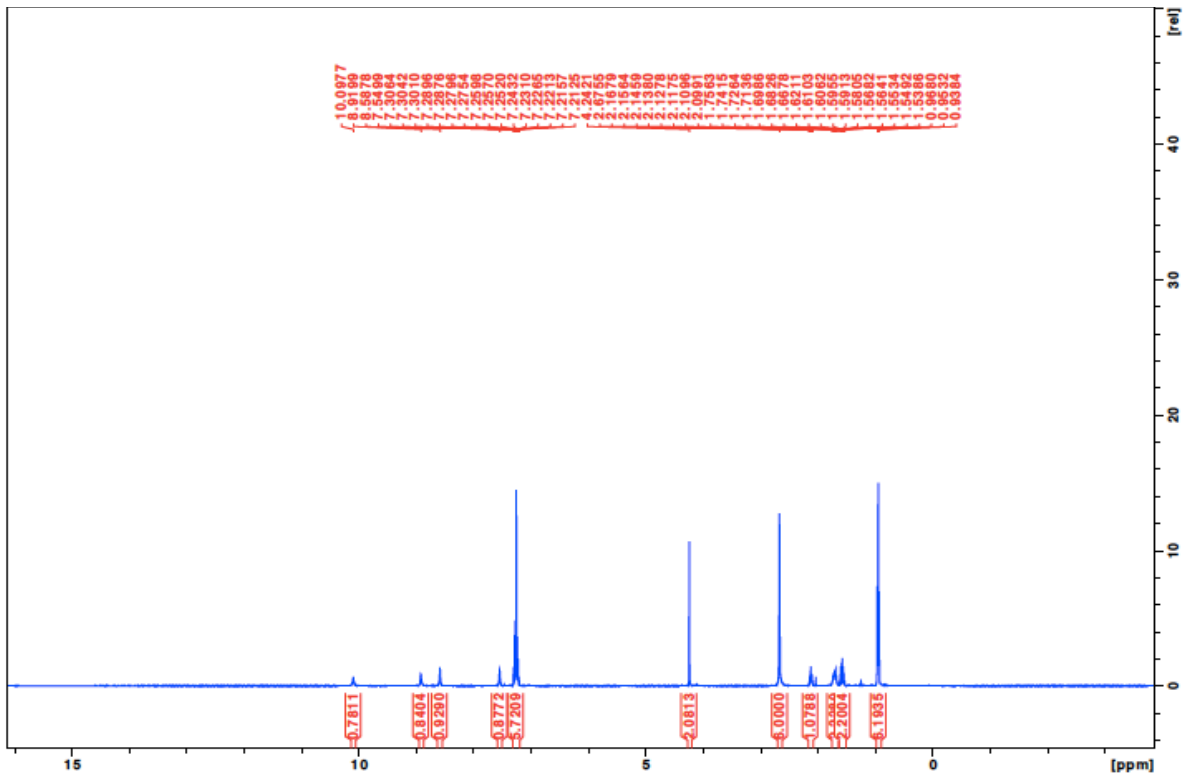


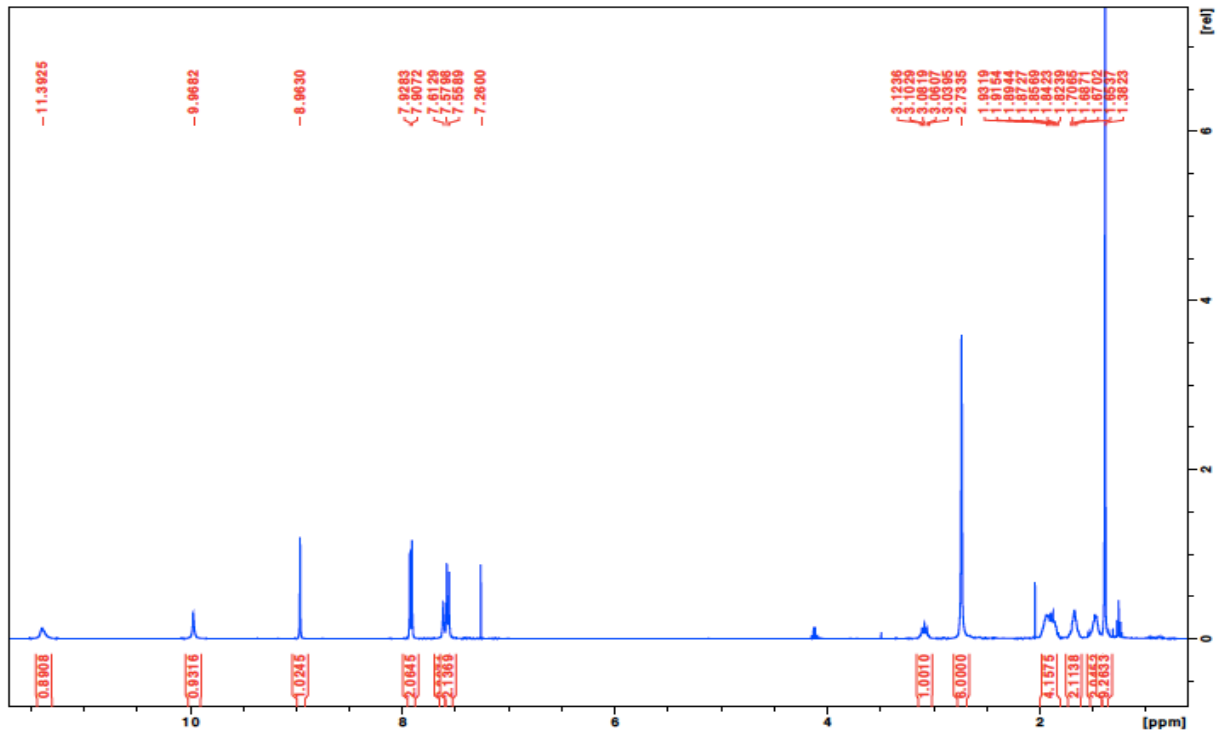
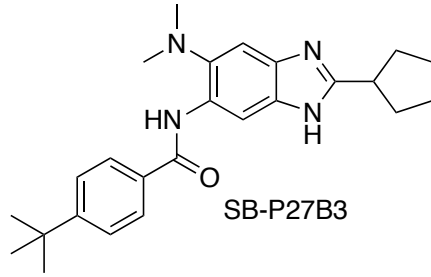


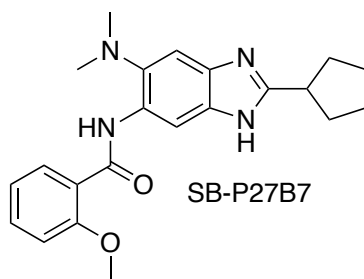
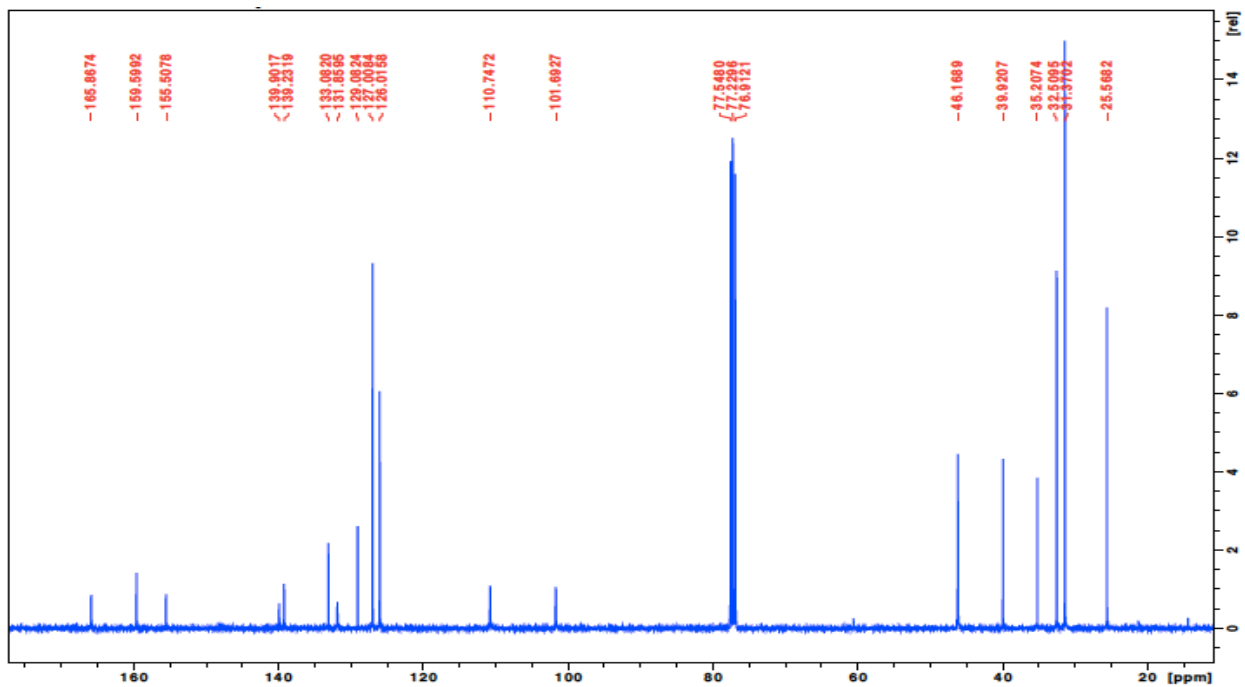


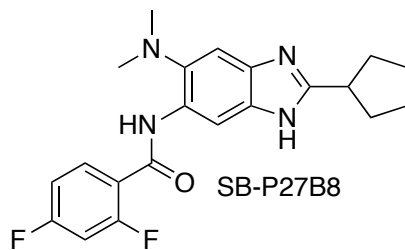
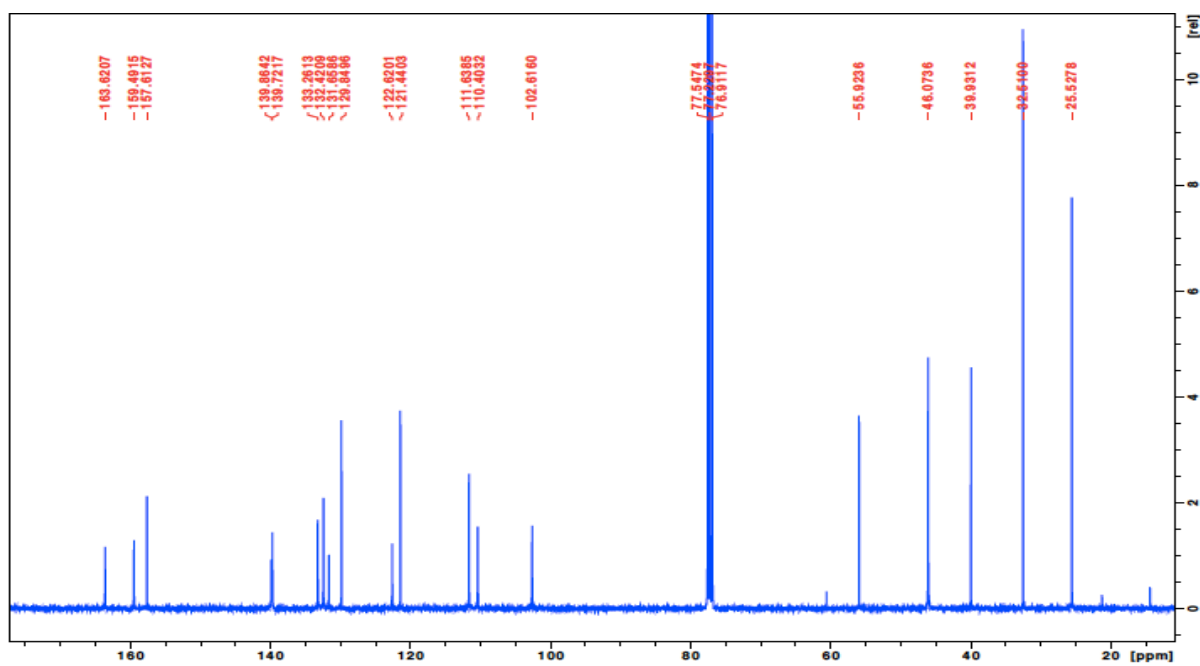
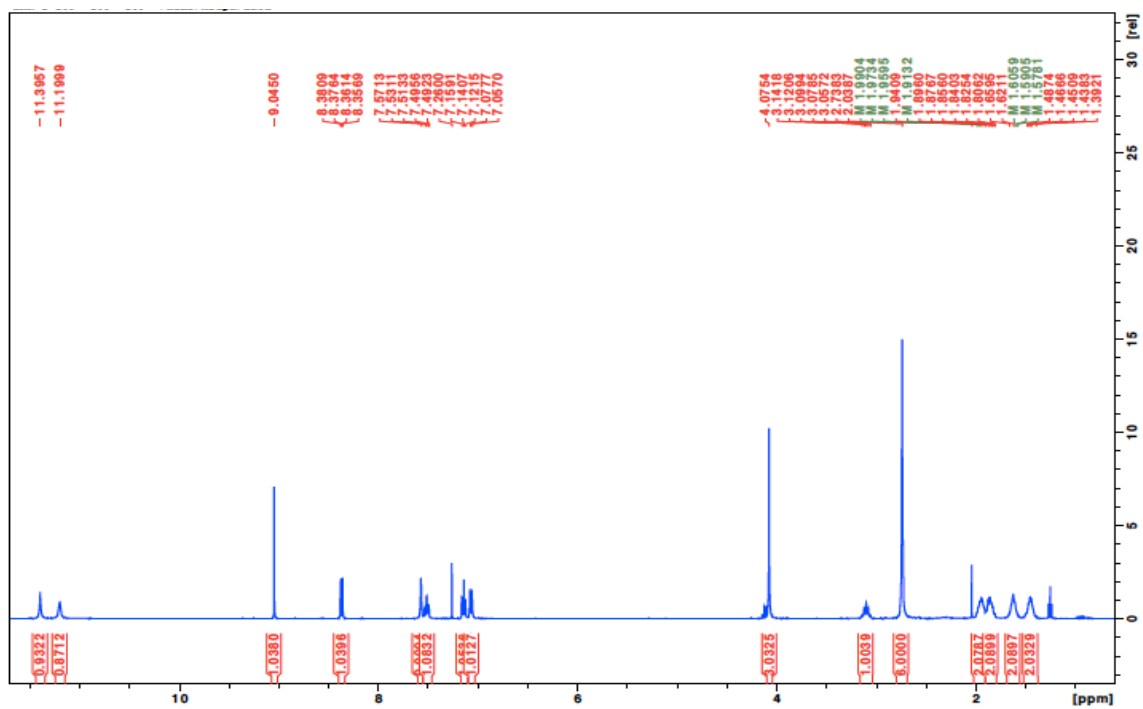


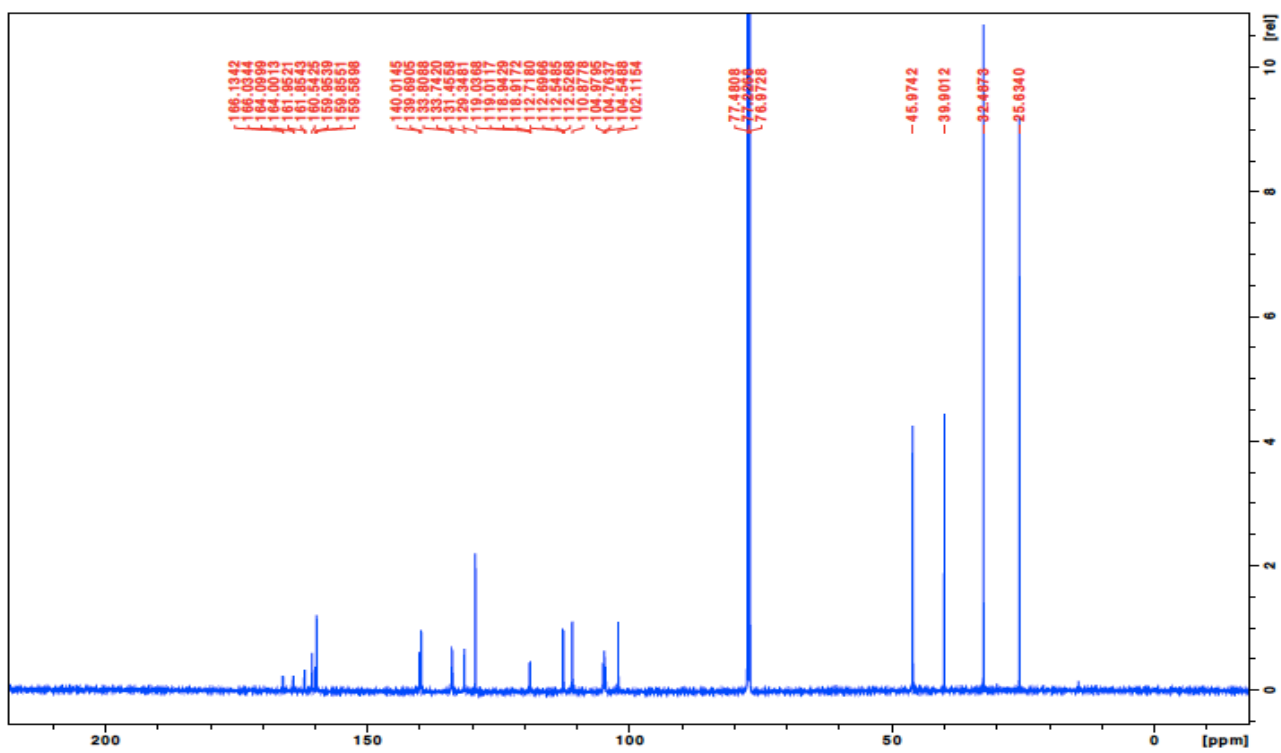
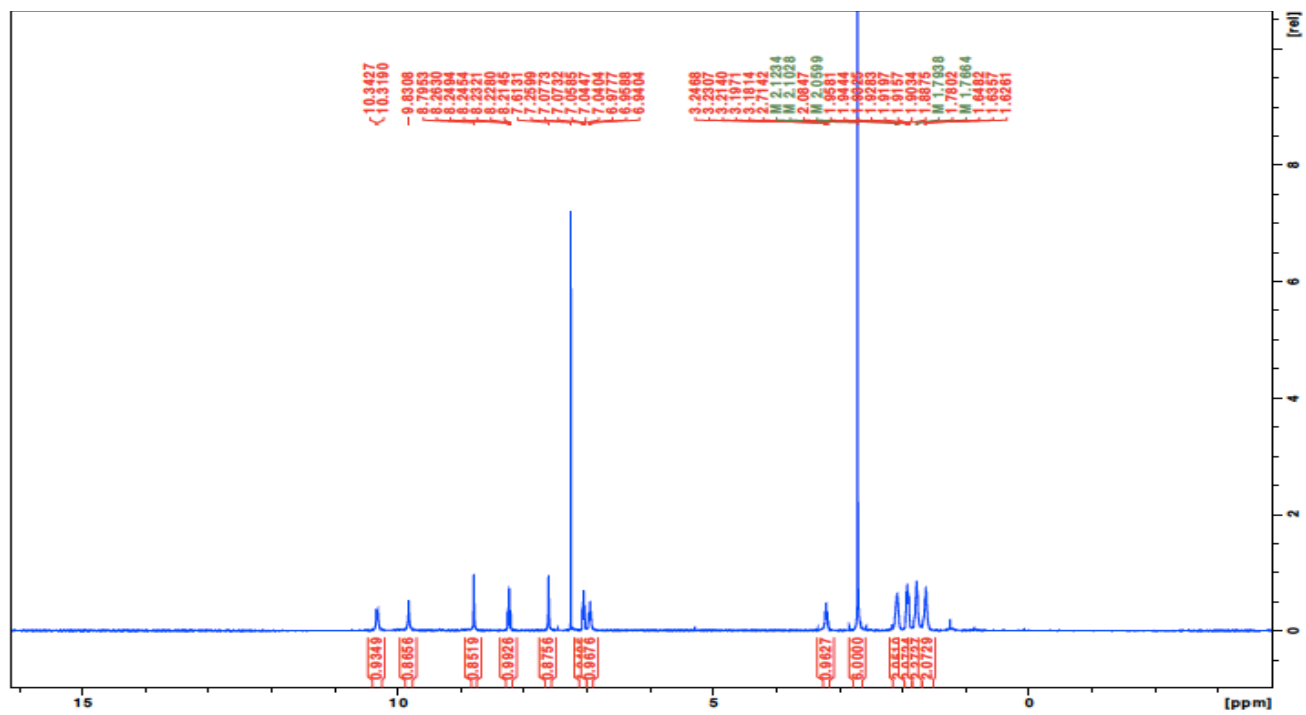


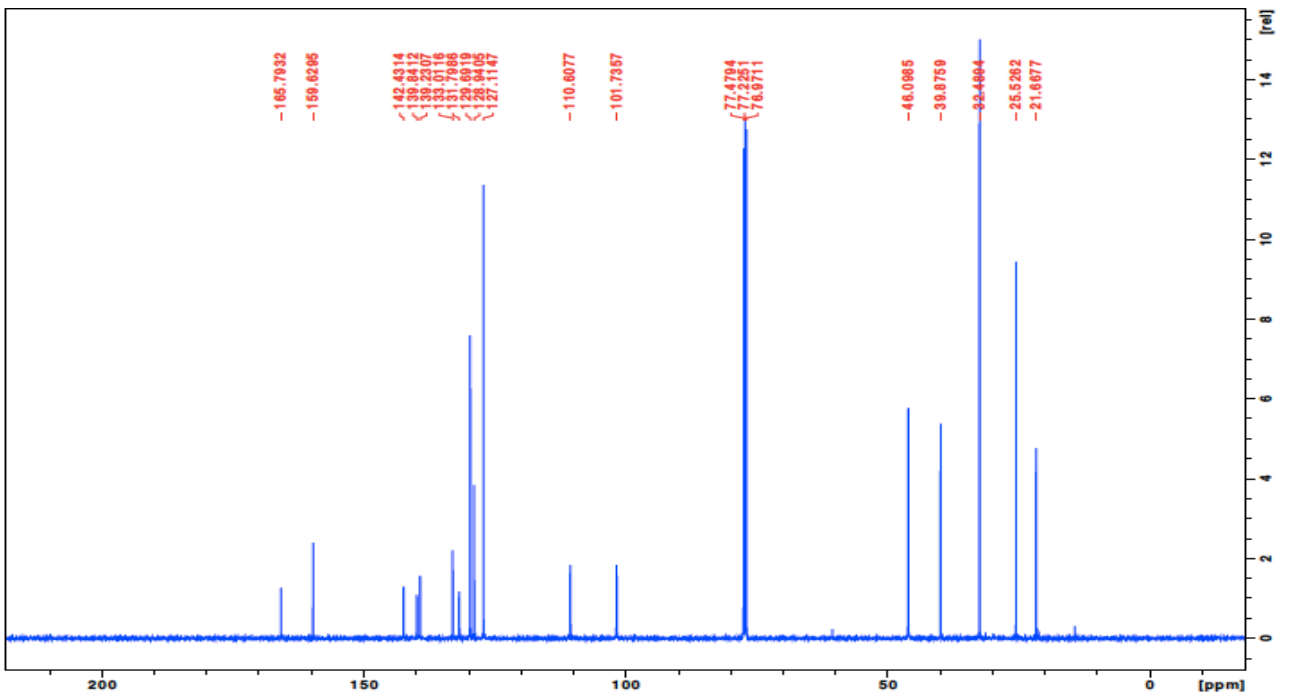
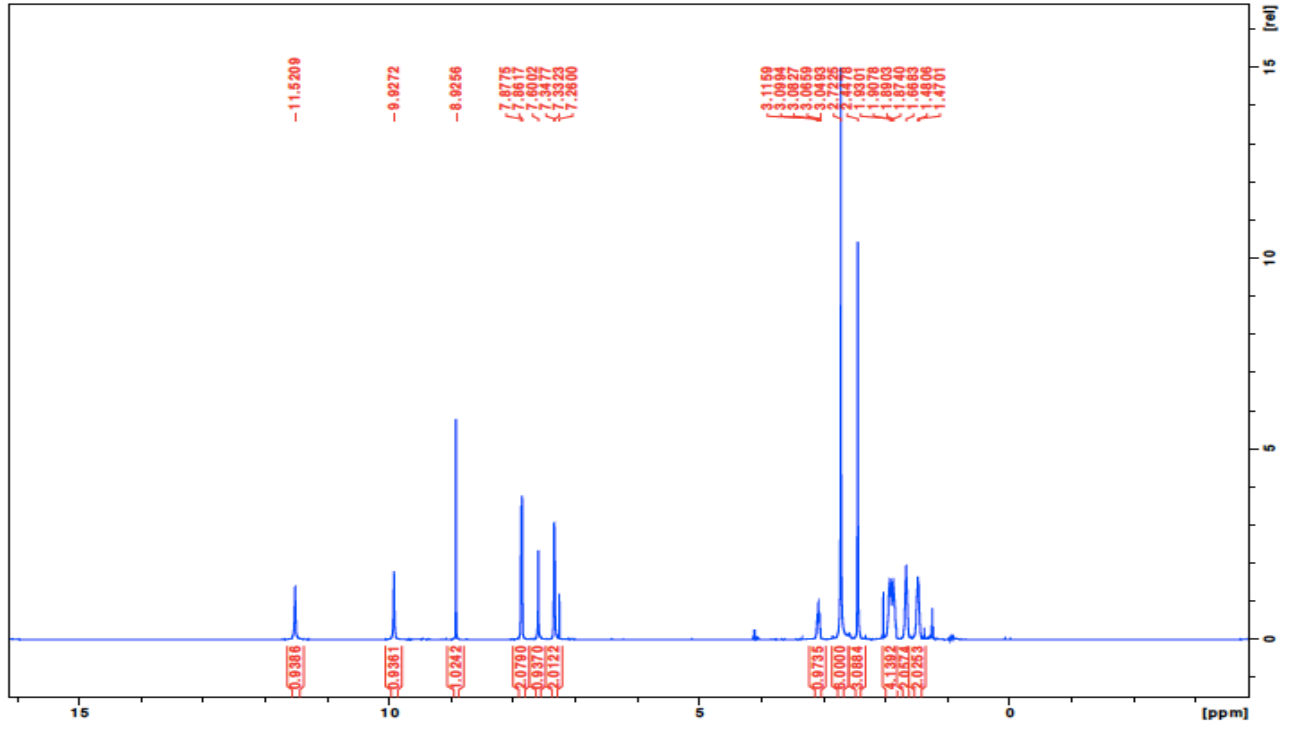
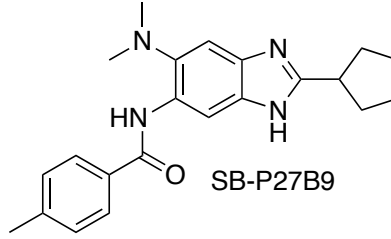


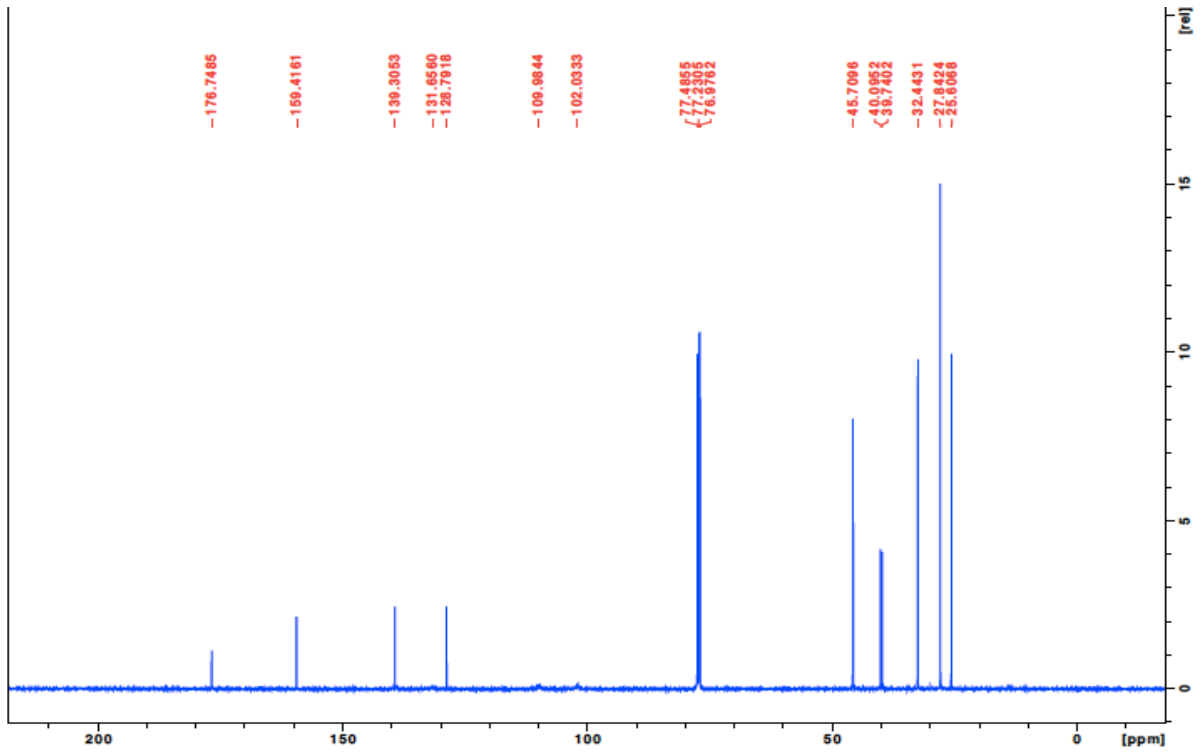
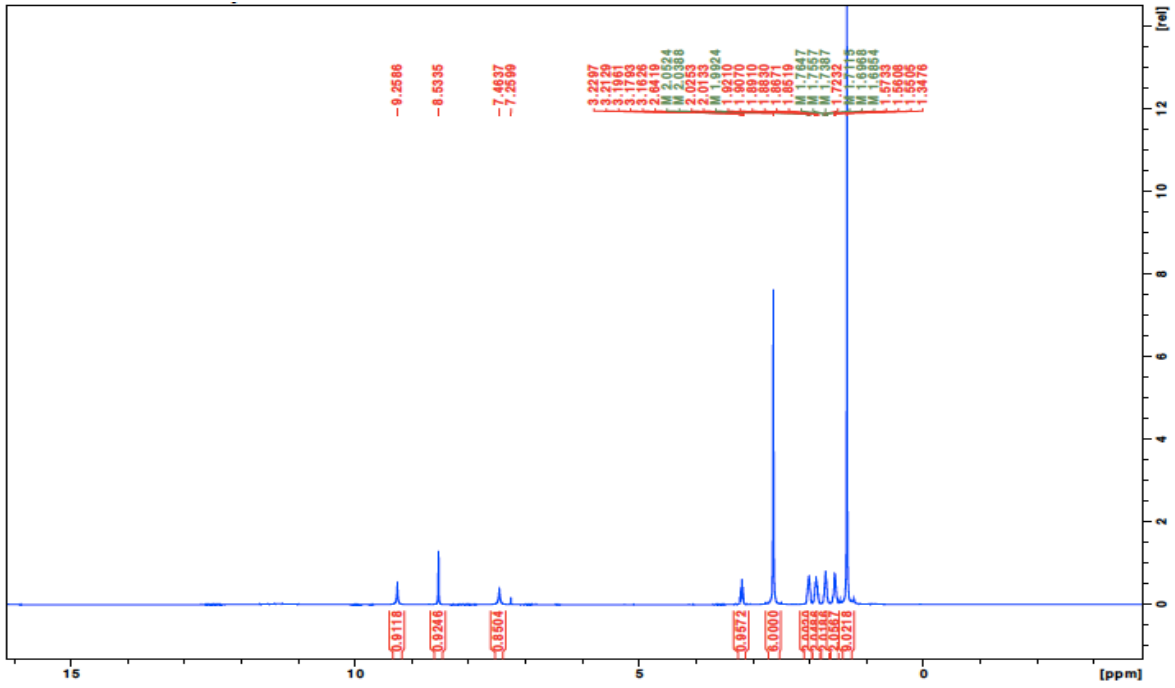
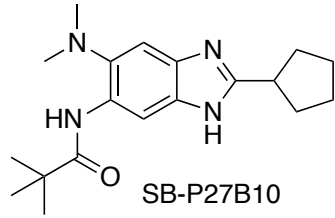


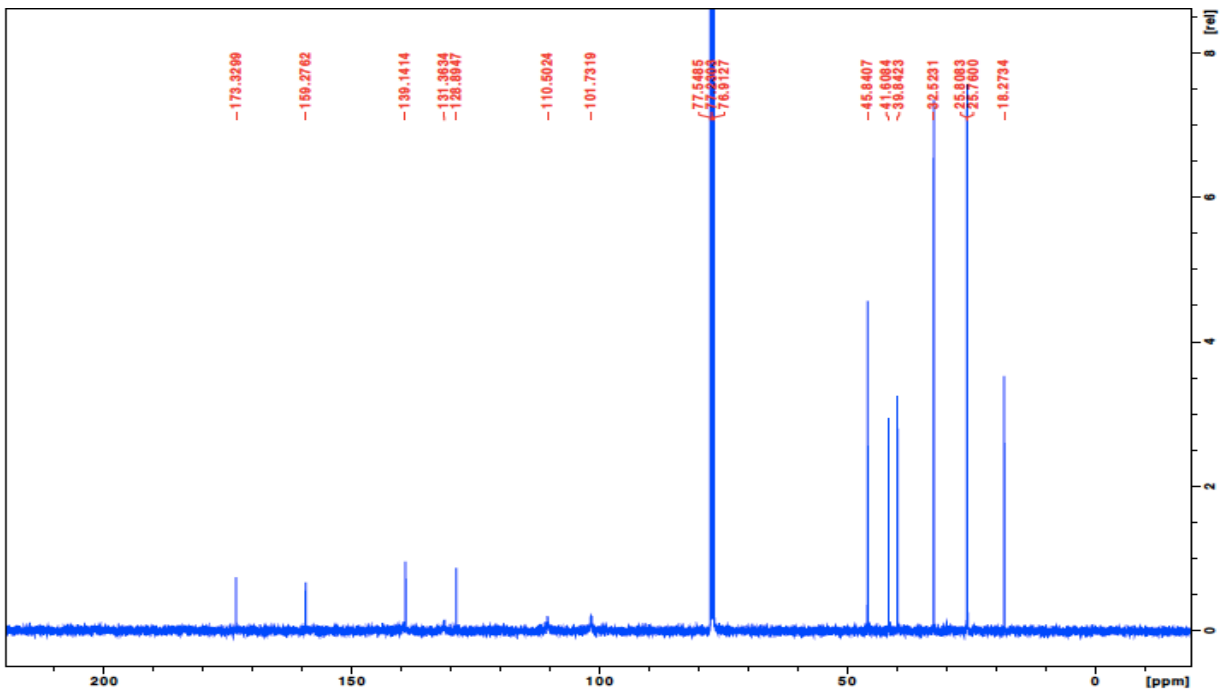
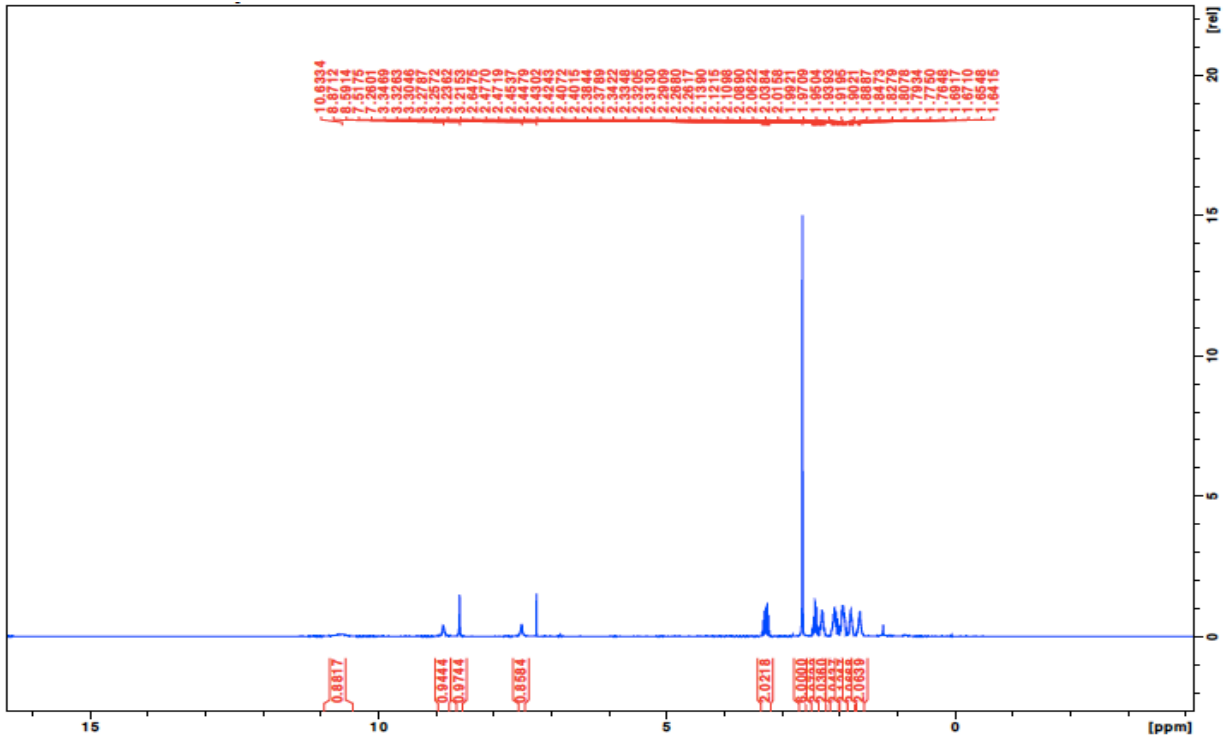
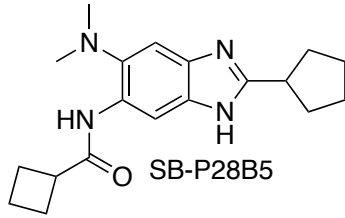


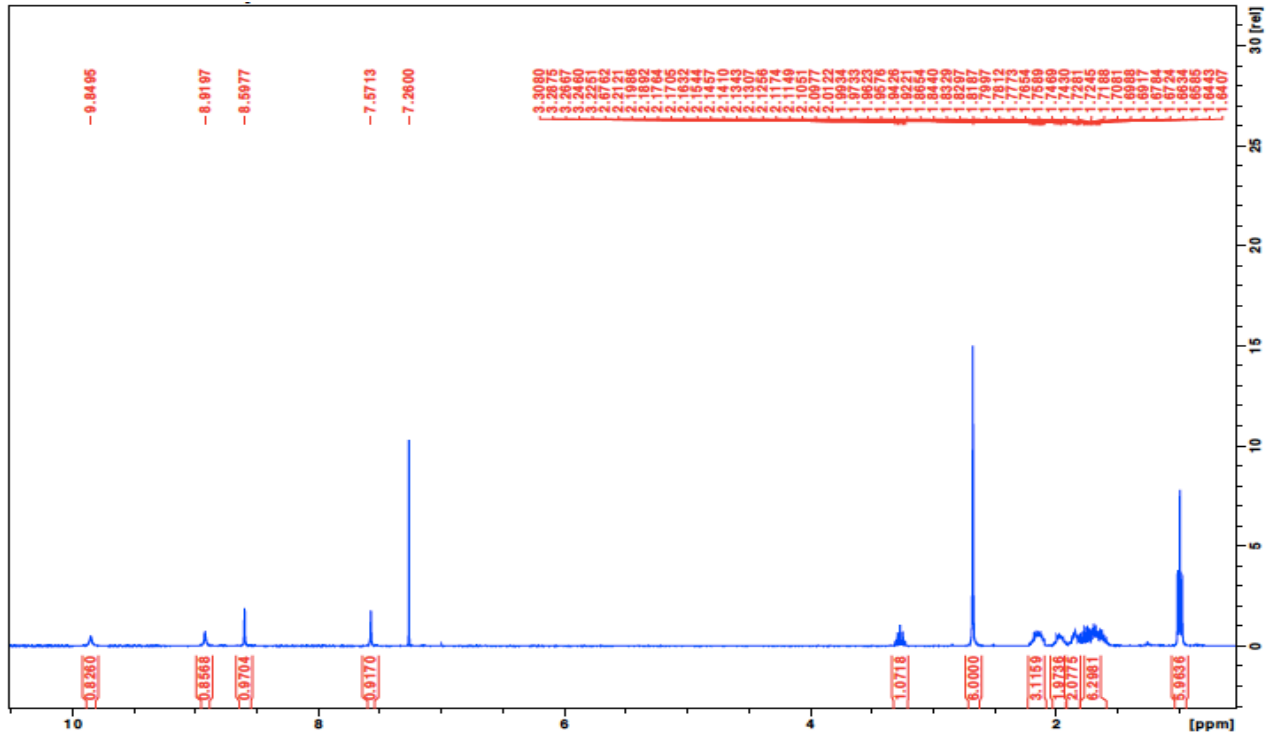
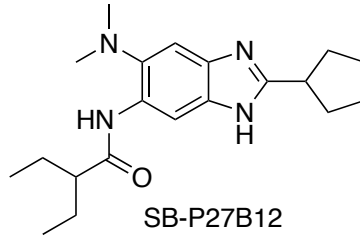


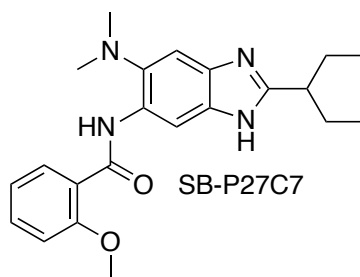
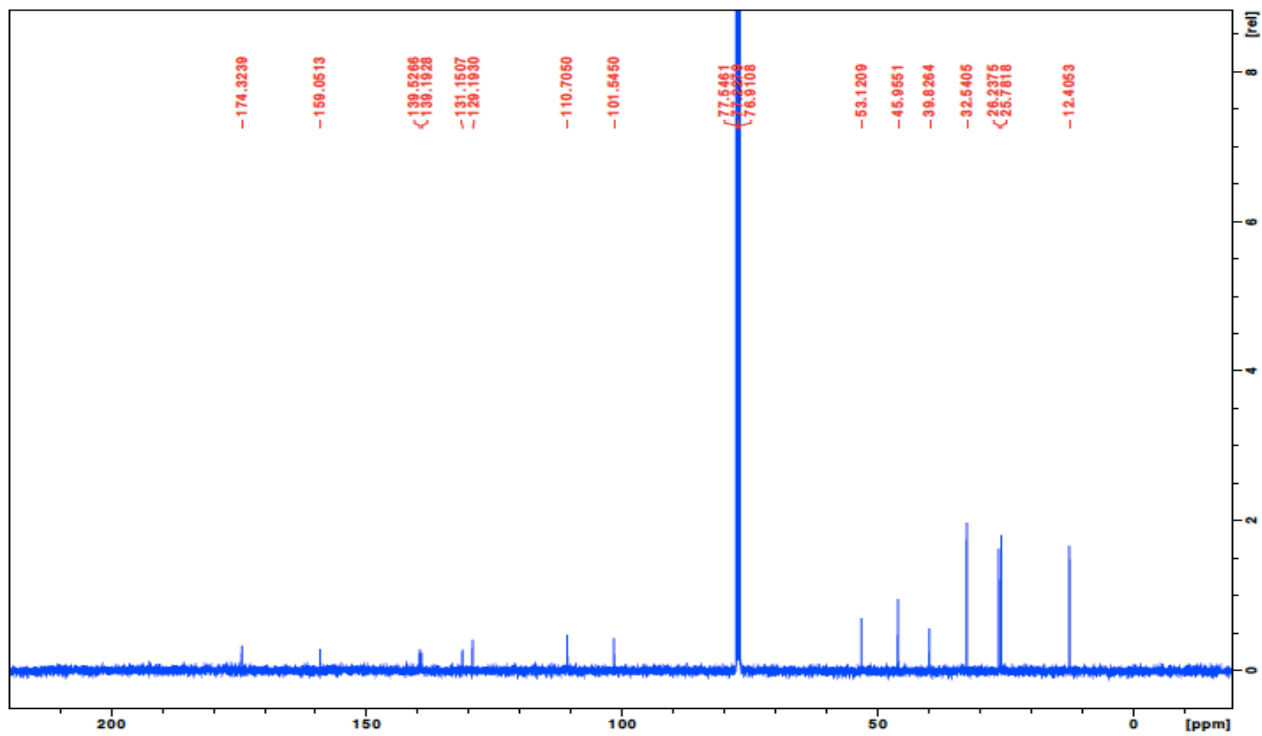


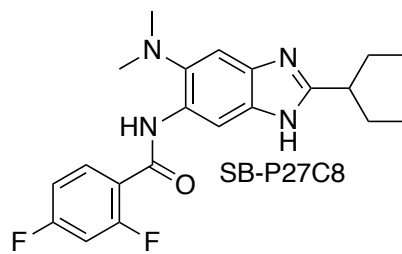
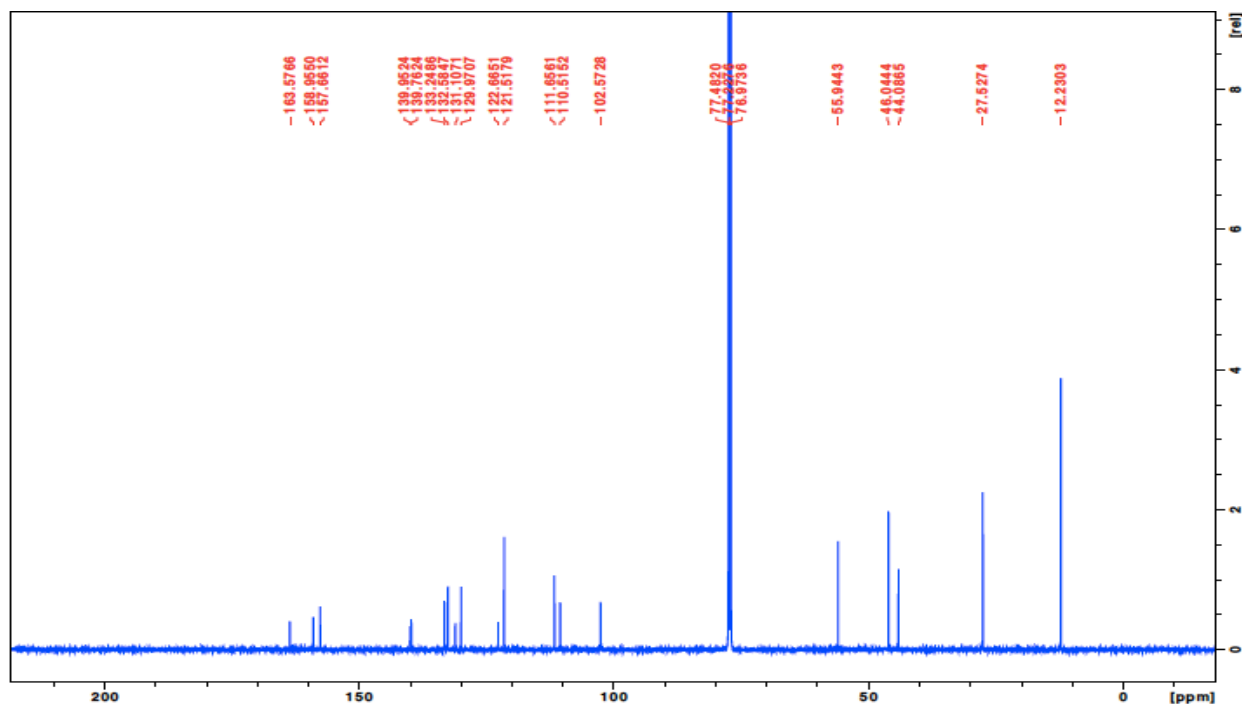
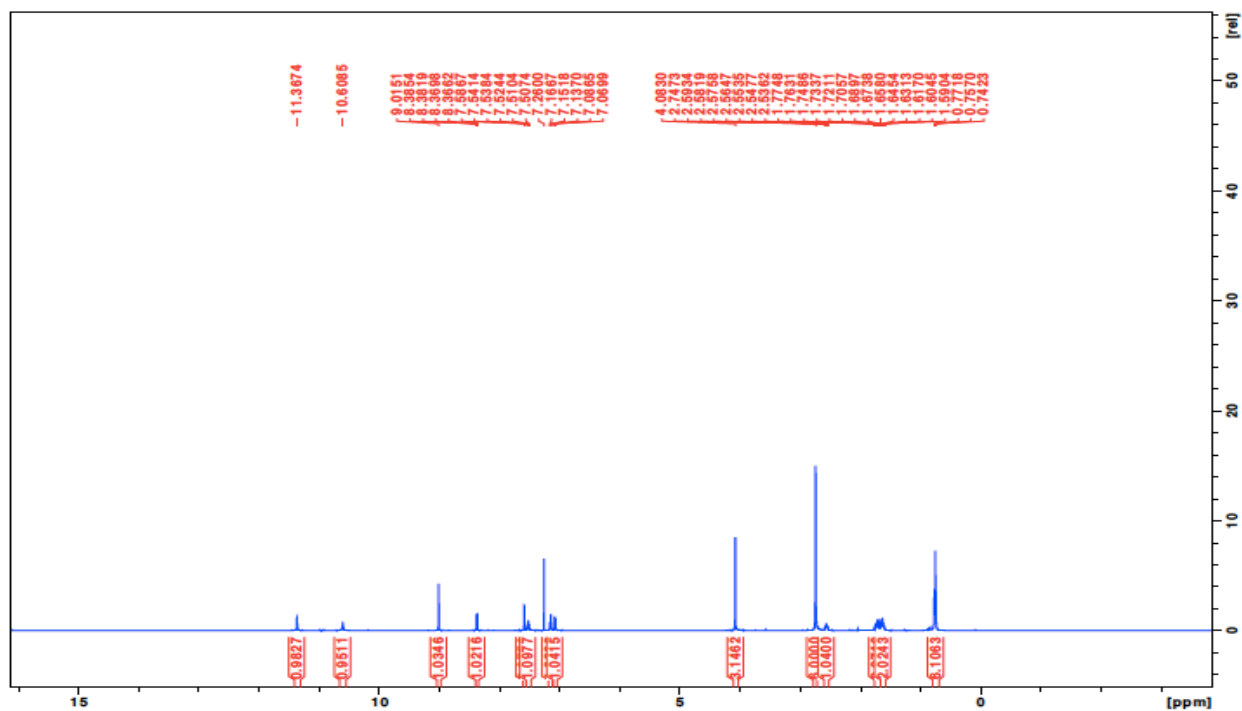


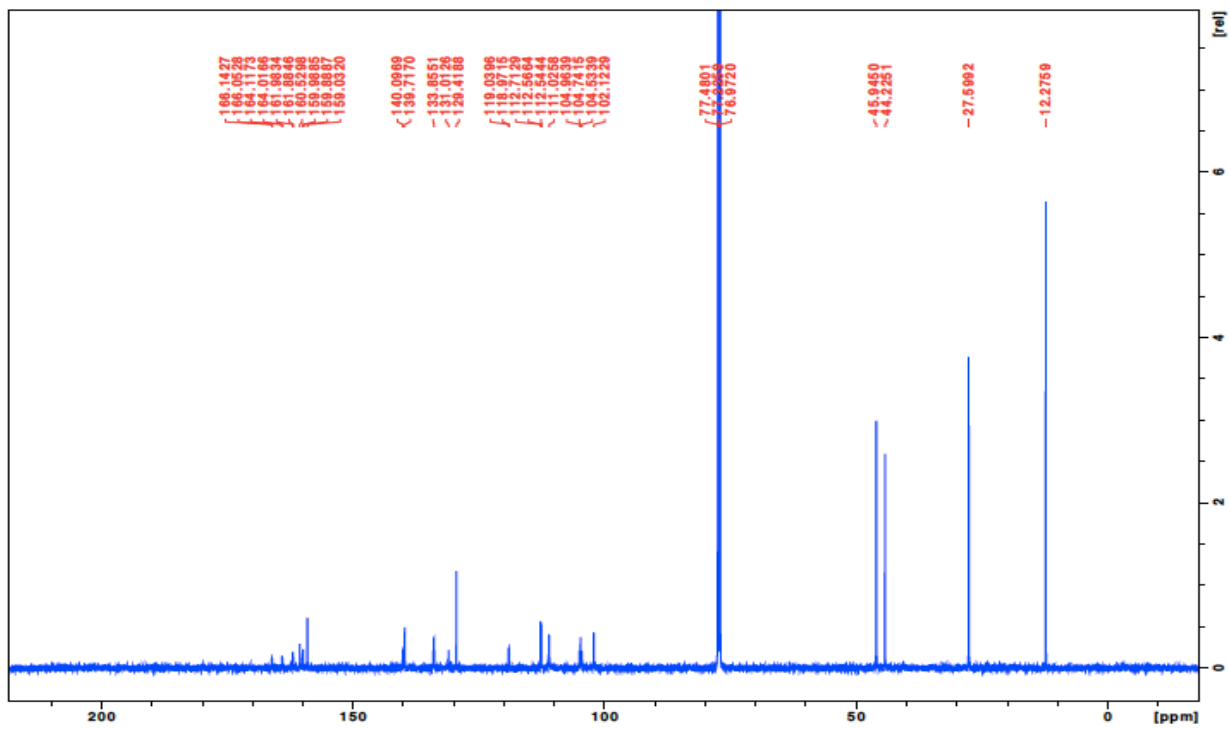
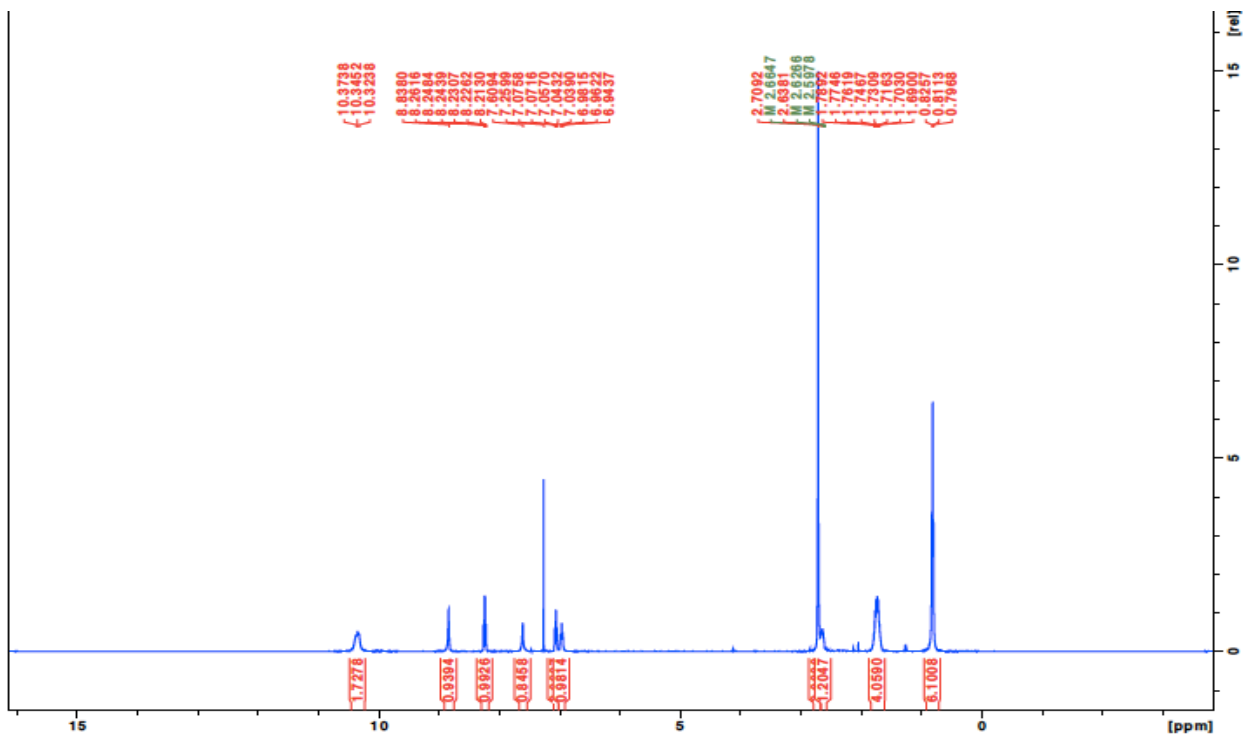


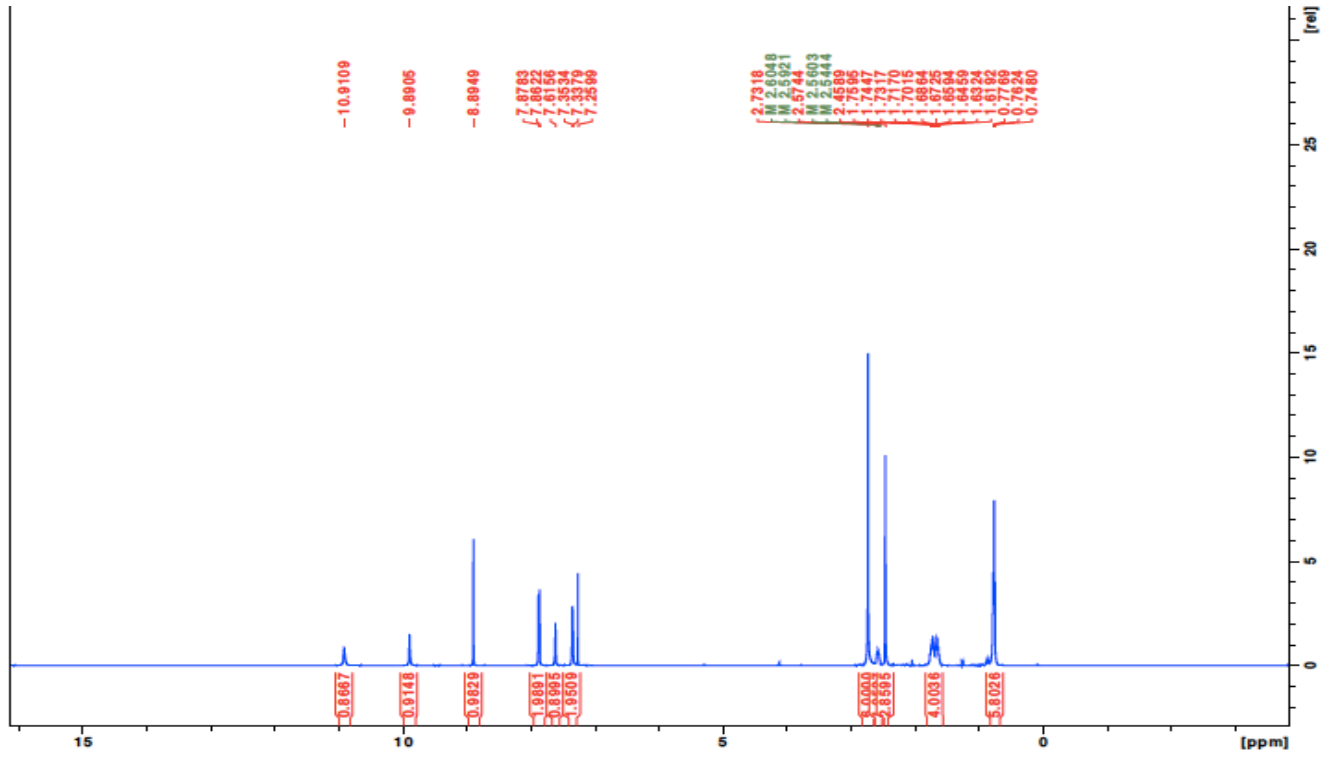
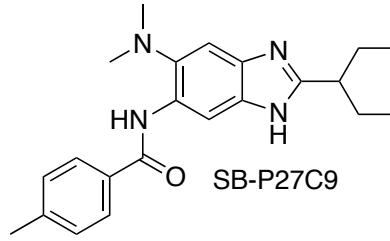


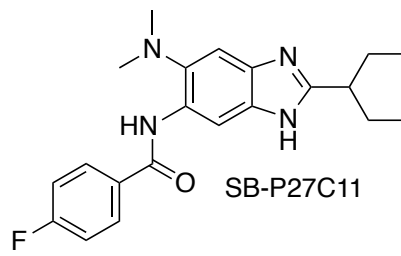
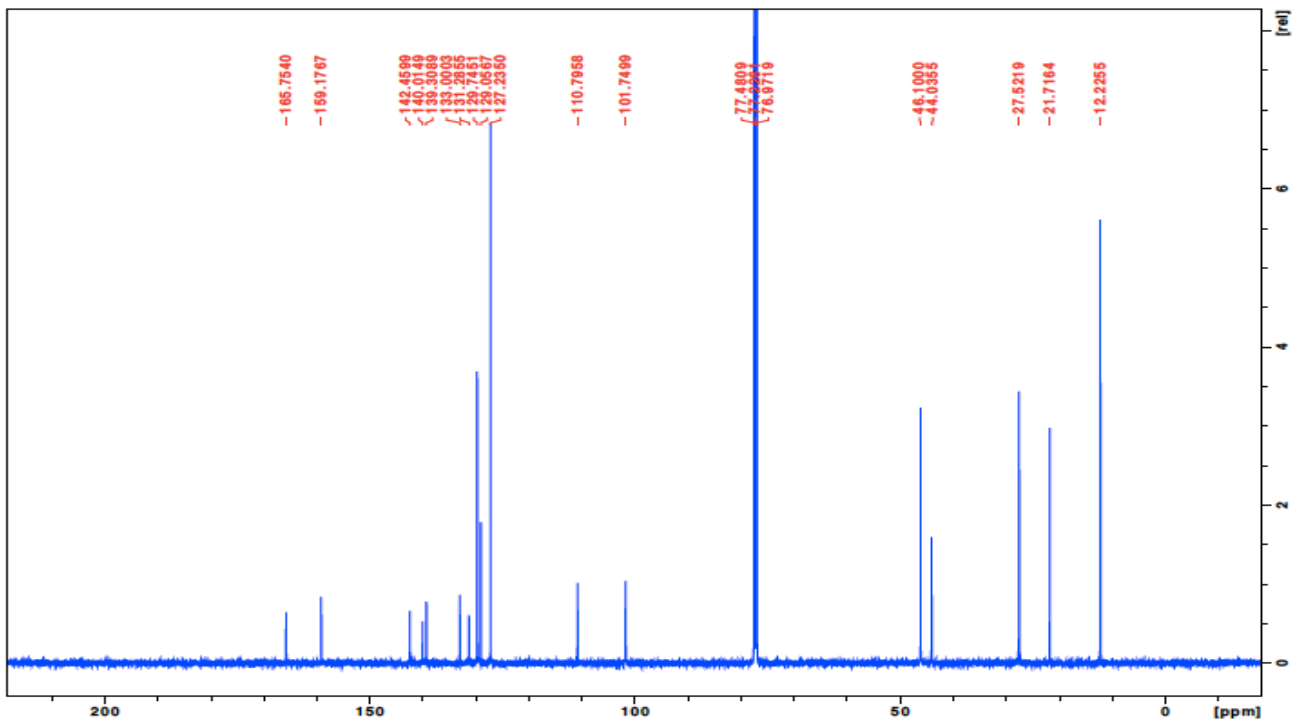


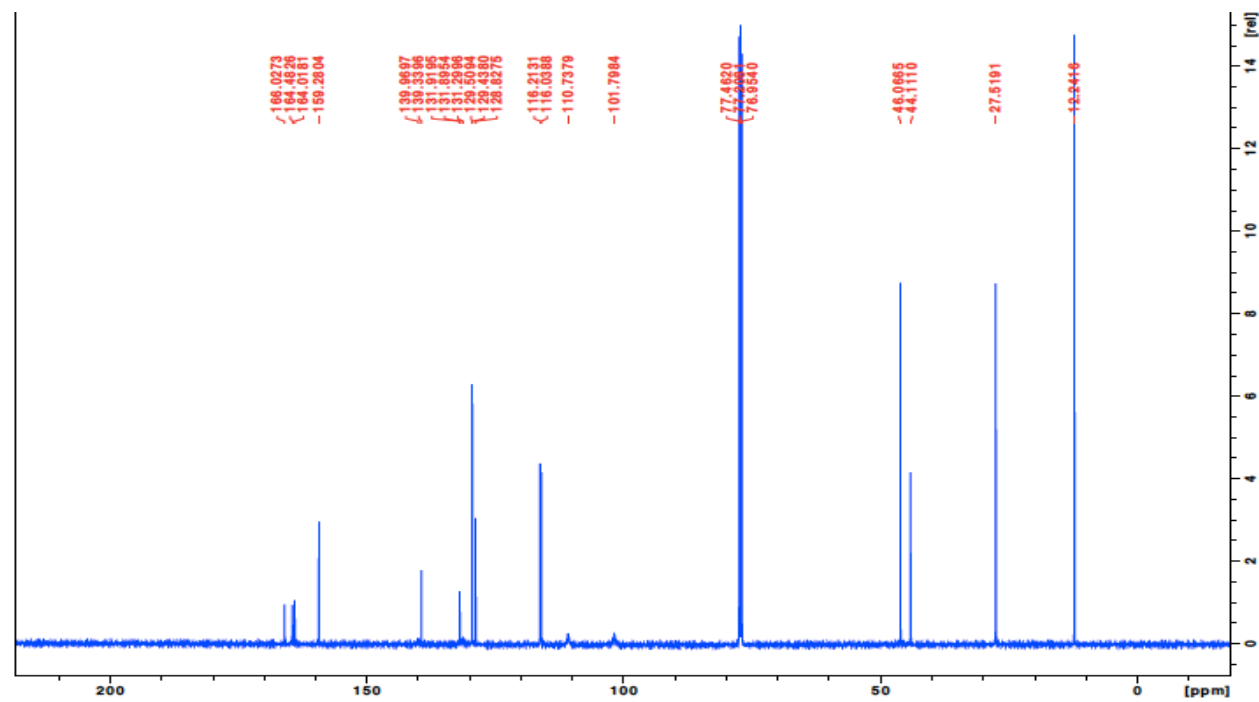
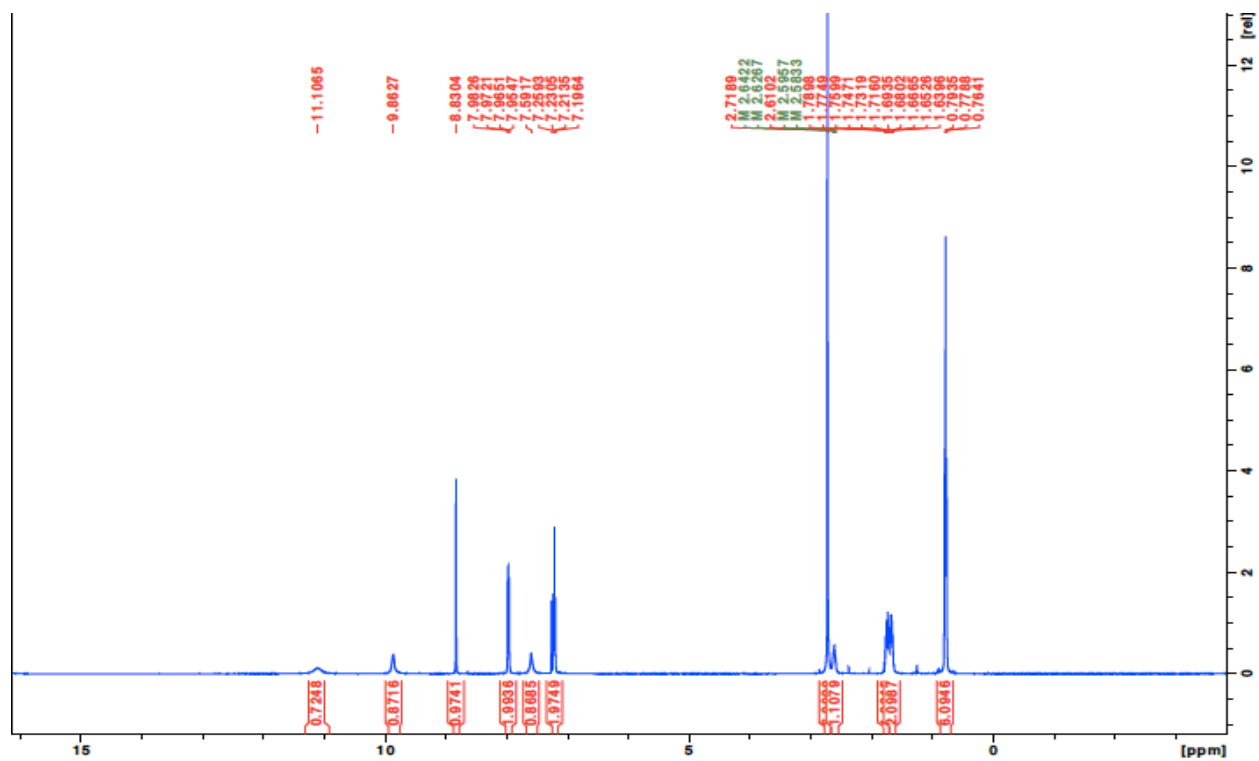


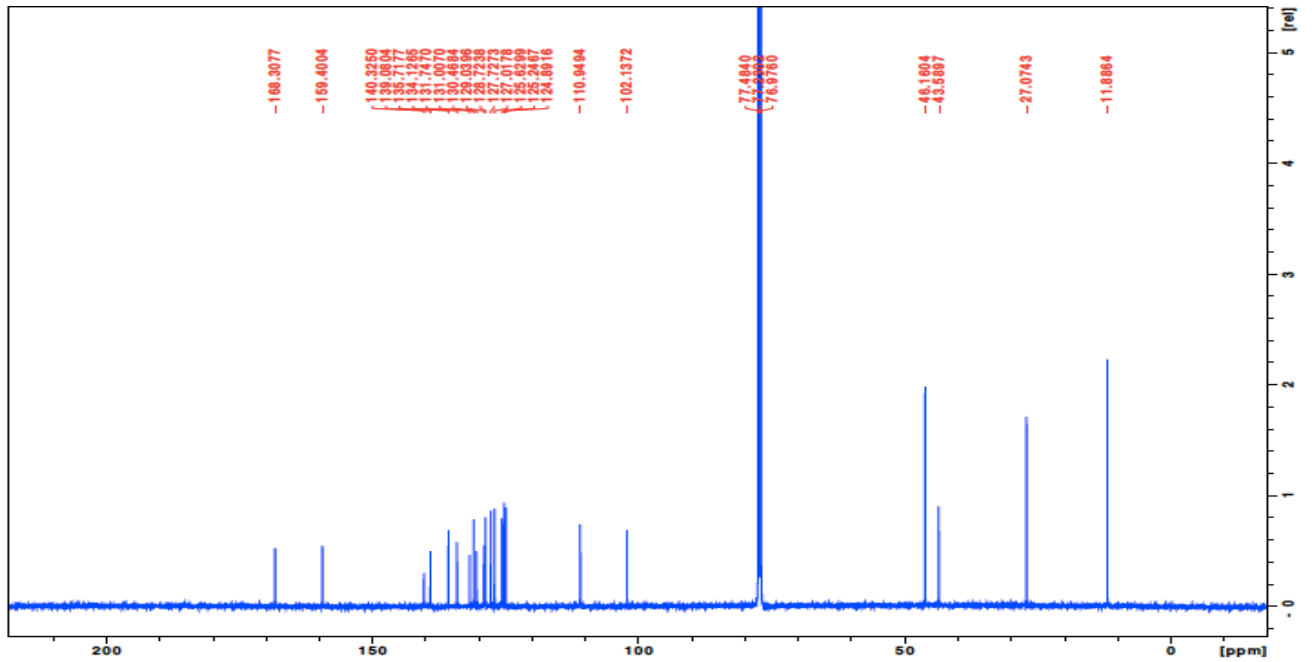
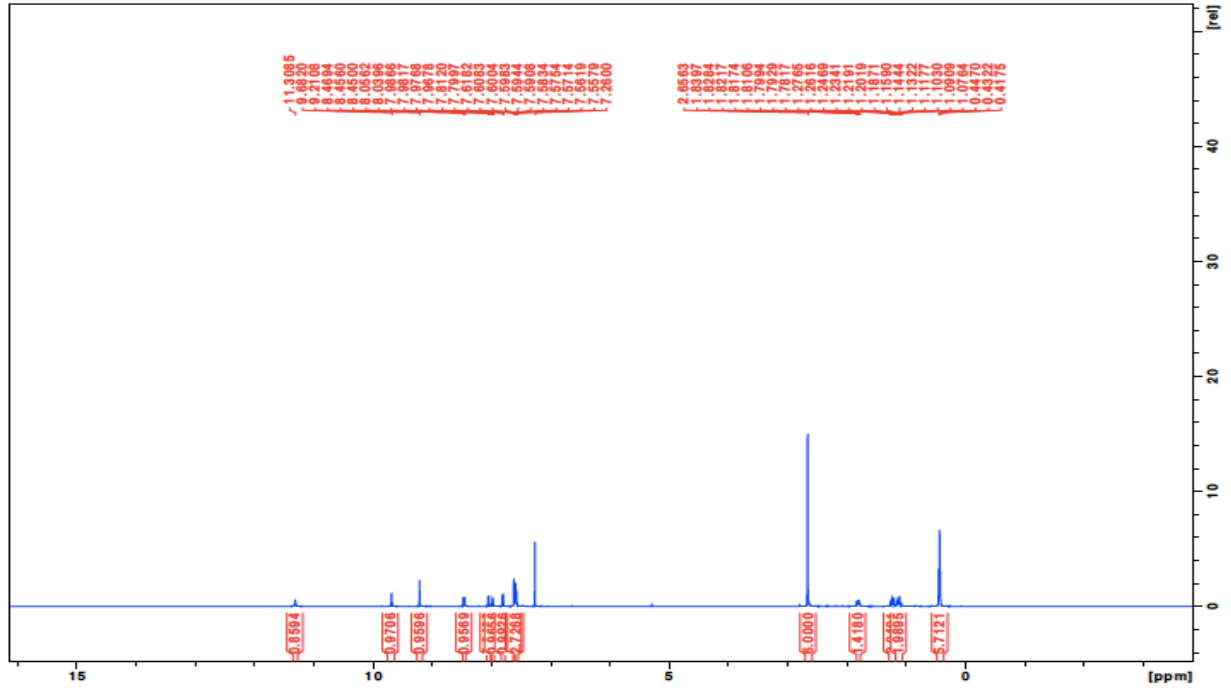
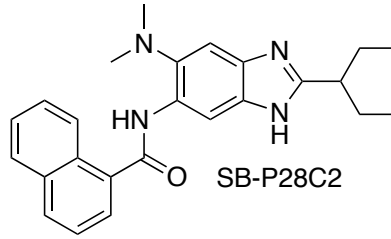


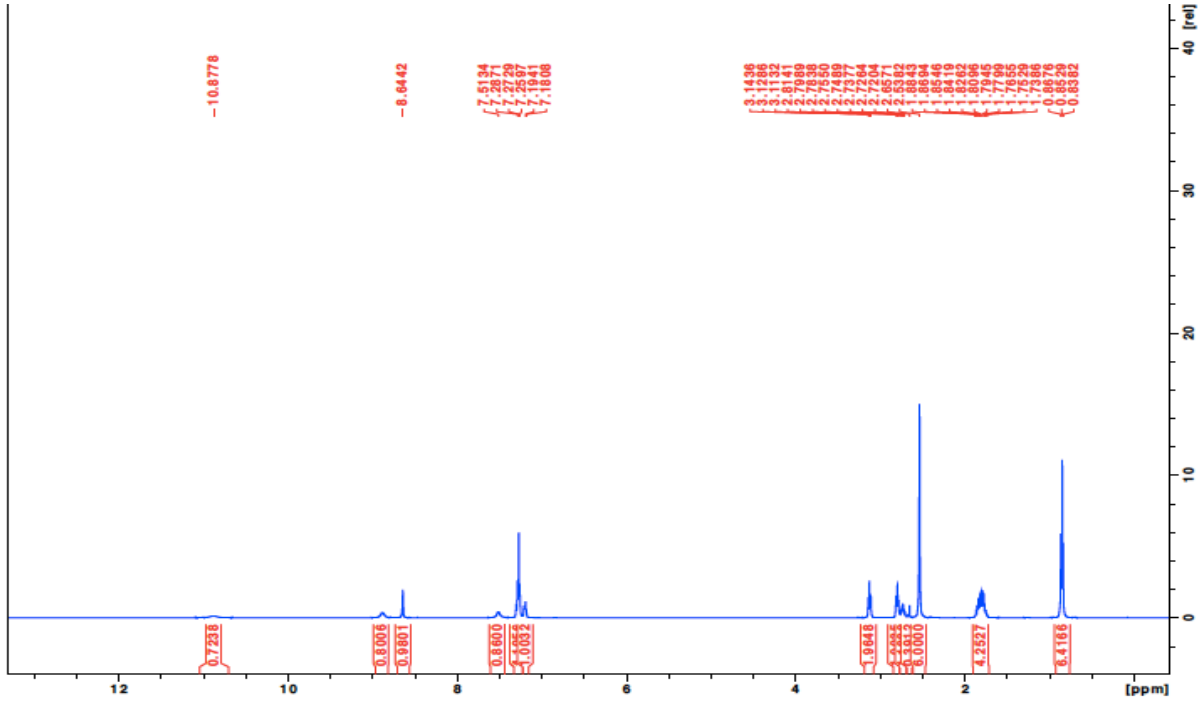
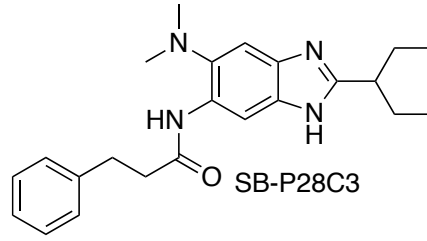


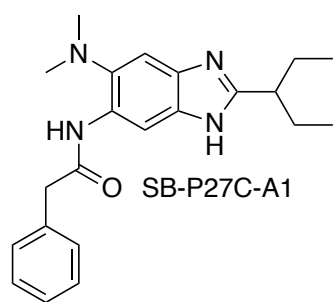
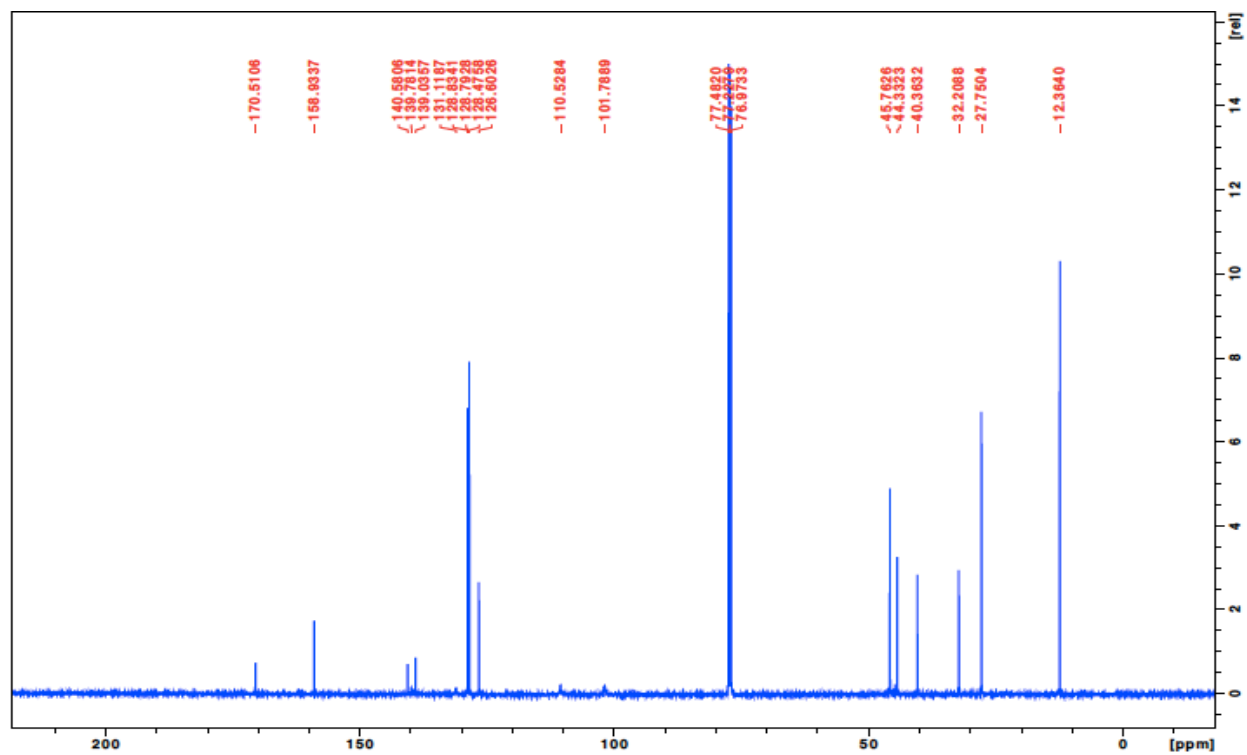


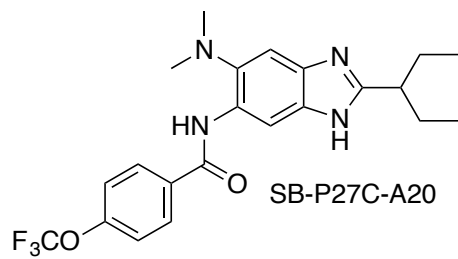
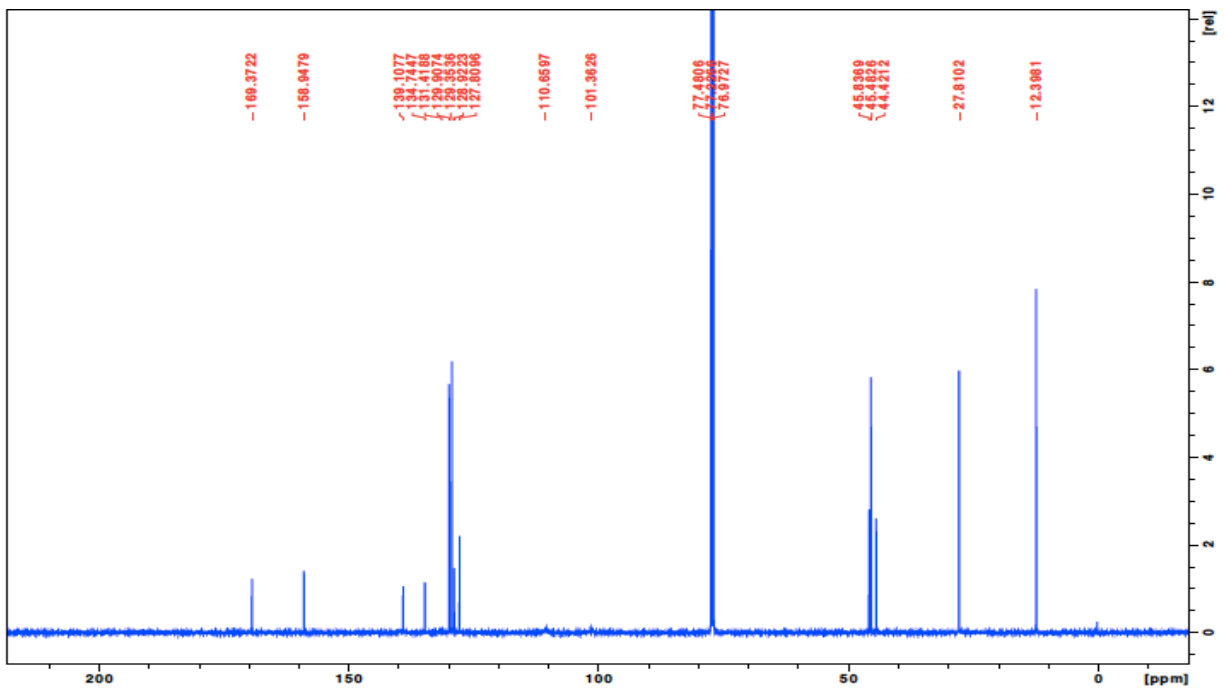
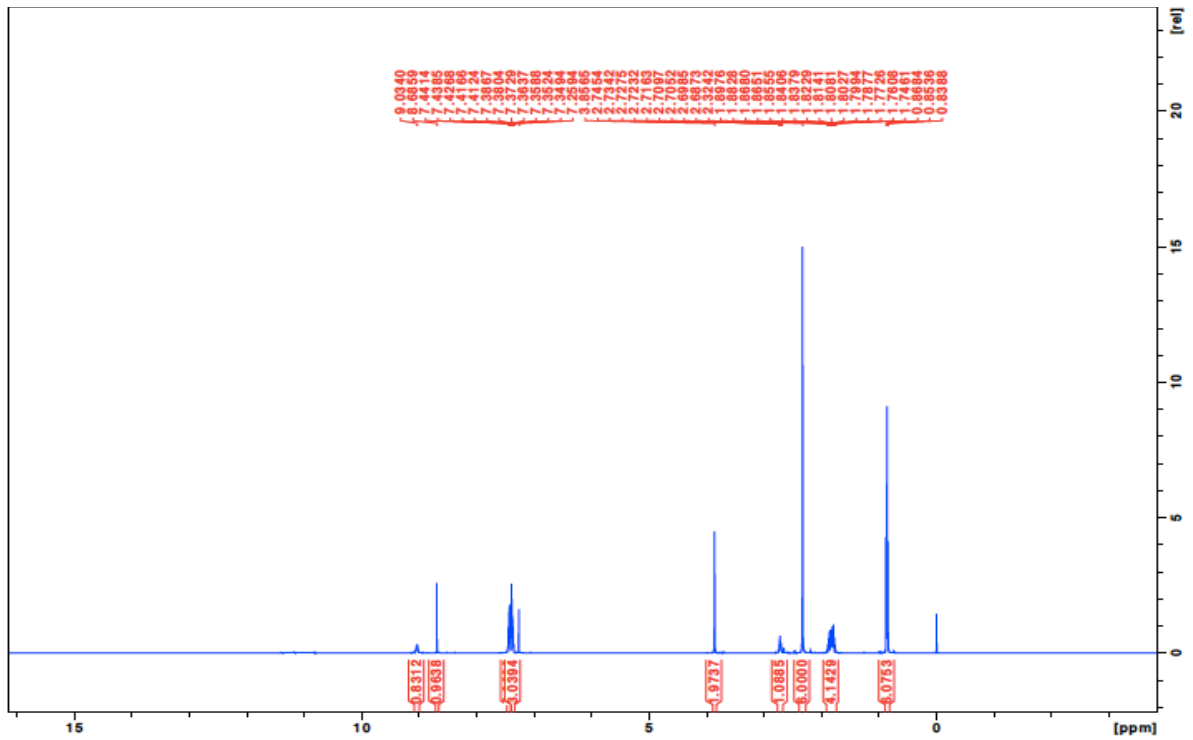


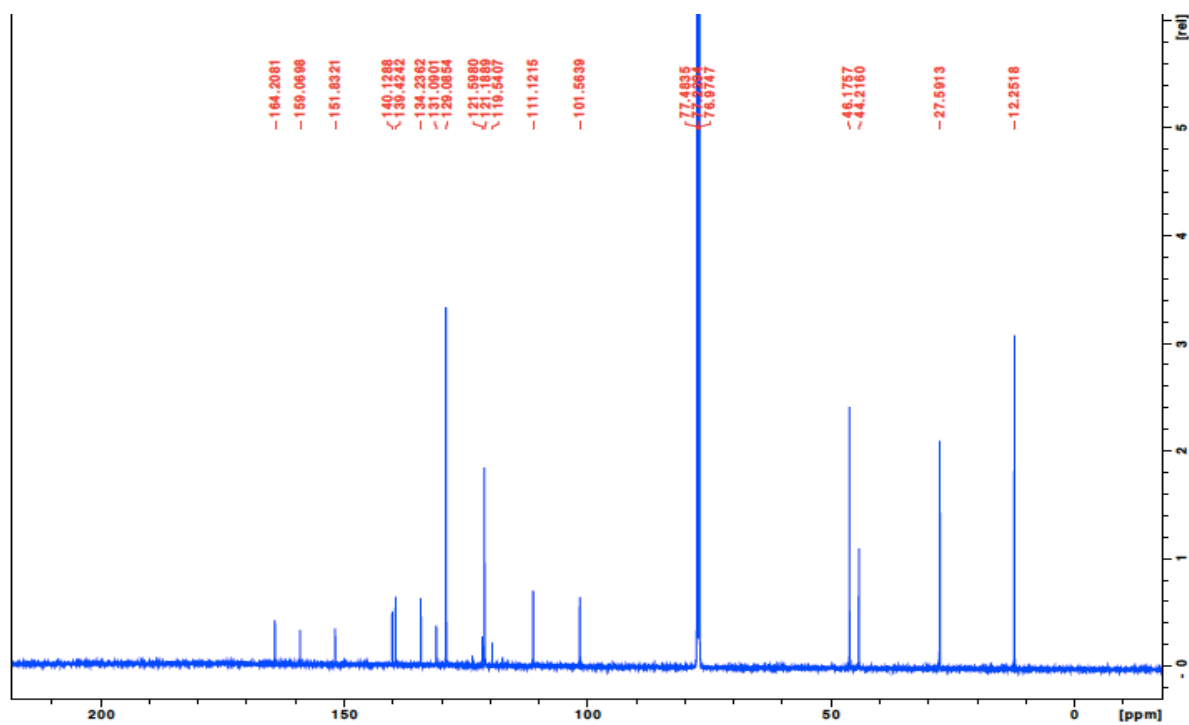
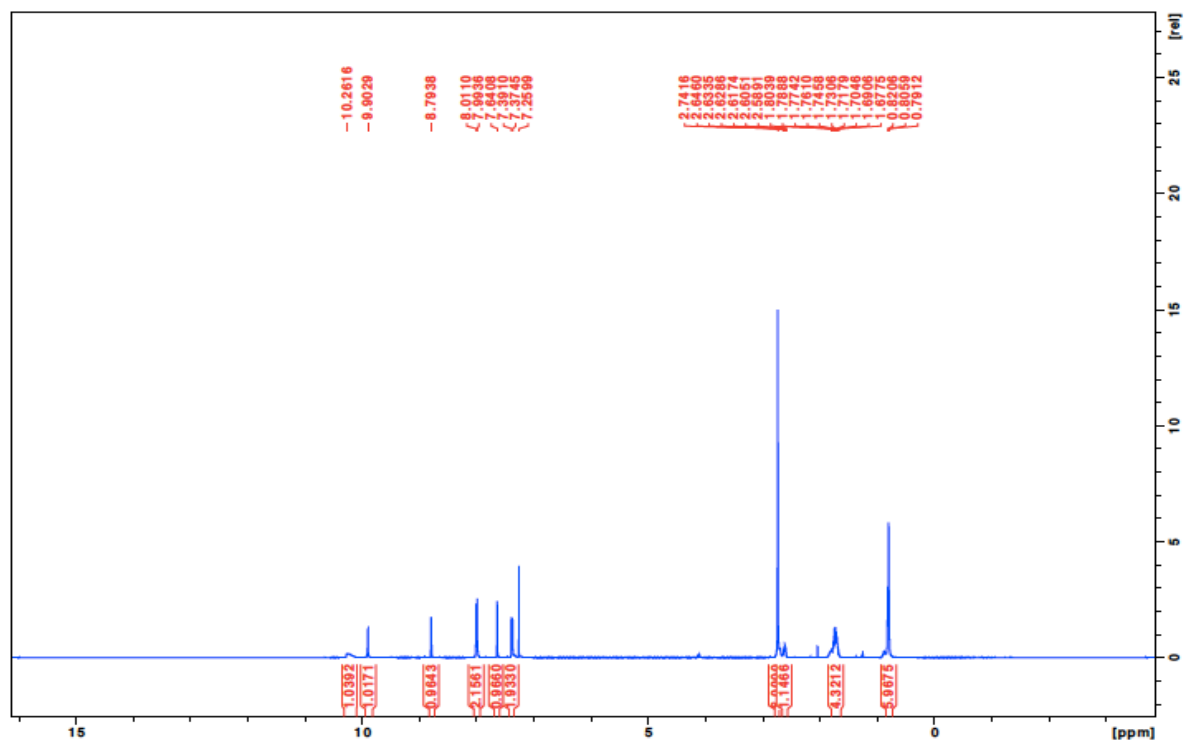


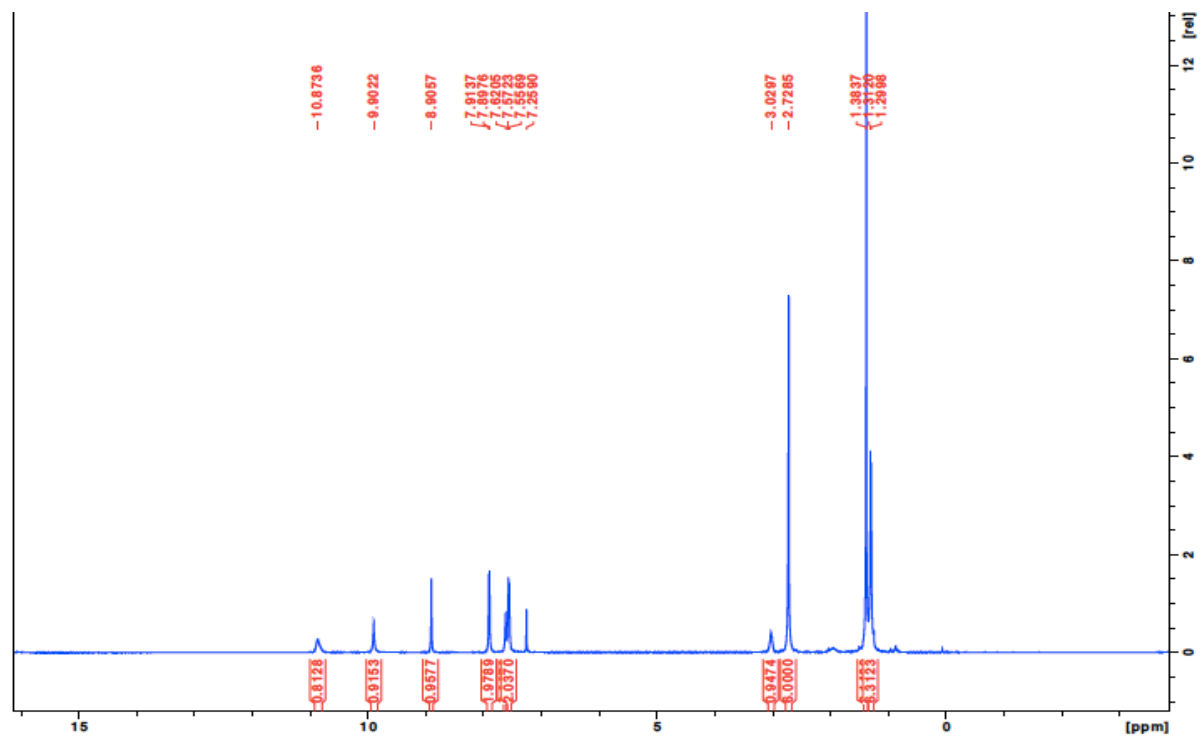
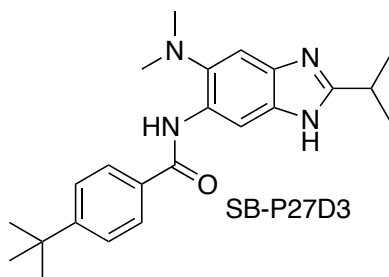


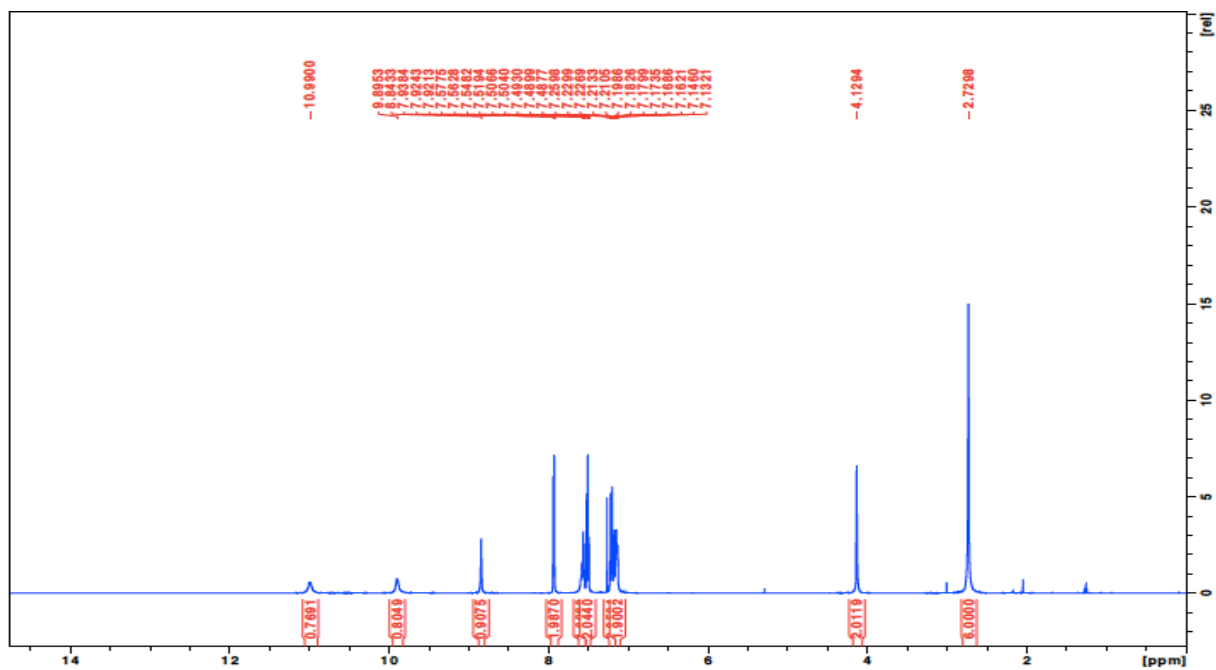
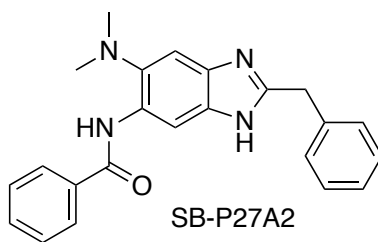
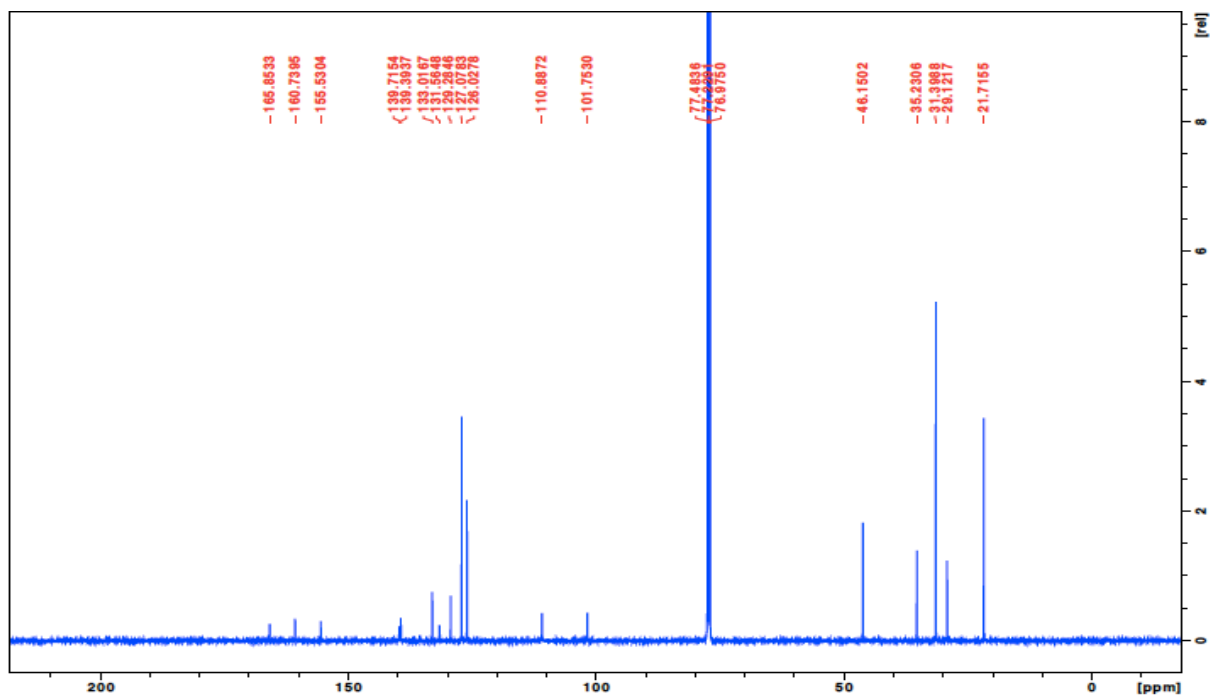


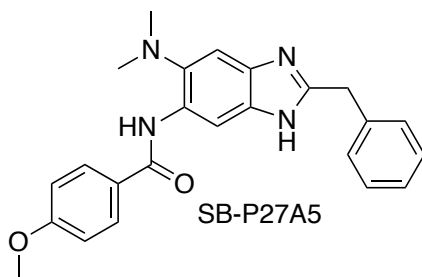
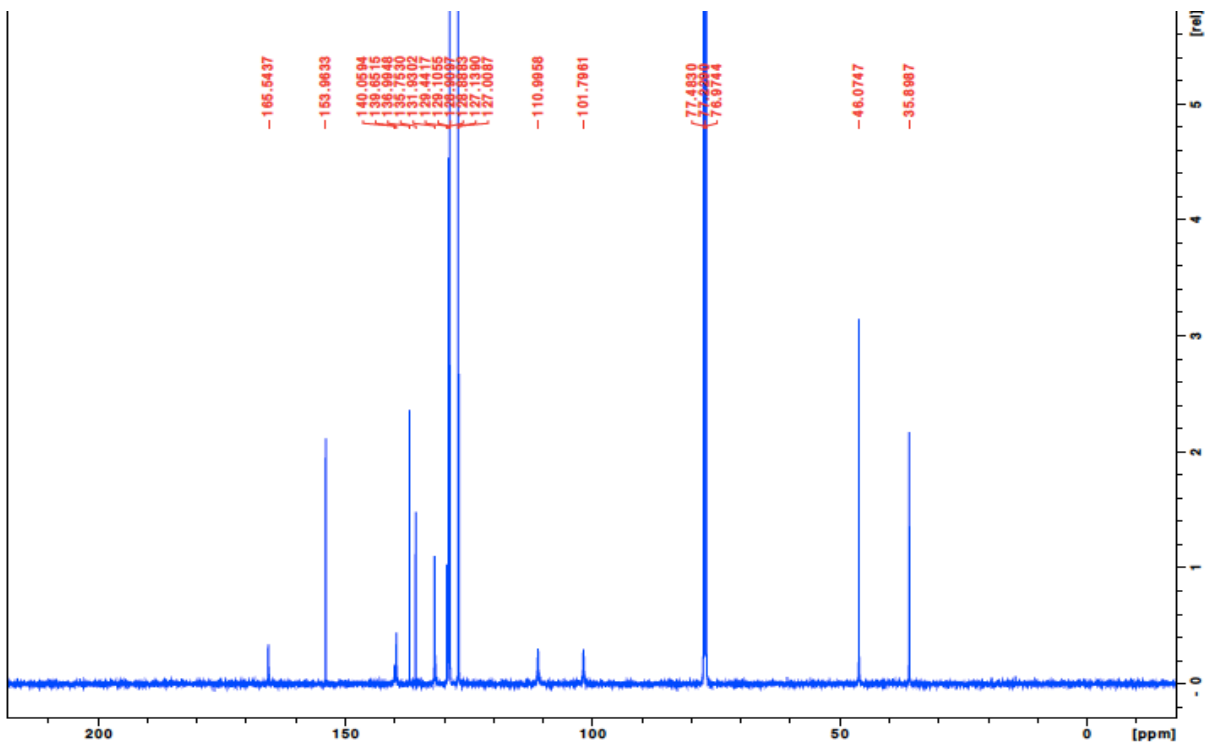


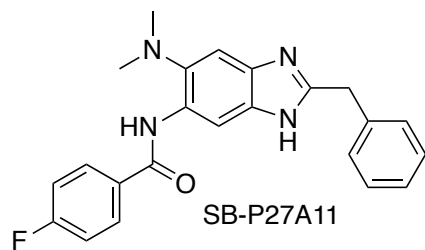
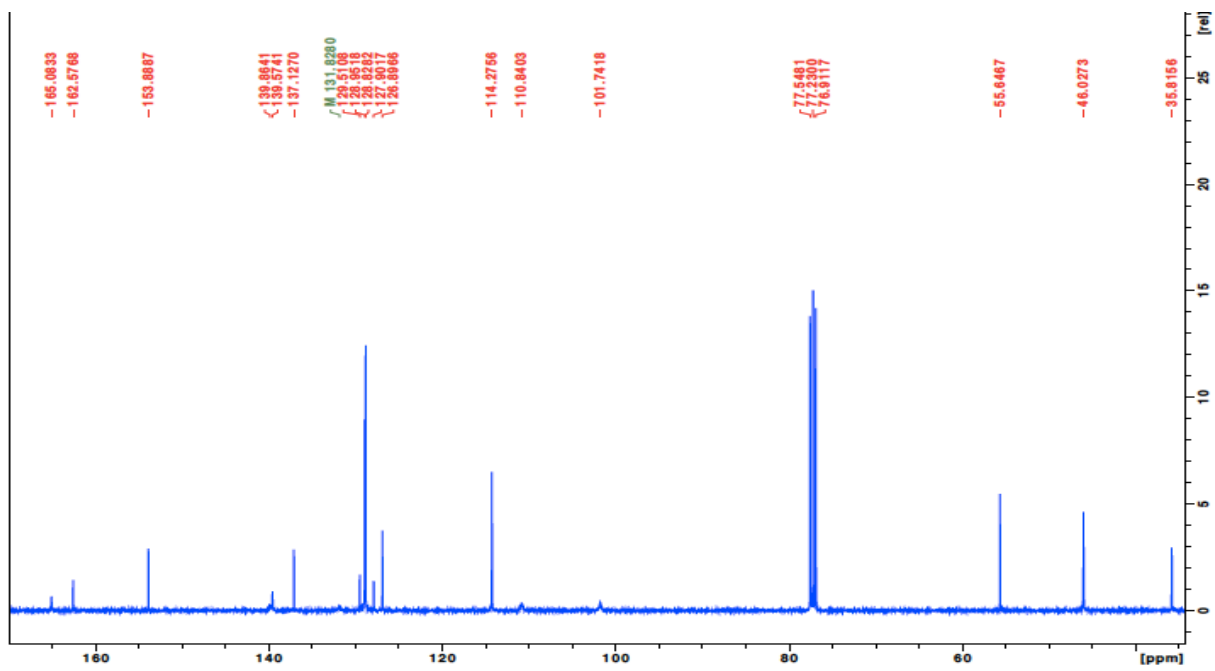
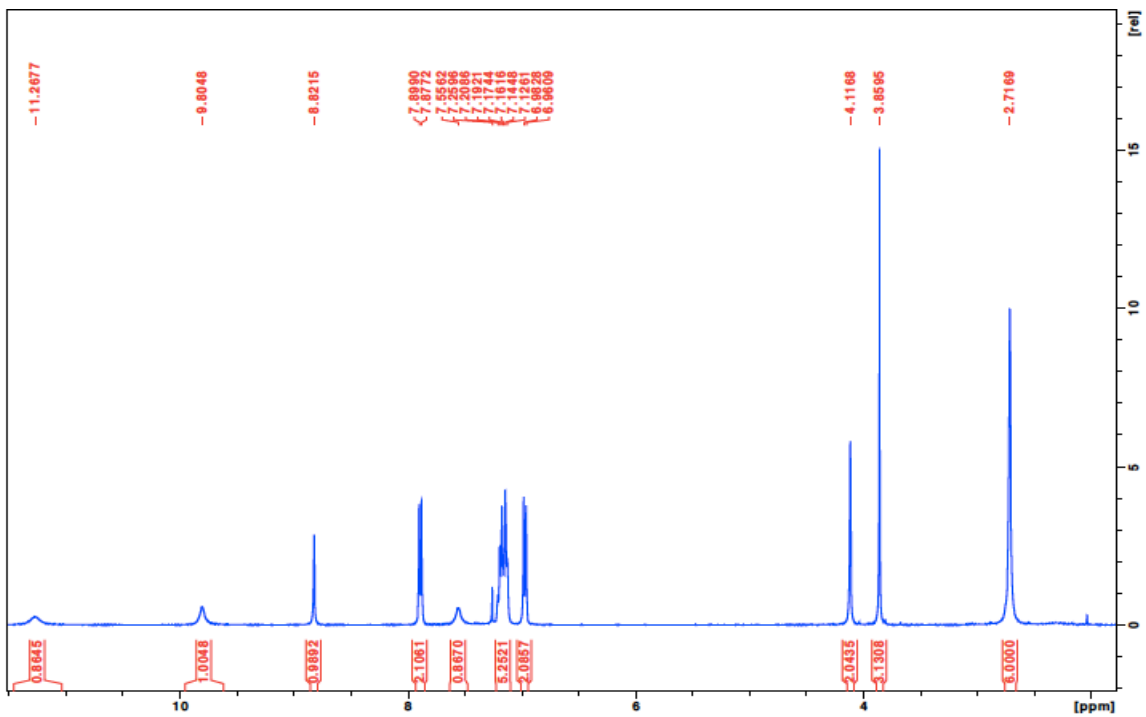


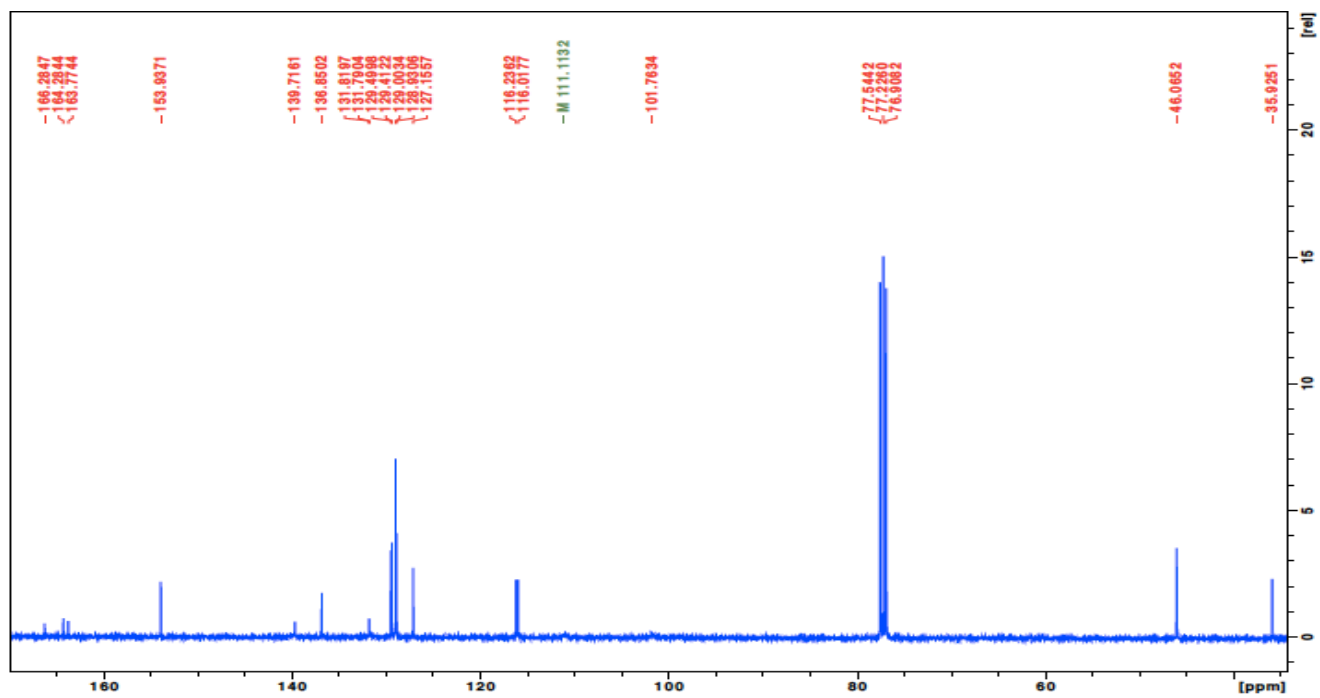
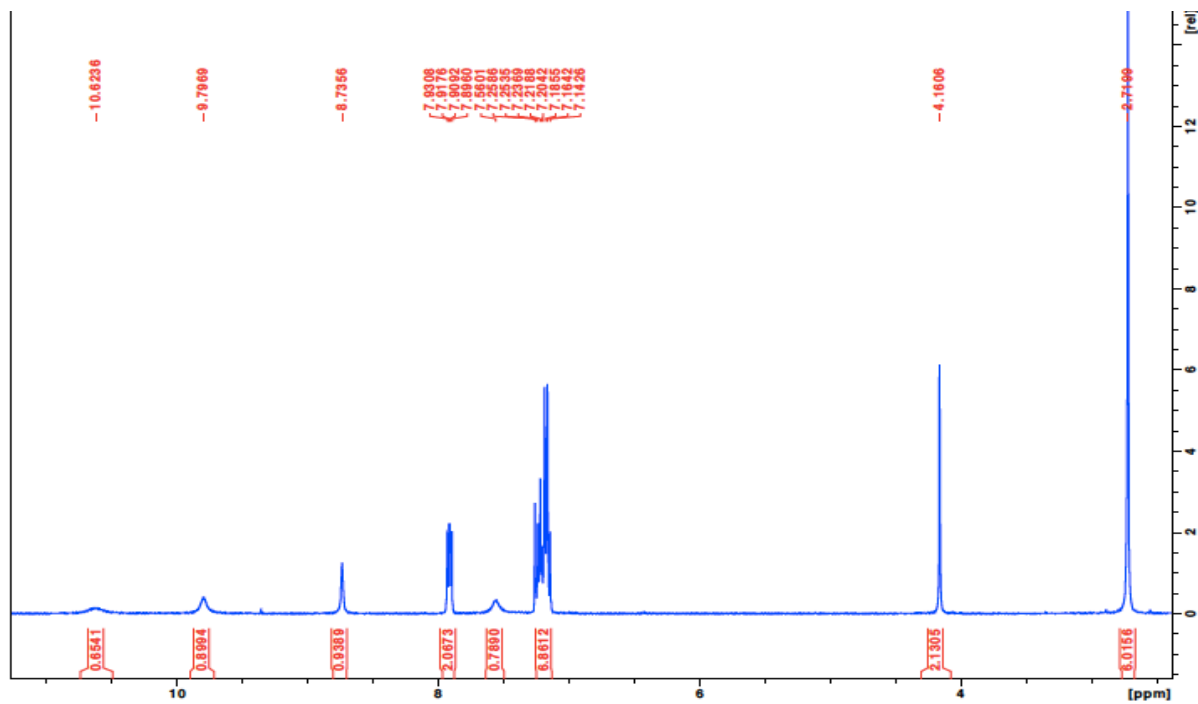


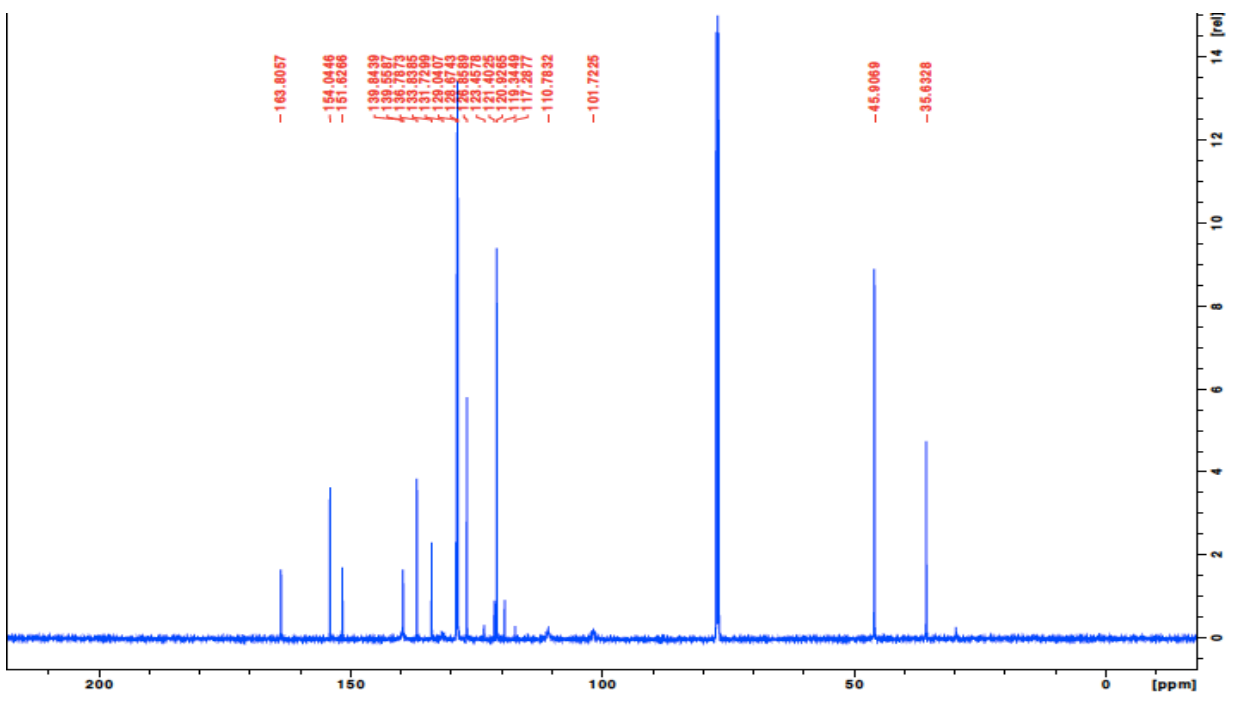
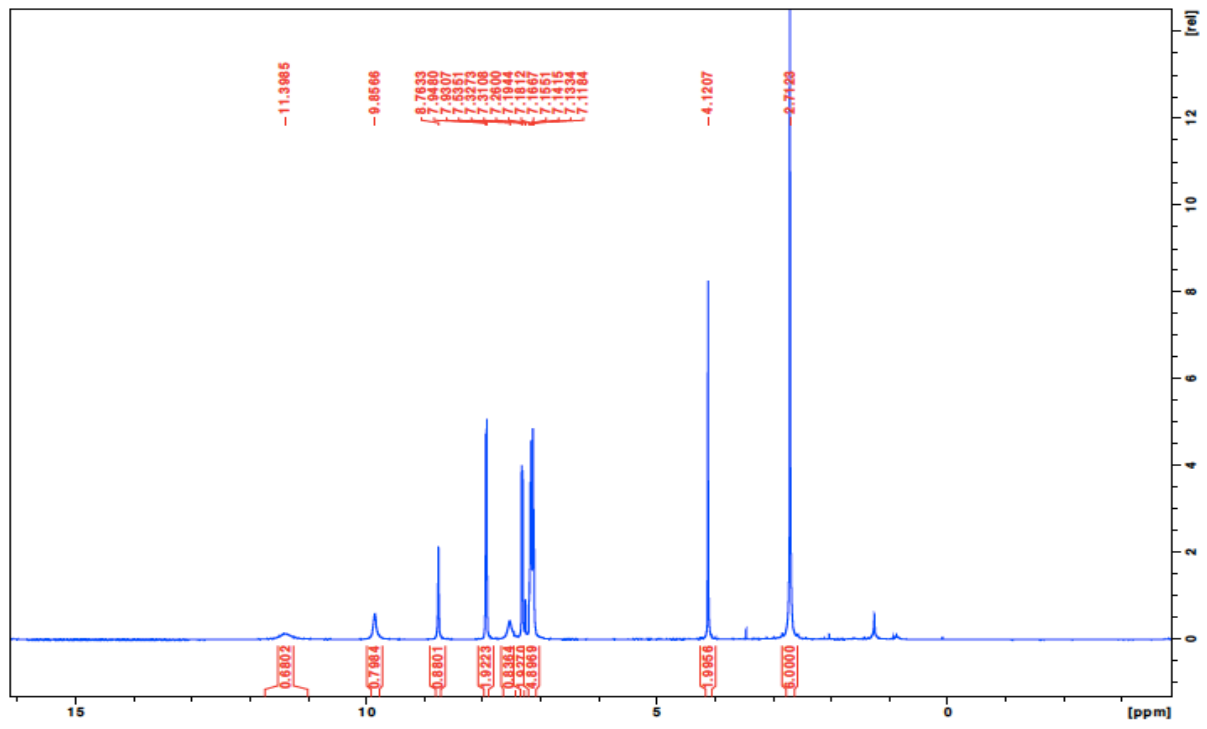
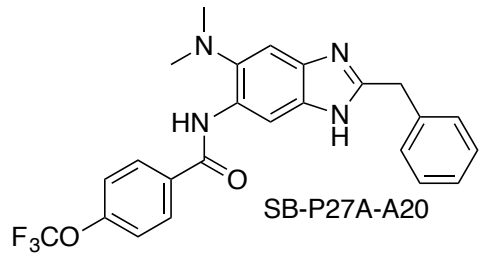


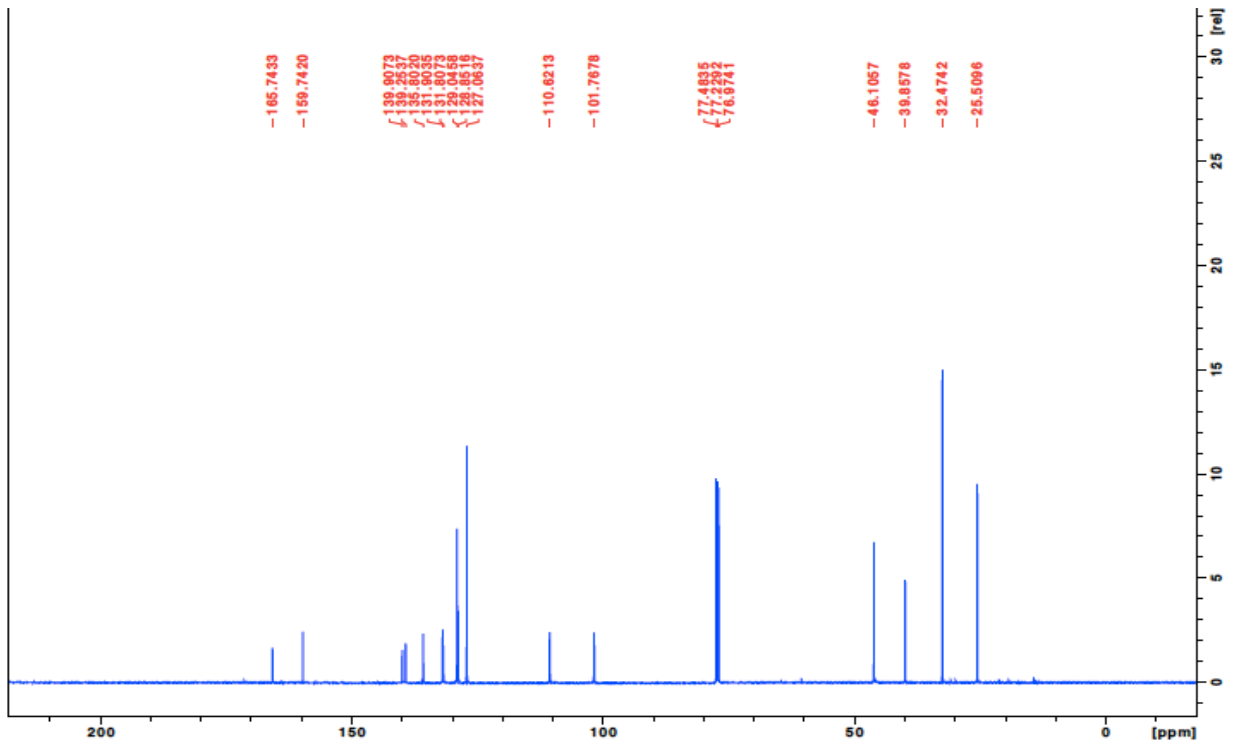
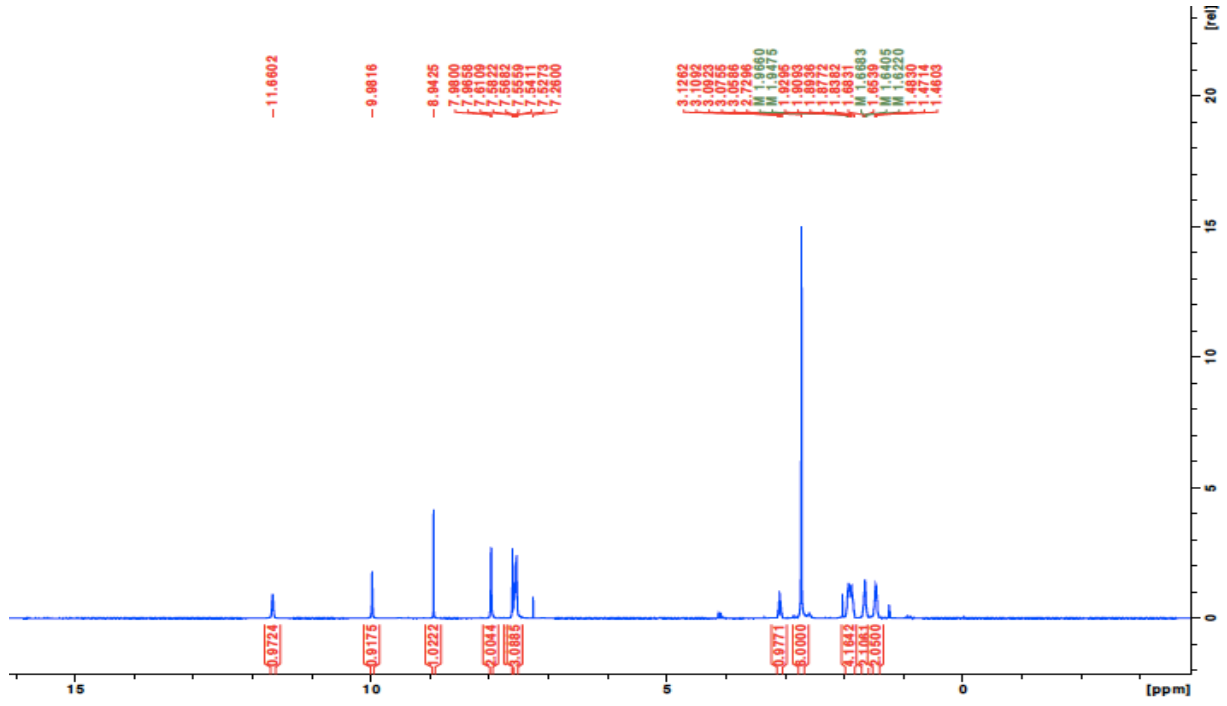
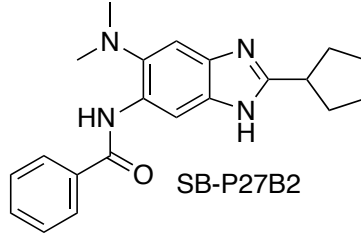


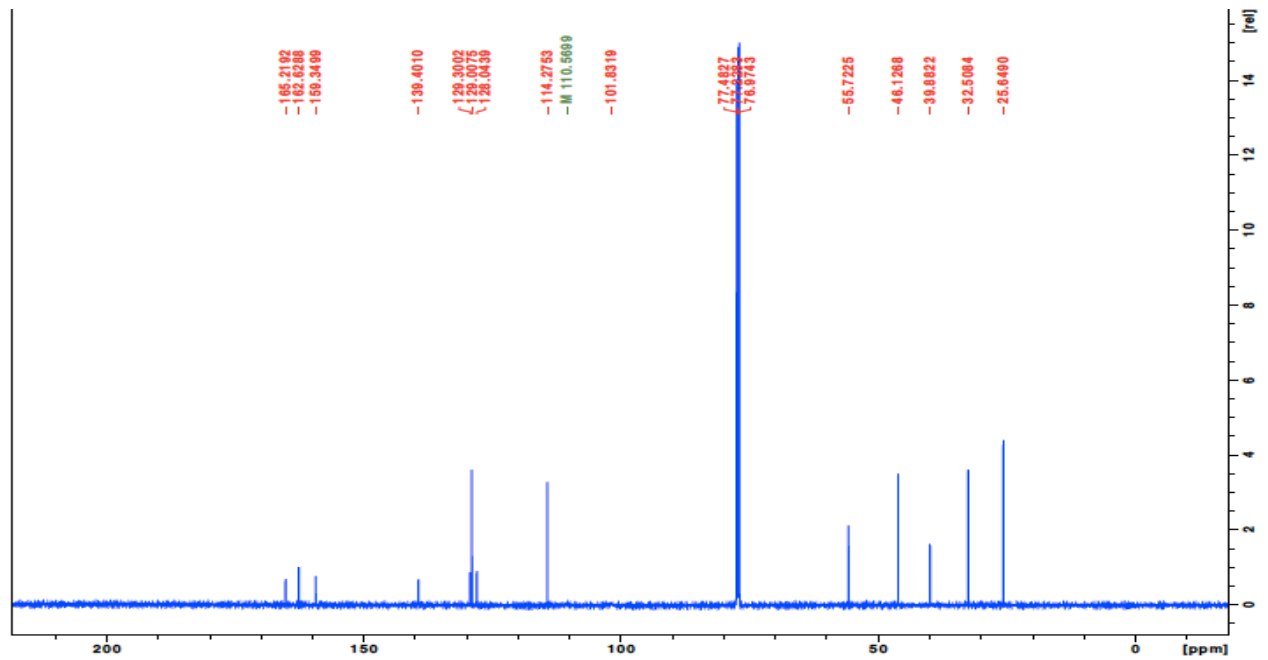
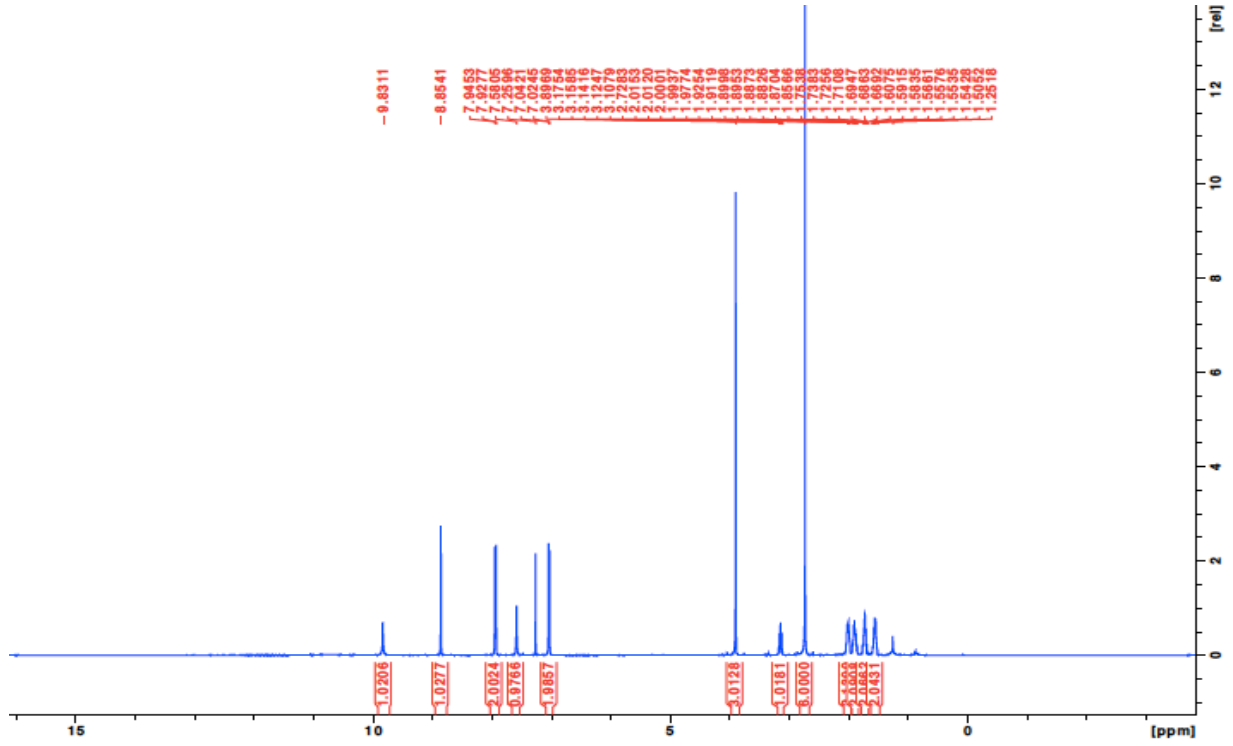
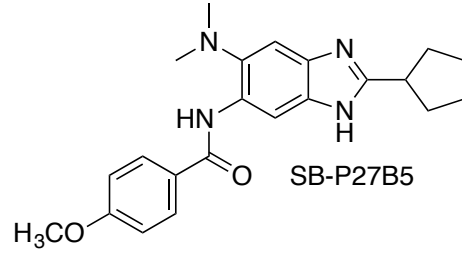


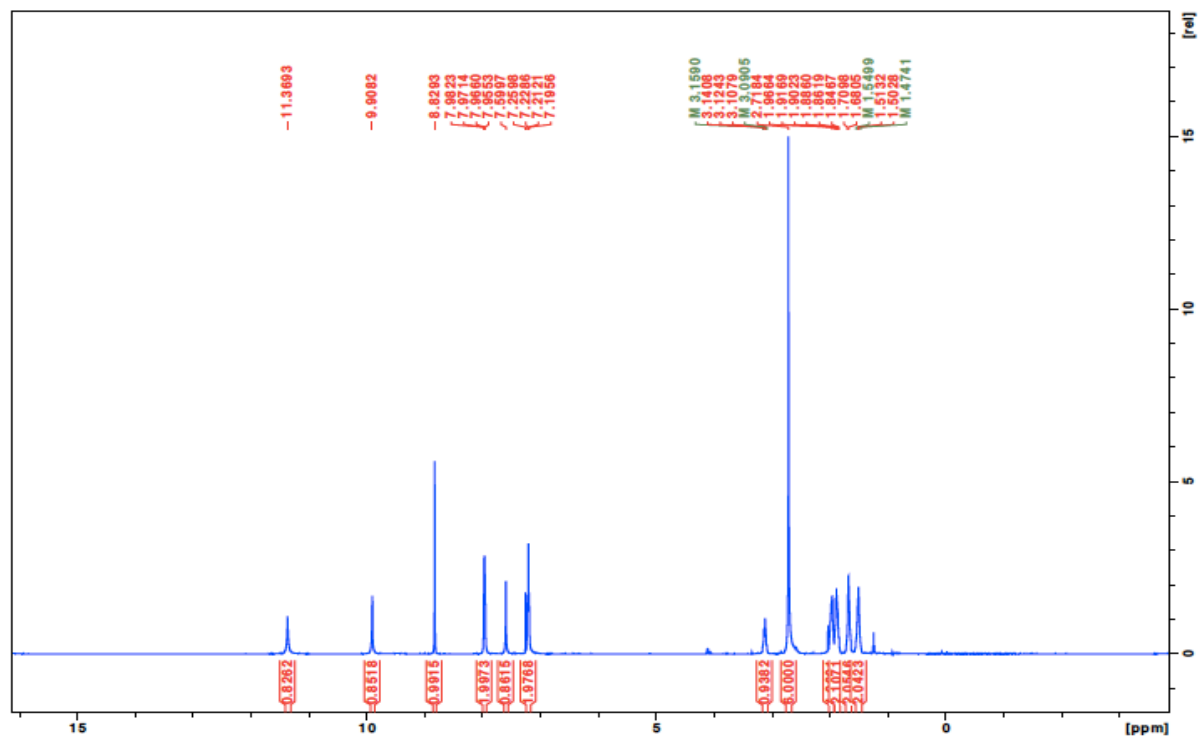
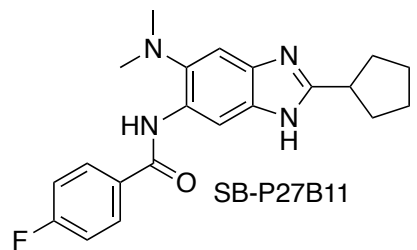


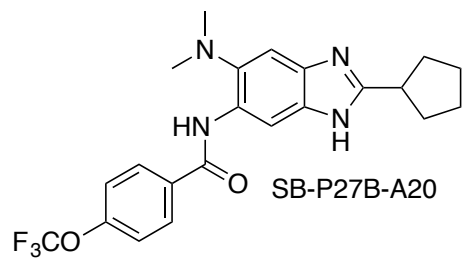
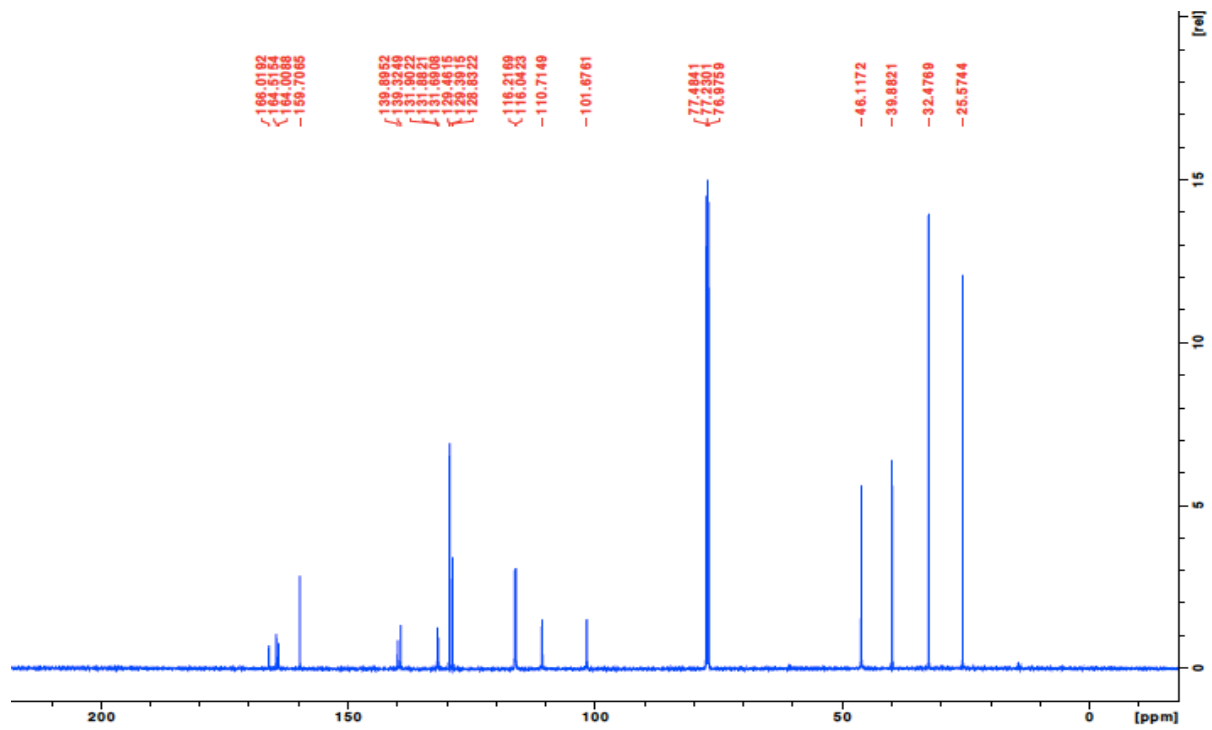


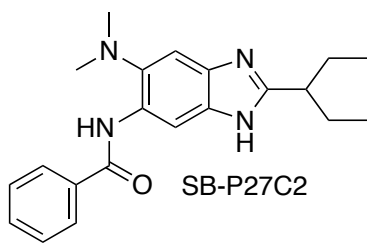
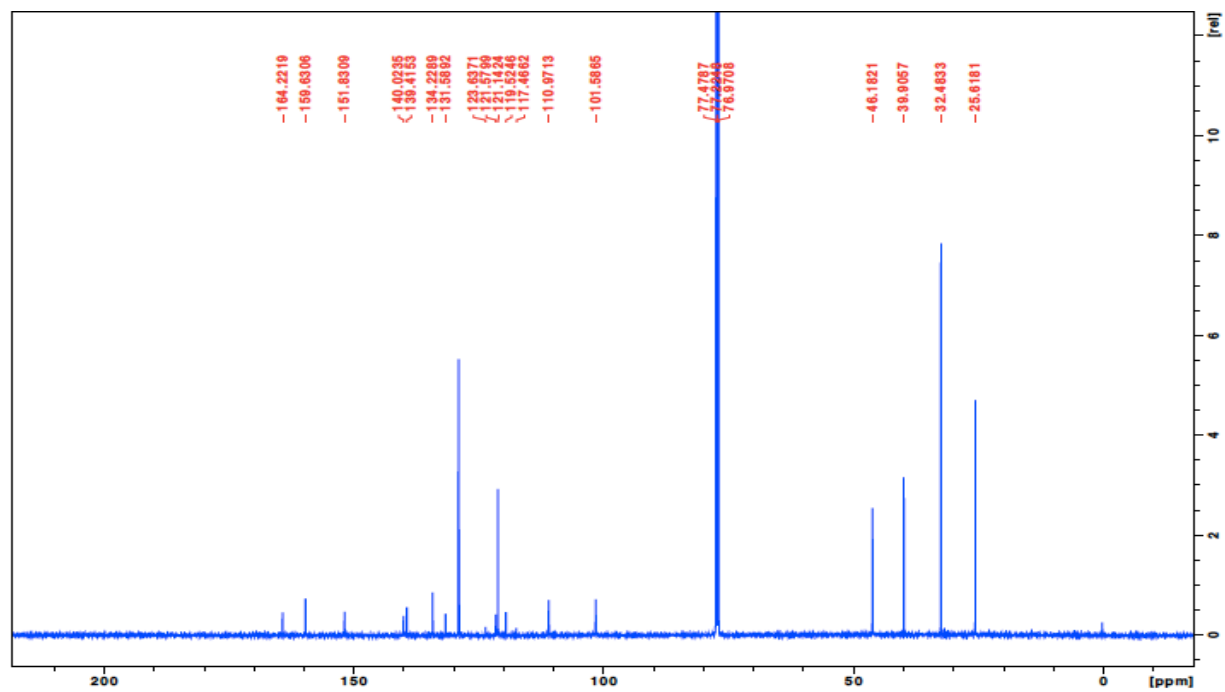
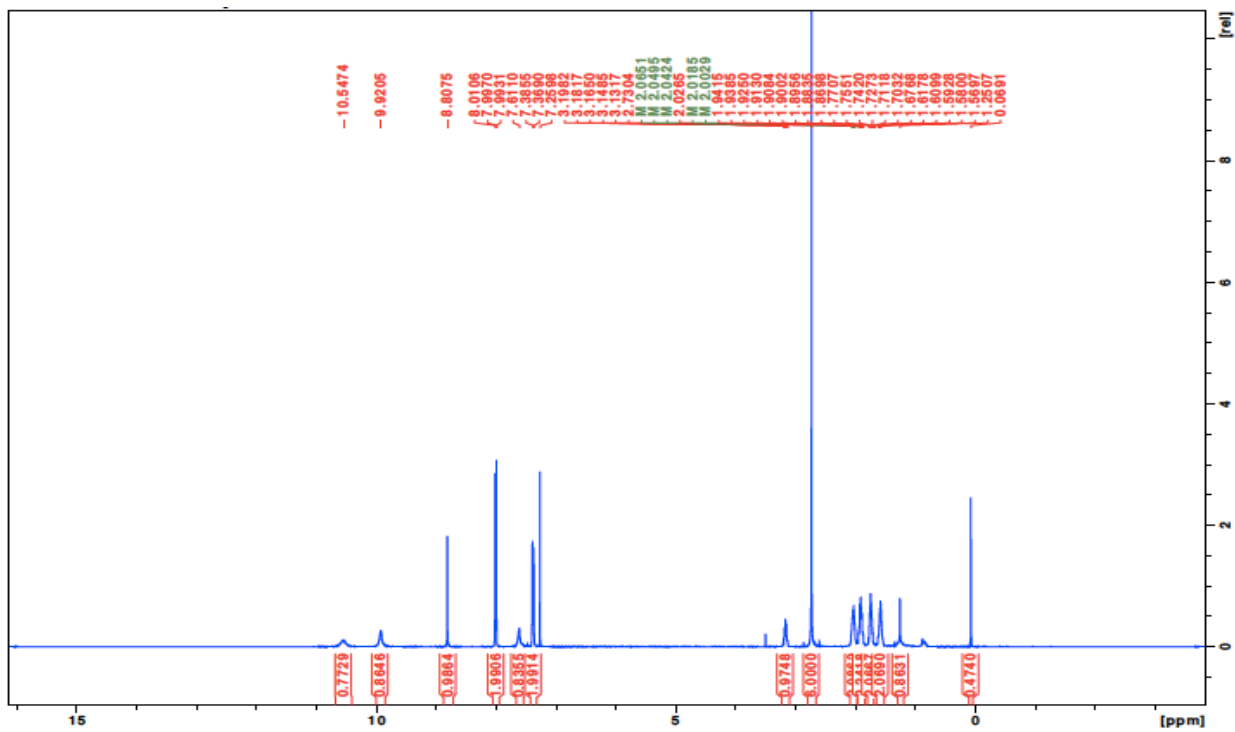


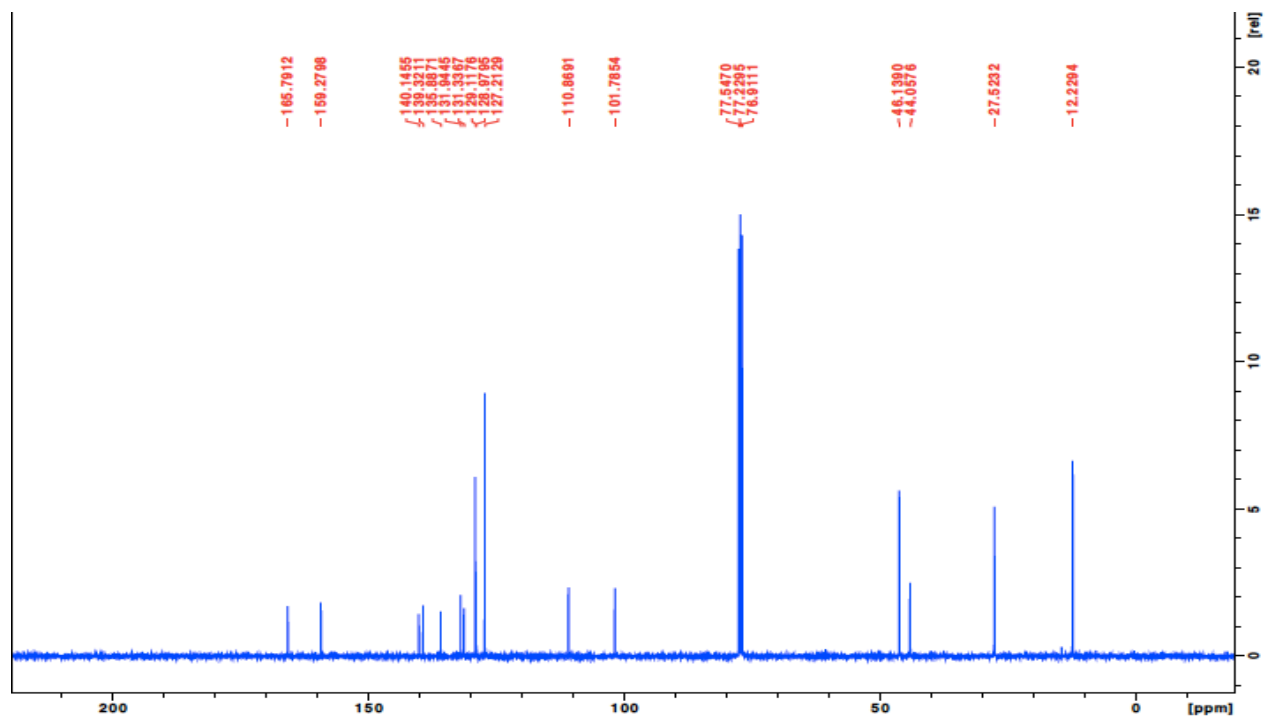
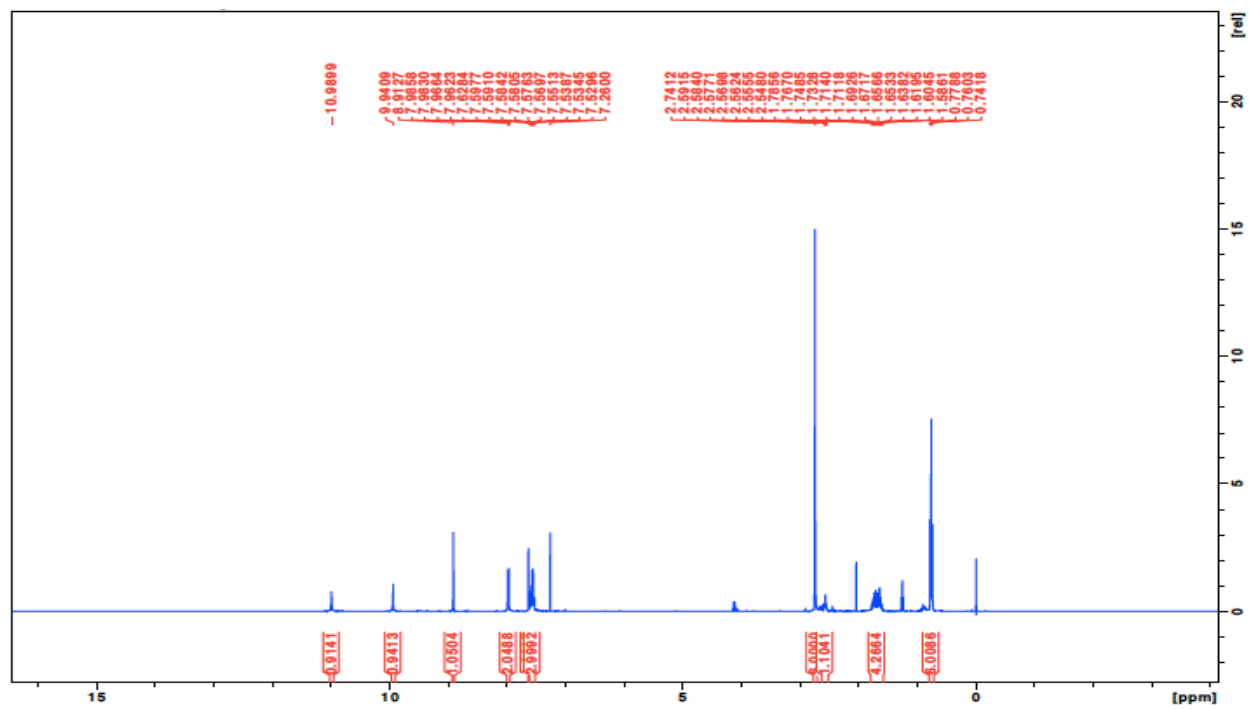


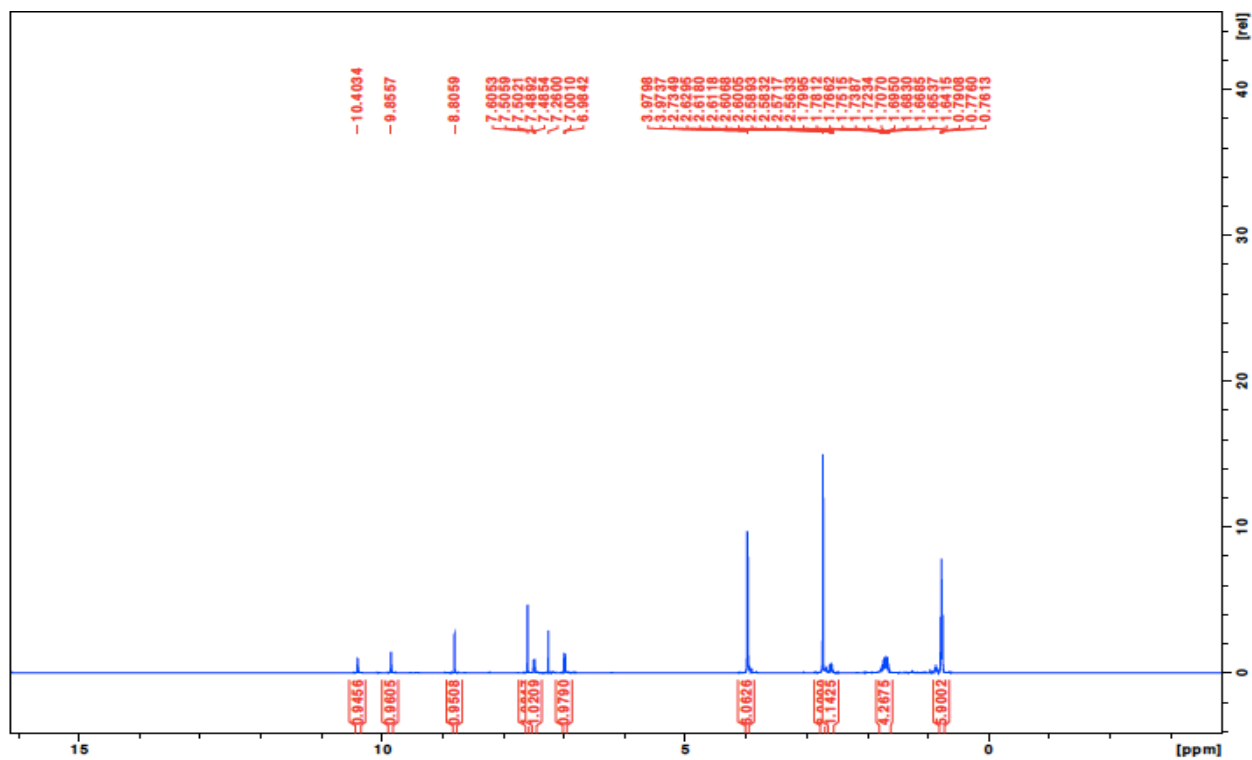
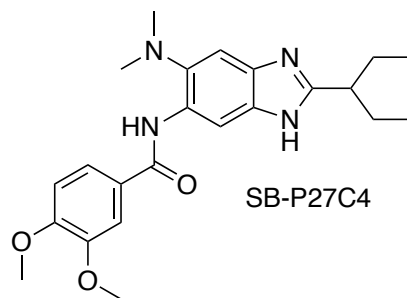


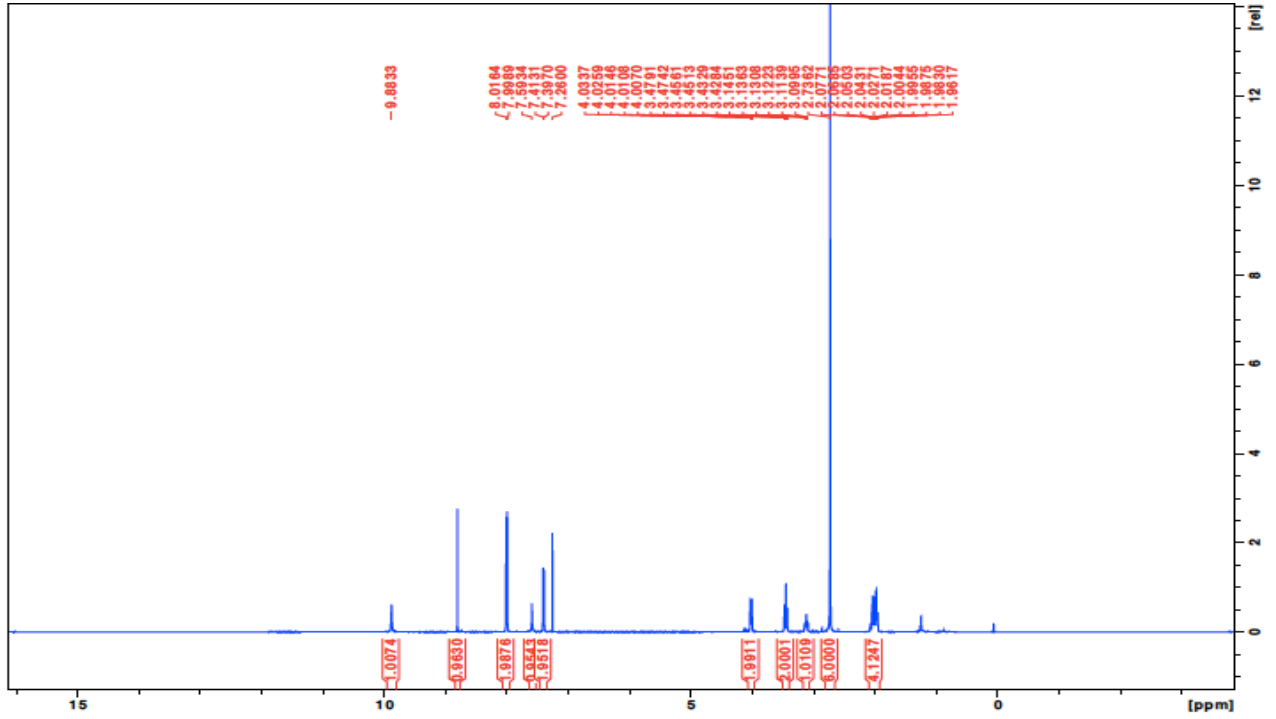
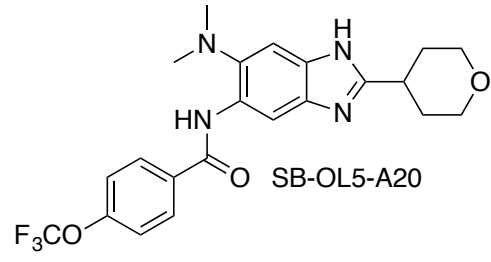


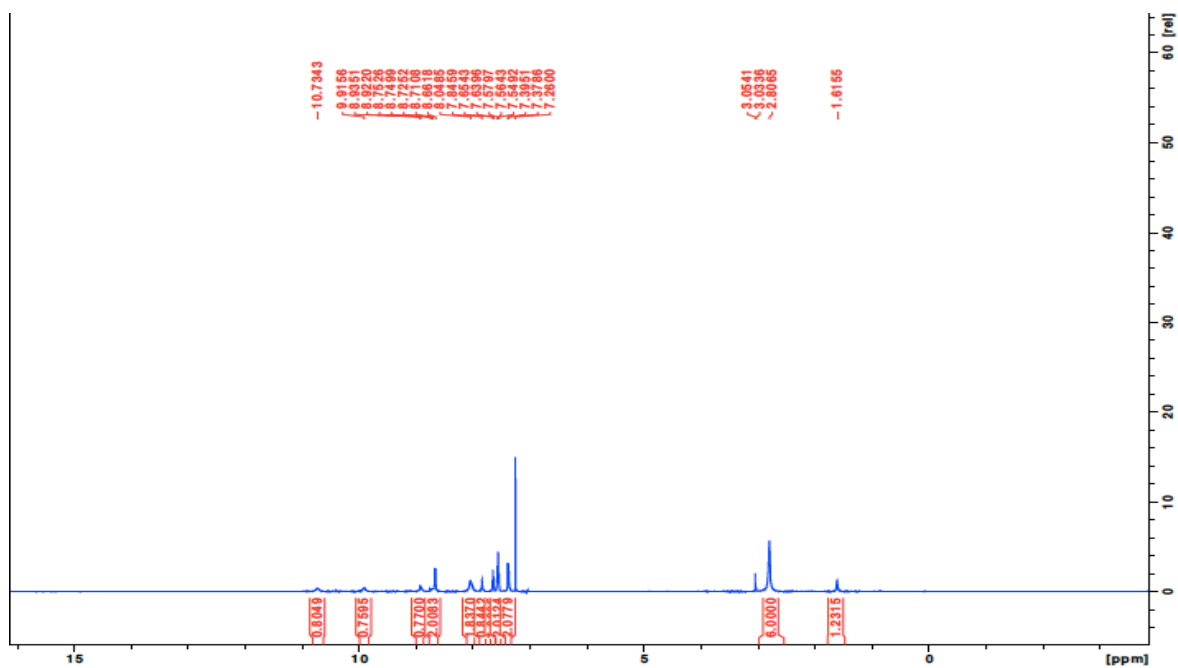
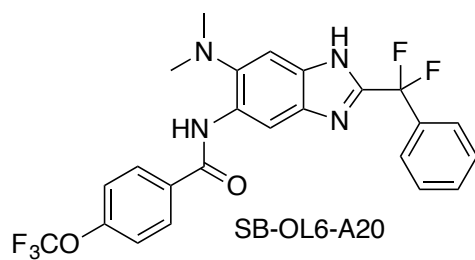
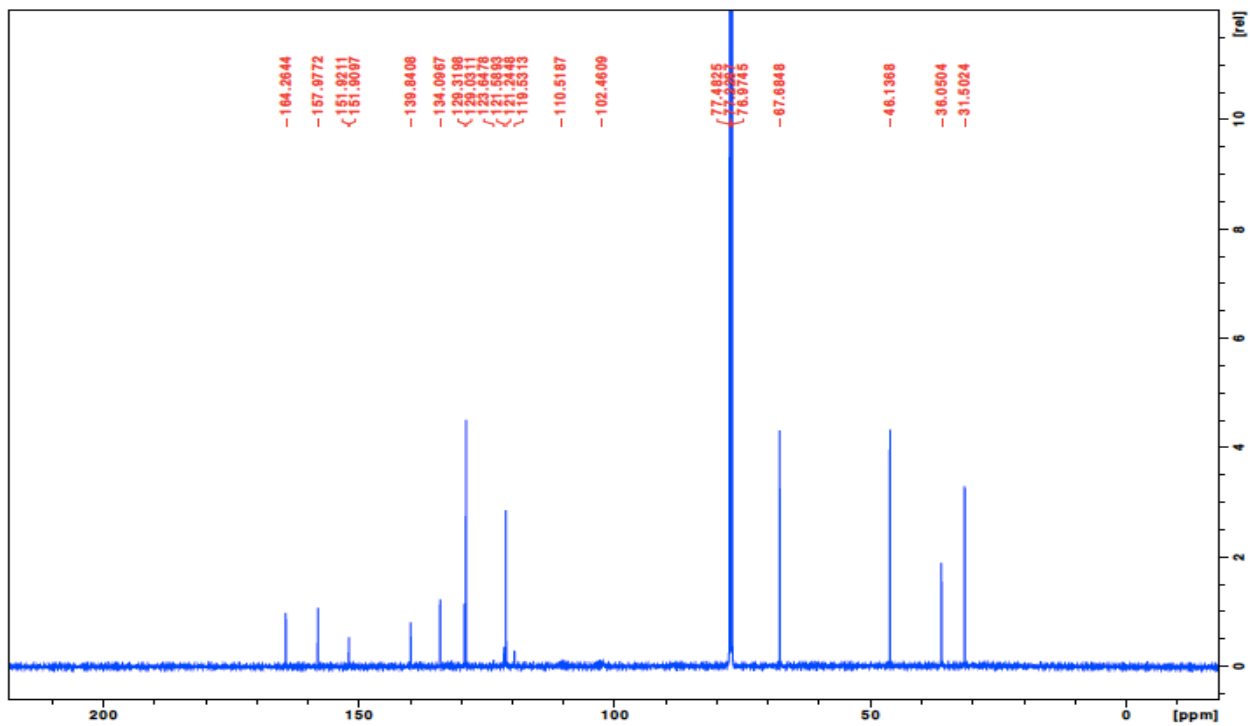


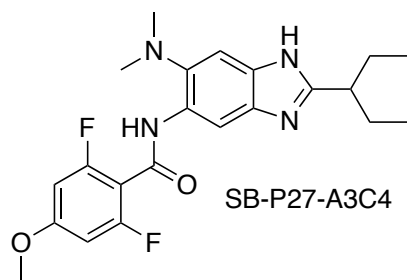
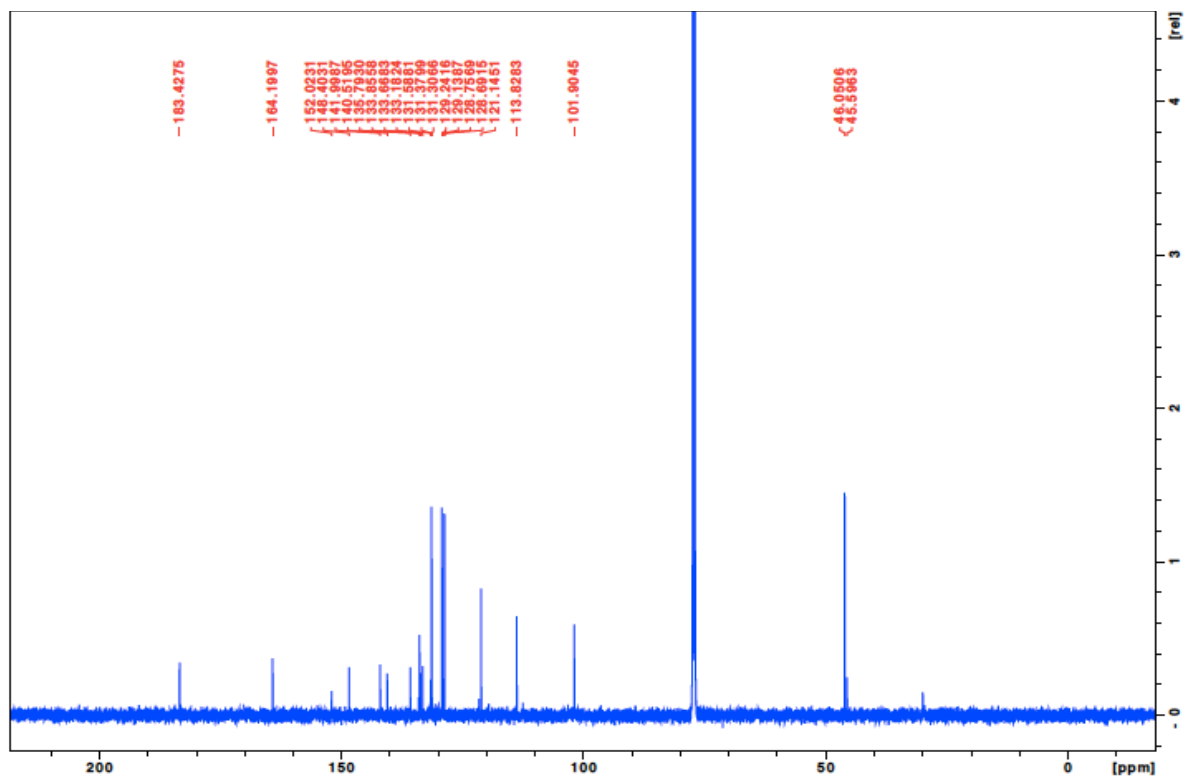


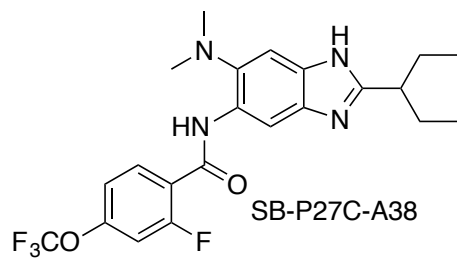
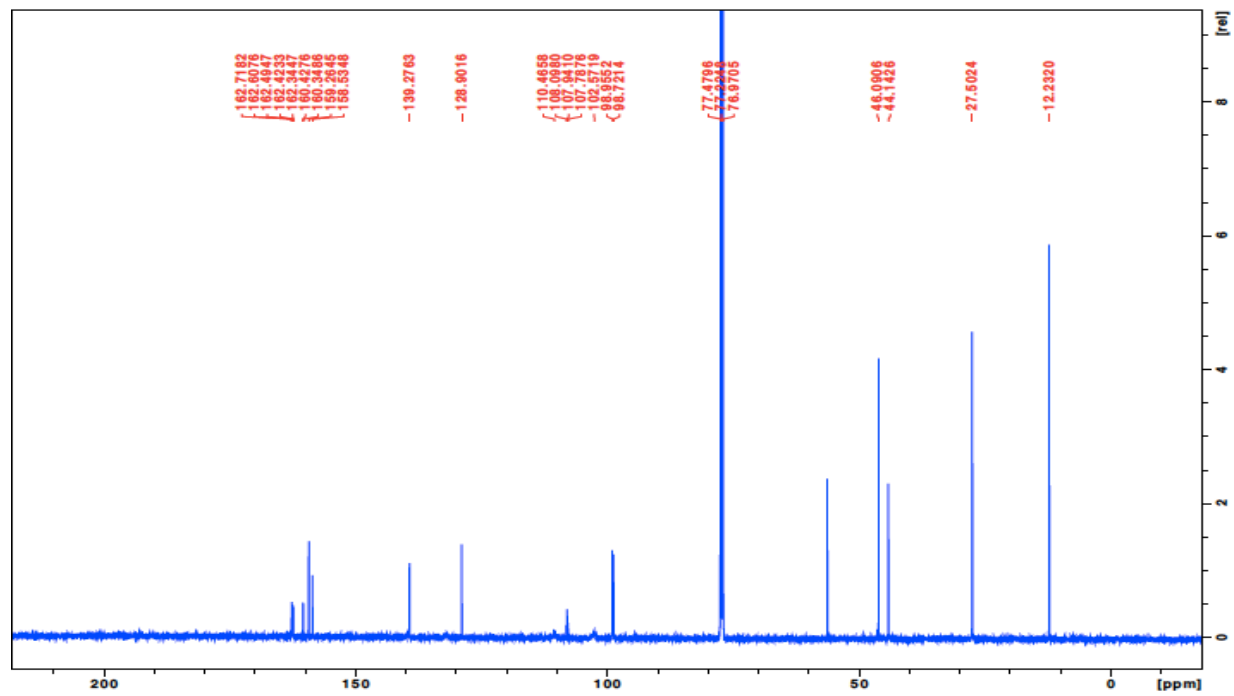
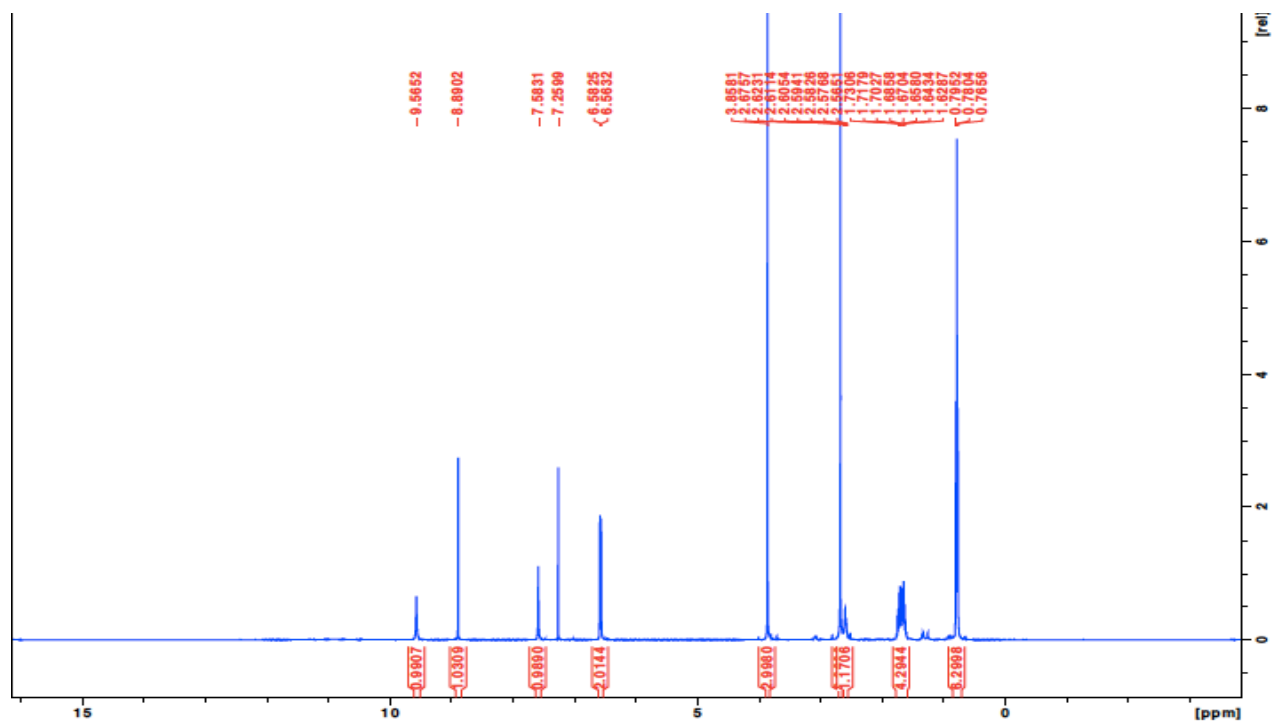


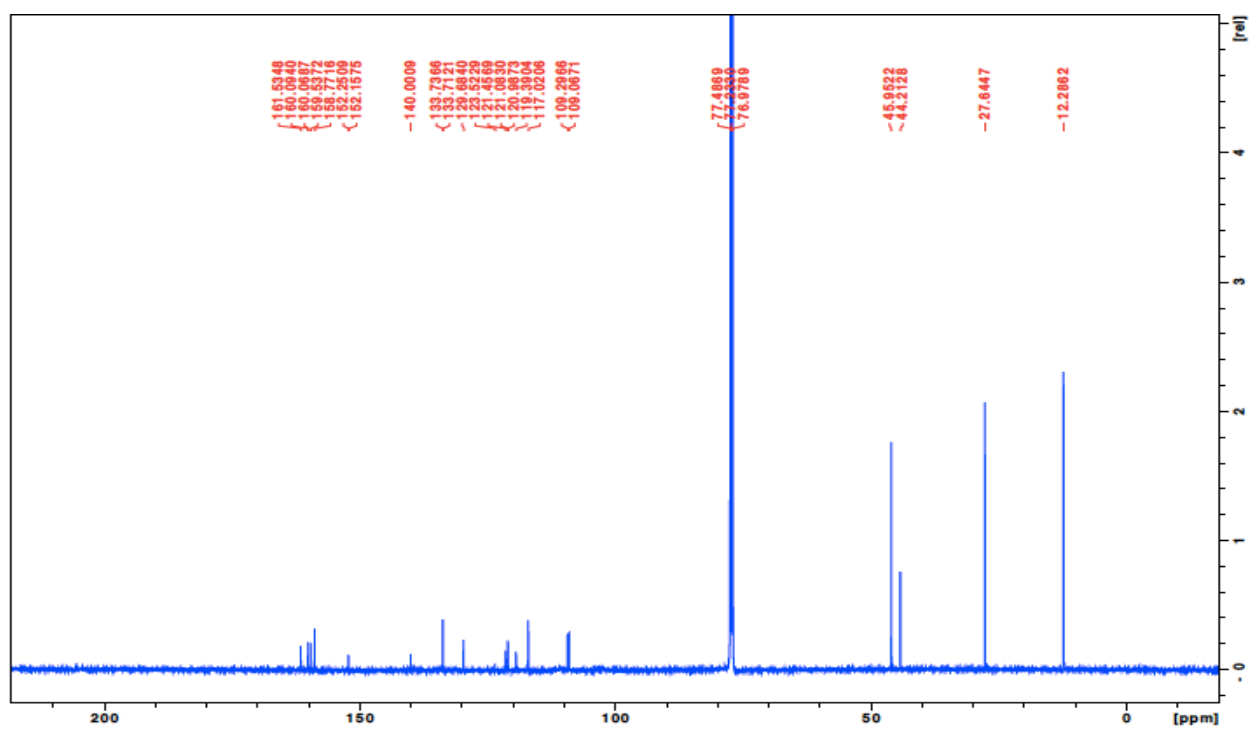
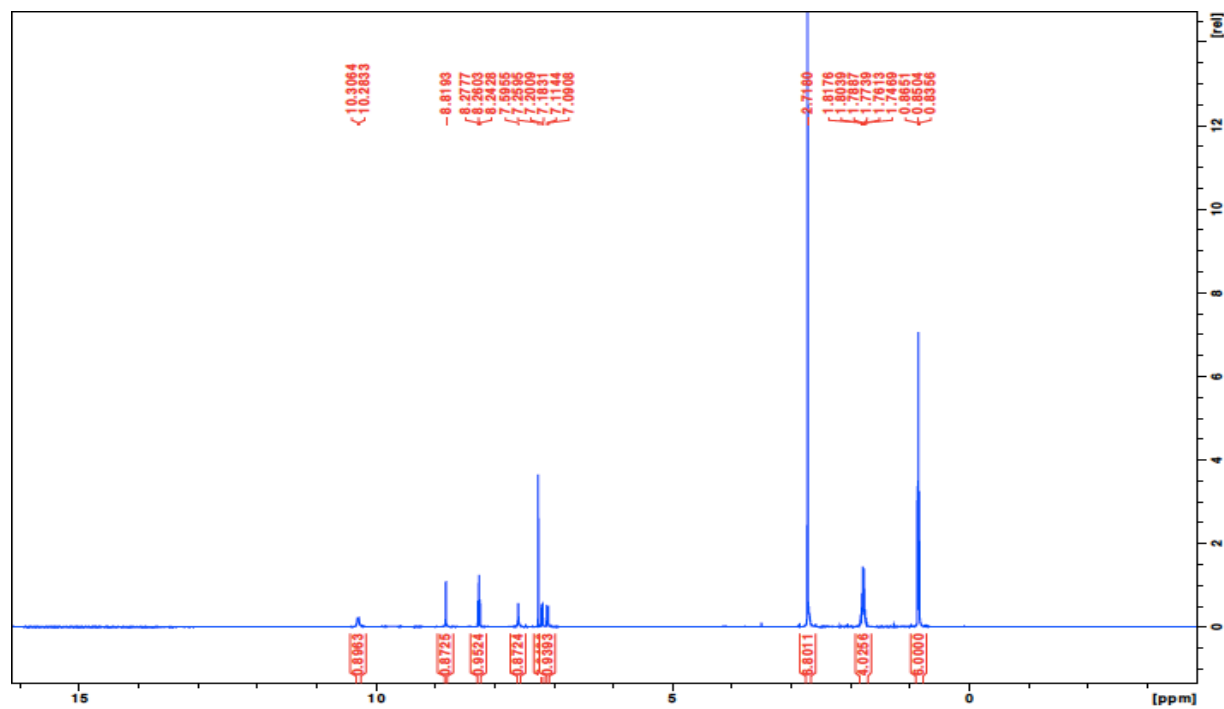


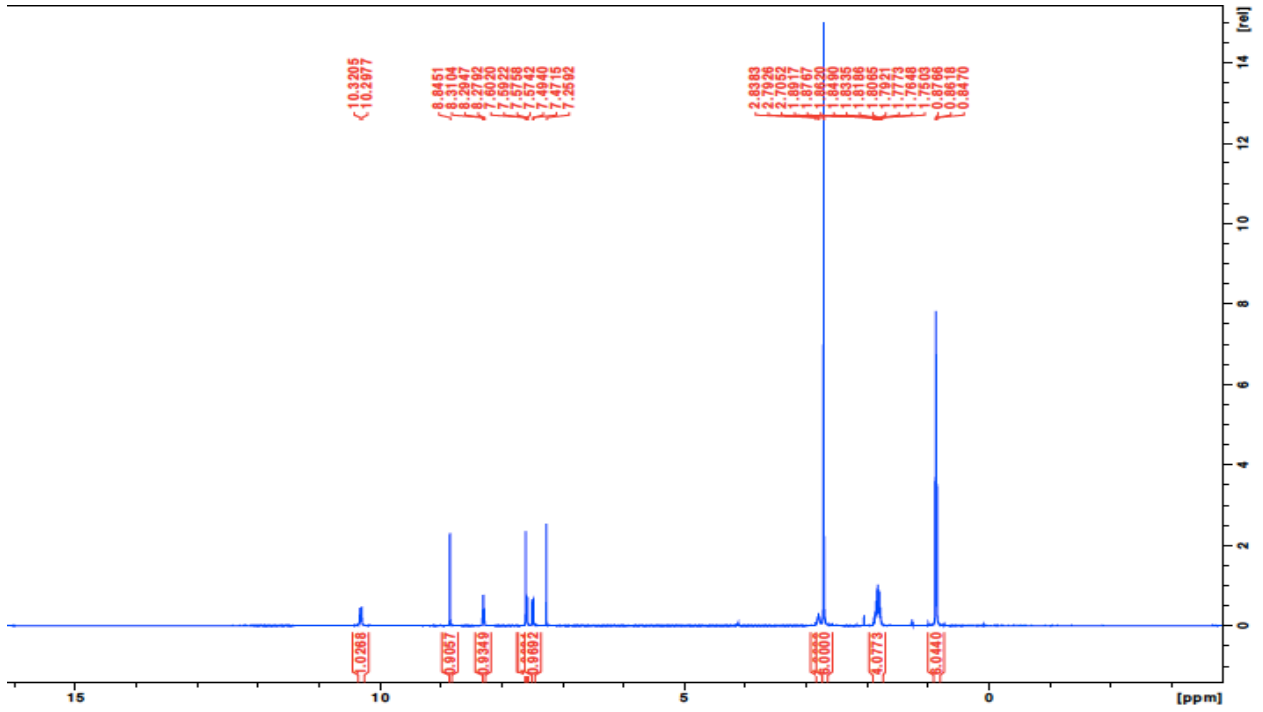
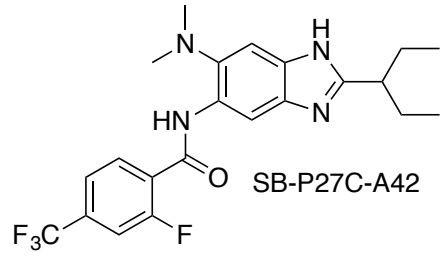


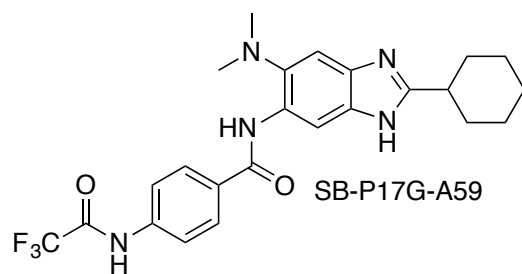
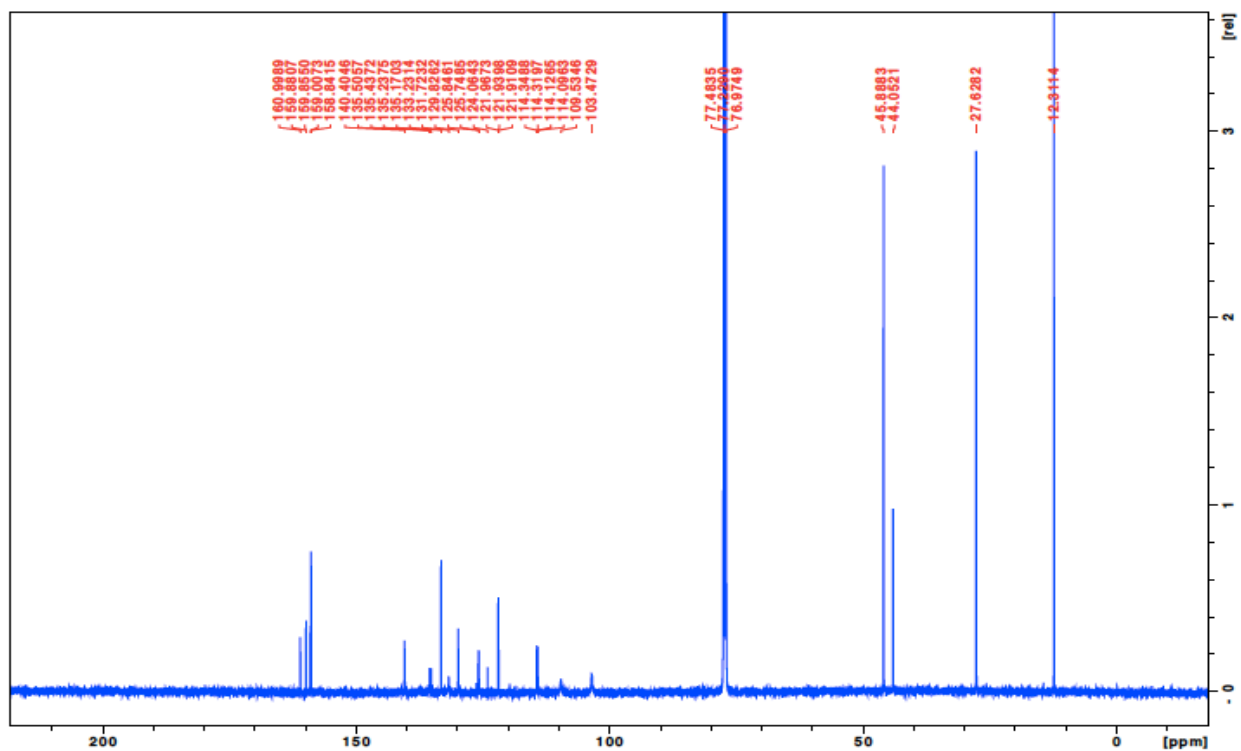


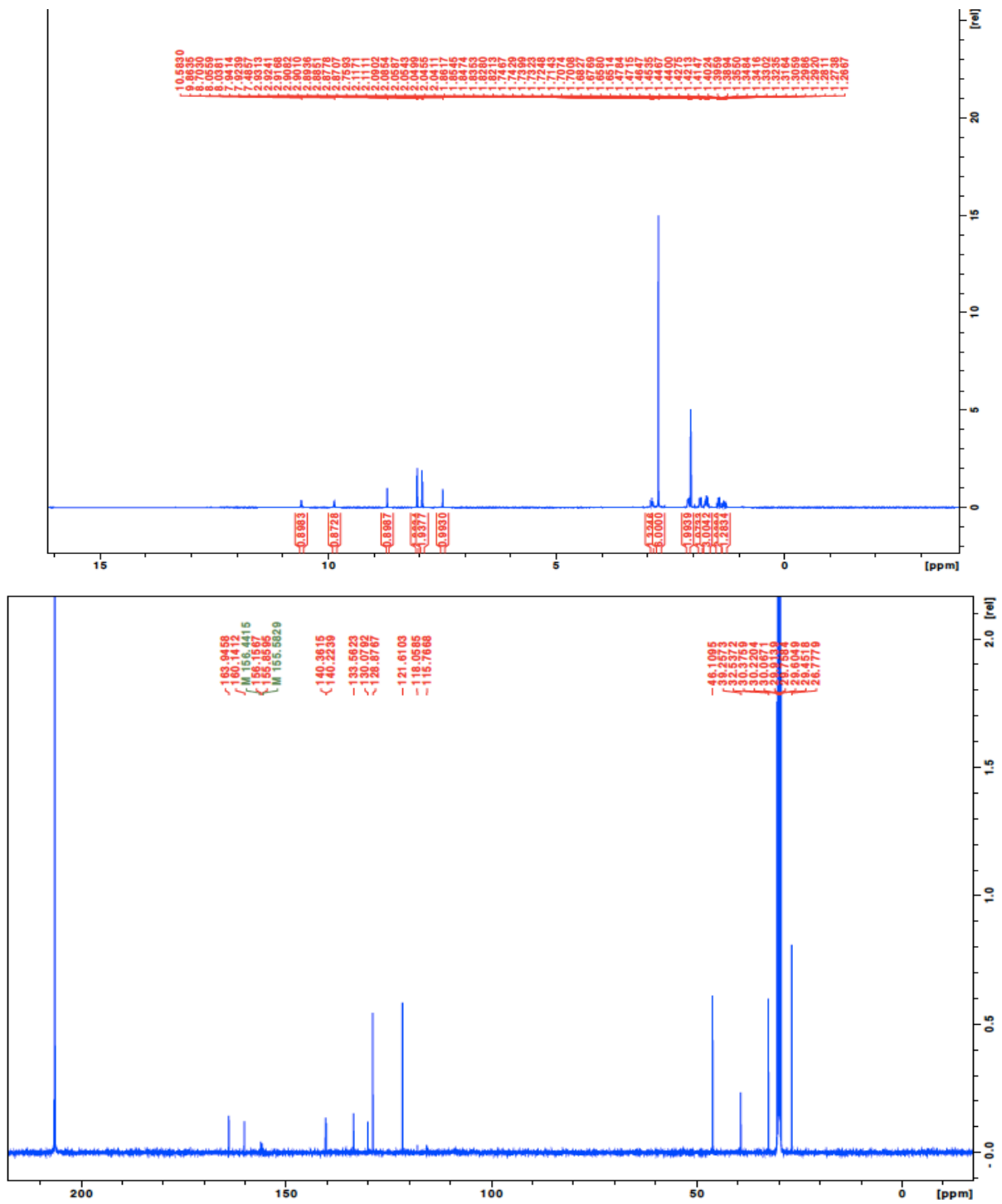


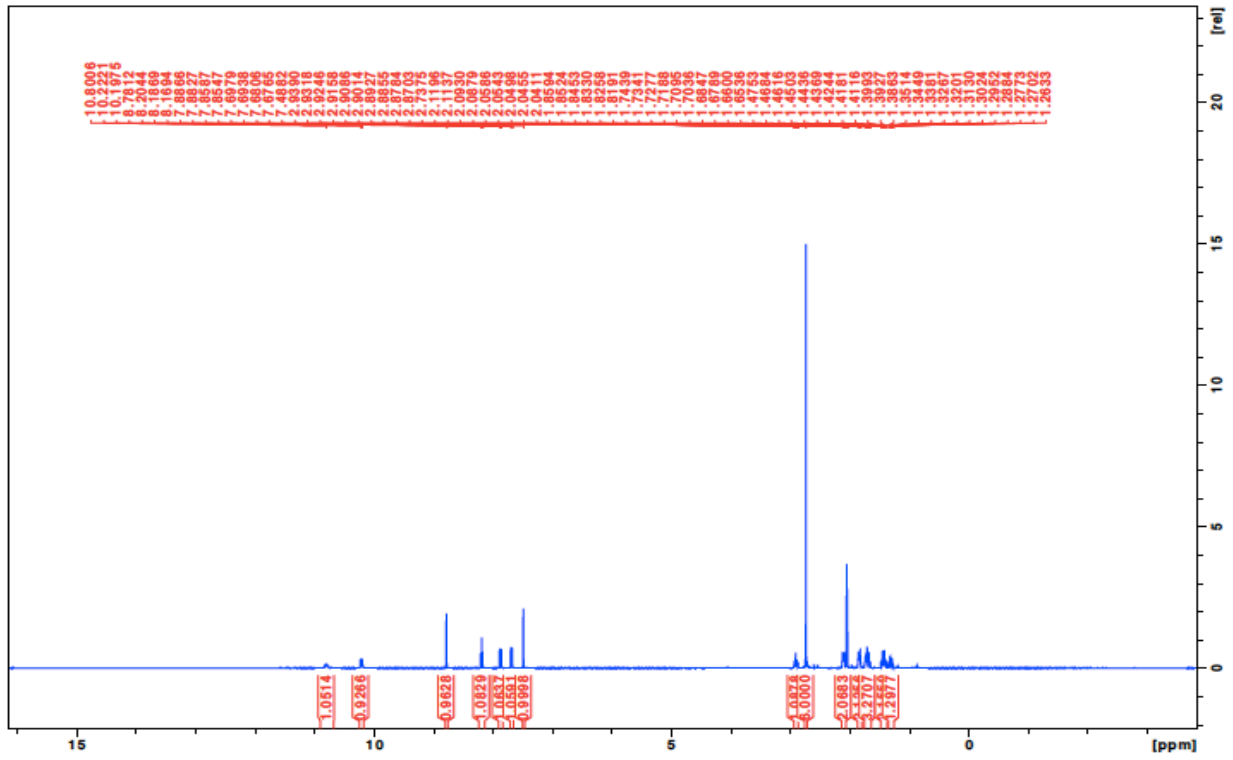
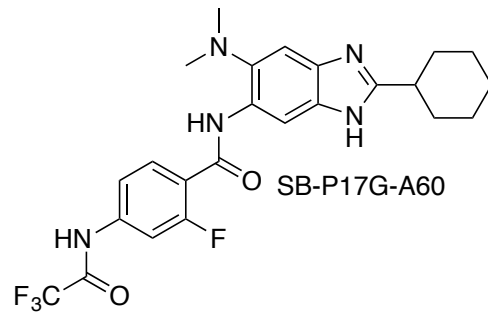


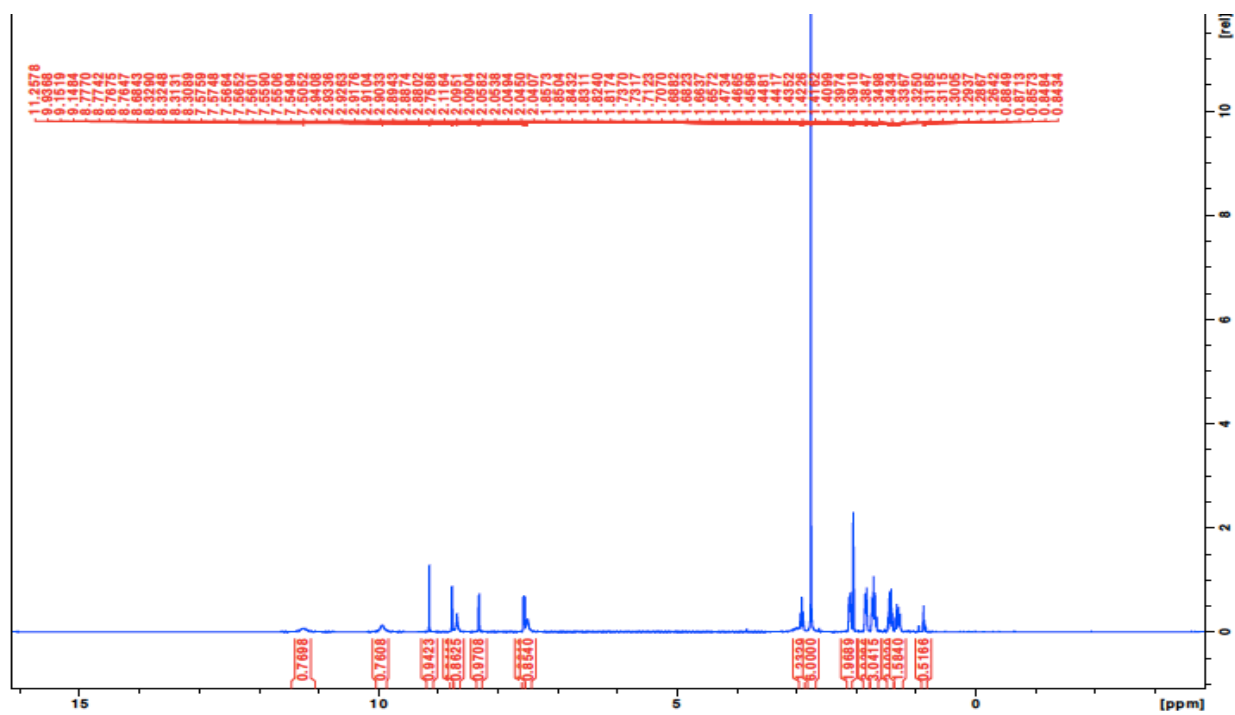
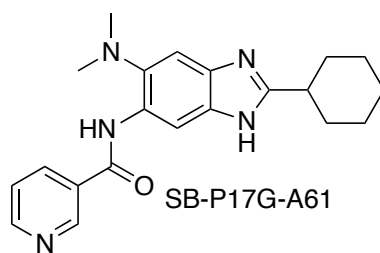
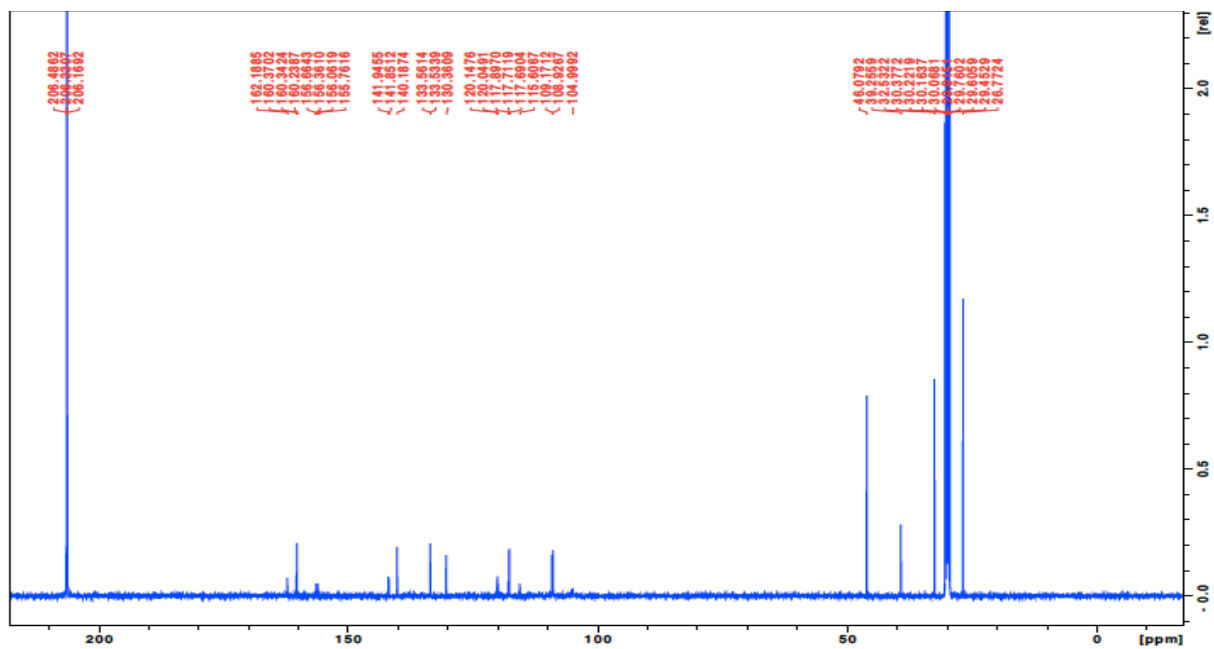


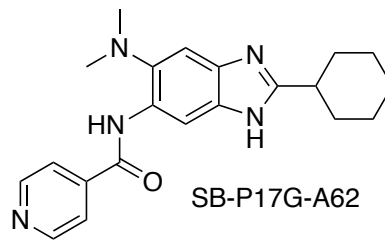
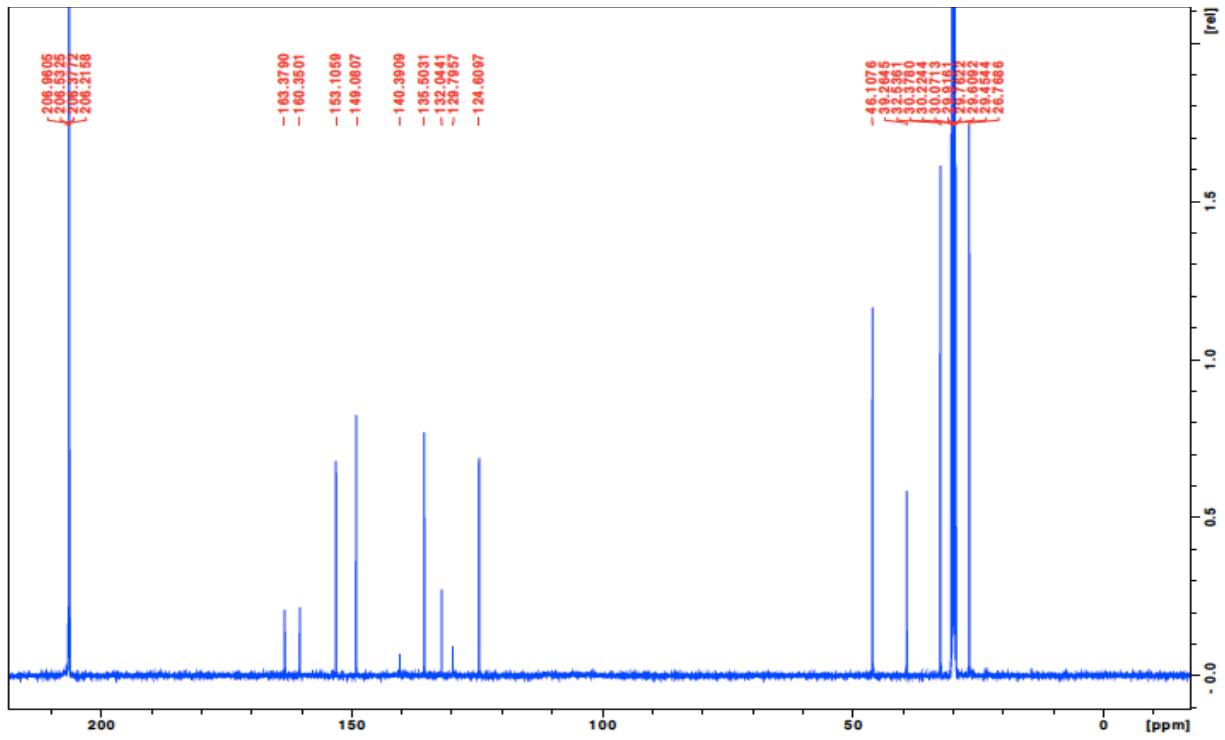


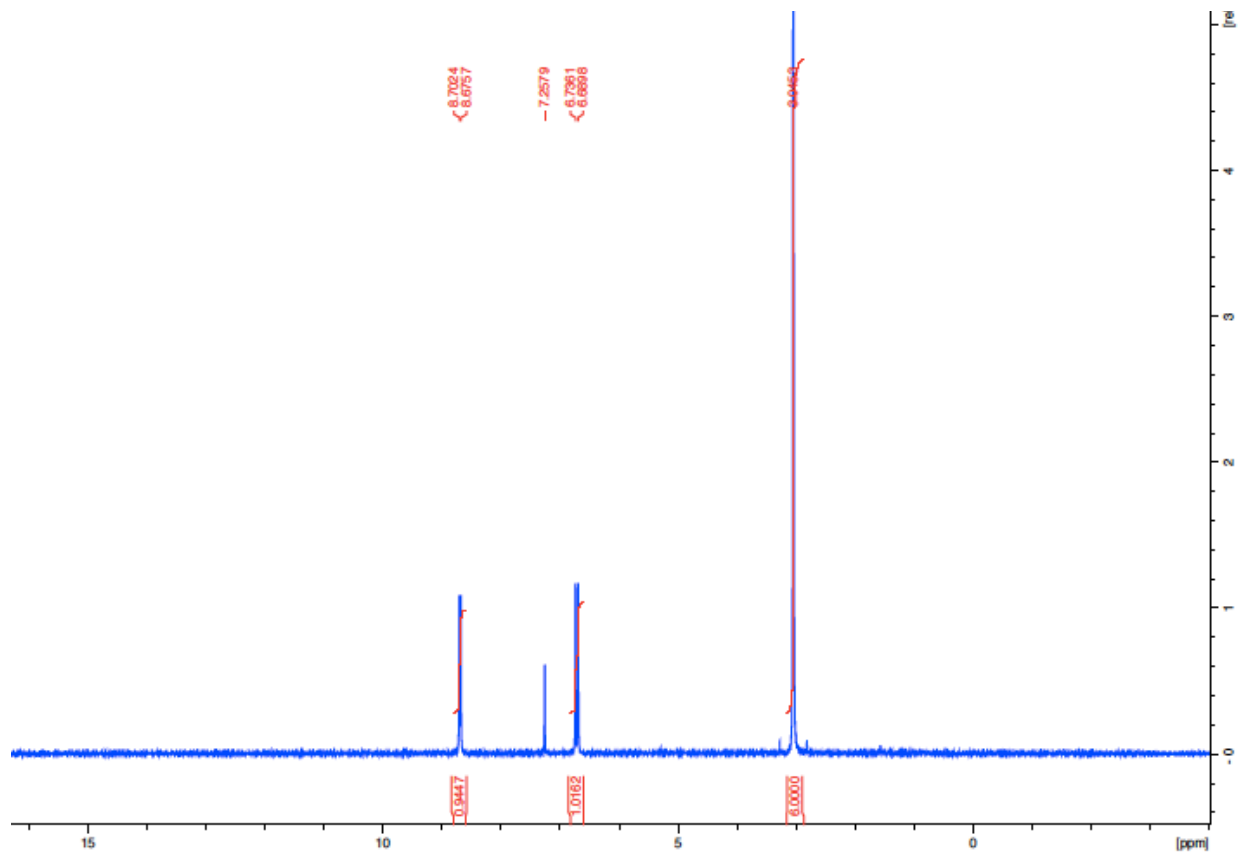


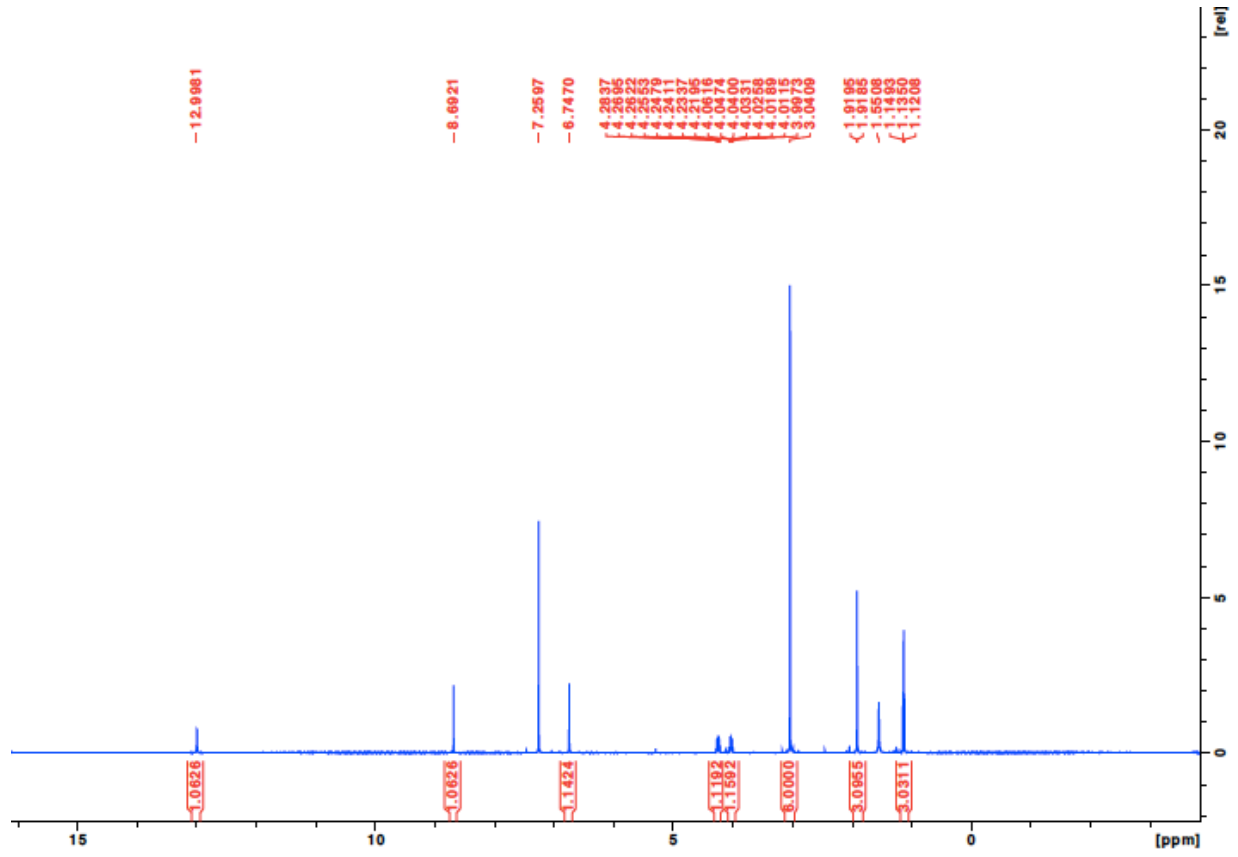
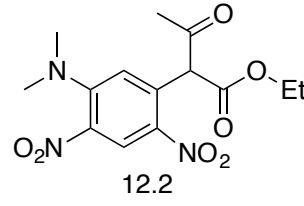


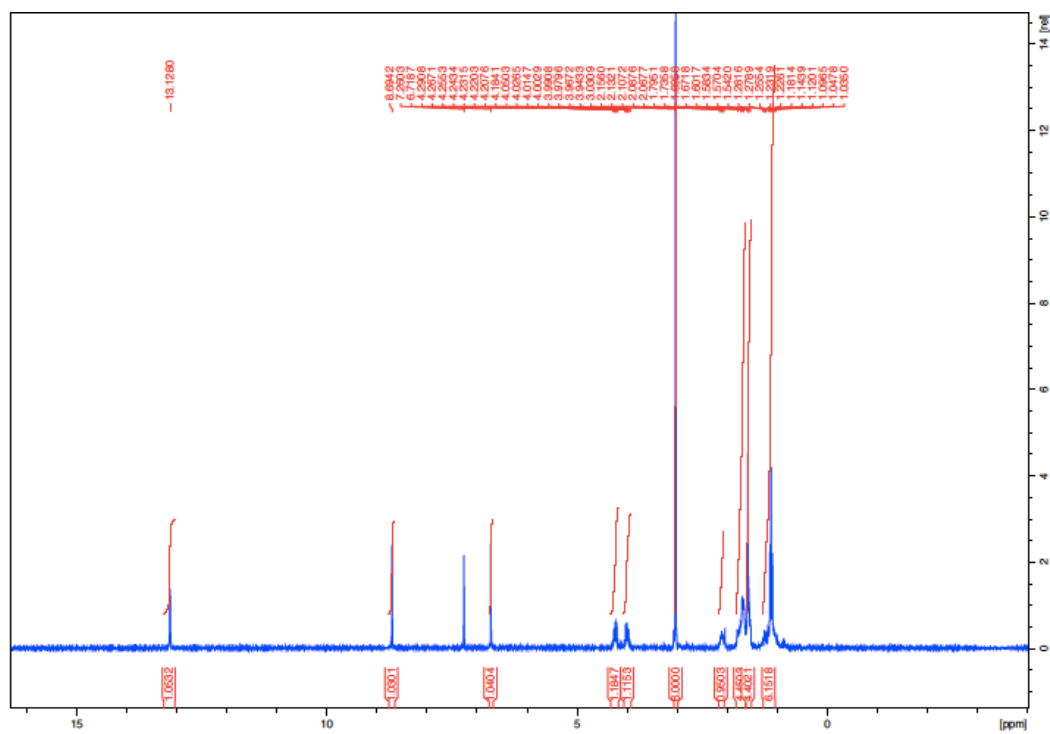
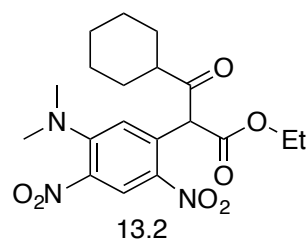


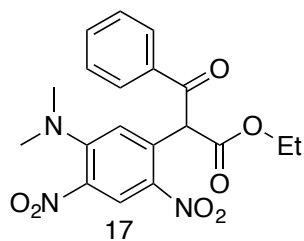
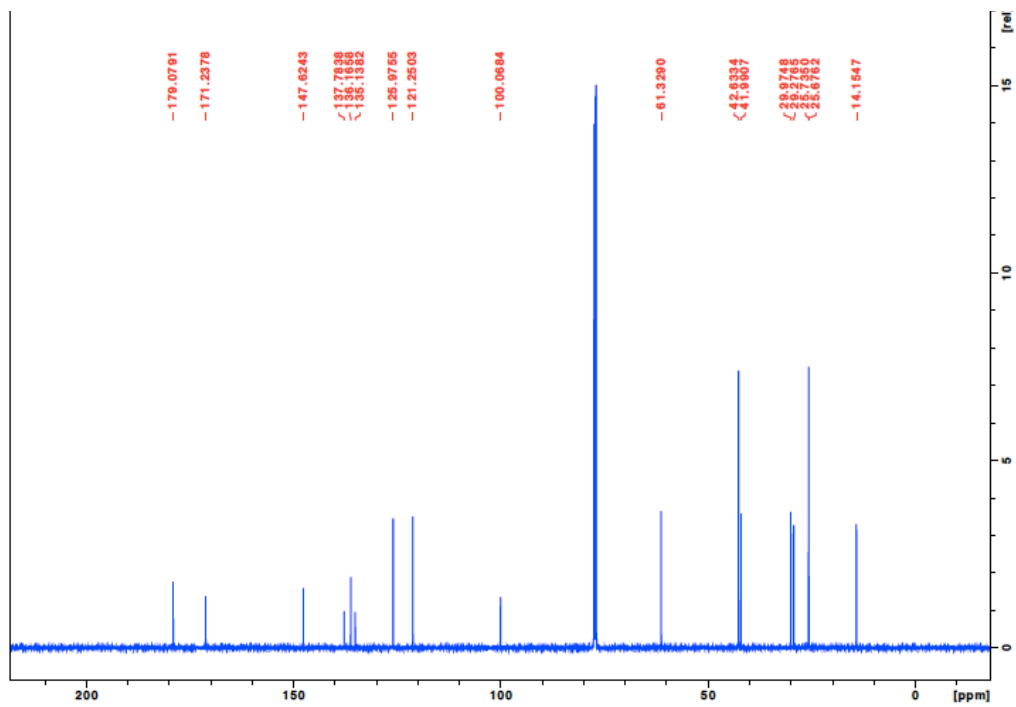


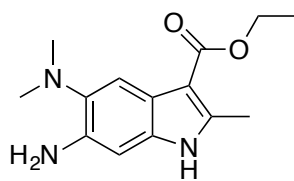
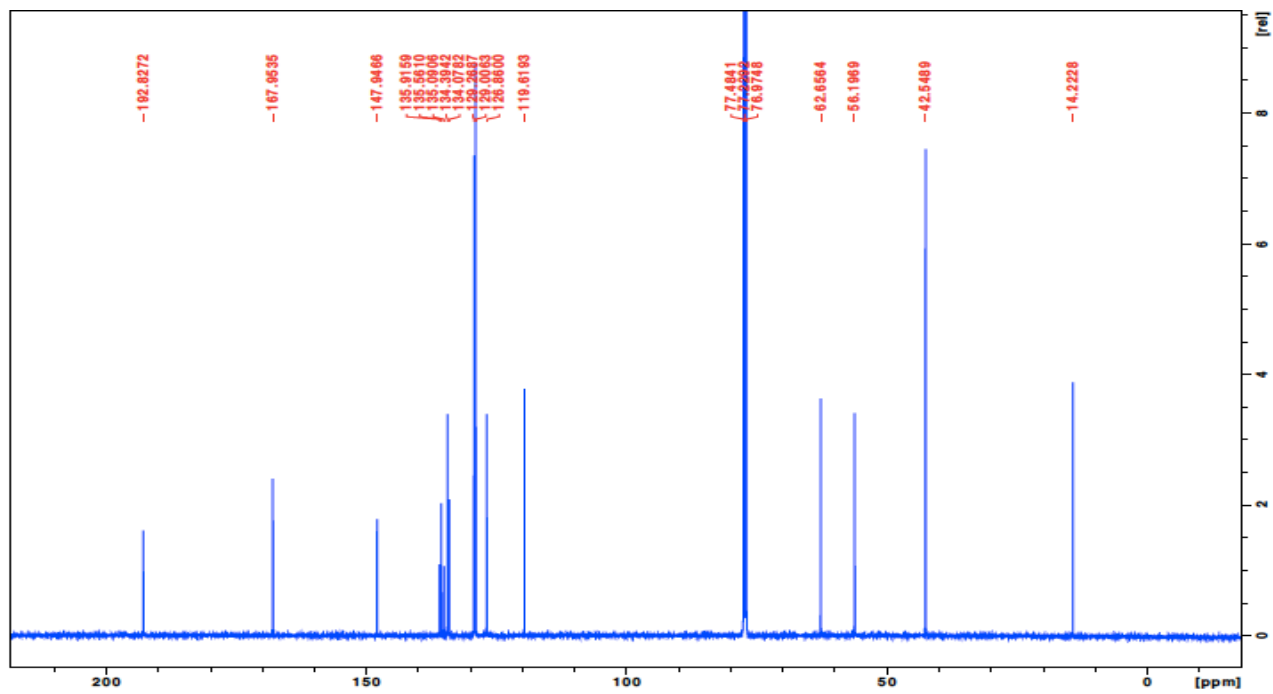
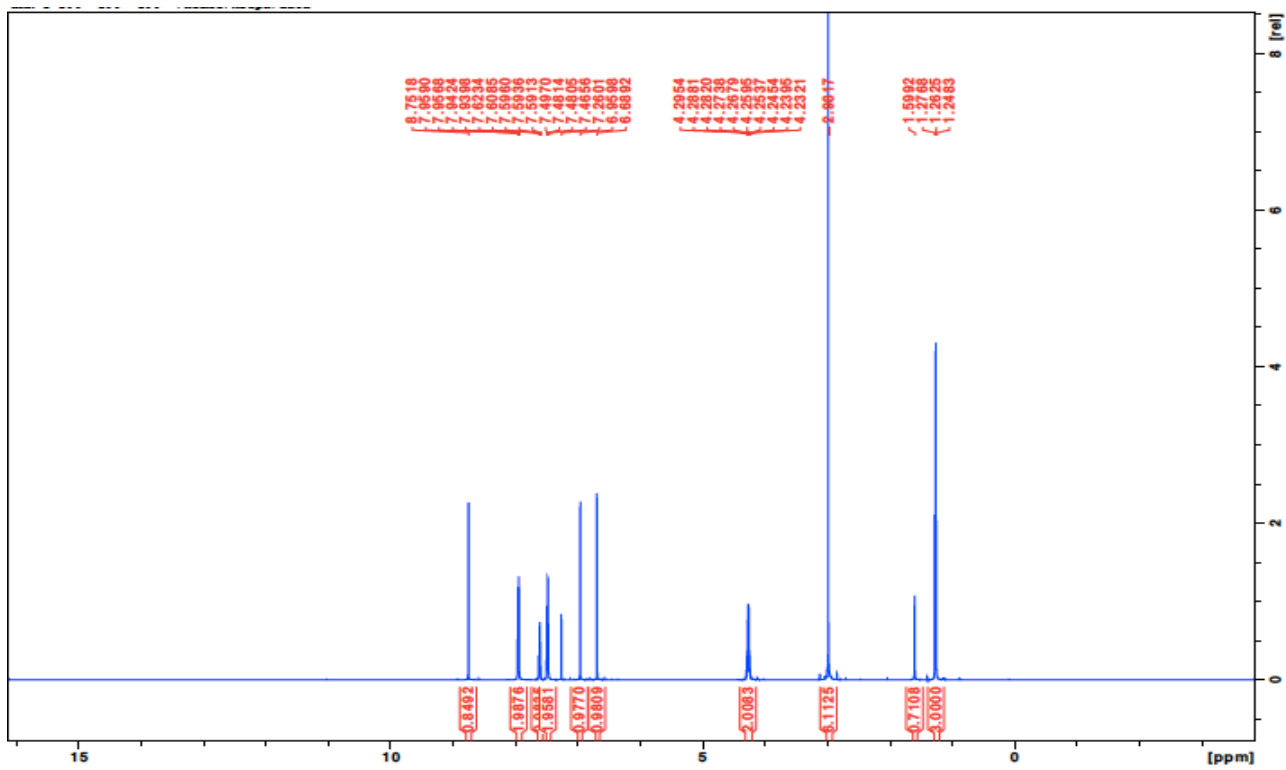




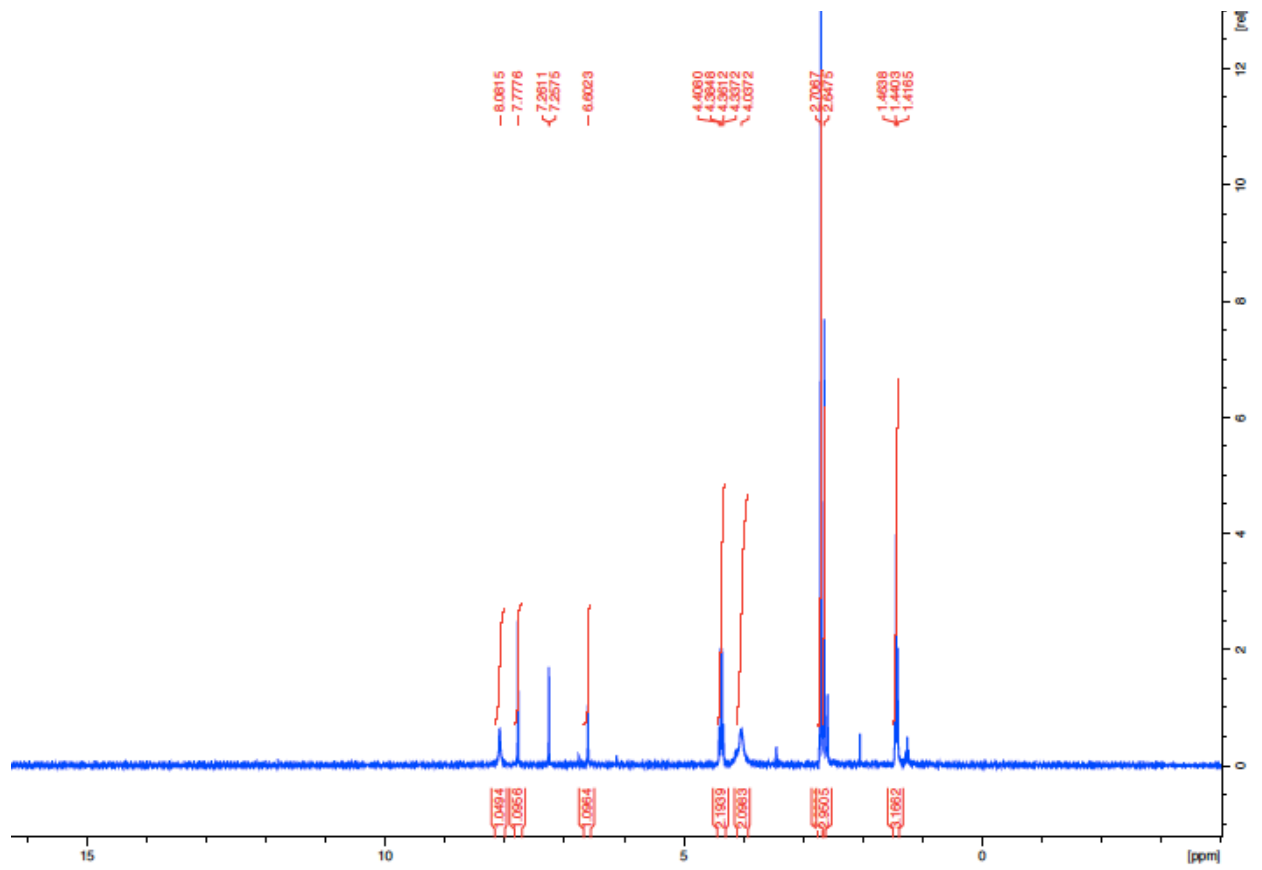


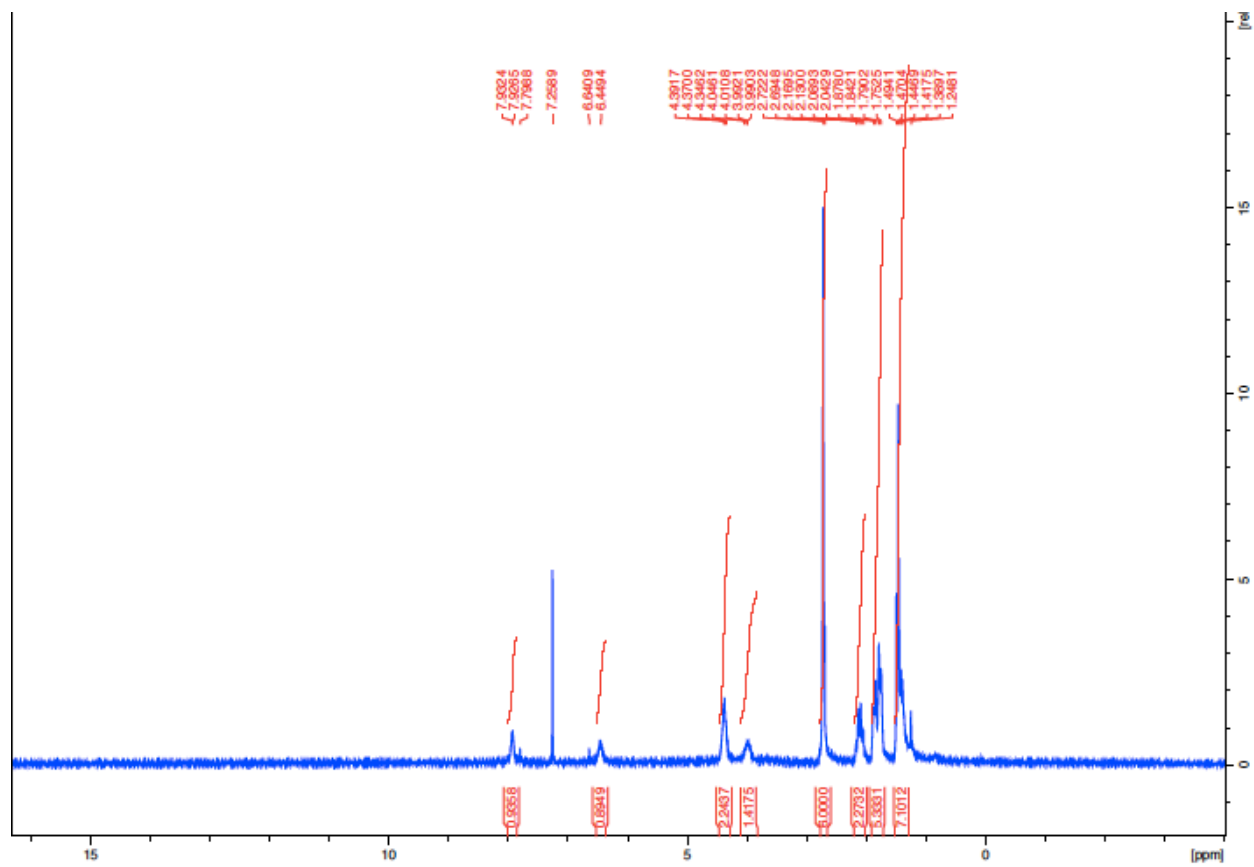
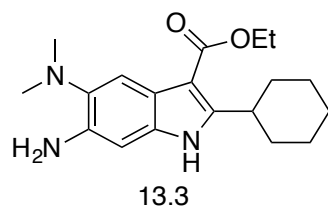


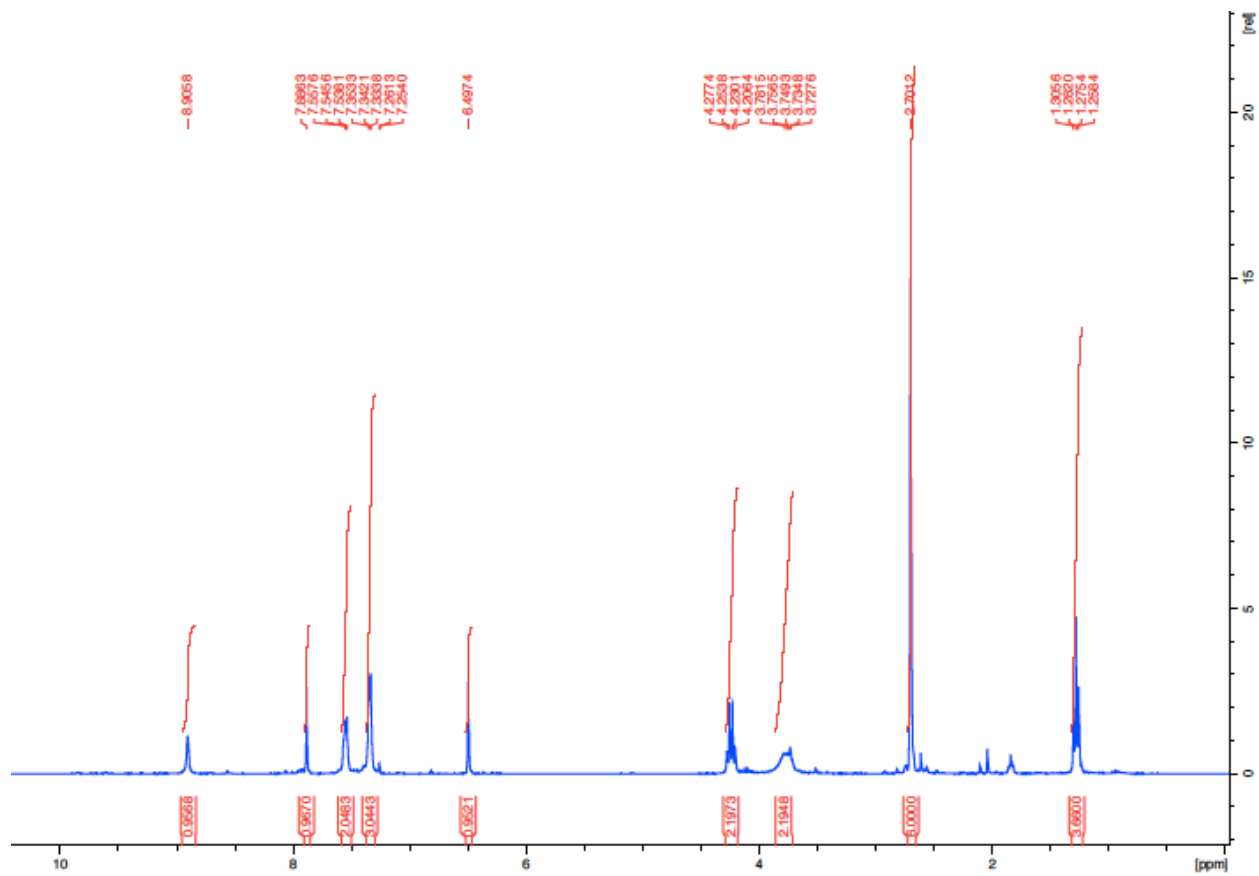
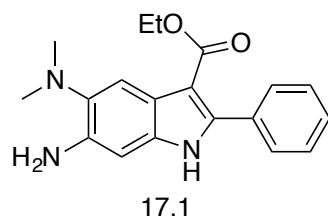


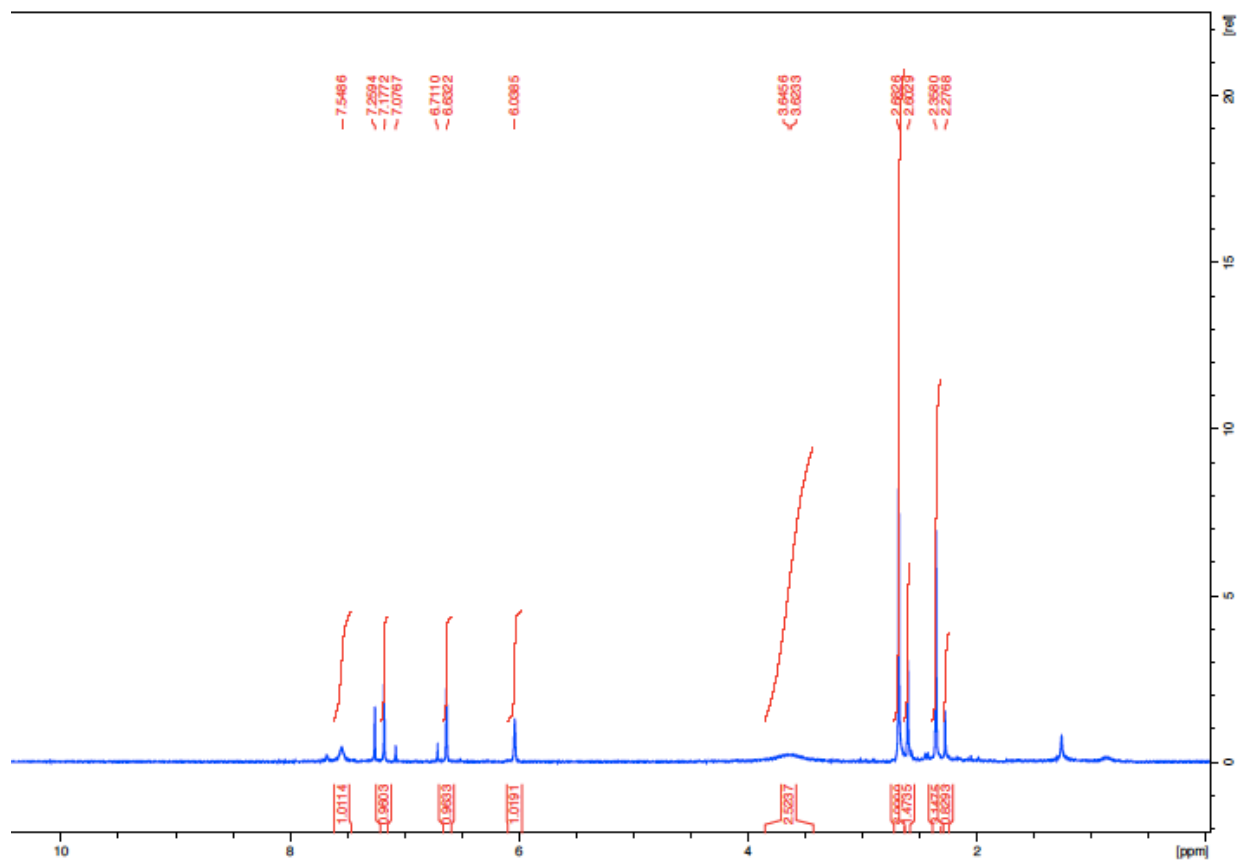
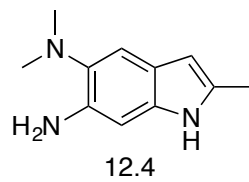


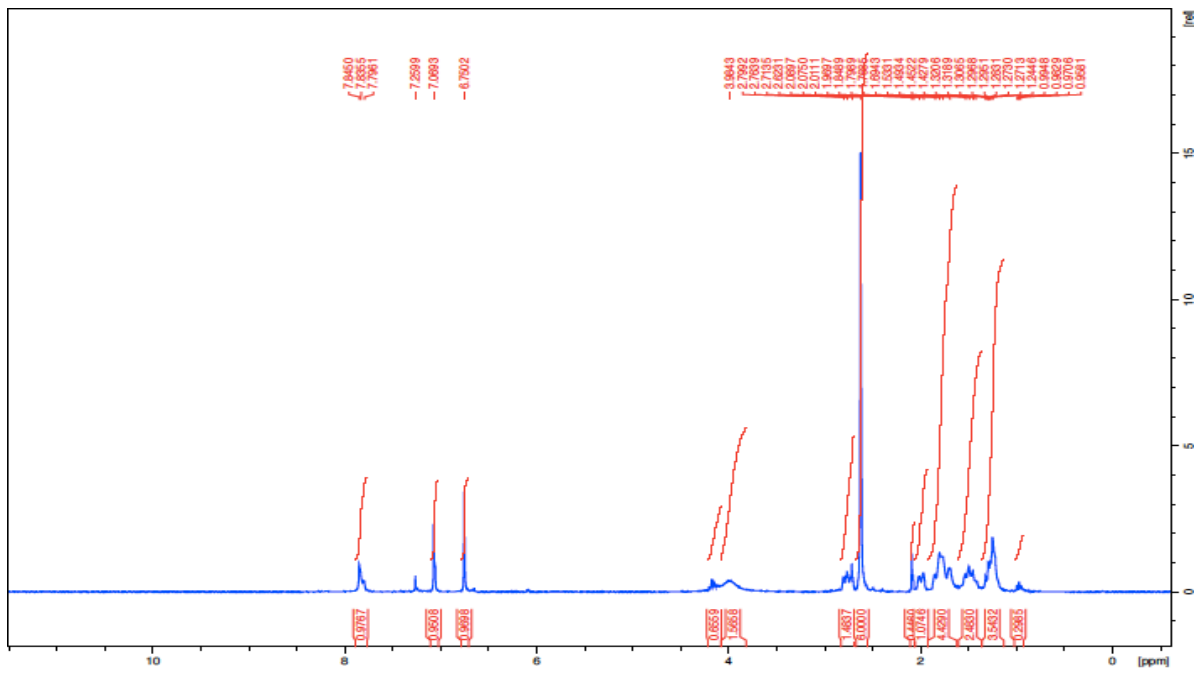
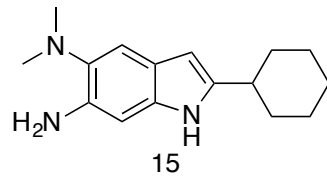
12.3

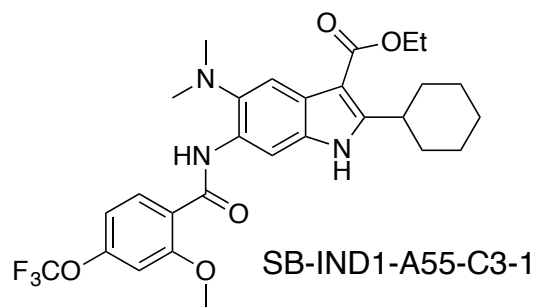
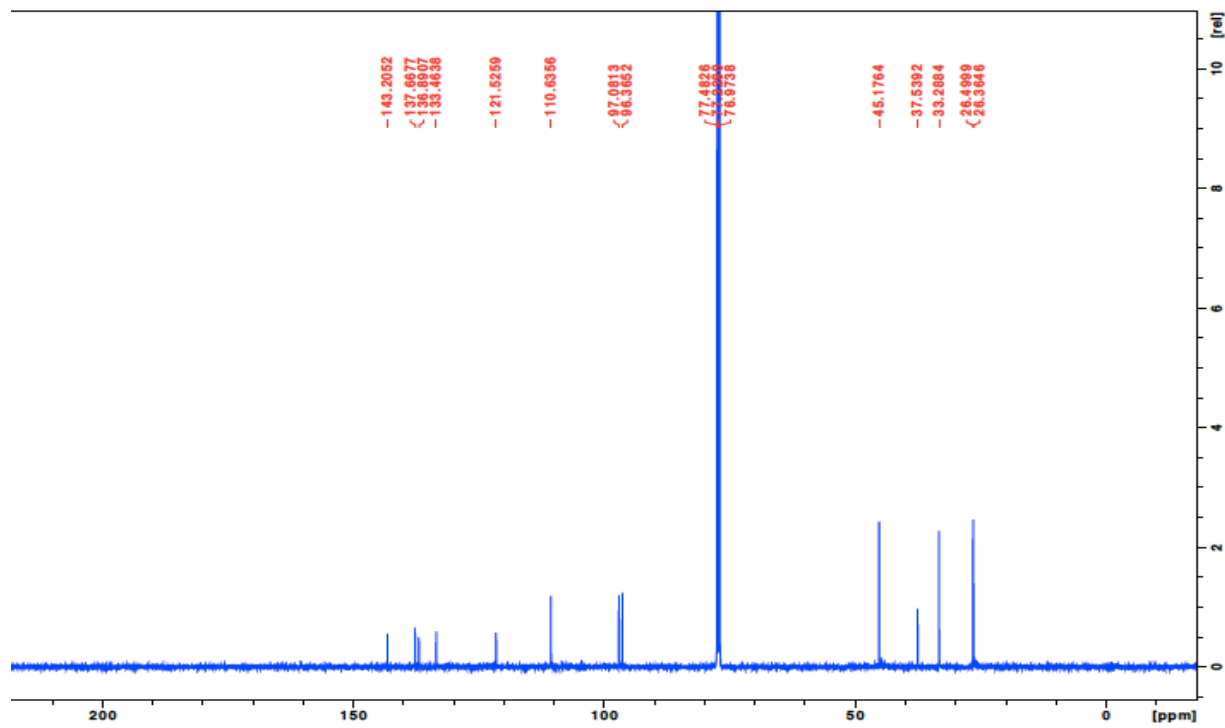


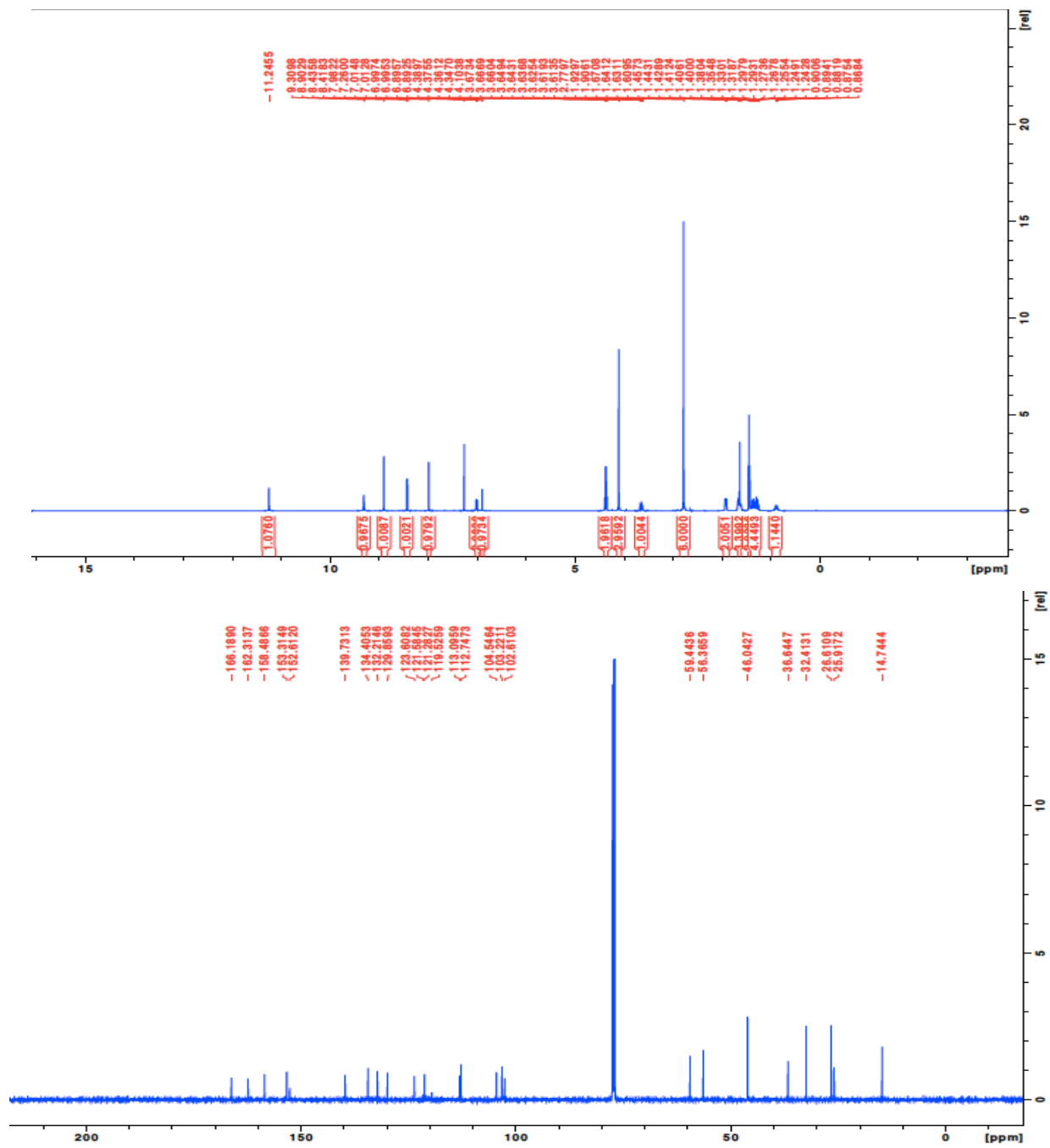




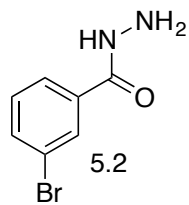


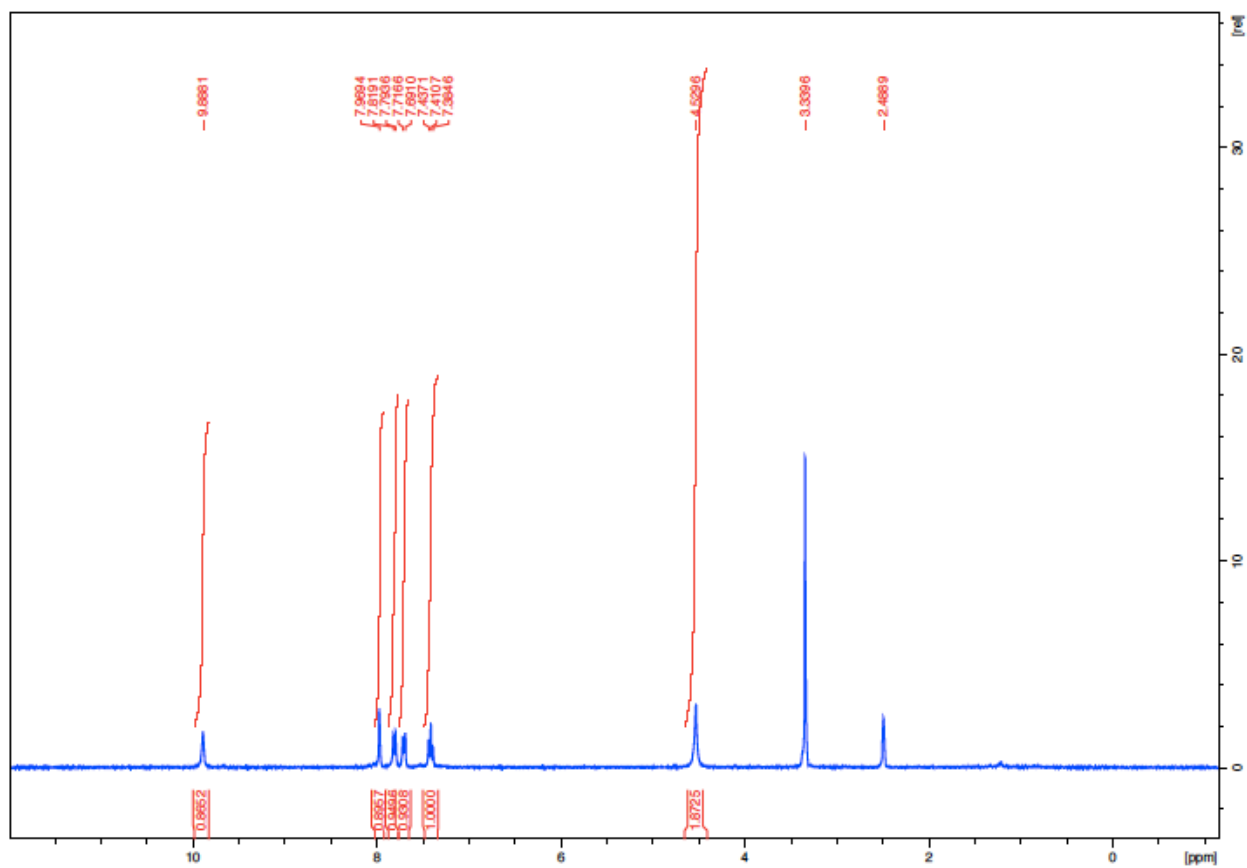


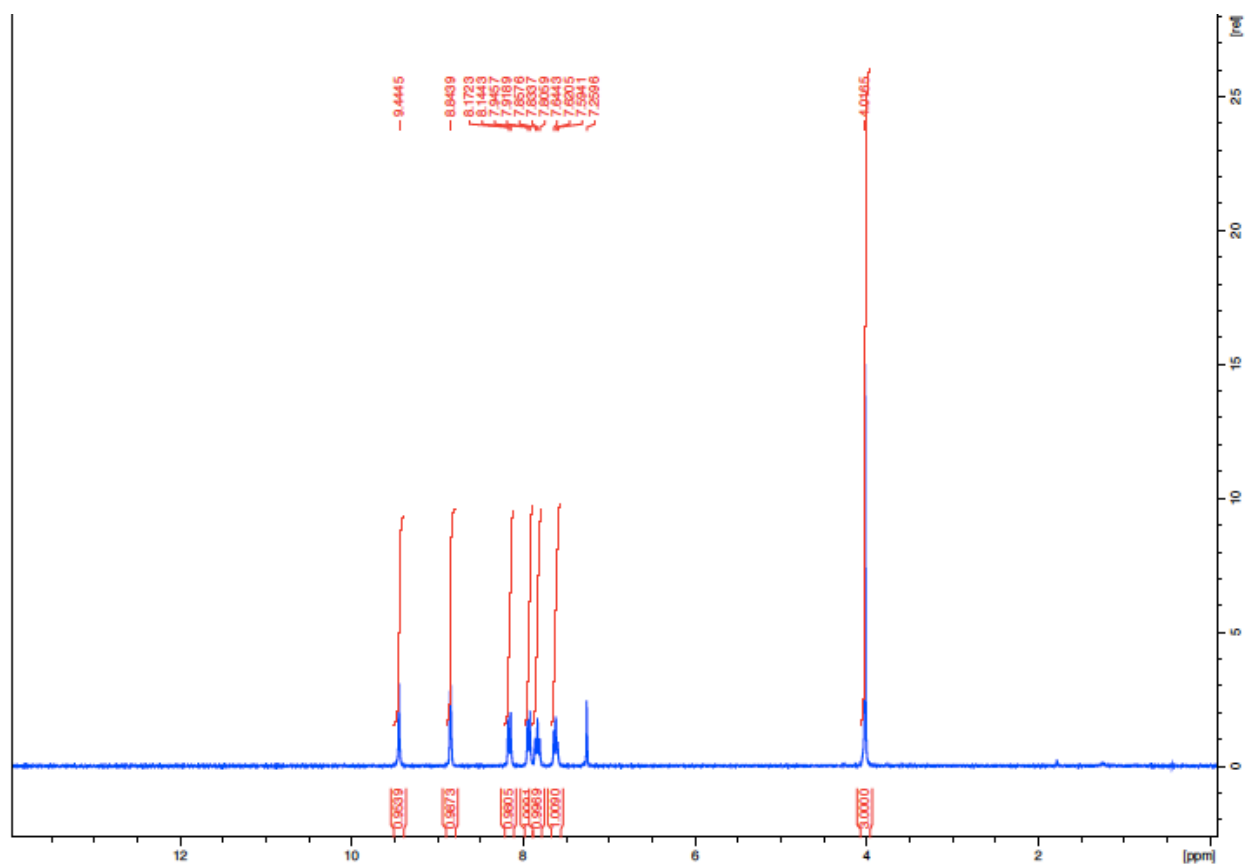
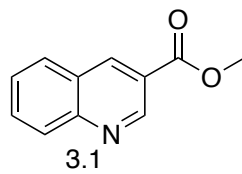


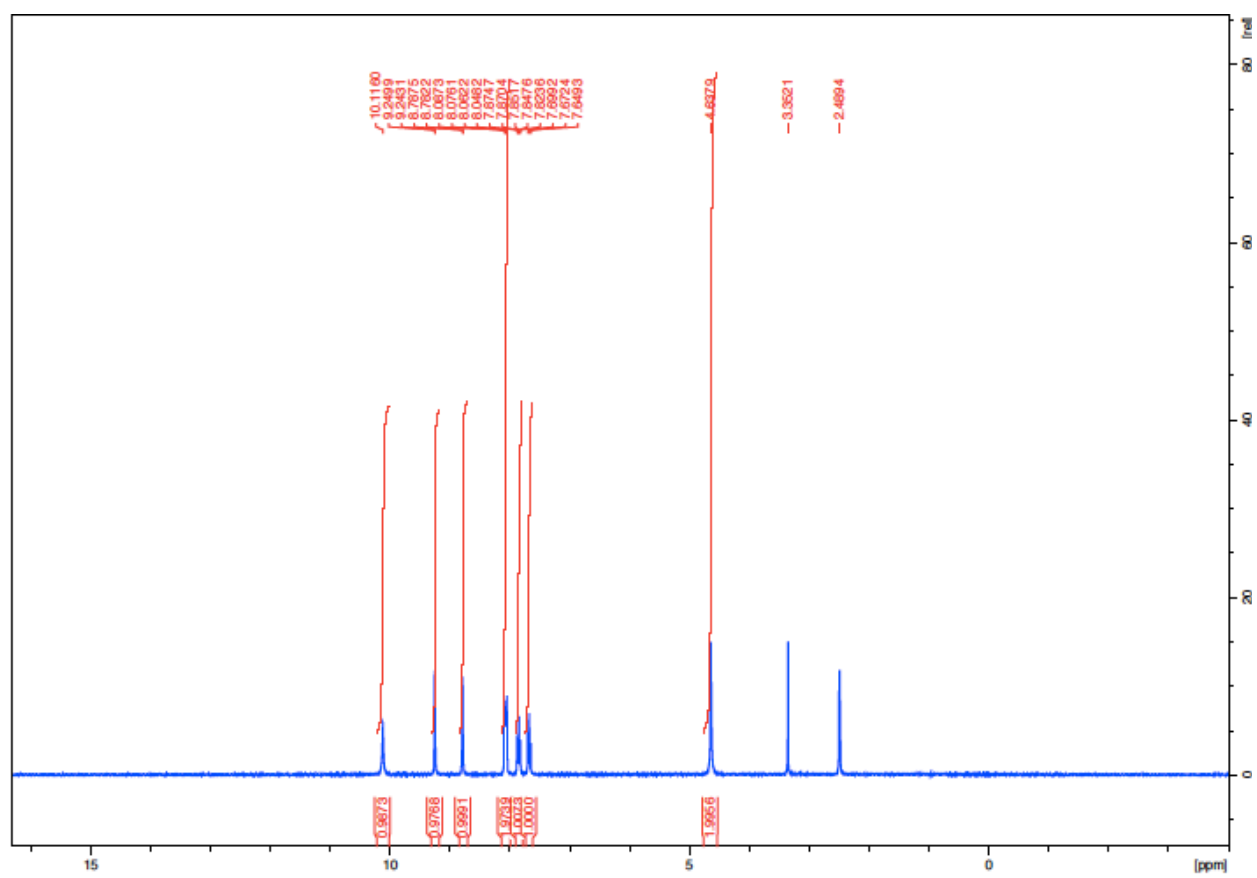
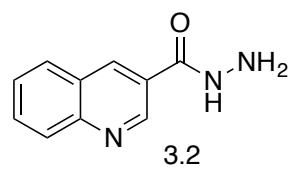


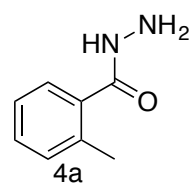
Chapter 2

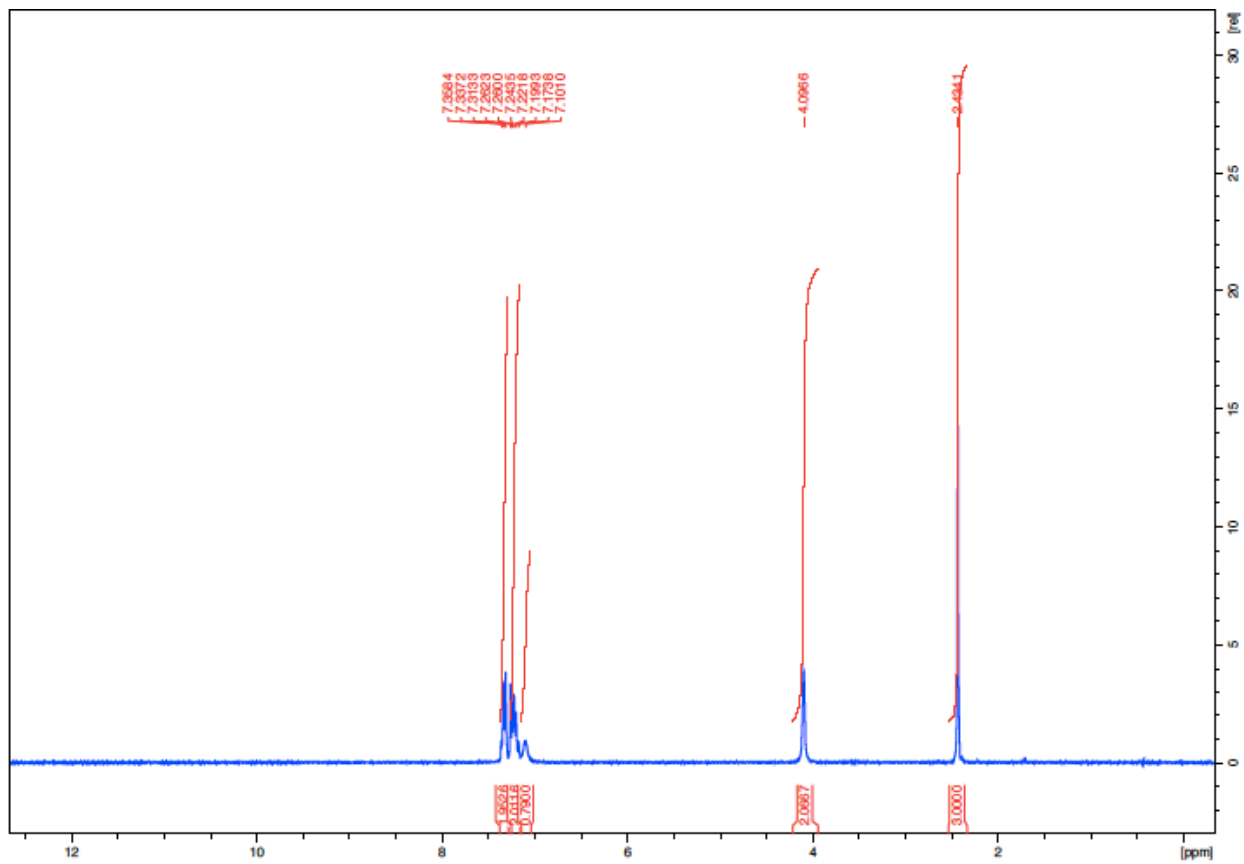


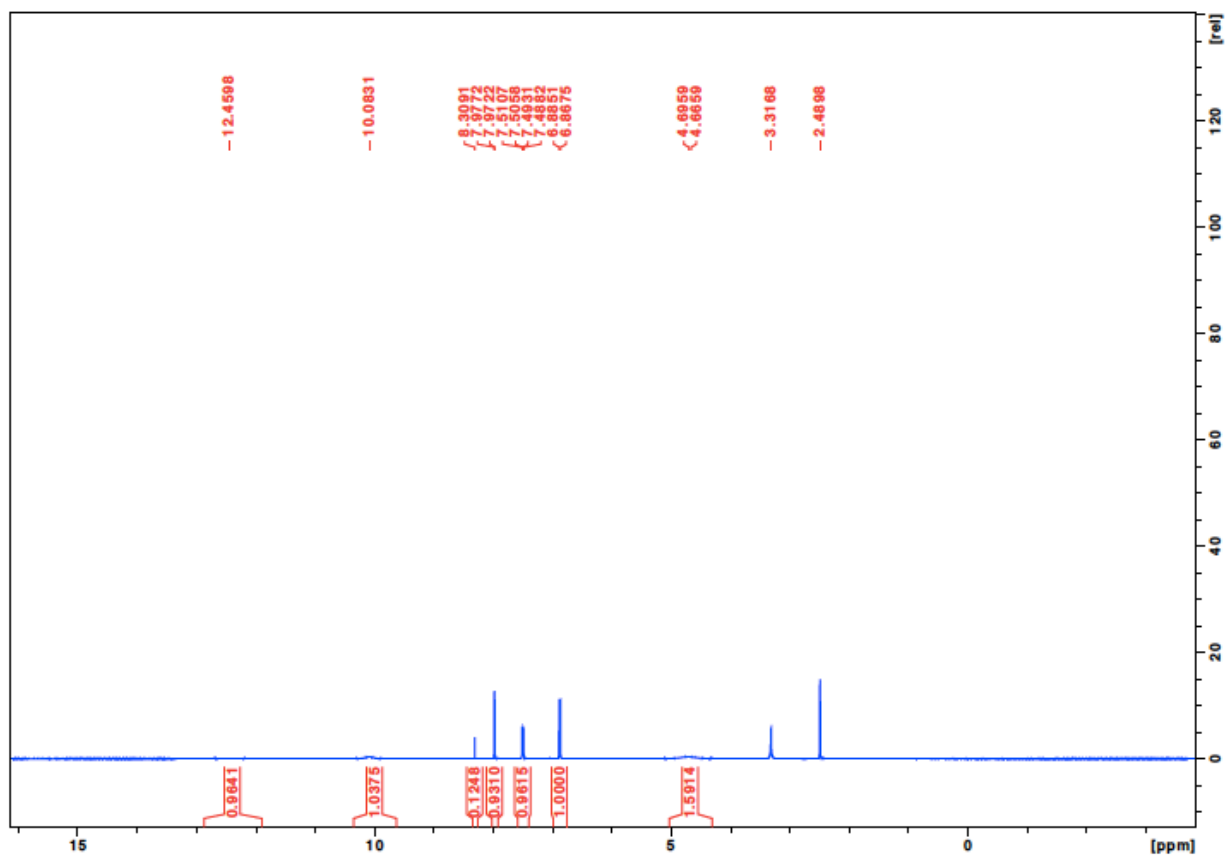
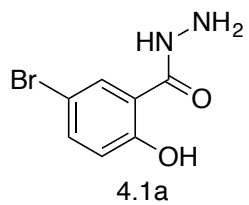


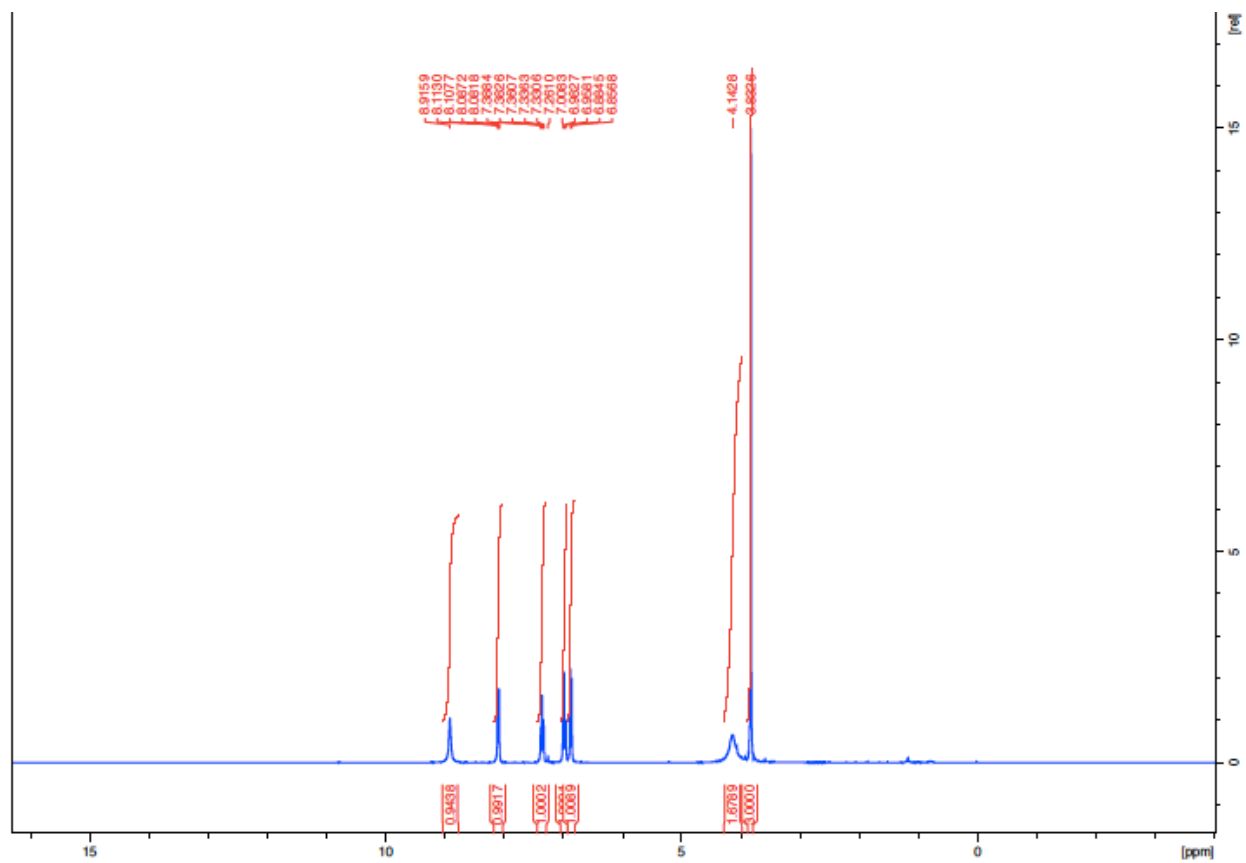
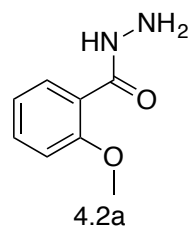


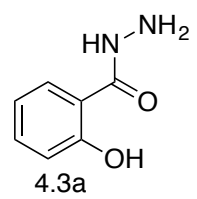


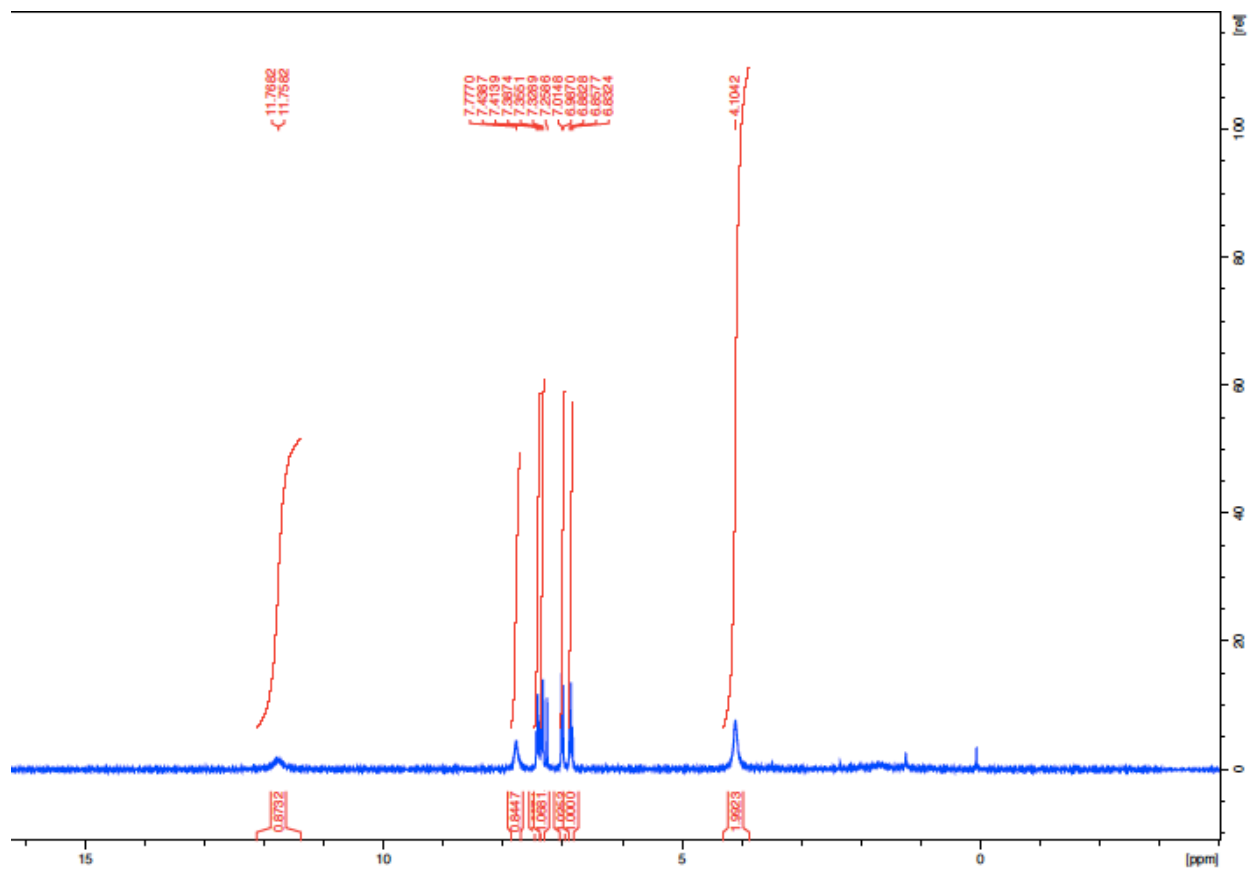


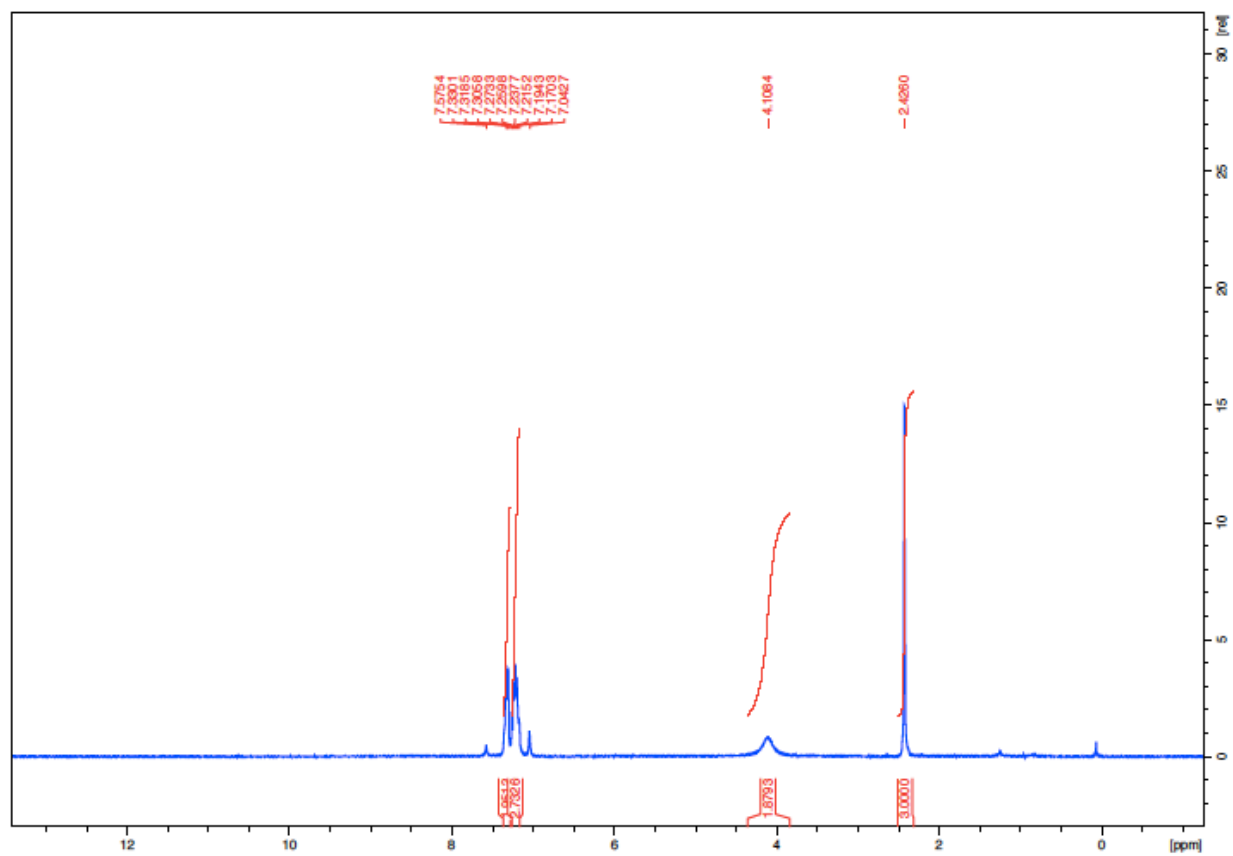
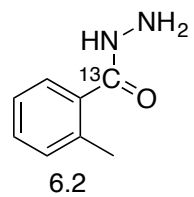


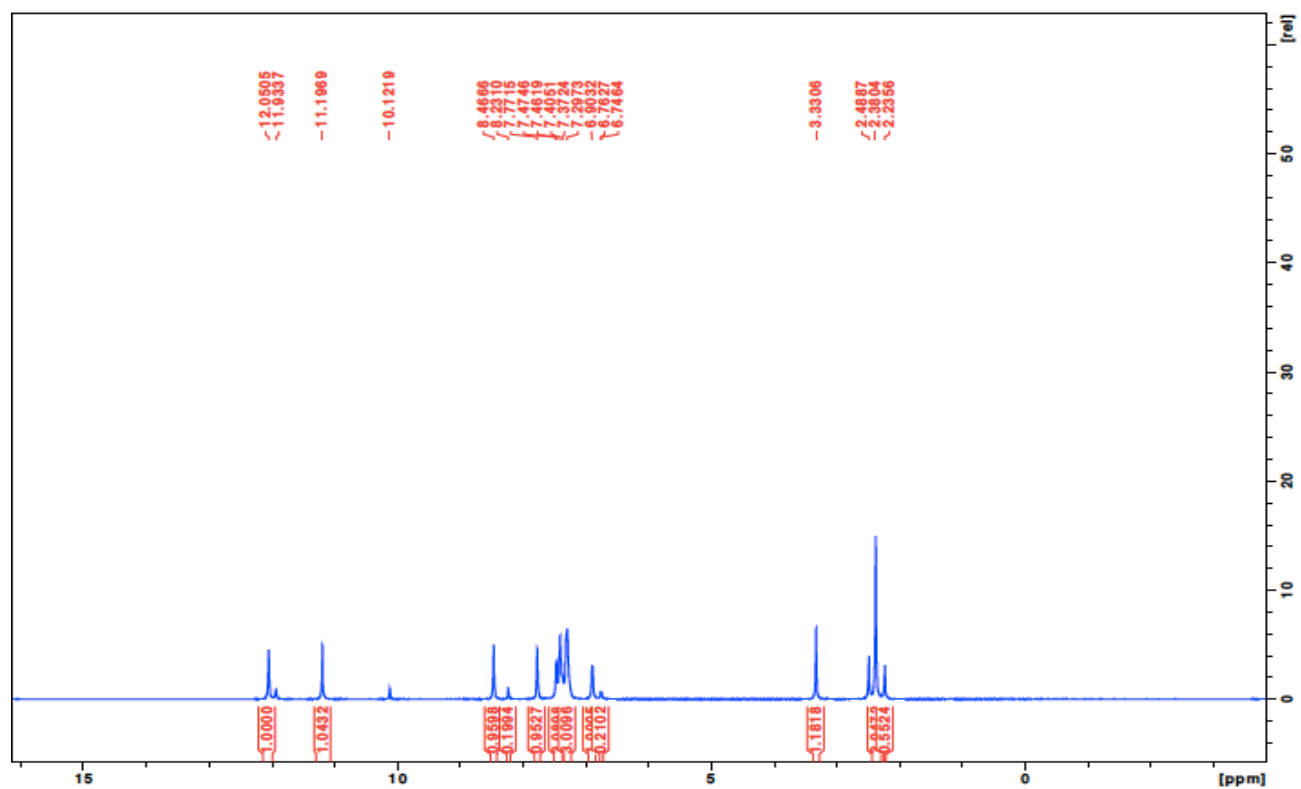
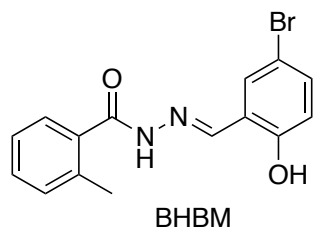


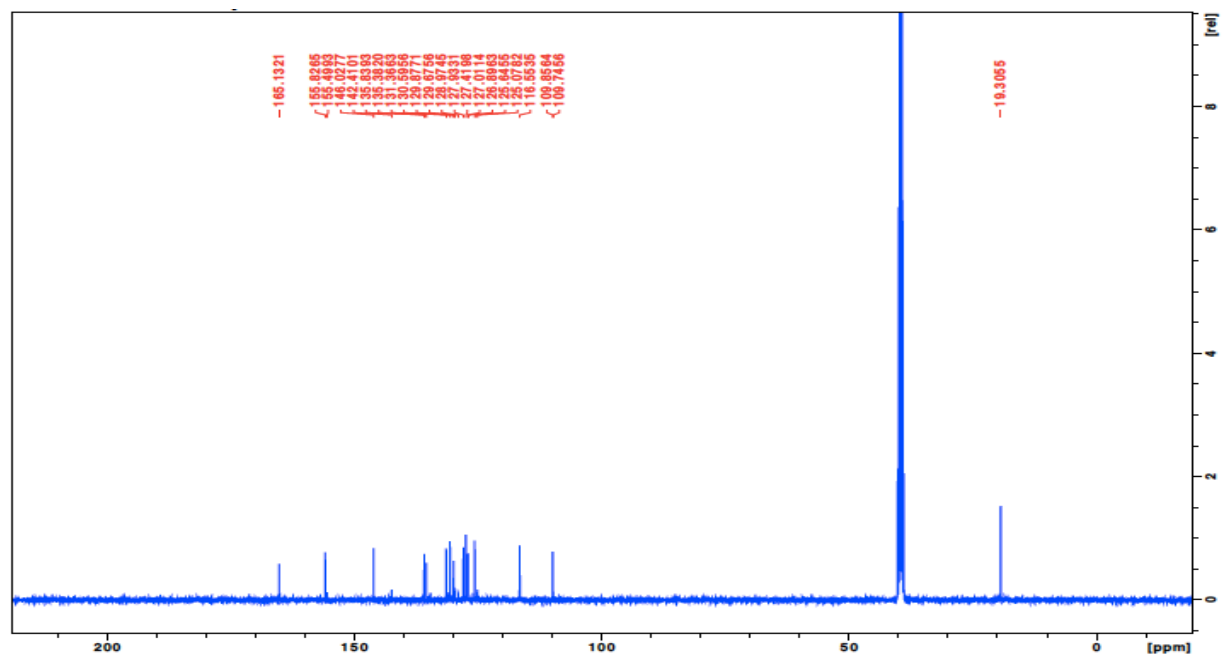
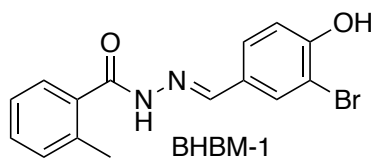
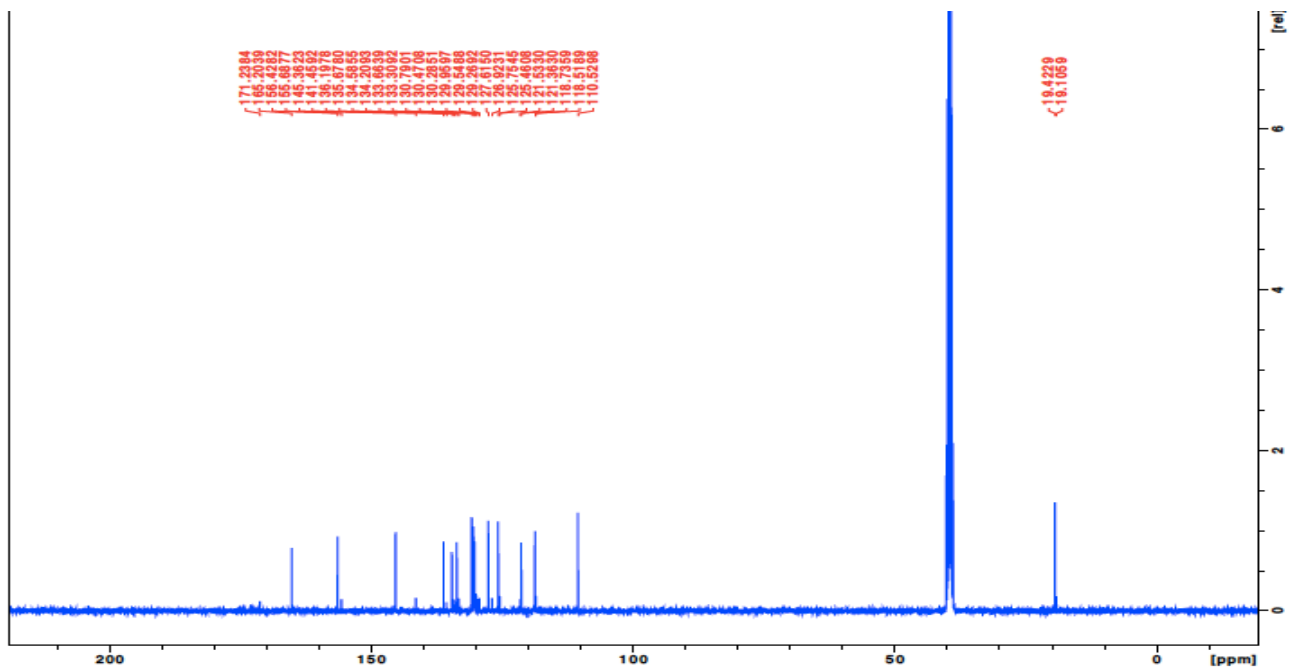


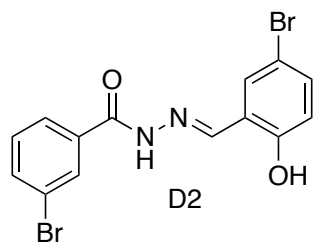
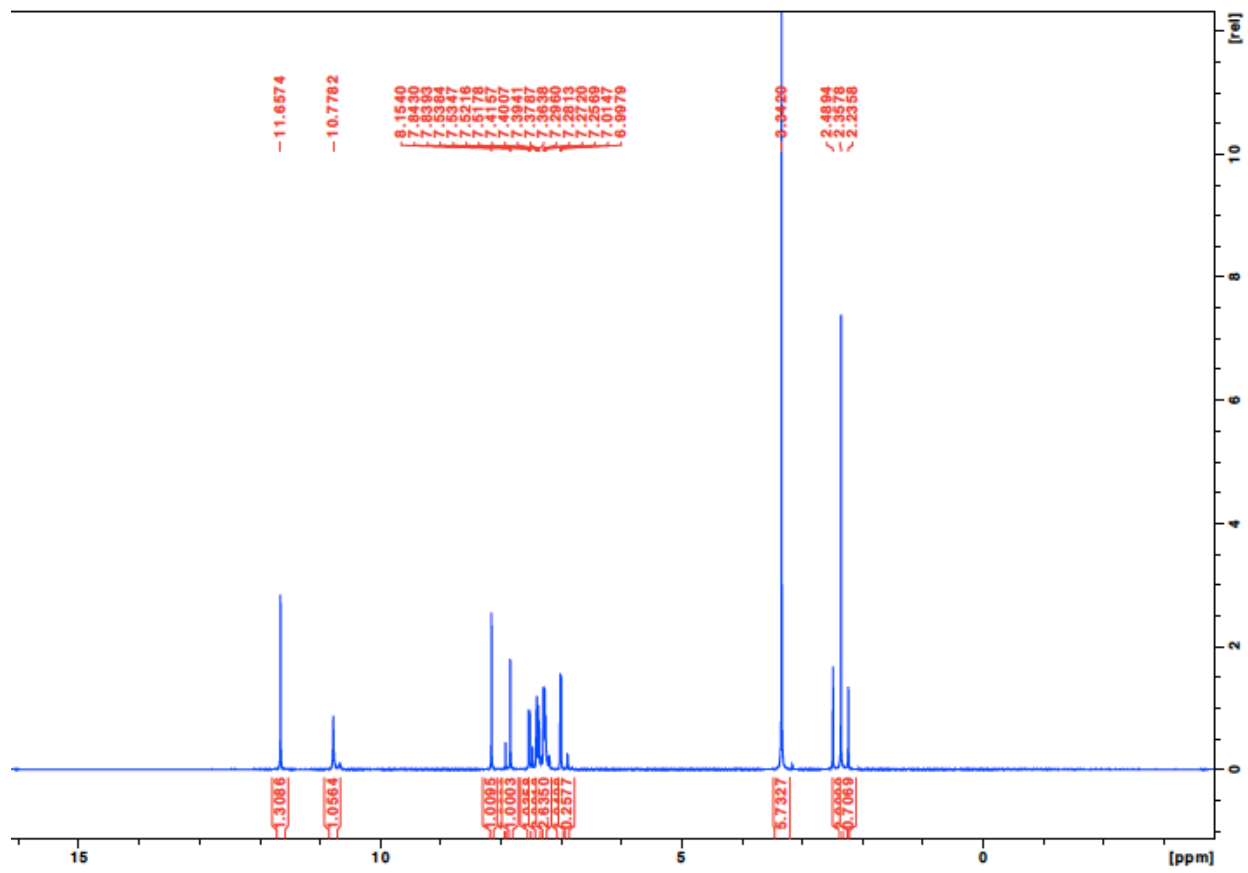


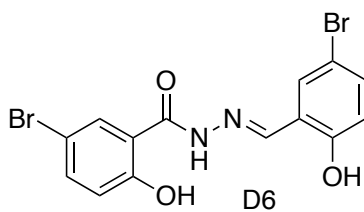
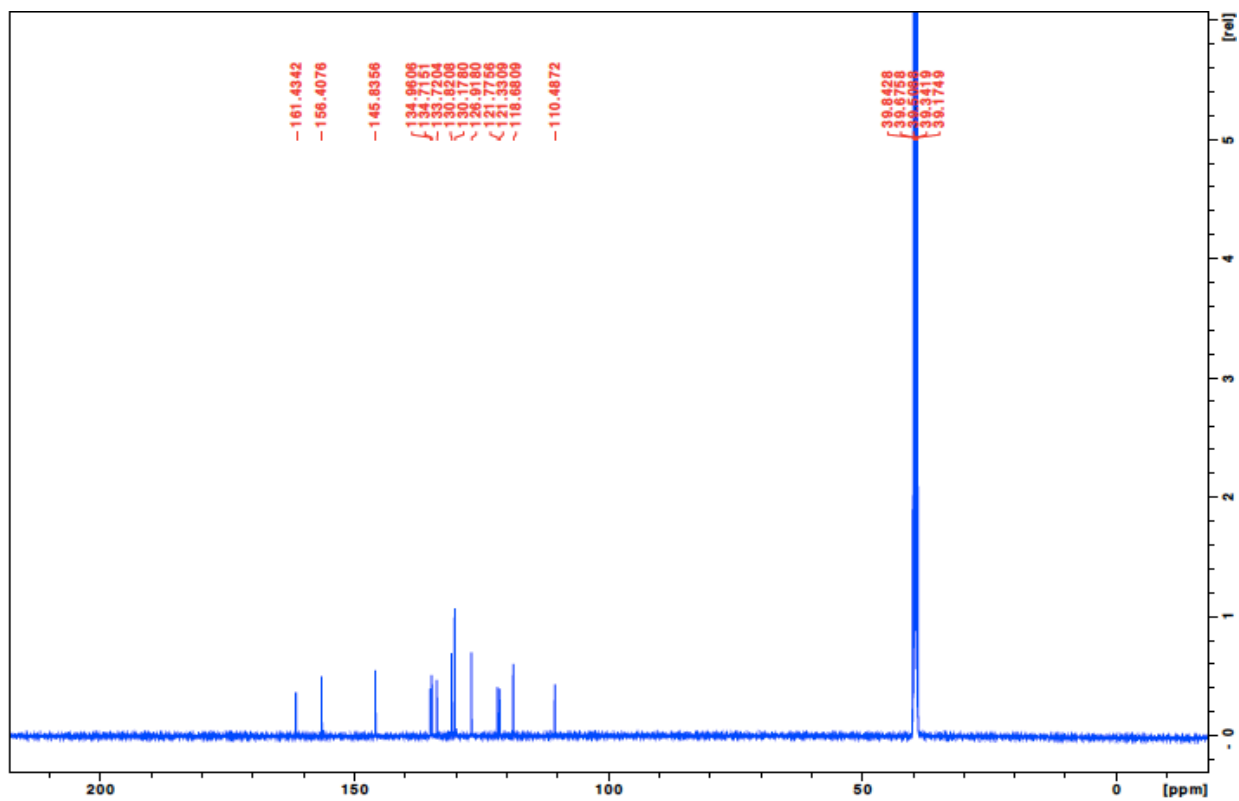
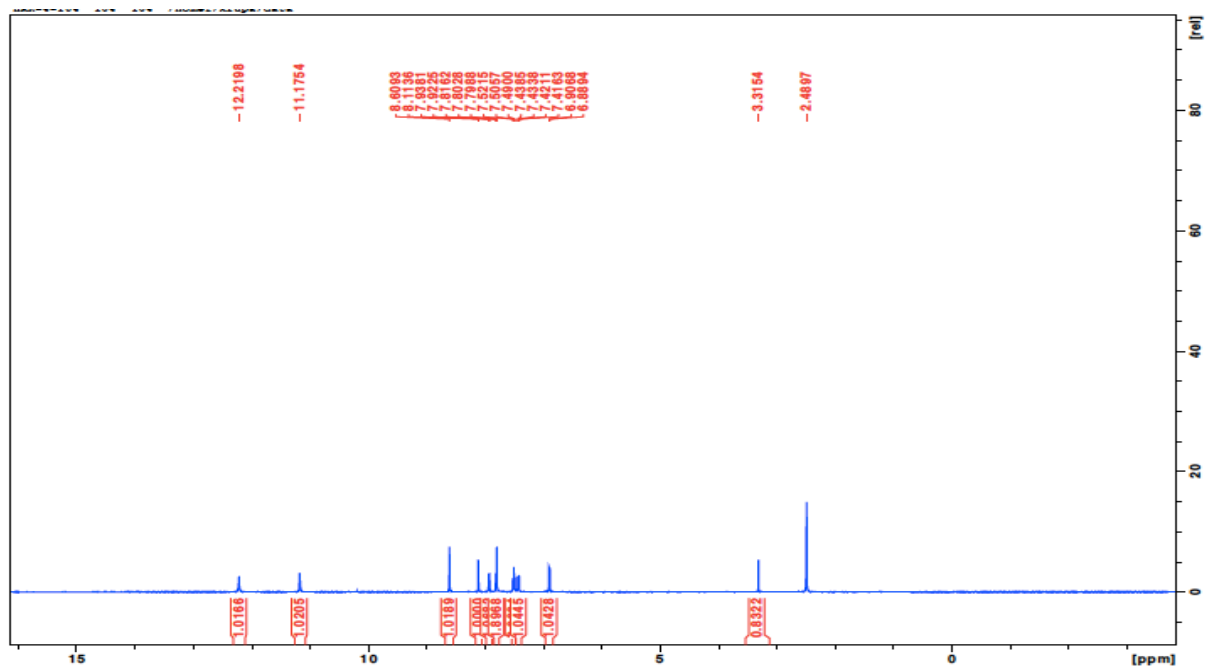


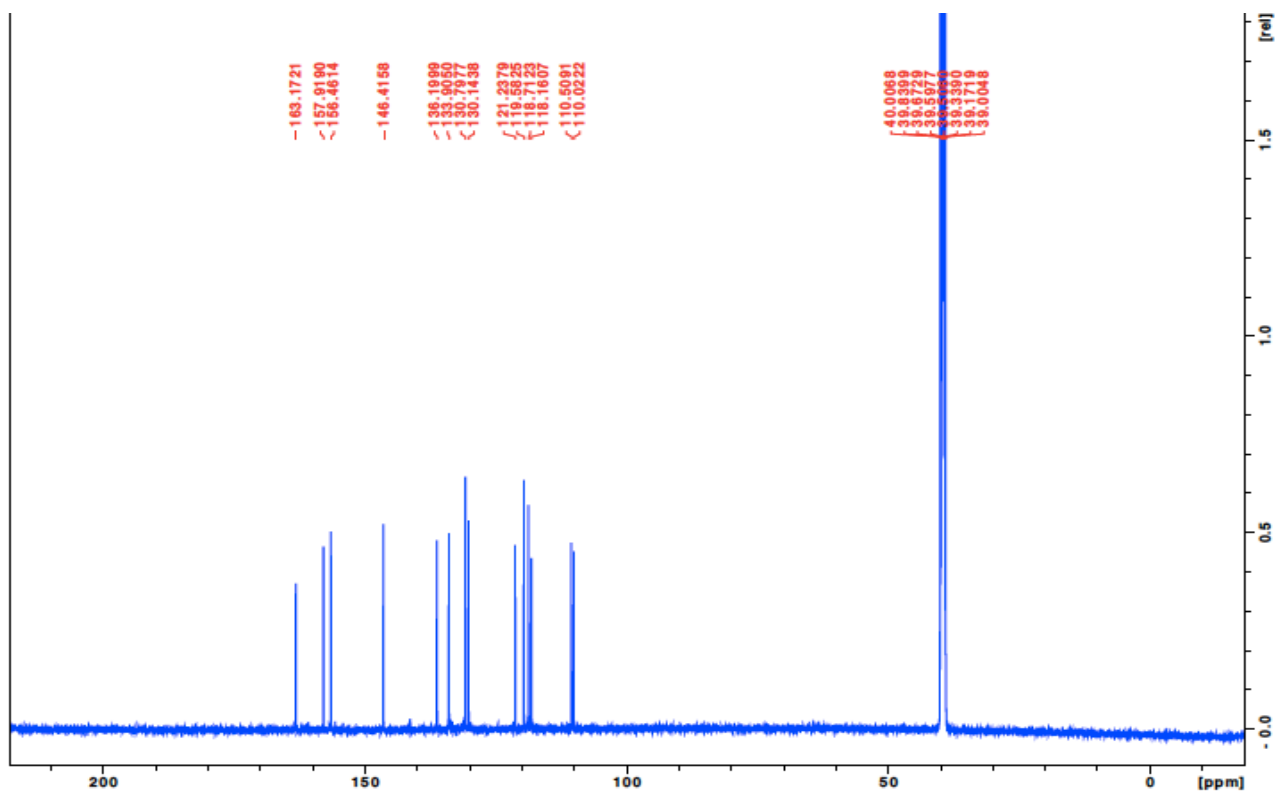
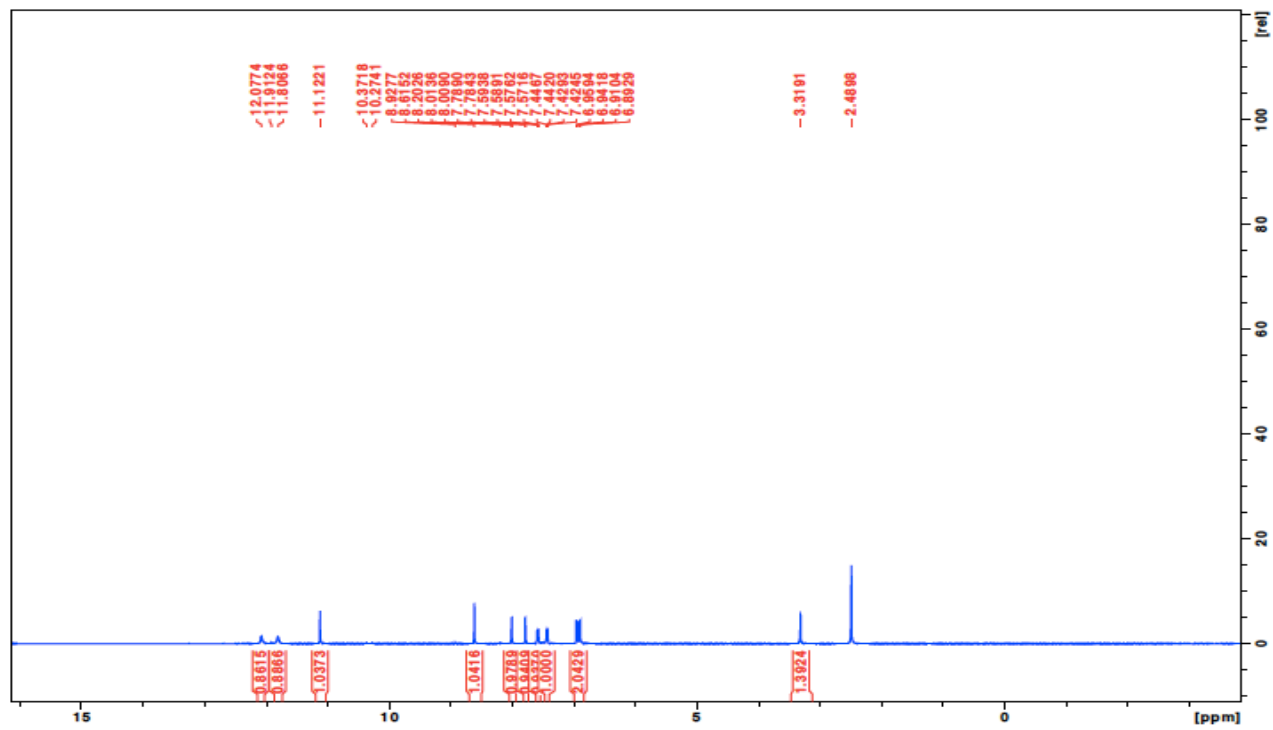


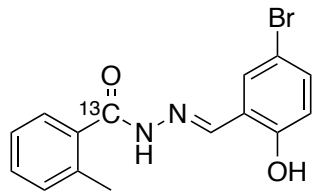




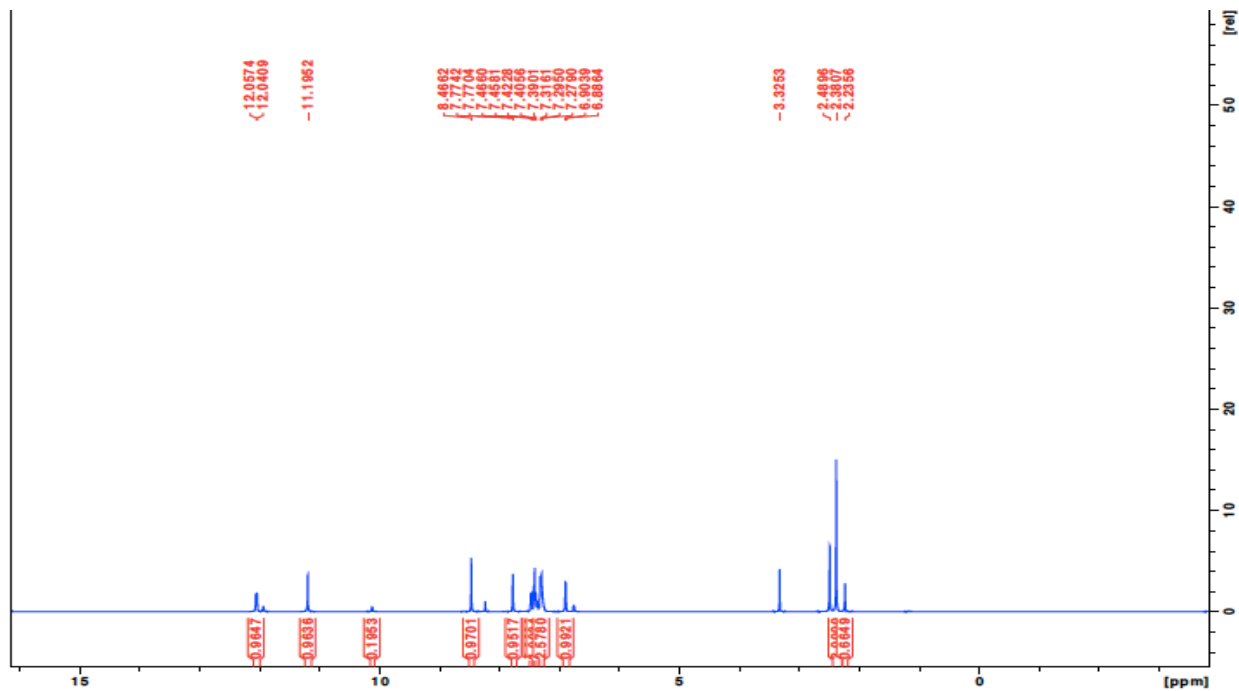


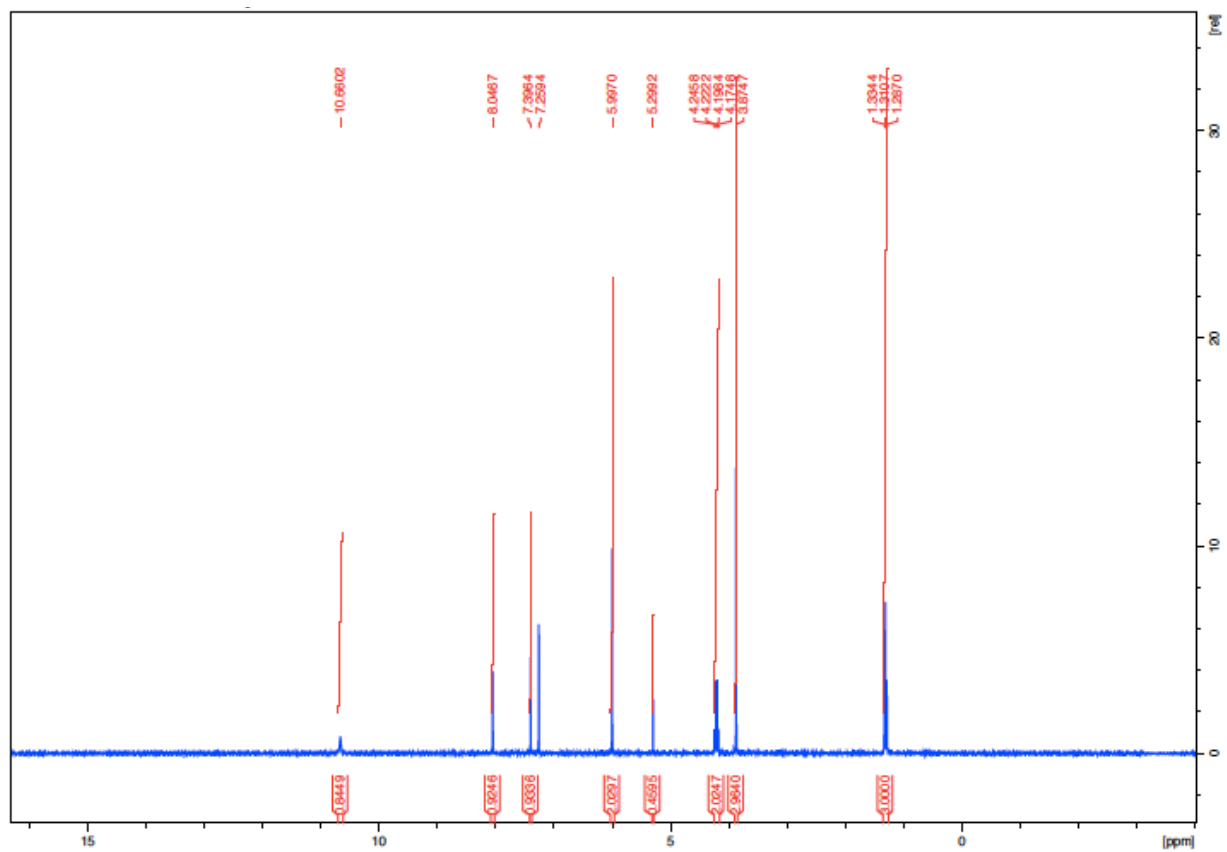


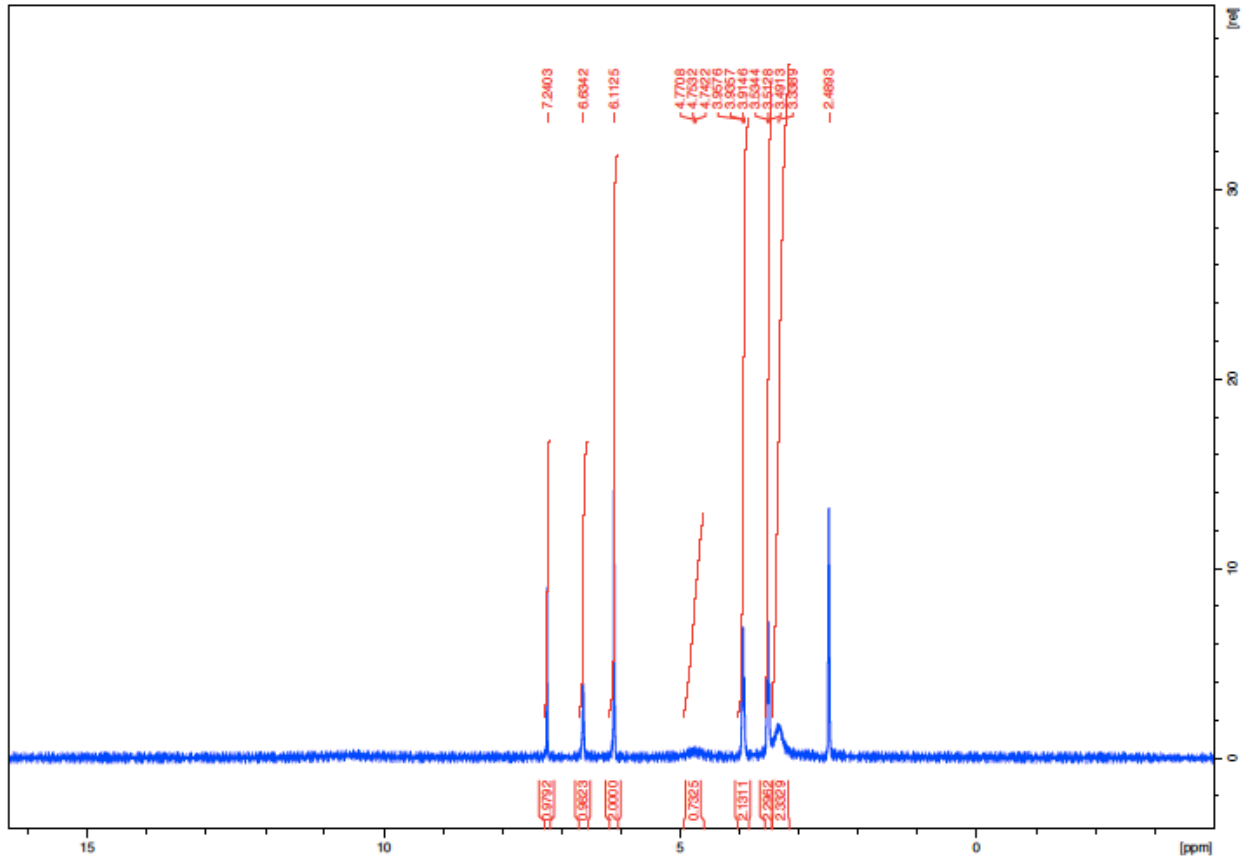
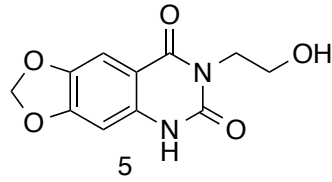


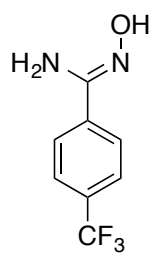


¹³C BHBM

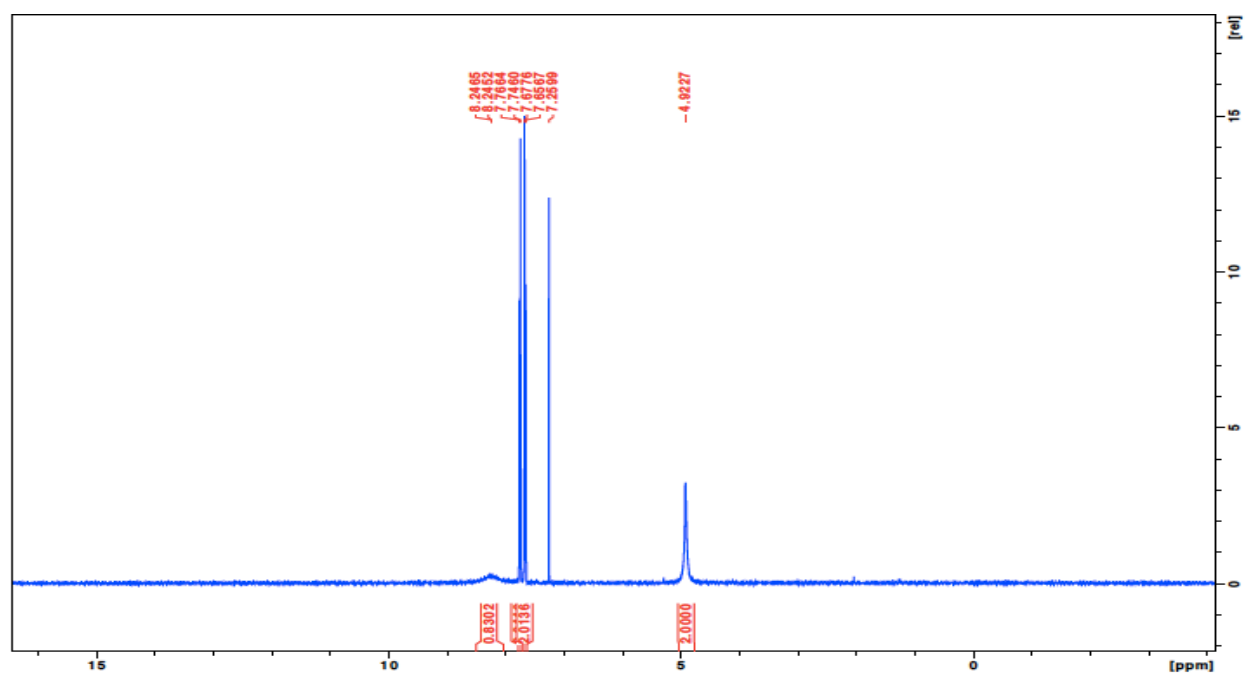


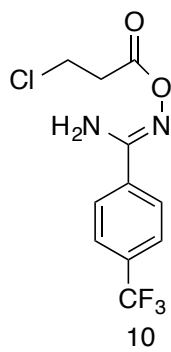
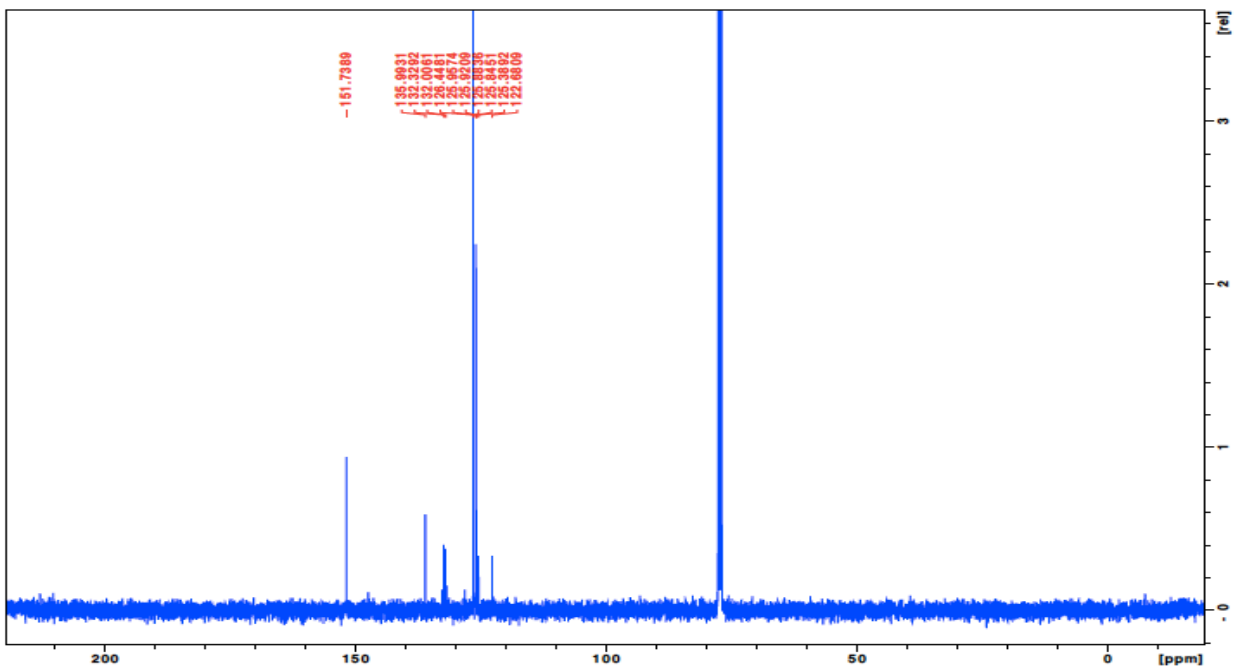


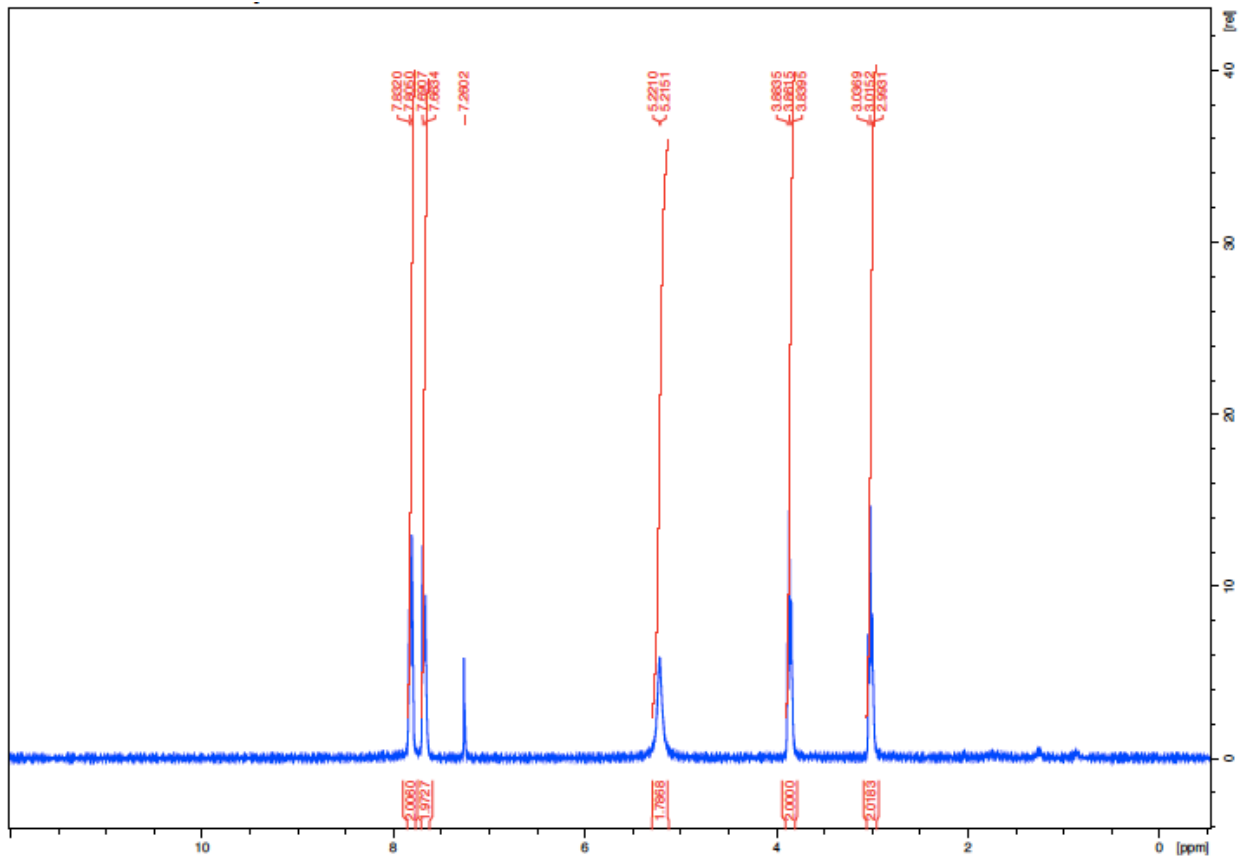


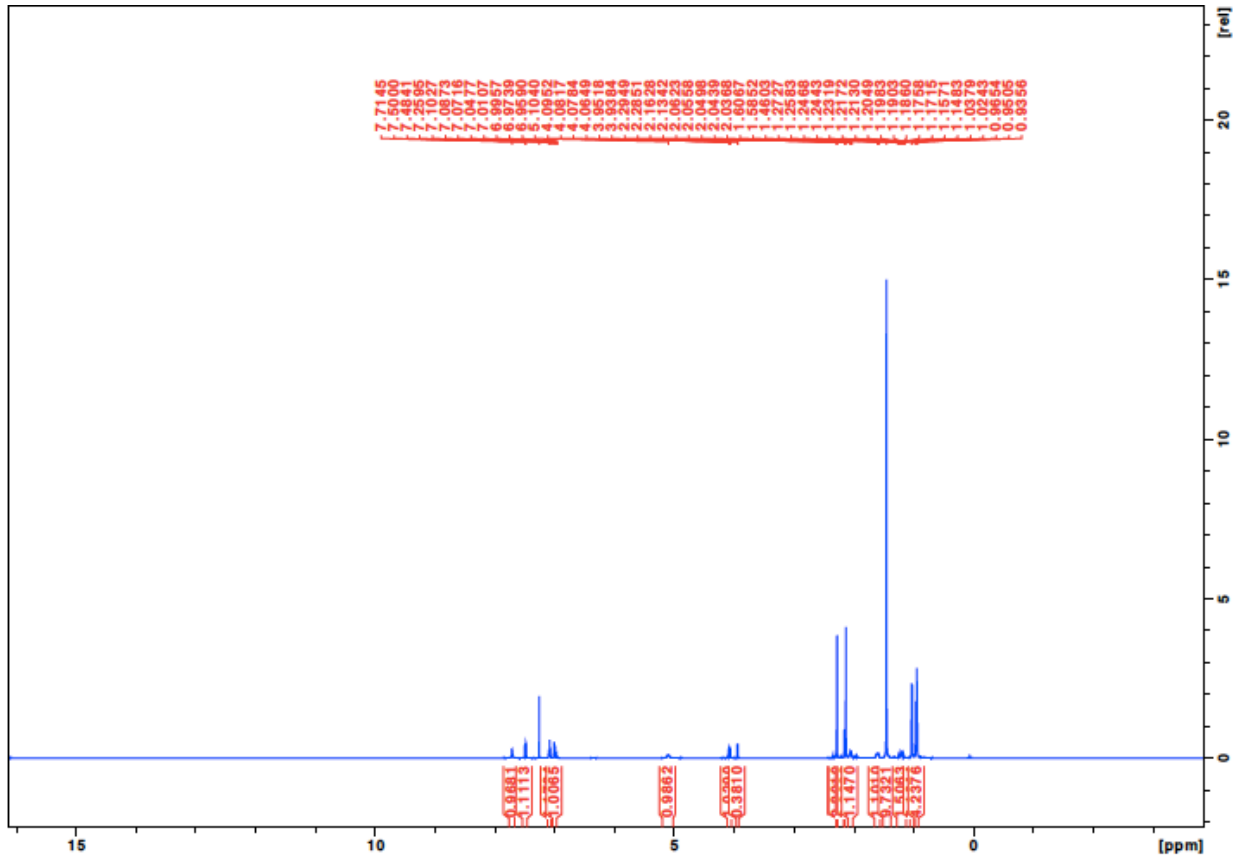
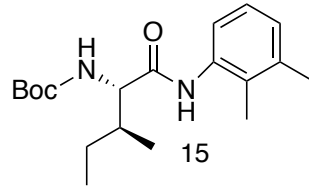


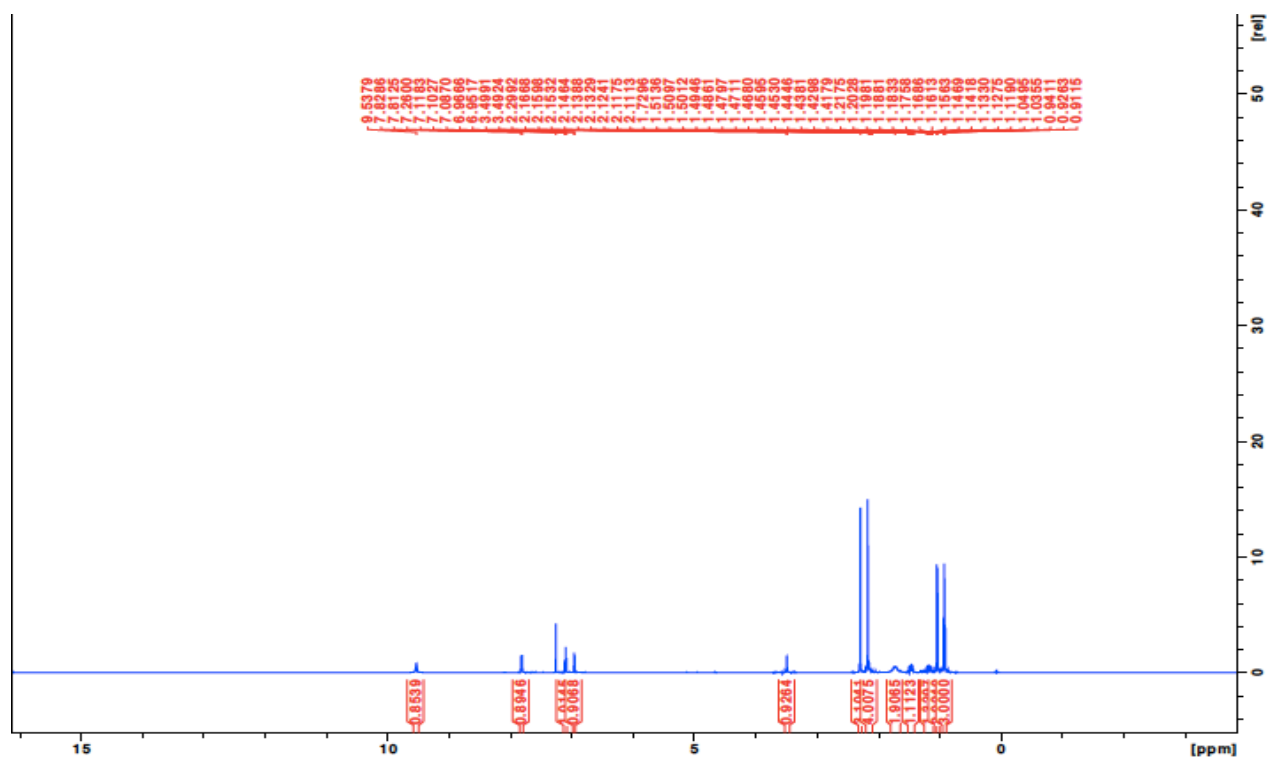
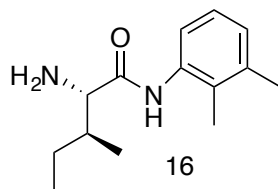
9

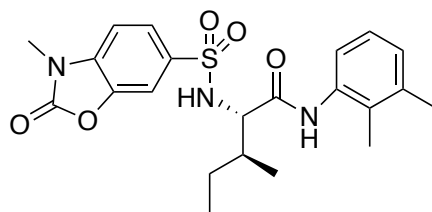
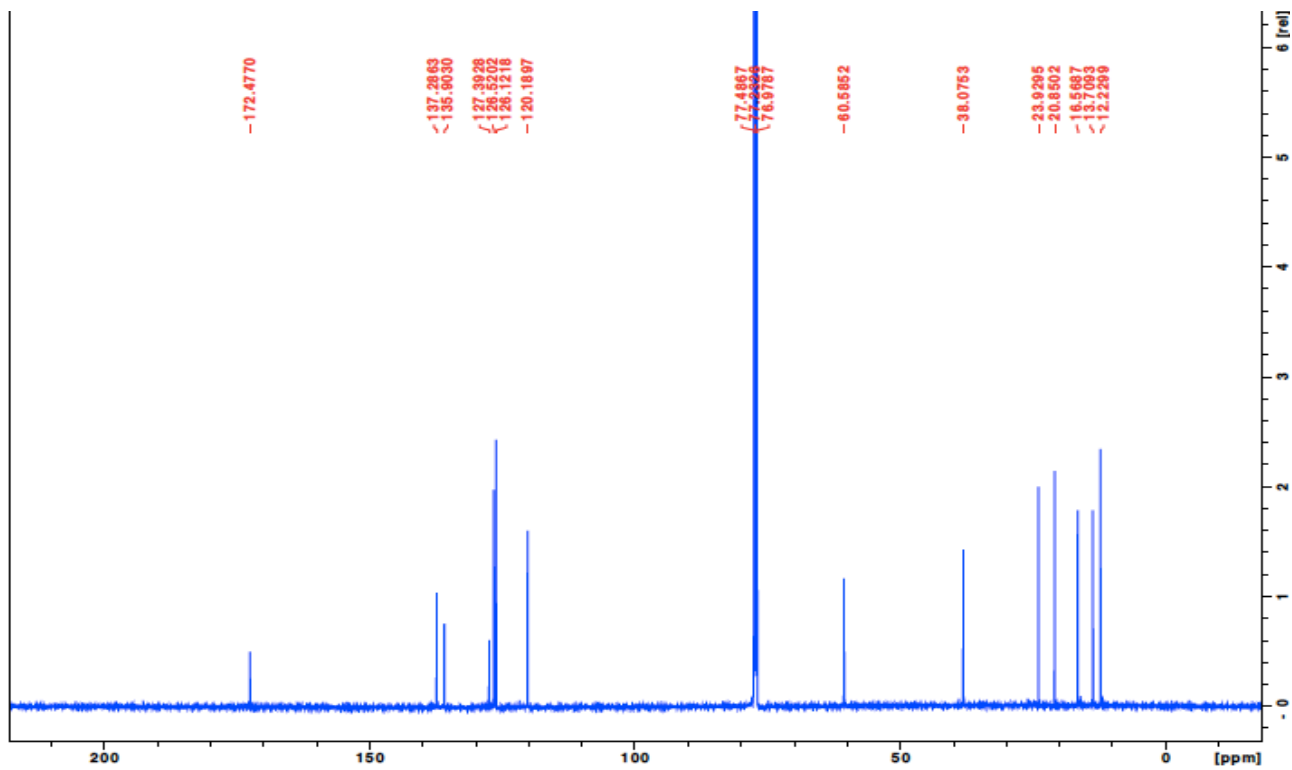












C562-1101-D-Ile

